Denture acrylic biofilms: microbial composition, interactions and infection

Thesis submitted in the part-fulfilment of the requirements of the degree of Doctor of Philosophy

Daniel James Morse
Oral and Biomedical Sciences
School of Dentistry
Cardiff University

2017

Acknowledgements

I would like to start by thanking my supervisory team; Prof. David Williams, Dr. Melanie Wilson, Dr. Xiaoqing Wei, Prof. Mike Lewis and Dr. David Bradshaw. There are no words to show my appreciation for giving me the opportunity to pursue my dream of completing a PhD, and for the continued support and positivity for these past four years. I am eternally grateful, and hope that I can someday begin to repay my debt! I am extremely grateful for the support of the Engineering and Physical Sciences Research Council, and GlaxoSmithKline Consumer Healthcare who funded this PhD with an EPSRC-GSK Case Award studentship. This funding provided many opportunities to pursue experimental ideas, and supported numerous trips to national and international conferences to present my work.

Secondly, a PhD is a task of developing research independence, but so much additional professional support happens behind the scenes. The PhD is a learning process, and along the way I have gained invaluable knowledge and skills. It is difficult to name everyone, but in particular I would like to thank Dr Yuri Cavalcanti, with whom I worked alongside during his visiting research year, Ms Lucy Marsh for her academic and personal support throughout my PhD journey, and Dr Rachael Jordan for taking me under her wings when I first started and making the most difficult times that much easier (and for answering my never-ending *Candida* questions). Dr Helen Rogers and Dr Jeff Wilson for collection of the clinical samples and clinical advice, Dr Ann Smith for support with the clinical study data analysis and interpretation. Dr Kirsty Sands, Dr Paola Marino, Dr Josh Twigg; all part of the DW research group. Also, my sincere gratitude for the support of Dr Craig Murdoch, Dr Helen Colley, Dr Lucie Hadley and Mr Luke Jennings during my visit to University of Sheffield. Of course, the professional and technical support from the 'Tech Team' at DENTL, and sorry to Dr Sarah Bamford for my inability to 'let go' of my old agar plates in the culture fridge.

Thanks to all the friends I have made along this arduous journey; particularly Jordanna (George), Elen, Rhiannon, Paul, Helen, Jabur, Daf, Hayley and Sue, and everyone who has ever expressed an interest and spoken to me about my research at conferences – I found inspiration in every conversation!

Finally, a massive thank you to my wife Lauren, without the support of whom I would not have been in a position to follow my dream of completing a PhD; my two sons, Ruben and Oliver who mean the absolute world to me, and give me a hundred reasons to smile every day; my parents Lynda and Chris, Ian, Jen, and extended families, and a special thank you to my mother in-law Shelley for her fantastic support at home. Also, to my late grandmother, Joan, who always believed in me – I hope that I have, and can continue to make you proud.

"If you think you can do it, you're probably right!" Mr Alan Bootle

Table of Contents

List of tables

List of figures

Chapter 3

Chapter 4

Chapter 5

List of abbreviations and units

AIDS	acquired immunodeficiency syndrome
AHL	*N*-acyl homoserine lactone
AI	autoinducer
ALI	air-liquid interface
ALS	agglutinin like sequence
ANOVA	analysis of variance
AS	artificial saliva (solution)
ATCC	American type culture collection
BA	blood agar
BHI	brain-heart infusion
BLAST	basic local alignment search tool
BM	basement membrane
cAMP	cyclic adenosine monophosphate
CBA	cytometric bead array
cDNA	complementary deoxyribonucleic acid
CFU	colony forming unit
CHC	chronic hyperplastic candidosis
CLSM	confocal laser scanning microscopy
d	day
DMEM	Dulbecco's modified Eagle's medium
DMEM-F12	Dulbecco's modified Eagle's medium supplemented with Ham's F12
DNA	deoxyribonucleic acid
dNTPs	deoxyribonucleoside triphosphates
DS	denture-associated stomatitis
eDNA	extracellular deoxyribonucleic acid
ELISA	enzyme linked immunosorbant assay
EPA	epithelial adhesin
EPS	extracellular polymeric substance
FAA	fastidious anaerobe agar
FBS	foetal bovine serum
FISH	fluorescence in-situ hybridisation
FITC	Fluorescein isothiocyanate
FT	full thickness (tissue models)
gDNA	genomic deoxyribonucleic acid
GlcNAc	*N*-acetyl-D-glucosamine

h	hour
HIV	human immunodeficiency virus
HKC	heat killed *Candida*
HTA	human tissue authority/human tissue act
HWP	hyphal wall protein
IL	interleukin
ITS	internal transcribed spacer
L	litre
LP	lamina propria
LPS	lipopolysaccharide
LTE	lysozyme tris-EDTA buffer
MIC	minimum inhibitory concentration
NaOH	sodium hydroxide
NCTC	National collection of type cultures
NGS	next generation sequencing
NRES	national research ethics service
OTU	operational taxonomic unit
PBS	phosphate buffered saline
PCR	polymerase chain reaction
PG	peptidoglycan
pH	potential of hydrogen
PhD	doctor of philosophy
PL	phospholipase enzyme
PMMA	poly(methyl methacrylate)
PNA	peptide nucleic acid
qPCR	quantitative polymerase chain reaction
QSM	quorum sensing molecule
REC	research ethics committee
RNA	ribonucleic acid
rRNA	ribosomal ribonucleic acid
RPMI	Roswell Park memorial institute (medium)
RT-PCR	reverse-transcription polymerase chain reaction
SAP	secreted aspartyl proteinase
SDA	Sabouraud dextrose agar
SD	standard deviation
SE	stratified epithelium
SEM	scanning electron microscopy/standard error of the mean

STAMP	structural time series analyser, modeller and predictor
TE	Tris-ethylenediaminetetraacetic acid (Tris-EDTA buffer solution)
v/v	volume per unit volume
w/v	weight per unit volume
YNB	yeast nitrogen base

Preface

All work unless otherwise stated was completed at the School of Dentistry, Cardiff University.

In vitro full thickness tissue model culture was completed in collaboration with Dr Craig Murdoch and Dr Helen Colley at the School of Clinical Dentistry, University of Sheffield.

The research presented in Chapters 2 and 4 were, in part, published as follows:
Cavalcanti, Y. W., Morse, D. J., da Silva, W. J., Del-Bel-Cury, A. A., Wei, X., Wilson, M. J., Milward, P., Lewis, M., Bradshaw, D. J., & Williams, D. W. (2015). Virulence and pathogenicity of *Candida albicans* is enhanced in biofilms containing oral bacteria. *Biofouling:Journal of The Bioadhesion and Biofilm Research*, *31*(1), 27–38

The research presented in Chapters 3 and 4 were, in part, published as follows:
Morse, D.J., Wilson, M.J., Wei, X., Lewis, M.A.O., Bradshaw, D.J., Murdoch, C. and Williams, D.W. (2018). Denture-associated biofilm infection in three-dimensional oral mucosal tissue models. *Journal of Medical Microbiology* [Online]:1–12. Available at: http://www.microbiologyresearch.org/content/journal/jmm/10.1099/jmm.0.000677.v1

Throughout the PhD, I have attended many conferences to present my research, and have received a number of awards. These are:

2017
British Society for Oral and Dental Research, Plymouth, UK
Oral Presentation: Contribution of oral bacteria to *Candida* virulence and denture stomatitis
Senior Colgate Prize Entry Winner

2016
Biofilms7, Porto, Portugal
Poster: Development of an *in vitro* oral mucosal tissue model for biofilm infection
Poster Prize Winner

2015
MITReG annual meeting, Canada Lake and Lodge, Cardiff, UK
Poster: Bacteria increase expression of *Candida* virulence factors in biofilms
Poster Prize Runner Up

Cardiff Institute of Tissue Engineering and Repair (CITER), Bristol, UK
Oral Presentation: Development of an *in vitro* tissue model for biofilm infection
Highly Commended

2014
Oral Microbiology and Immunology Group (OMIG) meeting, Gregynog, Wales
Poster: Development of an *in vitro* biofilm model on denture acrylic
Poster Prize Winner

Abstract

Denture-associated stomatitis (DS), a frequent infection in denture-wearers (up to 60%), presents as areas of palatal inflammation and is normally associated with denture biofilms containing *Candida albicans*. However, the contribution of co-existing bacteria in these biofilms to the infection remains unclear. As current DS management strategies are primarily directed towards *Candida*, research demonstrating the impact of specific bacteria upon infection prognosis is important to improve treatment regimes. This research evaluated the *in vitro* impact of bacteria on *Candida* virulence, and compared bacterial microbiomes at specific oral sites in DS and non-DS patients to determine associations with infection.

In vitro biofilm studies assessed expression of *C. albicans* virulence factors (morphological transformation, adhesins, hydrolytic enzymes) and their impact on pathogenesis in an infection model. In clinical studies, microbiological samples were obtained from the tongue, palate and denture-fitting surface of 19 denture-wearing patients (DS n=8, non-DS n=11). The presence of *Candida* was ascertained by PCR. Bacterial DNA was extracted and subjected to next generation sequencing using bacterial 16S rRNA gene targets, and differences in the bacterial microbiomes determined.

Certain bacterial species in acrylic biofilms significantly ($P<0.05$) increased the expression of *C. albicans* virulence factors, and subsequently, enhanced tissue damage in model systems. *Candida* was detected in clinical samples of 14 patients (DS n=6, non-DS n=8). Metataxonomic analyses revealed differences in relative abundance of bacterial species, but no significant differences in the bacterial microbiomes of the denture-fitting surface and palate between DS and non-DS patients. Importantly, a significant ($P=0.007$) increase in the number of bacterial species was evident for the tongue microbiome of non-DS patients.

The *in vitro* modulating capacity of bacteria toward *Candida* virulence, and the observed species-level differences in bacteria between DS and non-DS patients highlight the need for consideration of the bacterial composition of oral biofilms in the pathogenesis of DS.

Chapter 1

Literature review

1.1 Biofilms

1.1.1 Introduction to biofilms and their ubiquitous prevalence

1.1.1.1 The makeup and structure of biofilms

Microorganisms rarely exist in a free-living or planktonic state. Most often, microorganisms grow in the form of a biofilm, which can simply be defined as dynamically interacting aggregates of microorganisms, often attached to biotic or abiotic surfaces (Flemming & Wingender, 2010) (Fig. 1.1). Such biofilms may comprise of a single species (monotypic) or most often as a polymicrobial community of several species. A biofilm can have distinct three-dimensional components to its structure and will contain not only the microorganisms, but also a range of other components, detailed in Table 1.1, including biofilm-derived extracellular polymeric substances (EPS) (Flemming *et al*., 2007; Costerton *et al.*, 1999).

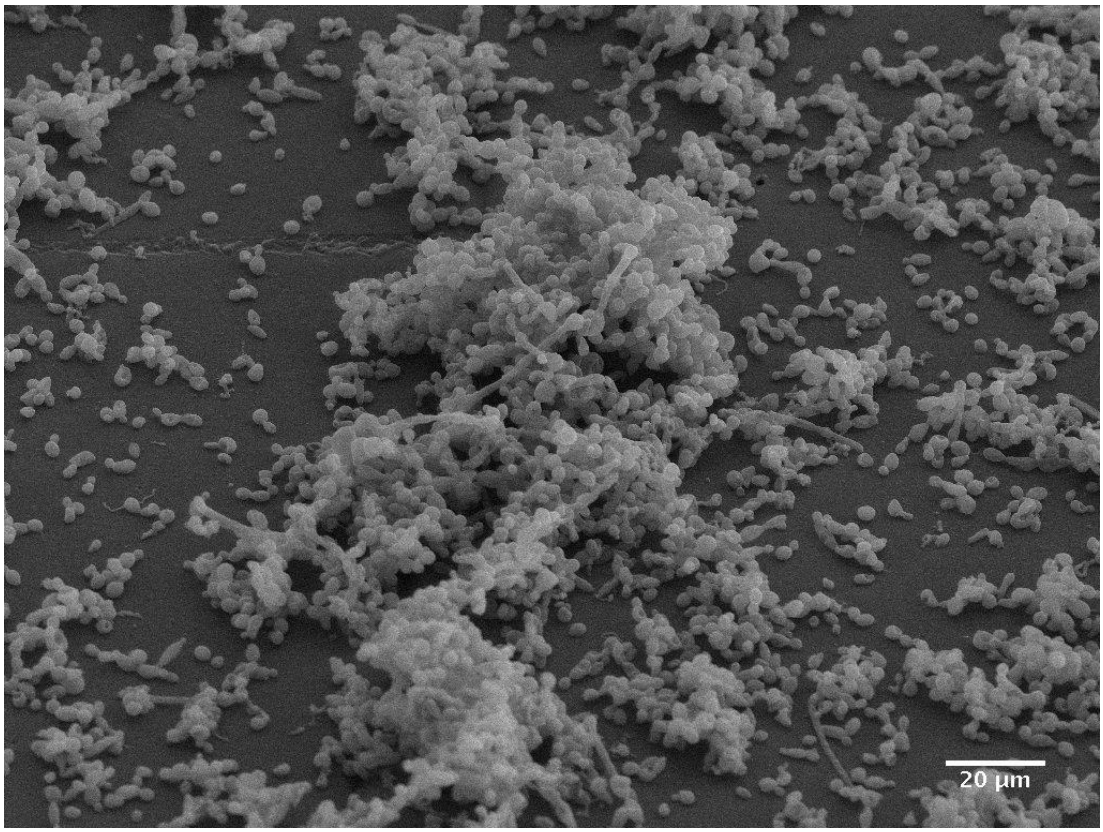

Figure 1.1 Representative scanning electron microscopy image showing example of *in vitro* polymicrobial biofilm grown on denture acrylic

Component	Proportion of matrix (%)
Water	Up to 97%
Microbial cells	2-5% (mixed-species)
Polysaccharides (homo- and heteropolysaccharides)	<1-2% (neutral and polyanionic)
Proteins (extracellular, and from cell lysis)	<1-2% (including enzymes)
DNA/RNA	<1-2% (lysed cells)
Ions	Unknown (bound and free)

Table 1.1 Typical components of biofilm matrices
Table used with permission from Sutherland (2001)

The EPS varies considerably in content depending on the environment in which it exists, and the microorganisms that make up the biofilm (often being species specific). For example, biofilms of the fungus *Candida albicans* typically contain a high percentage of carbohydrates (39.6%) relative to proteins (5%) or amino sugars such as hexosamines (3.3%). In contrast, *Candida tropicalis* biofilms contain much higher levels of hexosamines (27%) and lower levels of carbohydrates (3.3%) (Al-Fattani & Douglas, 2006). Paper mill-derived biofilms have also been shown to contain a substantial range of concentrations of various sugars, indicating the variability between biofilms formed by different microorganisms (Lindberg *et al*., 2001). This investigation found that the EPS of single-species biofilms of numerous different species of bacteria, including those of the genera *Burkholderia*, *Bacillus* and *Alcaligenes,* contained high levels and a large array of sugars including glucose, mannose, arabinose and galactose.

Although the chemical makeup in relative proportions of the different components of EPS may vary, the typical constituents of biofilm EPS are water, carbohydrates, proteins and extracellular DNA (eDNA), which are secreted by the biofilm cells. In addition to these, the contents from lysed cells; proteins, cytoplasmic material, genomic DNA and other cell components will also be present (Sutherland, 2001).

The EPS, eloquently referred to by Flemming *et al* (2007) as the “house of biofilm cells”, is multi-functional. EPS provides a physical function by providing a ‘material scaffold’ allowing biofilm maturation and expansion in a three-dimensional manner (Hall-Stoodley & Stoodley, 2002). The EPS protects biofilm cells from alteration of environmental factors including effects of temperature and pH. The EPS also serves as a source of nutrients for microorganisms (Flemming & Wingender, 2010). Additionally, increased tolerance of severe conditions, or the effects of antimicrobial compounds can be attributed to uptake of resistance genes by horizontal transfer of DNA from bacterium to bacterium, even of different genera, or by the active uptake of eDNA from the local environment (Hannan *et al*., 2010).

1.1.1.2 The role of extracellular DNA in biofilms

Extracellular DNA was originally thought to be present in biofilms as a result of previously interrupted horizontal transfer of DNA between microorganisms, or as a result of cell lysis, leading to externalisation of the DNA. However, it was more recently determined to be a much more significant contributor to biofilms, in that it supports structural integrity of biofilms as they develop (Mann *et al*., 2009; Hall-Stoodley *et al*., 2008; Jakubovics *et al*., 2013), enhances microbial attachment and co-aggregation, in addition to serving as a pool of genes of potential benefit to others for uptake as highlighted above. There are distinct sequential differences between eDNA and genomic DNA, further suggesting eDNA presence is not solely a result of cell lysis, but is actively produced and secreted by viable, metabolising cells (Flemming & Wingender, 2010). The presence of eDNA is also a requirement for some bacterial species to be able to form biofilms (Vilain *et al*., 2009).

As eDNA is negatively charged, it is thought to contribute to biofilm structure and integrity by acting as a bridging component, linking positively charged components within the EPS. The effects of bridging charged components could directly contribute to the active sequestering of similarly charged antimicrobial compounds, and provide some insight to explain their frequent inefficiency in treating biofilms.

Extracellular DNA is not restricted to bacterial biofilms, but has also been implicated in fungal biofilms involving *C. albicans* (Martins *et al*., 2010) where it serves a similar purpose as a contributor to biofilm structure and enhancement of genetic diversity of the biofilm community.

1.1.1.3 Biofilms in nature

Biofilms occur naturally in the environment, and are undoubtedly the outcome of microorganisms having millions of years of evolutionary experience for survival. Unsurprisingly, biofilms are ubiquitous in the natural world, and can be detected within environments such as The Great Barrier Reef (Witt *et al.*, 2011) and natural lakes (Fang *et al.*, 2014). Biofilms are also found in man-made locations such as paper mills (Al-Fattani & Douglas, 2006). Importantly, biofilms are also frequently detected in the human body where their presence can have a significant impact on human health both in a positive and negative manner, as discussed below.

1.1.1.4 Biofilms in medicine

Biofilm research is a relatively recent field of microbiology, with most research activity being from the 1980s and pioneered by the 'father of biofilms'; Dr JW Costerton. Given their significance in clinical infection, and their recalcitrance to treatment, biofilms are now of significant research interest. Approximately 65% of hospital acquired infections are estimated to have a biofilm origin (Costerton *et* al., 1999; Joo & Otto, 2013). It is well known that the impact of a biofilm-related infection can be highly significant, as highlighted in Fig. 1.2 and Table 1.2. Dental caries and periodontal disease affect a substantial portion of the global population, with caries present in approximately 35% of the general population, and severe periodontitis affecting 10% of people (Frencken *et al*., 2017). This high prevalence appears to be in decline in developed countries, with continually improving clinical intervention and global prevention strategies outlined by the World Health Organisation (WHO).

The necessary placement of medical devices, including endotracheal tubes in mechanical ventilation (Ramage *et al*., 2006; Sands *et al*., 2017), and use of

intravenous and urinary catheters (Donlan, 2001; Ganderton *et al*., 1992; Stickler *et al*., 1998), whilst vital for patient recovery can also serve as surfaces for biofilm formation, and therefore lead to increased patient morbidity, mortality and length of hospital stay (Sardi *et al*., 2013). Implanted devices also provide a route of access to additional locations within the body that would normally be inaccessible with the physical dermal barrier, and immune system as demonstrated in Fig 1.2.

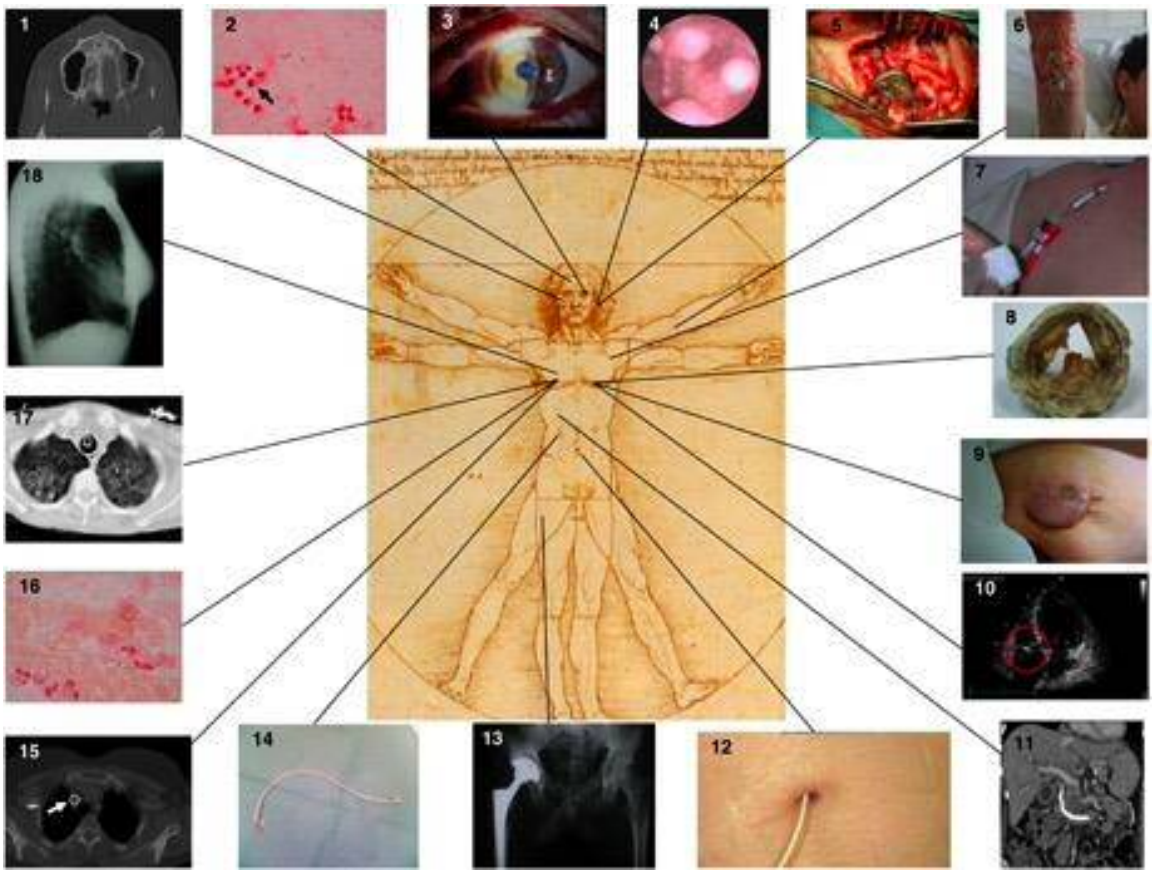

Figure 1.2 Diversity of biofilm-associated infections within the human body
Examples of the many locations within the human body that biofilms can exist, and subsequently, biofilm-related infections can occur including (1) chronic sinusitis, (2) central nervous system shunt (3) contact lense keratitis, (4) chronic otitis, (5) cochlear implant, (6) burn, (7) intravascular catheter, (8) prosthetic valve endocarditis, (9) pacemaker, (10) electrophysiological wire endocarditis, (11) biliary stent, (12) dialysis catheter, (13) prosthetic joint, (14) urinary stent, (15) intravascular stent, (16) pulmonary infection in cystic fibrosis patient, (17) ventilator associated pneumonia, (18) breast implant. Image used with permission from del Pozo & Patel, 2007

Biofilm-related infection/disease	Associated causative Microorganism(s)	References
Cystic fibrosis	*Pseudomonas aeruginosa*	Parsek & Singh, 2003; Lopes *et al*., 2012; Bagge *et al*., 2004
Dental plaque	*Streptococcus* spp., *Actinomyces* spp., *Lactobacillus* spp., *Veillonella* spp*, Fusobacterium* spp., *Prevotella* spp., *Porphyromonas gingivalis,* Firmicutes	Bradshaw & Marsh, 1995; Xie *et al*., 2010
Dental caries/periodontitis	Streptococci, Lactobacilli, *Actinomyces* spp., *P. gingivalis, Tannerella forsythia, Treponema denticola, Prevotella intermedia, P. nigrescens, Fusobacterium nucleatum*	Colombo *et al*., 2014; van Houte, 1994 Offenbacher *et al*., 2007
Medical device-associated infection		**Medical device-associated infection**
Denture-associated stomatitis	*C. albicans*	Samanarayake *et al*., 2002; Sitheeque & Samanarayke, 2003; Williams & Lewis, 2011; Rogers *et al*., 2013
Urinary catheters	*Proteus mirabilis, P. vulgaris, Klebsiella pneumoniae, Pseudomonas aeruginosa, C. albicans, Escherichia coli*	Stickler, 2014; Samanarayake *et al*., 2014;
Subdermal devices	Staphylococci	Otto, 2008;
Prosthetic joints	Staphylococci, *Enterococcus* spp., *Propionibacterium acnes*, *Streptococcus* spp.	Deva *et al*., 2013; Tande & Patel, 2014
Orthopaedic surgery	*P. aeruginosa, S. aureus, Staphylococcus epidermidis*	Veerachamy *et al*., 2014

Table 1.2 Biofilm related infections of the human body, and associated with medical devices

1.1.2 Development of biofilms – a dynamic series of events

The development of a microbial biofilm follows a distinct set of stages as outlined in Fig. 1.3 and include attachment and adherence, colonisation and recruitment, maturation, and dispersal, which are discussed below.

The makeup and structure of a biofilm is highly organised and typically incorporates open channels presumed to be used for transport of nutrients into and around the biofilm (Costerton *et al.*, 1999). The composition of local regions within a multi-species biofilm will vary depending on the requirements of the individual microorganisms in respect of nutrient and gaseous delivery. It is important, for example, that aerobic microorganisms have access to oxygen and other nutrients required for metabolism and growth, whereas fastidious or anaerobic microorganisms would not survive in the same conditions. Thus, biofilm channels provide a means of control in providing the necessary microenvironment for different regions in a biofilm (Christensen *et al*., 1998).

As biofilms are highly organised, 3D structured communities, it is necessary for the development to be an ordered and temporal process. Dental plaque is one such well-studied example of a polymicrobial biofilm, and serves as a perfect model to describe biofilm formation, development and maturation as detailed by Marsh & Bradshaw (1995). Figure 1.3 provides a schematic representation of biofilm formation and development within this distinct and structured process, highlighting the stages of formation; attachment and adherence, colonisation and maturation, and then mature biofilm and dispersal for secondary colonisation elsewhere.

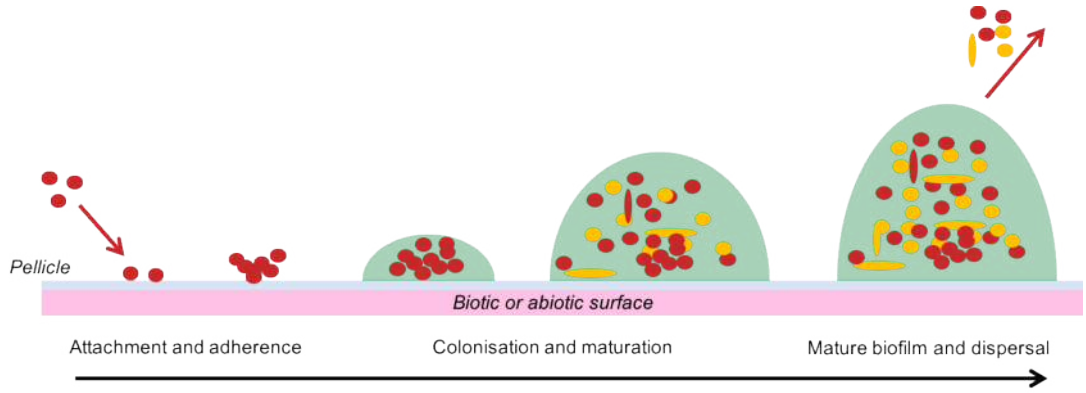

Figure 1.3 Diagrammatic representation of distinct stages of biofilm development; attachment and adherence, colonisation and maturation, mature biofilm and dispersal for secondary colonisation

1.1.2.1 Acquired surface pellicle, and subsequent microbial attachment and adherence of primary colonisers to the surface

Initial attachment and adherence of microorganisms to a surface is essential for successful colonisation, growth and maturation of the biofilm. Strictly speaking, surfaces in general are rarely 'naked', but most often are coated with a pellicle, which In the case of the oral cavity is typically saliva (de Paula *et al*., 2017). Whole saliva contains different substances including the main component, water; electrolytes including sodium, potassium, calcium, and phosphates, and host factors including enzymes, proteins, mucins, immunoglobulins (Humphrey & Williamson, 2001). The resulting coating film contains saliva-derived proteins, glycoproteins, lipids and glycolipids (Marsh & Bradshaw, 1995). Furthermore, other host components including cells; epithelial cells, immune cells and, of course, the constituents of the resident microbiome (Wade, 2013; Nasidze *et al*., 2009; Yang *et al*., 2012) are present. These components coat the surfaces, whereby proteins and mucins deposit onto the surface. This deposition determines the surface characteristics, particularly the charge of the surface, which can significantly influence microbial attachment.

The primary stage of biofilm development is the initial attachment of the microorganism to the surface which is a result of non-specific, reversible interactional forces such as van der Waals and electrostatic forces arising from charges on the surface and cells (Pascual, 2002). Microorganisms themselves have proteins on the surfaces of the cell; teichoic acid, pili, flagella antigens, and lipopolysaccharides (Eden & Hansson, 1978; O'Toole *et al.*, 2000; Scott & Zahner, 2006), which promote attachment to the surface via these non-specific forces by increasing surface area of the microorganism, thus increasing the relative force by which it can attach, and have also been implicated in subsequent biofilm formation (Tomaras *et al*., 2003). The forces are relatively weak, but if external influences do not break these bonds, the initial attachment persists and if the conditions are suitable, the microorganisms subsequently initiate processes of adherence of the cells to the surface. Surfaces are also rarely perfectly smooth, with the presence of microscopic ridges and other irregularities or imperfections that can influence

the initial attachment of microorganisms.

The subsequent adherence, considered an active process, is driven by specific binding arising from ligand-receptor interactions (Cotter & Kavanagh, 2000). The action of salivary flow in the oral cavity can remove loosely or non-adhered microorganisms from the surfaces, thus adherence to the oral surfaces is essential for successful microbial establishment and persistence. Adhesins such as Als1p, Als3p, and Hwp1p (Nobile *et al.*, 2006) for *Candida* species, and cell surface polypeptides such as SspA and SspB (Demuth *et al.*, 1996) for *Streptococcus* species and *Actinomyces* species. Once strongly attached to the surface, the microorganism can utilise nutrients on the surface or from the immediate environment to support growth.

In the case of dental plaque formation, the primary colonisers are typically streptococci and *Actinomyces* species. *S. sanguinis* and *S. mutans* are able to bind to terminal sialic acid residues; a component of saliva (McBride & Gisslow, 1977; Levine *et al*., 1978), and *S. oralis* and *S. mitis* expresse lectins that interact with galactose and trisaccharide structures containing galactose, sialic acid and *N*-acetyl-galactosamine (Murray *et al*., 1982; Murray *et al*., 1986). *Actinomyces* can bind to proline-rich proteins within the pellicle (Gibbons & Hay, 1988; Ruhl *et al*., 2004) via a β-galactoside-sensitive mechanism (Stromberg & Boren, 1992). Additionally, streptococci are known to bind to such proline rich proteins (Ruhl *et al*., 2004).

1.1.2.2 Biofilm maturation; arrival of secondary colonisers and development of 3D biofilm architecture

After the initial process of attachment and adherence, microorganisms begin to develop into microcolonies. The ability of microorganisms to adhere to one another (known as co-aggregation) is beneficial for subsequent biofilm development and maturation, thus sustained production of adhesins is important. Co-aggregation is an important characteristic of oral microorganisms, particularly secondary colonisers to establish a biofilm (Marsh & Bradshaw, 1995) and there are a number of mechanisms by which

co-aggregation can occur. Firstly, through ligand-receptor like binding of these secondary coloniser cells to primary colonisers on the surface, or secondarily as an already co-aggregated collection of cells adhering to a set of receptors. *Actinomyces* species have two functionally distinct fimbriae; type 1 which are necessary for the binding to salivary proteins (Gibbons *et al*., 1988), and type 2 which are associated with lectin-like interactions for co-aggregation with streptococci (Mishra *et al*., 2010).

Whilst the vast majority of oral microorganisms exhibit co-aggregation characteristics to some extent, not all are able to. However, these still form an important part of the biofilm community, and are able to do so by the presence of so-called bridging bacteria. Fusobacteria are a genera or bacteria that are important to facilitate the binding of non-co-aggregating bacteria for incorporation into biofilms, and particularly bridging anaerobic with aerobic bacteria, an example of a mutualistic microbial relationship (Bradshaw *et al*., 1998; Periasamy & Kolenbrander, 2009). *F. nucleatum,* specifically, bind extensively with most other oral bacteria, and facilitate the binding of early- and late-colonisers, to establish a more comprehensive community (George & Galfkler, 1992).

Whilst in close proximity, microorganisms can communicate, as discussed in 1.1.3, via secreted molecules as part of a quorum sensing system and are able to stimulate expression of virulence factors and other cell density dependent genes (Li *et al.*, 2002; Kruppa *et al.*, 2004). This allows the cells to adapt to changes in their environment quickly.

As these microcolonies form and develop, through both division and co-aggregation, the microorganisms produce EPS. Defined microenvironments also begin to form, allowing for the existence of diverse habitats and therefore supporting a range of microorganisms (Stoodley *et al.*, 2002). During biofilm maturation, if there is restriction in the availability of nutrients or gases around the biofilm matrix, cells can enter a ‘stationary phase’ where metabolic activity is significantly lowered until conditions alter (Fricks-Lima *et al.*, 2011).

As microcolonies grow in a structured manner, microenvironments within them become more defined in different regions of the biofilm as the penetration of nutrients and gases become more restricted. As oxygen availability is generally highest at the point of the biofilm furthest away from the attached surface, aerobic microorganisms tend to exist in this area, whereas anaerobic microorganisms are most likely to be found toward the base of the biofilm (Marsh, 2005; Monroe, 2007). Nutrients are supplied via channels (as previously described) in order to ensure diffusion within the EPS matrix is sufficient to enable sustained growth. Recruitment of additional microorganisms also occurs during this growth and maturation phase (Costerton *et al.*, 1987), as the presence of EPS provides a dynamic surface more likely to encourage adherence and integration of the new microorganisms into the biofilm, and this continued addition of microorganisms increases the likelihood of co-aggregation via ligand-receptor interaction (Hoyer & Cota, 2016).

Once the biofilm has an established structure, consisting of the early colonisers, and additional microorganisms recruited as part of the maturation phase, late colonisers join the biofilm through co-aggregation mechanisms and quickly integrate within the biofilm matrix and community (O'Toole *et al.*, 2000).

1.1.2.3 The mature biofilm, microbial cell dispersal and subsequent implications

The 'mature biofilm' typically exists after a number of days of growth and maturation, whereby the content of the community becomes more stable in physical size, distribution of microorganisms within the biofilm, and relative abundance of different genera and species. This is also known as the climax community. It is the phase at which the biofilm is in its most developed state, stable despite changes in local environmental stresses including dietary components, host defences, salivary flow and pH, the continues growth of which is most likely restricted by sheer forces imposed by salivary flow within the oral cavity (Marsh, 2006).

The final stage of biofilm development cycle is cell dispersal. It is thought that dispersal of cells occurs not by chance, but as part of a highly-regulated system influenced by physiological and environmental signals (Jackson *et al.*, 2002). It is necessary in order for the microorganisms to colonise and re-establish a biofilm development cycle at a different location, and is considered a major pathogenic factor. Numerous methods of biofilm dispersal have been observed such as planktonic cell dispersal via surface or liquid phase, and clumped cell dispersal (Hall-Stoodley *et al.*, 2004). Both types of dispersal can lead to relocating and establishing new microcolonies, which if the conditions are still suitable, have the potential to lead to further biofilm development and an increased infection state. Depending on the environment, shear force can also cause biofilm cell dispersal such as liquid flow (Rochex *et al*., 2008; Bearon, 2003).

The molecular process of dispersal is not completely clear, but one molecular method of biofilm dispersal in *E. coli* arises from induction of a global regulatory gene, *csrA*. Interestingly, this gene has also been implicated in the microbial invasion of host mucosa, and a plant homologue has been identified, which is involved in disease and host response (Jackson *et al.*, 2002). In *Candida* species, the production of the yeast wall protein (Ywp1p) has been implicated with anti-adherence properties, and linked to dispersal of cells from an established biofilm (Heilmann *et al.*, 2011; Granger, 2012).

The advantage of polymicrobial biofilms containing *Candida* species is that *Candida* has the ability to form hyphae (or pseudohyphae) depending on species. These morphologies are distinct and considered a significant virulence factor and indicator of pathogenicity (Santana *et al.*, 2013). The formation of hyphae is also implicated in tissue invasion, which inevitably increases the host immune response. Furthermore, the hyphae provide a structural advantage to the biofilm, allowing maturation and development in a 3D manner to occur (Seneveratne *et al*., 2008; Williams *et al*., 2011).

1.1.3 Microbial interactions and responses to environmental factors

Environmental awareness and communication between microorganisms are important features of successful mature biofilm development. Mechanisms for environmental sensing and inter-cellular communication are commonly known as quorum sensing systems or two component quorum sensing systems.

1.1.3.1 Quorum sensing

Quorum sensing is considered a major communication and environmental sensing mechanism of microorganisms. Distinct mechanisms exist for individual bacterial and fungal species (Ng & Bassler, 2009), but the overall concept of communication is similar. Gram negative bacterial quorum sensing, for example, is dependent on the autoinducer molecule *N*-acyl homoserine lactone (AHL), and the LuxI/LuxR system (or homologues to LuxI/LuxR), commonly found in bacterial genera including *Pseudomonas*, *Vibrio, Burkholderia (*Fux *et al.*, 2003*;* Ng & Basser, 2009; Spoering & Gilmore, 2008; Williams *et al*, 2007). The basic principle behind this mechanism is driven by cell density (Swift *et al*., 1996). Gram negative bacterial cells constitutively produce the small molecule, AHL, which is freely diffusible into the surrounding environment. This AHL can modulate specific gene expression and at lower cell densities, the threshold at which gene transcription occurs (as a result of protein binding and activation) is not met. Consequently, the genotypic and subsequent phenotypic profile of the bacteria follow a particular route. At higher cell densities however, the increased concentration of AHLs in the environment leads to increased diffusion into the cell. AHL then binds to LuxR and initiates transcription of alternative or additional operons. This results in a modified bacterial phenotype through the activation of expression of different genes, potentially changing cell behaviour.

This concept is similar through Gram positive, and fungal quorum sensing systems. The fungus *Candida*, utilises the molecule farnesol, which has a similar effect and mechanism to the AHLs mentioned above (Hornby *et al*., 2001, Ramage *et al*., 2002). Some characteristics of *Candida*, including the yeast to hyphae transition, are controlled by cell density in their ability to sense

the concentration of cells in the local environment, and adapt accordingly. The production of farnesol accumulates in the environment as it is actively and constitutively secreted, and above a certain threshold, modulates gene expression for induction of hyphae (Ramage *et al*., 2002).

1.1.3.2 Inter-kingdom interactions

It is beneficial for microorganisms to communicate with each other for the overall survival of the community. It is also beneficial for microorganisms of a different kingdom to be able to communicate, or at least sense communication between other microorganisms. These sensing and communication systems are mediated by small, diffusible molecules, including AHLs and autoinducer molecules (AIs). It is proposed that autoinducer 2 (AI2) is an inter-species communication molecule, which makes it distinct from AHLs, which are generally genus specific (Kolenbrander *et al.*, 2002). In addition to this, no evidence has been observed of AHL production by oral bacteria, indicating that these molecules are not used for microbial sensing or signalling. The production of both AHLs and AIs are cell density dependent. These molecules are produced in a continuous manner, such that changes in cell density can be detected, resulting in the production or up- regulation of virulence factors (Williams *et al.*, 2000) via cell-to-cell communication. AI2 has also been implicated in mutualistic polymicrobial biofilm development as a cell-density dependent molecule (Rickard *et al.* 2006).

Virulence factor regulation in streptococcal species has been described by Heath *et al.* (1999), resulting from the interruption of a gene encoding the response regulator *csrR*. The *csrR* gene is implicated in subsequent downstream processing events and regulation of other genes involved with pyrogenic exotoxin production, *speB,* and streptolysin production, *sagA*.

Candida are known to produce the quorum sensing molecule, farnesol, which is thought to directly influence or control morphological transition from yeast to hyphae (Ramage *et al.*, 2002; Chen *et al.*, 2004). Farnesol has been shown to enhance the growth and microcolony formation of *S. mutans* (Kim *et al*., 2017),

which is implicated in dental caries, but has also been shown to reduce formation of single and mixed (*Candida* and *S. mutans*) species biofilms (Fernandes *et al*., 2016). Whilst the evidence reports two polar effects of this single quorum sensing molecule, it suggests the resultant effects need to be considered as part of a wider, multi-component complex, and an overall net effect. In addition to farnesol, other sensing and communication molecules have been discovered and characterised such as tyrosol (Chen *et al.*, 2004), tryptophol and phenethyl alcohol (Lingappa *et al.*, 1968), and farnesoic acid (Oh *et al.*, 2001) as reviewed by Kruppa (2009).

1.1.4 Antimicrobials and their decreased efficacy against biofilms

It is generally accepted that microbial cells within biofilms possess a significantly higher tolerance to the effects of antimicrobials (Kumamoto, 2002). Studies estimate that biofilms can be in the region of 1,000 times more resilient to treatment with antimicrobials than their planktonic counterparts (Mah & O'Toole, 2001; Prosser *et al*., 1987). Furthermore, the knowledge that microbial cells do not behave in the same manner in planktonic states as they do in biofilms may have some influence on the mechanism of resistance or a method of developing tolerance towards the compounds (Hall-Stoodley *et al*., 2004).

A number of mechanisms are known to play a role in increased resistance to antimicrobials, some of which are shown in Fig. 1.4, and detailed below.

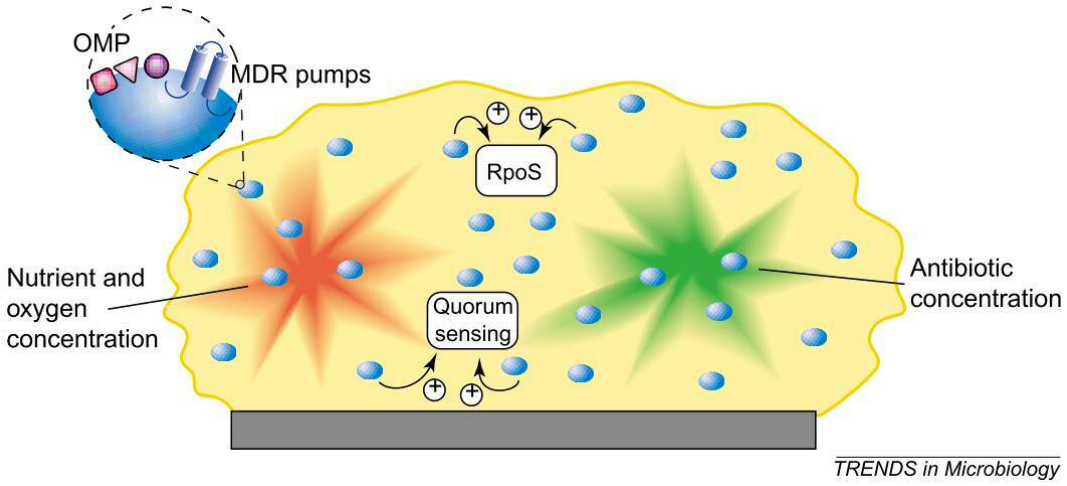

Figure 1.4 Diagrammatic representation of biofilm mechanisms of antimicrobial resistance.
Mechanisms include reduced penetration into the biofilm as a result of physical restriction by EPS; quorum sensing which modulate responses to environmental stresses, and can lead to phenotypic and metabolic changes; multi drug resistance pumps to actively sequester antimicrobials from within the biofilms; reduced nutrient and oxygen concentration, which impacts antimicrobial efficacy, and a reduced metabolism can alter efficacy as many antimicrobials are growth dependent by inhibiting cell wall production. Image used with permission from O'Toole (2001)

1.1.4.1 Physical mechanisms of biofilm protection

The makeup of biofilms includes EPS, which is a thick matrix of a mixture of components, which can physically restrict entry into the deeper segments of the biofilm structure, or by diluting the compounds once they have penetrated through and into the EPS (Sutherland, 2001). Stewart & Costerton (2001) suggested that, by their very nature, cells within biofilms, being embedded in a matrix of EPS, have a physical mechanism of protection, which was echoed in a review of biofilm resistance to antimicrobials by Mah & O'Toole (2001).

The inability of the antimicrobial to penetrate into the biofilm to a sufficient depth to be effective is important. The mechanism by which this occurs is complex and multifactorial. It is thought that as a result of opposite charges of the EPS and antimicrobial compounds, sequestration of the compounds within the EPS can arise. Furthermore, the effect of reduced oxygen availability and reduced metabolic activity of the microorganisms toward the centre of the

biofilm makes these cells more tolerant of antimicrobial activity (Walters *et al*., 2002).

The range of environments within the biofilm, and accumulation of waste products or by-products of metabolism can act as antagonists to the compounds. Biofilm mediated protection has been observed for *C. albicans* biofilms, where the effective concentration of antimicrobials (minimum inhibitory concentration, MIC) were up to 1,000 times higher for cells within a biofilm than the planktonic equivalent (Kuhn *et al*., 2002). This biofilm protective effect is also true for host-immune response assault of biofilms. Although antibodies may be raised against microorganisms at the biofilm periphery, most areas of the biofilm will be unaffected. It is likely that given the polymicrobial and localised microbial composition the antigens of some species may even be 'hidden' from the immune system. This response may be somewhat effective in an attempt to clear a small range of microorganisms, but the ability of antibodies or recruited immune cells to penetrate into the biofilm is severely reduced, as also observed with antimicrobial compounds (Fux *et al*., 2005).

1.1.4.2 Active mechanisms of protection

Antimicrobial compounds enter into the biofilm in what is an already arduous task of penetrating into and within the EPS, and subsequently into the depths of the metabolically active biofilm. As the drug reaches the cell, before it can have any effect, the cell can employ a number of mechanisms to avoid the effects of the compound. One such mechanism is to simply secrete the compound back into the environment. This is made possible by the employment of efflux pumps, which are membrane pores that control active transport of materials across the cellular membrane (Mukherjee *et al*., 2003). Efflux pumps are effective mechanisms of active secretion of antimicrobial compounds from cells, particularly within biofilms (Ramage *et al*., 2002; Mukherjee *et al*., 2003). Ramage *et al* (2002) showed up-regulation of genes known to be involved in formation and function of efflux pumps in *C. albicans*

biofilms, and a subsequent increase in antifungal resistance to fluconazole when these biofilms were challenged.

Furthermore, it was hypothesised by Mukherjee *et al*., (2003) that in addition to the involvement of efflux pumps in enhanced resistance, the reduction in overall cell membrane permeability also played a role. These factors, along with the ability for cells within biofilms to substantially reduce their metabolic activity, and thus become quiescent, lead to an enhancement of innate tolerance to the efficacy of targeted drugs. The role of quiescence in *C. albicans* biofilm resistance, however, is not clear in the literature, with studies suggesting that the majority of cells are metabolically active (LaFleur *et al*., 2006), and others suggesting they can exhibit a reduction in metabolic activity (Chandra *et* al., 2001; Lewis, 2005).

Microorganisms also have the ability to actively secrete DNA (extracellular DNA; eDNA) into the local biofilm environment (Okshevsky & Meyer, 2014; Hirota *et al*., 2016; Vilain *et al*., 2009; Jakubvics & Burgess, 2015). This eDNA has a structural role, supporting maturation and biofilm integrity, and a functional role, where portions of eDNA can then be taken up by surrounding microorganisms and integrated into their genome. Some genes in such eDNA fragments can code for antimicrobial resistance genes, and can give the new host an advantage in what is already a very competitive community. The presence of eDNA has also been attributed to inducing morphological transition from yeast to hyphae in *Candida* biofilms (Hirota *et al*., 2016).

1.1.4.3 Persister cells

An additional mechanism of antimicrobial resistance, and indeed tolerance to other environmental stresses such as extreme changes in local environment; temperature, pH, nutrient availability and desiccation, lie with the existence of persister cells (Lewis, 2001; Jenkinson, 2011; Percival *et al*., 2015). The cells exist in a state of substantially reduced metabolic activity. As discussed briefly above, the existence of cells that are considered dormant, or demonstrate reduced metabolic activity, have a significant advantage for these communities

at a time where the community is literally fighting for its life. Fig. 1.5 outlines the concept of persister cells, and their ability to avoid methods of treatment or removal which are important in the maintenance and recovery of biofilms.

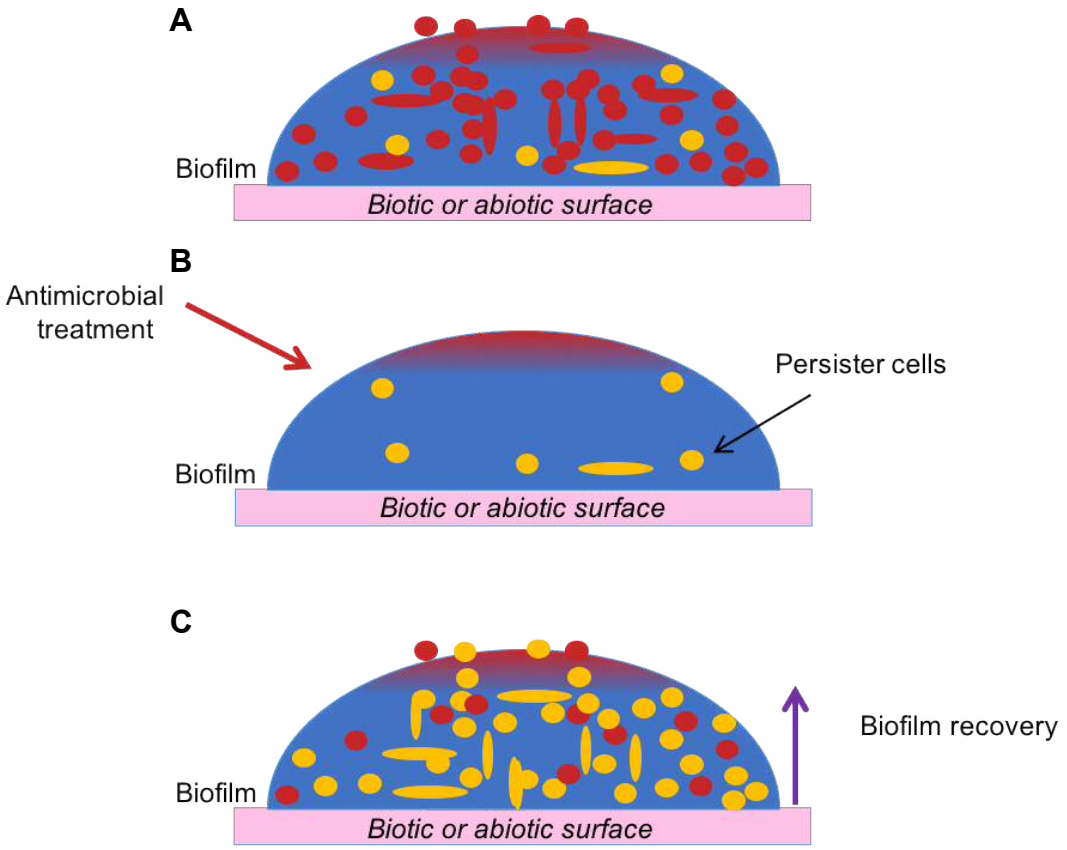

Figure 1.5 Diagrammatic representation of microbial persister cells, and biofilm recovery after ineffective initial antimicrobial treatment.
A) Polymicrobial biofilm exists on surface, embedded in extracellular polymeric substances, and after antimicrobial treatment B) few viable persister cells remain, which after antimicrobial treatment or challenge has subsided, re-establish and recolonise and re-establish the biofilm C), where it returns to its polymicrobial, mature state. These persister cells, and thus the biofilm in general now have increased tolerance for subsequent treatment or antimicrobial challenges.

1.2 The oral cavity

1.2.1 The anatomy of the oral cavity

The oral cavity is a portal to the body for the purpose of obtaining nutrients through food and drink. There are a number of anatomically distinct sites within the cavity, including the tongue, palate, teeth, and gingiva (Fig. 1.6); all with bespoke features and functions. There are a range of teeth with the same

primary functions, from tearing to crushing different foods to allow digestion. This chewing mechanism is facilitated by the production of whole saliva, mixed from the ducts of many salivary glands (de Paula *et al*., 2017), which contain a range of enzymes (Fabian *et al*., 2012), assisting the breakdown of substrates in the mouth and oesophagus. These enzymatic constituents of saliva, including lysozymes and phosphatases, also have a significant role in immunity of the oral cavity from microbial infection. The presence of the enzymes can prevent colonisation of surfaces by microorganisms. This, together with the presence of immunoglobulins and mucins, serve to maintain the inhibition of microbial colonisation and where necessary, establish an immune response to the potential infection. They also assist with mediating tolerance to commensal microorganisms, so as not to mount an inappropriate immune response, and constitutive localised inflammation (de Paula *et al*., 2017, Feller *et* al., 2013, Fabian *et al*., 2012).

In addition to teeth, other sites provide structural function to the oral cavity. The purpose of gingival tissue is to provide support to erupted teeth, and as it is comprised of mucosal tissue components, also acts as a barrier to potential infection. However, as a result of insufficient oral hygiene, it is common for dental plaque biofilms to accumulate above and below the gingival margin (supra- and sub-gingival respectively), where localised inflammation occurs, and can lead to destruction of the tissue (Marsh, 2005; Marsh & Bradshaw, 1995). This infection (periodontal disease) is dynamic, and depending on severity and length of sustained infection, can lead to severe tissue destruction, and ultimately bone destruction and tooth loss (Jenkinson & Lamont, 2005; Gendron *et al*., 2010).

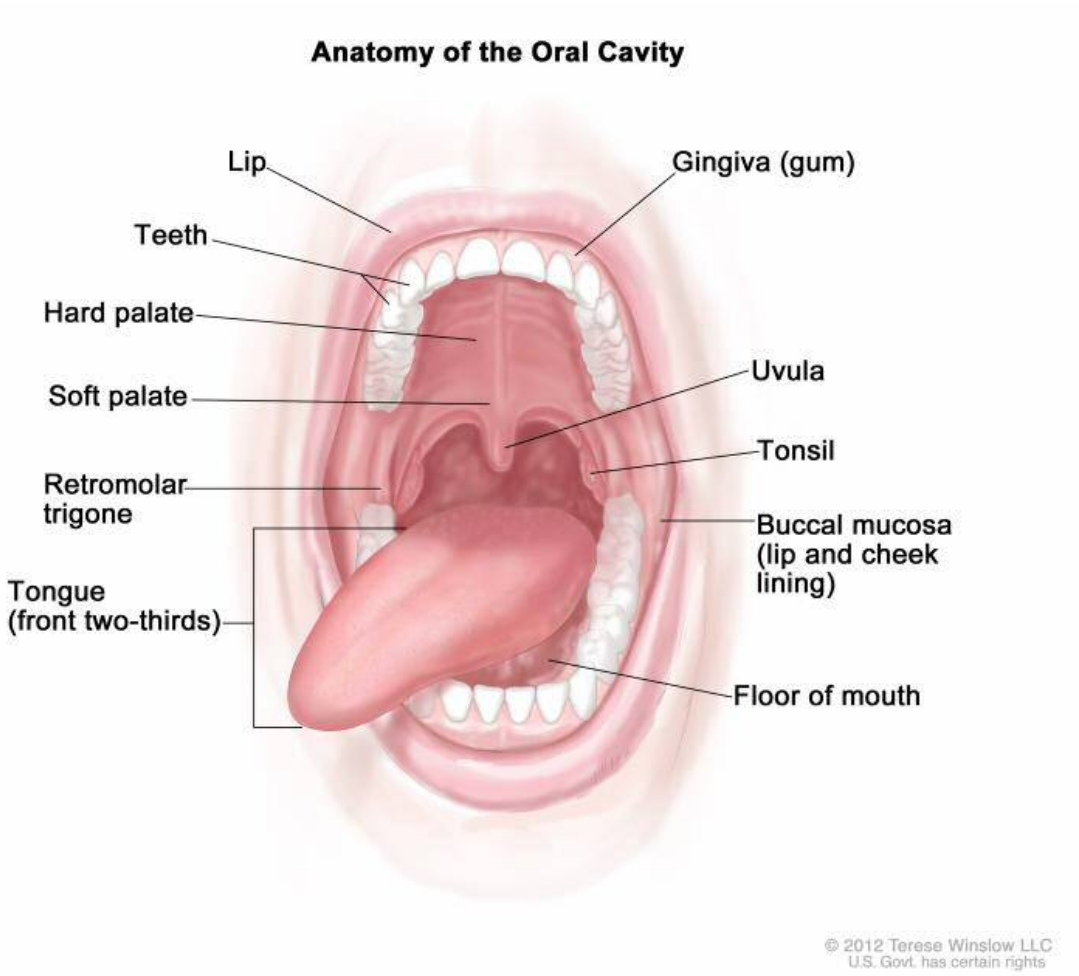

Figure 1.6 Schematic representation of sites within the oral cavity.
Image used with permission from Terese Winslow, For the National Cancer Institute © 2012 Terese Winslow LLC, U.S. Govt. has certain rights

The hard palate, a site of specific focus for this PhD, is a complex layered tissue (Fig. 1.7) analogous to other epidermal or dermal tissues. The most superficial layers of epithelial cells are keratinised, and the layers of cells beneath are well differentiated and stratified. These layers, moving from the superficial layer into the tissue are as follows: *stratum corneum*, *stratum granulosum*, *stratum spinosum*, and *stratum basale*. Again, as observed with skin, palatal mucosa provides a physical barrier to infection, whilst tolerant to colonised commensal microorganisms as discussed previously. Beneath the epithelial layer exists a final layer, *lamina propria*: fibrous connective tissue (Moharamzadeh *et al*., 2007) comprised of a fibroblast cell-populated matrix of collagen.

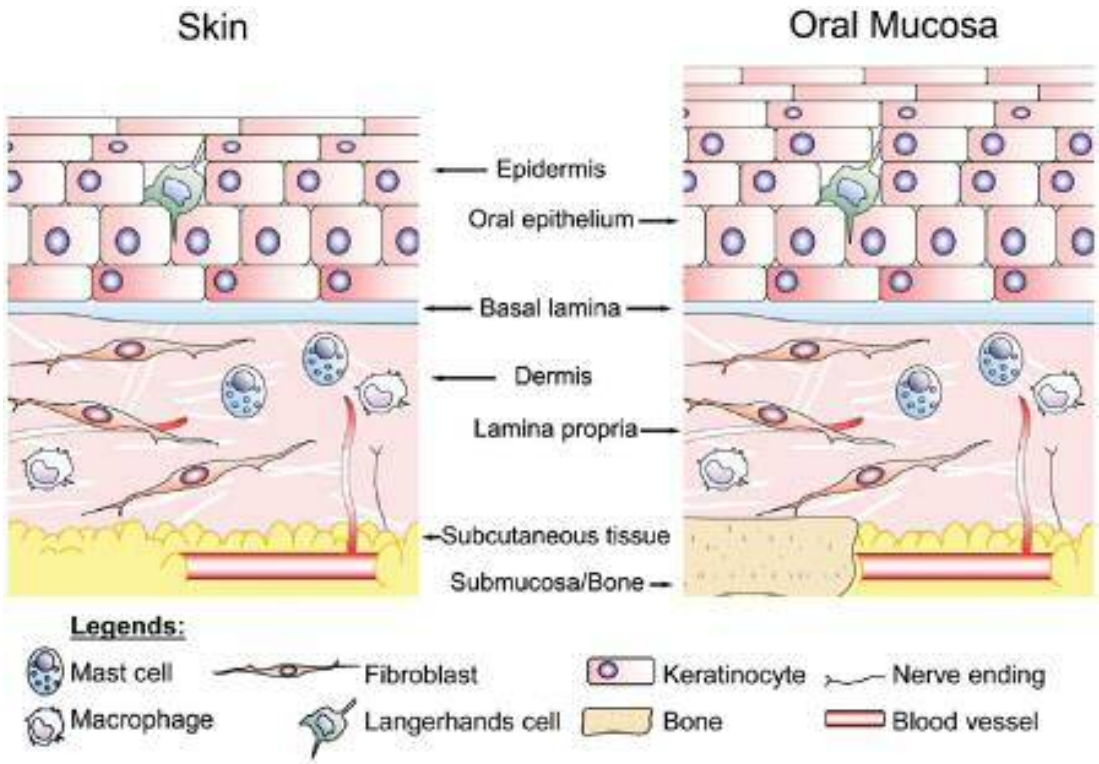

Figure 1.7 Diagrammatic representation of the oral mucosa and similarities in structure to skin
Image used with permission: Glim *et* al. (2013). Wound Repair and Regeneration
Volume 21, Issue 5, pages 648-660, 8 AUG 2013 DOI: 10.1111/wrr.12072

1.2.2 The oral microbiome

1.2.2.1 The journey to characterise the oral microbiome

Each of the surfaces in the oral cavity exhibit a variety of local environmental conditions including varying oxygen availability resulting in aerobic and anaerobic environments, but also different physical influences such as mechanical action caused by movement of the tongue and salivary flow. These varied local environments can support a vast array of microorganisms including bacteria and fungi. In fact, the oral microflora is second only to the colon in terms of microbial diversity in the human body, with over 1000 species reported to be present (Dewhirst *et al.*, 2010; Wade, 2013).

Studies of the oral cavity have previously relied upon culture-dependent methods to investigate the composition of the oral microbiome and organisms implicated in specific diseases (Bowden *et al.*, 1979). The advancement of technology and continued development of novel methodology has allowed

molecular techniques such as DNA analysis to be employed (Aas *et al.*, 2005; Ghannoum *et al.*, 2010; Wade, 2011). The use of molecular analysis has revolutionised our understanding of the oral microbiome. It is now known that there are far more microorganisms present in the oral cavity than originally thought based on culture-dependent methods.

Both culture-dependent and culture-independent analytical methods have provided valuable information into the range of microorganisms found in the oral cavity, and the creation of a central database (the Human Oral Microbiome Database; HOMD) to capture and collate results of characterisation studies was launched in 2010 (Chen *et al.*, 2010; http://www.homd.org). This database uses data from studies involving 16S rDNA sequencing, which, whilst providing information about the bacterial content, does not currently incorporate analysis of fungi (such as *Candida* species), which lack the 16S ribosomal subunit. This is significant as *Candida* species are known to be major causative agents of oral infections and diseases. However, all fungi, including *Candida,* have a similar ribosomal subunit, namely the 18S subunit, regions of which are highly conserved and can be analysed in the same manner as 16S rDNA for bacterial identification. In order to evaluate and compare *Candida* sequences, alternative databases are available, an example of which is the *Candida* Genome Database (Inglis *et al.*, 2012; http://www.candidagenome.org).

1.2.2.2 Characterisation of microbial hierarchy and their relationships

The most recent advances in this field highlight the issue that a significant proportion (as many as 35%) of oral microorganisms are not currently cultivable *in vitro* (Chen *et al.*, 2010). This may be due to the reliance of some microorganisms on enzymes, nutrients or cofactors produced by other microbes present in the locality. Many examples of symbiotic relationships between microorganisms growing as part of a biofilm have been reported. One such example of intra-kingdom, inter-species symbiotic relationships is the relationship between *Streptococcus gordonii* and *Veillonella atypica*. *S gordonii* utilises sugar for growth, the by-product of which is lactic acid, which is then used by *V. atypica* for energy production (Johnson *et al.*, 2009). In this

instance, both microorganisms benefit from the presence of each other. Without *V. atypica* the build-up of lactic acid would form part of a negative feedback signal transduction system leading to a reduction in *S. gordonii* sugar metabolism. Metabolism of lactic acid by *V. atypica* prevents this feedback occurring, allowing both organisms to benefit. Other relationships are not necessarily mutually beneficial, but may benefit just one microorganism, either at the expense of others (parasitic), or to no benefit or expense of others (commensal/neutral) and are detailed in Table 1.3.

A preliminary study investigated inter-kingdom *in vitro* relationships of mixed species culture, showing the effect of the presence of a range of bacterial species when grown in dual-species co-culture with *C. albicans* (Thein *et al.*, 2006). The study enumerated the number of viable cells after a period of time, and found that when maintaining a standardised inoculum of *C. albicans*, the effect of changing the inoculation rate of bacteria gave varied results. For example, *S. mutans*, a frequently isolated oral commensal microorganism, which is also commonly associated with oral infections, had no influence on the number of viable *C. albicans*. However, when *Porphyromonas gingivalis*

Relationship	Description	Example
Mutualistic	All organisms benefit from the relationship in some way	*S. mutans* and *C. albicans* sugar utilisation in co-culture: *C. albicans* is inefficient at sucrose breakdown, *S. mutans* has preference for sucrose. Sucrose breakdown results in glucose and fructose, which are utilised by *C. albicans*, producing lactate, further facilitating *S. mutans* growth (Kim *et al*., 2017)
Commensal/neutral	One (or more) organism(s) benefit with no benefit or harm to the host or others	Many gut and oral microorganisms operate a commensal relationship. Nutrients extracted from sources in the oral cavity or digestive tract are utilised for sole benefit, with no negative implications of surrounding environment or other microorganisms
Parasitic	One (or more) organism(s) benefit to the detriment of the host or others	Viral and parasite-associated infections are considered parasitic, with no host benefits as a result of presence, metabolism or behaviour of the microorganism

Table 1.3 Categories and descriptions of relationships between organisms

was added in co-culture with *C. albicans*, the number of viable *C. albicans* decreased. This study only investigated dual-species, so the effect of a true polymicrobial biofilm on the number of viable cells of both *C. albicans* and bacteria is of great interest. Furthermore, the study investigated biofilms grown only over 48 hours, a relatively short time period considering that oral infections can contain biofilms that will have grown over a significantly longer period than this. This is particularly true for denture wearers with poor general oral hygiene where biofilms may exist for many weeks or months. Overall, the study highlighted the fact that such mixed species relationships are complex with many variables affecting overall outcomes.

Our current understanding of the microbial composition of the healthy oral cavity indicates the presence of a vast and broad array of commensal microorganisms (Mager *et al.*, 2003; Aas *et al.*, 2005; Bik *et al.*, 2010; Dewhirst *et al.*, 2010; Ghannoum & Mukherjee, 2013). These studies found that commonly isolated or detected microorganisms in healthy individuals include bacteria such as *Porphyromonas*, *Streptococcus* and *Veillonella*, and yeast such as *Candida.* The characterisation of a healthy oral cavity is significant, as when we consider studies investigating oral diseases such as periodontitis, gingivitis, dental plaque and other oral infections, the same microorganisms found in healthy individuals are also identified as causative or supportive agents in disease progression. Consequently, it can be challenging to identify the aetiological agents within the commensal pool of microorganisms.

The current understanding of the roles of different microorganisms within biofilms is more complex than it just being a microbial collective. Each microorganism may have a distinct role to play, contributing to the overall community in some way. Different types of microbial roles can be classified into several types, more than just the typical commensal versus pathogen, as detailed in Table 1.4.

Microorganism role	Description	Example
Commensal	Normal microorganisms found in the typical microflora, indigenous microbiota	Streptococci in oral cavity, *S. epidermidis* on skin
Accessory pathogen	Typically commensal microorganisms, but contributes by nutritional/colonisation support to enhanced growth and/or virulence of other microorganisms, including pathogens	*S. gordonii* enhances virulence of *P. gingivalis* and *A. actinomycetemcomitans*
Keystone pathogen	Microorganisms whereby the influence they have on the microbial community is disproportionately large relative to their absolute abundance (Power *et al*., 1996)	*P. gingivalis* within the oral cavity; significant indirect contribution to development of gingivitis/periodontitis by inducing dysbiosis of the microbial community, thus enhancing inflammatory response and tissue damage
Opportunistic pathogen	Typically commensal microorganisms, but have the ability to adapt/change and cause infection under certain environmental conditions	*C. albicans*; commensal within the oral cavity of healthy individuals with no adverse effects, but in immunocompromised patients, can cause substantial localised and systemic infection
Pathobiont	Microorganisms whose effect, although similar to opportunistic pathogens, occurs indirectly via stimulation/activation of the host immune system	*P. gingivalis* induces systemic inflammation, segmented filamentous bacteria potent stimulation of host mucosal immune system (Hornef, 2015)

Table 1.4 Summary table of different roles of microorganisms within polymicrobial communities and hosts

1.2.3 Dysbiosis and development or progression of disease

The normal microbiome exists to maintain a state of health and homeostasis between commensal, and potentially pathogenic microorganisms, including bacteria, fungi and viruses (Wade, 2013; Zarco *et al*., 2012; Ghannoum *et al*., 2010). Several distinct advantages arise as a result of the presence of a distinct and diverse oral microbiome, including assistance with breakdown of substrates and nutrients within the oral cavity, and tolerance toward the presence of pathogenic microorganisms.

During the continual change in local environmental stimuli and conditions, and the stimulation of the immune system by the resident microflora, eventually the fine balance of homeostasis is tilted either by a local change or other factors such as diet or medication, and dysbiosis can occur. Dysbiosis refers to the shift from a homeostatic microbiome to one in favour of pathogenic and infection causing microorganisms. Dysbiosis is a serious concern, because not only can localised infection and inflammation occur (Zemanick *et al*., 2015), but also development of cancers and autoimmune diseases (Chen *et al.,* 2015, Li *et al*., 2014).

The onset or progression of disease is attributed to the reduction in diversity of the local microbiome, which in turn is responsible for maintaining tolerance of the immune response, and modulation of the local environment in which the microorganisms exist. This in turn requires adaptation of the host cells to changes in environmental conditions, and can lead to a change in genetic regulation. Interestingly, in the case of Crohn's disease as reported by Li *et al* (2014), the diversity of the gut mycobiome is inversely related to the diversity of the bacterial microbiome, and while there is an increase in the diversity of fungi, there is a subsequent reduction in the diversity of bacteria in this condition, leading to potentially severe inflammation. In this instance, it appears the modulation of the immune response is managed by the bacterial cells present, rather than the fungi, and thus, when keystone bacterial species change either in presence or relative abundance, the modulation of the inflammatory response is unregulated, leading to a proinflammatory response.

1.2.4 The role of saliva in the oral cavity, and changes with presence of oral prostheses

Salivary flow in the oral cavity is an important factor for normal function of the general oral cavity. As discussed previously, whole saliva contains many different components; water; electrolytes, host factors including enzymes, proteins, mucins, immunoglobulins (Humphrey & Williamson, 2001), epithelial cells, immune cells and, of course, the constituents of the resident microbiome (Wade, 2013; Nasidze *et al*., 2009; Yang *et al*., 2012). Saliva has a unique microbiome of its own, distinct from other sites in the oral cavity, with similar contributions to the normal function of the oral cavity as the presence of other microorganisms.

The primary function of saliva is lubrication and buffering of the environment, as well as antimicrobial activity through immunoglobulins, and antimicrobial peptides found in the saliva (Humphrey & Williamson, 2001). The functionality of saliva is altered with the presence of oral prostheses, such as dentures (Niedermeier *et al*, 2000), and where salivary flow is reduced, patients often experience dry mouth, or a burning sensation. The reduction in saliva, particularly between the denture-fitting surface, and epithelial cells of the palatal mucosa, can lead to an increase in the presence or persistence of biofilms on the denture-fitting surface, and indeed, the palate itself, where natural sloughing may be affected. This increased presence of biofilms can then lead to inflammatory responses, such as those observed in denture-associated stomatitis. Furthermore, the salivary microbiome can have implications for diseases of other sites of the body, particularly the gut (Acharya *et al*., 2017).

1.3 *Candida*

1.3.1 Taxonomical classification and characteristics of *Candida* species

The name *Candida* is derived from the Latin *toga candida,* which refers to the white robe (toga) worn by candidates for the Senate of the ancient Roman republic (Lynch, 1994), and relates to the white/off-white colour of the *Candida* colonies when cultured both *in vivo* and *in vitro*.

The fungal genus of *Candida* includes a diverse array of species, including the more clinically relevant species *C. albicans*, *C. tropicalis*, *C. parapsilosis*, *C. glabrata* and *C. dubliniensis* (Ramage *et al*., 2006), and *C. auris*, a multi drug resistant species of the *Candida* genus (Schelenz *et al.* 2016; Chowdhary *et al.* 2014). *Candida* species typically grow as waxy white/off-white colonies when cultured on Saboraud dextrose agar, and can differentially metabolise compounds in CHROMagar™ *Candida* to allow for presumptive identification of certain species (Williams & Lewis, 2000).

Candida species are generally considered commensal microorganisms, resident within the typical microflora in a range of many bodily sites in animals and humans, without any adverse implications, and are also associated with the natural environment (Skinner & Fletcher, 1960). Certain species, including *C. albicans*, *C. glabrata, C. parapsilosis*, *C. tropicalis* and *C. auris* however, are opportunistic pathogens, and can cause disease in immunocompromised individuals, under specific environmental conditions or as a result of external stimuli (Ramage *et al*., 2006; Deorukhkar *et al*., 2014).

1.3.2 *Candida* virulence factors

1.3.2.1 *Candida* polymorphism

Candida species (with the exception of *C. glabrata*) possess a unique, and very beneficial morphogenic trait. The ability of this polymorphogenic microorganism to exist as yeast cells, but also as distinct, elongated hyphae (or pseudohyphae) (Fig. 1.8) is considered an important virulence factor, and has been extensively studied and reviewed (Sudbery *et al*., 2004; Oh *et al.*, 2001; Ramage *et al.*, 2002; Nobile *et al.*, 2006; Santana *et al.*, 2013). Numerous factors are known to influence the morphogenic state of this microorganism. Factors that induce hyphae production include high temperatures, high CO_2 level relative to O_2 and poor nutrient supply, whereas the yeast form of this microorganism is the preferred phenotype when there is a more acidic pH in the local environment and lower temperatures (Oh *et al.*, 2001). Another important factor of morphogenic control is cell density. It has been shown that a cell density of $>10^6$ cells/ml results in the production of

budding yeasts, whereas a cell density of $<10^6$ cells/ml results in production of hyphae (Hornby, *et al.*, 2001). The production of the quorum sensing molecule farnesol has also been implicated in morphological transition, the higher concentration of which correlates with preference for the yeast form and an inhibition of production of hyphae. This is linked with viable cell density as farnesol is constitutively secreted as an environmental sensor.

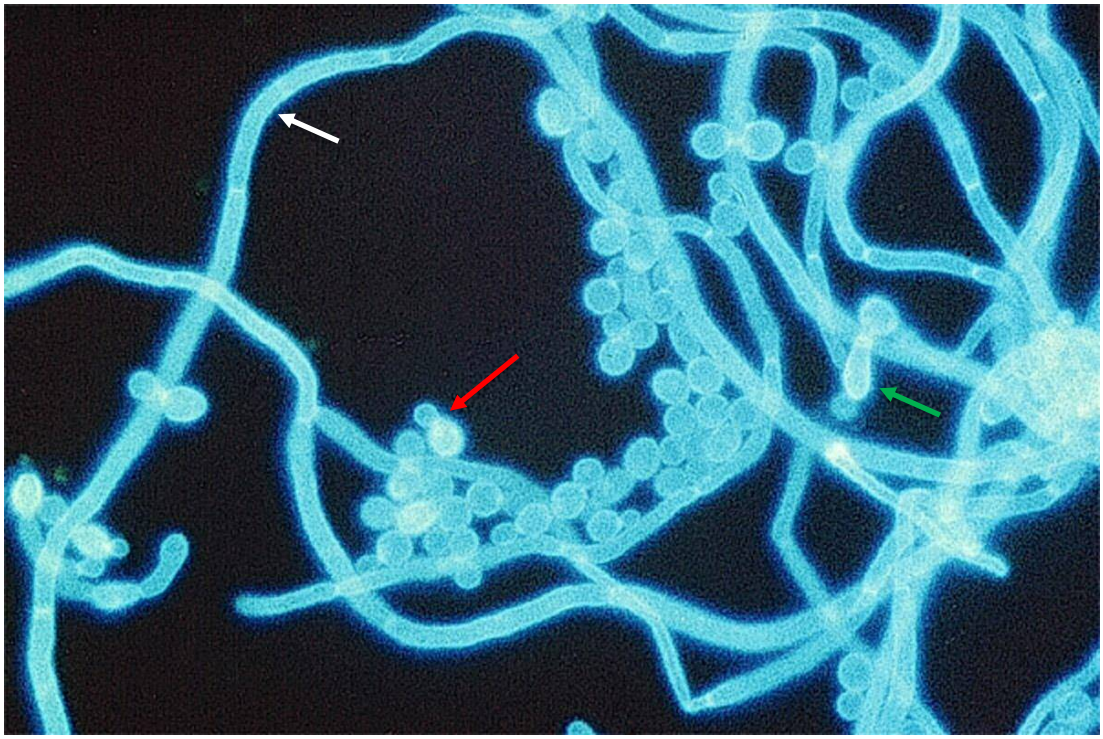

Figure 1.8 Fluorescence microscopy image of *C. albicans* morphological states.
Typical spherical yeast cells; considered the commensal morphology of *C. albicans*; budding yeast (red arrow), pseudohyphae (green arrow) and long, elongated hyphae (white arrow), representing the more virulent morphology.
Image used with permission from Dr Sladjana Malic.

1.3.2.2 Mechanism and regulation of yeast to hyphae morphological transition

The molecular mechanisms by which morphological transition and hyphal formation occurs are highly regulated. A number of stimuli can induce a signalling cascade leading to enhancement of the genes responsible for hyphal formation. Fig. 1.9 demonstrates the signalling pathways of a number

of typical stimuli including elevated temperature, pH, concentrations of quorum sensing molecules farnesol or homoserine lactones, among others (Sudbery, 2011).

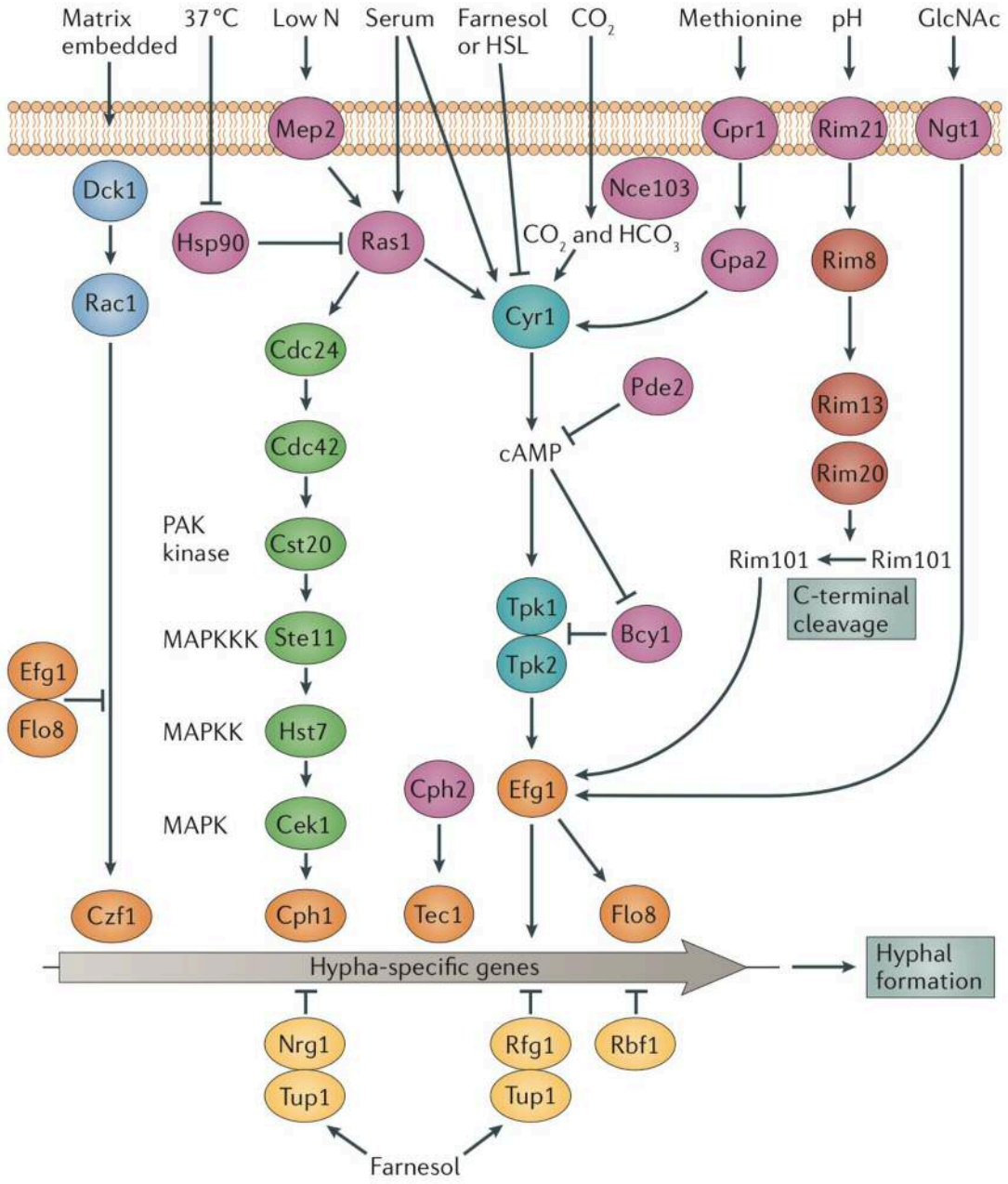

Figure 1.9 Summary of multiple hypha-inducing stimuli and subsequent signalling pathways leading to hyphal formation.
A number of environmental stimuli including changes in pH, concentration of quorum sensing molecules and concentration of CO_2 can lead to activation of specific signalling pathways including the mitogen-activated protein kinase (MAPK) pathway (green), pH sensing pathway (brown), matrix-embedded pathway (blue) and cAMP pathway (turquoise), activating a panel of transcription factors (orange). The general transcriptional regulator Tup1 (yellow) is responsible for negative regulation, by targeting the hypha-specific

gene promotors including Nrg1 and Rox1p-like regulator of filamentous growth (Rfg1). Image used with permission from Sudbery (2011).

Induction of hypha-specific gene expression is performed by a range of transcription factors including Efg1 (Stoldt *et al*., 1997; Lane *et al*., 2001; Kumamoto & Vinces, 2005) which is necessary for the formation of hyphae in response to serum, CO_2, neutral pH and *N*-acetyl-D-glucosamine (GlcNAc), Cph1 (Liu *et al*., 1994; Leberer *et al*., 1996; Kumamoto & Vinces, 2005), Cph2 (Lane *et al*., 2001), Tec1 (Lane *et al*., 2001) and Ndt80 (Sellam *et al*., 2010). The pathways to expression involve cyclic adenosine monophosphate (cAMP) and mitogen-activated protein kinase (MAPK) pathways. Induction of the pathways lead to activation of an array of hypha-specific genes including glycosylphosphatidylinositol (GPI)-anchored cell wall proteins *HYR1, IHD1* and agglutinin-like sequences *ALS3/ALS10* which are considered adhesins*,* hyphal wall proteins *HWP1, RBT1,* and secreted aspartyl proteinases *SAP4/SAP6* (Nantel *et* al., 2002; Kadosh & Johnson, 2005). Negative regulation of hypha-specific gene expression is provided by the corepressor Tup1 along with Nrg1 or Rox1p-like regulator of filamentous growth (Rfg1) (Kumamoto & Vinces, 2005; Sudbery, 2011).

1.3.2.3 Biofilm formation and important transcriptional regulators

The biofilm and cell wall regulator 1 (Bcr1) transcription factor is essential for both activation and repression of a number of genes related to biofilm formation in *C. albicans* (Nobile *et al*., 2011). Knockout studies have confirmed the relevance of the protein with regards to biofilm formation *in vitro* and *in vivo*, where Bcr1 deficient mutants were unable to produce biofilms (Nobile *et al*., 2006a; Dwivedi *et al*., 2011), and showed altered gene expression of *ALS1*, *ALS3*, *ECE1* and *HWP1 in vitro* (Nobile & Mitchell, 2005; Nobile *et al*., 2006a; Yano *et al*., 2016). Furthermore, Bcr1 deficient mutants were more susceptible to leukocyte-induced damage when grown *in vitro* or on mucosal tissues (Dwivedi *et al*., 2011).

Although Bcr1 is not critical for formation of hyphae, it is a positive regulator of a number of hypha-specific adhesins including *ALS3* and *HWP1* (Nobile *et al*.,

2006a), where overexpression of these targets partially restores biofilm formation in Bcr1 deficient mutants. Presence of a *TEF1-BCR1* construct restored expression of these genes, confirming the role of Bcr1, but Bcr1 acts downstream of the hyphal development activator Tec1, as studies involving Tec1 deficient strains also showed restored biofilm formation with the presence of the *TEF1/BCR1* construct (Nobile *et al*., 2006a).

Further to this regulator, other transcriptional regulators are known to modulate biofilm formation, where deletion of the *TEC1*, *EFG1* (Nobile *et al*., 2011) or indeed other regulators *NDT80*, *ROB1* and *BRG1* result in defective biofilm formation (Mayer *et al*., 2013). The transcriptional regulators control expression of a range of genes necessary for adhesion and biofilm formation, detailed in the following sections.

1.3.2.4 Adhesion

The first stage of biofilm formation for any microorganism is attachment and adherence to a surface. In many cases, this is primarily initiated by non-specific interactions with the surface by phenomena such as Van der Waals forces, or ionic bonding as a result of differences in charge between the cell and surface. However, if surface contact is maintained beyond this reversible phase, the expression of surface adhesins and the initiation of irreversible binding to surface receptors occurs. Adhesins are well documented in many microorganisms such as *P. aeruginosa*, *S. aureus* and also in *C. albicans* (Foster & Höök, 1998; Calderone & Fonzi, 2001; Verstrepen & Klis, 2006; Nobile *et al*., 2006, Ma *et al*., 2006; Silverman *et al*., 2010).

A number of *Candida* adhesins have been identified (select proteins of which are detailed in Table 1.5), including the agglutinin-like sequences family (including the proteins Als1-Als7 and Als9), hyphal wall protein 1 (Hwp1), and epithelial adhesin 1 (Epa1) (Sundstron, 1999; Zhao *et al*., 2004; Hoyer *et al*., 2008; Liu & Filler, 2011; Halliwell *et al*., 2012). Many of these, including Als3, Hwp1 and Epa1 are also associated with virulence of the fungus. Furthermore, it is known that a number of these adhesins are involved with the

morphological transition to hyphae, such as Als3 and Hwp1 and have additional functions including invasion into host cells (Phan, 2007; Liu & Filler, 2011) and subsequent pathogenesis of infections (Hoyer *et al*., 2008). However, anti-adhesive properties have also been identified with these adhesins, where in knockout studies, the deletion of Als5, Als6 or Als7 resulted in increased adhesion of *C. albicans* to human cells (Zhao *et al*., 2007).

Als3 is a known multifunctional adhesion, expressed specifically during hyphal formation and plays a crucial role in adhesion to biotic and abiotic surfaces, and invasion of host cells (Nobile & Mitchell, 2005; Argimon *et al*., 2006; Liu & Filler, 2011; Hoyer & Cota, 2016). It is a GPI-linked protein that localises to the surface of the cell wall and is activated by Bcr1 stimulation by the transcription factor Tec1. As detailed above, repression of *ALS3* gene expression by Tup1, Nrg1 and Rfg1, downregulates transcription via two repressor binding regions (Argimon *et al*., 2006; Liu & Filler, 2011), which results in growth in the yeast form. Folding of the N-terminal domain of Als proteins is reminiscent of bacterial adhesins, such as those observed in *Staphylococcus* species (Hoyer & Cota, 2016), indicating a conserved structure for adhesion to surfaces, indicating specific binding preferences despite the relative abundance of potential receptors on the surface.

Bcr1 is also necessary for candidal adherence, and the activation of *ALS3* expression contributes to, but is not solely responsible for subsequent biofilm formation once adhered to the surface (Nobile *et al*., 2006a) where Als3 deficient *Candida* retain biofilm formation capability., Overexpression of known Bcr1-regulated genes including *ALS1, ALS3* and *HWP1* result in some improvement in biofilm formation, highlighting the multi-gene contribution to biofilm formation.

Virulence attribute	Protein	Virulence role(s)	References
Adhesins	Als1	Adhesion to surface and colonisation. Associated with yeast form of *Candida*	Nobile *et al*., 2006b; Williams *et al*., 2011; Hoyer & Cota, 2016
	Als3*	Adhesion to surface and biofilm formation. Associated with hyphal form of *Candida*, can bind to fibronectin, collagen, E-cadherin, N-cadherin	Nobile *et al*., 2006b; Phan *et al*., 2007 Williams *et al*., 2011; Hoyer & Cota, 2016
	Hwp1*	Adhesion and formation of hyphae and involved in biofilm formation	Nobile *et al*., 2006b; Hoyer & Cota, 2016
	Epa1	Epithelial cell adhesion.	Haynes, 2001; Alves *et al*., 2014
Hypha formation	Ece1*	Epithelial infection; secreted toxin also known as Candidalysin, required for cell damage	Nobile *et* al., 2006b; Moyes *et al*., 2016
Hydrolytic enzymes	Sap4	Nutrient acquisition, tissue invasion/damage, associated with hyphae	Naglik *et al*., 2003; Schaller *et* al., 2005; Williams *et al*., 2011
	Sap5	Nutrient acquisition, tissue invasion/damage, breakdown of E-cadherin, associated with hyphae	Naglik *et al*., 2003; Schaller *et* al., 2005; Williams *et al*., 2011
	Sap6	Nutrient acquisition, tissue invasion/damage, associated with hyphae	Naglik *et al*., 2003; Schaller *et* al., 2005; Williams *et al*., 2011
	Pld1	Invasion during infection	Sanglard *et al*., 1997; Naglik *et al*., 2003; Schaller *et al*., 2005; Naglik *et al*., 2011; Hebecker *et al*., 2014

Table 1.5 Selected known virulence proteins and their associated roles in *Candida* virulence.

Adhesins including agglutinin-like sequences (Als1 and Als3), hyphal wall protein 1 (Hwp1), epithelial adhesion 1 (Epa1), extent of cell elongation 1 (Ece1), secreted aspartyl proteinases (Sap4, Sap5, Sap6) and phospholipase D1 (Pld1). *Als3, Hwp1 and Ece1 are implicated in both adhesion and formation of hyphae.

Hwp1 is a well-studied hypha-specific GPI-anchored cell surface adhesin (Staab *et al*., 1999; Nobile *et al*., 2006b; Nobile *et al*., 2011; Mayer *et al*., 2013). It is involved in the adhesion of *Candida* to surfaces including a salivary pellicle and fibrinogen (Haussler & Parsek, 2010; Nobbs *et al*., 2010), and formation of elongated hyphae (Staab *et al*., 1999; Hoyer *et al*., 2008; Williams *et al*., 2013). The adhesion of *C. albicans* cells to buccal epithelial cells and the involvement of interactions between *C. albicans* hyphae and keratinocytes via Transglutaminase cross-linkages has been reported (Staab *et al*., 1999).

1.3.2.5 Hydrolytic enzymes

Within its armoury, *Candida* has the ability to produce hydrolytic enzymes, including secreted aspartyl proteinase enzymes (Saps), and to a lesser but still significant extent, phospholipase enzymes as summarised in Table 1.5 (Sanglard *et al*., 1997; Schaller *et al*., 2000; Naglik *et al*., 2003; Naglik *et al*., 2011; Hebecker *et al*., 2014). These enzymes are not unique to *Candida*, or indeed fungi in general. They are known to be produced by a range of microorganisms including bacteria (Finlay & Falkow, 1997) and protozoa (McKerrow *et al*., 1993), in addition to fungi.

The enzymes are multifunctional: they have been associated with enhancing adherence to epithelial cells (Naglik *et al*., 2011), and active penetration and invasion of epithelial cells (Gow & Hube, 2012; Hebecker *et al*., 2014). This suggested increased virulence and pathogenicity of the microorganism. They have been observed in multiple *Candida* species, including *C. albicans*, *C. glabrata*, *C. tropicalis*, *C. krusei* (Haynes, 2001), indicating the conserved nature of these proteins and their widespread use. The production of these enzymes is typically associated with nutrient acquisition and infection/invasion of host tissues (Schaller *et al*., 2000; Naglik *et al*., 2003).

Secreted aspartyl proteinases are encoded by a family of 10 *SAP* genes and include two sub-families (Saps1-3, and Saps4-6) (Williams *et al*., 2013), and are considered key virulence traits of *C. albicans*. Other *Candida* species possess the ability to produce Saps, but which specific Saps are species

dependent (Naglik *et al*, 2003). Saps4-6, for example, result in permeabilisation of the lysosome, triggering caspase-1 dependent apoptosis (da Silva Dantas *et al*., 2016) and are linked with hyphal formation and invasion into the epithlium, while Sap5 is involves in breakdown of E-cadherin, a protein that maintains tight junctions between epithelial cells (Williams *et al*., 2013). Sap2 and Sap6 have been shown to produce inflammatory responses in the host (Pietrella *et al*., 2013; Gabrielli *et al*., 2015).

The proteinases are produced intracellularly before being packaged into secretory vesicles, and transported to the cell membrane and either released extracellularly, remains attached to the cell membrane, or anchored via a GPI anchor (Sap9 and Sap10) (Naglik *et al*., 2003).

Aspartyl proteinases have also been a target for treatments of *Candida* infection (Naglik *et al*., 2003), where aspartyl proteinase inhibitors showed good effects on the inhibition of these enzymes, and subsequently, reduce virulence in infections.

1.3.2.6 Candidal invasion of epithelium

In general, cells have a level of tolerance toward the presence and colonisation of a range of microorganisms. *Candida* is no exception to this tolerance, and is commonly observed as a commensal microorganism on mucosal surfaces. If and when environmental conditions allow it, *Candida* can activate virulence traits, one of which is the ability to invade colonised tissues (Felk *et al*., 2002; Naglik *et al*., 2003). The benefit in doing so is to seek nutrients in order to continue to survive, and potentially avoid factors that could lead to its demise such as environmental factors e.g. pH or factors secreted by the host and other microorganisms within the local community, or, within the oral cavity, salivary flow which could potentially physically remove it from the mucosal surface.

Candida can invade multi-layered tissues either by breakdown of E-cadherin to expose the junctions between epithelial cells (Nobile *et al*., 2006b; Phan *et al*., 2007 Williams *et al*., 2011; Hoyer & Cota, 2016) , or by physical penetration

of and invasion through cells themselves (Felk *et al*., 2002; Moyes *et al*., 2016; Wilson *et al*., 2016). The process by which *Candida* invade tissues is organised and relatively complex. Firstly, adherence to the cell surface is necessary, as with typical colonisation, which involves the *ALS* family of genes. This is typically followed by hypha formation involving *ALS3* and *HWP1* (as discussed above) and interestingly, cells deficient in the transcription factor Efg1, which is responsible for the control of hypha formation, do not invade tissues, indicating *HWP1* and formation of hypha are essential for the invasion (Stoldt *et al*., 1997; Lane *et al*., 2001; Felk *et al*., 2002; Kumamoto & Vinces, 2005). Hyphal invasion then occurs via one of two methods (Fig. 1.10); host-mediated endocytosis of the yeast/hypha, or hyphae induced inter- or intra-cellular active penetration (Wilson *et al*., 2016; Moyes *et al*., 2016). Inter-cellular invasion relies on the breakdown of E-cadherin in order for the hypha to physically move between the junctions of the cells, and involves the production of ALS3 and aspartyl proteinases known for their lytic capability.

During early intra-cellular invasion, as described by Moyes *et al*. (2016), an indwelling membrane pocket is formed by the physical action of penetrating hyphae, and the secretion of Ece1 occurs. This leads to cellular signalling as a response, calling for a localised immune response by the production of proinflammatory cytokines including IL-6, G-CSF, GM-CSF. Continued secretion of Ece1 leads to accumulation in the pocket, and the concentration reaches a threshold whereby it has a lytic effect. This causes membrane damage and allows lactate dehydrogenase to leak out of the cell, and calcium influx. Cell signalling pathways are maintained and induction of damage-associated cytokines occurs including IL-1α.

Sustained invasion provides an obvious route through epithelia to endothelia, whereby *Candida* can become disseminated throughout the host via the blood stream, known as systemic candidosis. Production of secreted aspartyl proteinases have also been linked to invasion of parenchymal organs in *in vivo* experiments (Felk *et al*., 2002).

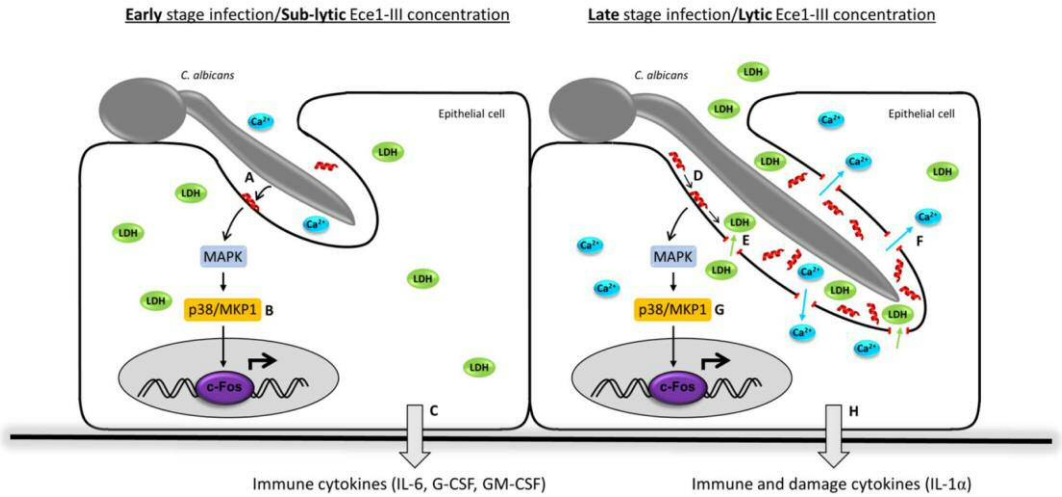

Figure 1.10 Early- and late-stage intra-cellular invasion of epithelial cells by candidal hypha
Penetration of the candidal hypha creates a pocket, into which (A) Ece1 is secreted leading to cellular responses (B, C). Continued secretion of Ece1 accumulates in the pocket (D), leading to membrane lysis (E, F) and sustained immune responses (G, H). Image used with permission from Moyes *et al*. (2016)

1.4 Candidoses

Candidoses have been recognised for thousands of years, and first known to be described by Hippocrates and published in 4th century BC (Lynch, 1994). *Candida* was then subsequently cultured some time later by Lagenbeck in 1839 (Knoke & Bernhardt, 2006), who described a culture similar to what we now consider to be *Candida*. The association between thrush (candidosis) and the microorganism was first reported by Berg in 1846 (Vazquez, 2003).

Opportunistic fungal pathogens of the genus *Candida* are frequently isolated from various sites of the human body and are considered causative agents of numerous medical conditions, commonly known as candidoses. Examples of infections caused or supported by *Candida* include vaginal candidosis (Heilmann *et al.*, 2011), oral candidosis and urinary catheter infections. *Candida* is more commonly implicated in conditions affecting the young or elderly, and those with current illness or immunological suppression (Scully *et al.*, 1994). The primary species involved in candidoses are considered to be *Candida albicans,* with other species including *C. tropicalis, C. glabrata,*

C. krusei and *C. parapsilosis* also implicated, but to a lesser extent (Odds, 1994).

1.4.1 Candidoses as human infections

The term candidosis (plural: candidoses) refers to an infection in a living organism as a result of infection by the fungus of the genus *Candida*. Such infections are also commonly, although incorrectly, referred to as candidiasis. The term candidosis stems from the Latin word *Candida*, and the suffix –osis from the Latin for 'state of disease'.

An array of distinct candidoses exist in humans, affecting almost every part of the human body. These can be categorised as superficial candidosis, which includes the most common form of candidoses, namely oral and vulvovaginal mucosal candidosis (Scully *et al*., 1994; Williams & Lewis, 2011; Samaranayake *et al*., 2002); cutaneous candidoses, including candidal folliculitis and onychomycosis (Deorukhkar *et al*., 2014); and systemic candidosis (Scully *et al*., 1994; White *et al*., 2005). Due to the distinct local environments in which the infection occurs, each category of infection has a different pathogenesis and prognosis, but similar treatment strategies which primarily rely on the use of local or systemic antifungals. Sub-groups within the categories exist. The primary subgroup of interest within the scope of this research topic was oral candidosis.

1.4.1.1 Localised *Candida* infections

Local *Candida*-associated infections present on almost every surface on the human body, ranging from cutaneous infections to mucosal, each with an array of sub-infection categories. The severity varies depending on the *Candida* species, the area of infection and health of the patient. Of course, the longer an infection is left without treatment, the more severe and more difficult it becomes to treat. This is true of any sort of infection, but as candidosis can be an invasive infection, with cells penetrating into tissues to establish themselves, a stronger and longer treatment regime may be necessary.

Localised *Candida* infections are typically treated with antifungal medication, such as azoles. However, systemic antifungal medications may be necessary in the scenarios discussed above.

1.4.1.2 Systemic *Candida*-associated infections

Compared with localised infections, systemic *Candida*-associated infections are potentially far more serious in terms of mortality. The innate ability to migrate and potentially re-establish themselves in any number of vital organs within the body, known as disseminated candidosis, is of significant concern when it comes to treatment options. A study by Wisplinghoff *et al* (2004) of almost 25,000 hospital patients with bloodstream infections implicated *Candida* species in 9% of cases, with an associated mortality rate of approximately 40% (47% of ICU patients, 29% of non-ICU patients).

1.4.2 Oral candidoses

Within the category of mucosal candidoses, oral candidosis is one of the most common forms of infection. Primary oral candidoses, depicted in Fig. 1.11, are recognised as the following; pseudomembranous, chronic hyperplastic, and acute or chronic erythematous candidosis, each clinical presentation accompanied with a distinct diagnosis and prognosis, but also strong similarities in factors affecting initiation development of the infection. There are numerous pre-disposing factors (Table 1.6) associated with all oral candidoses such as the use of broad-spectrum antibiotics or corticosteroids, immune system defects such as infection with human immunodeficiency virus (HIV) or the subsequent onset of acquired immunodeficiency syndrome (AIDS), diabetes, and natural physiological factors such as age and pregnancy (Scully et al. 1994; Samaranayake et al., 2002).

1.4.2.1 Chronic hyperplastic candidosis

Chronic hyperplastic candidosis, (CHC, Fig 1.11a), also known as candidal leukoplakia, is one of the less frequent forms of candidosis, and generally presents as bilateral candidal lesions of the buccal mucosa, close to the commissures of the oral cavity. The hyphae of these lesions penetrate into the

surrounding tissue (Webb et al., 1998a; Webb et al., 1998b), thus, the lesions cannot be removed by simple mechanical action (Sitheeque & Samanarayake, 2003).

Diagnosis of CHC involves observation of white plaques on the tissue, after which a swab for microbiological analysis or biopsy can be taken for histological analysis to confirm the presence of *Candida* (Williams *et al*., 1997; Sitheeque & Samanarayake, 2003). Treatment for CHC typically involves the administration of antifungals, and the recommendation for improvement of general oral hygiene. In cases where a more complex diagnosis is present, such as in the case of altered immune state, or systemic infections in addition to CHC, these are treated systemically.

1.4.2.2 Pseudomembranous candidosis

Pseudomembranous candidosis (Fig 1.11b), typically known as oral thrush, presents as white plaque lesions on the tongue and mucosa, also with evidence of erythema in the affected areas. The plaques, however, can be removed by physical scraping. This clinical presentation is the most commonly observed despite, like many of the candidoses, being influenced by a number of predisposing factors (Table 1.4) such as immunocompetence or use of medication. The infection can affect any gender, of any age, with similar presentation and pathology. Treatment for pseudomembranous candidosis is similar to others, with the administration of antifungal medication, both local and systemic.

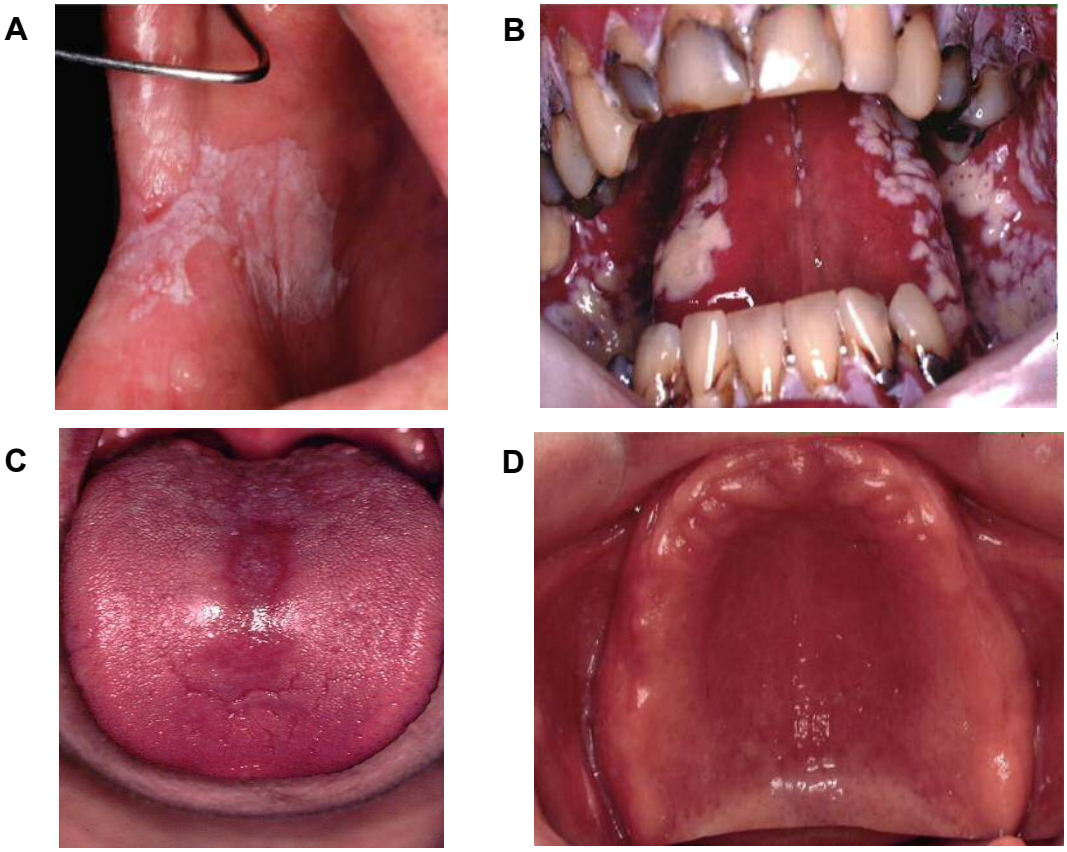

Figure 1.11 Clinical presentations of oral candidoses. **A)** hyperplastic candidosis, **B)** pseudomembranous candidosis, **C)** acute erythematous candidosis, **D)** chronic erythematous candidosis. Note the white lesions on the mucosal surfaces of A and B, the localised inflammation in the centre of the tongue in C, and diffuse inflammation of the palatal mucosa in D.
Image courtesy of Prof. Michael Lewis, School of Dentistry, Cardiff University

Host-associated factors	Miscellaneous factors
General oral/denture hygiene	Tobacco/alcohol use
Ill-fitting denture	Nocturnal denture use
Reduced salivary flow	Antibiotic use
Age	Steroid use
Health status: immunodeficiency, immunosuppression, diabetes mellitus	

Table 1.6 Predisposing factors associated with development of oral candidosis

1.4.2.3 Erythematous candidosis

Erythematous candidosis can either be acute or chronic in its persistence. Acute erythematous candidosis (as depicted in Fig. 1.11c) arises as a result of broad-spectrum antibiotic treatment. Antibiotics are active against bacteria, and will lead to a non-selective reduction of bacterial species within the microflora, many of which will be commensal species. *Candida* is unaffected directly by such antibiotic treatment and is then presented with an altered environment with less competition from other bacteria, and thrives, leading to a state of dysbiosis in that local area. Figure 1.11c shows a typical lesion in the centre of the tongue caused by the administration of a broad-spectrum antibiotic. This lesion is surrounded by an area of erythema. Upon completion of the antibiotic treatment, the homeostasis of the bacterial microflora and thus the equilibrium of the microflora will become re-established, and the lesion and area of erythema will resolve, as the immune response returns to a normal level. This emphasises the necessity of the commensal microorganisms to be present and in equilibrium for the health of the host.

Chronic erythematous candidosis (shown in Fig. 1.11d), is also known as denture-associated stomatitis (DS), and typically presents as areas of inflammation of the mucosa exclusively in contact with a denture-fitting surface (Rogers *et al*. 2013b). DS is discussed in more detail below. It is primarily associated with the use of a complete upper acrylic denture (Fig. 1.12), where biofilms exist on the surface and in prolonged contact with the palatal mucosa, resulting in inflammation of the epithelium.

Figure 1.12 Image of complete upper acrylic denture-fitting surface.
Image courtesy of Dr Helen Rogers, School of Dentistry, Cardiff University

1.4.2.4 Denture-associated stomatitis (DS)

Denture associated stomatitis (DS) is considered the most prevalent oral candidosis, affecting up to 67% of denture wearers (Arendorf & Walker, 1980). *Candida* species were first considered a potential causative agent in DS by Cahn in 1936, and both the clinical condition of DS and infecting *Candida* have since been extensively studied. The clinical presentation of DS can be sub-categorised according to the severity of the irritation based on Newton's classification. The classifications are characterised as the following: Type 0; no erythema, Type I; localised, pin-point erythema (slightly red or swollen tissue), Type II; diffuse erythema (moderately red or swollen mucosa covering part or all of the area of denture contact), and Type III; hyperplastic granular inflammation (severely red or swollen hard palate) (Samaranayake *et al*., 2002; Coco *et al*., 2008; Dar-Odeh *et al*., 2012). Where inflammation is present, all three classifications (Type I, II and III) can be observed simultaneously in differing locations of the palatal mucosa. Although DS is generally asymptomatic, some sufferers experience general discomfort, an itching or burning sensation, and occasional bleeding (Rogers *et al*., 2013b).

Predisposing factors to DS include those mentioned for other oral candidoses, but also include, among other factors, poor general oral hygiene, poor denture hygiene, tobacco use, nocturnal denture wearing, and an ill-fitting denture (Shulman *et al*., 2005; Rogers *et al*., 2013b). Immune status also plays a substantial role, with innate immunity responsible for management of the commensal state, and infection by the microorganisms (Feller *et al*., 2013). These predisposing factors lead to, or facilitate, a change in microenvironments within the oral cavity, which are also associated with oral candidosis. The ideal microenvironment conditions for candidosis include a low pH, increased temperature, increased carbohydrate concentration, reduction in or suppression of commensal bacterial population, and nitrogen and carbon starvation (Figueiral *et al*., 2007; Tobouti *et al*., 2015). *Candida* species tend to prefer these conditions, which can be too extreme for bacterial populations to survive, thus the equilibrium of the microbiome is shifted toward *Candida* growth leading to infection.

Interestingly, although immune status is a known predisposing factor for the development of DS in individuals, studies have observed that whilst the immune cells from patients with DS produce a suitable immune response, in upregulation of proinflammatory cytokines associated with (T-helper cell 1) Th1, Th2 and Th17 responses (Rogers *et al*., 2013b), a reduction in the amount of proinflammatory cytokines was produced in DS patients than those without DS, or non denture-wearers (Pinke, *et al*., 2016). These findings indicate that there are specific mechanisms related to immunocompetence that are affected during DS, that can lead to DS progression, despite calling for an immune response. Rogers *et al* (2013b) also determined that there appeared to be palatal clearance of *Candida* as a result of the immune response, but with no such mechanism possible on a prosthesis, a reservoir for subsequent infection persisted unless suitably removed through good denture care.

1.4.2.5 Microbial content of DS associated biofilms

Numerous studies have been undertaken involving analysis of the microbial content of biofilms implicated in DS (the findings of which are detailed in Table 1.7, and reviewed by Webb *et al*. (1998a, 1998b)). Geographical location, and subsequently the population analysed, appears to be a factor in differences of microbial content, as well as patient-to-patient variability, so it is difficult to achieve a consistent characterisation finding between studies. To date, subsequent studies arising from findings of these characterisation studies have involved single-species, dual-species or polymicrobial biofilms with only a few species, that is, dual-species or a limited number of microorganisms used at any one time (Jack *et al*., 2015; Cavalcanti *et al*., 2016). Whilst this provides some information about biofilm development from a physical and molecular perspective, it is not a completely true reflection of *in vivo* biofilms, and more complex biofilms need to be evaluated as each microorganism will contribute to the overall community.

Study	Sample/analysis method	Summary of findings
Kulak *et al*. (1997)	Swab, culture and presumptive identification	Higher frequency and density of *C. albicans* in DS patients (6/15 heathy patients. 45/45 DS patients) Increased density of α-haemolytic *Streptococcus, Neisseria* species in DS relative to healthy subjects
Barbeau *et al*. 2003	Agar imprint of denture, or agar culture of swab of denture surface	Significant increase in number of yeast in subgroups of DS; Newton's classification II and III than Newton's I, but no significant difference in carriage between healthy and DS overall (Newton's I, II and III)
Campos *et al* 2008	Molecular identification using 16S rRNA sequencing	82 bacterial species detected in all samples, 27 common to both healthy and DS, 29 exclusive to DS, 26 exclusive to healthy patients. Relative abundance of different species not determined, but phylogenetic relationships between species/genera determined
O'Donnell *et al* 2015	Swab and molecular identification using 16S rRNA sequencing	72% samples colonised by *Candida*, bacterial composition determined to phyla level Significantly fewer OTUs detected on denture surface compared with mucosa or teeth Predominantly colonised by actinobacteria and bacilli, more similar to microbiome of mucosa than teeth

Table 1.7 Summary of findings in a number of published studies to investigate biofilms associated with denture stomatitis

1.4.3 Treatment of candidoses

Current treatment strategies of candidoses in addition to the primary recommendation of improvement of general oral and denture hygiene, include the use of local or systemic antifungals, depending on the type and severity of infection (Pappas *et al*., 2016). Common treatments include azoles such as imidazoles, triazoles and thiazoles, and echinocandins such as Caspofungin (Sheehan *et al*., 1999), and polyenes such as Amphotericin B and nystatin (Baginski & Czub, 2009).

The mechanism of action of the azole group of antifungals is inhibition of the enzyme responsible for conversion of lanosterol to ergosterol, thus disrupting the fungal membrane structure and inhibition of cell growth. Echinocandins act by inhibiting production of β-1,3-glucan, which is a major component of the fungal cell wall (Sheehan *et al*., 1999), whereas polyenes bind to sterol (primarily ergosterol) in the fungal cell wall, modifying the porosity and causing leakage from the membrane (Baginski & Czub, 2009). The different compounds have the ability to target different mechanisms of the cell, which is useful when selecting treatment, and to limit the inevitable development of antifungal resistance of these fungi. Alternative treatment strategies may be of use in the future, with the recent advances and understanding of probiotics as a potential prophylactic and/or treatment for many microbial related diseases including intestinal infection (Isolauri *et al*., 2002; Resta-Lenert & Barrett, 2003) and diarrhoea (Szajewska & Mrukowicz, 2001).

1.5 Summary

Chronic erythematous candidosis is the most common denture-associated disease, affecting up to 67% of denture wearers. The disease presents as areas of inflammation on the palatal mucosa, which is in contact with the denture fitting surface. The inflammation is caused by the presence of polymicrobial biofilms that exist on the denture-fitting surface, leading to a host inflammatory response to attempt to clear the infection. There is no natural sloughing that occurs on dentures, thus the continued contact with the palate of the biofilms continues to induce an inflammatory response, leading to damage to surrounding tissues. Current treatment strategies are targeted toward the fungal component of the biofilm, but our knowledge of the role of *Candida* in candidoses is relatively comprehensive, and highlights the importance of bacteria within mixed species biofilms in these infections.

Existing knowledge of the role of bacteria in this disease, and the subsequent effect on *Candida* in terms of virulence factor expression, morphogenic influence and pathogenicity is poor. In order to address the gaps in our current knowledge, this study aims to investigate and further the understanding of microbial interactions within denture-associated biofilms, and determine the pathogenicity of such biofilms in infection models.

1.6 Project aims and objectives

Current understanding of chronic erythematous candidosis (denture-associated stomatitis; DS) is related primarily to the fungal component; *Candida*. The presence of bacteria in the oral cavity is well documented, but their role infection is unclear, thus this project aimed to further understand the role of bacteria with respect to expression of *C. albicans* virulence factors, and subsequent pathogenicity in infections of tissue models. The project has the following primary aims:

Chapter 2: To develop an *in vitro* biofilm model representing DS-associated biofilms using denture-acrylic as the substrate. Interactions between *Candida* and a number of oral bacterial strains, and subsequent effects on *Candida* virulence will be evaluated.

Chapter 3: To develop *in vitro* tissue models that can be used to evaluate biofilm-associated pathogenicity, and further our understanding of how bacteria affect *Candida* virulence and pathogenicity in polymicrobial biofilms.

Chapter 4: To evaluate the effects of DS-associated biofilms in an infection model using commercially available and *in vitro* 3D tissue constructs, and to investigate host immune cell responses to the presence of bacteria by use of LPS, and subsequent challenge with *Candida* cells.

Chapter 5: To characterise the bacterial microbiome of patients with and without DS using next-generation sequencing technologies, in order to determine whether differences exist in the bacterial species present that can be attributed to DS incidence.

Chapter 2

Denture-associated biofilm development and microbial interactions

2.1 Introduction

Biofilms are naturally occurring, complex phenomena. The concept of a biofilm has been investigated for some time and is currently defined as a polymicrobial community existing in distinct regions, that differ in respect of local environmental conditions such as oxygen or nutrient availability. Biofilm development progresses according to a series of distinct events (as described in detail in section 1.1.2). These events include initial attachment and adherence to the surface, formation of microcolonies followed by maturation of the biofilm and recruitment of additional microorganisms, and production of EPS, and finally when necessary, dispersal of microorganisms (Costerton *et al*., 1987; Costerton, 1995).

Our current knowledge of biofilms has been underpinned by the development of a range of *in vitro* biofilm models which have allowed investigations into an assortment of experimental concepts. These studies included basic investigation into the primary stage of biofilm development including microbial attachment and biofilm forming ability, where effects of surface pellicles can be evaluated, as in this study, or more detailed molecular analysis such as ligand-receptor interactions between microorganism and the surface (Dunne, 2002; Katsikogianni & Missirlis, 2004; Mandlik *et al*., 2008). Growth characteristics of single- and mixed-microorganism biofilms is an important field within biofilm research, with applications ranging from pure biological understanding of growth patterns of different species, and their biofilm forming capability, to the effects of antimicrobials in, for example, sub-minimum inhibitory concentration conditions, and the development of resistance to the compounds. Inter-species and inter-kingdom microbial interactions have also been shown to be crucial in determining the effects of co-culture, or polymicrobial interactions (Sztajer *et al.,* 2014; Montelongo-Jauregui *et al*., 2016). The polymicrobial nature of interactions within biofilms is essential to consider during *in vitro* analysis, as generally, biofilms that exist in nature, or more importantly for this project, in medicine, are most likely to be a mixture of many different types of microorganisms, with even more variety of species.

Further complex analyses have also included the sensing and adaptation of biofilms to environmental changes or external challenges (Polke *et al*., 2017), and evaluation of antimicrobial efficacy (di Luca *et al*., 2014). The extent of potential analyses is endless, and helps further our understanding of the behaviour of cells in biofilms compared with their planktonic counterparts. Furthermore, once a biofilm model has been developed, comparisons between similar types of biofilms with subtle changes including the use of different microorganisms or changing culture conditions can be completed relatively easily. Modifications of biofilm models or the microorganisms that are cultured can also help with determining those responsible for disease (keystone pathogens), or with the use of genetically modified microorganisms like knockout variants can facilitate a furthering of the molecular understanding of certain genes.

Biofilm models frequently use the bottom of multi-well plates, or glass cover slips as the substrate for growth, but the differences in material to clinically relevant surfaces like hydroxyapatite or dentine for dental-associated biofilms (Guggenheim *et al*., 2001), or mucosal tissues can substantially influence the behaviour of the microorganisms. Therefore, it is essential to develop biofilm models using the surface of interest, or at least a material that closely represents the surface of interest.

Microorganisms are known to behave differently in different environments, and when attached to different surfaces or other microorganisms (Bibel *et al*., 1982; Costerton *et al*., 1987; Hawser & Douglas, 1994). It is therefore important that the biofilms evaluated *in vitro* are as close as possible to the ones that they are meant to represent from *in vivo* clinical scenarios. Thus, the primary aim of this study was to develop an *in vitro* biofilm model using the most commonly used denture material; poly(methyl methacrylate), that represented denture-associated biofilms as closely as possible. Bacterial species commonly associated with colonisation of denture surfaces; *Streptococcus sanguinis* and *S. gordonii*, and *Actinomyces odontolyticus* and *A. viscosus*, along with the fungus *C. albicans* were deemed to be the most clinically representative

microorganisms to develop this biofilm model, and evaluate polymicrobial biofilm behaviour and interactions.

Interactions between microorganisms, particularly when in close proximity with each other, as is the case in biofilms, is essential for survival of biofilm cells. A number of environmental sensing mechanisms are known to be used by bacteria, and fungi, and even contribute to cross-kingdom interactions. These quorum sensing, or two component regulatory systems have been well documented in previous studies (Ramage *et* al., 2002; Parsek & Greenberg, 2005; Spoering & Gilmore, 2006; Hojo *et al*., 2009), and are discussed in section 1.1.3.1. The primary mechanism of communication and environmental sensing is quorum sensing, which exists in bacteria and fungi, but are unique to each. *Candida* species produce the molecule farnesol as their primary quorum sensing molecule (QSM). This molecule was determined to be produced in relation to controlling the morphological transition between yeast and hyphae, in a cell number dependent manner (Albuquerque & Casadevall, 2012). Furthermore, farnesol is also known to modulate biofilm formation of *Candida* species, by inhibiting genes responsible for hyphae formation, including HWP1 (Ramage *et al*., 2002). Bacterial QSM have also been shown to regulate biofilm formation with *C. albicans*, by disruption of the communication mechanism of the bacterium *S. gordonii* (Jack *et al*., 2015).

Investigations of direct contact between bacteria and fungi in biofilms have also demonstrated modulation of behaviour, observationally and at the molecular level (Bamford *et al*., 2015; Silverman *et al*., 2010; Cavalcanti *et al*., 2016). Studies by Silverman *et al* (2010) and Cavalcanti *et al* (2016) have demonstrated co-aggregation of bacteria with *Candida* in planktonic and biofilm investigations, indicating the importance of cell-to-cell contact in development of biofilms, both directly and indirectly by modulation of factors that promote biofilm formation.

Direct cell-to-cell contact is also known to contribute to genotypic and, subsequently, phenotypic changes as a result of interactions (Kolenbrander, 2000; Silverman *et al*., 2010). Both direct (in the case of cell-to-cell contact)

and indirect (in the case of secreted molecules) interactions can have a substantial influence on the phenotype of the specific microorganisms involved, which, in turn behave differently and can thereafter interact differently with additional microorganisms. This chain of events can modulate the behaviour of cells in local regions to entire biofilms, and can possibly modulate the virulence and pathogenicity of the biofilms.

A secondary aim of this chapter was therefore to evaluate the effect of the presence of bacteria in mixed-species biofilms on *C. albicans* virulence.

Specifically, the research sought to:

1. Develop single, and mixed-species biofilms on acrylic coupons, evaluating the effect of preconditioning the surface with an artificial saliva solution on subsequent microbial adherence and subsequent mature biofilm development
2. Evaluate the modulatory effect of bacteria toward *C. albicans* virulence
    a. Determine relative changes in expression of known putative *C. albicans* virulence genes between *C. albicans*-only and *C. albicans* plus bacteria (mixed-species) biofilms
    b. Evaluate the production of *C. albicans* hyphae in single versus mixed-species biofilms

2.2 Materials and Methods

2.2.1 Microorganisms and culture conditions

2.2.1.1 Overview of microorganisms used in this research

A number of clinically relevant oral microorganisms were used in the studies. These are detailed in table 2.1.

Microorganism	Reference Source	Reference ID
Candida albicans	ATCC	90028
Streptococcus sanguinis	NCTC	7863
Streptococcus gordonii	ATCC	10558T
Actinomyces viscosus	ATCC	1598
Actinomyces odontolyticus	NCTC	9935
Porphyromonas gingivalis	NCTC	11834

Table 2.1 List of microorganisms used in this research

ATCC: American Type Culture Collection, NCTC: National Collection of Type Cultures

A number of industrial funded research projects have used the strains in Table 2.1 to develop *in vitro* biofilms for evaluation of product formulations. *C. albicans* ATCC 90028 is a well-documented, characterised and widely published representative *C. albicans* strain, particularly for investigations into oral candidosis (Samaranayake *et* al., 2006; Thein *et* al., 2007; Jayatilake *et* al., 2007; Silva *et al*., 2010; Nithyanand *et al*., 2014). The bacterial strains listed in Table 2.1 have also been used in published studies, but this particular mixture was selected as it represents a range of oral microorganisms associated with the oral cavity, particularly denture surfaces. They have been used in industrial-sponsor funded studies by this research group for investigations into oral-associated biofilms.

2.2.2 Preparation of microorganisms, dental materials and experimental reagents

2.2.2.1 Microbial culture conditions

Candida albicans ATCC 90028 was cultured on Sabouraud Dextrose Agar (SDA, Lab M, Lancashire, UK) and incubated aerobically at 37 °C for 24 h. One colony was then aseptically transferred into 10 ml of sterile 1 × Yeast

Nitrogen Base (YNB; BD Difco, Oxford, UK) supplemented with 500 mM of sucrose (Fisher Scientific) or 100 mM of D-glucose (Fisher Scientific). The inoculated YNB was then incubated aerobically in sterile universals with the lids slightly loose at 37°C for 24 h with shaking at 180 rev/min. *Streptococcus* species were cultured on Blood Agar (BA; Blood Agar Base, Lab M) supplemented with 5% (v/v) defibrinated horse blood (TCS Biosciences, Buckingham, UK) and incubated aerobically at 37°C for 24 h. One colony was then aseptically transferred to 10 ml of Brain Heart Infusion broth (BHI; Lab M) and incubated aerobically at 37°C for 24 h with shaking at 180 rev/min. *Actinomyces* odontolyticus, *A. viscosus*, and *P. gingivalis* were cultured on Fastidious Anaerobe Agar (FAA; Lab M) supplemented with 5 % (v/v) defibrillated blood which was incubated anaerobically at 37°C for 24-48 h. One small loopful of an isolated colony was then aseptically transferred to 20 ml of BHI supplemented with 50 μg/ml of hemin (Sigma), 10 μg/ml of vitamin K (Sigma), and 5 μg/ml of L-cysteine (Sigma) (final in use concentrations), then incubated anaerobically at 37°C for a further 48 h.

2.2.2.2 Standardisation of inocula

Prior to inoculation for each experiment, the cultures were adjusted to a standardised inoculum level. Microorganisms were adjusted by optical density (OD_{600nm}) measurements using a spectrophotometer (DiluPhotometer™, Implen, Westlake Village, CA, USA). The equipment was calibrated at 600_{nm} to zero (blank) by using sterile uninoculated YNB or BHI medium. Subsequent sample readings were performed and diluted as necessary with sterile PBS to achieve a final OD_{600} of 1.00 (± 0.05) for *C. albicans* (equivalent to approximately 1×10^7 cells/ml), and an OD_{600} of 0.09 (± 0.01) for bacteria (equivalent to approximately 1.5×10^8 cells/ml (McFarland Standard 0.5)).

2.2.2.3 Denture acrylic (poly(methyl-methacrylate), PMMA) coupon preparation

Disc shaped poly(methyl methacrylate) (PMMA) coupons were prepared according to the manufacturer's instructions. Briefly, self-cure acrylic polymer (Bracon Ltd., Etchingham, UK) was added to self-cure acrylic monomer

(Bracon Ltd.) at a 2:1 ratio and mixed by hand until homogenous. The mixture was then carefully poured into a silicone mould (with pre-cut circular sections of approximately 10 mm diameter and 2 mm thickness) and left for approximately 15 s, after which, a thick glass cover was placed on top, and a 500 ml glass bottle containing approximately 250 ml water on top of the glass to apply pressure. The mixture was allowed to cure under ambient conditions overnight. The coupons were sanded to remove rough edges. The experimental surface (smooth upper surface left in contact with the glass during curing) was not manipulated or prepared in any way prior to use. The coupons were allowed to soak in water for a minimum of 7 d to allow excess monomer to leech out, before being sterilised by autoclaving at 121°C for 15 min. Coupons were stored in sterile distilled water prior to use, and as they are intended for single use only, used coupons were discarded after experimentation.

2.2.2.4 Preparation of artificial saliva (AS) solution

Artificial saliva (AS, Cavalcanti *et al*., 2015) was prepared by thoroughly mixing the following in sterile distilled water: 5.0 g/L proteose peptone (Oxoid) 2.5 g/L porcine stomach mucin (Oxoid), 2.0 g/L yeast extract (Oxoid), 1.0 g/L lab lemco powder (Oxoid), 0.35 g/L sodium chloride (Fisher Scientific), 0.20 g/L potassium chloride (Fisher Scientific), 0.20 g/L calcium chloride dihydrate (Fisher Scientific). Once homogenous, aliquots were prepared in glass bottles then the solution autoclaved at 121°C for 15 min. A 40% (w/v) urea solution was prepared in sterile distilled water and filter sterilised, then added to the artificial saliva solution at 1.25 ml/L immediately before each AS use.

2.2.2.5 Pre-conditioning PMMA coupons with AS

Sterile PMMA coupons were randomly selected and preconditioned by submersion in sterile artificial saliva solution for 16-20 h, incubated at 37°C. Randomly selected non-preconditioned PMMA coupons used as negative controls were submersed in sterile water and incubated overnight at 37°C. Immediately before transfer of the PMMA to the six-well plates for experimental

analysis, the AS preconditioned coupons were held vertically and excess AS allowed to aseptically drain to a waste container.

2.2.3 Adherence assay

To evaluate the effects of AS pellicle formation on adherence of microorganisms to the surface of PMMA, adherence assays were performed using *Streptococcus sanguinis* NCTC 7863; a representative species of oral bacteria commonly isolated from the oral cavity, and *C. albicans* ATCC 90028. All multi-well plates used in this project were polystyrene material (Starstedt, Nümbrecht, Germany).

2.2.3.1 Aseptic transfer and inoculation of microorganisms to PMMA

Sterile 24-well plates were used as containers for the PMMA coupons in each experiment. Aseptically, one preconditioned (PC) or non-conditioned (NC) PMMA piece was transferred into each individual well, with the smooth surface upwards, the total number of which was determined by the number of variables and replicates for each experiment. The lid of the 24-well plate was replaced immediately to avoid contamination.

A 100-µl volume of each standardised inoculum (prepared as described in section 2.2.2.2) was applied to the surface of the relevant PMMA coupons and the culture medium was added to give a 2 ml final volume. The 24-well plates were carefully moved to an aerobic incubator at 37°C for up to 90 min to allow adherence.

2.2.3.2 Enumeration of adhered microorganisms

Post-incubation, the PMMA coupons were aseptically removed, rinsed gently in PBS to remove any loosely or non-adherent cells, then transferred to a sterile plastic bijou container containing 5 ml of sterile PBS. The containers were vigorously vortex mixed for 1 min at 2500 rev/min to remove adhered cells. The solution was serially decimally diluted to 10^{-4}-fold in sterile PBS (100 µl sample to 900 µl PBS in sterile microcentrifuge tubes; Eppendorf). Four 10 µl samples of each dilution (including the original vortex mixed sample)

were plated according to the Miles and Misra drop count method (Miles *et al.*, 1938) on to agar plates appropriate for the target microorganism. Sabouraud dextrose agar was used for *C. albicans ATCC 90028* and BA for *S. sanguinis*.

Inoculated agar plates were incubated aerobically at 37°C until colonies had grown sufficiently (24-48h) to allow visual counting of individual colonies. The average colony count of the four 10 µl drops was determined and extrapolated to total recovered cells. The counts were analysed for statistical significance using unpaired two tailed T test at 95% confidence.

2.2.3.3 Fluorescence microscopy of adhered microorganisms

In addition to the enumeration of adhered microorganisms, direct determination of adherence was achieved by fluorescence microscopy. PMMA coupons were inoculated and microorganisms allowed to adhere as described in 2.2.3 Live/Dead *Bac*Light™ Bacterial Viability Kit (Life Technologies) was prepared as recommended by the manufacturer, and 20-30 µl of the fluorescent dye solution added to the surface of each PMMA coupon. The coupon was then overlaid with a glass cover slip for microscopy. The PMMA coupons were protected from light until use for microscopy.

Images of the PMMA surface were collected using an Olympus Provis AX 70 fluorescence microscope, using an Olympus U-MWIB3 filter cube (for Live/Dead staining) at ×200 and ×400 magnifications (×10 objective, with ×20 and ×40 lenses). Five fields of view were obtained for each microorganism and each condition (PC and NC), and representative images selected as visual representations.

2.2.4 Biofilm development and analysis

2.2.4.1 Single- and mixed-species biofilm development on PMMA surface

Microbial cultures were prepared according to sections 2.2.2.1 and 2.2.2.2, and PMMA coupons were preconditioned overnight according to section 2.2.2.3, after which the coupons were aseptically transferred to 24-well plates.

A 100 µl volume of each standardised inoculum was added to the PMMA coupons and sterile culture medium added to a final volume of 2 ml. The plates and coupons were then incubated aerobically or in 5% CO2 at 37°C for the microorganisms to adhere. After an initial adherence period of 90 min, the medium was removed, and replaced with 2 ml of fresh sterile culture medium. The well-plates were returned to the relevant incubator with shaking at 180 rev/min. After 24 h incubation, the well plates were removed from the incubator, the medium aspirated by pipette and replaced with 2 ml of fresh culture medium. This process was repeated again at 48 h, and the culture continued until 72 h, after which the biofilms were collected for analysis.

2.2.4.2 Culture enumeration of biofilms

Biofilms were removed from the coupon by vortex mixing in 5 ml PBS at 2500 rev/min for 1 min. The cell suspension was diluted by serial decimal dilution with each dilution plated according to the drop count method onto agar relevant for each microorganism. For mixed-species biofilms, BA, FAA and SDA were used to selectively culture bacteria or *C. albicans*.

The agar plates were incubated under conditions necessary for the growth of the relevant microorganism (for example, 37°C aerobically for *C. albicans* and *Streptococcus* species, or 37°C anaerobically for *Actinomyces* species). Once growth of colonies had been observed (sufficient to allow for visual counting), the colonies were enumerated, and extrapolated to determine total recovered cell numbers.

2.2.4.3 Confocal laser scanning microscopy (CLSM)

CLSM analysis was completed using an inverted Leica TCS SP5 confocal system, controlled by Leica Confocal software. PMMA coupons with biofilms were stained using one or more of the fluorescent dyes described in table 2.2. The biofilms were inverted onto a glass cover slip by using sterile forceps to invert the PMMA coupons and place them on top of the cover slip, and imaged at ×200, ×400 or ×630 magnification (×10 objective; ×20, ×40, ×63 magnification lenses). Z-stacks were obtained by imaging at varying depths of

the biofilm, creating a ‘pan-biofilm’ image. Emission windows were set according to the fluorescent stains used, and were set to at least 30 nm distance from the excitation of other lasers to avoid crossover.

2.2.4.4 Quantification of *C. albicans* hyphae

For the purpose of determining relative proportion of C. albicans hyphae within biofilms, confocal microscopy images were obtained and compressed into a single plane. The image was manipulated in order to use an automatic counting tool in Image J software (version 2.0.0-rc-64/1.51s), according to the following directions (originally developed by Larry Reinking Department of Biology, Millersville University Millersville, PA): images were converted into an 8-bit image, and then converted to a binary image. The ‘analyse particles’ tool was then used to identify individual circular yeast cells within the whole image area and enumerate them. Hyphae were counted manually. Validation of the method was confirmed by manual counts on two random images to ensure consistency between manual and automatic counts with good agreement between the two methods, thus automatic counting was determined to be suitable for this purpose.

Fluorophore/stain	Excitation/Emission (nm)	Intended target
Syto9	485/498	Live cells
Non-selective DNA specific		(active uptake)
Propidium iodide	535/617	Dead cells
Non-selective, DNA specific		(entry via permeable/compromised membrane only)
Calcofluor white	355/433	Fungi
		(chitin in candidal cell wall)
Concanavalin A	590/617	*Candida albicans*
Alexa Fluor® 594 conjugated lectin		(carbohydrate in candidal cell wall)
***Candida albicans* PNA**	490/525	*Candida albicans*
FITC conjugate		
Universal bacterial PNA	550/570	16S rRNA gene of bacteria
Cyanin-5 conjugate		

Table 2.2 Fluorescent dyes used for confocal microscopy analysis of biofilms

2.2.4.5 Scanning electron microscopy (SEM)

SEM was used to further image polymicrobial biofilms to determine biofilm structure and demonstrate *C. albicans* hyphal presence within the biofilms.

The biofilm samples were removed from multi-well plates, and immersed in 2.5% glutaraldehyde (diluted in sterile water) overnight. The biofilm coupons were washed gently with distilled water 2 × 10 min. The samples were then dehydrated using a gradient of increasing concentrations of ethanol: 30%, 50%, 70%, then 90%, for 10 min at each concentration, then 100% ethanol for 2 × 10 min. The samples were then immersed in hexamethyldisilazane for 10 min, then allowed to air dry.

Once dehydrated and prepared, the samples were sputter coated with gold, and imaged on a Tescan VAGA SEM system, at 5-10kV.

2.2.5 Quantitative PCR (qPCR) for *C. albicans* virulence genes

2.2.5.1 Extraction of RNA

Biofilms were suspended in 1 ml PBS, pelleted by centrifugation at 11,000 × *g* for 2 minutes and then resuspended in 200 µl TE buffer containing 10 mg/ml of lysozyme (LTE). RNA extraction was performed using phenol:chloroform:isoamyl alcohol solution (25:24:1, Sigma) and RNeasy Mini Kit (Qiagen) as described below. All centrifugation steps occurred at 11,000 × *g* unless otherwise stated.

The suspended biofilm cells in LTE were mixed with 350 µl RLT Buffer (Qiagen) with 1% (v/v) β-Mercaptoethanol and vortex mixed for 15 s. The suspension was transferred to a pathogen lysis tube (Qiagen) which contain sterile glass beads of an undisclosed diameter, and 500 µl of phenol:chloroform:isoamyl alcohol. The cells were disrupted using a Mini-BeadBeater-8 (Stratech Scientific Ltd., Suffolk, UK) for 1 min and placed on ice immediately, after which the suspension was centrifuged for 5 min. The solution separated into three distinct layers; a lower red coloured phenol rich layer, an intermediary white layer containing proteins and cell debris, and an

upper transparent layer rich in nucleic acids. The upper phase was carefully transferred on ice to a 1.5 ml microcentrifuge tube containing 700 µl of molecular biology grade 100% ethanol. This mix was stored at -20°C for 15 min to precipitate any proteins.

The lysate (700 µl maximum) was transferred to an RNeasy column (Qiagen) which was placed in a collection tube, and centrifuged for 1 min. The flow through was discarded and the centrifugation repeated for the remaining lysate. The pre-prepared DNase I solution (80 µl; Qiagen) was added to the column membrane and the membrane incubated at room temperature for 30 min. After incubation, 350 µl of RW1 buffer (Qiagen) was added and samples incubated at room temperature for a further 5 min, then centrifuged for 1 min. The flow through was discarded, then 500 µl RPE buffer (Qiagen) was added and the samples centrifuged for 1 min. The flow through was discarded, and a further 500 µl of RPE buffer was added and the samples centrifuged for 2 min. The flow through was discarded, and the column centrifuged for a further 2 min. The column was placed into a new collection tube and 30 µl of RNase-free water was added to the centre of the filter. The RNA was allowed to dissolve for 2 min before centrifugation for 2 min. The flow through was added onto the membrane and subjected to a second elution. The RNA solutions were stored on ice when being processed immediately, otherwise they were immediately frozen at -80°C until used.

RNA concentration and purity was quantified using a Nano-Vue Plus spectrophotometer (GE Healthcare) immediately prior to reverse transcription. Samples were diluted when necessary to achieve a standardised concentration.

2.2.5.2 Reverse transcription of RNA to cDNA (RT)

Quantified total RNA was subjected to a two-step reverse transcription to cDNA using the Precision nanoScript™ 2 reverse transcription kit (PrimerDesign, Southampton, UK) according to the manufacturer's instructions. Total concentrations used ranged from 500-1000 ng total RNA

(due to variability of total extracted RNA from biofilms). Step one involved annealing of random nonamer primers to the RNA. This was achieved by adding RNA (diluted as necessary in a final volume of 9 µl in RNase/DNase free water) to 1 µl of the random nonamer primers. This was then placed into a thermocycler at 65°C for 5 min, then immediately transferred to ice. The step two master mix was then prepared and comprised (for each reaction) of 5 µl nanoScript2 4× Buffer, 1 µl of dNTP mix (10 mM), 3 µl of RNase/DNase free water and 1 µl of nanoScript2 enzyme. The mixtures were vortex mixed for 5 s to homogenise and subjected to thermocycling of 25°C for 5 min, 42°C for 20 min, and a final heat inactivation step of 75°C for 10 min. The resulting cDNA was stored at -20°C until used.

2.2.5.3 qPCR analysis

Gene expression of samples was analysed by qPCR using a QuantStudio 6 Flex Real Time PCR system (Applied Biosystems). Each well contained a 20 µl reaction volume, and included 10 µl of 2× SYBR Green based Precision FAST qPCR master mix (PrimerDesign), 1 µl of each reverse and forward primer (detailed in Table 2.3), (10 mM), 3 µl of RNase/DNase free water and 5 µl of cDNA template.

The qPCR program used the following thermal cycling parameters: 95°C for 20 s, followed by 40 cycles of 95°C for 1 s and 60°C for 20 s. After completion of the cycles, a final melt curve stage was completed at 95°C for 15 s, and from 60°C for 1 min and final 95°C for 15 s. The cycle threshold for each sample was determined automatically by the software at the point of logarithmic amplification of the samples.

Target gene	Sequence (5' → 3')	Reference
ACT1	F – TGCTGAACGTATGCAAAAGG	Alves *et al*., 2014; Cavalcanti *et al*., 2015
Housekeeping Gene	R – TGAACAATGGATGGACCAGA	
ALS1	F – CCCAACTTGGAATGCTGTTT	Alves *et al*., 2014; Cavalcanti *et al*., 2015
Agglutinin-Like Sequence 1	R – TTTCAAAGCGTCGTTCACAG	
ALS3	F – CTGGACCACCAGGAAACACT	Bandara *et* al., 2012; Alves *et al*., 2014;
Agglutinin-Like Sequence 3	R – GGTGGAGCGGTGACAGTAGT	Cavalcanti *et al*., 2015
EPA1	F – ATGTGGCTCTGGGTTTTACG	Alves *et al*., 2014; Cavalcanti *et al*., 2015
Epithelial Adhesin 1	R – TGGTCCGTATGGGCTAGGTA	
HWP1	F – TCTACTGCTCCAGCCACTGA	Alves *et al*., 2014; Cavalcanti *et al*., 2015
Hyphal Wall Protein 1	R – CCAGCAGGAATTGTTTCCAT	
PLD1	F - GCCAAGAGAGCAAGGGTTAGCA	Alves *et al*., 2014; Cavalcanti *et al*., 2015
Phospholipase D 1	R – CGGATTCGTCATCCATTTCTCC	
SAP4	F – GTCAATGTCAACGCTGGTGTCC	Alves *et al*., 2014; Cavalcanti *et al*., 2015
Secreted Aspartyl Proteinase 4	R - ATTCCGAAGCAGGAACGGTGTCC	
SAP6	F – AAAATGGCGTGGTGACAGAGGT	Alves *et al*., 2014; Cavalcanti *et al*., 2015
Secreted Aspartyl Proteinase 6	R - CGTTGGCTTGGAAACCAATACC	

Table 2.3 Forward (F) and reverse (R) primers used for evaluation of *C. albicans* virulence genes via quantitative polymerase chain reaction (qPCR)

2.3 Results

2.3.1 Effect of preconditioning acrylic coupons with artificial saliva on microbial attachment and biofilm formation

The formation of a salivary pellicle on different surfaces has been reported to increase the attachment of certain microorganisms. Thus, to develop an optimised acrylic biofilm model, an evaluation of the effect of an artificial salivary pellicle on microbial attachment to PMMA and subsequent biofilm formation was undertaken.

2.3.1.1 Adherence of *Candida albicans* to PMMA

Fluorescence microscopy showed an increase in the number of adhered *C. albicans* cells to PMMA preconditioned (PC) with artificial saliva (AS) compared with PMMA conditioned in water (NC). Viable cell recovery and enumeration also demonstrated a significant (P=0.0075) increase in the number of adhered viable cells to the PC PMMA coupons (5.28 ± 0.25 $\log_{10}$ recovered CFU), compared with NC PMMA coupons (4.49 ± 0.11 $\log_{10}$ recovered CFU) (Figs. 2.1, 2.2; Table 2.4).

2.3.1.2 Adherence of *Streptococcus* species to PMMA

Similar to *C. albicans* adherence, a significant (P=0.0063) increase was observed in the recovery and enumeration of viable *S. sanguinis* from PMMA preconditioned with AS (PC; 5.32 ± 0.28 $\log_{10}$ recovered CFU) compared with non-preconditioned PMMA (NC; 4.47 ± 0.04 $\log_{10}$ recovered CFU) was observed (Fig. 2.3; Table 2.5). Differences in surface coverage by fluorescence microscopy were more subtle (Fig. 2.4)

Adherence of both microorganisms was homogenously distributed across the surface of the acrylic coupons, with no distinct clusters or aggregates of cells evident, irrespective of preconditioning status.

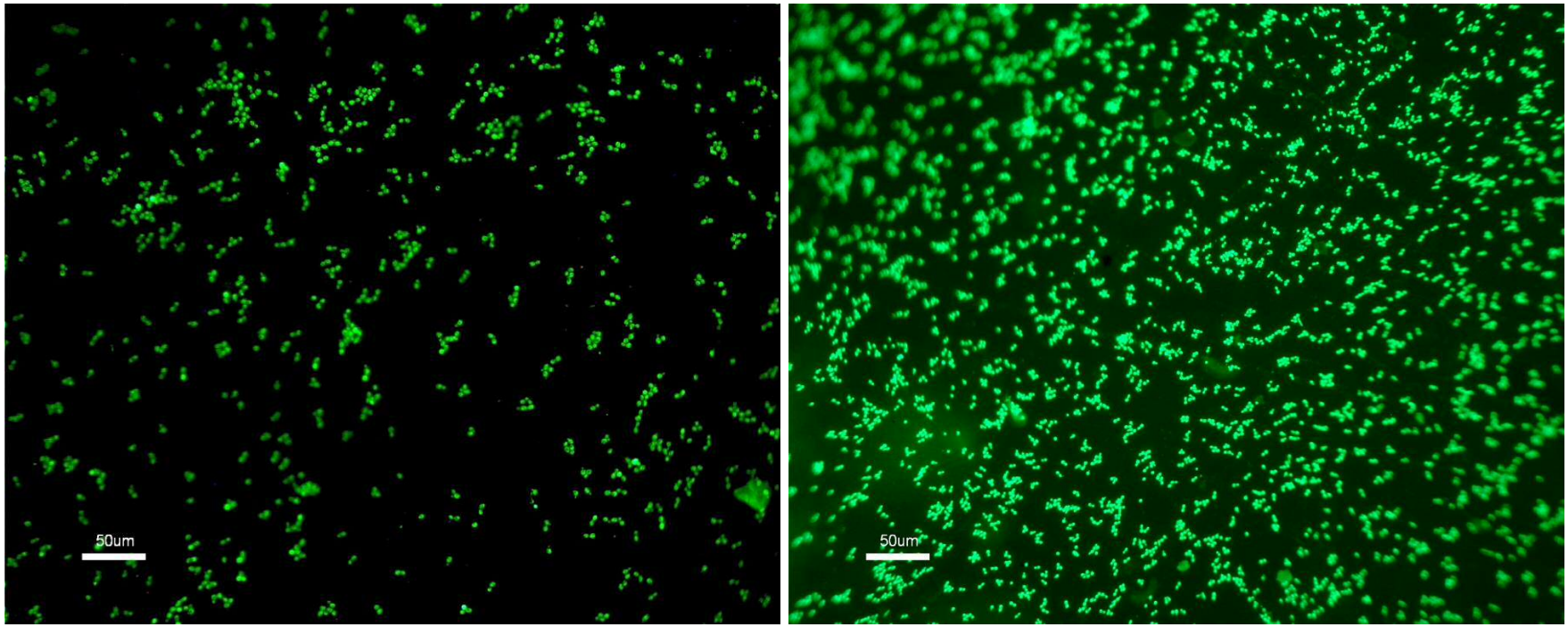

Figure 2.1 Effect of artificial saliva (AS) preconditioning of PMMA coupons on *C. albicans* adherence.
Typical fluorescence images of *C. albicans* adherence to acrylic coupons. Left: no preconditioning, right: artificial saliva preconditioning. Cells were stained with Syto-9. Scale bar represents 50 μm

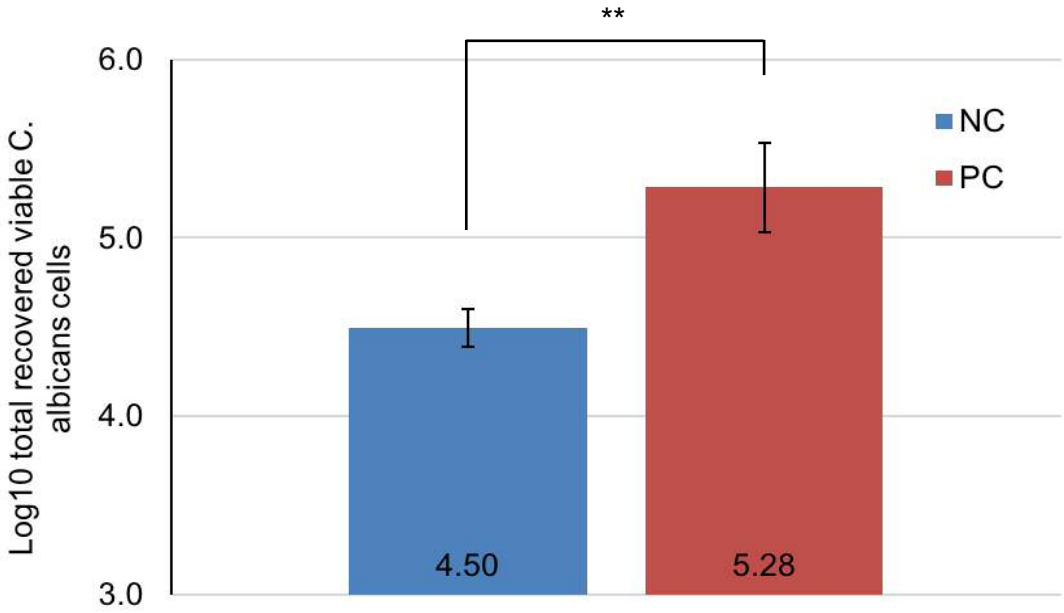

Figure 2.2 Effect of artificial saliva pre-conditioning of acrylic coupons on *C. albicans* adherence as measured by number of recovered viable *C. albicans.* Data expressed as mean of 3 experimental replicates (experimental n=3, 6 replicates). Error bars represent SD. NC= Non-preconditioned, PC=AS pre-conditioned.

Experimental replicate	Mean Log_{10} total CFU (± SD)	
	Non-conditioned	Pre-conditioned
1	4.60 (0.28)	5.57 (0.11)
2	4.39 (0.32)	5.10 (0.32)
3	4.50 (0.25)	5.18 (0.24)
Mean	4.49	5.28
SD	0.11	0.25
P value	0.0075	

Table 2.4 Effect of artificial saliva pre-conditioning of acrylic coupons on *C. albicans* adherence as measured by number of recovered viable *C. albicans*.

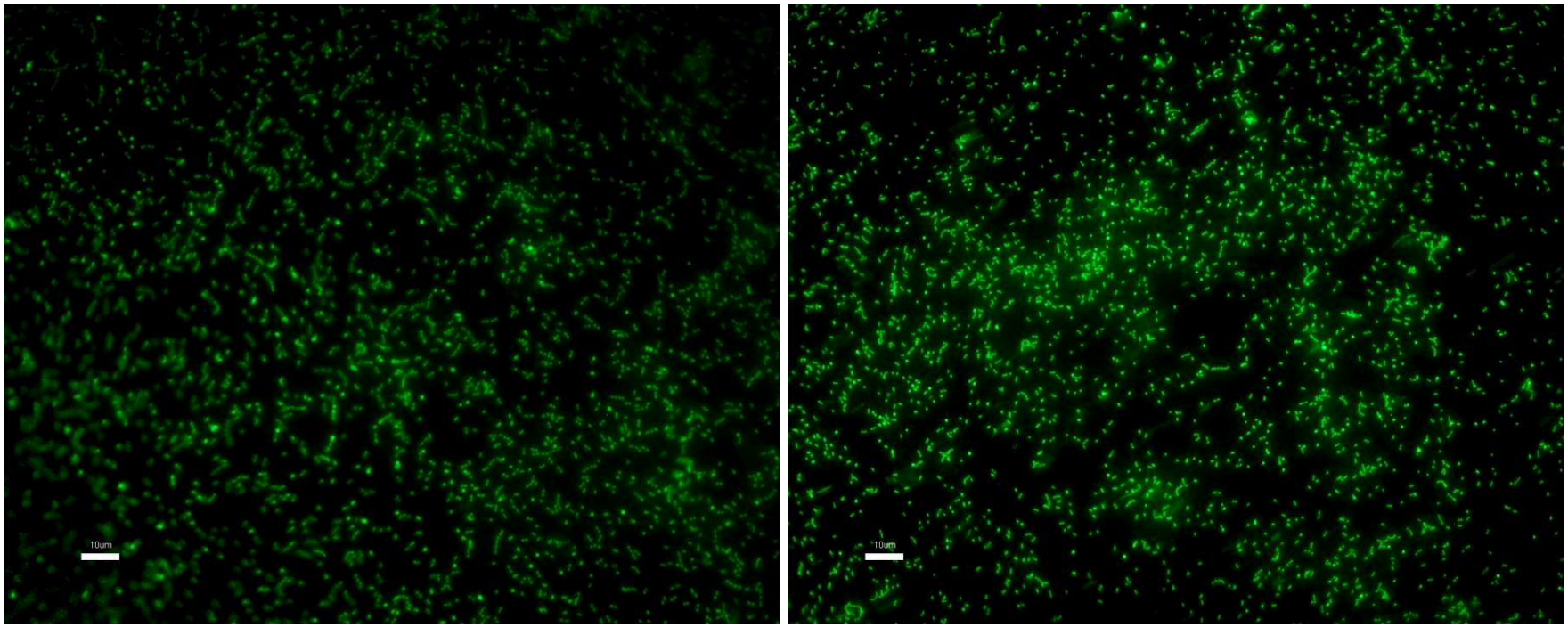

Figure 2.3 Effect of artificial saliva (AS) preconditioning of PMMA coupons on subsequent *S. sanguinis* adherence.
Typical fluorescence microscope images of *S. sanguinis* adherence to PMMA. Cells stained with Syto-9.
Left: Non-preconditioned, right: artificial saliva pre-conditioned. Scale bar represents 10 μm

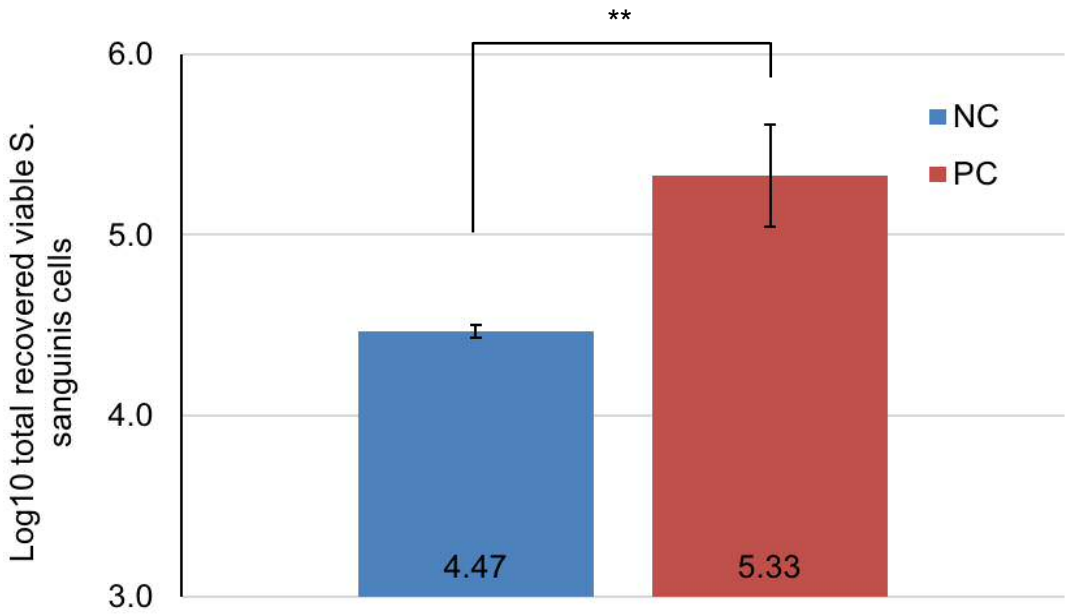

Figure 2.4 Effect of artificial saliva pre-conditioning of acrylic coupons on S. sanguinis adherence as measured by number of recovered viable S. sanguinis.

Data expressed as mean of 3 experimental replicates (experimental n=3, 6 replicates). Error bars represent SS. NC= Non-preconditioned, PC=AS pre-conditioned.

Experimental replicate	Mean Log_{10} total CFU (± SD)	
	Non-conditioned	Pre-conditioned
1	4.43 (0.47)	5.15 (0.35)
2	4.50 (0.23)	5.18 (0.56)
3	4.48 (0.76)	5.65 (0.28)
Mean	4.47	5.32
SD	0.04	0.28
P value	0.0063	

Table 2.5 Effect of artificial saliva pre-conditioning of acrylic coupons on S. sanguinis adherence as measured by number of recovered viable S. sanguinis.

2.3.2 Single and mixed-species biofilm formation on PMMA

Whilst no significant differences were observed in the adherence of microorganisms to the surface of PMMA coupons with the presence or absence of an AS pellicle, biofilm formation may have been influenced as well as potential interactions with microorganisms. Thus, formation of mature biofilms were evaluated with and without an AS pellicle.

2.3.2.1 Effect of artificial saliva pre-conditioning of PMMA on *C. albicans*-only and bacteria-only 72h biofilms

Using a batch culture biofilm system with daily medium changes, biofilm formation was measured by recovery and enumeration of viable microorganisms. The number of recovered viable *C. albicans* and *S. sanguinis* was not significantly (P>0.05) influenced by the presence of an AS preconditioning pellicle (Figure 2.5; Table 2.6).

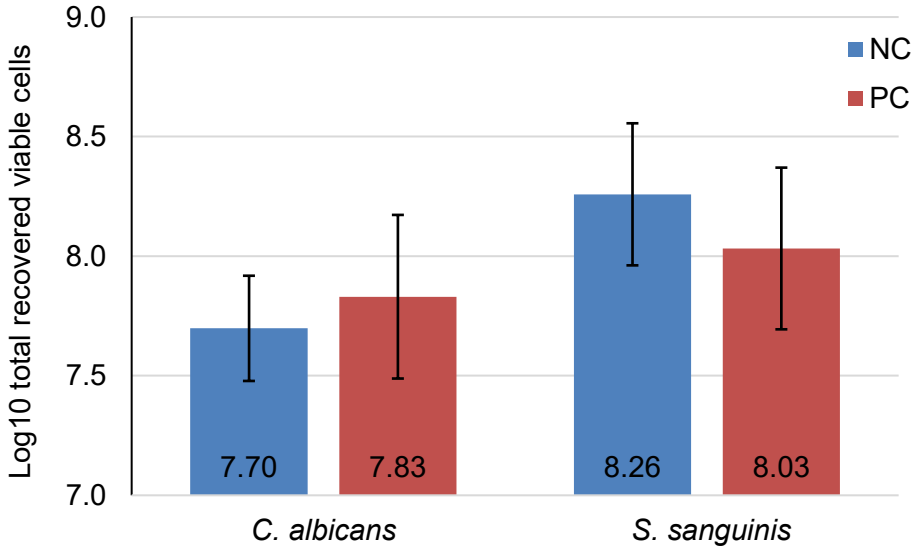

Figure 2.5 Effect of pre-conditioning acrylic coupons with artificial saliva on formation of single-species 72 h biofilms as measured by number of recovered viable cells.
Data expressed as mean of 3 experimental replicates (n=3, 4-5 replicates), error bars represent SD. NC= Non-preconditioned, PC=AS pre-conditioned.

Experimental replicate	Mean Log_{10} total CFU (± SD)			
	C. albicans		*S. sanguinis*	
	Non-conditioned	Pre-conditioned	Non-conditioned	Pre-conditioned
1	7.33 (0.10)	7.63 (0.14)	8.68 (0.09)	8.65 (0.17)
2	8.09 (0.39)	8.50 (0.17)	8.41 (0.08)	7.96 (0.23)
3	7.67 (0.19)	7.36 (0.10)	7.69 (0.11)	7.49 (0.05)
Mean	7.70	7.83	8.26	8.03
SD	0.38	0.60	0.51	0.58

Table 2.6 Effect of artificial saliva pre-conditioning of acrylic coupons on formation of single-species 72h biofilms as measured by number of recovered viable cells

The number of recovered viable cells of *C. albicans* was similar for both PC (7.83 ± 0.60 log_{10} recovered CFU) and NC (7.70 ± 0.38 log_{10} recovered CFU) conditions. Similarly, no significant differences in number of viable *S. sanguinis* was observed following PC (8.26 ± 0.51 log_{10} recovered CFU) and NC (8.03 ± 0.58 log_{10} recovered CFU) conditions. Furthermore, the extent of biofilm formation, as measured by enumeration of recovered viable cells, was similar for both *C. albicans* and *S. sanguinis*.

Confocal microscopy results of the mature single species biofilms (Figs. 2.6, 2.7) correlated with the findings presented in Table 2.6, in that no clear differences were evident due to AS conditioning. CLSM showed no clear visible differences in the observed biomass, coverage, or formation/structure of the biofilms irrespective of the presence or absence of an AS pre-conditioning pellicle.

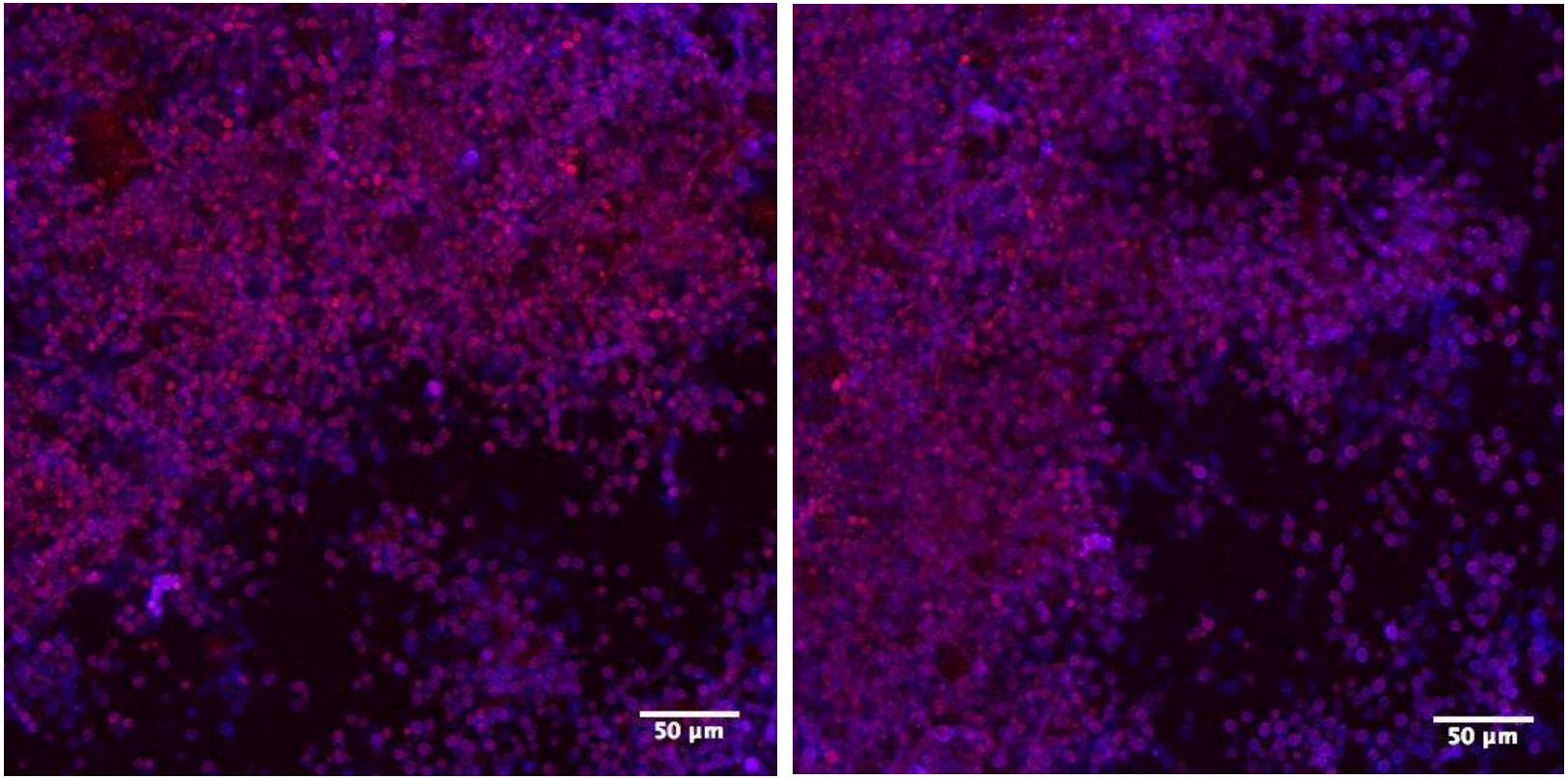

Figure 2.6 Typical confocal microscope images of *C. albicans*-only 72 h biofilms on acrylic coupons to evaluate the effect of artificial saliva pre-conditioning on development of mature biofilms, assessed visually for surface coverage and biofilm structure.
Candida albicans single-inoculum 72h biofilms with non-preconditioned acrylic coupon (left) and artificial saliva pre-conditioned acrylic coupon (right). Cells were fixed overnight with 10% (v/v) formal saline, then stained with propidium iodide (red) and calcofluor white (blue/purple).

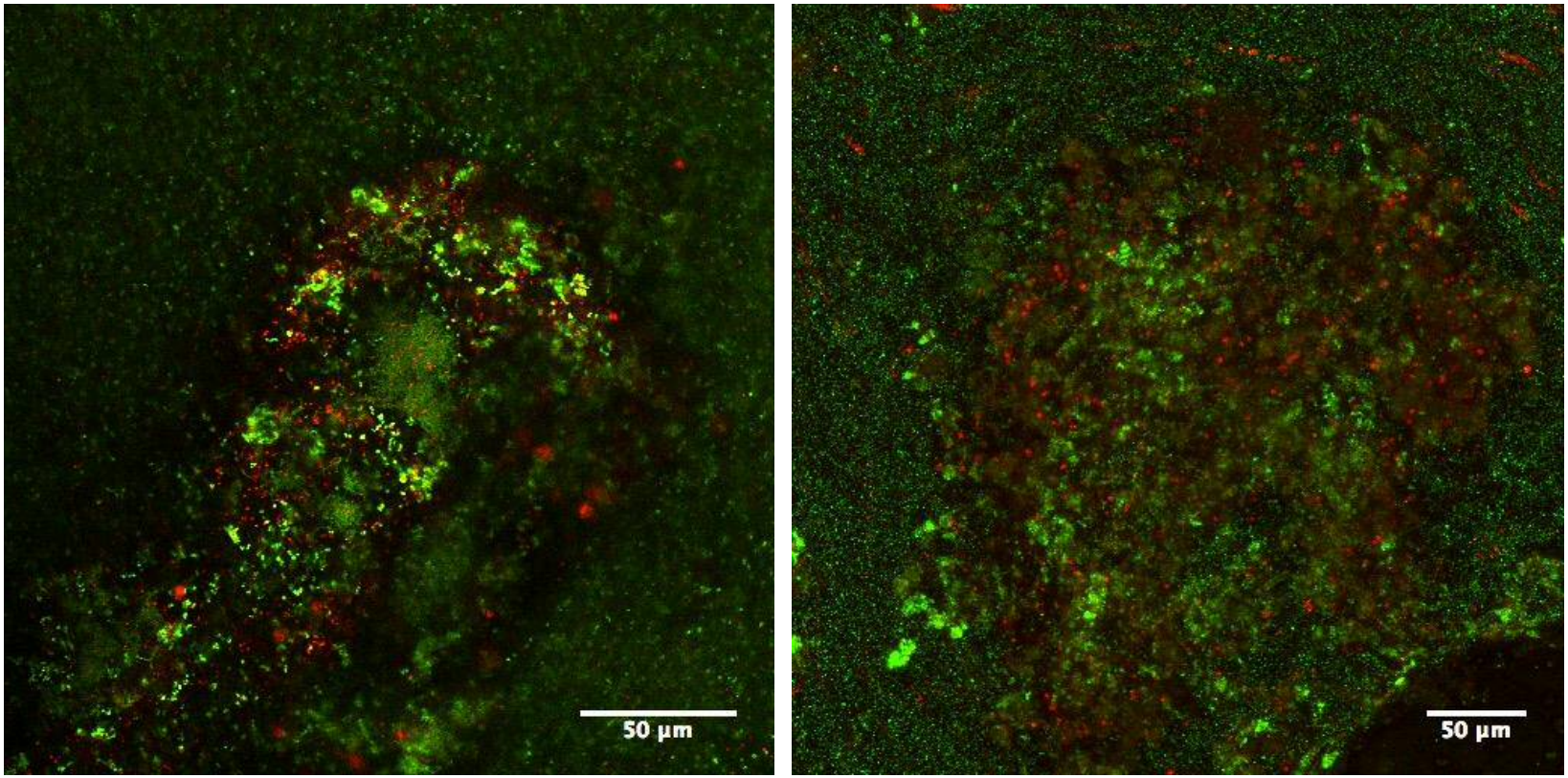

Figure 2.7 Typical confocal microscopy images of S. sanguinis-only 72h biofilms on acrylic coupons to evaluate the effect of artificial saliva pre-conditioning on development of mature biofilms, assessed visually for surface coverage and biofilm structure.
Bacteria-only 72 h biofilms with non-preconditioned acrylic coupons (left) and artificial saliva pre-conditioned acrylic coupons (right). Cells were stained with Live/Dead™ *Bac*Light™ bacterial viability kit (Syto-9, green; propidium iodide, red).

2.3.2.2 Effect of artificial saliva pre-conditioning on mixed-species (*C. albicans* and bacteria) biofilms

When mature biofilms were cultured using a mixed species inoculum (*C. albicans* with bacteria (*Streptococcus sanguinis, S. gordonii, Actinomyces odontolyticus* and *A. viscosus*), no significant (P>0.05) differences in the number of recovered viable cells, as a measure of biofilm formation, were evident (Fig. 2.8; Table 2.7).

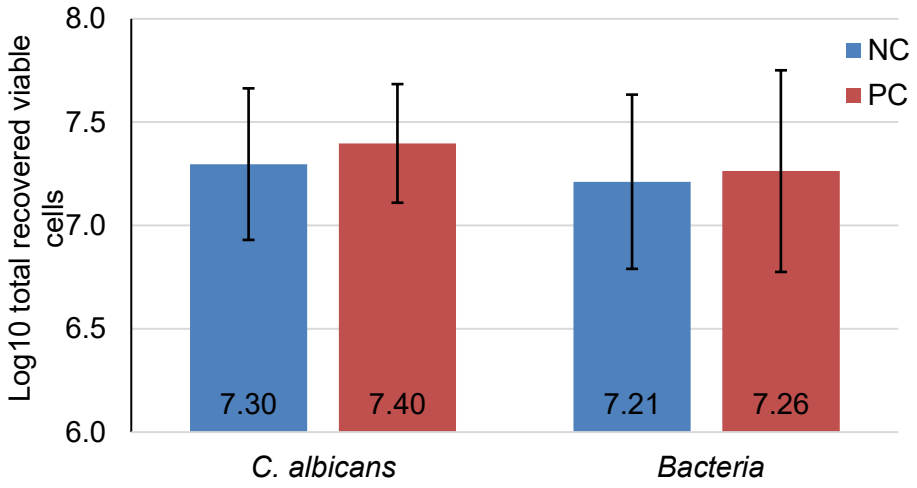

Figure 2.8 Effect of artificial saliva pre-conditioning of acrylic coupons in mixed-culture 72h biofilms as measured by number of recovered viable cells. Total recovered viable cell counts of *C. albicans* ATCC 90028, and bacteria[A] from mixed culture 72 h biofilms. Data expressed as average of 10 replicates, error bars represent SD. NC= Non-preconditioned, PC=AS pre-conditioned.

Experimental replicate	Ave Log_{10} total CFU (± SD)			
	C. albicans		*Bacteria*	
	Non-conditioned	Pre-conditioned	Non-conditioned	Pre-conditioned
1	6.93 (0.18)	7.68 (0.11)	6.79 (0.14)	7.75 (0.09)
2	7.66 (0.05)	7.11 (0.07)	7.63 (0.14)	6.78 (0.08)
Mean (SD)	7.30 (0.52)	7.40 (0.41)	7.21 (0.60)	7.26 (0.69)

Table 2.7. Effect of artificial saliva pre-conditioning of acrylic coupons in mixed-culture 72 h biofilms as measured by number of recovered viable cells

[A] *Mixed culture inocula included S. sanguinis and S. gordonii but enumeration data does not distinguish between species; presented as total bacteria*

Recovery of *C. albicans* from mixed species biofilms on NC coupons (7.30 ± 0.52 log_{10} recovered CFU) was very similar to that of PC (7.40 ± 0.41 log_{10} recovered CFU). Furthermore, high similarities were also observed with total recovered bacteria (NC=7.21 ± 0.60 log_{10} recovered CFU, PC=7.26 ± 0.69 log_{10} recovered CFU). Interestingly, the overall total number of bacteria in mixed-species biofilms was nearly 10-fold lower than that observed for the single-species bacteria-only biofilms.

Of note was that *C. albicans*-only and mixed-species biofilms were typical in biofilm structure and formation; characteristic aggregates of cells were evenly distributed over the surface where biofilm maturation developed as three-dimensional clusters. This was particularly evident at lower magnification, where a larger surface area was observed (figure 2.9).

2.3.3 Effect of oral bacteria within mixed species biofilms on expression of specific *C. albicans* virulence factors

Denture stomatitis (DS) is normally associated with polymicrobial biofilms including the fungus *Candida*, on the denture fitting surface. Whilst the presence of *Candida* subsequently leads to chronic palatal irritation and inflammation, other factors could impact the development of DS. One of these is the associated bacterial microbiome, which varies between individuals, and may have capacity to influence behaviour of *Candida*.

Using the developed acrylic biofilm model described in section 2.2.4, this study evaluated the effect of certain oral bacteria in mixed-species biofilms on expression of a range of putative virulence factors of *C. albicans.* These included morphological transition from yeast to hyphae, expression of virulence genes involved in adherence, biofilm formation, hyphal formation and production of hydrolytic enzymes

2.3.3.1 Use of a standardised microbial inoculum to develop biofilms for *in vitro* interactions

A standardised, reproducible microbial inoculum was used for evaluation of the influence of oral bacteria on *C. albicans* virulence as detailed in section 2.2.2.1. In addition to *C. albicans* ATCC 90028, the inoculum included the commensal oral bacteria *S. sanguinis* NCTC 7863*, S. gordonii* ATCC 10558T*, A. odontolyticus* NCTC 9935 and *A. viscosus* ATCC 1598. *Porphyromonas gingivalis* NCTC 11834 was also used as an additional bacterial species to evaluate differential regulation of *C. albicans* virulence compared with the former standardised bacterial inoculum.

2.3.3.2 Morphological transition from yeast to hyphae

Formation of hyphae is considered an important virulence factor of *C. albicans*. Whilst no significant differences were observed by culture in the quantity of viable *C. albicans* in either *C. albicans* only biofilms (7.83 $\pm$ 0.60 $\log_{10}$ recovered CFU, Table 2.6) or *C. albicans* with mixed oral bacteria biofilms (7.40 $\pm$ 0.41 $\log_{10}$ recovered CFU, Table 2.7), the relative proportion of hyphae (when compared with yeast form of the cells) was significantly ($P<0.001$) higher in mixed-culture biofilms compared to *C. albicans*-only biofilms (Figs. 2.10, 2.11, 2.12; Table 2.8). *Candida albicans* hyphae were not completely absent in *C. albicans*-only biofilms, but represented a very small proportion of the total cells (0.68% $\pm$ 0.56, expressed as % of the total yeast and hyphae cells combined). An increase of more than ten-fold in the average ($\pm$ SD) relative proportion of hyphae compared to yeast cells was evident in mixed-culture biofilms (8.29% $\pm$ 2.48) compared with *C. albicans*-only biofilms.

Scanning electron microscopy (Fig. 2.11) demonstrated location of hyphae within the biofilm, and these hyphae appeared to provide a ‘scaffold like structure’ within the biofilm, with yeast and many bacterial cells attached to them, and each other.

Interestingly, when *P. gingivalis* was included in the mixed-species bacterial inoculum, no enhancement of *C. albicans* hyphae production was observed.

The extent of hyphal production was similar to that observed in *C. albicans*-only biofilms (2.18% ± 0.06), where there was no significant (P=0.42) difference to that of *C. albicans*-only biofilms when analysed statistically using one-way ANOVA with Tukey's multiple comparisons test. However, the reduction in the relative proportion of hyphae compared with mixed-species biofilms was highly significant (P<0.001).

Differential modulation of *C. albicans* hyphal production in mixed-species including *P. gingivalis* biofilms was evident by confocal microscopy, where very few *C. albicans* hyphae were visible (Fig. 2.13).

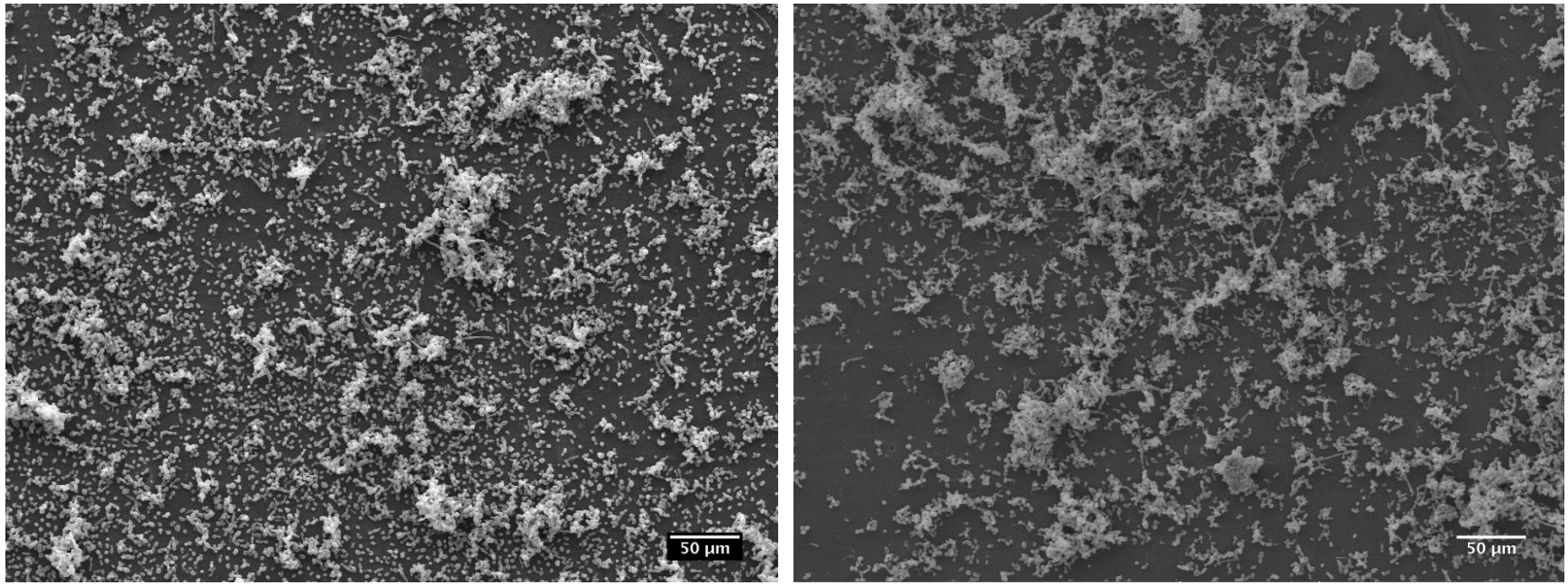

Figure 2.9 Scanning electron microscopy images of mature acrylic biofilms demonstrating distribution and formation of biofilms on the surface.
C. albicans-only (left) and mixed-species (right) 72 h acrylic biofilms representing typical distribution and clustering as a result of the three-dimensional formation of surface biofilms. Scale bar represents 50 µm.

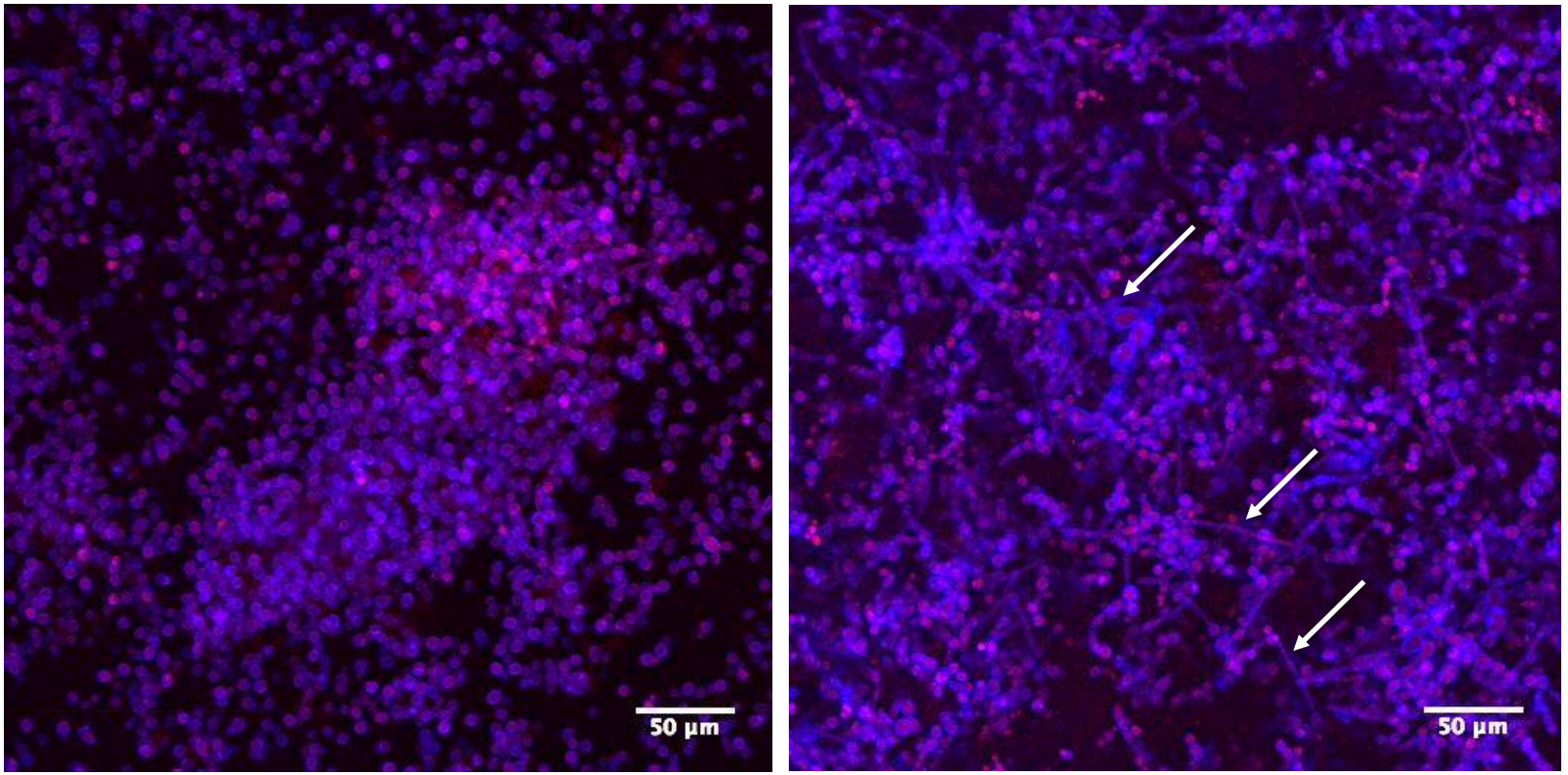

Figure 2.10 Confocal laser scanning microscopy images of *C. albicans*-only and mixed-species biofilms to quantify *C. albicans* hyphae.
Candida albicans hyphal presence in single (left) and mixed-culture (right) biofilms including *C. albicans* and oral bacteria. Arrows indicate hyphae. Cells stained with propidium iodide (red) and calcofluor white (blue/purple).

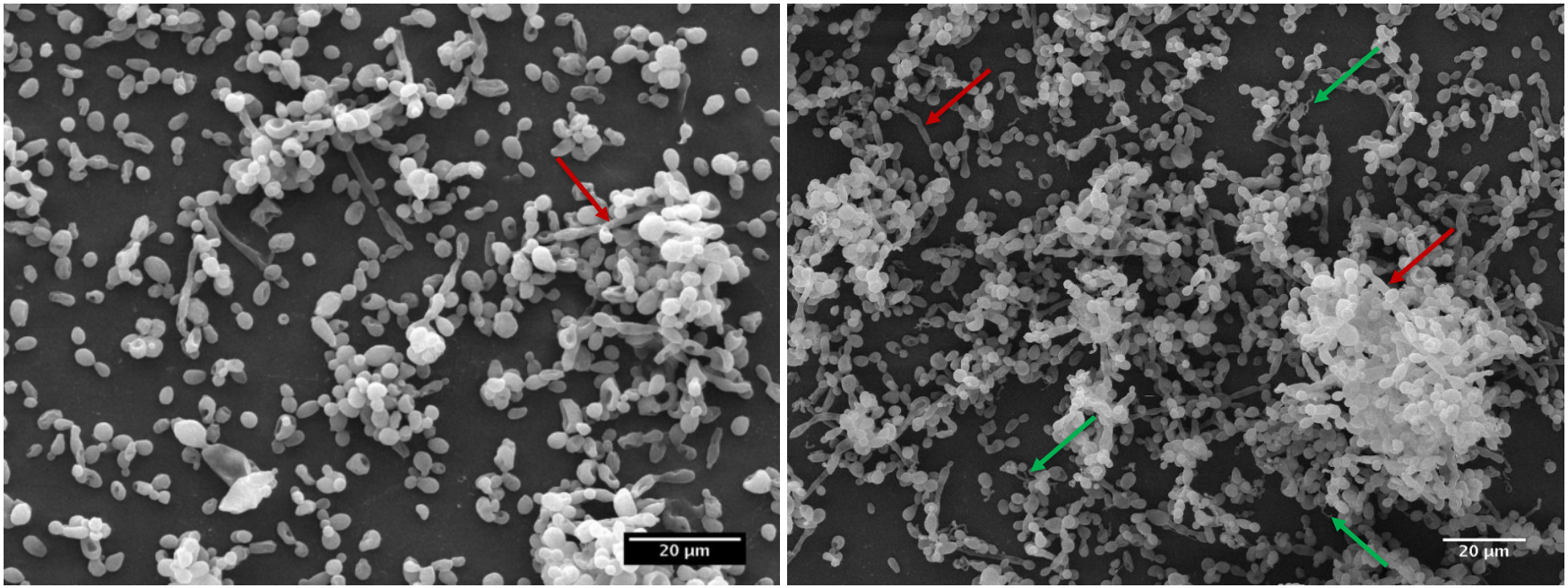

Figure 2.11 Typical scanning electron microscopy of *C. albicans*-only, and *C. albicans* with oral bacteria (mixed-species) biofilms to evaluate hyphal presence and bacterial attachment.
Typical scanning electron microscopy images of 72 h *C. albicans*-only biofilm (left) and 72 h mixed-species biofilm (right). Bacterial attachment appears to be primarily to the acrylic surface, but bacterial attachment to the *C. albicans* cells was also evident. Red arrows indicate *C. albicans* hyphae, green arrows indicate bacterial cells.

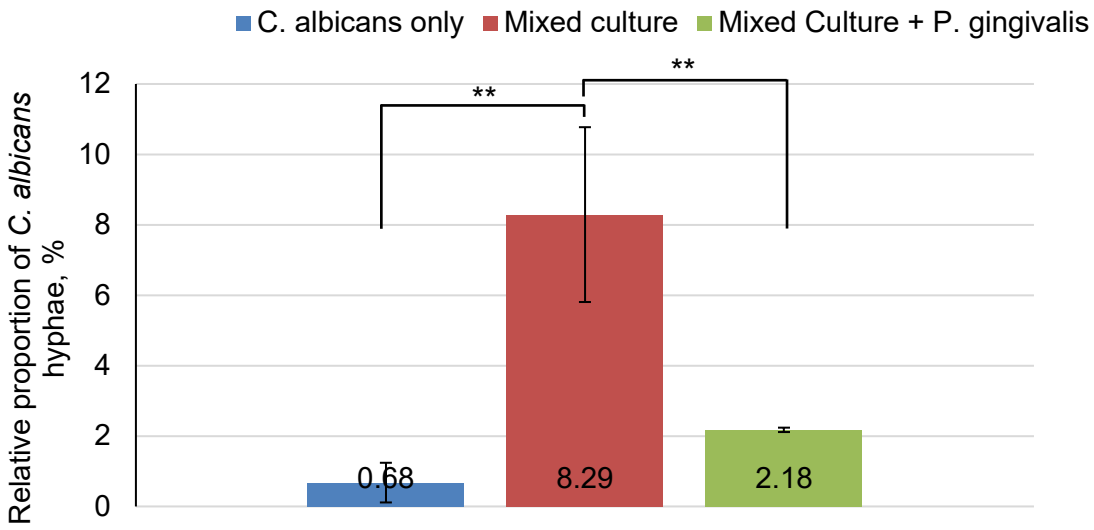

Figure 2.12 Relative proportion of *C. albicans* hyphae in *C. albicans*-only, mixed-species and mixed-species with *P. gingivalis* acrylic biofilms.
Proportion of *C albicans* hyphae in biofilms relative to total cells including yeast and hyphae. A significantly (P<0.001) higher proportion of hyphae was evident in mixed species biofilms than *C. albicans* only biofilms and mixed-culture biofilms also including *P. gingivalis*. No significant difference was observed (P=0.42) when comparing *C. albicans*-only biofilms with mixed-culture plus *P. gingivalis* biofilms.
Data expressed as mean of 4-5 replicates, error bar represents standard deviation.

Sample	Relative proportion of hyphae (%)		
	***C. albicans* only**	***C. albicans* plus bacteria**	***C. albicans* plus bacteria plus *P. gingivalis***
1	0.82	3.88	2.11
2	0.00	8.29	2.23
3	0.21	10.75	2.13
4	1.62	10.57	2.22
5	0.74	7.96	-
Mean (SD)	0.68 (0.56)	8.29 (2.48)	2.18 (0.06)

Table 2.8 Relative proportion of hyphae in *C. albicans*-only biofilms versus biofilms developed using *C. albicans* plus oral bacteria analysed with Image J.

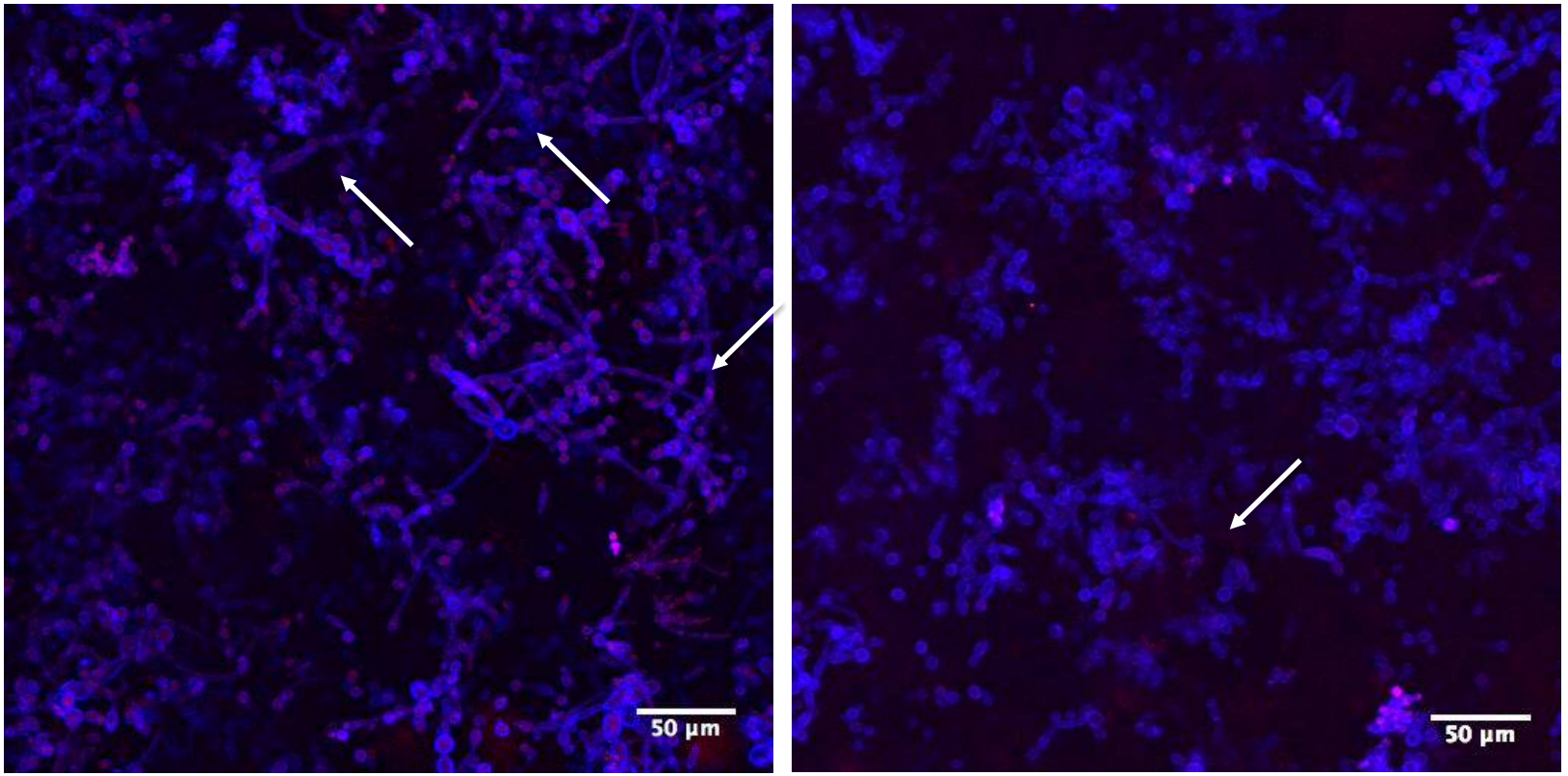

Figure 2.13 Typical confocal microscopy images demonstrating reduced *C. albicans* hyphal production in mixed-culture plus *P. gingivalis* biofilms compared with mixed-species biofilms.
Candida albicans hyphal presence in mixed-culture biofilms (left) and mixed-culture plus *P. gingivalis* (right). White arrows indicate presence of hyphae. Cells stained with propidium iodide (red) and calcofluor white (blue/purple).

2.3.3.3 Expression of *C. albicans* virulence genes

Changes in the relative expression of a number of *C. albicans* virulence genes was evident in mixed-species and mixed-species including *P. gingivalis* biofilms compared with *C. albicans*-only biofilms. These results are presented in Fig. 2.14 and Table 2.9.

Compared with *C. albicans*-only biofilm controls, mixed-species biofilms exhibited significantly increased expression of all the *C. albicans* virulence genes assessed in this study: agglutinin-like sequence (*ALS3*, $P<0.01$), epithelial adhesin (*EPA1*, $P<0.01$); hyphal wall protein 1 (*HWP1*, $P<0.001$), phospholipase D 1 (*PLD1*, $P<0.001$), secreted aspartyl proteinases 4 and 6 (*SAP4*, $P<0.001$; *SAP6,* $P<0.05$).

Despite the increases in *C. albicans* virulence observed with mixed-species biofilms, mixed-species plus *P. gingivalis* biofilms resulted in a different pattern of gene expression where, when compared to *C. albicans*-only biofilms, there was a significant down regulation of virulence genes including ALS3 ($P<0.01$) and SAP6 ($P<0.001$), and no significant ($P>0.05$) change in expression of EPA1, HWP1 or PLD1. Interestingly, despite levels of expression for many genes being similar between *C. albicans*-only biofilms and mixed-species plus *P. gingivalis*, a significant ($P<0.01$) increase was evident in expression of the SAP4 gene, to a level similar to that observed in mixed-species biofilms.

The pattern of increased gene expression, particularly for those genes involved in the formation of hyphae (*ALS3, ALS3*), correlated with observations by CLSM (Figs. 2.9, 2.10) of *C. albicans*-only and mixed-culture biofilms. Also, the down regulation of the expression of these same genes in mixed-species plus *P. gingivalis* biofilms correlated with a reduction in the number of hyphae when biofilms were analysed by CLSM (Fig. 2.13)).

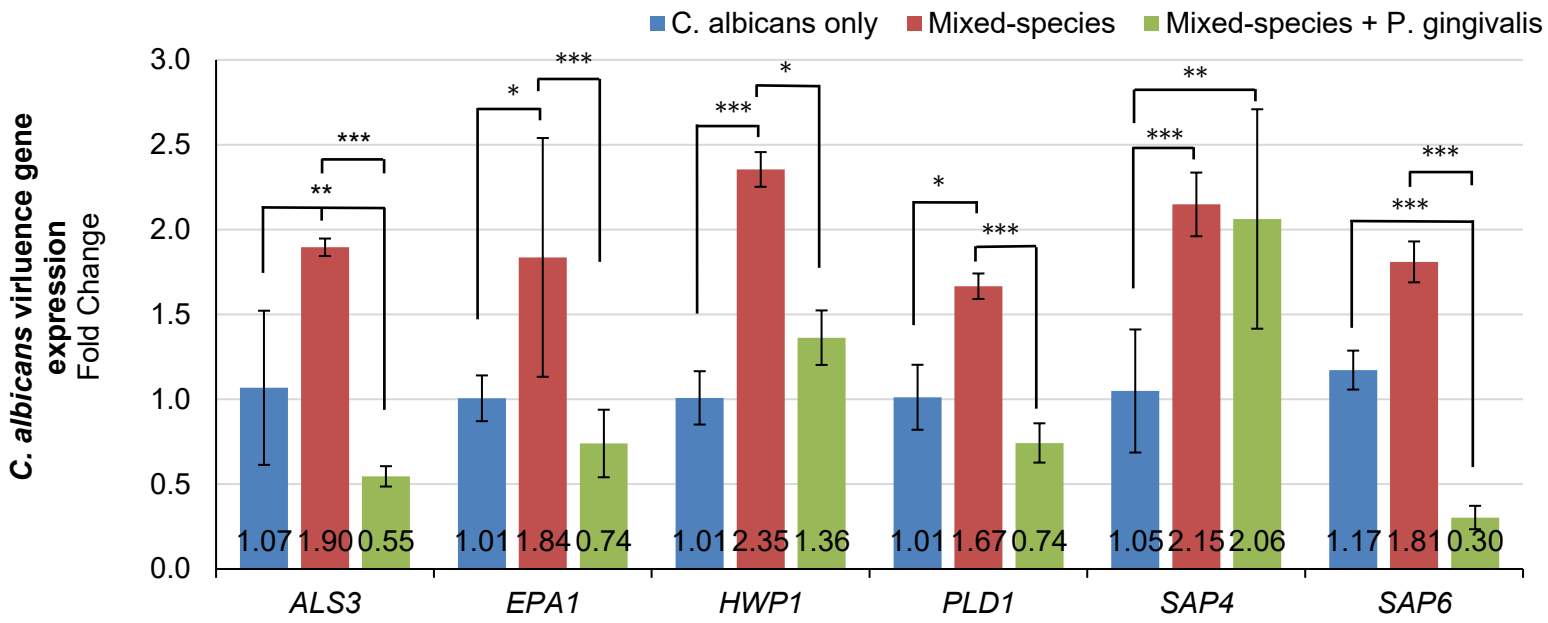

Figure 2.14 Changes in the expression of known putative *C. albicans* virulence genes, relative to the housekeeping gene *ACT1*, and compared with normalised *C. albicans* only biofilm controls.
Fold change in expression of *C. albicans* adhesin (*ALS3*, *EPA1*) genes, hyphal wall protein (*HWP1*) gene, phospholipase D (*PLD1*) gene and secreted aspartyl proteinase (*SAP4*, *SAP6*) genes. Data expressed as mean of 6 replicates, error bars represent SD. Analysis performed by $^{\Delta\Delta}$Ct method. Representative melt curves shown in Appendix I

C. albicans virulence gene	Change in expression, relative to *C. albicans*-only biofilms			
	Mixed-species	Sig.	Mixed-species + *P. gingivalis*	Sig.
ALS3	Increase	P<0.01	Decrease	P<0.01
EPA1	Increase	P<0.01	No change	P>0.05
HWP1	Increase	P<0.001	No change	P>0.05
PLD1	Increase	P<0.05	No change	P>0.05
SAP4	Increase	P<0.001	Increase	P<0.01
SAP6	Increase	P<0.05	Decrease	P<0.001

Table 2.9 Changes in *C. albicans* gene expression of mixed-species and mixed-species plus *P. gingivalis* biofilms relative to expression from *C. albicans*-only biofilms

2.4 Discussion

This research evaluated the effect of oral bacteria on *C. albicans* virulence in *in vitro* denture biofilms. Denture stomatitis (DS) is an inflammatory disease associated with the presence of *Candida*. However, whilst *C. albicans* is considered the primary causative agent of DS, the role of bacteria, which are normally present in denture biofilms, in this infection remains unclear.

Denture biofilms are complex in their microbial composition and physical structure, comprising many different microbial species and a range of extracellular polymeric substances (Chandra *et al*., 2001a). For species to survive, the community needs to communicate and respond to changes, and the ability of microorganisms to modulate the local environment to their benefit is a clear advantage within a biofilm community. Research into interactions between bacterial species, and indeed bacteria and fungi (in the case of this study), on the behaviour of *C. albicans* is important to further our knowledge of biofilm microbiology and associated infections

Specific oral bacteria were selected for this study and these were selected as they are commensal oral microorganisms and also associated with denture biofilms (Campos *et* al., 2008; Dewhirst *et* al., 2010; Jenkinson, 2011). These bacteria included *Streptococcus sanguinis* and *S. gordonii*, *Actinomyces viscosus* and *A. odontolyticus*, facultative anaerobic bacteria commonly associated with the oral cavity, and also specifically the denture surface. The fungus *Candida albicans* ATCC 90028 was used as the representative fungal component of the *in vitro* biofilm in these analyses. *Candida albicans* ATCC 90028 appears to be a hypovirulent strain that does not demonstrate the same extremes of behaviours as other *C. albicans* strains, including *C. albicans* SC5314, which is commonly used in biofilm studies as a wild-type strain. Lu *et al*., (2006) demonstrated this characteristic difference with a direct comparison between both of the aforementioned *C. albicans* strains, and found that ATCC 90028 demonstrated fewer hyphae and less invasion into tissue than SC5314 in an epithelium-only tissue infection model. Therefore, changes in virulence demonstrated in this study were testament to the significant influence of bacterial modulation of the factors.

The study developed an *in vitro* biofilm model comprising five microbial strains, which compared to the biofilms found *in vivo* is still somewhat simplistic, but one that is more representative of denture-associated biofilms than using single or dual-species as commonly utilised. The material used in these investigations to support biofilms is the most commonly used denture-base material namely poly(methyl methacrylate) (PMMA) (Vojdani & Giti, 2015; Singh *et al*., 2011). As saliva is a factor present in the normal oral cavity, and oral prostheses such as dentures are continually exposed to the saliva, its impact on microbial adherence for subsequent biofilm formation was evaluated. The AS formulation used in this study included mucins, proteose peptone and a number of salts, which could influence not only the surface charge of PMMA, but also the physical surface properties. Mucins are large glycoproteins present in normal human saliva (Namavar *et al*., 1998; Tabak *et al*., 1982; Tabak, 1995; Slomiany *et al*., 1996), that play a role in immune defence and contribute to lubrication of the mucosal surfaces. The presence of mucins in the AS formulation makes it more representative of *in vivo* human saliva, but also, from a physical perspective, the mucins can deposit onto the PMMA surface. The highly-charged structure is associated with increased viscosity and adhesiveness (Tabak, 1995), particularly of whole saliva, but mucin deposition onto surfaces has previously been associated with increased microbial adherence by *Streptococcus mutans, S. sanguinis* and by *C. albicans (*Gocke *et al*., 2002; Stinson *et al*., 1982).

A significant increase was observed in adherence of *C. albicans* in the presence of an AS pellicle, whereas no significant differences were observed with the adherence of *S. sanguinis* as the representative oral bacteria. An increase in adherence could be, in part, attributable to the deposition of proteins onto the PMMA surface, where the influence of ligand-receptor binding would override the far weaker non-specific bonding forces such as Van der Waals forces in the adherence of these microorganisms after the 90-min period. Previous studies have also reported varied results for microbial adherence, with reports showing increases in adherence (Edgerton *et al*., 1993), no differences (Jin *et al*., 2004), and even decreases in adherence of

bacteria (Samaranayake *et* al., 1980; Satou *et al*., 1991) to saliva coated surfaces.

Despite the differences in the effect of AS on microbial adherence to PMMA, the formation of mature biofilms was not influenced by the presence of AS preconditioning. Indeed, there were striking similarities between the total enumerated viable recovered cells of both total bacteria and *C. albicans* from single and mixed-species biofilms (Figs. 2.5, 2.8). This was likely due to the composition and complex physical structure of mature biofilms. As biofilms develop in a 3D manner, only the surface-bound cells would be subjected to the adherence forces of the preconditioning pellicle. Additional microorganisms that make up the biofilm, either as a result of cell division of already adhered microorganisms, or by co-aggregation from the planktonic phase of the surrounding environment, would not be in direct contact with the surface or pellicle, and therefore not influenced or restricted by the pellicle constituents. As a result, the majority of the biofilms could develop and grow as free entities, reaching a plateau phase of microbial growth and maximum support. This end-point of the 72 h culture in this study demonstrated this, with similarities between all biofilms in terms of visible growth and enumeration of recovered viable microorganisms from the biofilms.

A number of *C. albicans* virulence factors were investigated in single and mixed-species biofilms developed on PMMA. The virulence factors selected for analysis were based on previous findings from this research group. These factors included genes responsible for adhesins for attachment and adherence, and subsequent biofilm initiation and maturation (*ALS3* and *HWP1*), epithelial cell adhesin (*EPA1*), a key factor for adherence of *C. albicans* to epithelial cells, which, in the case of a DS model is essential for the infection, and a number of hydrolytic enzymes (*PLD1*, *SAP4* and *SAP6*). *ALS3*, *HWP1*, and *SAP4* and *SAP6* genes are also associated primarily with the hyphal morphology of *C. albicans*.

In this study, mature mixed-species biofilms containing *S. sanguinis, S. gordonii, A. viscosus* and *A. odontolyticus* resulted in significant

upregulation of *C. albicans* virulence genes (Fig. 2.14, Table 2.6). An increase of between 1.5 to 2.5-fold change was observed for each gene in mixed-species biofilms, indicating that the presence of bacteria either directly or indirectly, stimulated *C. albicans* to upregulate virulence gene expression.

The induction of hyphae production was also confirmed using confocal scanning laser microscopy (Fig. 2.10) and scanning electron microscopy (Fig. 2.11). Using these approaches many more hyphae were observed in mixed-species biofilms than *C. albicans*-only biofilms. Over a ten-fold increase in the number of hyphae was determined by image analysis that differentiated yeast cells from hyphae. The production of hyphae within the biofilms did not lead to an increase in the number of viable cells when enumerating by recovery of cells from the biofilms. However, hyphae were observed to be integral to the biofilm structure of mixed-species biofilms (Fig. 2.11), indicating the overall biofilm may be stronger structurally.

Streptococcus gordonii has previously been found to adhere to *C. albicans* hyphae, where expression of the ALS3 gene is known to play a critical role (Silverman *et al*., 2010). ALS3 expression is crucial in the development of *C. albicans* biofilms, and so the increase in its expression in this study correlated with this previous finding reported by Silverman *et al*., 2010. Adhesion of bacteria to the hyphae of *C. albicans* was also observed in this study, but it was also evident that the oral bacteria adhered to the PMMA surface, where they would be able to colonise and develop microcolonies, with the potential for additional biofilms of distinct microbial content. However, bacterial binding to hyphae has further implications when, for example, in an environment where the biofilm can cause infection to tissues.

Secreted aspartyl proteinases are expressed during *Candida* hyphal formation (Chen *et al*., 2002), and have also been associated with roles in tissue infection and damage (Silva *et al*., 2011; Alves *et al*., 2014). During investigations in this study, significant upregulation of *SAP4* and *SAP6* genes was observed in mixed-species biofilms (Fig. 2.14), indicating an increase in virulence. When extrapolating to an infection scenario, such a change could potentially lead to

an increase in pathogenicity. Furthermore, the phospholipase D1 gene was upregulated in mixed-species biofilms and this is also associated with yeast to hyphal morphological transition and is considered necessary for virulence (Dolan *et al*., 2004; Hube *et al*., 2001; Baker *et al*., 2002). Phospholipase D1 is more closely associated with tissue infection, as the enzyme is responsible for hydrolysis of phosphatidylcholine, a substantial component of cellular membranes (Baker *et al*., 2002), thus allowing *Candida* invasion into tissues, and a direct cause of cell damage. Additional phospholipases are also attributed to *Candida* virulence and pathogenicity, and required for invasion into tissues, and these include phospholipases B1 and B2, and C1 (Samaranayake *et al*., 2006), coded for by the *PLB1*, *PLB2* and *PLC1,* genes, respectively.

The oral bacteria used in this study are considered to be commensal microorganisms and thought to be primary (*Streptococcus* species) and later-phase (*Actinomyces* species) colonisers of the oral cavity. These bacteria are not typically associated with any specific disease, however, in these *in vitro* investigations, they appeared to modulate the local environment to an extent that *C. albicans* responded at a molecular level, stimulating induction of a range of virulence factors as discussed throughout this chapter. The oral cavity is diverse, and harbours hundreds of different bacterial species, and so to evaluate the differences that other bacteria have on *C. albicans* virulence, another common oral bacterial species was introduced to the mixed-species inoculum. This bacterial species, *P. gingivalis,* and has been implicated in periodontal infection, and is a known pathogen within the oral cavity.

Enhancement of *C. albicans* virulence by the co-existing bacteria in mixed-species biofilms may be contact-dependent or as a result of secreted molecules. The reverse modulation when *P. gingivalis* was included in the biofilms could be attributed to the production of gingipains; proteases secreted by *P. gingivalis* as a virulence trait. The gingipains are multifunctional, activating or degrading a range of host proteins and inhibiting the immune response to lipopolysaccharide (LPS) (Genco *et al*., 1999; Potempa *et al*., 2003; O'Brien-Simpson *et al*., 2003; Abe *et al*., 1998). It is through this

mechanism that gingival infection with *P. gingivalis* can so successfully lead to gingivitis and periodontitis, as the biofilms cannot be efficiently cleared by the host immune system. Gingipains may be modulating *C. albicans* virulence indirectly by either degradation of proteins related to the other bacteria, or a similar mechanism with receptors on the bacterial cell that could induce a response in direct contact with *C. albicans*

Farnesol is a quorum sensing molecule produced by *Candida*, and is known to enhance virulence of oral bacterial species including *S. mutans* (Kim *et al*., 2017). It is possible that the production and accumulation of farnesol is having a similar effect on other oral bacteria, particularly other streptococcal species included in the mixed-species biofilm model. This may have an antagonistic effect, leading to an increase in bacterial responses and an enhancement of virulence, subsequently leading to a further increase of *C. albicans* virulence factors. Furthermore, environmental stimuli play an important role in *C. albicans* virulence. *Streptococcus sanguinis, S. gordonii*, and *C. albicans* can tolerate some extremes such as low pH, which can arise as a result of utilisations of sugars. *C. albicans* has a preference for utilising glucose, whereas streptococci prefer sucrose. The initial breakdown of sucrose by *C. albicans* and streptococci creates glucose and fructose, which are then used by streptococci, resulting in production of acid (McCourtie & Douglas, 1984; Kim *et al*., 2017). In these environments, the extreme conditions act as stimuli, resulting in modified genetic regulation, and the subsequent expression of virulence factors as the microorganisms compete for nutrients, and to create an environment that suits them for their survival.

2.5 Conclusions

- The presence of an artificial saliva pellicle enhanced microbial adherence to the PMMA surface, but did not affect subsequent biofilm formation. The presence of the AS pellicle should remain an integral part of biofilm investigations, ensuring the surface is more closely representative of an *in vivo* scenario than a naked PMMA surface

- The presence of multiple bacterial species in co-culture mixed-species biofilms with *C. albicans* modulated *C. albicans* virulence; enhancing a range of putative virulence factors involved in adhesion, biofilm formation, and the production of hydrolytic enzymes, and substantially increased the formation of hyphae

- The addition of the opportunistic pathogen *P. gingivalis* to the mixed-species biofilm inoculum inhibited the previously observed enhancement of virulence, in some cases reducing the expression of the factors below the levels observed in *C. albicans*-only biofilms

Chapter 3

In vitro 3D oral mucosal tissue model development

3.1 Introduction

Candida are generally considered the main causative agents of denture associated stomatitis (DS). Current clinical treatment strategies where intervention in addition to improvement of general oral and denture hygiene is necessary, are targeted toward this fungal component of the denture biofilm. However, it is becoming increasingly apparent that interactions between *Candida* and bacteria within *in vitro* biofilms occurs and therefore is an important consideration when understanding the infection process (Jack *et al*., 2014; Cavalcanti *et al*., 2015). As demonstrated in Chapter 2, *in vitro* virulence of *C. albicans* can be modulated by the presence of specific bacterial species within mixed-species biofilms, and therefore the role of bacteria in the pathogenesis, and thus prognosis and subsequent management of DS requires further evaluation.

Analysis of pathogenicity would be best represented using *in vivo* animal or human models. These are costly, require substantial ethical consideration, and are becoming less favoured, particularly by funders (such as the National Centre for the Replacement, Refinement and Reduction of Animals in Research (NC3Rs)) who wish to reduce the use of animals for scientific analysis unless absolutely necessary.

Oral mucosal tissue models have been used to undertake investigations including the pathogenicity of microorganisms and associated host cell responses (Silva *et al*., 2009; Silva *et al*., 2011; Yadev *et al*., 2011; Cavalcanti *et al*., 2015). This work is crucial to gaining insight into the complex relationship between host and microbes, particularly biofilm infections, but little work has been applied to biofilms with the aim of evaluating pathogenicity or host responses toward infection, where, in the case of DS, this is essential.

Tissue models are, therefore, valuable tools for a range of *in vitro* analyses. The concept of three-dimensional constructs representing skin were pioneered in the 1970s by Rheinwald & Green who began by successfully culturing keratinocytes *in vitro*, and establishing novel protocols in order to maintain cellular viability. This was then taken forward by O'Connor *et al* (1981), Burke *et al*., (1981), and Cuono *et* al., (1986) who prepared autologous epithelium and dermal allografts for grafting onto burns patients, with great success during the observational period of approximately 8 months or more. Later work included the further development of models to incorporate different cell types, particularly fibroblasts, and understand the pivotal role they play in revascularisation and repair/remodelling (Dermanchez *et al*., 1992). From this concept, a range of commercial models were developed. Many of these models incorporate a scaffold or dressing; either bovine collagen (Integra™, Apligraf™, OrCel™, Varkey *et al*., 2015) or acellular dermal scaffold, and are seeded with autologous cells in order graft onto patients with various needs. Some models include a mixture of cell types; epithelial cells and fibroblasts (Tiscover™, Permaderm™, denovoSkin™, Varkey *et al*., 2015).

Several different types of 3D tissue constructs are commercially available, including those representing dermal (as reviewed by Varkey *et* al., 2015), vaginal, lung (Braian *et al*., 2015), corneal (Yang *et al*., 2015; Ghezzi *et al*., 2017), and of interest in this project, oral tissues. In particular, this study focuses on the palatal mucosa, where two different types of tissue models are available; a keratinocyte-only tissue model (SkinEthic™ RHOE, EpiSkin, Lyon, France), representing the oral epithelium, and a full-thickness tissue model (EpiOral FT, MatTek Corporation, Ashland, MA, USA); more closely representing human oral mucosa, comprising a *lamina propria* overlaid with an epithelium.

Commercially available constructs are popular within research, but have some limitations. Keratinocyte-only models are comparatively simplistic, containing the epithelial layer developed using a cancer-derived cell line; TR146, originally isolated from a buccal squamous cell carcinoma, which is cultured at the air-liquid interface for 5 days. A 3D structure develops with maturation of the TR146 cells and culture in a 3D manner, but full differentiation is typically absent with these cells under these conditions (Nor *et al*., 2016). These tissue models have been used in numerous studies of microbial infection, particularly for investigations into furthering understanding of virulence and/or pathogenesis related to candidosis (Yadev *et al*., 2011; Alves *et al*., 2014; Silva *et* al., 2009; Silva *et al*., 2011; Jayatilake *et al*., 2005). The responses of these tissues may be somewhat limited relative to other tissue models that incorporate additional cells such as fibroblasts, as found in full thickness tissue models. However, as the first line of defence, the epithelial cells produce a wide array of proinflammatory cytokines to attract and engage immune cells (Waelti *et al*., 1992; Jayatilake *et al*., 2005), which are possible to detect in the supernatant of the cell culture. Detection and quantification of the cytokines depends on the type and duration of the infection, as it takes some time for the cytokines to accumulate in the supernatant to a level that is detectable with typical methods of analysis like enzyme linked immunosorbent assays (ELISAs). This is particularly important when trying to identify differences between infection types.

There are also advantages and disadvantages of the full thickness tissue model. The full thickness tissues (EpiOral) comprise both a *lamina propria;* a fibroblast populated collagen matrix, and an epithelium. A significant advantage of this tissue model is that the presence of both cell types will allow for cell-to-cell communication in the form of cytokines and chemokines. This crosstalk between the cell types is vital for normal immune responses and function, and should therefore ensure the responses of the cells are more representative of normal oral mucosa, as a result of the feedback mechanism the cytokines play on stimulating other cytokines or chemokines (Galley & Webster, 1996; Dinarello, 2000). The primary responses by epithelial cells occurs in the form of interleukin-1α (IL-1α) IL-1β, IL-8 and IL-18, some of which are also shared with fibroblast cells, including IL-18 (Dongari-Bagtzoglou & Ebersole, 1996) and IL-6. Fibroblast cells, importantly, are substantial producers of IL-6, also a proinflammatory cytokine, which occurs in response to stimuli including a number of interleukins. This increased production of IL-6 further stimulates epithelial-associated interleukins in a positive feedback mechanism, driving inflammation (Ansel *et al*., 1990; McKenzie & Sauder, 1990; Netea *et al*., 2006). Furthermore, the cells used in the model are normal primary oral cells, and so expected to more closely represent normal mucosa when cultured than the cancer-derived cell lines. The epithelium is typically well structured and layered, and some keratinisation present, further adding to the defence of the tissue from potential infection. The primary disadvantage is cost of the tissues. For the minimum quantity of tissues (24), the batch cost is approximately $4,000, plus transport and import costs. This is a major limitation for many research laboratories, where consumable budgets are very modest relative to this.

All commercially available tissue models are considered ‘static’, in that no modification of the tissue can be performed post-culture. There is scope to further develop these tissue models to incorporate additional cell types, such as immune cells. There are clear advantages of adding additional cell types, primarily in the ability to evaluate the call for an immune response to infections,

and the ability to monitor migration of immune cells through the tissue model in response to stimuli. Furthermore, the lifespan of these tissue constructs is limited to just a few days after receipt, due to cornification of the models, and rapid loss of cell viability. It is important, therefore, to be aware of the physical limitations of working with a large number of tissue models, where additional time for actual use may be necessary, but not available.

The tissue models are reproducible and consistent between batches, but very expensive, which can be prohibitive in many cases to the quantity of infections that can be evaluated.

In order to overcome the restrictions of the tissue models imposed by the financial, and 'static' nature of the models, the primary aims of this study were to establish and optimise an *in vitro* alternative to commercially available constructs. Specifically:

- Develop and optimise culture conditions for an alternative to SkinEthic™ RHOE, using TR146 keratinocytes.

- Establish a full-thickness oral mucosal tissue model;
    - develop and optimise a *lamina propria*, by varying levels of collagen and seeding number of cells
    - comparing the use of TR146 cancer-derived cells with normal oral-derived cells in the culture of the model, as an alternative to EpiOral FT.

3.2 Materials and methods

3.2.1 Cell types and culture conditions

A range of cells were used for this study and the details of each cell type and origin are presented in Table 3.1.

Cell name	Cell type	Source/details
TR146	Keratinocyte	Buccal squamous cell carcinoma (Rupniak *et al*., 1985)
HCA-2	Fibroblast	Neonatal dermal fibroblasts (foreskin) (Wyllie *et al*., 2000)
3T3	Fibroblast	Mouse embryonic (Todaro & Green, 1962)
FNB6	Keratinocyte	hTERT immortalized normal oral keratinocytes (McGregor *et al*., 2002)
NOF806	Fibroblast	Normal oral fibroblasts (Colley *et al*., 2011)

Table 3.1 Overview of cell types used in this research
Details of the cell name, type and source or description of cell origin

Normal oral fibroblasts (NOF806) were kindly provided by Dr Helen Colley, University of Sheffield. All tissues were collected with written, informed consent (ethical approval was granted by the University of Sheffield Ethics Committee ref: 3463) and processed according to Colley *et al*., (2011).

Normal oral fibroblast cells, hTert immortalised HCA-2 fibroblasts, and FNB6 and TR146 keratinocyte cells were cultured and maintained in Dulbecco's Modified Eagle Medium (DMEM; Life Technologies, UK) supplemented with 10% (v/v) foetal bovine serum (FBS), 4.5 g/L glucose, and 2 mM L-glutamine; this medium was changed every 2-3 d of incubation. Each cell type was split at approximately 85-90% confluence (approximately 4-7 d). To provide suitable culture conditions for FNB6 keratinocytes, γ-irradiated mouse 3T3 fibroblast cells were also co-seeded at a density of approximately 400,000 cells per flask as feeder cells, and 3T3 and FNB6 cells were co-cultured as described above. The incubation parameters for all cells were 37°C, 5% (v/v) CO_2 with high humidity.

3.2.2 Type I collagen extraction

Type I collagen extraction from the tails of euthanised rats was performed at the University of Sheffield (during a research secondment by the candidate). Briefly, rat tails were surgically removed and stored at -20°C until sufficient numbers were obtained for batch collagen extraction. The rat tails were broken in sections by hand, twisted to break the skin and then gently pulled apart to reveal collagen strands. These strands were cut using a scalpel and placed in 500 ml of sterile PBS. The collagen strands were washed thoroughly by mixing the container by hand. The PBS was removed and the collagen was dissolved in 1 L of 0.1 M acetic acid. The collagen solution was then mixed at 4°C for approximately 2 weeks. Once sufficiently dissolved (where no visible aggregates remained), the collagen mixture was freeze dried in 150 ml aliquots. The dried collagen was weighed and stored at -20°C prior to dissolving in 0.1 M acetic acid at a final concentration of 5 mg/ml for approximately 1 week prior to use in tissue models.

3.2.3 Development of an in vitro keratinocyte-only oral mucosal tissue model

The development of an *in vitro* keratinocyte-only model was performed as detailed below and outlined in Fig. 3.1

3.2.3.1 Cell preparation and seeding

To obtain keratinocyte cells for 3D culture, the culture medium was removed from the flasks and adhered cells washed (×1) with sterile PBS. The PBS was aspirated and 3 ml of 0.25% trypsin-EDTA (Life Technologies) added to detach the cells. The flasks were incubated at 37°C for 5 min for enzymatic detachment of cells. A 10-ml volume of culture medium was added to the detached cells to dilute the enzyme in solution, thus reducing activity to negligible levels. The cell suspension was aseptically transferred to a sterile universal and the cells were pelleted by centrifugation at 330 × *g* for 5 min (Durafuge 200 Precision, Thermo Scientific). The medium was carefully removed by decanting to a waste container, and the remaining pelleted cells

were agitated gently by flicking the universal to suspend. The cells were suspended in 5 ml of Dulbecco's Modified Eagle Medium supplemented with Ham's F12 medium (DMEM/F12, Life Technologies), then gently mixed to ensure homogeneity and a 10 μl sample of cells counted using a haemocytometer.

The cells were resuspended at twice the required seeding density, ranging from 2×10^5 to 2×10^6 cells/ml. Free standing cell culture inserts (PIHP01250, Merck Millipore) were aseptically placed in a sterile 12-well plate, and 500 μl of the suspended keratinocyte cells added to the inside of the insert. One ml of DMEM/F12 (supplemented with 10% (v/v) of FBS and keratinocyte culture supplements (detailed in Table 3.2)) was added to the outside of the inserts, and the well plate was incubated for 24 h at 37°C in 5% (v/v) CO_2.

Component	**Final in-use volume/concentration**	**Supplier**
DMEM/F12	450 ml	Life Technologies
FBS	50 ml	Life Technologies
Penicillin	100 U/ml	Life Technologies
Streptomycin	100 U/ml	Life Technologies
Human epidermal growth factor	10 ng/ml	R&D Systems (Abingdon, UK)
Cholera toxin	1.8×10^4 U/ml	Sigma
Insulin	0.5 μg/ml	Sigma
Adenine	5 μg/ml	Sigma

Table 3.2 Composition of DMEM culture medium with added culture supplements for keratinocyte-only tissue model development

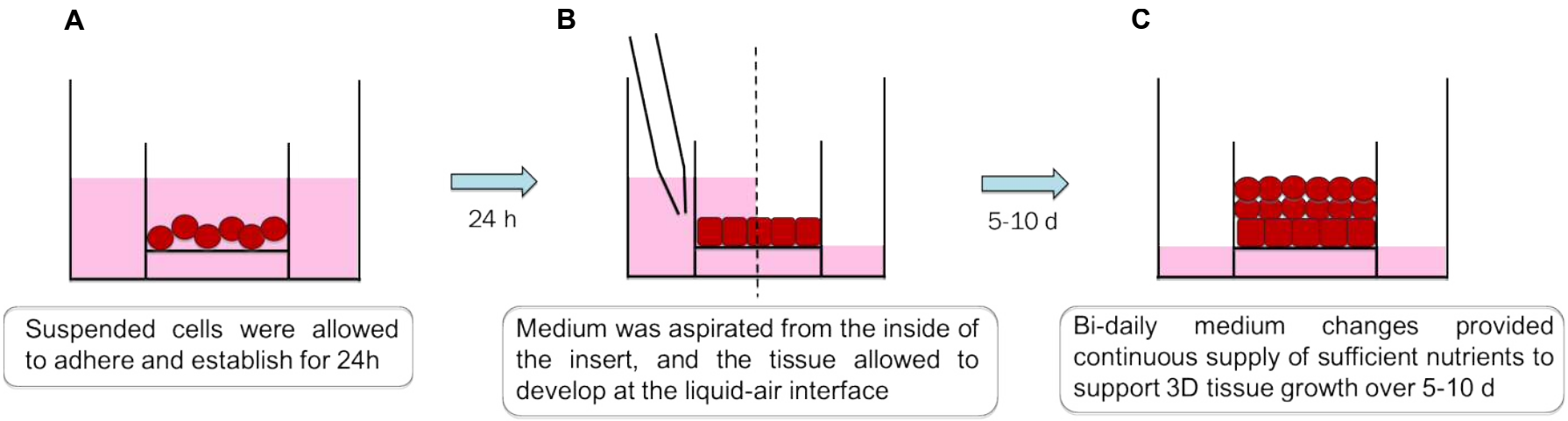

Figure 3.1 Diagrammatic representation of the stages of *in vitro* keratinocyte-only tissue model culture
A) Establishment of monolayer, then **B)** raised to air-liquid interface. Cultures were maintained through **C)** maturation and 3D culture, resulting in a multi-layered tissue structure.

3.2.3.2 Establishing air-liquid interface and tissue model maintenance

Once the cells were established on the insert membrane (after approximately 24 h), the used culture medium was aspirated from inside the cell culture insert, and from the well. Six hundred µl of fresh DMEM/F12 culture medium was added to the well, ensuring the surface of the medium was in contact with the cell culture insert, but not above the level of the cells. It was important to maintain an air-liquid interface (ALI) for the cells, to allow stratification. The well plate was returned to the incubator and the culture medium replaced every other day, for a total culture period of 5-10 d.

3.2.4 Development of a full thickness in vitro oral mucosal tissue model

The full thickness oral mucosal tissue model was cultured in three distinct stages. Establishment of the lamina propria (fibroblast cell-populated collagen matrix), seeding of the keratinocytes, and maintenance of the tissue model culture at the ALI. A diagrammatic representation outlining the method is shown in Fig. 3.2.

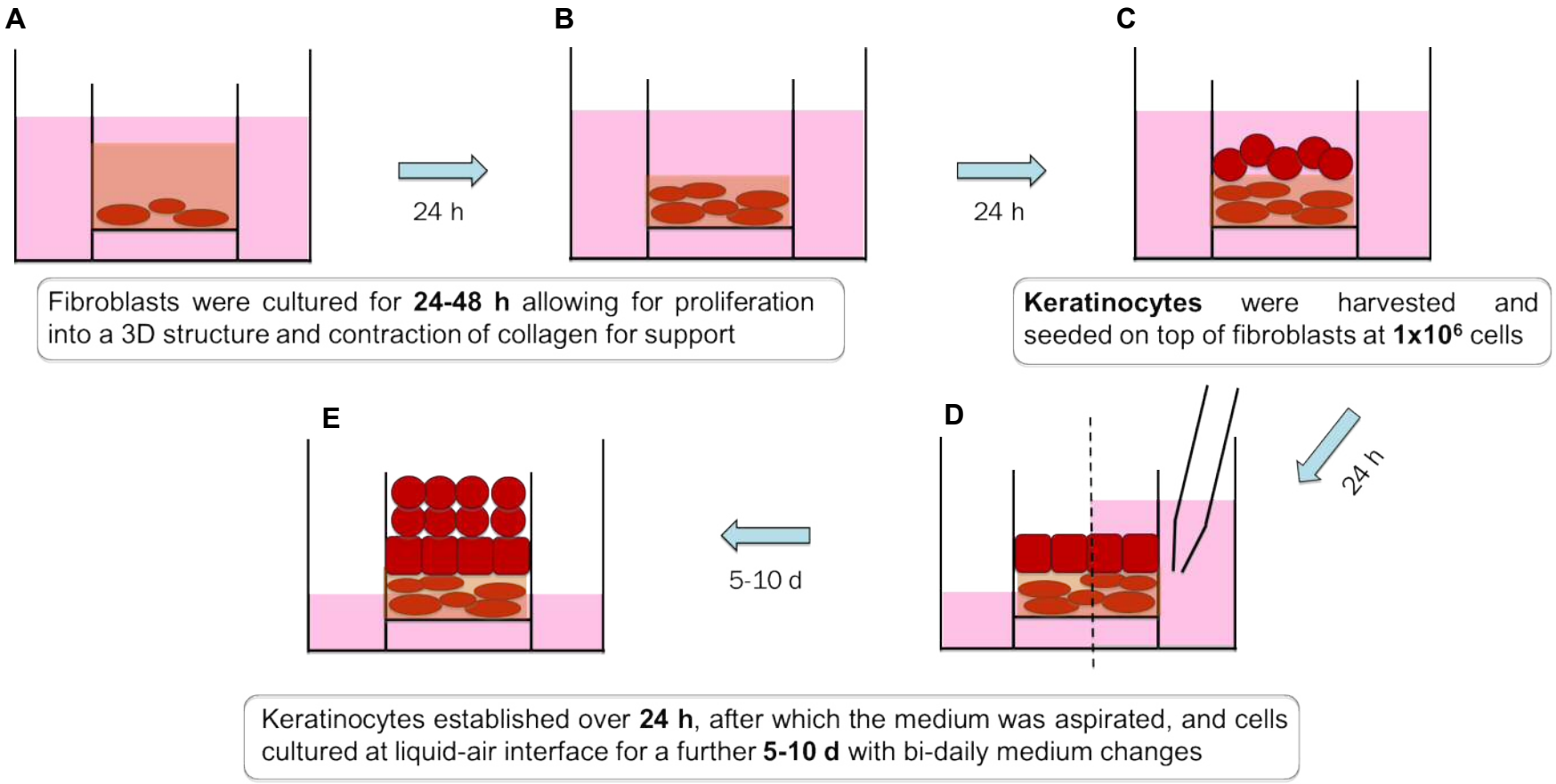

Figure 3.2 Diagrammatic representation of the stages of *in vitro* full-thickness tissue model culture
A) Fibroblasts in collagen matrix added to cell culture insert, and allowed to set, then **B)** collagen contracted, after which **C)** keratinocyte cells were added and allowed to establish a monolayer. **D)** The cultures were brought to air-liquid interface and **E)** maintained to culture into a 3D tissue structure

3.2.4.1 Establishment of the lamina propria

A collagen mixture was prepared on ice in a 30 ml falcon tube, and this mixture contained the following (sufficient volume for 10 tissue models): 1 ml of 10 × DMEM (D5648, containing 4.5 g/L of glucose, 2 mM of L-glutamine, Sigma), 1 ml of reconstitution buffer (comprising 0.02 M of HEPES buffer, 0.062 M of sodium hydroxide), 0.83 ml of FBS, and 6.73 ml of 5 mg/ml collagen. The solution was mixed gently but thoroughly by hand, avoiding the formation of bubbles within the mixture. Due to the acidity of the collagen solution, a bright yellow colour was formed. The pH was adjusted to pH 7 using 1 M sodium hydroxide with gentle mixing by hand between addition. The colour of the solution changed to red, and was re-adjusted to approximately pH 7 after 10 min once the mixture equilibrated.

The fibroblast cells were detached from the T75 flasks as described in section 3.2.3.1, and resuspended to a final cell seeding density of 6.25×10^6 cells/ml in a volume of 800 µl (equivalent to 2.5×10^5 cells per 40 µl cell suspension). The high cell density was necessary to avoid introducing excess medium into the collagen solution, and thus influencing the final pH.

Hanging cell culture inserts (PIHP15R48, Merck Millipore; 0.4 µm pore size, PET membrane) were aseptically placed into each well of a 12-well plate using sterilised forceps. The suspended fibroblast cells were then added to the collagen mixture, and mixed gently by hand. Immediately after mixing, 1 ml of collagen/cell mixture was added to each insert. The inserts and collagen were transferred to an incubator (parameters as above) for 60 min to allow the collagen mixture to solidify. Once suitably solidified, 500µl of DMEM Green's medium (as detailed in table 3.3) was added to the insert, and 2 ml to the well outside of the insert. The plates were returned to the incubator and incubated for approximately 44 – 48 h.

Component	Final in-use volume/concentration	Supplier
DMEM/F12	450 ml	Life Technologies
FBS	50 ml	Life Technologies
Penicillin	100 U/ml	Life Technologies
Streptomycin	100 U/ml	Life Technologies
Adenine	0.025 pg/ml	Sigma
3,3,5-tri-iodothyronine	1.36 ng/ml	Sigma
Apo-transferrin	5 μg/ml	Sigma
Human epidermal growth factor	5 ng/ml	R&D Systems (Abingdon, UK)
Cholera toxin	8.47 ng/ml	Sigma
Insulin	5 μg/ml	Sigma

Table 3.3 Composition of DMEM Green's culture medium for full thickness tissue model development

3.2.4.2 Keratinocyte seeding and establishment of epithelial layer

FNB6 or TR146 keratinocyte cells were detached from the culture flasks with 3 ml of 0.25% (w/v) trypsin-EDTA as described in section 3.2.3.1. The cells were washed, pelleted and resuspended to 5×10^5 cells/ml in DMEM Green's medium, and 500 µl of the cell suspension added to each insert. The medium on the outside of the well was replaced with 2 ml fresh DMEM Green's medium. The plates were returned to the incubator for a further 48 h, after which, significant contraction of the collagen was evident (Fig. 3.2b).

3.2.4.3 Establishing the air-liquid interface to initiate tissue maturation in a 3D manner and stratification

After 48 h culture, the tissue models were removed from the incubator, and the liquid medium aspirated from inside the insert and wells. Fresh DMEM Green's medium was added only to the well for the remainder of the tissue model culture. The volume used was sufficient to allow feeding of the cells from below, but was small enough to allow an air-liquid interface of the keratinocyte cells on the outermost section of the tissue model. The tissue model was

maintained at the ALI for a further 14 d with culture medium replenished every other day

Prior to infection, the final medium change (2 d before use) used culture medium devoid of antimicrobial compounds (penicillin or streptomycin).

3.2.5 Tissue processing and preparation for analysis

Tissues were processed overnight using a Leica ASP300S processor, prior to paraffin wax embedding using Leica EG115OH embedding equipment. The processing protocol was as follows: dehydration in ethanol (90% (v/v) for 1 h, 95% (v/v) for 1 h, absolute for 4 × 1 h), immersion in xylene (3 × 1 h), and embedded in paraffin wax for 1 h, 1.5 h, and 2 h. The tissues were transferred to a paraffin wax container in a Leica EG115OH embedder. To section transversely, each tissue was orientated on the sectioned edge, then submersed in paraffin wax, which was allowed to solidify. The samples were trimmed and sectioned at 5 μm thickness using a rotary microtome (Thermo Shandon Finesse ME +, Thermo Scientific). The sections were attached to Thermo Colorfrost Plus microscope slides (Thermo Scientific), and heated at 60 °C for at least 1 h to ensure strong attachment to the slides

3.2.6 Histological staining

The sections were stained with haematoxylin and eosin using automated staining equipment (Thermo GLX Linistainer, Thermo Scientific). Briefly, the sections were dewaxed in a series of xylene baths (×4, decreasing concentrations), dehydrated in alcohol (×2, increasing concentrations), then rinsed with tap water and stained with haematoxylin (×5, VFM Harris Haematoxylin (Acidified), CellPath Newtown, UK). The samples were then rinsed with tap water, and subjected to acid alcohol rinse (5% (v/v) acetic acid in 70% (v/v) ethanol), and rinsed again with tap water. The blue colouration (nuclei) was enhanced by rinsing in Scott's tap water substitution, followed by a further rinse using tap water and then counterstained with Shandon aqueous eosin (Thermo Scientific). Finally, the sections were dehydrated through a

series of alcohol baths (×3), then xylene (×2) and stored in xylene until they were covered with a glass coverslip using DPX (CellPath)..

3.2.7 Observational analysis of tissue models

Analyses for the tissue models were primarily observational, which includes visual analysis by microscopy of sections for the different cultured tissue models to evaluate a number of parameters: tissue depth, morphology of cells, maturation and establishment of layers of cells, and keratinisation.

3.2.7.1 Keratinocyte-only tissue model analysis

Sections of keratinocyte-only tissue models were evaluated visually, to determine relative tissue depth by number of layered cells in the epithelium, and cellular morphology. The morphology TR146 cells in continued culture in culture flasks was determined to be the typical cell morphology. This morphology was then compared with the morphology of the cells within the 3D constructs, to determine whether culture in the 3D manner influenced morphology.

The typical morphology for TR146 in flasks was described as polygonal in shape, with a distinct large nucleus.

3.2.7.2 Full-thickness tissue model analysis

As the full-thickness tissues comprised 2 distinct sections, each were considered when analysing development of the structures.

The *lamina propria* contained fibroblasts, which were compared with typical fibroblast cells, and their characteristics when cultured in culture flasks. Fibroblasts grow as elongated cells, with a central nucleus, and fibrous spindle-like characteristics outwards from the centre.

Epithelial cell morphology was also evaluated visually, similar to that described in section 3.2.7.1. FNB6 keratinocytes have similar cell morphology to TR146 when cultured in culture flasks; polygonal shape with large distinct nucleus

typically around the centre of the cell. Maturation of cells that behave normally when cultured at the ALI should show a transition from ‘block’ like cells at the innermost layer, becoming more spherical to the outermost layer, where they begin to keratinise. Tissue models were compared to the typical morphology of cells in a biopsy of normal palatal mucosa to determine whether cells follow the anticipated maturation pathway.

3.3 Results

3.3.1 Commercially available epithelial tissue model

The SkinEthic™ RHOE tissue model (EpiSkin, Lyon, France) comprised of multi-layered epithelial cells (TR146 cell line; originally isolated from a squamous cell carcinoma of the buccal mucosa) cultured in a well plate culture insert, which had a porous polycarbonate membrane of 10 mm in diameter, with 4 μm-sized pores.

A number of models from each batch undergo quality control checks prior to dispatch from the manufacturer, which ensures consistency. The requirements for the tissues to successfully 'pass' quality tests are for the tissue depth to be greater than 4 cells, and to exceed a baseline cell viability level assessed by a 3-(4,5-dimethylthiazol-2-yl)-2,5-diphenyltetrazolium bromide, MTT assay. The tissue models are also checked for bacterial, fungal and viral contamination. Each batch of tissue models received met these criteria.

A number of batches of the commercial tissue models were received, and varied in tissue depth across the membrane of individual models, with most areas thicker than the 4 cells as specified in the quality control specifications. There were some areas that were just 4 cells thick and other regions that did appear thinner than the specified minimum. Overall, when considered as a whole, the tissues did exceed the minimum average cell depth as specified by the manufacturer. The structure of the model differed slightly from the quality control image provided in terms of cellular morphology, as the cell-to-cell junctions were less defined in the slides observed after receipt and processing at the University.

No keratinisation of the epithelium was evident microscopically (Fig. 3.4A). Furthermore, there was no distinct maturation or stratification of the cells throughout the 3D epithelium as would be expected with normal keratinocytes. The morphology of the cells through the layers was consistent. The lack of differentiation of the cells was anticipated as the cells

were originally derived from a cancer, and these typically do not mature or differentiate as normal cells would.

3.3.2 *In vitro* development of epithelial tissue model

3.3.2.1 Effect of cell seeding density on tissue model development

The manufacturer, EpiSkin, states that the SkinEthic™ RHOE tissue model is cultured for 5 d at the air-liquid interface (ALI), however further information is considered proprietary by the company, and as such, not publically available. Therefore, for *in* vitro tissue model development, a range of initial cell seeding densities were evaluated from 1×10^5, 2×10^5, 5×10^5 and 1×10^6 cells total. These were seeded into a cell culture insert of similar surface area as the SkinEthic™ RHOE tissue model (10 mm^2).

At lower cell seeding densities of 1×10^5 and 2×10^5 total cells, the keratinocytes that attached to the membrane were too few to establish a confluent single layer, and subsequently did not develop into a 3D structure to be considered a tissue model, despite the culture period of 5-10 d (Fig. 3.3).

At higher seeding densities of 5×10^5 and 1×10^6 total cells, sufficient numbers of cells attached to the membrane, and when cultured at the ALI, developed into a 3D structure (Fig. 3.4). There was a clear difference in the observed tissue depth (number of layers of cells) (Figs. 3.4a, 3.4c) with the higher seeding density of 1×10^6 cells providing the thickest tissue model at the end of the 5-d culture period. The depth of tissue observed appeared consistent across the membrane for each model cultured, but did show some variation between models.

3.3.2.2 Effect of culture period on tissue model development

Two culture periods for the *in vitro* models were evaluated by light microscopy. This assessment was based on the number of layers of cells of the models, and consistency across the membrane for each model evaluated. At the lower seeding density of 5×10^5 total cells, an increase in

the number of cell layers, and tissue model depth occurred between 5 and 10 days of culture (Figs. 3.4b, 3.4c). This was in contrast to the models seeded with 1×10^6 total cells, where no increase in the number of cell layers (and thus, depth of tissue model) was observed between 5-10 d culture (Figs. 3.4d, 3.4e)..

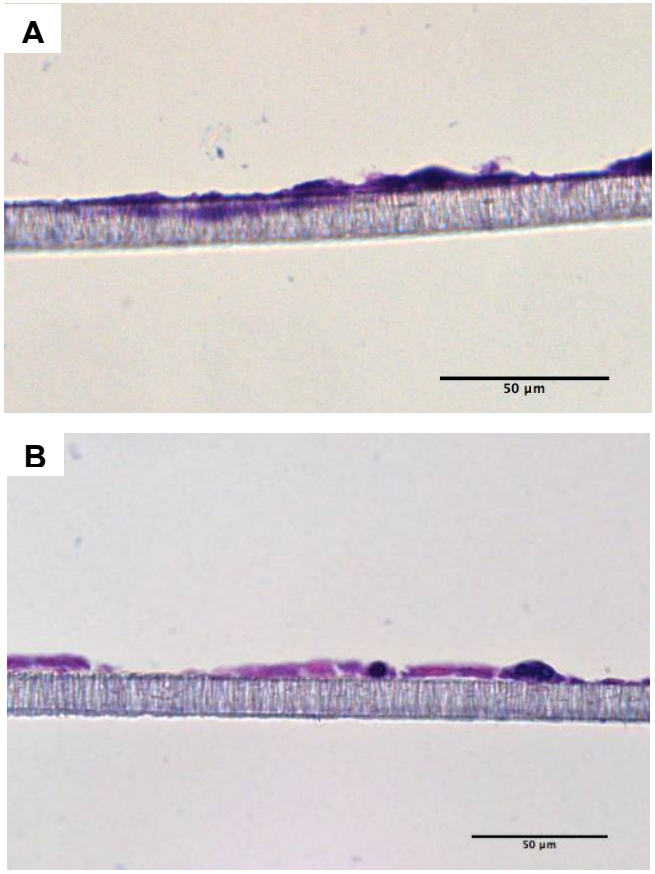

Figure 3.3 Lower keratinocyte cell seeding densities (2×10^5 cells) did not result in a stratified epithelium, irrespective of culture period
A) 5d culture, 2×10^5 cells, **B)** 10d culture, 2×10^5 cells. Sections stained with haematoxylin and eosin. Scale bar represents 50µm.

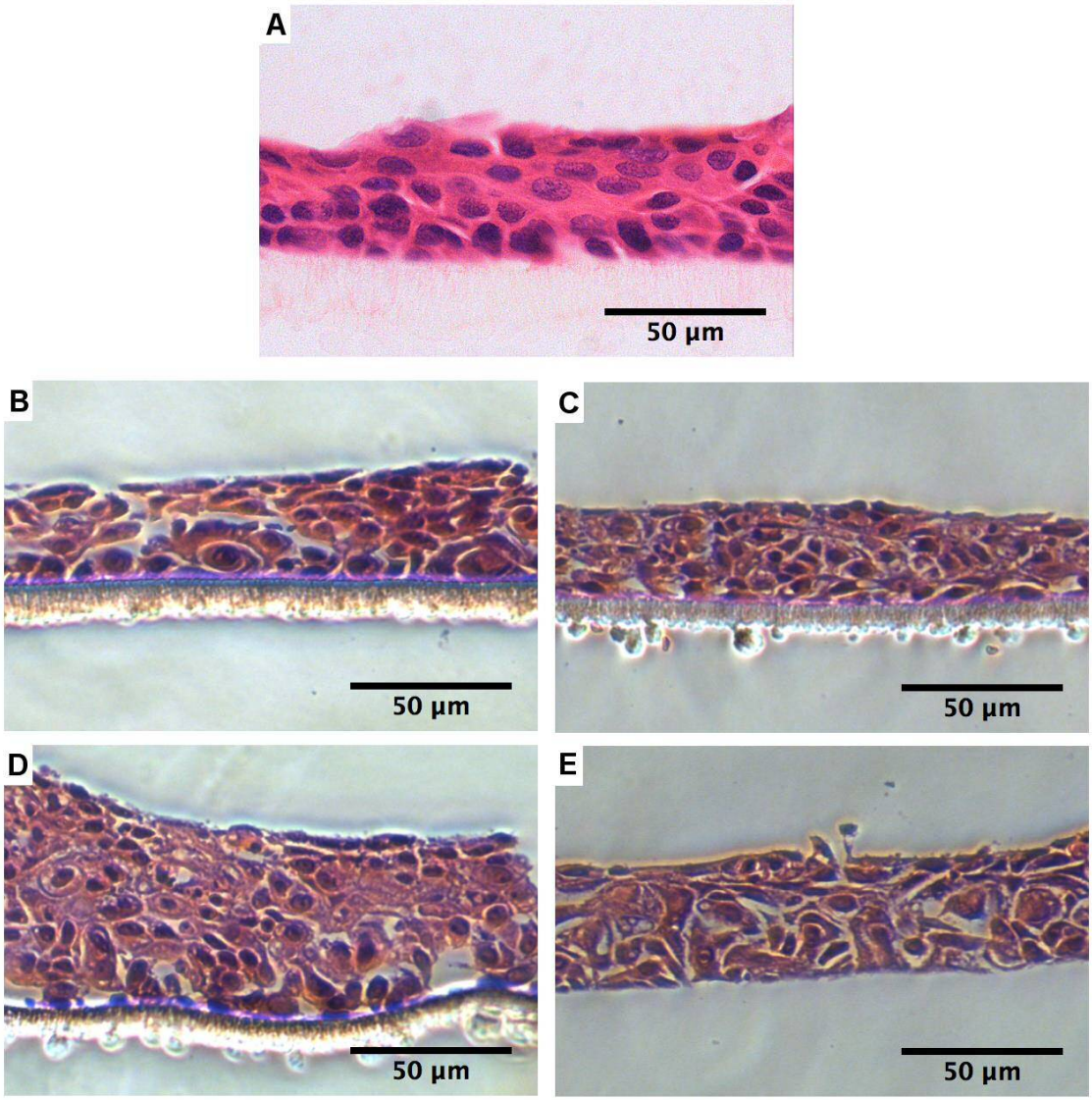

Figure 3.4. Effect of initial cell-seeding density and culture periods on final 3D epithelial tissue model thickness and structure.
Light microscopy images demonstrating the effect of varying cell seeding density and culture periods on epithelial tissue model thickness, cell morphology and tissue structure. **A**) SkinEthic™ RHOE, **B)** 5 d culture, 5×10^5 cells, **C)** 10 d culture, 5×10^5 cells, **D)** 5 d culture, 1×10^6 cells, **E)** 10 d culture, 1×10^6 cells. Stained with haematoxylin and eosin.

3.3.3 Development of full thickness tissue models

3.3.3.1 MatTek models as 'gold standard'

A range of 3D tissue models are available from MatTek Corporation, including the EpiOral™ models or oral mucosa. These 'full thickness' tissue models comprise a *lamina propria* of fibroblasts in a collagen matrix, overlaid with a stratified and slightly keratinised epithelium.

The fibroblast cells in the *lamina propria* showed typical morphology with 'spindle-like' cells sparsely populating the collagen matrix (Fig. 3.7). Good 3D culture and maturation of the epithelial cells was evident, with 'block' like cells making up the *stratum basale*, and the outermost cell layers more representative of keratinised epithelial cells, but somewhat limited in quantity. The maturation process was evident in the layers of keratinocytes in the model, with changes in cellular morphology evident from the *stratum basale* to the *stratum corneum*.

Histologically, the depth of the epithelial layer was relatively consistent across the model. Toward the edges of the insert (closest proximity to the cell culture insert wall), the depth of both the collagen matrix and the epithelial tissue noticeably decreased, to an extent where there were no cells or matrix evident. Although, this was not a sudden change, the depth tapered off, beginning far from the centre of the tissue model.

3.3.3.2 Establishment of lamina propria

A commercially available collagen solution (Bornstein and Traub Type I, extracted from rat tails, pepsinised extraction method, Sigma) was initially evaluated to develop a method or establishing a *lamina propria* of fibroblast cells contained within a collagen matrix. The concentration of the collagen within the solution varied between batches, but was 3.76 mg/ml for these experiments. The collagen was dissolved in acetic acid, and thus was required to be diluted, and pH adjusted by addition of 1 M sodium hydroxide prior to use, to avoid immediately killing the cells. Two final collagen concentrations were evaluated; 1.88 mg/ml and 0.94 mg/ml (1:1 and 1:3 dilution of the collagen solution, respectively).

The concentration of the collagen solution used in this study was not suitable for establishing a scaffold in which the fibroblast cells could embed for structural support of a 3D tissue model. Figure 3.5 illustrates the effect of cell seeding density and culture period on establishment of the fibroblast cells in a 3D structure. A clear pattern was evident concerning the cell

seeding density with increased cell seeding density resulting in a histologically thicker model with an increase in the number of cell layers. Furthermore, increasing the culture period from 24 h to 48 h, irrespective of the concentration of collagen used, resulted in better establishment of the cells in the collagen matrix, which appeared more fibroblast-like in morphology, with elongating filaments.

At the lower seeding density of 2×10^5 cells, few cells were observed on the membrane after 24 h culture, whereas more cells were observed after 48 h culture, and these exhibited better layering and cell morphology. At the cell seeding density of 5×10^5 cells, a similar pattern was observed, but more cell layers were evident after 24 h, and more layers were formed after 48 h culture. The highest cell seeding density of 1×10^6 cells yielded the greatest number of cell layers, with little difference between 24 h and 48 h culture. Morphologically, the cells after 48 h culture were fibroblast-like, whereas after 24 h culture, they were poorly established and did not have a typical fibroblast phenotype.

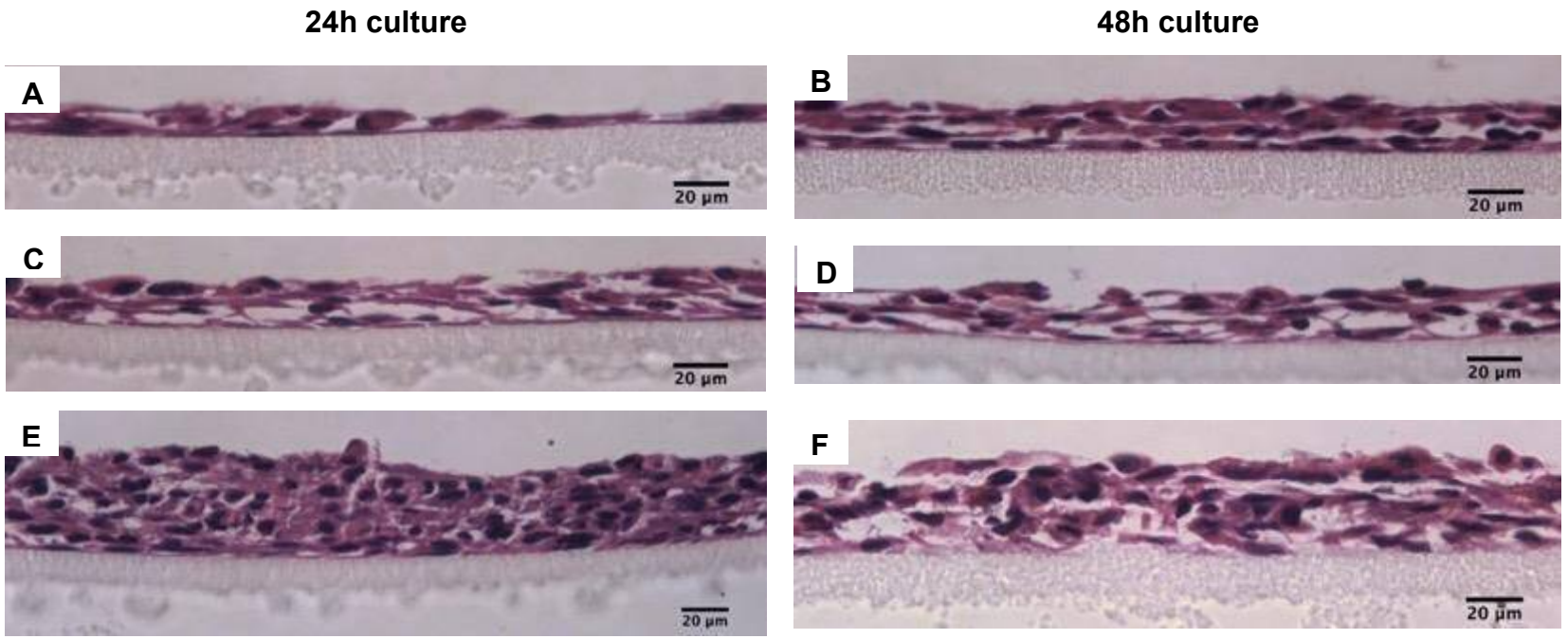

Figure 3.5 Effect of varying cell seeding density and culture period on establishment of a *lamina propria* layer.
Light microscopy images of HCA-2 fibroblasts in a collagen matrix (0.88 mg/ml). Cell seeding density **A+B)** 2×10^5 total cells, **C+D)** 5×10^5 total cells, **E+F)** 1×10^6 total cells. The depth of the layer and cell morphology was dependent upon both culture period and cell seeding density. Increased thickness was observed with a higher cell seeding density, but no difference between 24-48 h culture periods.
Sections stained with haematoxylin and eosin. Scale bar represents 20 μ.

Building upon the evaluation of cell seeding density, and using the highest cell seeding density of 1×10^6 cells, the effect of varying the collagen concentration was investigated. The purpose of the collagen matrix was to provide a scaffold for fibroblasts to establish, on which, keratinocytes could be overlaid, and subsequent adherence to the collagen matrix could be established. Figure 3.6 demonstrates the effect of doubling the collagen concentration from 1.88 mg/ml to 0.94 mg/ml final concentration, which resulted in no clear visible differences in terms of *lamina propria* thickness; there was however an apparent effect on cellular morphology and definition of the layer. The cells seeded into the higher concentration of 1.88 mg/ml collagen appeared histologically more structured, with a more defined outer layer at the ALI. There were little differences between 24 h and 48 h culture periods for this collagen concentration, but the surface definition persisted after 48 h culture. Additionally, no differences in the thickness of the layer was evident when comparing the collagen concentrations, and no contraction of the collagen layer was evident at any seeding density, nor culture period.

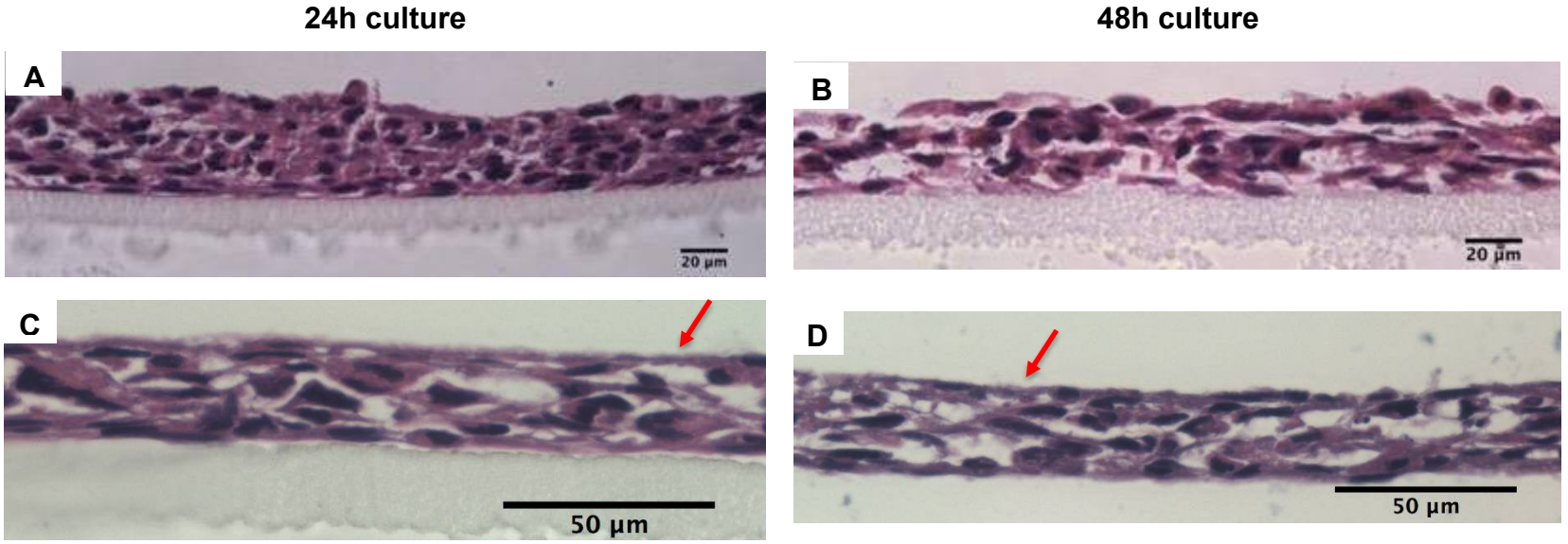

Figure 3.6 Effect of varying collagen concentration for production of an *in vitro lamina propria* layer comprising 1×10^6 fibroblast cells Light microscopy images demonstrating the effect of collagen concentration on subsequent lamina propria layer development, measured observationally. **A+B)** 0.94 mg/ml collagen, **C+D)** 1.88 mg/ml collagen. Tissue depth (number of layers) was not affected by collagen concentration. but a more defined border at the higher collagen concentration was evident compared with rugged outermost layer in 3.6A and 3.6B (highlighted with red arrows). Sections stained with haematoxylin and eosin. Scale bar represents 20 μm in images 3.6A and 3.6B, 50 μm in 3.6C and 3.6D.

3.3.4 Initial *in vitro* studies to develop full thickness tissue model

Initial studies employing the knowledge acquired from the *in vitro* keratinocyte-only tissues were completed to establish a co-culture full-thickness tissue model. This used a fibroblast populated collagen matrix, overlaid with keratinocytes that would stratify into a 3D epithelium.

Fig. 3.7 demonstrates a representational section of MatTek full thickness tissue model that more closely represented the target tissue structure. Initial studies building on the establishment of an *in vitro lamina propria* used this knowledge and overlaid it with keratinocyte cells to establish the epithelium.

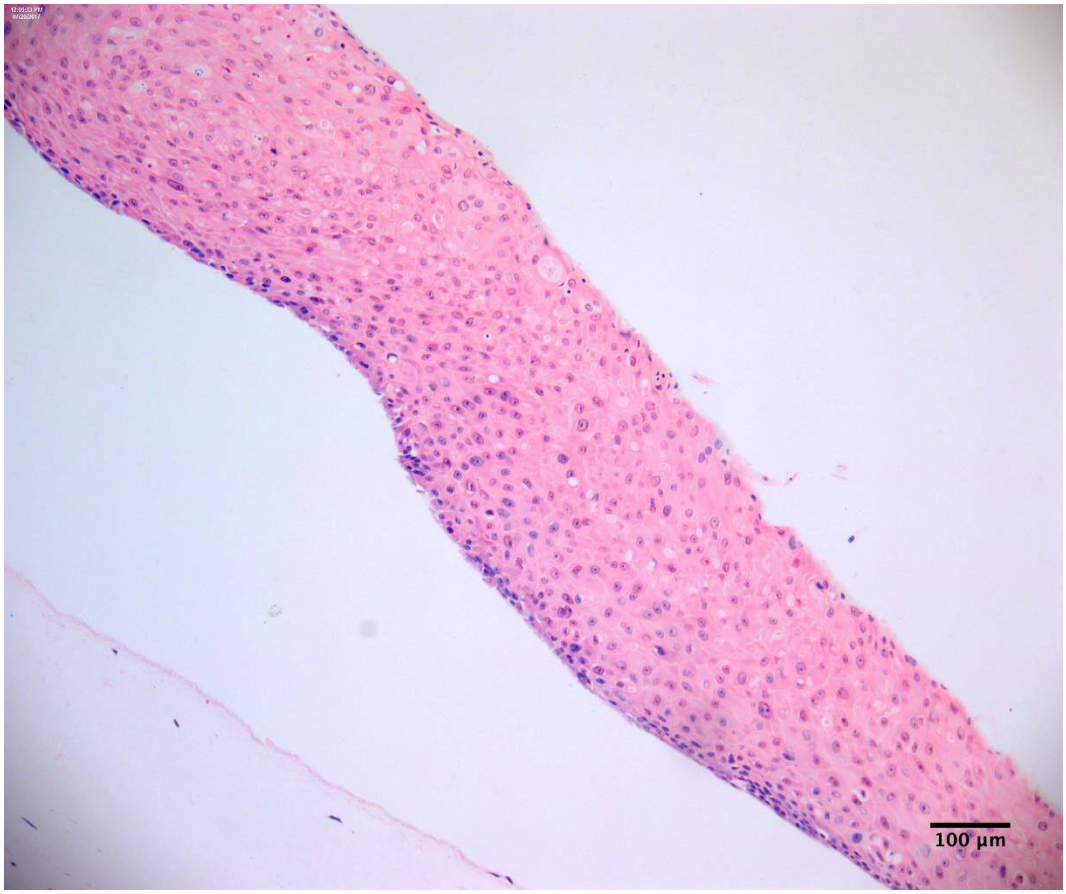

Figure 3.7 Typical representation of MatTek EpiOral full thickness tissue model section by light microscopy
Representative image of typical MatTek EpiOral full-thickness tissue model. Stained with haematoxylin and eosin. Scale bar represents 100 µm.

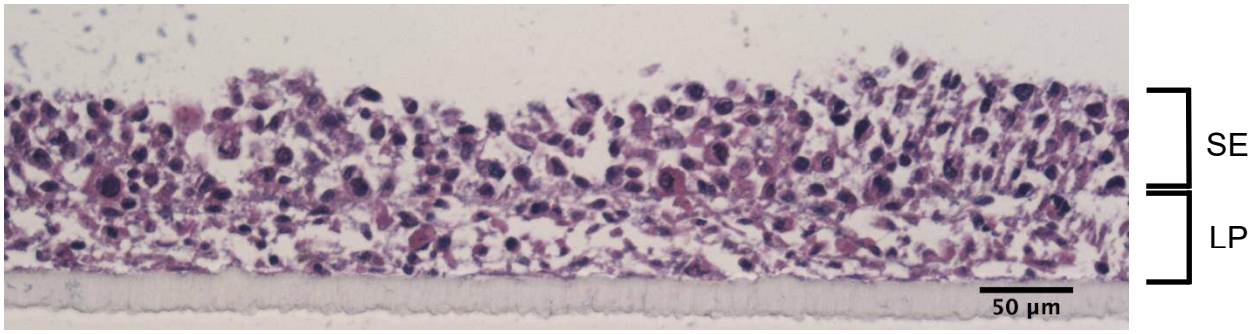

Figure 3.8 Initial *in vitro* full-thickness tissue models developed with 1.88 mg/ml collagen in conjunction with non-normal oral cell lines
SE, multi-layered keratinocyte-containing epithelial layer; LP, *lamina propria* comprising fibroblasts in collagen matrix. Cells stained with haematoxylin and eosin. Scale bar represents 50μm.

A somewhat defined fibroblast-populated *lamina propria* layer was evident, with multi-layered epithelium. However, the definition of cell morphology for the *lamina propria* was poor, with very little depth of the matrix structure, and was very densely populated by fibroblast cells. Additionally, the epithelial stratification was limited, with no defined differentiation of the keratinocyte cells, as was anticipated with the use of this TR146 cell type.

The *lamina propria* was cultured with HCA-2 fibroblast cells: hTert immortalised diploid fibroblasts, and although viable, did not show typical fibroblast-like morphology. The cells appeared very densely populated, with a myofibroblast-like appearance.

The epithelium showed a number of cell layers, indicating keratinocytes did develop into a 3D epithelium, but no maturation of the cells was evident. This was also observed in Fig. 3.4, where the same cells were used in the keratinocyte-only tissue model. No definition of *stratum basale*, or other anticipated layers were visible, although the viable cell morphology was similar to that expected with the TR146 cell line.

3.3.5 Full thickness model culture

Development of a full thickness tissue model was completed as part of a collaboration with Dr Craig Mudroch, and Dr Helen Colley at the School of

Clinical Dentistry, University of Sheffield. Some time was spent at the University of Sheffield to obtain the relevant technical knowledge and skills to culture the full thickness tissues at Cardiff University for this research.

Use of normal oral fibroblast cells to establish the *lamina propria*, which was then overlaid with immortalised normal oral keratinocytes, yielded the most representative oral mucosa full-thickness tissue of all models in this study, as represented in Fig. 3.9A. There was a very thick *lamina propria*, which in some areas was greater than 700 μm from the membrane to the *stratum basale*.

The fibroblast cells were spindle-like, with typical normal healthy fibroblast morphology, and sparsely populated within the collagen matrix. The higher concentration (5 mg/ml) of collagen used in this full thickness model protocol provided a much stronger and more stable physical structure in which the fibroblasts were able to establish and contract the matrix, but still maintain good integrity of the *lamina propria*.

The overlaid epithelium of immortalised normal oral keratinocytes showed excellent stratification, with many cell layers. The number of cell layers was greater than both in the *in vitro* keratinocyte-only and SkinEthic™ RHOE tissue models. The maturation of the *in vitro* epithelium showed defined layers with distinct cell morphologies, and some keratinisation of the outermost layers, as evident in normal histological palatal mucosa samples.

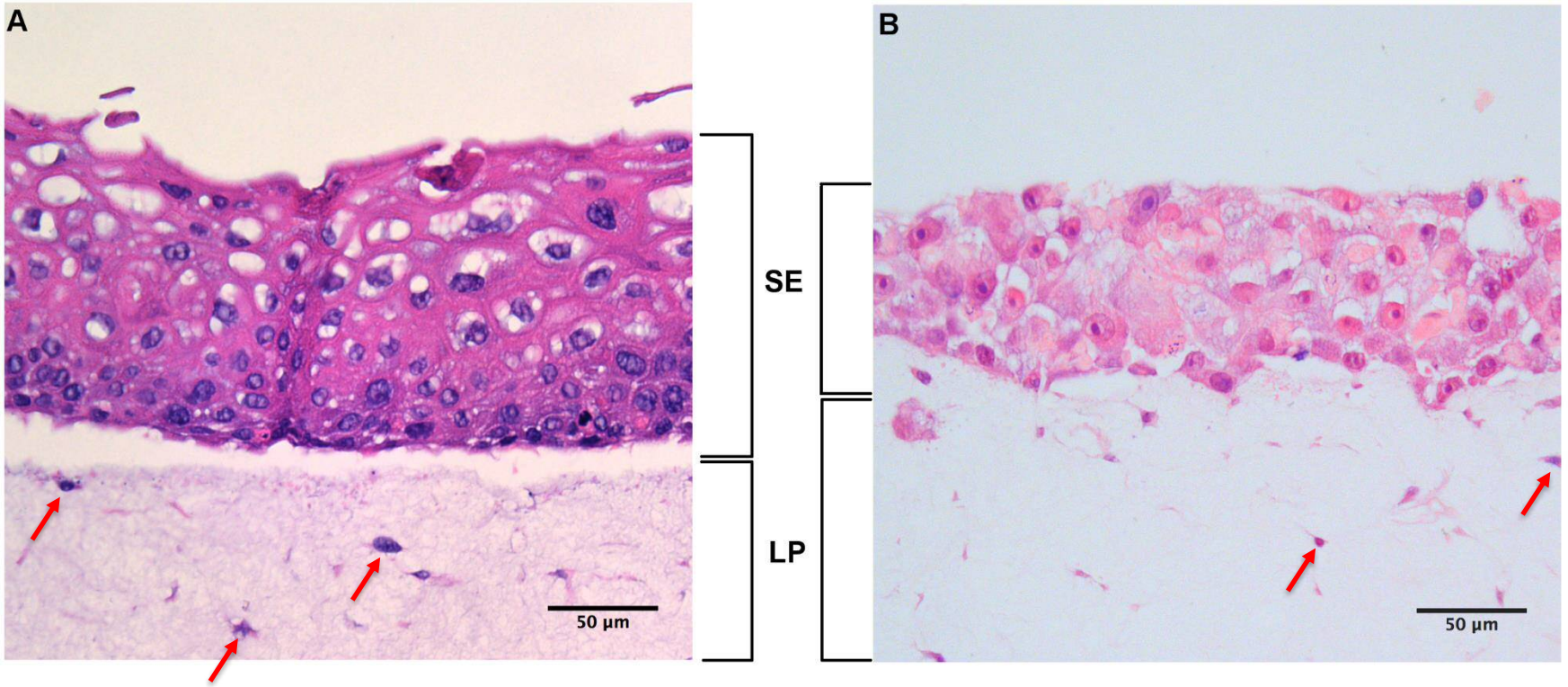

Figure 3.9 *In vitro* full-thickness tissues using normal oral fibroblasts and **A)** immortalised normal oral keratinocytes, and **B)** TR146 cancer-derived keratinocytes.
Typical light microscopy images of *in vitro* full thickness oral mucosal tissues in a collagen matrix (5 mg/ml) comprising a *lamina propria* (LP), sparsely populated with fibroblasts (red arrows), and layers of epithelial cells (SE). Tissues cultured for 10 d at ALI. Cells were stained with haematoxylin and eosin. Scale bar represents 50 µm.

The use of TR146 cancer-derived keratinocytes in place of immortalised normal oral keratinocytes (Fig. 3.9B) resulted in some interesting changes to the epithelium. The structure of the *lamina propria* remained similar with the TR146 cells as the FNB6 cells, indicating a similar response to environmental stimuli by the fibroblasts, and therefore they contracted in the normal manner. However, epithelial maturation and stratification were significantly affected. Little maturation of the keratinocyte cells was observed, despite many cell layers being present within the model. It was also noted, however, that the extent of epithelial stratification was less in the tissues using TR146 cells, than when using FNB6 cells.

3.4 Discussion

Commercially available tissue models have been widely used for a number of different types of investigations, from chemical cytotoxicity, to evaluation of candidosis (Jayatilake *et* al, 2005; Dongari-Bagtzoglou & Kashleva, 2006a; Silva *et* al, 2009; Silva *et* al, 2011; Yadev *et al*, 2011; Cavalcanti *et al*, 2015). The tissue models are relatively consistent and reproducible, as are the responses to infection between batches. There are, however, substantial limitations to each of the commercially available models, primarily associated with cost, but also the type of cells used. This study aimed to develop *in vitro* models equivalent to the commercially available constructs, in order to allow a higher throughput of analyses in future studies, but substantially reducing costs.

The SkinEthic™ RHOE tissues have been widely used for infection analyses, but primarily using planktonic cells, as opposed to biofilms which were of primary interest in this project. The SkinEthic™ RHOE tissue comprised solely of keratinocyte cells, in particular, TR146 cells, which were originally derived from a squamous cell carcinoma. The very nature of cancer cells, in that they are considered 'non-normal', can dictate the way they behave and respond to different stimuli. The responses to infection, expression of surface receptors may be different in cancer cells, compared with their non-cancerous equivalent. This study also used TR146 keratinocytes to establish a keratinocyte-only epithelial tissue model. The manufacture of the SkinEthic™ RHOE is proprietary; the culture period of commercial RHOE tissue models is published as 5 d at the ALI, but it was not known whether this was due to limitations of the model in terms of continued culture, part of the optimisation process, or due to the commercial nature of the model and wanting to reduce culture time to provide a greater number of models more frequently. Additionally, the cell seeding density, and specific details of the culture medium and supplements are not disclosed.

Previous preliminary, but unpublished work by the research group of Xiaoqing Wei at Cardiff University established culture medium supplements that support

the culture of keratinocytes and encourage stratification and development in a 3D manner. The evaluation of cell seeding density resulted in different tissue depths, increasing with the number of seeded cells (Fig. 3.1). The effect of culture period did not appear to influence tissue depth, with no substantial increase in depth despite doubling the culture period from 5 d to 10 d. The morphology of the cells within the 3D structure was similar in the *in vitro* tissues to that in the SkinEthic™ RHOE tissues. Tight, defined cell-to-cell junctions were evident in both *in vitro* and RHOE tissues, with typical TR146 cellular morphology. Previous work has been undertaken using TR146 to establish a 3D tissue, but this cultured for a significantly longer period (23 d), and the resulting tissues did not show as much stratification of the epithelial cells (Jacobson *et al*., 1999).

The keratinocyte-only tissue model is limited as it contains only keratinocytes, and no other cell types. The typical responses to infection or local environmental stresses of tissues is complex and includes many different cell types, such as keratinocytes, fibroblasts, Langerhans cells, immune cells, with a vast array of cytokine and chemokine signals being produced and sensed. Pro- and anti-inflammatory cytokines are critical to mount a suitable immune response to infection, and the limitation of cell types present in the model may not result in the same responses, as the production of the cytokines are known to further stimulate or suppress subsequent responses. Keratinocyte cells produce a range of cytokines, including interleukin-18 (IL-18), IL-1α, IL-1β, IL-3, IL-6, IL-8, and Tumour necrosis factor alpha (TNFα) (Waelti *et al*., 1992; Yadev *et al*., 2011; Jayatilake *et al*., 2005). These cytokines can have subsequent effects on monocytes and fibroblast cells, which subsequently produce cytokines of their own to mount an immune response to the stimulus, which in this case would be the infection. Fibroblasts, particularly in co-culture with keratinocytes are known to produce IL-6, which in turn further stimulate keratinocytes to produce pro-inflammatory cytokines (Ansel *et al*., 1990; McKenzie & Sauder, 1990; Netea *et al*., 2006).

To develop upon the relatively simple keratinocyte-only tissue model, a co-culture model was established, comprising both epithelial cells and a fibroblast-populated collagen matrix. The first stage was to evaluate the effect of collagen concentration on establishment of a *lamina propria*. Two concentrations of type I collagen were evaluated in this study; 1.88 mg/ml and 0.94 mg/ml, and were based on the commercial availability of a rat tail collagen solution. The pre-dissolved collagen was selected for use in preliminary studies due to the great expense of purchasing collagen in powder form, when considering the quantities required for such studies. For example, the lowest concentration of collagen used in these studies was 0.88 mg/ml for each tissue model, thus while making the cell suspension volume necessary for a batch of tissues (12 tissues), this equated to approximately 1 mg/ml. The price for collagen powder as a raw material was approximately £4-£9 per mg, which equates to a minimum of £12 per single batch. Taking into account that multiple batches were cultured at any one time, and the concentration of collagen used in the models varied from the equivalent of 1 mg/ml-approximately 6 mg/ml for each model, the cost very quickly becomes significant. For a single batch of full-thickness tissue models for infection studies, for example, the collagen cost alone equates to up to £1,296. Despite this, the *in vitro* tissue models are still significantly cheaper than the commercially available equivalent models, at approximately $4,000 (US dollars) for 24 tissues.

When the collagen solution was mixed with fibroblasts and allowed to set, neither produced a structure resembling a typical *lamina propria*, which is typically relatively thick compared to the epithelium, and contains fibroblasts that are sparsely populated within the matrix. A number of fibroblast seeding densities were also investigated, to determine an optimum seeding density for sufficient contraction of the collagen, whilst maintaining structural integrity. A slight increase was observed in *lamina propria* depth with increasing numbers of seeded cells. Observationally, there was however, little difference in cellular morphology. The cells retained the same spindle-like, elongated phenotype, indicating there were no benefits in using a higher number of cells to achieve a thicker fibroblast-collagen layer. Increasing the concentration of type I

collagen in the mixture also did not significantly affect tissue thickness, or structure of the *lamina propria*. The higher concentration of collagen (1.88 mg/ml) resulted in a more defined outer layer which was smoother than that evident with the lower concentration. The outermost edge of the lower concentration of collagen (0.94 mg/ml) was visibly rough, whereas the outermost edge when using the higher concentration (1.88 mg/ml) of collagen had a more uniform appearance with fewer peaks and troughs. These concentrations of collagen were still ultimately lower than were used in the final *in vitro* full-thickness tissue development protocol.

A preliminary *in vitro* co-culture tissue model was developed with 1.88 mg/ml collagen, and the highest seeding density of HCA-2 fibroblasts (1×10^6 total cells), followed by the highest seeding density of TR146 keratinocytes (1×10^6 total cells) as deemed optimal in this study. The resulting culture at the ALI showed a 3D culture of the *lamina propria* and epithelium, but no true stratification. The epithelial depth was similar to that observed in *in vitro* keratinocyte-only tissues, and was consistent across the membrane. The depth was similar between batches, indicating there may be a maximum thickness that can be supported by both the HCA-2 and TR146 cells in these models. The TR146 cells are limited in the potential extent of maturation and stratification of the resulting epithelium, as previously observed, which in turn may influence the cellular responses to infection.

In addition to the substantial contribution made to the development of *in vitro* replacements for grafts by researchers including Rheinwald & Green (1975, 1977), O'Conner *et al*., (1981), Gallico *et al*., (1984), continued development and optimisation of a co-culture mucosal tissue model protocol has been completed at the University of Sheffield by the group of Dr Craig Murdoch. Dr Helen Colley and Dr Craig Murdoch kindly shared their expertise which allowed substantial progress for this project for infection analyses. The protocol used by the University of Sheffield was adopted for this project, where the use of normal oral fibroblasts and immortalised normal oral keratinocytes yielded a very histologically different tissue model to those developed when

using cancer-derived cells. Fig. 3.7A demonstrates the resultant tissues when using normal oral cells, compared with TR146 keratinocytes in Fig. 3.7B. There was considerable difference between the two cell types when cultured in the full-thickness tissue model. The primary difference is the maturation of cells, where, TR146 cells do not show any maturation within the epithelial layer. The same cellular morphology was evident throughout the epithelium, with no distinct 'block'-like *stratum basale*, through to keratinised outer epithelium as would be anticipated. However, distinct cell morphologies were evident in the model containing normal oral keratinocytes; a dark *stratum basale*, after which, the cells matured and differentiated, to the outermost layer which some keratinisation.

There were some observed differences between the *in vitro* full thickness tissues, and EpiOral full thickness tissues. The extent of keratinisation was slightly higher in the EpiOral tissues, and such keratinisation may serve as a physical barrier to damage or infection. The cellular morphology of the fibroblasts was very similar, as were the keratinocytes in the epithelium. Distinct cell morphologies were visible for both models, indicating the similarities in culture, despite using cells from different sources. Upon consultation with Dr Adam Jones (Oral Pathologist, Cardiff Dental Hospital), who has expertise in histopathology, it was observed that some of the MatTek full thickness tissue models had a dysplastic-like appearance. It is not known whether this was a true representation of the cells, or an artefact during culture of the models, or indeed during the processing of the samples prior to sectioning.

Furthermore, this study did not evaluate the expression of cell markers such as those known to be expressed on keratinocytes of different stages of maturation and differentiation, nor did the study evaluate additional collagen types produced by fibroblasts in the full-thickness model. These would be interesting factors to evaluate in future work, but the limitations of time within the development and use of the models in this study were prohibitive to this undertaking. Expression of cell markers has previously been confirmed for the

in vitro full-thickness tissue model used in this study by Yadev *et al* (2011), as part of the development of the model at the University of Sheffield.

3.5 Conclusions

- An *in vitro* keratinocyte-only tissue model was developed, using TR146 cells, and optimised to achieve tissue depth equivalent to that of the SkinEthic RHOE tissue model. Cellular morphology was similar between the two tissue models, as was tissue depth and overall appearance.

- An *in vitro* full thickness tissue model was developed with normal oral fibroblasts and immortalised normal oral keratinocyte cells. The *in vitro* tissue model was considered superior to the MatTek EpiOral full thickness tissues, which were dysplastic in appearance when evaluated histologically.

- The use of cancer-derived keratinocyte cells resulted in a non-normal appearance epithelium respectively, whereas a normal phenotype with typical maturation and differentiation characteristics were observed with immortalised normal cells.

Chapter 4

Biofilm infection of oral mucosal tissue models and host immune responses

4.1 Introduction

In vitro interactions between microorganisms, either in planktonic culture, or as biofilms can be evaluated in several ways, but these analyses represent only part of the story, particularly when studies also have clinical implication. In Chapter 2, the development of single- and mixed-species biofilms was reported, and interactions between *Candida albicans* and a range of oral bacteria associated with denture stomatitis (DS) were studied. The presence of bacteria within these mixed-species biofilms increased the expression of a range of *C. albicans* virulence factors, and whilst this indicates increased pathogenic potential as a result, the actual pathogenicity (amount of damage caused) by these biofilms in an infection situation is not known.

To better understand the pathogenicity of mixed species biofilms *in vivo*, we need to further our basic understanding of events and interactions taking place in *in vitro* infection models. In addition to providing insight into the behaviour and prognosis of the infection, these models will allow better understanding of associated host responses. Previously simple interactions between cell monolayers and micro-organisms have been used to evaluate the responses of cells to stimuli, but more recent development of *in vitro* 3D tissue models provide an opportunity to build upon that, with more complex, but much more representative models of tissues and the host responses to infection.

The surfaces provided by the human body for colonisation or infection by micro-organisms vary histologically. For example, areas such as the skin or palatal mucosa include keratinised epithelial cells, primarily comprised of keratins (McLean & Irvine, 2007), which can resist microbial invasion, effects of chemicals, and harsh environments (Bibel *et* al., 1982; McLean & Irvine, 2007). However, non-keratinised epithelium lacks this robustness of the initial physical barrier for the other layers of stratified epithelial cells.

A number of 3D tissue models are commercially available including those that represent mucosal, epidermal, and vaginal tissues, and these have been used in a number of published studies (Schaller, 2002; Silva *et al*., 2009; Williams *et al*., 2013; Cavalcanti *et al*., 2015). In addition to evaluating cytotoxicity of

chemicals or formulated products, these tissue models are a good system for evaluating microbial infections, particularly, in the case of this PhD, infections using denture-associated biofilms. The use of 3D tissue models can provide benefits over monolayer cell studies including being more histologically representative of *in vivo* tissues for infection studies. This is important, because, the 3D structure compared with monolayers results in a reduction of effective local concentration of the compounds due to reduced penetration of the compounds to the inner-most cells, reducing their efficacy (Sun *et al*., 2006). This is also the case with biofilm infection studies; physical damage occurs initially on the outermost epithelial cells through direct-contact mediated pathogenicity factors, and secreted components such as hydrolytic enzymes. This damage then leads to lysis of the cells, allowing access to the next layer of cells, whereby the process repeats. Cells within tissues tend to have tight cell-to-cell junctions, thus permeability of solutions or secreted factors into the tissue is typically limited. Microbial invasion into tissues and secretion of compounds including hydrolytic enzymes are important virulence factors of many biofilms, and provide an opportunity for pathogens to cause substantial damage in order to obtain nutrients to continue to thrive and obtain nutrients critical for their survival including iron (Weinberg, 1975).

Whilst pathogenicity in tissue models is of great interest, previous studies investigating infections of these models have typically used planktonic cells as the inocula, whereas, in the case of DS, the infection originates from biofilms. Existence of microorganisms in a biofilm is known to change the behaviour of the cells compared with their planktonic counterparts (O'Toole *et al*., 2000). It is likely that researchers will continue to use planktonic inocula, because of the ease of preparation, and more precise standardisation between experimental replicates, where biofilms may vary slightly more. Additionally, the design of previous and likely future investigations follows a similar pattern of outcomes; analysis of microorganism-induced cell damage and histological analyses as part of an infection and host response (Silva *et al*., 2009; Yadev *et al*., 2011). There are substantial costs involved in the use of commercially available tissue models in large scale infection studies, hence the development and evaluation

of *in vitro* models that may be used in place of the commercially available constructs.

Previous *in vitro* studies of candidosis have relied upon the evaluation of the causative agent *Candida* alone (Yadev *et al*., 2011; Silva *et al*., 2009), but have not considered the contribution of other microorganisms that are also present in such conditions, such as the many different types of bacteria also present in denture biofilms. Whilst *Candida* species are indeed the causative agents of candidosis, bacteria are inevitably present and as this thesis has shown in Chapter 2, the presence of bacteria can influence the virulence of *Candida* in biofilms. The careful selection of bacterial species to use, along with the overall presence of both bacteria and *Candida* may influence subsequent pathogenicity and therefore influence mechanisms by which actions occur.

Host responses to infection are the most important factors in clearing infections *in vivo*. The initial call for an immune response through production of cytokines and chemokines that trigger infiltration of immune cells to the site of infection, and the sustained proinflammatory responses by epithelial cells, fibroblasts and dendritic cells. Cellular recognition of microorganisms occurs by detection of one of several conserved molecular patterns; lipopolysaccharide (LPS) from the cell walls of Gram-negative bacteria, or peptidoglycan (PG) present in cell walls of Gram-positive bacteria (Philpott *et al*., 2001), and β-glucans in the cell wall of fungi (Gow *et al.,* 2007). These are collectively known as pathogen associated molecular patterns (PAMPs), and the detection of these results in production of an array of inflammatory cytokines, which depends on the cell producing them, but can include IL-8, IL-1, IL-18, IL-6 and TNFα. These cytokines then induce leukocyte recruitment to clear the microorganisms.

As discussed in Chapter 3, the different types of tissue models have different abilities to produce cytokines, influenced by the type of cells used; cancer-derived cell lines, or normal cells, and determined by the type of tissue model used. Full thickness tissues, which comprise both epithelium and *lamina propria*, in theory could produce a full range of cytokines, and may be more

representative of an *in vivo* response as a result of cytokine-induced feedback mechanisms, controlling cytokine production by other cells.

It was therefore necessary for this PhD project to evaluate the pathogenicity of denture-associated biofilm infections toward commercially available and *in vitro* tissue models; to determine the effects of biofilms with differing microbial composition on the biofilm induced damage and invasion into the tissues. Interleukin-18 is a representative proinflammatory cytokine produced by keratinocyte cells in response to microbial infection, and the expression of the gene responsible for its production was selected for evaluation in this analysis, as the production of the cytokine to a detectable level may not be sufficient for the analysis methods employed. Furthermore, monocyte cells were selected to represent the immune cell responses to infection, as would be the case *in vivo*. These cells were primed and challenged with LPS and heat killed *C. albicans* cells, in order to determine the responses from both a bacterial cell wall component, as would be the case *in vivo*, and whole *C. albicans* cells. A number of studies have evaluated specific proinflammatory cytokines with stimulation solely with LPS, including a comparison between THP-1 cells and whole blood or peripheral blood monocytes (Schildberger *et al*., 2013), and LPS with additional compounds (Harrison *et* al., 2005; Chanput *et* al., 2010).

It is known that in order for immune cells to control fungi and any fungal-related infection, dectin-1 expression on the cell surface is an essential receptor for recognition of β-glucan (Brown *et al*., 2003). Taylor *et al*., (2007) demonstrated that monocytes deficient in dectin-1 rendered mice susceptible to fungal infection, highlighting the necessity for the receptor in recognition to restrict infection occurring. It is known that members of the IL-12 family are involved in proinflammatory responses to infection (Wei *et al*., 2011), particularly with fungi, thus the production of IL-23, a monocyte-associated pro-inflammatory cytokine was selected for evaluation to this priming and challenge. In order to evaluate immune responses with a perspective of DS, where both bacterial cells and *Candida* are implicated, investigations related to both LPS (representative of bacteria) and heat killed *C. albicans* need consideration.

The aims of this study were to evaluate the pathogenicity of single and mixed-species biofilms developed in Chapter 2 within *in vitro* 3D tissue models. Specifically, this research involved:

1. Evaluating biofilm-induced tissue model infection:
    a. Determining the extent of biofilm-induced damage of 3D tissue models, using a lactate dehydrogenase assay to quantify relative damage caused by different single- and mixed-species biofilms formed on acrylic surfaces.
    b. Histological analysis of tissues to observe physical damage to the epithelial layers, and invasion of *C. albicans* and bacteria within the layers of epithelial cells.
    c. Assessment of host tissue pro-inflammatory (IL-18) responses.
    d. Assessment of *C. albicans* virulence gene expression.

Evaluating immune cell responses as a result of stimulation with bacterial lipopolysaccharide (LPS) and/or heat killed *C. albicans* cells (HKC)

4.2 Materials and Methods

4.2.1 Commercially available tissue models and culture conditions

Commercially available three-dimensional tissue models were used to evaluate *in vitro* pathogenicity of polymicrobial biofilms on acrylic surfaces. These tissue models were cultured by the manufacturer and transported to the School of Dentistry, Cardiff University for use in this study. Upon receipt, the tissue models were prepared as detailed below.

4.2.1.1 EpiSkin SkinEthic Reconstituted Human Oral Epithelium (RHOE)

Keratinocyte only (TR146 cells originally isolated from a squamous cell buccal carcinoma) based oral mucosal tissue models (EpiSkin, Lyon, France) were cultured in cell-culture inserts on polycarbonate membranes with 0.4 μm diameter pores to allow free circulation of nutrients to the cells. The models were cultured at the air-liquid interface (ALI) for 5 d by the manufacturer prior to shipping. For shipping, the medium was replaced with an agar-based cell culture maintenance medium (of proprietary formulation) to restrict movement of the inserts during transport but provide nutrients to the cells.

Upon receipt, the models were moved to a new well plate and 2 ml of fresh sterile cell culture maintenance medium devoid of the phenol-red indicator (proprietary formulation) added. The volume of medium added ensured the tissues were maintained at the ALI during this period. The tissues were incubated at 37°C, 5% (v/v) CO_2, 95% air in a humidified incubator until use (minimum of 4 h after receipt).

4.2.1.2 MatTek EpiOral tissue model

The EpiOral tissue models were cultured for an undisclosed period using a proprietary protocol at the MatTek laboratories (Ashland, MA, USA). Similar to the EpiSkin transportation method, the EpiOral full thickness tissue models were shipped in an ‘agar-like’ medium. Upon receipt, tissue models were carefully removed from the agar and each model placed into a new tissue plate well with a sterile aluminium ring to elevate the model from the base of the well. Five ml of fresh cell culture maintenance (phenol-red free) medium was

added to each well, and the models incubated at 37°C, 5% (v/v) CO_2, 95% air in a humidified incubator until use (minimum 4h after receipt).

4.2.2 Tissue model preparation for biofilm infection

Immediately prior to infection, tissue models were transferred to new well plates containing 1 ml of cell maintenance culture medium and returned to the incubator momentarily to avoid potential adverse effects of a fully aerobic environment.

The tissue model infection was performed as depicted in Fig. 4.1. Biofilms (developed as described in section 2.2.4) were carefully lifted with sterile forceps, then inverted so the biofilm was on the underside of the coupon. The biofilm surface was carefully placed in contact with the tissue models. It was important to minimise inducing physical damage to the tissue from addition of the biofilm coupons, or by touching the tissue models with the forceps. The infected tissue models were returned to the humidified incubator (37°C, 5% (v/v) CO2, 95% air) for 12-14h.

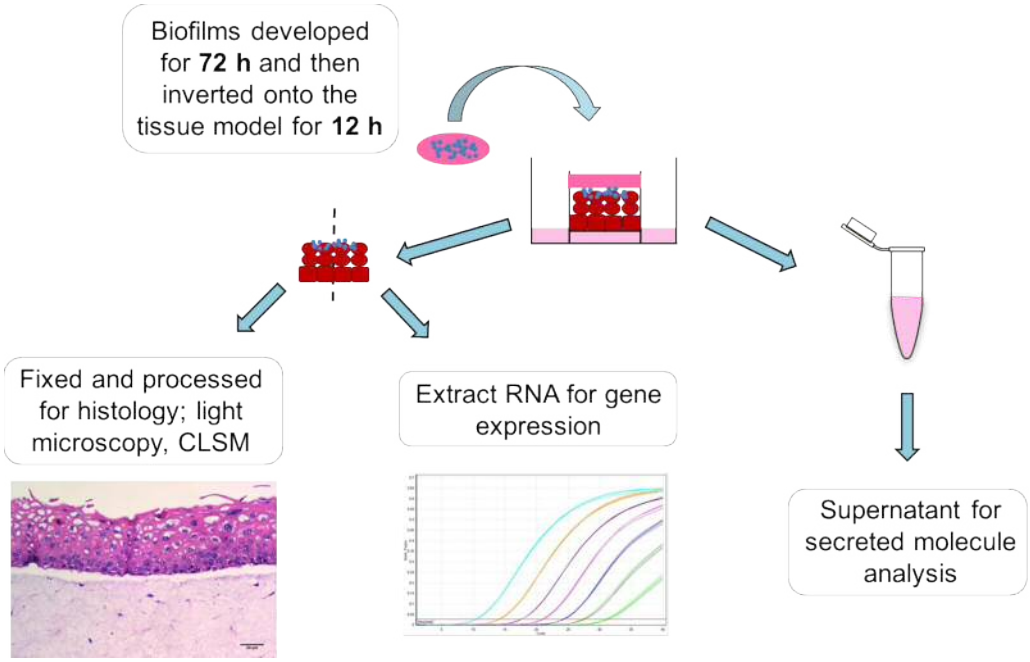

Figure 4.1 Diagrammatic representation of protocol for biofilm infection of tissue models
Biofilms developed on PMMA are placed in contact with tissues and incubated overnight. Tissues are removed, bisected and processed (total RNA extraction, and histology), and supernatant collected for cell damage analysis.

4.2.3 Post-infection processing of tissue models

After 12-14 h incubation, tissue models were removed (one well plate at a time to reduce the atmospheric exposure during removal and processing) from the incubator for processing.

4.2.3.1 Tissue model removal and preparation for analysis

The PMMA coupon supporting the biofilm, was carefully removed from the tissue using forceps, and the membrane/tissue model was carefully cut from the cell culture insert with a scalpel. The tissue was bisected with a clean scalpel, and half was placed in a sterile pathogen lysis tube (Qiagen) containing glass beads (undisclosed diameter), 350 μL RLT buffer (Qiagen) with 1% (v/v) β-mercaptoethanol, 500 μL of phenol:chloroform:isoamyl alcohol (25:24:1) and 200 μL TE buffer containing lysozyme (10 mg/ml) for RNA extraction and purification as described in section 2.5.1. The remaining half of the tissue was carefully wrapped in Surgipath® Bio-Wrap to maintain model integrity during processing, and securely placed into a pathology cassette. The

cassettes were immersed and stored at room temperature in neutral buffered formalin overnight prior to being processed for analysis by microscopy (as described in section 3.2.7).

The used cell culture supernatant was transferred to a centrifuge tube and placed on ice prior to analysis of lactate dehydrogenase (LDH) activity. The remaining portion was stored at -20°C until necessary for further analyses.

4.2.3.2 Histological preparation, analysis and fluorescence *in situ* hybridisation (FISH) analysis via confocal microscopy

Preparation and histological analysis was completed as described in sections 3.2.5 and 3.2.6.

Sections of the SkinEthic™ RHOE tissues were used as the preliminary tissue model for infection analysis, and were also stained for fluorescence microscopy for publication.

Wax embedded tissue sections were cut at 20 μm thickness and dewaxed with xylene, then dehydrated with 70% then 100% (v/v) ethanol. The tissues were rehydrated with distilled water immediately prior to processing. A 50-100 μl volume of lysozyme (10 mg/ml) was added to each section, and incubated at 37°C for 30 min in a humidified container. After incubation, the slides were washed twice with PBS. A 50-100 μl volume of 1 × citrate buffer (Sigma) was added to the sections, and the slides incubated in a humidified container at 55°C for 30 min. The sections were then washed twice with PBS.

Pan cytokeratin (C11) antibody (SC8018, Santa Cruz Biotechnology, Heidelerg, Germany) was added at 20 μg/ml, followed by an Alexa Fluor® 488-conjugated goat anti-mouse IgG secondary antibody (Life Technologies) at 5 μg/ml. The sections were protected from light and incubated at 55°C for 60 min. The sections were then washed with pre-warmed (55°C) fluorescence in situ hybridisation (FISH) washing solution and incubated at 55°C for 15 min. The cell nuclei were stained with Hoechst 33342 solution (Life Technologies)

at 1 μg/ml. Additionally, Yeast Traffic Light kit (AdvanDX, Vedbaek, Denmark), and a universal bacterial Cy3 labelled peptide nucleic acid (PNA) probe (Bac-Uni1CY3; 300 nM; probe sequence: CTGCCTCCCGTAGGA) specific for bacterial 16S rRNA (Malic *et al*., 2009) were mixed at a 1:1 ratio, and 30 μl of the solution added to the sections. Finally, 20 μl of Alexa-594 conjugated concanavalin A lectin (0.025% w/v in PBS) solution was added to the sections at room temperature, and the sections washed again with 200 μl FISH washing solution. The slides were then mounted with 20 μl Vectashield™ (H1100), and analysis performed by confocal microscopy

Despite two targets using Alexa-594 conjugates, they were to stain different components. Both bacterial cells and the cell wall of *C. albicans* cells are stained and visualised using the 594 nm wavelength excitation (red). The distinct cellular morphology (size and shape) of the bacterial and *C. albicans* cells, along with the inclusion of a co-stain for *C. albicans* with the Yeast Traffic Light kit (green). The co-stain for *C. albicans* allows differentiation between yeast and hyphae when evaluating tissue invasion.

Prior CLSM work was performed with 3D tissue models to ensure suitable conditions and protocol for FISH staining, and whilst no blocking solution was used, use of primary or secondary-antibody only resulted in no fluorescence staining, indicating the specificity of binding to the targets within the tissue model sections.

4.2.3.3 Biofilm-induced tissue model damage

Measuring LDH activity can provide an indirect quantitative measurement of cell damage, as the enzyme is released when cells lyse. In the case of biofilm infections of 3D tissue models, the released enzyme collects in the supernatant, which can be used in a colorimetric LDH activity assay to determine relative quantities.

The Pierce LDH activity assay kit (Thermo Fisher Scientific) was used according to the manufacturer's instructions. Briefly, the assay buffer and

substrate mix were combined to prepare the reaction mixture, after which 50 μl of the tissue model supernatant was added in triplicate to wells of a 96-well plate. A 50-μl volume of the reaction mixture was then added to all of the wells and mixed gently. The plate was incubated at room temperature for 30 min, then 50 μl of the stop solution was added. As the colour change of the solution was clear to red, the absorbance of the wells was analysed at 490 nm (background absorbance) and 680 nm (target absorbance) wavelengths. The background absorbance values were subtracted from the target absorbance values, and differences in colour intensity relative to the uninfected PMMA only infection control were calculated.

4.2.4 Expression of human genes

4.2.4.1 Nucleic acid extraction and purification

RNA was extracted and purified, and reverse transcribed to cDNA as described in sections 2.5.1 and 2.5.2.

4.2.4.2 Quantitative PCR

Quantitative PCR was used to measure relative level of expression of genes associated with the proinflammatory cytokine IL-18, and monocyte cell receptors; Dectin-1, and Toll Like Receptors 2 and 4 (TLR2, TLR4) as host responses to infection. Keratinocytes (as used in the tissue models tested in this chapter) are major producers of interleukin-18; a proinflammatory cytokine, which can mediate subsequent T cell responses. Dectin-1 is a cell surface receptor for β–glucans as found in the *C. albicans* cell wall, and TLR2/TLR4 are pattern recognition receptors involved in candidal cell clearance.

Target genes are detailed in table 4.1, along with the forward and reverse primer sequences.

Each qPCR reaction contained reagents as described in 2.2.5.3, and the following thermal cycling parameters: 95°C for 20 s, followed by 40 cycles of 95°C for 1 s and 70°C for 20 s. After completion of the 40 cycles, a final melt

curve stage was completed at 95°C for 15 s, and from 60°C for 1 min then 95°C for 15 s. The cycle threshold for each sample was determined automatically by the QuantStudio™ Real Time PCR software (version 1.2, Thermo Fisher Scientific) at the point of logarithmic amplification of the samples.

Calculation of fold change was completed according to the $^{\Delta\Delta}$Ct method described by Levak & Schmittgen (2001). Statistical analysis was performed using the $^{\Delta\Delta}$Ct values, using students T-test or one-way ANOVA..

Target gene	Sequence (5' → 3')
β-actin	F – GAGCACAGAGCCTCGCCTTTGCCGAT
Housekeeping gene	R – ATCCTTCTGACCCATGCCCACCATCACG
IL-18	F – CCTTCCAGATCGCTTCCTCTCGCAACAA
Interleukin 18 (pro-inflammatory cytokine)	R – CAAGCTTGCCAAAGTAATCTGATTCCAGGT
Dectin-1	F – ACAGCAATGAGGCGCCAAGGAGGAGATG
Cellular membrane receptor	R – GGAGCAGAAAGAAAAGAGCTCCCAAATGCT
Toll Like Receptor 2	F – GGAGCATCCGAATTGCATCACCGGTCAGA
Cellular membrane receptor	R – GGCCATCACACACCCCAGAAGCATCACA
Toll Like Receptor 4	F – GGCACTGTTCTTCTCCTGCCTGACACCA
Cellular membrane receptor	R – AGGGACTTTGCTGAGTTTCTGATCCATGC

Table 4.1 Human gene primer sequences for qPCR analysis of tissue model infection and host cell response

4.2.5 Monocyte cell responses to challenge with *Candida*

4.2.5.1 Monocyte cell culture conditions and preparation

THP-1 monocytes were cultured in RPMI 1640 medium (Life Technologies, UK), supplemented with 10% (v/v) FBS and 2 mM L-glutamine. The culture medium was changed every 2-3 d and cells were split when cultured to a cell density of no greater than 1×10^6 cells/ml.

The cells were collected by aspirating the suspended cells into a sterile universal container, then subjecting them to centrifugation (Durafuge 200 precision, Thermo Fisher Scientific) at 330 × *g* for 5 min to pellet the cells. The culture medium was removed and the cells enumerated using a haemocytometer, and resuspended to a density of 1×10^6 cells/ml.

4.2.5.2 Preparation of bacterial lipopolysaccharide (LPS) and heat killed *Candida albicans* (HKC)

Bacterial LPS (isolated from *Escherichia coli*, Sigma) was prepared at a stock concentration of 1 mg/ml in PBS, and diluted in RPMI 1640 culture medium (supplemented with 10% (v/v) FBS, 2 mM L-glutamine) immediately prior to use.

Candida albicans ATCC 90028 was cultured in Yeast Nitrogen Base (BD Difco) supplemented with 100 mM glucose (as previously described in section 2.2.2.1). The cells were centrifuged at 2879 × *g* (Thermo IEC CL10, Thermo Fisher Scientific) for 5 min to pellet and washed in PBS, then resuspended in PBS at a density of 1×10^9 CFU/ml. The suspended cells were heated in a water bath at 95°C for 10 min. Heat killing efficacy was assessed by adding 100 µl of the suspended cells to a Sabouraud Dextrose Agar plate in triplicate and incubating for 48 h. The heat killed *Candida* (HKC) cells were then retained at 4°C for short term storage, or -20°C for longer term storage.

4.2.5.3 Monocyte priming and challenge with *Candida*

THP-1 monocyte cells were seeded at a density of 2×10^5 cells/ml in 6-well plates. LPS was added to each of the wells at the necessary concentration,

and the plates were incubated overnight (37°C, 5% (v/v) CO_2). Dilutions of HKC were prepared at various densities (ranging from 1×10^5 to 1×10^8 cells/ml), and 100 µl of each concentration was added to the respective wells (1×10^4 to 1×10^7 cells/ml final density of HKC).

The plates were incubated for 24 h, after which the cells were suspended by repeat pipetting, and the suspension transferred to a 1.5 ml microcentrifuge tube. The tubes were centrifuged (Durafuge 200 precision) at 330 × *g* for 5 min to pellet the cells, after which, the supernatant was aspirated and transferred to a new microcentrifuge tube for cytokine analysis. The cells were resuspended in 1 ml PBS and stored at -20°C for flow cytometry.

4.2.5.4 Interleukin-23 cytokine ELISA

IL-23 cytokine quantification was performed using a sandwich enzyme linked immunosorbent assay (ELISA), with the Human IL-23 Ready-SET-Go® kit (eBioscience, Thermo Fisher Scientific), according to the manufacturer's instructions. All reagents were provided (except those stated) in the assay kit and diluted to a 1× concentration when initially provided in a concentrated form.

Each well of a 96-well plate was coated with 100 µl of capture antibody (pre standardised by the manufacturer but of undisclosed concentration, prepared in diluted coating buffer), and mixed on a shaking plate for 30 s to ensure homogeneous coating of the base of the wells. The plate was sealed with an adhesive seal, and incubated at 4°C overnight to ensure optimal coating of the antibody to the well.

After incubation, the antibody solution was removed and the wells washed (×5) with Wash Buffer (0.05% tween 20 in PBS). The plate was then washed (×5) with wash buffer, and 200 µl Assay Diluent added to all of the wells for 2 h at 37°C to block remaining non-specific binding sites. The protein standard was prepared in Assay Diluent at a concentration of 1 ng/ml, and added to the wells in triplicate. Two-fold dilutions of the protein standard in triplicate were

performed to a final concentration of 15.625 pg/ml. Triplicate wells containing Assay Diluent-only (to establish baseline absorbance) were included. Samples were added to wells in triplicate (100 µl volume) and the plate incubated overnight at 4°C to allow binding of any target protein to the capture antibody.

The plate was washed (×5) with Wash Buffer and biotin-conjugated detection antibody was then added. The plate was incubated at room temperature for 2 h and then washed (×5) with Wash Buffer. Fifty µl of diluted HRP-conjugated StreptAvidin (1:1000 dilution) was added to each well, and the plate incubated for 1.5 h at 37°C, after which it was washed (×6) with Wash Buffer. Fifty µl of tetramethylbenzidine (TMB) solution was added to each well and the plate was stored for 15-30 min at room temperature in the dark to allow colour development. The reaction was stopped with 50 µl Stop Solution (0.16M sulphuric acid) and the absorbance (at 450 nm wavelength) of the wells determined.

4.2.6 Flow cytometry for monocyte Dectin-1 cell surface receptors

Collected monocyte cells (all cells from each well independently) were resuspended in 50 µl of ice cold flow cytometry buffer (5% (v/v) FBS, 0.05% (w/v) sodium azide in PBS), and 1 µl of anti-human PE conjugated Dectin-1 antibody (20 µg/ml), then the solution incubated on ice for 30 min. The cells were pelleted by centrifugation (Durafuge 200 precision) at 330 × *g* for 5 min and washed (×3) with wash buffer (0.05% (w/v) sodium azide in PBS). The cells were finally resuspended in 200 µl flow cytometry buffer (2% (v/v) FBS, 0.05% (w/v) sodium azide in PBS) for flow cytometry.

Samples were analysed in a BD FACSCanto II (BD Biosciences, Oxford, UK) flow cytometer using the following parameters: FSC voltage, 250V; SSC voltage, 435V; PE voltage, 250V, with medium flow rate, and counting a minimum of 10,000 events.

4.3 Results

4.3.1 Effect of bacteria in mixed-species biofilms on subsequent pathogenicity and tissue damage in tissue model infections

Using tissue models constructed solely with keratinocytes, the effect of infecting with biofilms on acrylic surfaces was assessed. The biofilms analysed included *C. albicans*-only biofilms, oral bacteria-only biofilms and *C. albicans* plus oral bacteria species biofilms (mixed-species). Controls of sterile uninfected PMMA acrylic coupons were included with all experiments. Analysis of tissue infections and pathogen responses include measurement of lactate dehydrogenase (LDH) activity, expression of genes for human IL-18 and dectin-1, and *C. albicans* virulence genes (as previously analysed in *in vitro* biofilms in section 2.3.3.3), and histological examination of the infected tissue.

4.3.2 Epithelial tissue model infection

Epithelium- only tissue infections were evaluated using two 3D tissue models. These tissues were a SkinEthic™ Reconstituted Human Oral Epithelium (RHOE; EpiSkin, Lyon, France), and an *in vitro* keratinocyte-only tissue model which has previously been described (section 3.3.2).

4.3.2.1 Infection of SkinEthic™ Reconstituted Human Oral Epithelium

LDH activity to measure cell damage was expressed as fold-change relative to tissues overlaid with acrylic coupons devoid of biofilms. Infection of the RHOE (Figure 4.1A) with bacteria-only biofilms resulted in a small, increase in tissue damage which was however not significantly different to the control. However, a significant ($P<0.05$) increase in tissue damage was observed with *C. albicans*-only biofilms, and a further significant ($P<0.01$) enhancement in tissue damage occurred using mixed-species biofilms.

Host inflammatory responses (Figure 4.2B) to infection were evaluated by expression of the *IL18* gene relative to the response of tissues to uninfected acrylic coupons. A slight increase in expression of the *IL18* gene was observed in tissues previously infected by bacteria-only biofilms. A further increase in the expression of the *IL18* gene was found with tissues infected by *C. albicans*-

only biofilms. These increases were however determined not to be significantly increased compared to controls, whereas in the case of tissues infected with mixed-species biofilms, a significant ($P<0.01$) increase in expression of the *IL18* gene was evident compared with controls.

Histological analysis was used to assess structural damage to the epithelium and the location of microorganisms during the infection. Fig. 4.3 shows a post-infection cross-sectional representation of each of the biofilm infections by confocal microscopy.

Fig. 4.3A shows a tissue that had been overlaid with an acrylic coupon devoid of a biofilm where, for this tissue, good cellular structure that was typical of TR146 cells was evident with no observable damage to the cells.

Fig. 4.3B shows tissue previously overlaid with an acrylic coupon supporting a bacteria-only biofilm. For this tissue, a bacterial biofilm was evident on the surface of the epithelium with the bacteria seen as clustered aggregates. Some damage to the tissue was evident, as seen by lesions in the epithelium, and there was atypical morphology of the cells.

Similarly, Fig. 4.3C shows a tissue previously overlaid with an acrylic coupon supporting a *C. albicans*-only biofilm. For this tissue, the biofilm could be detected on the surface of the epithelium, although little visible damage was evident. Interestingly, the *C. albicans* were primarily in the yeast form.

Mixed-species biofilm infection of tissues (Fig. 4.3D) illustrate the substantial differences between the biofilms during infection. Extensive biofilm invasion of all layers of the epithelium was observed and significant tissue damage was evident, although in this representative image, it did visually appear somewhat less than bacteria-only (Fig 4.3B). Furthermore, *C. albicans* hyphae were clearly seen to invade through to the lower layers of the epithelium, and this was seemingly both between and penetrating through cells. The bacterial cells within the biofilm appeared to adhere to the hyphae, and therefore were also

found within the epithelium itself. Lesions occurred in the tissue and an atypical morphology of the keratinocyte cells was also apparent.

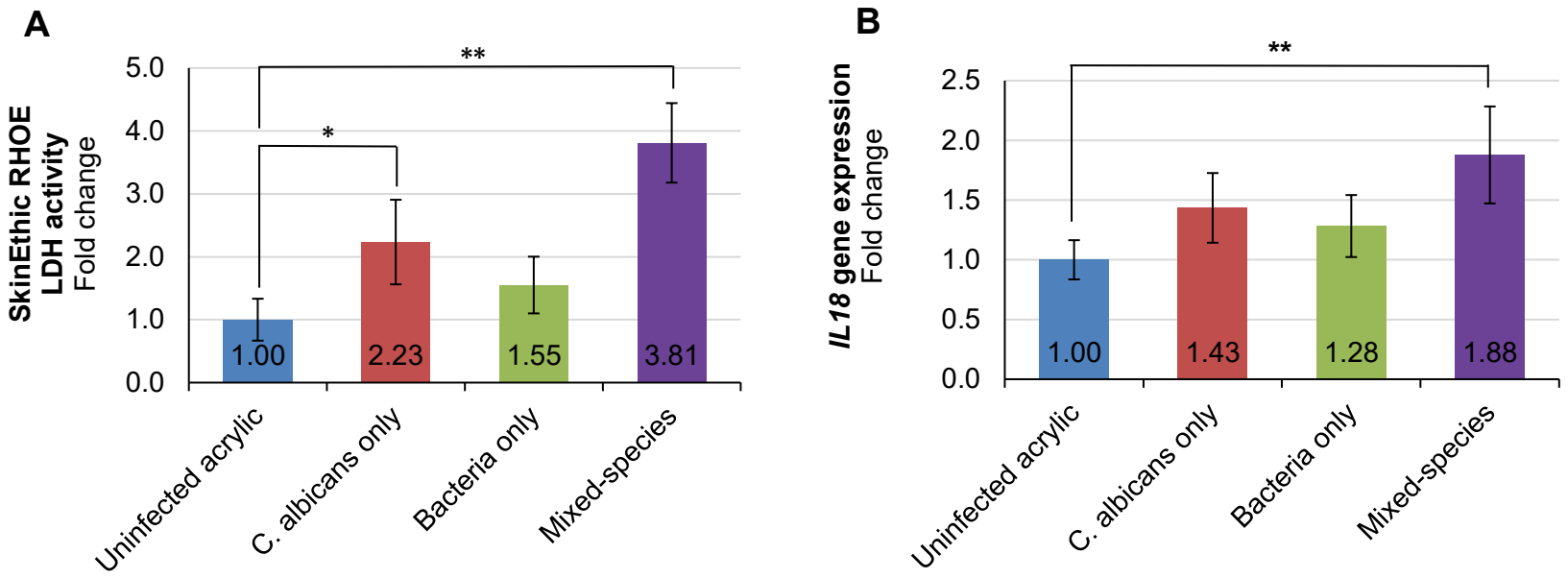

Figure 4.2. Acrylic biofilm-induced damage of SkinEthic™ RHOE tissue models as measured by lactate dehydrogenase (LDH) activity and IL-18 gene expression.

A) Fold change of biofilm-induced cell damage measured by LDH in collected supernatant post-infection relative to a normalised uninfected acrylic-only control. A significant increase in cell damage was caused by *C. albicans*-only biofilm, and this was further increased in tissues infected with mixed-species biofilms. **B)** Host pro-inflammatory interleukin-18 (IL-18) cytokine gene expression as a result of infection. Mixed-species biofilms led to a significantly increase expression of the *IL-18* gene. Data expressed as mean of 6 replicate experiments. Error bars represent standard deviation. *P<0.05, **P<0.01. Representative melt curves are provided in Appendix 1.

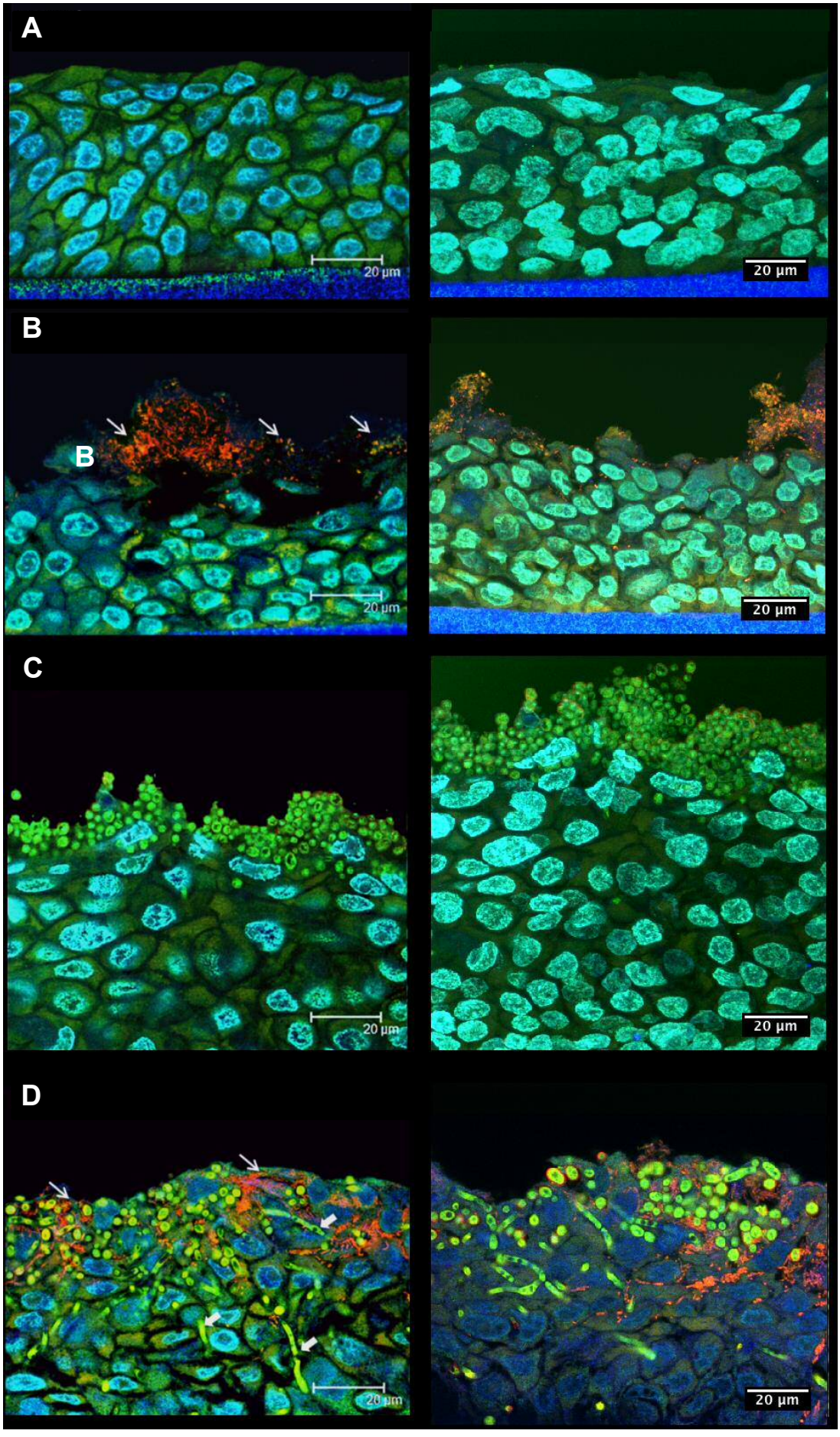
A
20 µm
20 µm
B
B
20 µm
20 µm
C
20 µm
20 µm
D
20 µm
20 µm

Figure 4.3 Fluorescence *in situ* hybridisation images of sections taken from 3D tissue models post-biofilm infection.
Fluorescently stained tissue model sections of **A)** uninfected acrylic only, **B)** oral bacterial biofilm infection, **C)** *C. albicans*-only biofilm infection and **D)** mixed-species biofilm post-infection.
Epithelial cells were stained with Hoechst 33342 dye (nuclei, blue) and a fluorescently labelled pan-cytokeratin antibody (cytoplasm, green). Bacteria were stained with a universal-bacterial peptide nucleic acid (PNA) probe (red), and *C. albicans* was stained using a Yeast Traffic Light PNA probe (AdvanDX, bright green). Light arrows indicate bacteria, bold arrows indicate invading *C. albicans* hyphae.Scale bar represents 20 μm.

4.3.2.2 Infection of in vitro keratinocyte models

A similar pattern of tissue damage (LDH release) to that of the RHOE was observed when biofilm infection was assessed in the 'in-house' developed *in vitro* keratinocyte model (Fig. 4.4A). Compared with the uninfected acrylic coupons, only a very slight increase in biofilm-induced tissue damage was observed with bacteria-only biofilms, although a significant ($P<0.01$) increase was apparent using *C. albicans*-only biofilms and this was further enhanced ($P<0.001$) when tissues were infected with mixed-species biofilms. It was also observed that the relative extent of damage for the *in vitro* epithelial tissue models was lower than previously encountered for the commercial epithelial tissue models, but this may be due the quantity of tissue present rather than the relative effect of the biofilms on the respective tissues.

The induction of an inflammatory response (*IL18* gene expression) of the *in vitro* keratinocyte-only tissues followed a very similar pattern to the SkinEthic™ RHOE tissues (Fig 4.4B).

Light microscopy images demonstrated a similar visual progression of the infection as previously observed with the SkinEthic RHOE tissue infections (Fig. 4.5); an intact epithelium when using PMMA coupons only with no infection (Fig. 4.5A), some visible damage with bacteria-only biofilms (Fig. 4.5B), and similar with *C. albicans* biofilms (Fig. 4.4C), but *C. albicans* remain on the outer surface, whereas substantial tissue damage was observed with mixed-species biofilms (Fig. 4.5D).

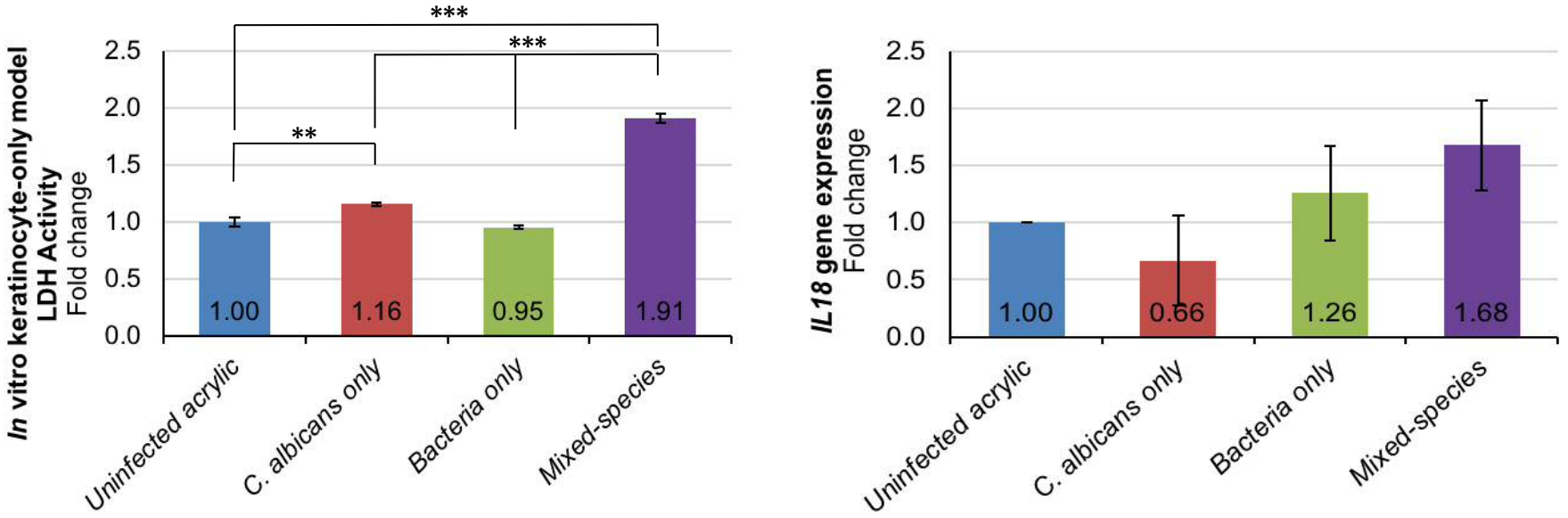

Figure 4.4 Acrylic biofilm-induced damage of *in vitro* keratinocyte-only tissue models as measured by lactate dehydrogenase (LDH) activity, and *IL18* gene expression.
A) Fold change of biofilm-induced cell damage measured by lactate dehydrogenase (LDH) in collected supernatant post-infection relative to a normalised uninfected acrylic-only control. Slight increase in damage caused by *C. albicans*-only biofilms, and significant increase in cell damage caused by mixed-species biofilms **B)** Host pro-inflammatory interleukin-18 (*IL18*) cytokine gene expression as a result of infection. Mixed-species biofilms induce significant increase of *IL18* gene expression. Data expressed as mean of 6 replicates. Error bars represent standard deviation. *P<0.05, **P<0.01

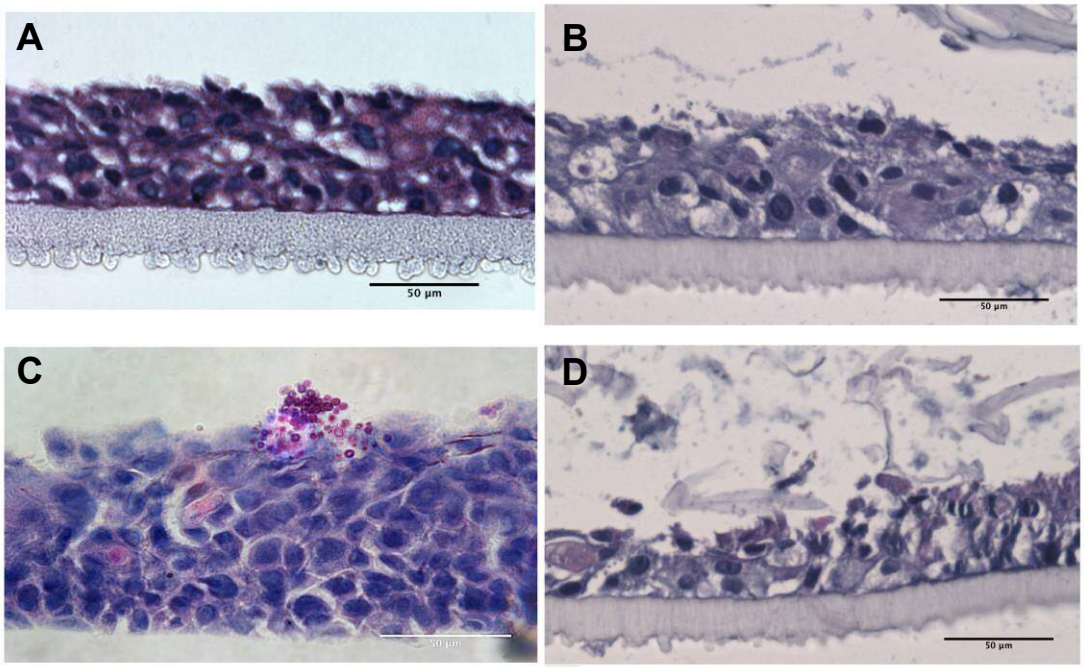

Figure 4.5 Light microscopy images of histological sections of *in vitro* keratinocyte-only tissue infections with different biofilms
A) uninfected acrylic only, **B)** oral bacterial biofilm infection, **C)** *C. albicans*-only biofilm infection and **D)** mixed-species biofilm infection.
Stained with periodic acid Schiff. Scale bar represents 50µm

4.3.3 Full-thickness tissue model infections

Biofilm infections of full-thickness tissue models included a commercially available full-thickness oral mucosal tissue model (EpiOral), purchased from MatTek Corporation, and a full-thickness tissue model cultured at Cardiff University as described in section 3.3.5.

4.3.3.1 Infection of MatTek full-thickness tissue models

Biofilm infection of commercial full-thickness (FT) tissues (MatTek) (EpiOral, MatTek Corporation) resulted in a similar pattern of damage (Fig. 4.6A) as observed with the previously described keratinocyte-only tissue models, but not to the same extent. This was despite significant histological differences between the two model types and the cells used to develop them. The MatTek tissues comprised a lamina propria, as well as layered epithelial cells (Fig. 4.7A)..

Tissue damage was measured by LDH activity assay (Fig. 4.6A), and the extent of damage caused specifically by biofilm infections were expressed as fold change relative to the uninfected acrylic coupons. When compared with tissues overlaid with uninfected acrylic coupons, tissue damage was observed with *C. albicans*-only and mixed-species biofilms. There was, however, no difference in LDH activity caused by uninfected control coupons and bacteria-only biofilms. However, despite evident increases in damage, none of the differences were statistically significant.

The observed differences in biofilm-induced MatTek tissue damage (Fig. 4.6A) were not obvious histologically (Fig. 4.7). The morphology of the cells after the 12h duration of biofilm infection (Figs. 4.7B, 4.7C, 4.7D) were similar to that of tissues exposed to uninfected control acrylics (Fig. 4.7A). Histology revealed keratinised epithelial layers with normal cell morphology and anticipated stratification with few indications of substantial epithelial damage caused by the biofilms. Additionally, biofilms were evident on the tissue surface after overlaying with *C. albicans*-only and bacteria-only biofilms, and, in the case of mixed-species biofilms, areas of invasion into the tissue were evident (Fig. 4.7D), but not to the same extent as seen in the mixed-species biofilm infection of SkinEthic RHOE tissues (Fig. 4.3D.

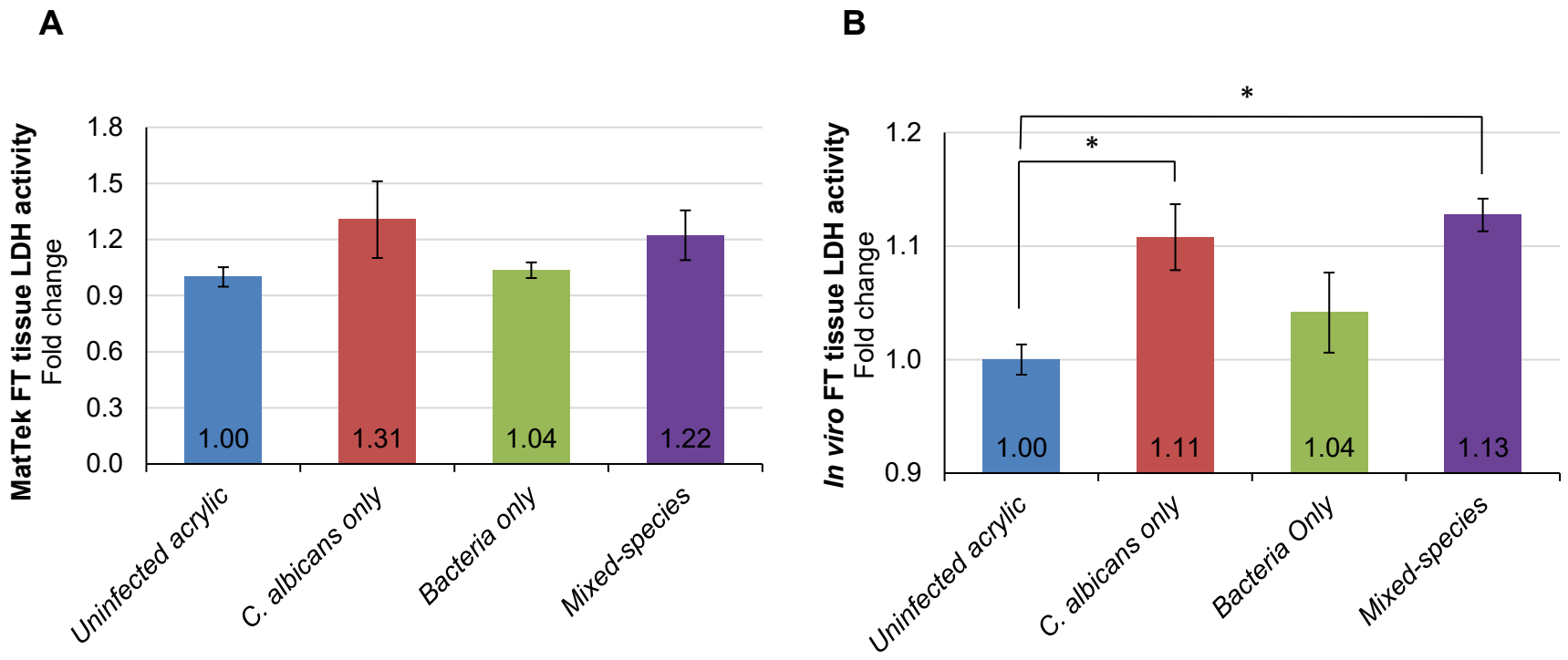

Figure 4.6 Biofilm-induced tissue damage as measured by lactate dehydrogenase (LDH) activity assay
A) Relative to an uninfected acrylic control, biofilm infections of MatTek EpiOral tissues resulted in slight increases in damage caused by mixed-species biofilms, and a greater increase caused by *C. albicans*-only biofilms, but no increase in damage by bacteria only biofilms. However, no observed increase was significant. **B)** Biofilm infections of *In vitro* full-thickness tissues resulted in a significant increase in damage caused by *C. albicans*-only biofilms, and a similar increase again by mixed-species biofilms, however as observed with MatTek tissue infections, no difference in damage caused by bacteria-only biofilms was observed. Data expressed as mean of 9 replicates, error bars represent standard deviation. *P<0.05, **P<0.01

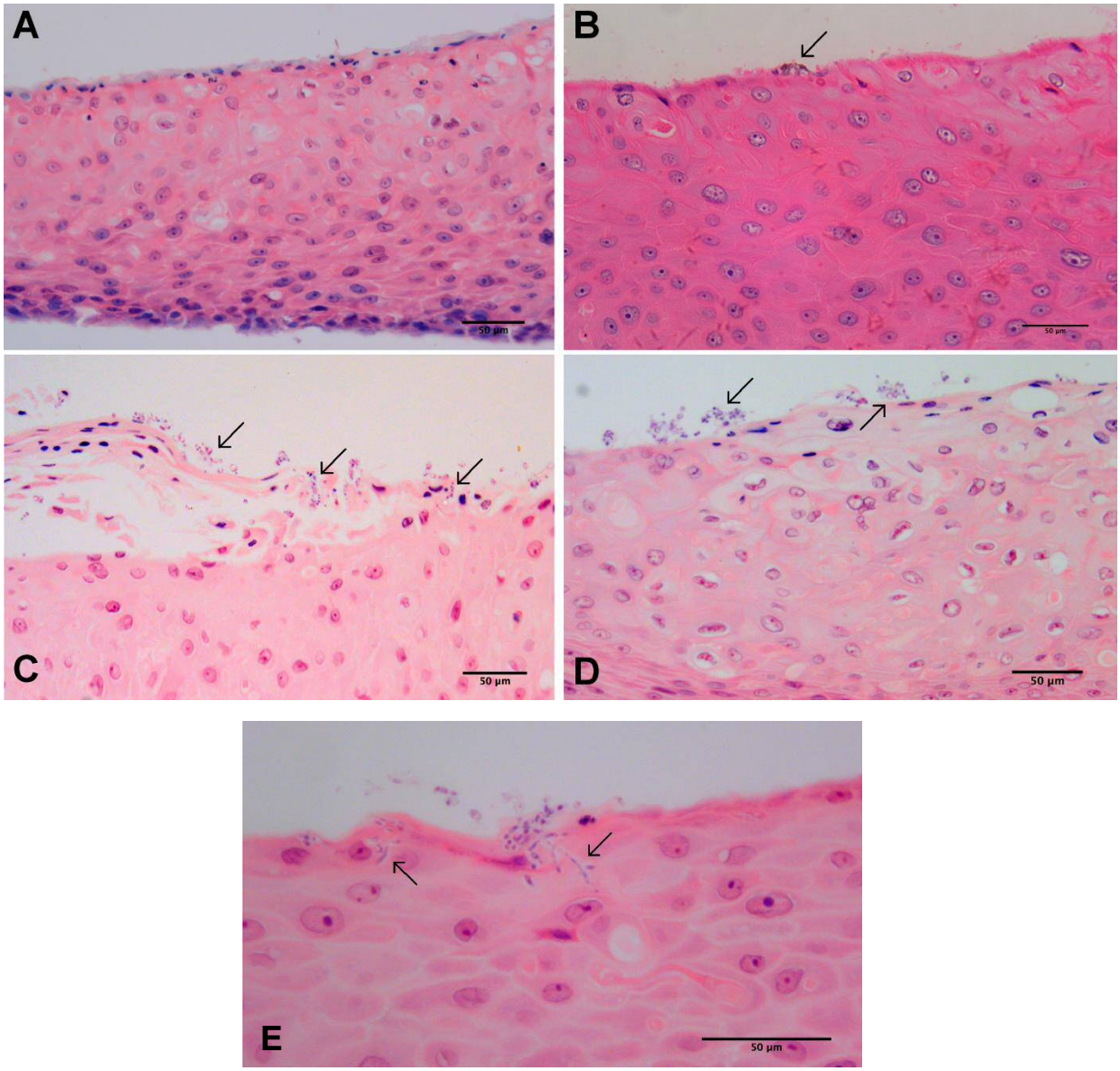

Figure 4. 7 Histological sections of biofilm-infected MatTek EpiOral tissues
Typical light microscopy images of histological sections of **A)** Uninfected acrylic coupons, **B)** bacteria-only biofilms, **C)** *C. albicans*-only biofilms and **D)** mixed-species biofilms, and **E)** mixed-species biofilms showing hyphal invasion.
Sections stained with haematoxylin and eosin. Arrows indicate biofilms. Scale bar represents 50µm

4.3.3.2 Infection of *in vitro* full-thickness (FT) tissue models

Biofilm-induced tissue damage of *in vitro* full thickness tissues, as measured by LDH activity (Fig. 4.6B), followed the same pattern as previously observed (section 4.3.3.1); a significant ($P<0.05$) increase in tissue damage was caused by *C. albicans*-only biofilms, and this was further significantly ($P<0.01$) enhanced in tissue infections by mixed-species biofilms relative to the uninfected acrylic coupon controls. The overall levels of tissue damage were smaller than that previously observed with infection of either keratinocyte-only or MatTek tissues.

Despite the smaller differences observed by LDH, substantial damage was observed visually by histological analysis of the tissues (Fig. 4.8). The tissues exposed to uninfected acrylic coupons did not show any signs of damage (Fig. 4.8A); no disruption to the keratinised epithelium, nor any clear signs of damage to the cells deeper within the epithelium. Bacteria-only biofilm infected tissues (Fig. 4.8B) showed some extent of cell damage to the keratinised outer layer, with evidence of biofilms existing on the outer surface. A large extent of damage was evident in *C. albicans*-only biofilms (Fig. 4.8C), with some invasion within the layers of the epithelial section, and considerable destruction of the epithelial cells. It is also evident that the *C. albicans* cells were primarily in the yeast form, as previously observed. Furthermore, tissue infection with the mixed-species biofilms resulted in extensive destruction of the epithelium, and a large extent of invasion of the microorganisms into the tissue. Interestingly however, no infection of commercial or *in vitro* tissue models showed any damage to the lamina propria layer. It is not known whether the viability of these cells was affected by the production of hydrolytic enzymes, but there appeared to be maintained structural integrity and normal cellular morphology.

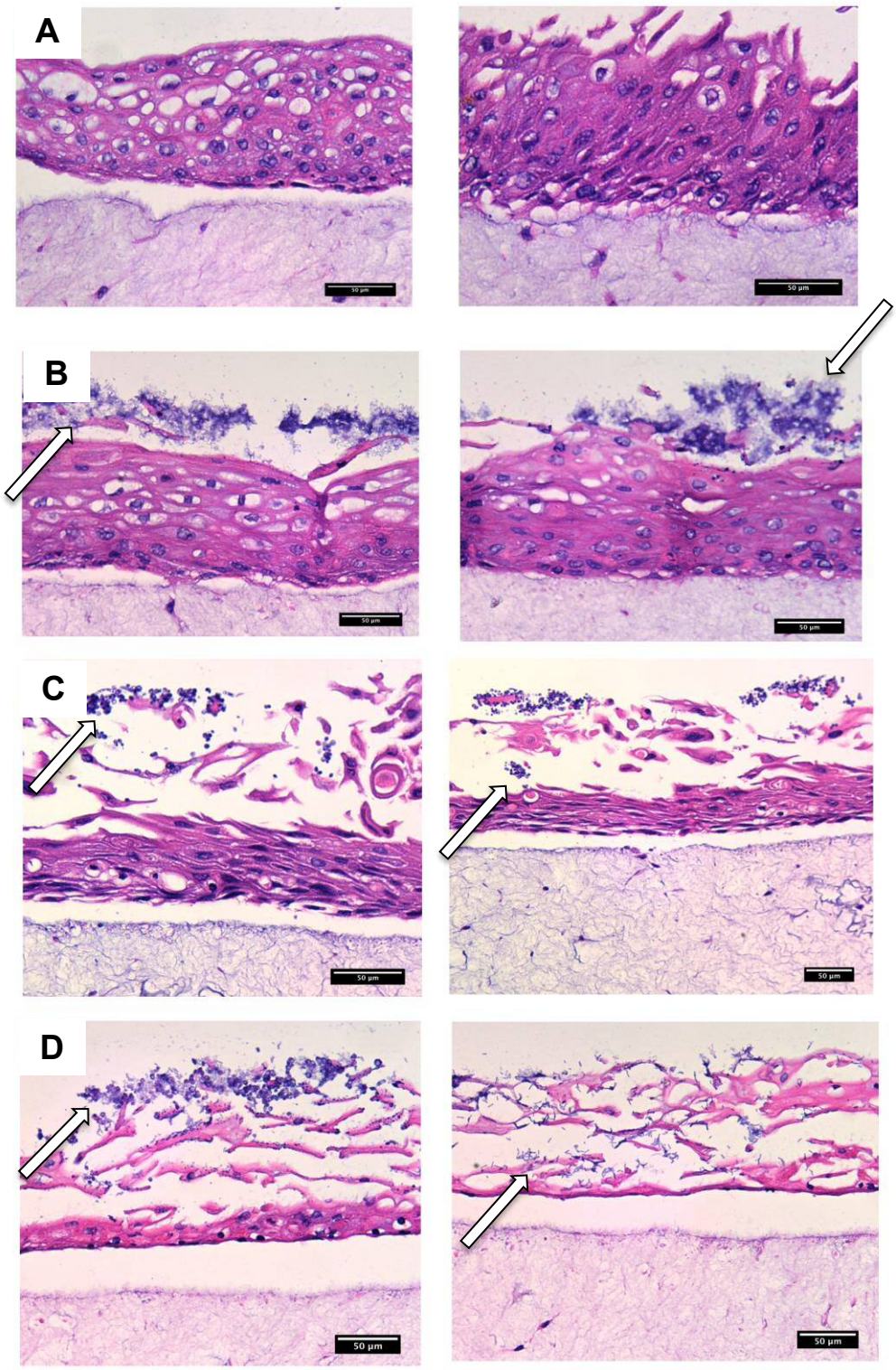

Figure 4.8 Histological sections of biofilm-infected *in vitro* full-thickness tissues stained with haematoxylin and eosin

Typical replicated (left and right) light microscopy images of histological sections of **A)** Uninfected acrylic coupons, **B)** bacteria-only biofilms, **C)** *C. albicans*-only biofilms and **D)** mixed-species biofilms, stained with haematoxylin and eosin. Arrows indicate biofilms. Scale bar represents 50µm

Infected tissue model type	Mean LDH absorbance raw values (blank adjusted 490nm wavelength) (± SD)			
	Uninfected acrylic	**Bacteria-only**	***C. albicans*-only**	**Mixed-species**
SkinEthic RHOE	0.218 (0.040)	0.339 (0.087)	0.488 (0.149)	0.832 (0.179)
***In vitro* keratinocyte only**	0.233 (0.032)	0.222 (0.014)	0.269 (0.015)	0.444 (0.034)
MatTek EpiOral FT	0.295 (0.004)	0.305 (0.006)	0.338 (0.011)	0.386 (0.017)
***In vitro* full thickness**	0.430 (0.013)	0.448 (0.035)	0.476 (0.029)	0.485 (0.014)

Table 4.2 Raw absorbance values for tissue model post-biofilm infection lactate dehydrogenase assay

Raw data (mean of 6-9 replicates) of adjusted absorbance values (490 nm wavelength) for each infection type with each tissue model type. Data shown as mean of test conditions minus negative/blank samples (culture medium only). SD=standard deviation.

4.3.4 *C. albicans* virulence gene expression during tissue model infection

Figures 4.9 and 4.10 detail the expression of a range of *C. albicans* virulence genes across the infected tissue models, expressed as a fold change in gene expression of mixed-species biofilm infections relative to a *C. albicans*-only control.

An increase was observed in the expression of *ALS3, EPA1, SAP4, SAP6* and *PLD1*, although no increase in the expression of *HWP1* was evident. The expression of *HWP1* has previously shown to be upregulated in mixed-species biofilms (Chapter 2), and despite there being no upregulation shown here, it is considered that the expression was not consistently up regulated once hyphae formation ceased, e.g. in the case where sufficient hyphae are formed within the environmental conditions. Results in Chapter 2 and in Fig. 4.8 show substantial hyphae within the biofilms and infected tissues. There was consistency in the extent of gene expression between the infections of different tissue models, and the expression profile was also similar to that observed in *in vitro* biofilms (section 2.3.3.3), but interestingly, the increase in relative expression of the epithelial adhesin *EPA1* was considerably greater in this study than was observed in *in vitro* biofilms.

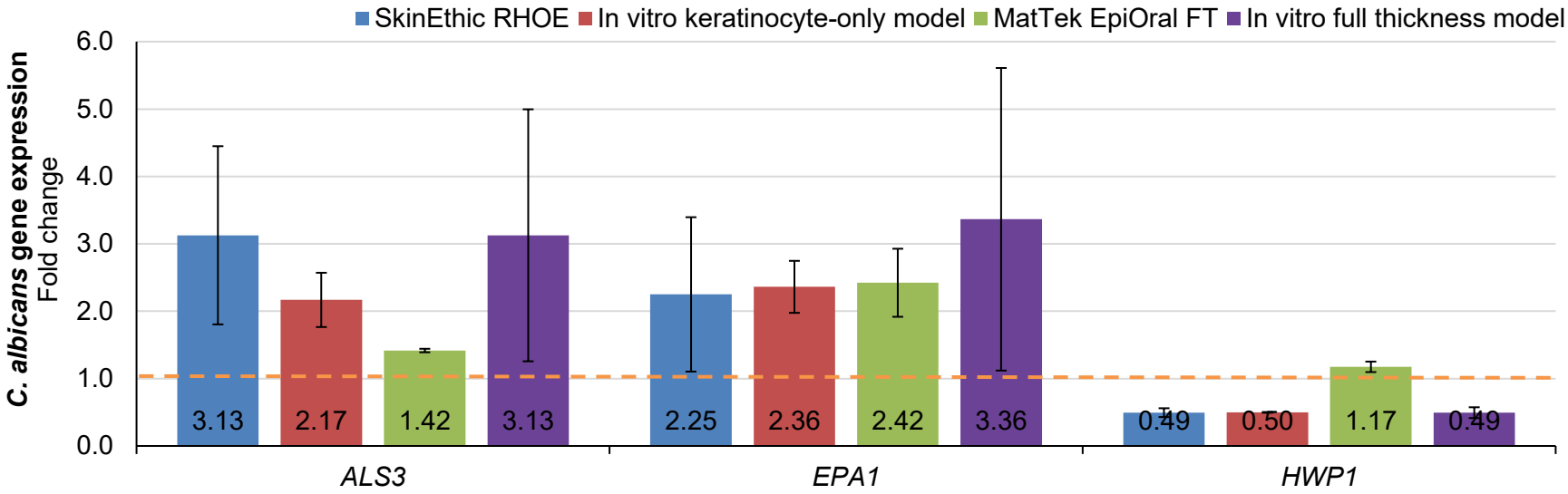

Figure 4.9 *C. albicans* virulence gene expression of mixed-species biofilm infections of tissue models.
Candidal adhesin (*ALS1*, *ALS3*, *EPA1*) genes, hyphal wall protein (*HWP1*) gene, phospholipase D (*PLD1*) gene and secreted aspartyl proteinase (*SAP4*, *SAP6*) genes. Gene expression relative to *C. albicans*-only infection control
Data expressed as mean of 6 replicate experiments; error bars represent SD. Analysis performed by $^{\Delta\Delta}$Ct method. Orange dashed line represents normalised *C. albicans*-only biofilm infection control.

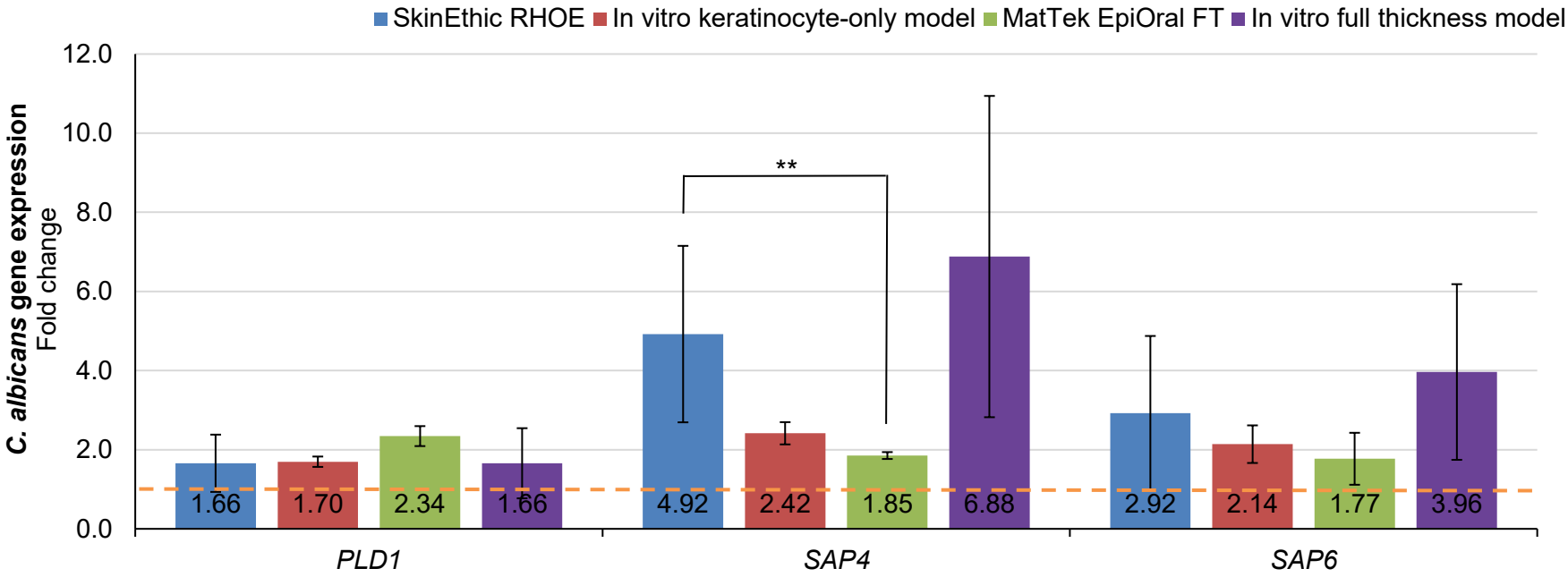

Figure 4.10 *C. albicans* virulence gene expression of mixed-species biofilm infections of tissue models.
Candidal adhesin (*ALS1*, *ALS3*, *EPA1*) genes, hyphal wall protein (*HWP1*) gene, phospholipase D (*PLD1*) gene and secreted aspartyl proteinase (*SAP4*, *SAP6*) genes. Gene expression relative to *C. albicans*-only infection control
Data expressed as mean of 6 replicate experiments; error bars represent SD. Analysis performed by $^{\Delta\Delta}$Ct method. Orange dashed line represents normalised *C. albicans*-only biofilm infection control.

4.3.5 Immune cell responses to bacterial LPS and *C. albicans*

THP-1 monocyte cells were used to evaluate host immune responses to bacterial lipopolysaccharide (LPS), Short-term (0-24h) monocyte cell responses in the form of expression of the genes responsible for the two subunits of the interleukin-23 cytokine; *IL12p40* and *IL23p19*, and dectin-1, and sustained responses (>24h) by measurement of released IL-23 protein in the culture supernatant were evaluated

4.3.5.1 THP-1 monocyte cell gene expression when stimulated with LPS

Previous work by our group has shown that secretion of the IL-12 family of cytokines is up regulated during monocyte challenge, therefore IL-23 was selected as a representative proinflammatory cytokine within this family. The expression of genes responsible for the production of the two IL-23 subunits (*IL12p40* and *IL23p19*) when stimulated with 100 ng/ml LPS (Fig. 4.11) showed some increases after 24h stimulation relative to the unstimulated control cells for both subunits, but these were not statistically significant.

LPS stimulation of THP-1 cells resulted in an immediate decrease in dectin-1 gene expression (Fig. 4.12) relative to unstimulated cells immediately after LPS stimulation and at 4h, whereas following continued stimulation at 24h, a significant ($P<0.05$) increase was then observed. There was some variation in the gene expression of samples at 2h, and although it showed a trend toward a repression of expression, the difference was not statistically significan.

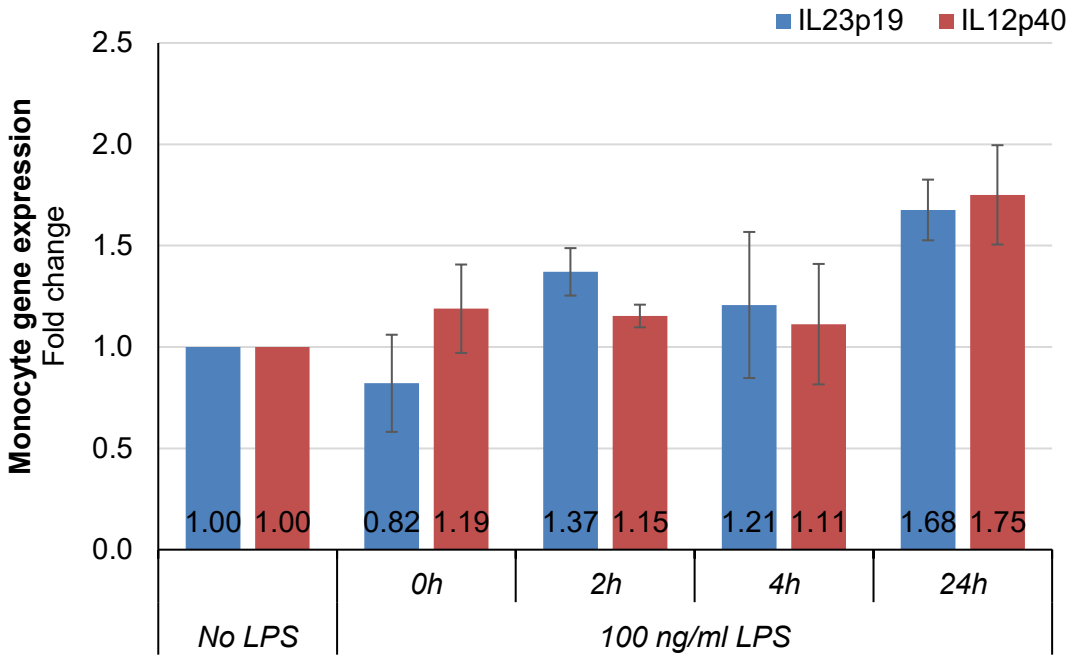

Figure 4.11 Gene expression of monocyte cells in response to stimulation with lipopolysaccharide (LPS)
Expression of the genes coding for the two subunits of IL-23 (*IL23p19* and *IL12p40*) significantly increased over 24h when stimulated with 100 ng/ml LPS

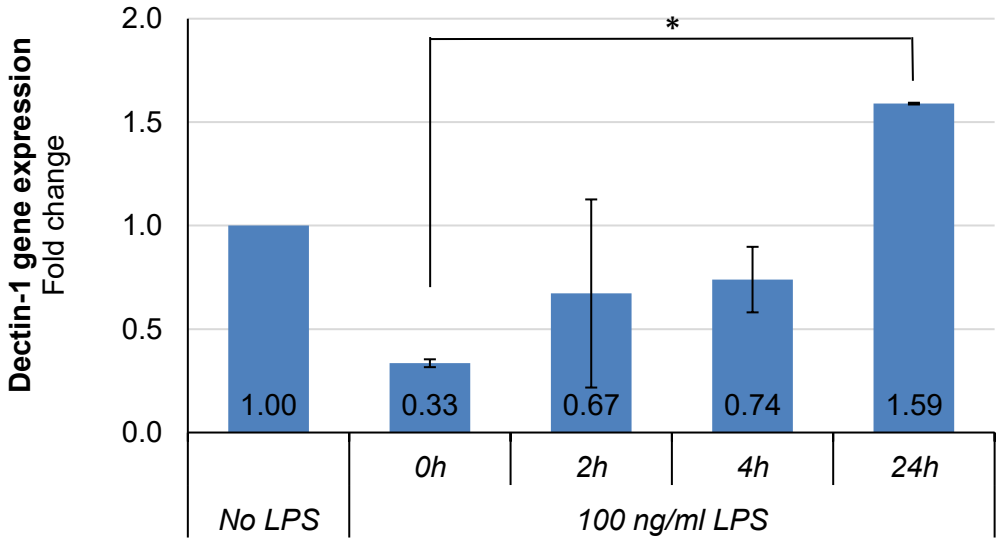

Figure 4.12 Monocyte cell expression of *dectin-1* gene in response to lipopolysaccharide (LPS) stimulation
Expression of the *dectin-1* gene decreased immediately after stimulation, but then increased over time, and showed a significant increase at 24 h compared with 0h cells. *P<0.05

Furthermore, flow cytometry analysis to determine the quantity of dectin-1 surface receptor positive cells resulted in no observed differences between the number of unstimulated and LPS-stimulated cells showing no detection of dectin-1 on the cell surface, irrespective of LPS concentration (Fig. 4.13).

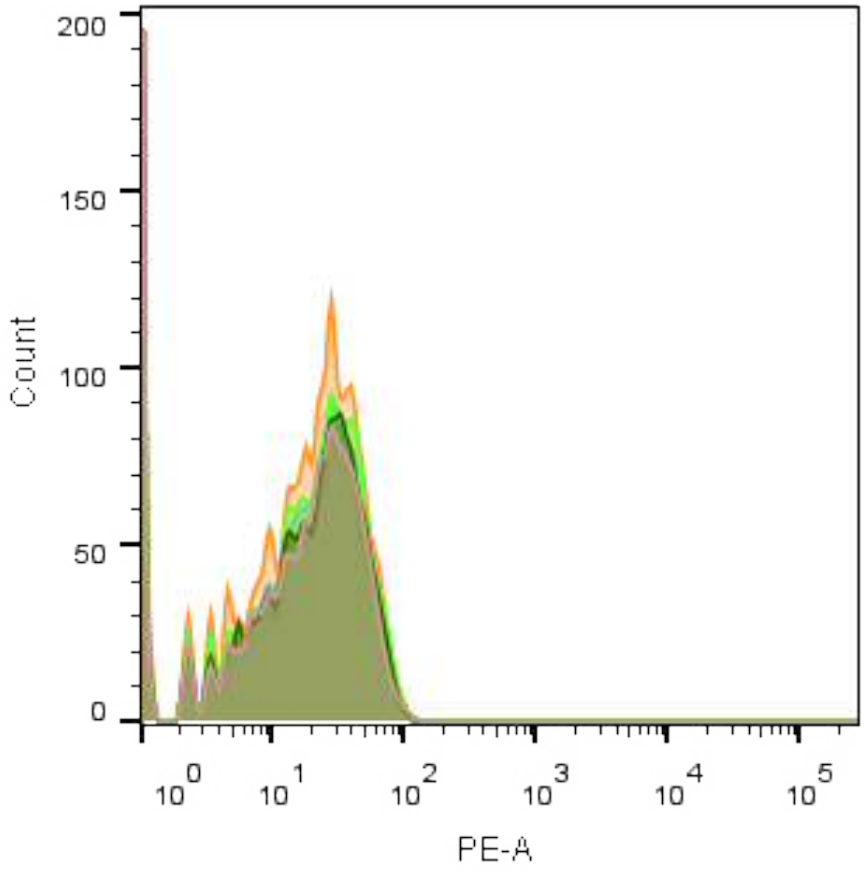

	Sample Name	Subset Name	Count
	Specimen_001_200 LPS 2.fcs	live cells	6560
	Specimen_001_100 LPS 2.fcs	live cells	6545
	Specimen_001_10 LPS 2.fcs	live cells	7419
	Specimen_001_0 LPS 2.fcs	live cells	8528
	Specimen_001_Unstained 2.fc	live cells	6982
	Specimen_001_Isotype 2.fcs	live cells	6131

Figure 4.13 Flow cytometry of THP-1 monocyte cells staining for dectin-1 surface receptor expression
THP-1 monocyte cells were analysed for expression of the *C. albicans* surface receptor dectin-1. Flow cytometry analysis showed no differences in the intensity of fluorescence, and thus the quantity of cells showing expression of the receptor between unstimulated and LPS-stimulated cells, irrespective of the overnight (12-14h) LPS stimulation concentration.

The genes responsible for toll like receptors 2 and 4 (*TLR2*, *TLR4*) showed little change of expression in LPS stimulated cells over the 24h stimulation period (Fig. 4.14). A slight, but not significant, increase in expression was evident at 24h stimulation for *TLR4*, but the overall relative expression returned to a similar level as unstimulated cells thereafter.

4.3.5.2 IL-23 production when stimulated with LPS and *heat* killed *C. albicans*

The production of IL-23 in response to LPS followed a dose dependent pattern. Figure 4.15 demonstrates the responses of monocyte cells to stimulation with LPS and HKC. No IL-23 was detected in unstimulated cells, but in the presence of heat killed *C. albicans* (HKC), a low level was detected (6.31 pg/ml $\pm$ 0.82). When the cells were stimulated with 10 ng/ml LPS, a significant ($P<0.001$) increase in the production of IL-23 was observed (124.98 pg/ml $\pm$ 3.13), and increasing the concentration of LPS to 100 ng/ml resulted in a five-fold increase of the detected IL-23 in the supernatant (689.98 pg/ml $\pm$ 3.09) which was also statistically significant ($P<0.001$).

Co-stimulation of the monocyte cells with 10 ng/ml LPS and HKC resulted in slight fluctuations in the level of detected IL-23 similar to that of the cells stimulated with LPS alone, but no clear pattern with increasing numbers of HKC. However, co-stimulation of cells with 100 ng/ml LPS and HKC resulted in an increase with increasing numbers of HKC, and statistical significance ($P<0.001$) when comparing 100 ng/ml LPS alone, and LPS with 10^7 HKC cells. The biological significance is likely to be limited, as the increase between 10 and 100 ng/ml LPS is far more substantial, whereas the difference of 100 pg/ml of IL-23 is likely to have less of an effect.

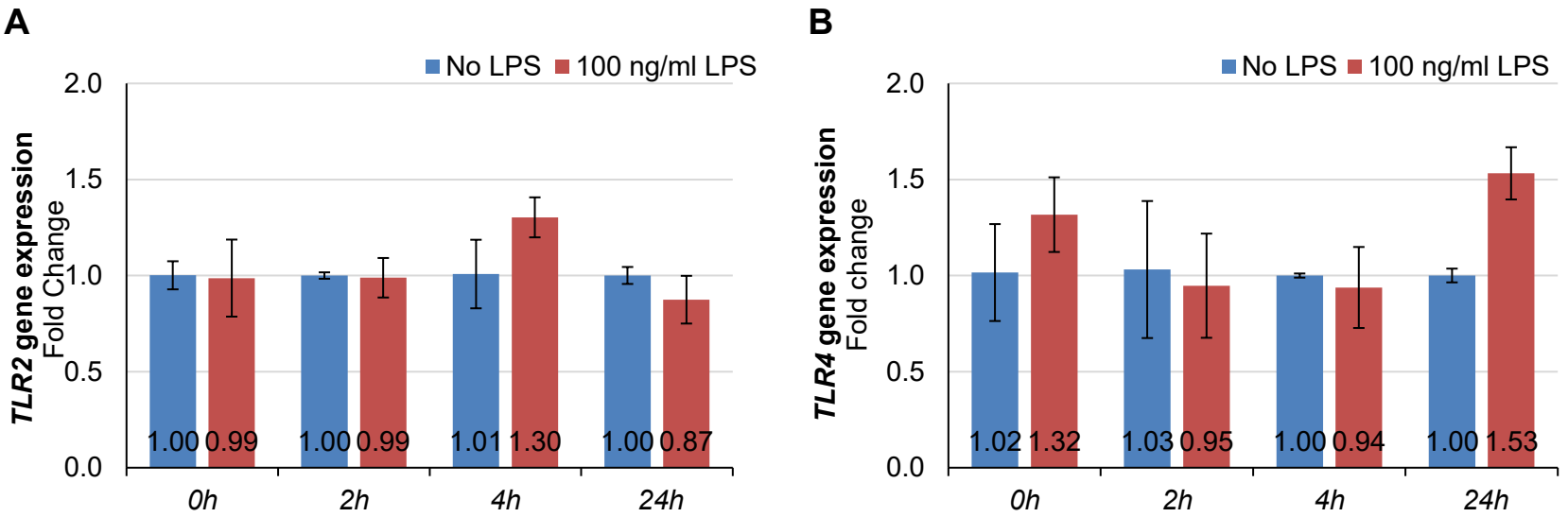

Figure 4.14 Expression of toll like receptors 2 and 4 (*TLR2, TLR4)* genes by monocyte cells in response to lipopolysaccharide (LPS) stimulation.
A) Toll-like receptor 2 gene expression of LPS stimulated cells remained constant relative to an unstimulated control for the 24h period with no significant differences over time. **B)** Toll-like receptor 4 gene expression remained constant up to 4h, but then showed an increase after 24h.
Data expressed as mean of 4 replicates, error bars represent standard deviation.

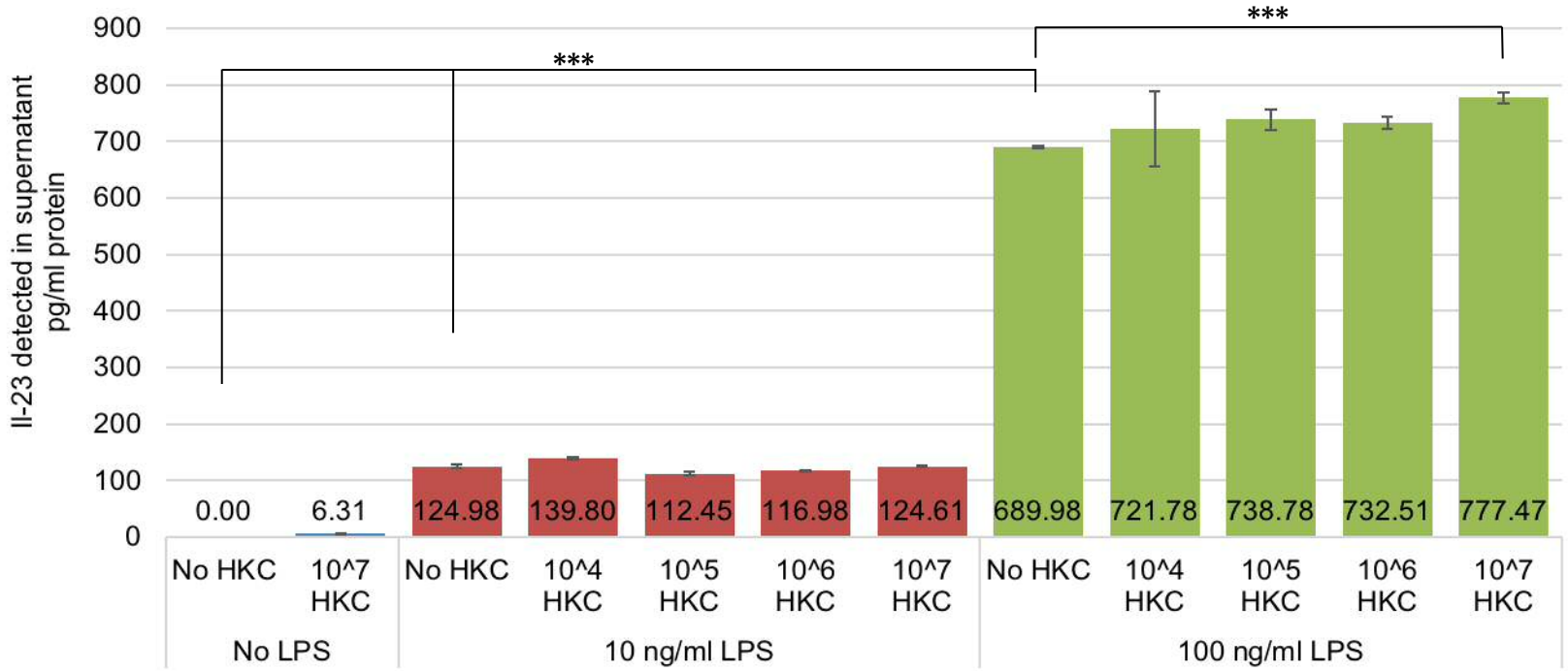

Figure 4.15 Interleukin-23 (IL-23) cytokine release as a result of stimulation of monocyte cells, protein quantification measured by enzyme linked immunosorbent assay (ELISA).
Release of IL-23 cytokine increased in a dose dependent manner with stimulation using LPS, relative to the basal level expression of IL-23 cytokine in unstimulated cells. Stimulation with the higher LPS concentration resulted in a further small increase with increasing numbers of heat killed *C. albicans* (HKC).
Data expressed as mean of 3 replicates, error bars represent standard deviation. ***P<0.001

4.4 Discussion

The use of *in vitro* biofilms is essential to investigate microbial behaviour and interactions, the findings of which can provide many benefits to our basic understanding. The results obtained in Chapter 2 demonstrated that mixed-species biofilms including *C. albicans* and several oral bacterial species can enhance the *in vitro* virulence of *C. albicans*, as suggested by an increase in the proportion of hyphae and an increase in the expression of a number of virulence genes. As denture stomatitis (DS) arises as a result of polymicrobial biofilms on the denture-fitting surface in contact with the palatal mucosa, it was necessary to evaluate these *in vitro* biofilms during infection of tissues, to ascertain whether the observed effects during *in vitro* biofilm interactions, and the upregulation of a range of virulence factors translates to a more destructive and more inflammatory infection. Experiments using monolayers of cells would have been useful, but not as clinically representative as a 3D tissue model, that more closely represents the oral mucosa.

There are a number of tissue models commercially available that could be used for such infection analyses, and have been used extensively by others (Schaller, 2002; Samaranayake *et* al., 2006; Silva *et al*., 2009; Silva *et* al., 2011; Williams *et al*., 2013; Yadev *et al*., 2011) for the investigation of many infections including candidosis. The work in this chapter evaluated infections of 3D tissue models using the *in vitro* biofilms developed in Chapter 2, and certain associated host responses.

The infection of tissue models using biofilms developed *in vitro* the most simplistic representation of the oral mucosa; SkinEthic™ RHOE showed an interesting pattern of results. Relative to the tissues infected with acrylic coupons only (no biofilm), slight tissue damage was induced with bacteria-only biofilms, a further increase in damage, which was statistically significant, caused by *C. albicans*-only biofilms, and a further increase in damage, which was also statistically significant caused by mixed-species biofilms. This pattern of biofilm-related pathogenesis correlated with the expression of *C. albicans* virulence factors in *in vitro* biofilm analyses (Chapter 2). The strong correlation

between virulence and pathogenicity was highlighted by microscopic analysis of histological sections of the infected tissues, where the uninfected tissue model showed no signs of damage, but each of the infections showed some damage, the extent of which is determined by the biofilm used.

Both *C. albicans*-only and bacteria-only biofilm infections induced some damage, and this was evident in the tissue model sections, but the residual biofilms after removal of the acrylic coupon were clustered on the surface of the tissues. The mixed-species biofilms showed substantial damage and extensive invasion through the epithelium. The increase in *C. albicans* hyphae observed in *in vitro* biofilm studies, was also evident in the tissue infections, where the hyphae appear to be responsible for penetration through the cells. It was interesting, however, that there was no upregulation of the *HWP1* gene when evaluating the *C. albicans* virulence genes used throughout this PhD. Hyphae were evident in all mixed-species infections, which correlated with the upregulation of genes involved with hyphae formation, but *HWP1* was not upregulated during these infections. It is known that a number of genes are collectively involved with the regulation of hyphal formation, including *ALS3*, *HWP1* and *HYR1* (Bailey *et al*., 1996), *EFG1* (Sohn *et al*., 2003), the transcriptional regulator *UME6* (Banerjee *et al.,* 2008), *UME6* and *HGC1* (Zheng *et al*., 2004; Lu *et al*., 2015). The expression of *HWP1* is not exclusively responsible for the development of hyphae (Sundstrom, 2006), and therefore, although the expression was not elevated at the time of sampling in this study, and the presence of hyphae was clearly demonstrated in microscopy images, the relative level of expression may have been influenced by other factors in this case. The aim of this study was to compare relative levels of expression of virulence genes between infections of commercial and *in vitro* tissue models of the same type, and there were no significant differences observed with this perspective. Relative abundance of gene expression is important to consider when interpreting qPCR data. Small fold changes in genes with low relative abundance can lead to more substantial phenotypic changes than small changes in genes that are typically highly expressed. The Ct values between qPCR runs can vary due to the differences in starting RNA concentration, but relative values are the same as RNA concentration is standardised within each

reverse transcription. With respect to gene expression of mixed-species biofilm infection of SkinEthic RHOE tissues, *EPA1* (Ct=28.739 ± 0.343) and *HWP1 (*Ct=28.738 ± 0.540) mean Ct were very similar to that of the housekeeping gene *ACT1* (Ct=28.907 ± 0.658). Other virulence genes including *ALS3* (Ct=24.055 ± 0.255), and *PLD1* (Ct=26.157 ± 0.413) had Ct values much lower than *ACT1*, whereas *SAP6* (Ct=23.535 ± 0.263) was substantially lower again indicating an increase in abundance of the gene relative to the *ACT1* gene. The abundance of the *SAP4* gene, however, (Ct=30.274 ± 0.413) was higher than *ACT1* indicating the expression was not what would be considered high in relative abundance.

Adhesion of bacteria to *C. albicans* hyphae, which has been reported previously (Bamford *et* al., 2014; Silverman *et* al., 2010) was evident in *in vitro* biofilms, and is also evident in the tissue models. In the tissue models, the bacteria appear to be invading the tissue along with the *C. albicans* hyphae, in close proximity, suggesting they remain adhered through the invasion process. It is not known which of the bacterial species are adhered, but the sustained adherence could be continually inducing contact-dependent responses and a possible increase in *C. albicans* virulence. This increased virulence may be similar to that observed in Chapter 2, an increase in hydrolytic enzymes, and responsible for the observed tissue damage, or it may be a cooperative effort between bacteria and *C. albicans* and their respective secreted factors

This pattern of biofilm-infection related tissue damage was also evident when using an *in vitro* keratinocyte-only tissue model, where an increase in damage caused by bacteria-only and *C. albicans*-only biofilms, but a further increase in mixed-species biofilms was observed. The correlation between the *in vitro* keratinocyte-only tissue model, and the SkinEthic™ RHOE, show strong similarities between the tissue models in their behaviour during biofilm infection. This was further confirmed with evaluation of the expression of the gene responsible for the pro-inflammatory cytokine IL-18, known to be produced by keratinocytes (Dinarello, 1999). In the case of both SkinEthic™ RHOE, and the *in vitro* keratinocyte tissues, infection with mixed-species

biofilms stimulated an increase in gene expression of the *IL18* gene, more so than was observed with *C. albicans*-only or bacteria-only biofilms.
Full thickness mucosal tissue models included both the epithelium and *lamina propria*. Not only is the physical structure more representative of human oral mucosa *in vivo*, which is more complex than just an epithelium, both the EpiOral FT and *in vitro* full-thickness tissues were cultured using normal human cells, that lack the limitations of cancer-derived cells as used in the epithelial model. However, despite the improvement of the epithelium-only models, these models still do not take into account many other factors present *in vivo*. Langerhans or other immune-associated cells, nerves, endothelial cells all contribute to the structure and normal function of mucosa, but are absent in these tissue models. Subsequent infection responses, while still of academic interest, may not necessarily be entirely representative of an *in vivo* response.

This study evaluated MatTek EpiOral full thickness tissue models, as a representative commercially available full thickness tissue model. Additionally, an *in vitro* full thickness tissue model, established in the School of Clinical Dentistry, University of Sheffield was adopted for use in biofilm infection studies at Cardiff University through collaboration with Dr Craig Murdoch. The same biofilm model was used for the full thickness infections as with keratinocyte-only tissues, and the results follow a remarkably similar pattern. The *C. albicans*-only and bacteria-only biofilms resulted in some tissue damage as evidenced by LDH release, but an increase in damage caused by mixed-species biofilms was evident when compared to these. The characteristic profile of tissue damage was consistent across all tissue models, with invasion only occurring in mixed-species biofilm infections, indicating the increased *C. albicans* virulence did indeed directly lead to increased pathogenicity, irrespective of the infection model used. Similarly, this indicates good comparability between all the tissue models used in this study, within the scope of the analyses completed.

Histological sections of the biofilm-infected full thickness tissues also followed a similar pattern of epithelial damage when analysed by microscopy, but there

was some variation between the *in vitro* and MatTek EpiOral full thickness models. There was significantly more visible damage to the tissues in the *in vitro* full thickness tissues than was observed with the MatTek tissues. The MatTek tissues had been transported for 3 d prior to receipt, which can adversely affect the integrity and viability of the cells within the tissues. MatTek recommend using the tissues immediately, although they suggest tissue viability up to 5 days after shipping, but there is a substantial risk of cornification of the tissues (Eckhart et al., 2013), increasing with time. This is one possibility for this batch of tissues, as there was less visible damage, and less microbial penetration in the mixed-species biofilms than observed in the *in vitro* full thickness tissues, despite there being no initially obvious signs of cornification.

The development of the tissue models, as discussed in Chapter 3, was primarily to overcome the substantial financial costs involved with the use of the commercially available models, to allow a higher throughput of infection analyses. There were similarities between the models in terms of physical structure, progression of infection and associated host responses, but the *in vitro* model appeared more normal in its appearance, where the MatTek EpiOral model had more of a dysplastic appearance..

Microbial penetration and subsequent invasion into tissue models has also been observed by other groups investigating candidosis. Samaranayake *et* al (2006) showed that *C. albicans* can induce damage of SkinEthic™ RHOE tissues, but very little invasion into the tissues was observed in this study, which was also observed in a similar study but using an alternative strain; *C. parapsilosis* completed by Silva *et al*., (2009). Yadev *et al*. (2010) also evaluated RHOE, and MatTek and *in vitro* full thickness tissue models, but not with biofilms as the inoculum. This study found that the hyphae of *C. albicans* SC5314 (which forms hyphae more readily than ATCC 90028, which was used throughout this project) could invade into the tissues, and cause damage. *Candida albicans* was the sole inoculum in this study, and appeared not to invade into the SkinEthic™ RHOE tissues, and although the RHOE showed

responses by production of TNFα, they did not show a significant increase in the production of IL-1β or CXCL8, both of which are also pro-inflammatory, as observed with the other full thickness tissue models. These observations confirmed that the type of tissue model that should be used in any study is dependent upon the anticipated analysis, and driven by the experimental question. In this project, initially, the restricted analysis of tissue damage, microscopic analysis and mRNA analysis for gene expression are sufficient, but in the future, it would be useful to be able to characterise the responses of tissues to different types of biofilm infection. The development of these *in vitro* models therefore allow more analyses to be completed in a more cost effective manner, and these additional parameters can be evaluated.

The responses of full-thickness tissue models, should, in theory, be more representative of normal oral mucosa than keratinocyte-only tissues. The presence of both an epithelium and fibroblast cells would allow for cell-to-cell communication as a result of stimulation by the microorganisms, and the distinct cytokines the different cells produce are known to regulate the production of subsequent cytokines as part of a rounded inflammatory response.

This study did not evaluate additional cytokines known to play a role in inflammatory responses to microbial infection, such as IL-6, IL-10, IL-12, IL-1β, CXCL8, TNFα (Yadev et al., 2011; Wei et al., 2011; Akira et al., 2006; Waelti et al., 1992), but it would be of great interest to characterise the cytokine profile of tissue model responses, particularly with a view to using different biofilm inocula. The work in Chapter 2 also showed that presence of different microorganisms in addition to the mixed-species inoculum can differentially modulate the virulence of *C. albicans*. This bacterial modulation directly influences *C. albicans*, but it is not known whether it can also modulate the host responses. The work in this chapter also showed that immune cells can respond to components of the bacterial cell wall to induce gene expression for cell surface receptors intended to recognise *C. albicans*, so microbial

modulation of host responses would be a beneficial trait for promoting clearance of other organisms, leaving opportunity for some to thrive.

In vitro tissue models used in this study did not contain immune cells, which of course, play a crucial role in clearing infections, and without them, humans would not survive. However, the development of *in vitro* tissue models has not yet reached a point at which they can be viably included in such a model system. It would be very beneficial for these cells to be incorporated into such a system, as their response to cytokines or direct stimuli can be monitored alongside the parameters measured here. Currently, methods of analysis using immune cells are limited to adhered or suspended cells in multi-well plates. This method still has advantages, as the immune cells can be directly stimulated in isolation and their responses evaluated, but in a more complex tissue model, these responses may differ.

This study evaluated host immune responses using suspension cells in multi-well plates described above. The study examined the effects of lipopolysaccharide (LPS, a common component of the cell wall of Gram negative bacteria, of which contribute to denture-associated biofilms within the oral cavity) on the responses of THP-1 monocyte cells. These cells were then also subsequently challenged with heat killed *Candida albicans* (HKC) to evaluate production of a common proinflammatory cytokine, IL-23. An increase in the expression of the genes responsible for both subunits of IL-23 (*IL23p19* and *IL12p40*) were observed (Fig. 4.11) at 24h post-stimulation with LPS, but these were not statistically significant. This increase in gene expression was also observed in the quantification of IL-23 protein when stimulated with the same concentration of LPS. Rogers *et al*. (2013) showed that stimulating monocyte cells with LPS primed them for recognition of *Candida*. A basal level of IL-23 was established with HKC challenge only relative to the normalised unstimulated cells. Significant increases were evident with stimulation with LPS at increasing concentrations, and a further significant increase again was observed at the higher LPS concentration, between LPS alone and 10^7 HKC cells. Interestingly, despite the recognition

of *Candida*, and the increase in the production of IL-23 protein, no differences were evident when evaluating Dectin-1 surface receptor.

Dectin-1 is a c-type lectin membrane-bound receptor for recognition of *Candida*. The receptor recognises β-glucans, which make up approximately 40% of the *Candida* cell wall (Gow *et al*., 2007; Netea *et al*., 2008) and mannans (Shibata *et al*., 2007) which are also targeted by the immune system through receptors such as toll-like receptors 2 and 4 (TL2 and TLR4). The expression of the genes responsible for the dectin-1, TLR2 and TLR4 receptors in monocyte cells was also evaluated. Following stimulation with LPS, statistically significant increases in the expression of genes responsible for dectin-1 and TLR4 were observed after 24 h. Interestingly, no significant increase was evident in the expression of *TLR2*. Furthermore, despite an increase in the expression of the gene responsible for dectin-1, no differences were observed in the presence of the specific surface receptor on the cells, irrespective of stimulation with varying concentrations of LPS. This suggests the cells did not respond to LPS in the expected way. LPS is a very common molecule, and may have contaminated the cells at some point in the past, which may also explain the limited increase in upregulation of the gene observed in the study, although the cell still responds in an anticipated manner with respect to production of cytokines.

There were a number of interesting findings from this study, primarily the differential infection profile of the bacteria-only and *C. albicans*-only versus mixed-species biofilms, and the resultant damage and invasion into the tissues. There are clear directions of future work that have arisen: as discussed in Chapter 2, it is not known which single/dual-species of bacteria result in the increased expression of *C. albicans* virulence factors, and it was shown in this chapter that the mixed-species biofilms, where *C. albicans* virulence factors are enhanced, result in greater tissue damage and invasion into the tissue. Therefore, it is of interest to evaluate not only the monospecies versus mixed-species biofilms in terms of their inter-microbial interations, but also in the tissue infection model. The development of the model in Chapter 3,

and subsequent evaluation of the tissues compared with commercially available models in this chapter, has confirmed the suitability of the tissues, and thus will allow a higher throughput of investigations related to the single-species influence and infection prognosis. Chapter 2 also showed that inclusion of an additional bacterium *Porphyromonas gingivalis* resulted in inhibition of enhancement of the *C. albicans* virulence factors observed with use of the other bacterial species. *P. gingivalis* is a known keystone pathogen, and results in tissue damage in its own right in the case of gingivitis and periodontitis. It would therefore be very interesting to evaluate these biofilms in the tissue infection to see whether the biofilms still had the same level of pathogenicity relative to the mixed-species, or monospecies, and whether the gene expression profile of *C. albicans* virulence factors was the same as *in vitro* biofilms.

Further to this, cytokine and receptor responses are of major interest in order to fully understand the host response to the infection. I would like to follow this up more comprehensively from the perspective of the mixed-species biofilms used in this chapter, that is, to use a screening tool to evaluated an array of cytokines produced by the tissues. This would include other pro and indeed anti-inflammatory cytokines to profile the responses to the different infections. Additionally, inclusion of *P. gingivalis* would also be interesting to establish whether the host responses are further enhanced due to the known pathogenicitiy of *P. gingivalis*, or whether the host response is more toward *C. albicans* in the biofilms, and as such, as the *C. albicans* virulence factors were not upregulated when including *P. gingivalis* in biofilms, the host response would be limited.

Use of THP-1 monocyte cells did not appear to yield much of an insight into whether the cells respond to *C. albicans* and/or LPS in this chapter, but other cell lines are known to respond to stimulation by *C. albicans* and/or LPS, and could be of use in future studies. U937 is another monocytic cell line that has been used to evaluate *C. albicans* infections (Heidenreich *et al*., 1996; Lopez *et al*., 2014), but it would of course be more representative to use primary human monocytic cells as investigated by Lopes *et al*., 2015). As a screening

tool, however, cell lines are good representations of cells that can be used as the primary investigative tool. Further development of the *in vitro* tissue models described in Chapter 3 could incorporate such monocyte cells, and thus, infection with monospecies and mixed-species biofilms could then be used to investigate a more comprehensive range of host responses and tissue infection.

4.5 Conclusions

- Mixed-species biofilms that demonstrated enhanced *C. albicans* virulence also demonstrate increased pathogenicity in oral mucosal tissue model infections
    - Increases in damage, and substantial tissue invasion were observed in mixed species biofilms compared with *C. albicans*-only or bacteria-only biofilms

- The type of tissue model used for infections did not influence *C. albicans* virulence gene expression

- Monocyte stimulation with LPS resulted in increased production of the pro-inflammatory cytokine IL-23, and also when challenged with heat killed *Candida*, but showed little increase in dectin-1 gene expression or expression of the dectin-1 surface receptor when analysed by fluorescent antibody immuncytochemistry

Chapter 5

Metataxonomic analyses of bacterial communities at sites within the oral cavity of denture-wearing patients, presenting with and without denture-associated stomatitis

5.1 Introduction

There is ever increasing interest in the understanding of the microbiomes of various higher organisms, particularly humans, and identifying the changes within the microbiome that leads to the onset of disease or infection. This interest is, in part, fuelled by the view that whilst communities of microorganisms exist naturally at sites in the human body without any negative impact on the host, subtle or substantial changes in the composition of the microbiome can lead to development of infection (Jenkinson *et al*., 2005; Avila *et al*., 2009; Zarco *et al*., 2012; Wade, 2013).

There has been significant recent interest in the influence of the microbiome in maintaining normal bodily function and overall health, particularly concerning the gut or intestinal microbiome (Turnbaugh *et* al., 2009; Turnbaugh & Gordon, 2009; O'Brien *et al*., 2013). Radical treatments have also been offered to 'replenish' the microbiome of sites of interest such as these, including faecal transplantation whereby the colon is cleaned, and processed faecal matter is introduced from a 'normal' or 'healthy' individual with the aim to re-establish a 'normal' microbiome (Turnbaugh & Gordon, 2009; Turnbaugh *et al*., 2009). The efficacy of these treatments appears to be beneficial in the short period that has elapsed since they were introduced, but induced changes of this magnitude of the resident microbiome and the subsequent longer-term effects need to be considered with caution, with little evidence supporting any benefit in the longer-term as yet. Additional human microbiome studies investigating other key sites such as the skin and oral cavity have been completed as part of the Human Microbiome Project (Methé *et al*., 2012).

The oral cavity is an area of extensive interest with respect to the microbiome in health and disease. Various distinct environments and surfaces within the oral cavity can harbour a large array of microorganisms, with each site potentially accommodating a unique microbiome of bacteria, fungi and viruses (Dewhirst *et al.*, 2010; Wade, 2013). Several benefits to the host associated with the presence of microorganisms are known, related to modulation of the local environment which has a subsequent indirect inhibition of the

development of disease including caries (Burne & Marquis, 2000). Additionally, the competition within biofilms that exist at the various locations within the oral cavity help maintain a stationary level of potentially pathogenic microorganisms (Wade, 2013; Kilian *et al*., 2016). Additionally, direct inhibition of pathogenic species has been demonstrated in the intestine (Buffie & Pamer, 2013), where despite distinct microbiomes, the concept of direct microbial self-modulation could also be a factor in play in the oral cavity. The distinct composition of the microbiomes at each oral site shows the adaptability of microorganisms to different surfaces and environmental conditions. Different sites within the oral cavity share common microbial species, but overall have distinct characteristic microbiomes, when compared with other sites of the human body (Costello *et* al., 2009; Bik *et al*., 2010).

The development of Sanger sequencing and related technological advances has allowed microbiome analyses that can identify the composition of microbial communities to species level. Studies indicate that more than 1000 bacterial species have been detected using molecular methods from samples of the oral cavity; including on the surfaces of teeth, oral mucosa, and within saliva (Palmer, 2014; Wade, 2013; Acharya *et al*., 2017), and a database established known as the Human Oral Microbiome Database (HOMD; Dewhirst *et al*., 2010) to facilitate analysis of the substantial data sets. The higher detection of species by molecular methods compared with culture-dependent methods, partly relates to the latter's reliance on specific suitable culture media, specific culture conditions, and the potential requirement for the presence of additional microorganisms to facilitate growth. Furthermore, dying or non-replicating microorganisms may not grow *in vitro* thus limiting their detection by culture. Identification by molecular methods, and indeed using other recent technological advances including proteomics and pyrosequencing (Jenkins, 2011), bypass the requirement of culture, and the microorganisms present even at relatively low proportions can be detected and identified.

Several oral diseases have been attributed to specific microorganisms including *Candida* (causative agent of candidosis), *Streptococcus mutans* (a causative agent of dental caries) and Porphyromonas gingivalis (a species

associated with onset of periodontal disease) (Axelsson & Lindhe, 1981). Detection of these keystone pathogens has focussed treatment strategies toward the pathogenic component, rather than pursuing a broad-spectrum treatment, avoiding potentially untargeted and unnecessary manipulation of the resident microflora.

In addition to our understanding of the importance of the resident microflora in maintaining a state of symbiosis and health in the host, it has been hypothesised that a shift in the prevalence of certain bacterial species within the microbiome of a particular site can contribute to disease progression, as in the case of periodontal disease (Marsh & Bradshaw, 1995). This change of state from symbiosis to dysbiosis can lead to an inflammatory response, subsequently changing environmental conditions in which many other microorganisms can flourish, or conversely, undergo a stress response. These responses and changes in the conditions further exacerbate the disease and can lead to a substantial inflammatory scenario. Tissue damage can occur, and if allowed to persist, can lead to significant tissue destruction and a great burden on the host. Furthermore, the oral microbiome has also been implicated in non-oral diseases (Scannapieco, 1999; Wade, 2013). It is possible for oral microorganisms to bypass typical mucosal membranes and enter the bloodstream through, for example, local trauma to the gingiva or other mucosal site, and serious subsequent infections can occur. Examples of such serious infections include endocarditis (Mylonakis & Calderwood, 2001), and respiratory infections (Sands *et al*., 2017).

Most oral microbiome studies have been focused on the bacterial species of the different sites within the oral cavity, and justifiably so as many oral conditions are attributed to bacteria; periodontitis and caries associated with *P gingivalis* and *S. mutans* respectively (Axelsson & Lindhe, 1981). Fungal and viral infections of the oral cavity are also important, especially in the case of the many clinical presentations of candidosis. In candidoses, the causative agent *Candida* are attributed to the disease, and there are multiple additional factors that also contribute, but the fungal composition of the oral cavity often takes a backseat in *in vitro* and *in vivo* studies. This was the case with the

creation of the oral microbiome database, where bacterial species were solely included in the draft database, and subsequently added to through the years that followed its creation. Some studies have investigated the fungal component of the oral cavity (Ghannoum *et al*., 2010; Ghannoum *et al*., 2013; Mukherjee *et al*., 2014; Dupuy *et al*., 2014), but very few specifically of candidosis-associated dentures (O'Donnell *et al*., 2015; Shi *et al*., 2016). The overall microbiome, including both bacteria and fungi, is necessary for it to be a true representation of the 'microbiome', which strictly speaking should additionally include other microorganisms such as viruses and protozoa. The role of the presence of bacteria in ecological niches such as dentures is an important factor to consider alongside other predisposing factors like diabetes or immune status. As certain bacteria are known to contribute to *C. albicans* virulence as demonstrated in this thesis, it highlights the need to understand the mycobiome and microbiome of dentures as equals.

To further understand the role of the bacterial microbiome in the case of denture-associated stomatitis (DS), was the aim of this study. The approach employed molecular analysis by next generation sequencing of appropriate oral samples. Such samples were obtained from patients with and without clinical presentation of DS and therefore comparisons in the relative microbiomes between these patient cohorts could be made.

The specific aims of the study were:

1. To obtain microbiological samples from patients with and without DS, and use next generation sequencing technologies to characterise the bacterial microbiome of microbiological samples of the tongue, palatal mucosa and denture-fitting surface (in contact with the palate).

2. To determine whether differences in the bacterial microbiome of patients with and without clinical presentation of DS occurred and was assessed by:
    a. Determining whether differences exist in number of unique bacterial species present in patients of each disease grouping.

b. Evaluating richness and evenness of the distribution of bacterial species in patients of each disease grouping.
c. Identifying any species that undergo substantial changes in the relative abundance of each disease grouping that could be attributed to causation of the disease.

5.2 Materials and Methods

Informed consent and recruitment of patients to the clinical study was completed by certified clinicians Dr Helen Rogers and Dr Jeff Wilson.

Processing of the obtained samples was completed by Daniel Morse with assistance from Ms Lucy Marsh (Research Technician, Cardiff University). This included microbiological culture analysis on agar plates and extraction of fungal/bacterial DNA from samples.

Next generation sequencing analysis; sample preparation and sequencing according to the two step protocol detailed in Section 5.2.7 was completed by Research and Testing Laboratories, (RTL, Texas, USA). The sequence data was processed by Dr Ann Smith (Postdoctoral Research Associate, Cardiff University), and data analysed by Dr Smith and Daniel Morse together and independently.

5.2.1 Ethical approval and patient recruitment

5.2.1.1 Research ethics approval

Research ethics committee approval was sought prior to the collection of clinical samples for analysis in this study. Ethical approval was obtained on the 12th February 2014 with the following reference information: Study title: Denture acrylic biofilms: microbial composition, interactions and prevention; *REC reference*: 14/WA/0023*; Protocol number*: SPON 1265-13*; IRAS project ID*: 137108 (Appendix II).

Training courses for the Human Tissue Act, and Principles of Good Clinical Practice were attended prior to the start of clinical sample collection.

5.2.2 Patient recruitment and sample collection

Patients attending the Oral Medicine clinic at the Dental Hospital, Cardiff and Vale NHS Trust, for normal, routine treatment were recruited following informed consent, according to the inclusion/exclusion criteria detailed in Table 5.1. Patient details were recorded and stored along with the signed and dated consent form, and each individual patient assigned a unique identifier, which remained anonymous to the researcher throughout the study. A limited

amount of clinical information was recorded about each patient, and included: gender, age, smoking status, and the presence and the extent of denture stomatitis according to Newton's classification. The clinician then performed a clinical assessment of the palate, and if denture stomatitis was evident, then collected clinical samples for processing in the laboratory. Clinicians who contributed to this aspect of the study included Dr Helen Rogers and Mr Jeff Wilson.

Inclusion Criteria	Exclusion criteria	Period prior to study
≥18 years of age	Antibiotic use	30 days
Able and willing to consent	Steroids (systemic, inhaler)	30 days
Complete upper acrylic denture	Immunosuppressant drugs	30 days
	Receipt of investigational drug	30 days
	Participation in other clinical study	30 days

Table 5.1 Selection criteria for patient recruitment

5.2.3 Clinical sampling

Following recruitment, and before any clinical intervention, swabs and imprint cultures of the patient's tongue, palate and denture fitting surface were obtained by qualified clinicians as detailed above. Sterile Transwab® Amies Charcoal swabs (Medical Wire and Equipment (MWE), Wiltshire, UK) were used to recover microorganisms for DNA extraction, and for isolation of microorganisms for future studies. The swabs were rubbed across the denture fitting surface, tongue and hard palate for 15 s, placed into a sterile container, sealed and transported to the microbiology laboratory for microbial DNA extraction as detailed in the clinical protocol in Appendix I.

For microbial culture, sterile square foam pieces (imprint cultures; measuring approximately 2 cm × 2 cm) were pre-soaked in PBS, then pressed against the denture fitting surface, tongue and hard palate for approximately 30 s, then

overlaid on to SDA and transported to the microbiology laboratory where it was processed immediately upon receipt according to section 5.2.4 and 5.2.5.

Laboratory processing of samples was performed with occasional practical assistance from Ms Lucy Marsh.

5.2.4 Laboratory processing of swab samples

The tip of the swab was carefully separated from the stem (the latter was then discarded), and placed into a sterile bijou container containing 1 mL PBS. The bijou was vortex mixed at 2,500 rev/min for 1 min. The supernatant was collected by pipette, thoroughly mixed and transferred into a sterile centrifuge tube and centrifuged for 2 min at 13,000 × *g* to form a pellet. The supernatant was discarded and 300 µl of sterile PBS was added, and the suspension homogenised by pipetting. The suspension was aliquoted in three sterile microcentrifuge tubes. DNA was extracted from one aliquot as described in section 5.2.4.1, to another was added 20 µl glycerol. All samples were stored at −80°C according to HTA regulations until required for use.

5.2.4.1 Total microbial DNA extraction from clinical swab samples

Bacterial genomic DNA was extracted using a Gentra PureGene Bact/Yeast DNA extraction kit (Qiagen, USA) according to the manufacturer's instructions, and using the Gram-positive bacteria extraction protocol. In brief, the samples were centrifuged for 5 s at 16,000 × *g*. The pellets were re-suspended in 300 µL of Cell Suspension Solution and homogenised by repeat pipetting. Once homogenous, 1.5 µL of Lytic Enzyme Solution was added and the mixture inverted (×25). The tubes were then incubated at 37°C for 30 min. After incubation, the tubes were centrifuged at 16,000 × *g* for 1 min to pellet the cells. The supernatant was carefully removed, then 300 µL of Cell Lysis Solution and 1.5 µL of RNase A Solution added. The solutions were thoroughly mixed to lyse the cells and 100 µL Protein Precipitation Solution was added. The tubes were vortex mixed at 2,500 rev/min for 20 s and then centrifuged for 3 min at 16,000 × g. The supernatant was then aspirated into a clean 1.5 mL microcentrifuge tube containing 300 µL of isopropanol. The tubes were

mixed by inverting (×50) and the mixtures then centrifuged for 1 min at 16,000 × *g*. The supernatant was discarded and the tubes drained on to an absorbent paper. A 300-µL volume of 70% (v/v) ethanol was added to each tube to wash the DNA. The tubes were then centrifuged again for 1 min at 16,000 × *g*, the supernatant discarded and the tubes drained again on absorbent paper, before allowing to air dry for 5 min. Once suitably dry, 100 µL of DNA Hydration Solution was added and the tubes were vortex mixed for 5 s at 1,000 rev/min. The tubes were then incubated at 37°C for 1 h, after which the tubes were transferred to a water bath set to 65°C to dissolve the DNA. The tubes were then placed on an orbital shaker overnight at room temperature (15-25°C), and stored at -20°C prior to subsequent next generation sequencing (NGS). Immediately prior to shipment for NGS, the samples were moved from -20°C and placed into an appropriate transport container on dry ice.

In addition to culture based methods, the presence or absence of *Candida* was evaluated by molecular analysis. The remaining portion of the swab sample for DNA analysis, was used for extraction of yeast DNA for PCR using the Gentra PureGene Bacteria/Yeast DNA extraction kit. The DNA was extracted using the according to the yeast/fungi extraction protocol, which was similar to that of the Gram-positive bacterial extraction protocol, except that the RNase A solution was added after the DNA Hydration Solution as opposed to immediately after Cell Lysis Solution in the Gram-positive bacterial DNA extraction protocol.

5.2.5 Laboratory processing of imprint cultures

The foam imprints were received already placed on the surface of SDA, and were then gently pressed on the agar for 30 s to ensure optimal contact of the foam with the agar. The foam square was then aseptically transferred with sterile tweezers to a blood agar plate and pressed for 30 s and then aseptically transferred to fastidious anaerobe agar. After contact with the FAA surface the imprint was then discarded.

The SDA and BA plates were incubated aerobically at 37°C, and FAA incubated anaerobically at 37 °C until sufficient growth was achieved to isolate and presumptively identify individual colonies by colour and appearance. For samples that were deemed culture positive for *Candida*, representative colonies were further sub-cultured on to CHROMagar® *Candida* medium for presumptive identification of *Candida albicans*.

5.2.6 Identification of microorganisms from clinical samples by molecular methods

The methods described below were performed with the assistance of Ms Raquel Posso under the supervision of Dr Lewis White (Department of Medical Microbiology and PHLS, University Hospital of Wales, Cardiff).

5.2.6.1 Pre-amplification of pan-fungal DNA

Extracted fungal DNA was pre-amplified in a general nested PCR using the RenDX Fungiplex Amplification Kit (Renishaw Diagnostics Ltd, Glasgow, UK) with a final reaction volume of 50 μL. The kit targets a region on the fungal 18S rRNA gene. Each reaction mix contained 5 μL of 10 × PCR buffer, 1 μL $MgCl_2$ (7.5 mM), 4 μL dNTPs (10 mM each nucleotide), 10 μL primer mix (10 mM), 19.5 μL molecular grade water, 0.5 μL *Taq* polymerase enzyme (5 U/μL) and 10 μL of the extracted DNA template. Target DNA was amplified using the following thermal cycling protocol: 95 °C for 15 min, followed by 45 cycles of 94°C for 30 s, 58°C for 30 s and 72°C for 30 s. A final elongation step of 72°C for 7 min was also performed. The samples were held at 4°C until required for the next stage of amplification.

5.2.6.2 Real-time PCR of pre-amplified DNA

Amplified samples were subjected to a second round of probe-based real-time PCR to amplify regions of the internal transcribed spacer (ITS) region (located between 18S and 5.8S rRNA genes) that were specific to *C. albicans*, *C. krusei* and *C. glabrata*. The primers are detailed in table 5.2.

Primer/probe name (target)	Sequence (5' → 3')	Melting temp. (°C)
L18R	GCC-TGC-TTT-GAA-CAC-TCT	54.0
L18F	CTC-GTA-GTT-GAA-CCT-TGG	54.0
Pan-*Candida*	ATC-TTT-TTG-ATG-CGT-ACT-GGA-CCC-TG	52.9
C. glabrata	GGC-TAA-CCC-CAA-GTC-CTT-GTG-GCT-T	55.9
C. krusei	TAC-CTA-TGG-TAA-GCA-CTG-TTG-CGG-C	54.2

Table 5.2 Primer sequences for *Candida* detection of clinical samples by nested-PCR

Primers L18R and L18F, and probes pan-*Candida*, *C. glabrata*-specific and *C. krusei*-specific

DNA samples were amplified using LightCycler FastStart DNA Master HybProbe (Roche Diagnostics, Sussex, UK), and contained 2.5 μL of hybridisation mix, 3 μL $MgCl_2$, 15 μL nuclease free, molecular grade water, 2.5 μL primer/probe mix and 2 μL template DNA. The preparations were homogenised by brief vortex mixing. The DNA was amplified using the following thermal cycling protocol: 95°C for 15 min, followed by 30 cycles of 95°C for 15 s, then 58°C for 30 s. Amplicons were detected using the following fluorescence probes FAM (green), JOE (yellow) and ROX (orange) for detection of pan-*Candida* species, *C. glabrata* and *C. krusei*, respectively.

5.2.7 Metataxonomic profiling of bacterial microbiome of clinical swab samples using the Illumina MiSeq two stage amplification protocol

Bacterial DNA samples were transported on dry ice to Research and Testing Laboratories (RTL, Texas, USA) for NGS, and upon receipt, were processed according to a standard operating procedure used by RTL. The method was based on an Illumina 2-step protocol as outlined below by trained staff members at RTL. The resulting sequence data was provided in fasta file format, and analysed in conjunction with Dr Ann Smith (Postdoctoral Research Associate in bioinformatics, School of Biosciences, Cardiff University).

5.2.7.1 Primary stage amplification

The forward primer was constructed with (5'-3') the Illumina i5 sequencing primer (TCGTCGGCAGCGTCAGATGTGTATAAGAGACAG) and the 28F primer (GAGTTTGATCNTGGCTCAG), and the reverse primer was constructed with (5'-3') the Illumina i7 sequencing primer (GTCTCGTGGGCTCGGAGATGTGTATAAGAGACAG) and the 388R primer (TGCTGCCTCCCGTAGGAGT). Reactions were performed using ABI Veriti thermocyclers (Applied Biosystems, California, USA) in a 25 μL final volume comprising 22 μL Qiagen HotStar *Taq* master mix (Qiagen Inc. California, USA), 1 μL of each primer (5 μM) and 1 μL DNA template. The thermal cycling protocol was: 95°C for 5 min, then 25 cycles of 94°C for 30 s, 54°C for 40 s, 72°C for 1 min, followed by one final cycle of 72°C for 10 min, then the products were held at 4°C. This primary amplification generated multiple 250 bp sequences, which overlap at the V4 region of the 16S rRNA gene.

5.2.7.2 Second stage amplification

Products from the first stage amplification were added to a second PCR, based on qualitatively determined concentrations. Primers for the second PCR were designed based on the Illumina Nextera PCR primers and were as follows: Forward - AATGATACGGCGACCACCGAGATCTACAC[i5index]TCGTCGGCAGCGTC and Reverse - CAAGCAGAAGACGGCATACGAGAT[i7index]GTCTCGTGGGCTCGG. The thermal cycling protocol for this second stage amplification was the same as the first, but involved 10 cycles.

5.2.7.3 Standardisation of PCR products for next-generation sequencing

Amplification products were initially visualised with eGels (Life Technologies, New York, USA). Products were then pooled at equimolar concentrations and each pool was size selected in two rounds using Agencourt AMPure XP (BeckmanCoulter, Indiana, USA) in a 0.7 ratio for both rounds. Size selected pools were then quantified using the Quibit 2.0 fluorimeter (Life Technologies)

and loaded on an Illumina MiSeq (Illumina, Inc., California, USA) 2 × 300 flow cell at 10 pM.

5.2.7.4 Preparation of sequence library

The sequencing data was obtained in FASTA file format, and processed according to the MOTHUR pipeline (Schloss *et al*., 2009). Briefly, the forward and reverse sequences for each unique sample were aligned, made into contigs and enumerated; then ambiguous sequences were removed. The remaining sequences were re-aligned and counted again, then aligned to a reference database. The sequences were then trimmed to remove ambiguous base calls, chimeras or sequences outside of the required base pair length. The undesirable sequences (those that were not specific for bacteria) were then filtered to identify, and removed. Sequences were clustered into operational taxonomic units (OTUs). Using the USEARCH algorithm and the Ribosomal Database Project (RDP) database (Edgar, 2010), the resulting taxonomy was determined to 97% similarity at species level. Those OTUs with less than 97% sequence similarity to a bacterial species in the database were classified only to genus level

5.2.7.5 Data analysis

Once the data was taxonomically assigned, a number of analyses were completed using a range of statistical programs. Firstly, the shared OTU file was used to determine the frequency at which each OTU was observed in the samples, and thus the occurrence of each bacterial species. The analyses included the Shannon and Chao indices using R (version 3.3.1, R Development Core Team, 2008), where samples were compared according to diversity, species abundance and similarities. Bray-Curtis distance measure (measurement of dissimilarity) using the STAMP program script (Parks & Beiko, 2010) was also used to create dendograms of phylogenetic trees. Weighted Unifrac distance matrices were analysed in R using non-metric multidimensional scaling (NMDS) plots, where OTUs were grouped by similarity, and clustered to determine whether there is a distinction between the different patient groupings.

5.2.7.6 Community analysis of individual bacterial species

After phylotypic assignment to bacterial species, the absolute occurrence (number of sequence reads) of the OTUs was transformed into relative occurrence for comparison with other samples.

Relative proportions of specific bacterial species expressed as a percentage of the overall community were compared within each sample site, to determine whether changes in the abundance of specific bacterial species could be attributed to the incidence of DS.

5.3 Results

5.3.1 Patient demographics

Tables 55.3 and 5.4 summarise the demographics and recorded clinical information of the 19 patients recruited to the study. More females (n=11, 57.9%) were recruited to the study than males (n=8, 42.1%), and similar average ages 69.64 yrs (±13.84) and 64.88 yrs (±7.14) were evident for females and males, respectively. Of the recruited patients, eight (42.1%) were current smokers.

Eight (42.1%) patients showed clinical presentation of DS to varying extent, of which six were female (75%, 31.58% of total) and two were male (25%, 10.53% of total). Eleven (57.9%) individuals had no signs of DS (Female n=5, 45.5%, 26.32% of total; Male n=6, 54.5%, 31.58% of total).

Samples from each patient were assigned an anonymised reference number (S001-S019) upon sampling, to which each patient is referred herein.

5.3.2 Detection of *Candida* species in samples

Both swab and imprint culture methods for determining *Candida* in clinical samples resulted in varied detection of *Candida* species as shown in table 5.5. The agar culture method from foam imprints resulted in positive detection of *Candida* species in 9 (47.37%) individuals, whereas the molecular method of nested real-time PCR resulted in detection of *Candida* species in 11 (57.89%) individuals. Samples of the tongue, palate and denture surface from 3 individuals of the overall cohort were not tested using the molecular method. Samples of the palate from patients 9, 11 and 12, and the denture surface of patients 10 and 14 were also not tested by this method due to the requirement of additional samples for next generation sequencing.

Interestingly, several samples that did not yield *Candida* growth by agar culture, did ultimately result in positive detection using nested real-time PCR. These samples were S003D, S006P and S006D, S007T and S007D, S008T, S008P and S008D, S0013D, S0014P and S0015D (where T refers to tongue

sample site, P is palatal mucosa sample site, and D is denture surface). Additionally, although sample S0014T was positive for *Candida* by agar culture, it was not detected using the nested real-time PCR method.

	Total n	Female	Male	Mean age		*Candida* presence	Smoker
				Female	Male		
DS	**8** (42.11%)	**6** (75%) (31.58% of total)	**2** (25%) (10.53% of total)	**67.00** (±17.57)	**70.00** (±7.07)	**6** (75%)	**5** (62.5%)
NS	**11** (57.89%)	**5** (45.45%) (26.32% of total)	**6** (54.54%) (31.58% of total)	**72.80** (±8.38)	**63.17** (±6.88)	**8** (72.72%)	**3** (27.27%)
Total	**19**	**11**	**8**	**69.64** (±13.84)	**64.88** (±7.14)	**14**	**8**

Table 5.3 Demographics and key outcome measures of recruited individuals.

Total number of patients recruited n=19 (Female n=11, Male n=8)

Patient ID	Gender	Age (yrs)	Tobacco smoker	Denture stomatitis	
				Present	Newton's Classification
S001	Female	59	Yes	No	0
S002	Female	66	No	Yes	1
S003	Male	66	No	No	0
S004	Male	66	No	No	0
S005	Male	52	Yes	No	0
S006	Male	64	No	No	0
S007	Female	67	No	Yes	1
S008	Female	75	No	No	0
S009	Male	72	Yes	No	0
S010	Female	74	Yes	Yes	2
S011	Female	36	Yes	Yes	1
S012	Female	81	No	No	0
S013	Male	75	Yes	Yes	3
S014	Male	65	Yes	Yes	2
S015	Female	72	No	No	0
S016	Female	90	No	Yes	2
S017	Male	59	No	No	0
S018	Female	77	No	No	0
S019	Female	69	Yes	Yes	2

Table 5.4 Patient specific clinical information recorded during recruitment

Patient ID	*Candida* presence			Presumptive *Candida* species identification (CHROMagar/RT-PCR)
	Tongue (Culture/PCR)	Palate (Culture/PCR)	Denture (Culture/PCR)	
S001	+ / NT	+ / NT	+ / NT	*C. albicans*
S002	- / NT	- / NT	- / NT	-
S003	- / -	- / -	- / +	*C. albicans*
S004	+ / +	+ / +	- / +	*C. albicans*
S005	+ / +	+ / +	- / -	*C. albicans*
S006	- / -	- / +	- / +	*C. albicans*
S007	- / +	- / -	- / +	*C. albicans*
S008	- / +	- / +	- / +	*C. albicans*
S009	- / +	+ / NT	- / +	*C. albicans*
S010	- / +	- / +	+ / NT	*C. albicans*
S011	+ / +	+ / NT	+ / +	*C. albicans*
S012	+ / +	+ / NT	+ / +	*C. albicans*
S013	- / -	- / -	- / +	*C. albicans*
S014	+ / -	- / +	+ / NT	*C. albicans*
S015	- / -	- / -	- / +	*C. albicans*
S016	- / -	- / -	- / -	-
S017	- / -	- / -	- / -	-
S018	- / -	- / -	- / -	-
S019	+ / NT	+ / NT	+ / NT	*C. albicans*

Table 5.5 Evaluation of *Candida* presence and presumptive identification by culture and PCR

Candida presence (+) or absence (-) determined by positive agar culture and real-time PCR identification. Samples not tested by real-time PCR are denoted by NT. Samples that were positive by culture were further subcultured onto CHROMagar® *Candida* for presumptive identification of *Candida* species

Those samples that were positive for *Candida* species either by culture and/or nested real-time PCR (n=14) were subsequently used for analyses by next generation sequencing. It is accepted that for the infection to be considered candidosis, that *Candida* species will be present, as opposed to other causes of palatal inflammation.

5.3.3 Identification of detected *Candida* species

From each sample type (*e.g.* tongue, palate or denture) on Sabouraud dextrose agar, several typical colonies were subcultured on to CHROMagar® *Candida* agar as described in section 5.2.5. The agars were incubated for 48 h, after which, a turquoise/green colour was observed for each subculture streak, indicating the presumptive presence of *Candida albicans* within samples. No other colour was observed for any streak cultured on this agar.

The molecular method of nested real-time PCR also used primers to amplify the ITS regions of the 18S rRNA considered to be conserved within species, and thus identify *Candida* in samples to species level. Amplicons were observed in the pan-*Candida* channel for numerous samples, but no detection was evident in the *C. glabrata* or *C. krusei* probe channels, thus eliminating the presence of these species. These results, in addition to those of culture, indicated the presence of *C. albicans* within all *Candida* positive samples.

5.3.4 Metataxonomic profiling of bacterial species present in swab samples

The raw data obtained from the next generation sequencing analysis, post-processing and phylotypic assignment can be found in Appendix III.

5.3.4.1 Primary analysis of sequence reads

From the 57 samples from 19 patients, 2 were not analysed by sequencing (these samples were pooled together in the laboratory and thus not available for NGS), and 5 failed to yield amplicons at the primary step. A total of 2,194,967 sequence reads were obtained from the remaining 50 samples prior to quality control of the FASTA file data.

Quality control steps resulted in the removal of some sequence reads, and the total number of final reads was 1,864,575. The number of reads for each sample ranged from 133,846 (S003_D) to 10,995 (S019_P), and to normalise the data between samples and to avoid sample size bias, the operational taxonomic units (OTUs) were sub-sampled to the lowest read count (S019_P) of 10,995 reads.

Once normalised, patients were grouped based on the presence or absence of DS (groupings named DS and NoDS, respectively) and analysed. In total, 2,411 OTUs were identified, 353 of which had more than ten sequence reads. Bacterial species with a minimum of ten sequence reads were included in the analysis, as the OTUs with read counts below this were not considered truly representative of bacterial species content. Some OTUs when phylotypically assigned were determined to be the same bacterial species, but resulted due to intra-strain sequence variation. Thus,
for analysis of the composition of communities to species-level, such multiple OTUs representing the same bacterial species were consolidated into a single species unit, so the number of bacterial species present in the samples was lower than that of the number of OTUs detected.

5.3.4.2 Analysis of OTUs between sample sites

Each distinct OTU was considered specific to a single bacterial species for the purpose of this analysis. However, multiple OTUs can be assigned to a single bacterial species (different strains of the same species can generate different sequences), therefore the analysis was separated into OTU-wide (Shannon and Chao indices, section 5.2.8.5) analysis and post-consolidation species-specific analysis (section 5.2.8.6).

The Chao index is an indicator of ecological diversity within a sample and compares the number of unique OTUs present between sample groups; the Shannon diversity index characterises the community diversity by taking into account the abundance and the evenness of spread of the OTUs. The values associated with the Shannon diversity index are an indication of the

commonality of, in this case, OTUs. Thus, the more unequal the abundances of the OTUs in the samples, the larger the weighed value, and so the resultant Shannon index value is smaller. For example, if the vast majority of samples were associated with one OTU, with very few others, irrespective of total number of the other OTUs, the Shannon index would be close to zero, whereas in cases where there was a more even distribution of frequency of OTUs, the Shannon index would be higher.

Non-metric multidimensional scaling (NMDS), a method for determining differences between the microbial communities of individual samples was also performed for the OTUs using the UniFrac weighted matrix (a measure of phylogenetic community distances). The data was presented as a scatter plot, and grouped by denture, palate, and tongue site. Additionally, phylogenetic heat maps of the microbiome to species level were compiled to further assess community distances in each sample within the groups.

5.3.4.3 Diversity of bacteria detected at each sample site

A large number of unique OTUs were detected for all sample sites, but it was also noted that there was a large range variation between samples and sample sites. The number of unique OTUs in denture samples ranged from 145 to 382 (DS: 145-359, NoDS: 156-382), whereas a much larger range was observed in the palate (overall: 88-549; DS: 88-207, NoDS: 181-549) and the tongue (overall: 89-448; DS: 89-311, NoDS: 136-448). Interestingly, despite only having a small cohort of DS samples from the denture (n=5), three of these showed a very similar number of unique species (203, 216, 223), with the remaining two showing a much higher (359) or lower (146) number of OTUs. However, this was not evident in the palatal NoDS samples (also n=5), which showed a more even spread of values between the highest and lowest. It appeared as though the DS samples of each site not only showed a narrower range of the number of unique OTUs, but also a lower overall number of OTUs than the NoDS samples.

Figures 5.1A, 5.2A and 5.3A show the Chao indices for the denture, palate and tongue respectively. Comparing DS samples with NoDS samples, T-tests (at 95% confidence) showed no significant differences in either the denture (P=0.806) or palatal (P=0.104) samples, whereas the tongue did show a significantly (P=0.007) larger overall number of unique OTUs in the NoDS samples compared with the DS samples.

Additionally, when evaluating differences in the bacterial microbiome profiles within patient groups with STAMP software using Fisher's exact test with Benjamini-Hochber corrections, no significant differences were observed for any sample site.

5.3.4.4 Bacterial diversity by abundance and evenness of spread – Shannon index

Analysis with the Shannon index resulted in no significant differences when comparing DS with NoDS samples and for all sites (denture P=623, palate P=0.318, tongue P= 0.222). NoDS samples, in general, appeared to show an overall Shannon index value higher than that of DS samples, indicating the frequency of OTUs were more evenly distributed across the whole population, thus less clustering of higher relative abundance associated with a smaller group of bacterial species.

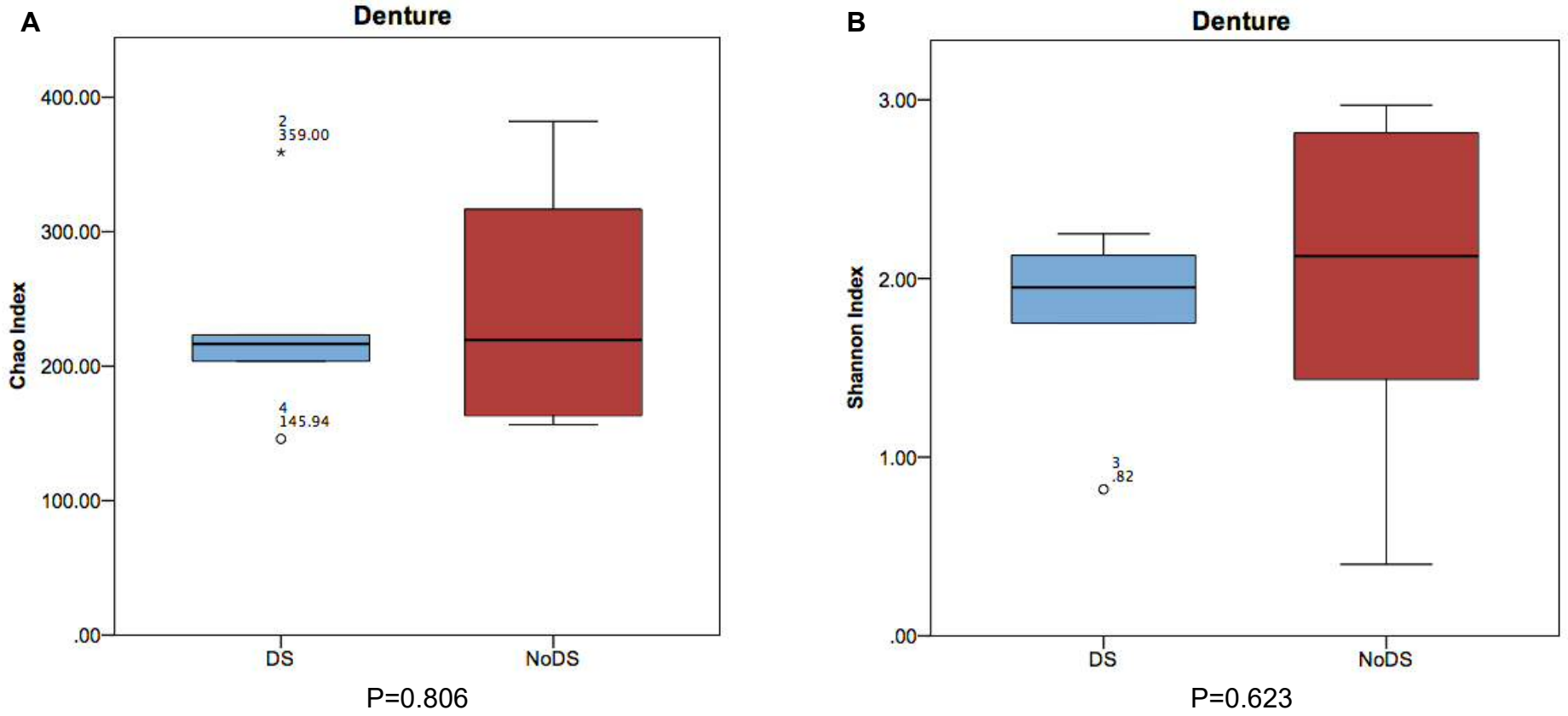

Figure 5.1 Box and whisker plot comparing the number of unique bacterial species (Chao index) and diversity (Shannon index) detected in samples of the denture-fitting surface between DS and NoDS patients

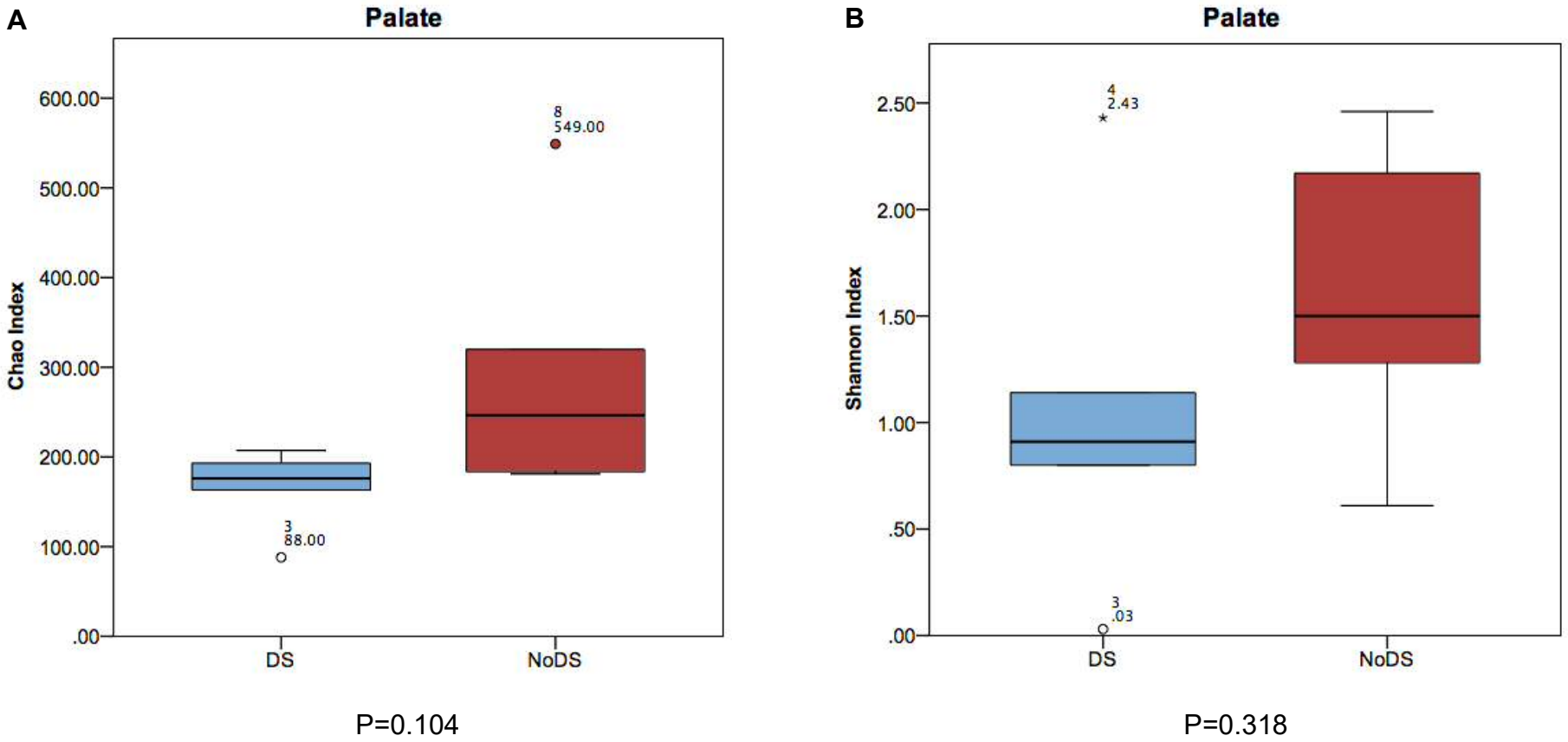

P=0.104

P=0.318

Figure 5.2 Box and whisker plot comparing the number of unique bacterial species (Chao index) and diversity (Shannon index) detected in samples of the palatal mucosa surface between DS and NoDS patients

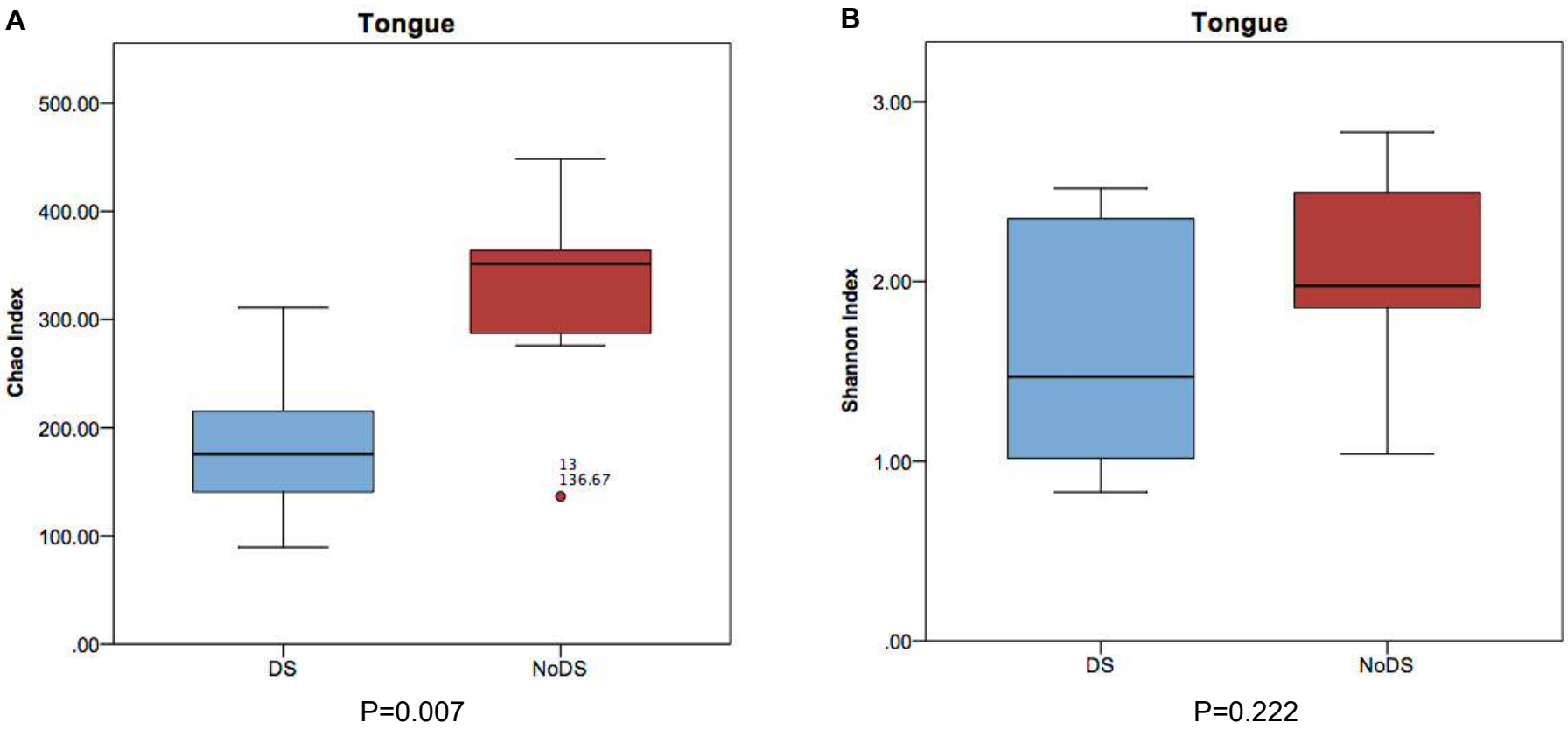

Figure 5.3 Box and whisker plot comparing the number of unique bacterial species (Chao index) and diversity (Shannon index) detected in samples of the tongue between DS and NoDS patients.

5.3.4.5 Similarity of patient groups by grouping using non-metric multidimensional scaling (NMDS) plots

The NMDS scatter plots provided an indication of the cluster groupings of the sample within groups, to determine whether they were distinct from each other. Fig. 5.4 shows the DS and NoDS groups overlap to a large extent with respect to samples of every sample site, suggesting that they were not dissimilar in diversity.

It also appeared as though there is less general bacterial diversity for DS samples than NoDS for when considering all OTU analyses performed.

5.3.4.6 Phylotypic distancing analysis demonstrated with Bray's heatmap dendograms to determine group similarities

Similarity or distinctness of the bacterial microbiomes for each specific sample site was determined with the use of dendograms. The tree-like structure indicated similarities by grouping those phylotypically most closely related to each other (Figs. 5.5, 5.6, 5.7).

The overall finding with all sample sites was that there were no distinct groupings of samples from patients with or without DS. This suggested that the microbiomes were not that distinct from each other, although there were more defined clusters of samples in samples of the tongue (Fig. 5.7).

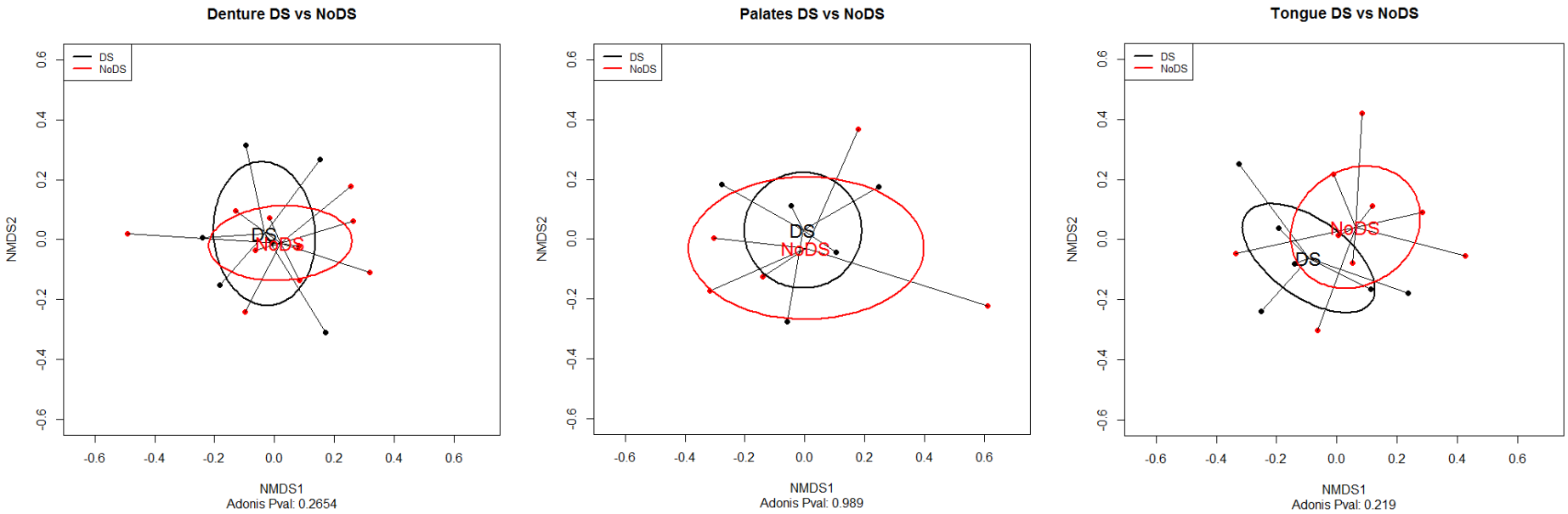

Figure 5.4 Nonmetric multidimensional scaling (NMDS) comparison of the bacterial microbiomes of denture surfaces for patients with (DS) and without (NoDS)
Scatter graph showing differences of samples by patient groups. Overlapping clusters indicated strong similarities between DS and NoDS samples when considered as a group.

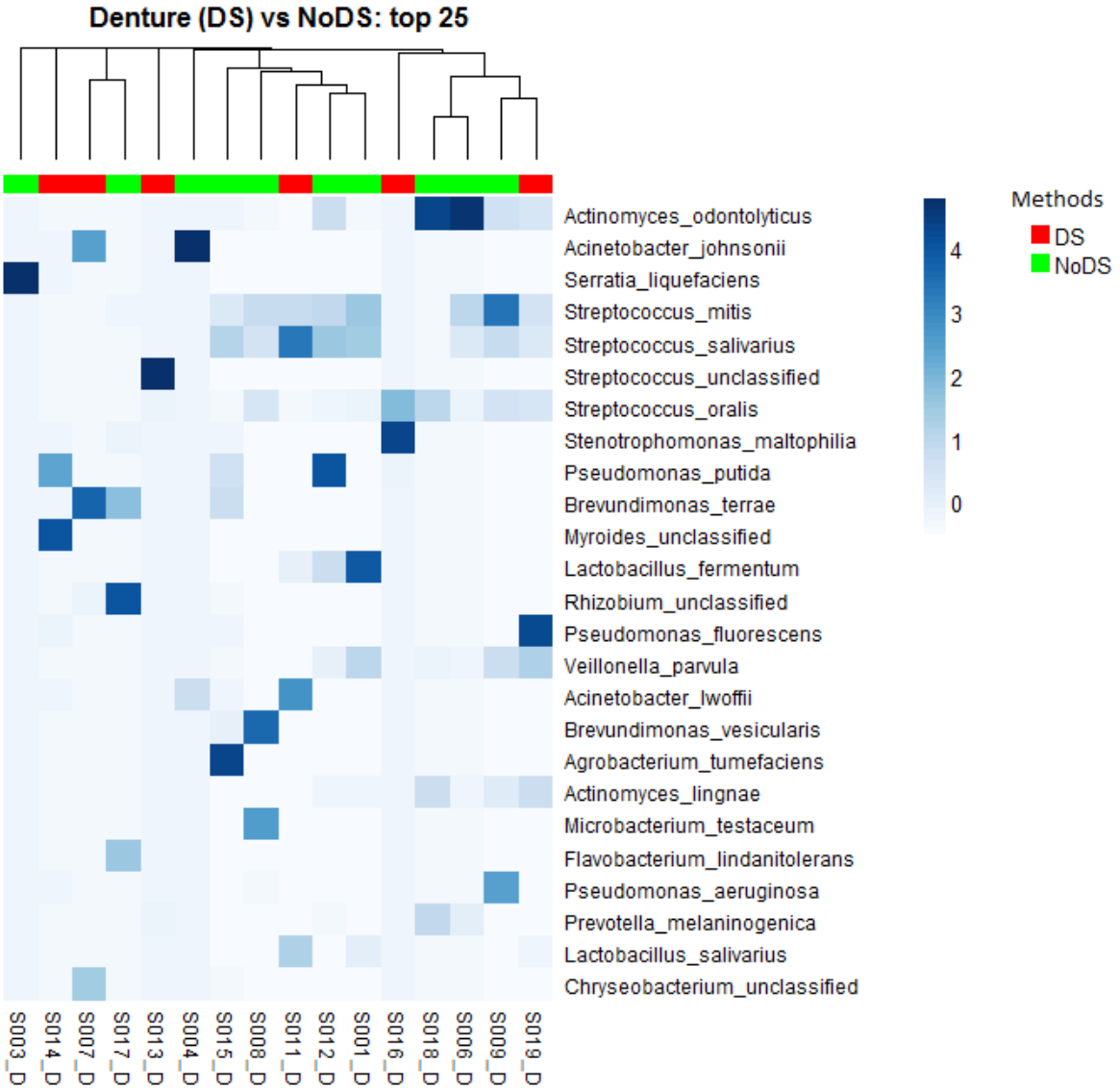

Figure 5.5 Heat map and dendrogram according to the relative abundance and overlap of OTUs in samples of the denture-fitting surface
Relative abundance ranges from low abundance (pale blue) to high abundance (dark blue).

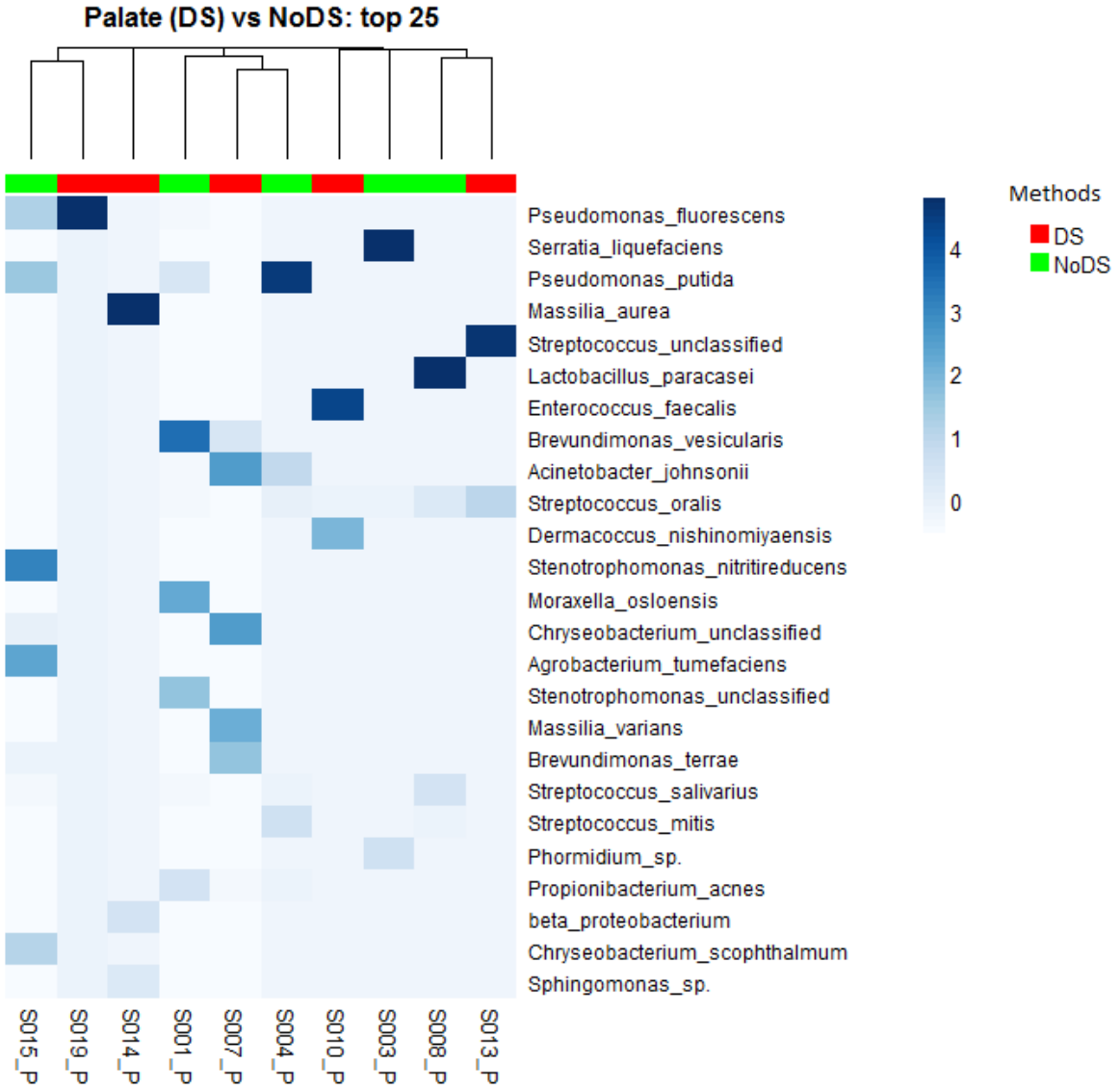

Figure 5.6 Heat map and dendrogram according to the relative abundance and overlap of OTUs in samples of the palatal mucosa surface
Relative abundance ranges from low abundance (pale blue) to high abundance (dark blue).

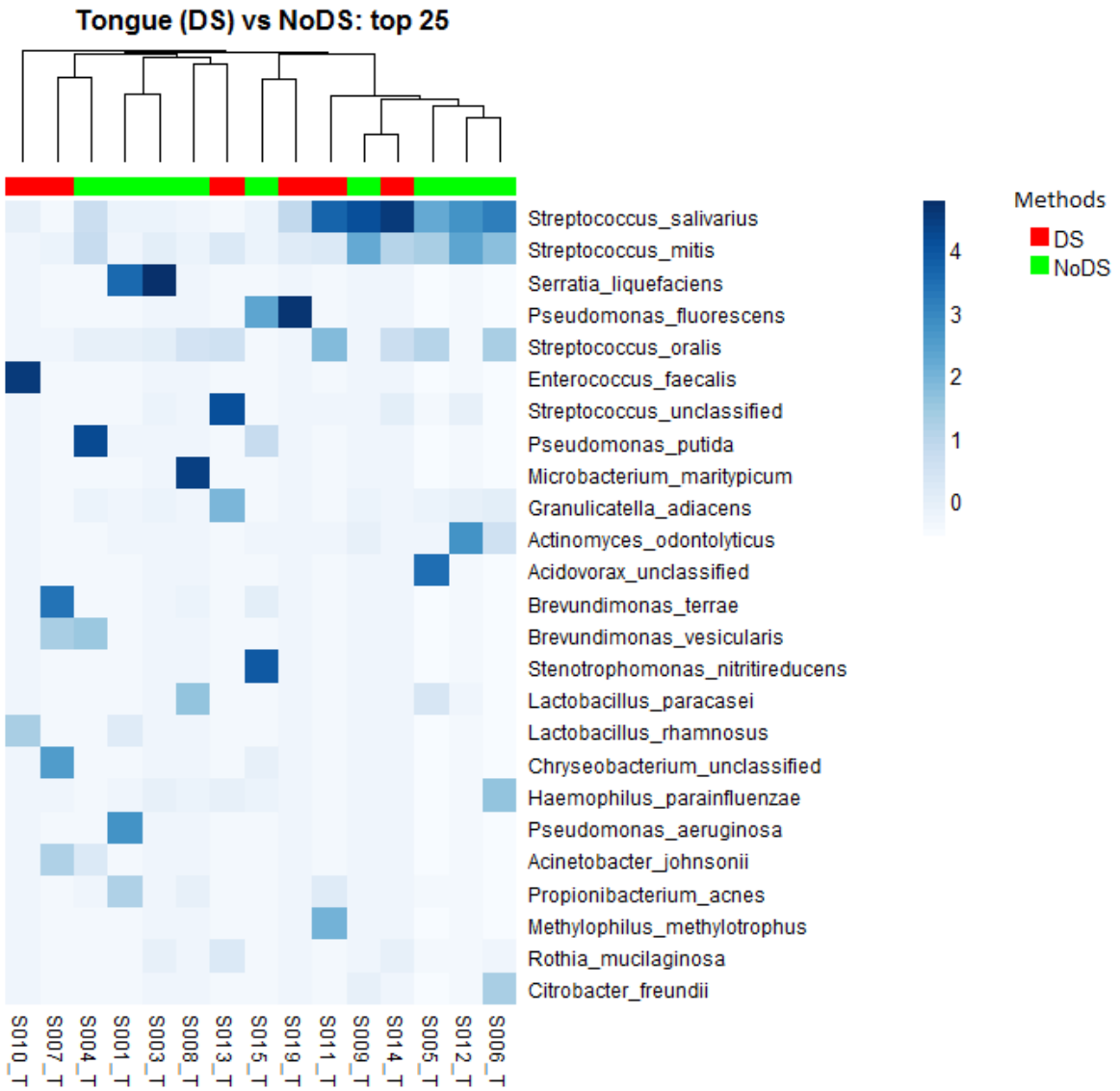

Figure 5.7 Heat map and dendrogram according to the relative abundance and overlap of OTUs in samples of the tongue
Relative abundance ranges from low abundance (pale blue) to high abundance (dark blue).

5.3.5 Presence and differences in relative abundance of bacterial species detected at each sample site

The top 25 bacterial species present at each sample site (*i.e.* denture, palate, and tongue) were compared for DS and NoDS (Tables 5.6, 5.7, 5.8) to determine whether occurrence of DS was associated not only with *Candida* but also the presence or absence, or abundance of certain bacterial species. Differences were evident in the top 25 bacterial species for all sample sites. Additionally, the top ten common species (which, for some samples in the groups included bacterial species outside of the top 25) also varied in abundance.

5.3.5.1 Bacterial species on the denture surface

In total, 338 bacterial species were identified from all samples obtained from the palate; 166 in DS samples, of which 60 (36.1%) were unique to the DS group, and 172 in NoDS samples, of which 64 (37.2%) were unique to the NoDS group. As detailed in table 5.6, the top 25 bacterial species by average abundance (%) represented approximately 92% (DS) and 85% (NoDS) of all bacterial species identified within the samples. The highest average abundance of individual bacterial species was similar between DS (*Streptococcus species,* 14.24%) and NoDS (*Serratia liquefaciens*, 13.59%), and there were five bacterial species unique to the DS group, compared with two unique species to the NoDS group.

Of the top 25 bacterial species in each DS and NoDS groups, 10 common species were detected in both groups (Fig. 5.8), but differences in the relative abundance of each species was evident. *Acinetobacter johnsonii, Streptococcus mitis* and *Actinomyces odontolyticus* were greater in abundance in the NoDS group compared with DS, and slight increases in abundance of *Veillonella parvula* and *S. oralis* were also observed in the NoDS group. However, *Pseudomonas putida, Acinetobacter lwolffii, Lactobacillus salivarius* and *Actinomyces lingnae* had higher abundance in the DS than NoDS samples.

Interestingly, the bacterial species with the highest average abundance; *S. salivarius,* was present at very similar levels in each group of denture samples (DS, 6.79%; NoDS, 6.83%), and was detected at the highest average abundance in tongue samples, and also exhibited similar average abundance between DS and NoDS.

DS		NoDS	
Bacterial species	**Average abundance (%)**	**Bacterial species**	**Average abundance (%)**
Streptococcus unclassified	14.238	*Serratia liquefaciens*	13.591
Myroides unclassified	8.518	*Acinetobacter johnsonii*	10.645
Pseudomonas fluorescens	7.209	*Streptococcus mitis*	10.143
Streptococcus salivarius	6.786	*Actinomyces odontolyticus*	9.590
Brevundimonas terrae	6.477	*Streptococcus salivarius*	6.831
Pseudomonas putida	6.180	*Lactobacillus fermentum*	6.185
Agrobacterium tumefaciens	4.545	*Brevundimonas vesicularis*	4.637
Acinetobacter lwoffii	3.933	*Pseudomonas putida*	3.731
Acinetobacter johnsonii	3.733	*Microbacterium testaceum*	3.481
Streptococcus mitis	3.490	*Veillonella parvula*	3.397
Chryseobacterium unclassified	2.470	*Streptococcus oralis*	2.680
Veillonella parvula	2.411	*Pseudomonas aeruginosa*	2.620
Lactobacillus salivarius	2.158	*Acinetobacter lwoffii*	1.915
Actinomyces lingnae	1.671	*Haemophilus parainfluenzae*	1.716
Massilia varians	1.621	*Prevotella histicola*	1.649
Actinomyces odontolyticus	1.505	*Propionibacterium acnes*	1.457
Streptococcus oralis	1.490	*Streptococcus anginosus*	1.297
Lactobacillus rhamnosus	1.333	*Actinomyces lingnae*	0.986
Streptococcus sobrinus	1.264	*Streptococcus sanguinis*	0.796
Devosia unclassified	1.222	*Prevotella melaninogenica*	0.790
Lactobacillus paracasei	1.186	*Granulicatella adiacens*	0.775
Stenotrophomonas nitritireducens	1.006	*Leptotrichia unclassified*	0.668
Acinetobacter junii	0.953	*Lactobacillus salivarius*	0.658
Delftia tsuruhatensis	0.947	*Actinomyces graevenitzii*	0.630
Empedobacter brevis	0.734	*Lactobacillus unclassified*	0.623
Total	**91.929**	**Total**	**84.884**

Table 5.6 Top 25 bacterial species in samples of denture-fitting surfaces of patients with (DS) and without (NoDS) grouped by disease status.

Red text indicates unique bacterial species in the top 25 detected bacterial species of either group, blue indicates common bacterial species within the top 25, and species in black text may or may not be present in both sample sets but are outside the top 25 detected species.

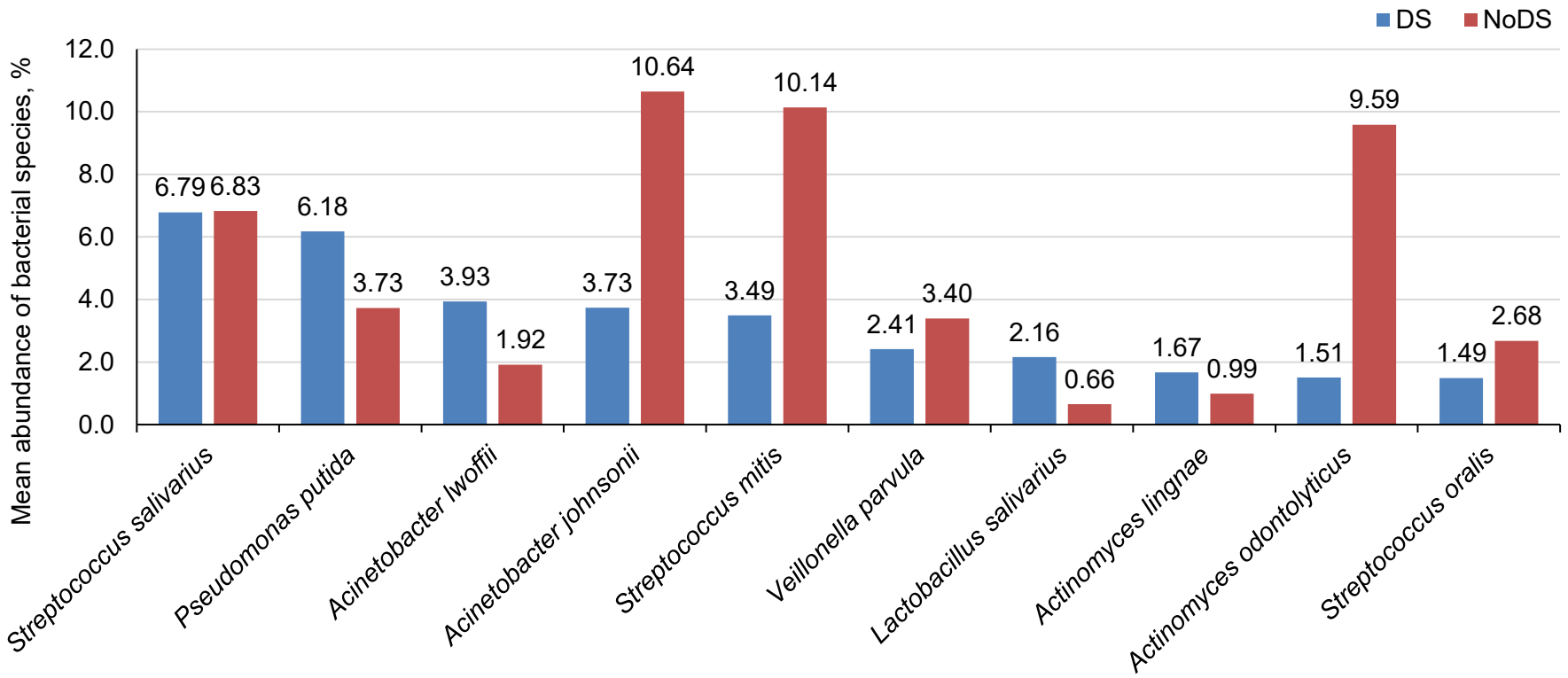

Figure 5.8 Mean relative abundance of the top 10 common bacterial species of patients with (DS) and without (NoDS) of the denture-fitting surfaces

Comparison of mean relative abundance for the top 10 common bacterial species detected in samples from the denture-fitting surface of DS (blue columns) and NoDS (red columns) patients as determined by NGS.

5.3.5.2 Bacterial species on the palatal mucosa

In total, 352 bacterial species were identified from all samples obtained from the palate; 131 in DS samples, of which 54 (41.2%) were unique to the DS group, and 129 in NoDS samples, of which 52 (40.3%) were unique to the NoDS group.

The top 25 bacterial species (table 5.7) of the palate represented a more significant proportion of the total number of bacterial species than that found in the denture fitting surface samples, totalling approximately 98% (DS) and 95.5% (NoDS). Eleven bacterial species detected were unique to the DS samples, compared with 7 unique to NoDS, and 8 bacterial species in the top 25 common to both groups.

Pseudomonas fluorescens was the bacterial species common to both DS and NoDS groups (Fig. 5.9) with the highest representation in DS samples, and was also common in the NoDS samples. The difference in the mean relative abundance was also the highest of any bacterial species between the two sample groups, with 19.99% relative abundance in DS samples, compared with just 2.34% in NoDS samples. Furthermore, the other most common bacterial species in both groups; *S. oralis, A. johnsonii, Brevundimonas terrae*, and *Chryseobacterium* (unknown species) were higher in abundance in DS samples than NoDS. The abundance of *Brevundimonas vesicularis* was greater in NoDS than DS, whereas only small differences in abundance between groups were observed for the remainder of the top ten common bacterial species.

Fifteen of the top 25 bacterial species detected in DS samples from the denture fitting surface were also found in DS samples of the palatal mucosa site. However, 22 of the top 25 bacterial species of NoDS samples from the palate were also detected in NoDS denture samples. A higher level of similarity between sample sites in NoDS than DS groups.

DS		NoDS	
Bacterial species	**Average abundance (%)**	**Bacterial species**	**Average abundance (%)**
Pseudomonas fluorescens	19.992	*Serratia liquefaciens*	16.698
Massilia aurea	15.572	*Pseudomonas putida*	16.583
Streptococcus unclassified	15.338	*Lactobacillus paracasei*	13.869
Enterococcus faecalis	12.754	*Brevundimonas vesicularis*	6.516
Dermacoccus	6.297	*Stenotrophomonas nitritireducens*	4.532
Streptococcus oralis	4.016	*Moraxella osloensis*	4.477
Acinetobacter johnsonii	3.839	*Agrobacterium tumefaciens*	3.611
Chryseobacterium unclassified	3.819	*Stenotrophomonas* unclassified	3.366
Massilia varians	3.334	*Acinetobacter johnsonii*	3.182
Brevundimonas terrae	2.646	*Streptococcus salivarius*	2.794
beta proteobacterium	2.252	*Phormidium species*	2.781
Sphingomonas species	1.576	*Streptococcus mitis*	2.759
Devosia unclassified	1.541	*Streptococcus oralis*	2.562
Brevundimonas vesicularis	1.016	*Pseudomonas fluorescens*	2.344
Massilia unclassified	0.732	*Chryseobacterium scophthalmum*	2.014
Rhizobium unclassified	0.712	*Propionibacterium acnes*	1.914
Acidovorax unclassified	0.664	*Luteimonas cucumeris*	1.411
Propionibacterium acnes	0.393	*Stenotrophomonas maltophilia*	0.836
Veillonella parvula	0.232	*Streptococcus sanguinis*	0.639
Delftia tsuruhatensis	0.229	*Chryseobacterium* unclassified	0.551
Streptococcus sanguinis	0.223	*Brevundimonas terrae*	0.498
Brevundimonas unclassified	0.201	*Rhizobium* unclassified	0.443
Rhizobium mesosinicum	0.198	*Streptococcus infantis*	0.420
Massilia alkalitolerans	0.198	*Pseudoxanthomonas mexicana*	0.413
Methylobacterium unclassified	0.186	*Acinetobacter lwoffii*	0.322
Total	**97.959**	**Total**	**95.531**

Table 5.7 Top 25 bacterial species in samples of palatal mucosa of patients with (DS) and without (NoDS) grouped by disease status.

Red text indicates unique bacterial species in the top 25 detected bacterial species of either group, blue indicates common bacterial species within the top 25, and species in black text may or may not be present in both sample sets but are outside the top 25 detected species.

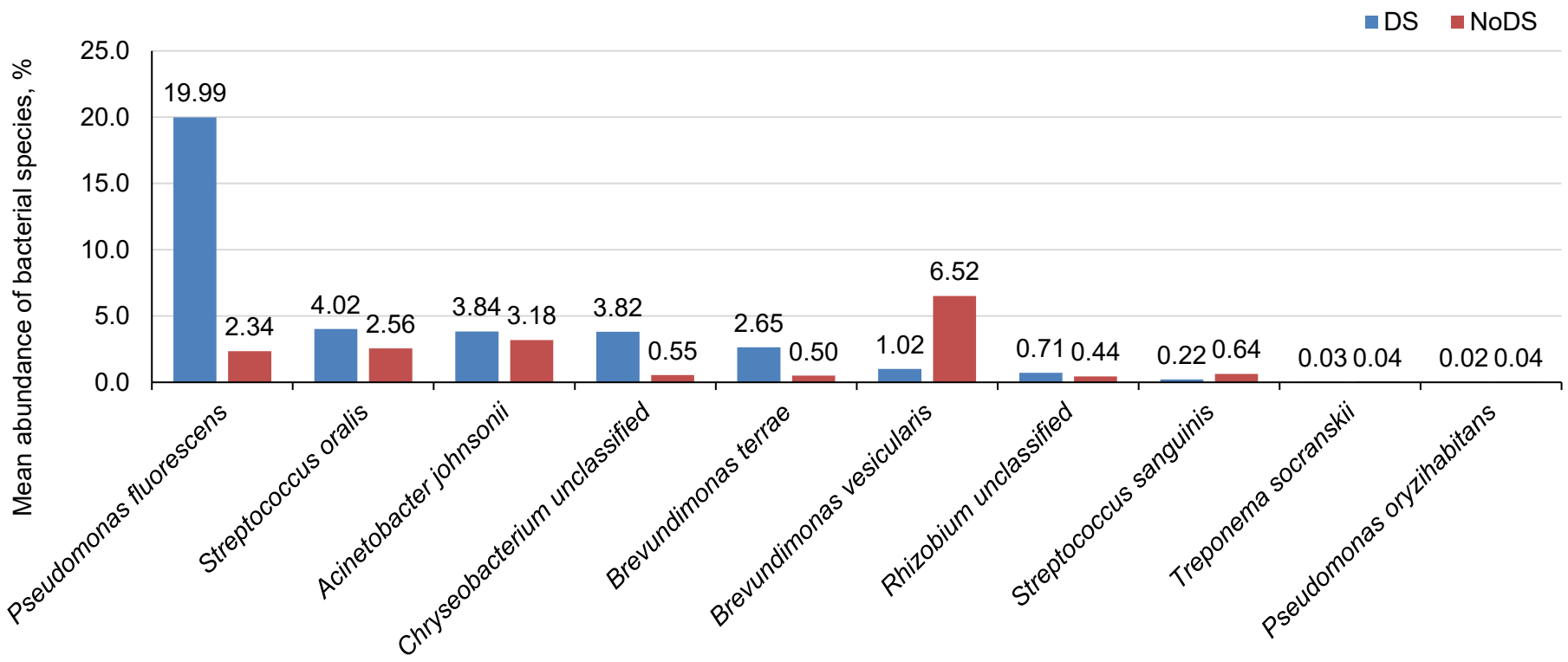

Figure 5.9 Mean relative abundance of the top 10 common bacterial species of patients with (DS) and without (NoDS) of the palatal mucosa surfaces

Comparison of mean relative abundance for the top 10 common bacterial species detected in samples from the denture-fitting surface of DS (blue columns) and NoDS (red columns) patients as determined by NGS.

5.3.5.3 Bacterial species on the tongue

In total, 352 bacterial species were identified from all samples obtained from the tongue, which was a similar finding to the other sample sites in this study; 157 in DS samples, of which 35 (22.2%) were unique to the DS group, and 195 in NoDS samples, of which 73 (37.4%) were unique to the NoDS group. Interestingly, a higher number of unique bacterial species were present in the NoDS samples than were observed in DS samples.

Also, similar to the denture samples, table 5.8 shows the top 25 bacterial species of NoDS samples represented less of the overall bacterial presence than that of DS samples (NoDS 88.153%; DS 95.656%). This was also observed in the Shannon index values of the samples, which indicated a more even distribution of abundance, rather than being high relative abundance being clustered to a smaller group of bacterial species. However, the top 25 species still make up a very significant proportion of the overall bacterial microbiome of the sample site in both patient groups, common in all sample sites.

Interestingly, of the top 10 bacterial species common to both DS and NoDS, 4 species of *Streptococcus* were present (Fig. 5.10), all of which are frequently isolated from the oral cavity, and are considered commensal bacteria. The species with highest abundance in both patient groups was *S. salivarius*, with only small differences in relative abundance between DS (18.412%) and NoDS (15.372%) samples.

DS		NoDS	
Bacterial species	**Average abundance (%)**	**Bacterial species**	**Average abundance (%)**
Streptococcus salivarius	18.412	*Streptococcus salivarius*	15.372
Pseudomonas fluorescens	12.481	*Serratia liquefaciens*	11.432
Enterococcus faecalis	11.527	*Streptococcus mitis*	11.185
Streptococcus unclassified	8.806	*Pseudomonas putida*	5.940
Streptococcus oralis	6.500	*Microbacterium maritypicum*	5.205
Streptococcus mitis	6.091	*Streptococcus oralis*	4.725
Brevundimonas terrae	4.958	*Actinomyces odontolyticus*	4.017
Granulicatella adiacens	4.199	*Acidovorax* unclassified	3.828
Chryseobacterium unclassified	3.814	*Stenotrophomonas nitritireducens*	3.311
Lactobacillus rhamnosus	3.709	*Lactobacillus paracasei*	2.978
Methylophilus methylotrophus	2.873	*Pseudomonas aeruginosa*	2.315
Brevundimonas vesicularis	2.224	*Haemophilus parainfluenzae*	2.167
Acinetobacter johnsonii	2.017	*Pseudomonas fluorescens*	2.060
Rothia mucilaginosa	1.688	*Brevundimonas vesicularis*	2.033
Prevotella tannerae	0.853	*Propionibacterium acnes*	1.637
Streptococcus sanguinis	0.754	*Citrobacter freundii*	1.635
Devosia unclassified	0.730	*Granulicatella adiacens*	1.605
Propionibacterium acnes	0.635	*Chryseobacterium scophthalmum*	1.464
Pseudoxanthomonas mexicana	0.634	*Veillonella parvula*	0.843
Haemophilus parainfluenzae	0.575	*Afipia broomeae*	0.796
Lactobacillus plantarum	0.515	*Microbacterium testaceum*	0.782
Prevotella oris	0.509	*Actinomyces lingnae*	0.753
Dermacoccus nishinomiyaensis	0.405	*Acinetobacter johnsonii*	0.729
Streptococcus sobrinus	0.379	*Rothia mucilaginosa*	0.705
Veillonella parvula	0.370	*Prevotella melaninogenica*	0.637
Total	**95.656**	**Total**	**88.153**

Table 5.8 Top 25 bacterial species in samples of the tongue of patients with (DS) and without (NoDS) grouped by disease status.

Red text indicates unique bacterial species in the top 25 detected bacterial species of either group, blue indicates common bacterial species within the top 25, and species in black text may or may not be present in both sample sets but are outside the top 25 detected species.

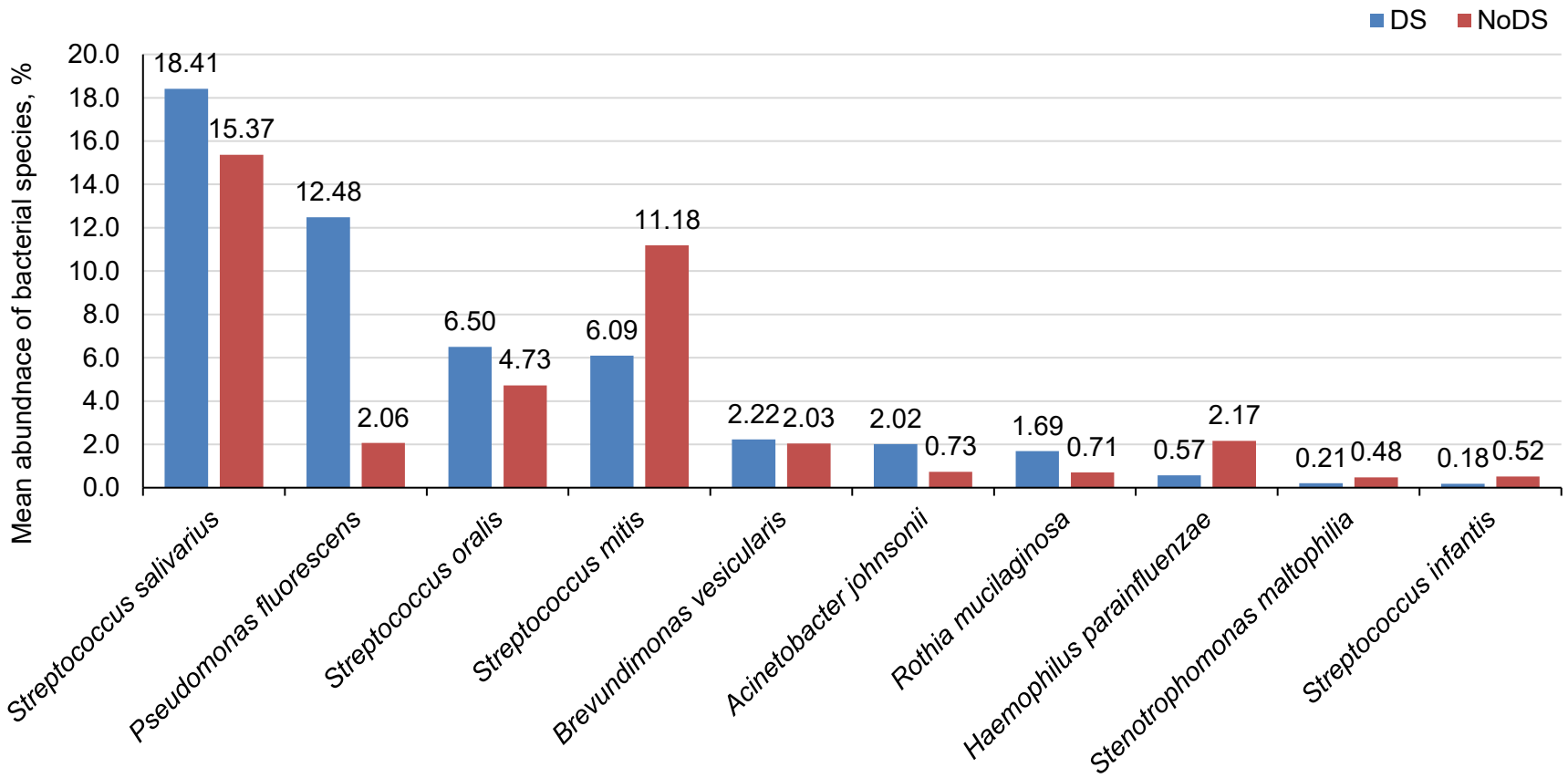

Figure 5.10 Mean relative abundance of the top 10 common bacterial species of patients with (DS) and without (NoDS) of the tongue

Comparison of mean relative abundance for the top 10 common bacterial species detected in samples from the denture-fitting surface of DS (blue columns) and NoDS (red columns) patients as determined by NGS.

5.3.6 Sample size power calculation

Based on the data obtained within this chapter, a power size calculation was performed by Dr Damian Farnell (Lecturer in Statistics, School of Dentistry, Cardiff University) to determine sample size necessary to provide confidence in the differences determined in these results. As analysed above, the sample groups were DS versus Non-DS for each sample site. Power was set at 0.8 for the purpose of these calculations.

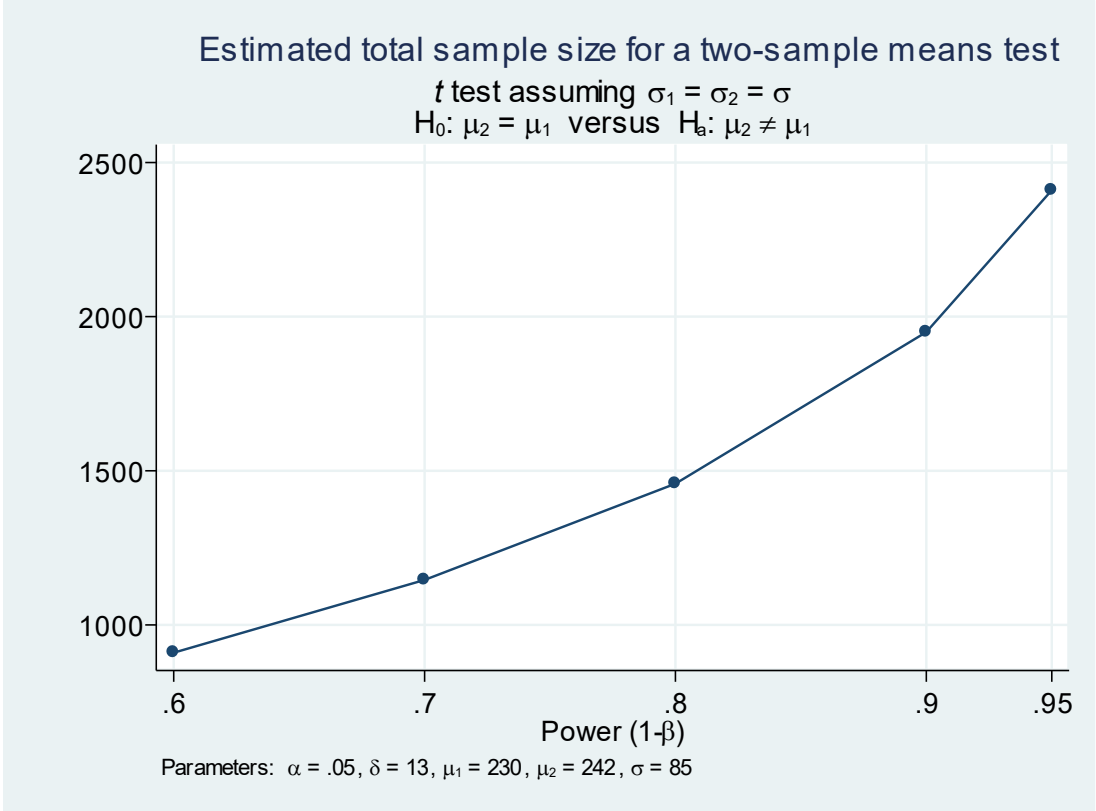

Figure 5.11 Sample size power calculation plot showing required n for samples of denture-fitting surface

The number of samples required to achieve a power of 0.8 was calculated to be approximately 1500 recruited patients.

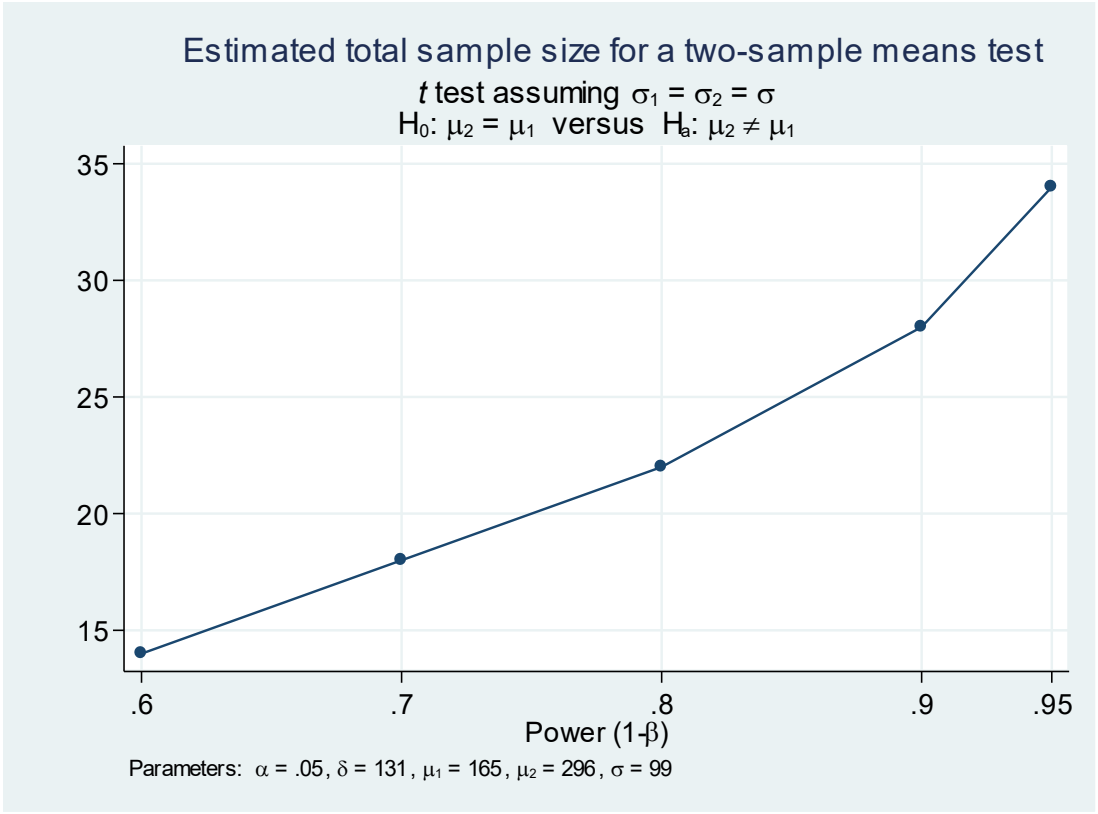

Figure 5.12 Sample size power calculation plot showing required n for samples of palatal mucosa

The number of samples required to achieve a power of 0.8 was calculated to be 22 recruited patients.

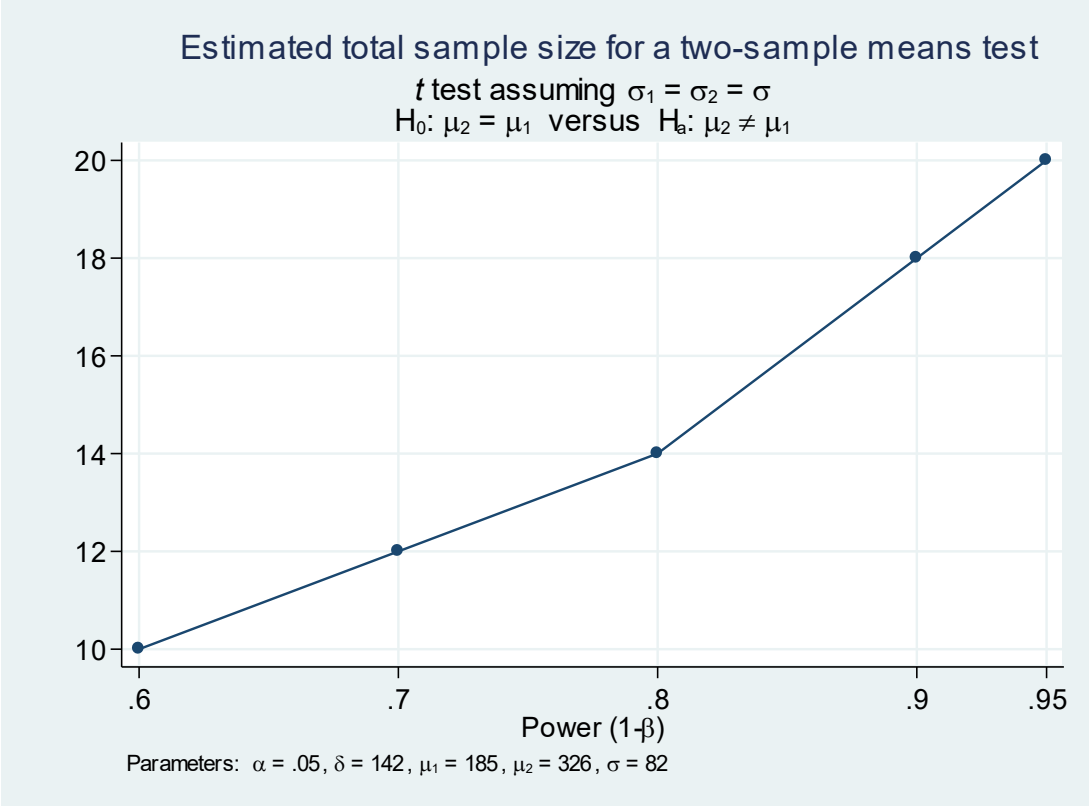

Figure 5.13 Sample size power calculation plot showing required n for samples of tongue
The number of samples required to achieve a power of 0.8 was calculated to be approximately 14 recruited patients.

The threshold for true reflection of results using the samples of the tongue was met within this study, thus observed differences are statistically robust and a true reflection of the differences within these samples

5.3.7 Effect of smoking status on bacterial microbiome

Microbiological samples taken and analysed by NGS in this study showed some differences in the bacterial microbiome of patients when grouped by smoking status.

No significant differences (P>0.05) were observed in the number of unique bacterial species of the denture-fitting surface, irrespective of smoking or DS status (Fig. 5.14), where the number of bacterial species in the samples were very similar between groups. This was also the case with samples of the palate, but a decrease, although not statistically significant, was evident for smokers with DS compared with each of the other groups.

Significant differences were observed between groupings from samples of the tongue (Fig. 5.15). A significant increase in the number of unique bacterial species was evident for each group compared with the smokers with DS (smokers NoDS=$P<0.01$, non-smokers DS=$P<0.05$, non-smokers NoDS=$P<0.05$). Interestingly, no significant differences were evident when comparing within each of the other three groups ($P>0.05$).

The pattern of results of the tongue and palatal mucosa were very similar; a lower number of unique bacterial species present in smokers with DS, compared with each other group, but the extent of differences was more pronounced in the results from the tongue samples.

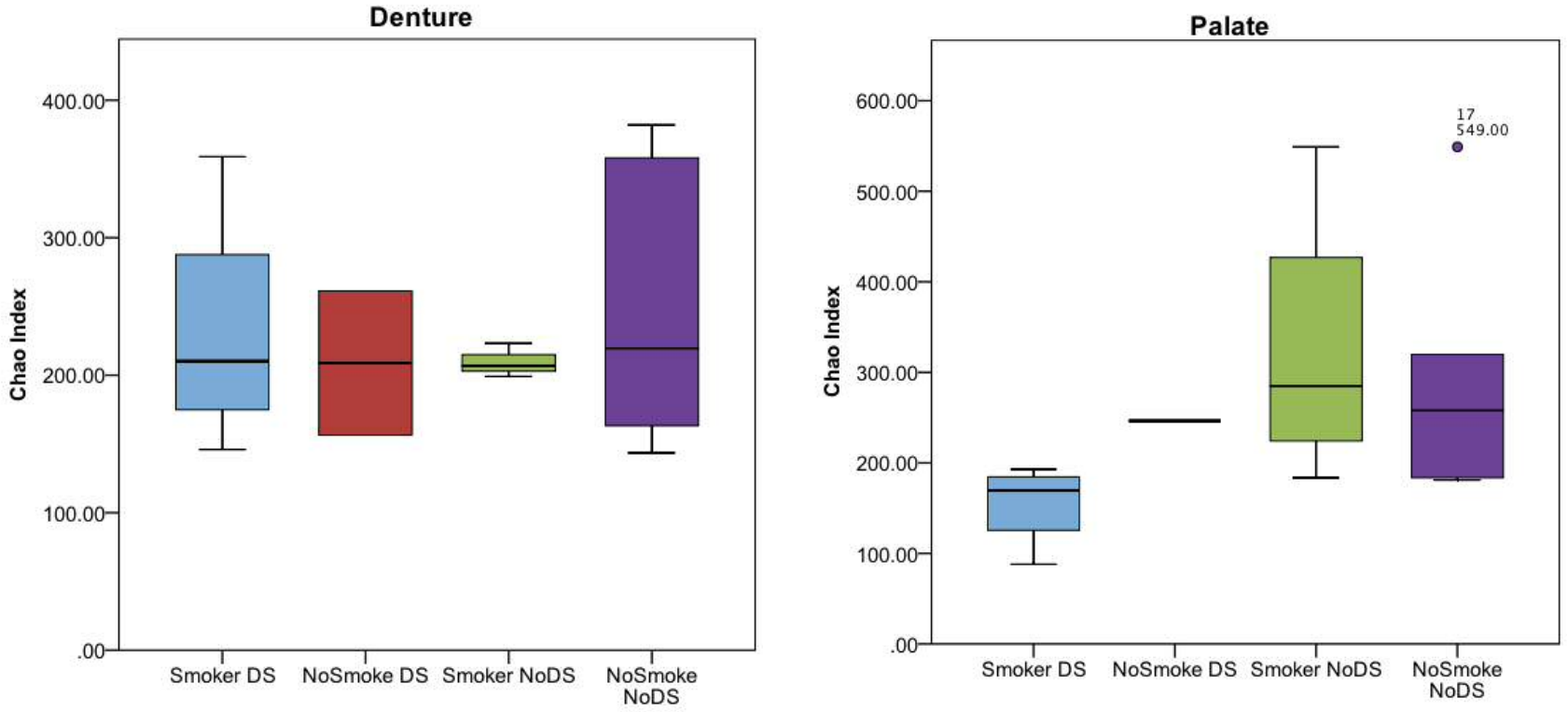

Figure 5.14 Effect of smoking status on the bacterial microbiome of DS and NoDS patients as measured by Chao index
Comparison between the number of unique bacterial species detected in samples from the denture-fitting surface and palatal mucosa of patients grouped by smoking and DS status. No significant differences in the number of unique bacterial species were observed between any of the groups.
Denture: smoker DS n=4, smoker noDS n=2, no smoker DS n=3, no smoker noDS n=8
Palate: smoker DS n=4, smoker noDS n=1, no smoker DS n43, no smoker noDS n=6

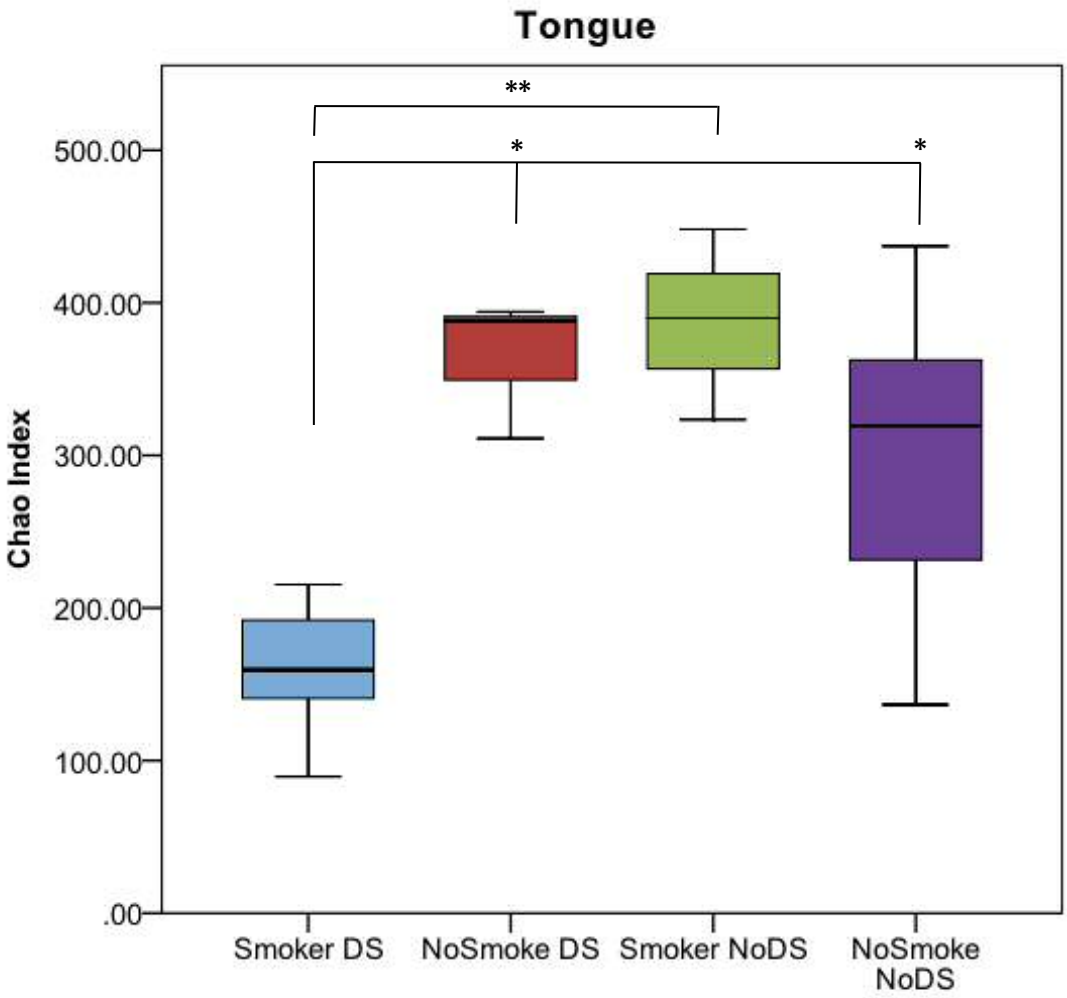

Figure 5.15 Comparison of effect of smoking status on bacterial microbiome of the tongue

Comparison between the number of unique bacterial species detected in samples from the tongue of patients grouped by smoking and DS status.

*P<0.05, **P<0.01

Smoker DS n=5, smoker noDS n=3, no smoker DS n=3, no smoker noDS n=8

5.4 Discussion

This research represents the first study to use next generation sequencing to characterise denture-associated biofilms from patients with and without clinical presentation of DS, with a specific view to characterise the bacterial microbiome to species level. The aim was to investigate whether relationships existed between the bacterial composition of denture-associated biofilms, and DS disease progression. Previous studies in this area have used molecular biology methods, but these have typically identified bacteria to genus level (O'Donnell *et al*., 2015; Shi *et al*., 2016). The study of microbial diversity and its association with health status in many niches, including the oral cavity is an increasing area of research (Paster *et al*., 2001; Cho *et al*., 2014).

Interestingly, Campos *et al* (2008) performed a similar study to the one reported here, but used pooled swab samples of DS versus non-DS patient groups. Additionally, when reporting the data, they only described differences of detected bacteria between DS and non-DS groups at genus level. Furthermore, no statistical analysis was done, making it difficult to evaluate the significance of the detected differences in the bacterial composition. The data reported in this chapter is based at species level, where substantial differences can exist, even within the same genus.

Different bacteria species (even of the same genus) will likely also behave differently at a particular site and whilst relative abundance of a genus may be an interesting factor in a study, the influence of a particular species may have a significant impact on the infection status, which may be missed in cases where genus level results are reported. For example, there are many species of *Streptococcus* including *S salivarius* and *S. mutans*, which are distinct, particularly in their disease-causing ability. *Streptococcus salivarius* is a commensal microorganism, and not associated with oral infection, whereas *S. mutans* is a known pathogen, associated with development of dental caries. Interestingly, *S. mutans* has also been associated with an increase in virulence when co-cultured with *C. albicans* (Kim *et al*., 2017), where the production of the candidal quorum sensing molecule, farnesol, leads to increased *S. mutans* microcolony formation. As an acidogenic microorganism, increased

colonisation subsequently results in increased sugar utilisation and thus acid production, which is destructive to enamel.

This study considered each patient's bacterial microbiome individually, grouping them according to disease status only after characterisation of the bacterial microbiome, and then analysing the differences, after which, results were reported as differences at species level.

This study included a number of strict patient recruitment criteria. In order to be deemed suitable for inclusion in the study, patients were not to have taken antibiotics or used steroids, or administered any immunosuppressive drugs investigational drugs in the previous 30 days to recruitment for the study. These factors have the ability potentially influence the composition of the microbiome, either directly as in the case of antibiotics, or indirectly in the case of steroids as a modulator of inflammation, and thus the normal immune response to the presence of microorganisms, particularly on the palatal surface. To standardise recruitment of patients, it was deemed necessary to employ these strict criteria. However, the modulating capacity of each of these factors, would be an interesting area for future study.

Use of antibiotics is obviously commonplace in medicine and whilst often necessary, their over prescription has led to increased antimicrobial resistance. This occurs when common microorganisms that were previously controllable with the use of antibiotics develop tolerance or resistance to the mechanism of action of the drugs, rendering them far less effective. This in turn leads to a requirement for the use of alternative agents, that may also have different side effects. Importantly, cases of antibiotic resistance against last resort drugs *e.g.* carbapenems, are increasingly reported. Antibiotic use has previously been correlated with onset of acute erythematous candidosis, and is thought to arise because of the reduction of the resident bacterial microflora (Williams & Lewis, 2011). This in turn, provided an environment where *Candida* has less competition, and thus can grow to a level that provokes an immune response and causes local tissue damage. The modulatory effect of steroids on the immune response may also play a role in

Candida-associated disease progression, as studies have also shown a relationship between immune status and *Candida* colonisation in DS (Rogers *et al*., 2013). As antibiotics and steroids have an influence on the bacterial microflora, either directly or indirectly, it would be interesting to assess use of these agents in future studies. Use of antibiotics would inevitably reduce bacterial load, and possibly modify the overall composition of bacterial species present, the changes of which could lead to progression of DS. However, this may not necessarily have been the case, as the modulatory capacity of specific bacteria for *C. albicans* virulence may have been left in-tact with the remaining bacteria, and subsequent progression to DS may not have occurred. This would potentially have allowed the identification of bacterial species that could be attributed to progression of DS. Alternatively, the lowered competition caused by antibiotics could have a greater effect than the inter-species modulatory factors, thus including this as an exclusion criteria does provide a more representative environment in which these modulatory factors could be determined. Furthermore, a longer-term study would also be of interest to monitor the bacterial microflora of DS patients, and a follow-up post-treatment analysis of the microbiome would provide additional evidence into species-specific contributions to DS.

The patient exclusion criteria employed in this study had a negative impact on the number of patients recruited. As patients attending the Cardiff School of Dentistry are generally referred for treatment from local dental clinics, they likely had already received some form of intervention treatment prior to attending. An additional criterion for recruitment was use of a full upper acrylic dental prosthesis. These are becoming increasingly less common, not only with the improvement in dental health for the general public, but also due to the introduction of alternative materials to produce the prostheses such as cobalt chromium, but also, the somewhat recent introduction of dental implants to replace missing teeth. Furthermore, the inclusion of partial dentures would have also created an additional level of complexity, as there would be remaining teeth that are known to harbour a distinct bacterial microbiome of their own. This may have further clouded the results obtained, making the subtle differences that were observed, even less so.

Whilst the medical history and lifestyle history of the patients recruited to this study was limited, the incidence of HIV/AIDS, diabetes or nutritional factors on bacterial microbiome and incidence of DS would have been interesting to determine. The only 'lifestyle factor' recorded in this study was tobacco smoking, which has been attributed to changes in the microbiome of a number of sites in the human body, including the oral cavity (Kenney *et al*., 1975), and lungs, and some associations with development of microbial-related diseases have been made. DS is one such disease, the prognosis of which has correlations with smoking status.

Whilst smoking is a key risk factor in oral candidosis (Shulman *et* al., 2005; Williams & Lewis, 2011) and other oral infections, no significant difference in the bacterial microbiome of denture surfaces of patients with or without DS, irrespective of smoking status was observed for denture and palatal mucosa samples. However, a significant (P=0.005) increase in the number of unique OTUs (*i.e.* bacterial species) was observed in tongue samples of Non-DS patients compared with DS patients (Fig. 5.15), which although a distinct surface, and within the oral cavity, it is separate from the denture and palatal mucosa surfaces. Normally, in the absence of a dental prosthesis, the influence of the tongue may be more significant, as the two surfaces can contact directly, but the physical material of the denture renders this not possible (unless dentures are removed). The tongue is also considered a reservoir for microorganisms, and although the presence of anaerobes is much higher on the tongue (Seerangaiyan *et al*., 2017), it can also act as a provider for other oral sites.

Although only 19 patients were recruited to this study, the distribution of disease status between patients DS and non-DS was similar (DS n=8, NoDS n=11). Despite the lower than anticipated number of recruited patients, the sequence data generated was of excellent quality. The next generation sequencing data was sub-sampled at 10,995 reads, which allowed for bacterial species at the lower detection to be represented, even with a relatively small sample volume used for the NGS process. Some samples did contain a much

higher quantity of reads (*e.g.* S003_D with 133,846 reads). Sub sampling, although necessary to normalise samples for inter-sample comparisons of relative abundance of species, does render a portion unusable. In this case, approximately 12% of the data was used for analysis, leaving 88% unusable.

Interestingly, relatively large differences were observed by culture between sample site and between patients. Images of the cultured agar plates were not collected for all samples analysed, and thus were not used to compare relative colonisation as an indicator of DS status or bacterial load.

Some differences between culture and molecular detection of *Candida* was observed. Each foam imprint was placed onto a section of a Sabouraud's dextrose agar (SDA) plate, and cultured in the laboratory. Where yeast-like colonies developed on SDA, the sample was considered *Candida*-positive. Random selections were further cultured on chromogenic agar (CHROMagar™ *Candida*) (Williams & Lewis, 2000; Perry & Freydière, 2007) for presumptive identification of *Candida* species. There are a number of limitations with this method for identification. Firstly, SDA does not discriminate between species of *Candida*. Secondly, not all colonies cultured on SDA were subcultured on CHROMagar™ *Candida*, thus depending on the number of *Candida*-like colonies that were cultured from the original foam imprint sample, there are several opportunities for missed colonies, as of those with many colonies, only a small portion were subcultured. Additionally, it was not always possible to differentiate between different colonies on the original SDA plate due to the close proximity in which they grew, and eventually merged together. The CHROMagar™ *Candida* claim to clearly differentiate different species by colony colour is true to a certain extent, but different species can, and do grow as the same colour. This is true for *C. albicans* and *C. dubliensis*, both of which grow as green-coloured colonies. As a result of these numerous limitations, the use of molecular methods was therefore employed to alleviate this uncertainty.

Further detection of *Candida* species was performed using a nested PCR, which, briefly, involved DNA extraction, pre-amplification with a fungal-specific PCR reaction, then using species-specific primers to further amplify the samples to detect the presence or absence of different *Candida* species. The results of the nested PCR showed presence of *Candida* based on a primer set that was not species-specific. However, no presence of *C. glabrata* or *C. krusei* was detected using primers specific for these species. As *C. albicans* is the most frequent cause of *Candida*-related infection, the absence of the detection of *C. glabrata* or *C. krusei* species is as important as the positive identification and confirmation of *C. albicans*. For this purpose, it was determined that the positive indication of *C. albicans*-like colonies by CHROMagar™ *Candida* and the absence of other common *Candida* species by nested PCR, implied that the samples had *C. albicans*. These samples were included in the NGS analysis, as presence of *C. albicans* was regarded as a pre-requisite for classification of DS, rather than an associated issue such as ill-fitting denture caused palatal irritation.

Although sensitivity or limit of detection for these sample types was not performed, it appeared as though the molecular method of nested PCR was more sensitive than the culture method, even with the use of chromogenic agar. White *et al* (2003) determined the limit of detection for *Candida* species in blood samples using the same PCR method as used here was 5 CFU/ml. Although in theory, the culture sensitivity only requires one CFU per area measured (2cm^2 in this case) the foam imprint culture method relies on good contact firstly between the foam imprint and the sample-site, and sufficient collection of the microorganisms. It also relies on good contact between the foam imprint and the agar surface, to efficiently transfer cells to the agar. This is then followed by culture of the microorganisms. The foam imprints do have the advantage of being porous, thus allowing surface fluids to be drawn into the foam, and for microorganisms to be drawn into the imprint along with it, but depends on the user and method of imprint sample collection. The use of a swab, which is less porous and in closer overall contact when streaked across the sample surface, may result in a higher yield of microorganisms collected

overall. This again depends on the collection of the sample, and the assumption that the area size for the samples were the same between the $2cm^2$ area of the imprint, and the swab streaks. Variation in microbial load on each of these surfaces was evidenced by the differences in read numbers from the NGS data, and such differences were also observed in a similar study performed by Rogers *et* al., (2013b) where although differences were observed between sample sites, generally, patients with DS showed a higher *Candida* load on the denture-fitting surface and tongue, but lower on the palatal mucosa compared with NoDS patients.

The order in which the samples were taken, which is important, was not specified in the sampling protocol. If the imprint and swab samples were taken from the same area of the sample site, and the swab was taken first, the resulting collection of viable and representative microorganisms for DNA extraction would inevitably have been higher than the foam imprint sample, as many microorganisms will already have been removed, and *vice versa*. This can affect subsequent culture or molecular analysis, depending on the order of sampling.

The NGS data did not show any significant overall differences ($P>0.05$) in the bacterial microbiome between patients with or without DS for the denture-fitting surfaces or palatal mucosa. In fact, high similarities of DS and NoDS results for both number of unique bacterial species detected (Chao index), and the richness and evenness of spread of these species (Shannon index) was evident in samples of the denture-fitting surface. A slight trend toward a higher number of unique bacterial species was evident in NoDS patients than DS for samples of the palatal mucosa. A similar trend was also observed in the Shannon index of samples of the palatal mucosa, and of the tongue, where the distribution and abundance of bacterial species was more even (as demonstrated by the higher Shannon index values for NoDS patients compared with DS for each group). A significant increase in the number of unique bacterial species was observed in samples of the tongue from patients without DS compared with those with DS. This difference in bacterial diversity is in line with previous reports that suggest that when a community becomes

less diverse, or there is a trend toward dysbiosis, community-modulation of the environment is no longer maintained (Marsh, 2005). Microorganisms that can exist in more extreme environments subsequently thrive, and can cause damage to their local environment, such as the host (Takahashi, 2005; Matsubara *et al*., 2016). Similarity between DS and NoDS samples was also observed with other analyses including non-metric multidimensional scaling, in which, samples were weighted by relationship and distances assigned, but showed no distinct clusters of either DS or NoDs groups. The substantial overlap indicated high similarity between the groups. Furthermore, heatmaps and dendrograms assigned by phylogenetic distances of bacterial species between samples showed few correlations between individual samples, and only loose groupings by disease state, further indicating no strong distinctions by disease for abundance of particular bacterial species in samples.

There were some striking differences when considering the abundance of individual bacterial species within sample groups. For example, when considering samples of the denture-fitting surface, a bacterial species within the genus *myroides* (species unknown) was found exclusively in the DS sample group, at approximately 8.5% relative abundance. *Myroides* (specifically the species *odoratimimus*) have been implicated in soft tissue infections of immunocompetent patients (Maraki *et al*., 2012), and linked with cases of bacteremia in those suffering with diabetes (Endicott-Yazdani *et al*., 2015). It is therefore possible that the presence of this microorganism in the DS group is contributing to the palatal inflammation observed when recruiting the patients. Alternatively, the presence of the bacteria is contributing to the local microbial community (biofilms) residing on the denture surface, and modulating *Candida* virulence, thus resulting in the observed palatal inflammation.

P. fluorescens was also detected exclusively in the DS group of denture samples with an abundance of approximately 7%, but also detected in both DS and non-DS samples of the palate and tongue, indicating its presence is not necessarily by chance, but it has successfully colonised each of these sites. There were quite significant differences in the abundance of

P. fluorescens between DS and non-DS of the palate (DS = 20%, non-DS = 2.3%) and tongue (DS = 12.5%, non-DS = 2%). This indicates that at both biotic sites (palate and tongue), there is a basal level of presence of approximately 2% of the overall bacterial microbiome. There are a number of possibilities as to why this relative abundance then shifts, but it is not clear whether the shift is due to changes in the local environment, saliva, diet, immunocompetence, or whether it is indeed due to inflammatory conditions in the local area, or whether other factors within the biofilm due to accessory pathogens or other species that contribute different by-products can result in a better environment for *P. fluorescens*, which encourages its enhanced growth. It is also not clear whether the change in the abundance is due to the DS state of infection, or if the increased level of *P. fluorescens*, and indeed other bacterial species either unique to or increased in the microbiome of DS patients results in the disease. It is a very complex environment, with many influencing factors, with likely no single factor contributing solely to the incidence or development of the disease.

Interestingly, when the patients were sub-grouped by smoking status (an important predisposing factor of DS incidence (Williams & Lewis, 2011)) there was a significant decrease in the number of unique bacterial species on the tongue detected in DS patients who smoked compared to DS patients that did not smoke, and non-smokers irrespective of DS status. A similar trend was observed in analysis of samples of the palate, but these were not statistically significant. Both biotic surfaces in this study, although distinct in location and histology show the same pattern of results, whereas on the denture-fitting surface, the number of unique bacterial species was similar between all sub-groupings irrespective of disease or smoking status. The abiotic surface is in contact with the palate for a significant portion of the day (and not infrequently, also during the night), and this contact with the palate does not appear to allow for immunological management of the microbial content of biofilms. The relatively unchallenged biofilms may be present in similar quantities, and are similar in characterisation and profiling as observed in this study, whereas the palate and tongue are biotic, and subject to natural sloughing and other immunological management. The use of tobacco has long been attributed to

disease progression, including infections (Kinane & Chestnutt, 2000; Arcavi & Benowitz, 2004; Bagaitkar *et al*., 2008; Mehta *et al*., 2008), cancers (Blot *et* al., 1988; Winn, 2001; Johnson, 2001) and general but substantial immunosuppression (Sopori, 2002).

5.5 Conclusions

- Although species-level differences of the relative abundance of common bacterial species were evident, no significant differences were observed in the bacterial microbiome of the denture-fitting surface or the palatal mucosa between patients with or without DS,

- Phylogenetic distance analysis showed overlapping groupings, correlating with the primary analysis in that the DS and NoDS groupings showed little distinction between bacterial microbiomes.

- A significant increase in the number of unique bacterial species, and thus bacterial diversity was evident in the tongue microbiome of patients without DS, further suggesting a reduction in diversity results in a loss of microbial homeostasis, and possible onset of disease.

Chapter 6

General discussion

6. General discussion

Biofilms are defined as multi-layered aggregates of microbial cells, attached to a surface and/or each other, with the cells often embedded in a matrix comprised of self-produced polymeric substances. Biofilms are ubiquitous in their distribution, occurring in natural and man-made environments (Häussler & Parsek, 2010). Of particular interest and relevance to this research is the presence of biofilms in the human body, where they can cause important clinical infection. To highlight this, an estimated 65% of hospital-acquired infections are thought to have a biofilm origin (Costerton *et* al., 1999; Joo & Otto, 2012).

Microorganisms present in biofilms can be up to 1000-fold more tolerant to antimicrobials than their planktonic counterparts. The mechanism(s) of this increased tolerance is likely multifactorial. The biofilm community itself is typically embedded in a matrix of extracellular polymeric substances (EPS) (Flemming *et al*., 2007), which serves to reduce the cidal effects that would otherwise be caused by desiccation of the biofilm matrix. The EPS also provides a physical barrier to movement of antimicrobial compounds through the biofilm, and mitigates the impact of changing environmental variables such as temperature and pH (Flemming & Wingender, 2010). Furthermore, the polymicrobial nature of most biofilms provides many benefits for the resident microorganisms. The close proximity of the microorganisms and the constitutive use of quorum sensing molecules can stimulate stress responses from others around them, inducing virulence factors and increasing tolerance to extremes of conditions or external challenges. Many microorganisms, including bacteria and fungi actively secrete DNA to their surrounding environment and this provides a structural function to the biofilm (Mann *et al*., 2009; Hall-Stoodley *et al*., 2008; Jakubovics *et al*., 2013; Martins *et al*., 2010). Furthermore, certain nucleic acid sequences may be taken up by other microorganisms, which is a potential method of acquiring additional genetic information.

The biofilm matrix is complex, containing channels for nutrient transport (Costerton *et al.*, 1999), and providing a range of different conditions in the

biofilm. This means that a diverse array of species may inhabit the biofilm but not all at the same location. For example, in a location exposed to air, anaerobic bacteria would be able to survive in an area of the biofilm where oxygen levels are lowest; potentially deep in the biofilm or near the attachment surface. Resistance to toxic chemicals including some antimicrobials can be mediated in the biofilm by the action of microbial efflux pumps (Costa *et al*., 2014; Ramage *et al*., 2002; Mukherjee *et al*., 2003; Lewis, 2007), which actively remove antimicrobial compounds once they have been taken up by the cells. While efflux pumps are not unique to biofilm cells, they are up regulated during antimicrobial challenge to increase resistance (Costa *et al*., 2014; Webber & Piddock, 2003). The biofilm matrix itself can sequester antimicrobials through hydrophobic or electrostatic interactions, and indeed physical cell wall components which can then impede a diffusion gradient through the biofilm (Fux *et al*., 2005; Van Acker *et al*., 2014; Mah *et al*., 2003). A reduced growth rate and metabolic activity of biofilm embedded cells can also contribute to this increased resistance (Fux *et al*., 2005). Similarly, persister cells within a biofilm are viable cells that remain after antimicrobial treatment has eradicated the majority of other microorganisms. These persister cells can then re-establish the biofilm following completion of the treatment regime (Lewis *et al*., 2001; Seneviratne *et al*., 2008; Monroe, 2007.

Biofilms are very common in clinical environments. Some of the most frequent and widely cited examples of biofilms occur in the lungs of cystic fibrosis patients (Stewart & Costerton, 2001; Lewis, 2001; Donlan & Costerton, 2002) and in this respect, *Pseudomonas aeruginosa* and *Burkholderia cepacia* are often implicated bacteria. Within the oral cavity, the most obvious example of a biofilm is dental plaque (Marsh & Bradshaw, 1995; Marsh, 2004; Marsh, 2005; Rosan & Lamont, 2000). Dental plaque biofilms occur on the tooth surface and are comprised of hundreds of different bacterial species. Plaque colonised with *Streptococcus mutans* are associated with dental caries (Kim *et al*., 2017), whilst subgingival dental plaque containing proteolytic anaerobic bacteria such as *Porphyromonas gingivalis* are linked to periodontal disease (Marsh *et al*., 2011).

Members of the fungal genus *Candida*, are also frequently associated with human infection, and often these occur in biofilms in the oral cavity. Infections caused by *Candida* are termed candidoses, with four primary clinical presentations of oral candidosis described (Scully *et al*., 1994). These include pseudomembranous candidosis, chronic hyperplastic candidosis, and acute and chronic erythematous candidosis. Chronic erythematous candidosis (also referred to as denture-associated stomatitis, DS) was the focus of research in this PhD. DS is seen as areas of inflammation of the palatal mucosa in close proximity to the denture-fitting surface, on which, biofilms are present (Williams *et al*., 2011). The sustained contact of the denture-associated biofilms with the palate can lead to an inflammatory response from the host. Importantly, as the abiotic denture surface is not subject to natural renewal, and is not readily accessible to the reach of immune cells, the inflammation is chronically sustained, leading to subsequent tissue damage.

Current treatments of DS target either improving general oral and denture hygiene, or treating the fungal component of the infection, with little consideration for the bacterial component of the biofilms. Several studies have shown that hundreds of different bacterial species are present in the oral cavity, including the denture-fitting surface, each of which could have a substantial influence toward the incidence or progression of the infection, as they exist in co-culture with other species and *Candida*.

The overarching aim of this PhD was to investigate the relationship between the bacteria within denture biofilms and *Candida albicans*. Specifically, an evaluation of the impact of microbial interactions on *Candida* virulence was investigated. Initially, the research sought to develop an *in vitro* polymicrobial biofilm model using poly(methyl methacrylate) (PMMA) as the biofilm supporting surface, as this is the most commonly used material for complete dentures. The biofilm model incorporated several species as an inoculum. These species included representative oral bacterial species namely the facultative anaerobic early colonisers of *Streptococcus sanguinis* and *S. gordonii*, and the anaerobic secondary colonisers *Actinomyces odontolyticus* and *A. viscosus.* In addition, *Porphyromonas gingivalis,* which is an oral

bacterial species primarily associated with gingivitis and periodontitis was also utilised.

Initial studies involved optimising biofilm model development, through the evaluation of the effects of pre-conditioning the PMMA surface with artificial saliva (AS) on subsequent adherence and biofilm formation. The AS formulation comprised of a range of chloride salts, in addition to proteose peptone, yeast extract, and most importantly, mucins. Despite the numerous compounds included in the formulation, the AS was still relatively simplistic compared with whole saliva which contains additional compounds including host cells, enzymes and peptides (Wade, 2013; Nasidze *et al*., 2009; Yang *et al*., 2012; Fabian *et* al., 2012; Humphrey & Williamson, 2001). This pre-conditioning did not appear to influence overall microbial adherence nor biofilm formation by single- or mixed-species. This was interesting because the presence of saliva in such studies has shown a wide range of results, from an increase in adherence (Edgerton *et al*., 1993) to a decrease in adherence (Samaranaye *et al*., 1980; Satou *et al*., 1991).

Saliva is a key component of the oral cavity, and also contains mucins and other proteins that may influence adherence *in vivo*, particularly as there is a constant flow of saliva in the oral cavity, whereas in the *in vitro* experiments, the pellicle is formed prior to addition of microorganisms. This flow was represented *in vitro* through agitation of the specimens during adherence of the microorganisms. Interestingly, this shear flow has also been linked with an increase in adherence *in vitro* (Thomas *et al*., 2002), but this was not observed in this study. It is thought that the deposition of mucins onto the surface modify the charge and adhesiveness, and this has previously been associated with an increase in adherence of oral bacteria to surfaces (Tabak, 1995; Gocke *et al*., 2002; Stinson *et al*., 1982). In the present study, biofilm was evident as multi-layered structures sporadically growing across the surface which was not uniformly covered and this pattern of biofilm growth was not affected by pre-conditioning with AS.

It has been hypothesised that candidosis may occur due to elevated numbers of *C. albicans*, and in this study, the effect that bacterial presence had on the numbers of *Candida* and virulence factor expression was studied. Bacteria in mixed-species biofilms increased several putative *C. albicans* virulence factors including expression of genes involved in surface adhesion, biofilm initiation and maturation (ALS3, HWP1), and genes encoding hydrolytic enzymes involved in tissue invasion and damage (secreted aspartyl proteinases 4 and 6 (SAP4, SAP6) and phospholipase D (PLD)). These genes, some of which are involved in morphological transition of *C. albicans* from yeast to hyphae state were up-regulated. This was also reflected by microscopic analysis of *C. albicans*-only and mixed-species biofilms. In these studies, in excess of 10-fold increase in the number of *C. albicans* hyphae was evident in mixed-species biofilms compared with *C. albicans*-only biofilms. The observed enhancement of putative *C. albicans* virulence genes, and the increase in the presence of *C. albicans* hyphae could not be attributed specifically to direct-contact with a specific bacterial species, or to specific secreted molecules. There were no significant difference in the number of viable *C. albicans* in *C. albicans*-only biofilms and mixed-species (bacteria plus *C. albicans*), confirming that the increase in gene expression and formation of hyphae were due to the genotypic/phenotypic changes, rather than associated with more *C. albicans* cells.

When mixed-species biofilms were developed incorporating *P. gingivalis*, most of the *C. albicans* virulence factors were no longer up-regulated. A significant decrease in genes involved in production of adhesins and hyphae was observed in mixed-species biofilms with *P. gingivalis* biofilms, and at a level similar to or lower than *C. albicans*-only biofilms. The differences in virulence factor expression highlighted the complexity of the microbial interactions, either through direct contact or by secreted molecules. Both mechanisms have previously been shown to affect virulence. Direct-cell contact has been demonstrated in oral bacteria, including *S. gordonii* and *P. gingivalis* (Kuboniwa & Lamont, 2010), and between *S. gordonii* and *C. albicans* (Bamford *et al*., 2015), but modulation of *Candida* phenotype is also associated with quorum sensing molecules including its own, farnesol, but also

those produced by bacteria including a homoserine lactone molecule produced by *P. aeruginosa* (Hogan *et al*., 2004). Although *P. aeruginosa* is not normally associated with colonisation of the oral cavity, the fact that a homoserine lactone molecule has been shown to modulate *Candida* morphology, indicates that other similar molecules, produced by other bacterial species may have comparable effects.

Studies have shown that streptococci can bind to *C. albicans* hyphae (Silverman *et al*., 2010), and subsequently induce virulence factor expression. Direct binding of cocci-shaped bacteria to *C. albicans* was also detected by SEM of *in vitro* mixed-species biofilms in this PhD. This co-adhesion was more evident on hyphae, in comparison to yeast cells, indicating that direct cell-to-cell contact may be playing a role in inducing responses that lead to an enhancement of *Candida* virulence. At the time of writing, this was the first study that had evaluated the effects of oral bacteria on the modulation of *C. albicans* virulence in *in vitro* biofilms. It is of great interest to determine the mechanism behind the modulation of virulence, as this may provide insight into possible targets for prophylactic strategies for individuals at increased susceptibility for DS, or management of established infection.

The *in vitro* biofilm model developed in this project provided valuable insight into the modulatory capacity of what are considered commensal bacteria on *C. albicans* virulence factor expression. However, as DS is an infection of the palatal mucosa, it was important to also develop a tissue infection model. A number of commercially available 3D tissue models exist, but these all have a number of limitations, not least of which is their high cost. Furthermore, there is an inability to further modify these tissue models to incorporate additional cell types, thus somewhat limiting the models as clinically and histologically representatives of normal mucosa.

The two main types of tissue models are epithelial-only (comprised of stratified keratinocyte cells), and full-thickness (which includes both the epithelium and a *lamina propria*). In an effort to overcome some of the limitations outlined above, Chapter 3 of this thesis describes the development of two types of *in*

vitro tissue models as alternatives to those commercially available, thus allowing a greater number of analyses to be completed in a cost-effective manner. The research involved creating both an alternative tissue model to the SkinEthic™ RHOE (EpiSkin), and a full thickness tissue model similar to EpiOral full thickness tissues (MatTek). The *in vitro* and commercially available tissues were also used in biofilm-infection studies in Chapter 4 to investigate the pathogenicity of the different types of *in vitro* biofilms.

SkinEthic™ RHOE used TR146 keratinocytes, which were originally isolated from a buccal squamous cell carcinoma. These cancer-derived cells are not normal in their genotype, and as such, may not behave as normal oral keratinocytes should. This was evident in both the SkinEthic™ RHOE and *in vitro* keratinocyte-only tissues, where TR146 cells were used. Although 3D culture was evident in both the commercially available and *in vitro* tissues, to a similar extent in each model, no differentiation or stratification of the keratinocytes was evident. Normal mucosal epithelium typically has several distinct cell morphologies. These include block-like basement epithelial cells which then differentiate as they stratify toward the outer layer, where they keratinise as longer spindle-like, keratin rich cells. The differences between the model and *in vivo* tissues highlight the limitations of the *in vitro* tissue models. Furthermore, there is no possibility of fully representing immune responses, due to the lack of *lamina propria* and immune cells. On the other hand, the relatively short culture period of 5 d, and the relative ease of culture in the laboratory facilitates the high throughput of analyses that can be completed in a relatively short period, with very little associated costs.

Previously, keratinocyte-only tissues have been used to study *in vitro C. albicans* infection using planktonic inocula (Schaller, 2002; Samanarayake *et al*., 2006; Silva *et al*., 2009; Silva *et al*., 2011; Williams *et al*., 2013; Yadev *et al*., 2011). No studies had evaluated the use of biofilms as the starting inoculum, and specifically, the effect of a mixed oral bacterial species inoculum. The biofilms developed in this research, whilst simplistic in

composition were deemed to be appropriate to evaluate effects on virulence and pathogenicity of *C. albicans*.

Full thickness tissue models, which are considerably more expensive than the keratinocyte-only tissues, are more (histologically) representative of oral mucosa. This was demonstrated by the presence of both an epithelium and *lamina propria*, with the advantage of being able to evaluate a more complex tssue response, as a result of cell-to-cell communication between the epithelial cells and fibroblasts. These cells produce distinct cytokine profiles to modulate immune responses to infection, and these self-produced cytokines are known to have a regulatory function for further production or inhibition of cellular production of other cytokines. Due to the substantial costs of the EpiOral full thickness tissues, another aim of this research was to develop an alternative full thickness tissue. As previously discussed, this model could be used to perform a greater number of infection analyses in a cost-effective manner. In addition, the model could facilitate the incorporation of additional cells, including immune cells such as dendritic cells, monocytes and Langerhans cells, making the model even more representative of *in vivo* oral mucosa.

The successful culture of a full-thickness tissue was achieved using normal oral fibroblasts in a collagen matrix, overlaid with immortalised normal oral keratinocytes. The histological analysis of the tissues showed excellent structure of the tissues. The *lamina propria* showed a sparsely populated matrix, which had contracted during culture, and a thick stratified epithelium, with good differentiation of the cells, and some keratinisation. Interestingly, when TR146 cells were used in place of immortalised normal oral keratinocytes, this differentiation was lost, and despite the better stratification in the full thickness tissues than in the keratinocyte only tissues, no maturation or keratinisation of the cells was observed. This finding confirms the abnormal behaviour and culture of the cancer cells, and highlights the importance of using normal, or immortalised normal cells to represent normal tissues.

To culture the immortalised normal oral keratinocytes *in vitro*, a feeder layer of fibroblast cells was required. The by-products of fibroblast metabolism allows

the keratinocytes to grow. Without the feeder layer, keratinocytes will initially adhere to the flask, but then grow very slowly, where the rate of cell death is quicker than the new cell growth, and ultimately no viable cells remain. For this reason, the use of immortalised normal oral keratinocytes were not used for the keratinocyte-only tissue model. It is possible that the fibroblast feeder cells could be seeded into the well of a plate, and keratinocytes seeded into an insert, thus providing an opportunity for free movement of by-products in the culture medium. In this way the cells could maintain viability, and when cultured at the air-liquid interface, could stratify into a 3D tissue structure. Many published research articles for candidosis-associated infections use the SkinEthic™ RHOE keratinocyte only models, but the advantages of using normal cells over the cancer-derived TR146 do warrant further investigation into this possibility of 3D tissue development. This would potentially reduce the necessary culture time for the tissue models, and could provide the same tissue structure as the RHOE, but with normal cells. In this instance, as the RHOE is a widely accepted tissue model for *in vitro* analyses, the new keratinocyte-only model could be adopted as the new standardised, and more representative model.

The *in vitro* biofilm models developed in Chapter 3 were used for infection analyses in both the simplistic keratinocyte-only tissues, and full thickness tissues, using commercially available constructs and *in vitro* equivalents. In all cases, a similar pattern of biofilm-induced damage was observed, but the extent did differ between models. Slight damage was caused by *C. albicans*-only and bacteria-only biofilms, whereas the mixed-species biofilms induced a greater amount of damage to the tissues. Additionally, the expression of the *SAP4*, *SAP6*, *PLD1*, and *ALS3* genes was up-regulated, also correlating with previously observed results. The upregulation of *SAP4*, *SAP6* and *PLD1* could indicate production of hydrolytic enzymes, the effects of which were clear when analysing the sections by microscopy. Mixed-species biofilms showed substantial damage to the tissues, and extensive invasion of *C. albicans* hyphae and bacteria. Previous studies have also implicated the production of

SAPs and PLs with tissue damage and invasion into epithelial layers of tissues (Villar *et al*., 2007; Schaller *et al*., 2005; Naglik *et al*., 2003).

In some studies that investigated candidosis using tissue models, *C. albicans* was inoculated as planktonic cells. Interestingly, even when the wild-type *C. albicans* strain (CAF2-1) was used, the damage induced by this planktonic inoculum was not visibly as apparent as when using mixed-species biofilms in this study. Yadev *et al* (2011) observed the vast majority of the *C. albicans* cells remained on the surface of the tissues, with relatively few invading into the tissues. Although no quantification of damage was reported, it appears as though there was relatively little visible damage to the tissues, as the integrity of the tissues appeared similar to that observed with tissue infections using *C. albicans*-only biofilms in this study. The observed differences between the CAF2-1 strain, and ATCC 90028 could indicate substantial strain variability, but the differences in method inoculum also elude to differences in culture state, between planktonic and biofilm forms. Moreover, throughout this PhD, a strain was used that produced virulence factors less readily, including formation of hyphae (Lu *et al*., 2006). Thus, the induction of *C. albicans* virulence factors within biofilms indicated the strong extent of bacterial modulation of *C. albicans* virulence.

A component of this PhD project was to characterise the bacterial microbiomes of specific sites in the oral cavity of patients with and without clinical presentations of DS (Chapter 5). The research recruited denture wearing patients attending the Cardiff University School of Dentistry for routine treatment or appointments. Strict recruitment criteria were imposed to ensure a specific group of patients were recruited and to allow for the anticipated subtle differences to be observed where evident. However, this also resulted in fewer patients being recruited than was desirable.

Analysis of the bacterial content of samples from the tongue, palate and denture-fitting surface yielded interesting results. The only significant difference in the number of unique bacterial species, as analysed by the Chao index of the next generation sequencing data, was the microbiomes of DS and

NoDS patients in samples of the tongue. However, using STAMP analysis to determine microbiome profiles between patient groupings, there were no significant differences at any sampling site.

Analysis of the microbiome data at species level demonstrated some substantial differences of particular bacterial species between DS and NoDS. For example, the presence of *Pseudomonas fluorescens* was detected exclusively in samples of the denture-fitting surface of DS patients and at nearly 6 and 10 times the level in DS patients compared with non-DS patients in samples of the tongue and palate respectively. Furthermore, *Acinetobacter johnsonii* was increased approximately 3-fold in patients with DS compared with patients with no DS. This was similar to the findings for *S. mitis*. *Acinetobacter johnsonii* was also present on the palates of both DS and NoDS patients, but at similar levels between the disease groupings, and a similar level to the denture samples. Thus, the only increase in presence of this bacterial species was in the denture samples of DS patients. Furthermore, the presence of *S. mitis* was also increased approximately 2-fold, in samples from the tongue. The presence of *Actinomyces odontolyticus* was also higher in DS patients, more than 6-fold, and was one of the selected oral bacteria used in the mixed species biofilms experiments in this PhD. Both *S. mitis* and *A. johnsonii* are opportunistic pathogens (Mitchell, 2011; Shelburne *et al*., 2014) and common residents of the oral cavity. *Actinomyces odontolyticus* has also been deemed an opportunistic pathogen, although it is only rarely associated with bacteraemia (Cone *et al*., 2003). The differences in the presence of particular bacterial species, and their apparent correlation with DS warrants further *in vitro* analyses to investigate the effects of these particular bacterial strains. Furthermore, it would be useful to evaluate a clinically relevant mixed-species biofilm, by incorporating not only the specific species, but also the relative proportions at which they were detected, and evaluate subsequent modulation of *C. albicans* virulence in biofilms. The difficulty in doing this, is that other bacteria that may not necessarily be present at substantial quantities, but still contribute to the overall community. Ultimately the whole biofilm will adjust to a balance according to the environment in which it is cultured. This factor is not easily controlled, but the starting inocula is the

easiest factor to control. Whether the resulting biofilm is then relatable to an *in vivo* scenario warrants further investigations.

The presence of *Candida* is a pre-requisite for DS, but the mere presence of *Candida* does not necessarily lead to onset of DS. The bacteria and their effects on *Candida* virulence were the primary interests in this PhD, but further work using clinical strains of *C. albicans* isolated from patients with and without DS to varying extents (according to Newton's classification of DS), is of great interest. Studies have demonstrated that there is significant intra-strain phenotype variation, and this may well be another mitigating factor in the incidence or severity of DS. In addition to the multiple predisposing factors already attributed to DS incidence, if a strain of *Candida* is present that is particularly virulent, or avirulent, it may determine the prognosis of the modulation, and thus the subsequent infection by the denture-associated biofilms. Furthermore, the absolute numbers of different bacterial species present, or microbial load may not be as influential to the microbial community or modulation of virulence as the actual species themselves. This project has shown that certain bacterial species can differentially modulate *C. albicans* virulence factors *in vitro*, and it is likely that this will continue *in vivo*, with more comprehensive modulation with a greater diversity of mciroorganisms.

At the time of writing, there was only one published article detailing an investigation of the oral bacterial microbiome between patients with and without DS, published late into the duration of this project (Shi *et al*., 2016). The findings were very similar to this project, in that no significant differences in the overall bacterial microbiome were observed between patients with and without DS. No other studies have specifically looked at the bacterial component of these biofilms in this context. The study within this PhD however, analysed the bacterial content to species level, and found some substantial differences in presence of individual specific bacterial species, that may be attributed to the incidence of DS. Further studies are warranted, particularly with the limited patient numbers achieved in this study, to increase confidence in the associations of particular bacterial species with incidence.

The similarities of the overall bacterial communities determined in individuals with and without DS demonstrate that subtle changes in the composition down to specific bacterial species may have an influence on the incidence of DS. A larger cohort of patients would be necessary to further evaluate the bacterial microbiome, and to identify these subtle changes with more certainty.

This research confirmed the inherent complexity of microbial interactions, particularly in mixed-culture biofilms. Although many infections are associated with a limited number of 'keystone' pathogens, the inevitable co-existence of additional microorganisms may, as demonstrated in this research, contribute to overall modulation of virulence of these pathogens, or indeed, local opportunistic pathogens.

Subtle differences were observed in the clinical study, but these differences may be substantial when considering the modulatory capacity of bacteria on *C. albicans* virulence shown in the *in vitro* research. Small variations in the bacterial composition of biofilms may heavily influence the pathogenicity of the biofilms, and subsequent inflammatory response *in vivo*.

These findings have implications for most, if not all polymicrobial biofilm-associated infections. The modulatory influence that each microorganism has in the overall community needs to be considered carefully, and although there may be specific pathogens associated with disease or infection, attention should be given not necessarily to eradicating the pathogen, but potentially managing them. This could be by use of alternative antimicrobial compounds, or even the application or introduction of probiotics into the environment.

The observational studies in this project have indicated a number of future opportunities and interests that could further our understandings of microbial interactions, and microbial modulation within biofilms. These include the following:

- Determining the bacterial strain(s) responsible for up-regulation of the *C. albicans* virulence factors

- Continue to develop *in vitro* biofilm models that are more representative of denture-associated biofilms using the results of the clinical study. The use of clinically relevant species, and inclusion at a level that corresponds with the relative proportions detected in patients with and without DS to strengthen understanding of *in vitro* interactions and modulation of *C. albicans* virulence

- Understanding the mechanisms underpinning the enhancement of *C. albicans* virulence in mixed-species biofilms, and the reasons behind the reversal of virulence after the inclusion of the keystone pathogen *P. gingivalis* within the mixed-species biofilms

- Building upon the foundations of the *in vitro* 3D tissue models, to develop a normal oral keratinocyte-only tissue model, and incorporate additional cells to make the models more closely representative of normal oral mucosa. This is necessary to more comprehensively understand the host responses to infection when considering cell-to-cell communications and responses of epithelial cells to the potential varying virulence of the strains.

- Evaluating the *in vitro* virulence profiles of the *C. albicans* isolates from patients with and without DS, to determine whether intra-strain variability of virulence can be associated with the susceptibility to candidosis infection. This can be achieved by incorporating the clinical isolates in the *in vitro* biofilm model, and evaluating the virulence genes used in this study. The mature biofilms can also be used to infect *in vitro* and/or commercial tissue models to profile the infection progression and host responses to the different *C. albicans* strains.

- Investigating efficacy of antimicrobial compounds and commercial denture-cleansing products against denture-associated biofilms

An *in vitro* polymicrobial biofilm model was developed to evaluate interactions between bacteria and the causative microorganism of DS; *C. albicans*. The biofilm model was used to determine the effects of a mixture of oral bacterial species on the production of a range of *C. albicans* virulence factors, including the morphological transition from yeast to hyphae, and the expression of a number of putative virulence-associated genes. An up-regulation of the expression of the virulence genes involved in adhesion, biofilm formation, formation of hyphae and production of hydrolytic enzymes was observed, and a visual increase in the proportion of hyphae compared with yeast cells in mixed-species biofilms. When the biofilm inoculum was modified to include an additional strain of oral bacteria; *P. gingivalis*, a reverse of the enhancement of *C. albicans* virulence was observed, highlighting the intricacy and complexity of polymicrobial interactions and modulation of virulence.

The research also developed two *in vitro* 3D mucosal tissue models for the purpose of evaluating the biofilm-associated pathogenicity in an infection model. A keratinocyte-only tissue and a full-thickness tissue were developed as alternatives for commercially available constructs of equivalent types. Biofilm infections of the *in vitro* tissue models were compared with infections of commercially available models, evaluating biofilm-induced damage, and behaviour of the biofilms, with similarities between the *in vitro* and commercially available constructs of both types.

A clinical study was completed to characterise bacterial microbiomes at various sites within the oral cavity of patients with and without denture-associated stomatitis (DS). Some differences in the relative abundance of bacterial species were detected between patients with and without DS, but the overall microbiomes for each sample site were not significantly different. The identification of several bacterial species that may be associated with DS incidence is of great interest, but further studies would be required to increase confidence in these subtle differences.

The key findings and outcomes of this study are:

- Certain oral bacterial species when co-cultured in acrylic biofilms

significantly increased the expression of *C. albicans* virulence factors, and subsequently, enhanced tissue damage in model systems.

- Enhancement of *C. albicans* virulence was reversed with the inclusion of an additional oral bacterial species, *P. gingivalis*. This highlights the complexity in predicting how bacterial communities as a whole might modulate *C. albicans* virulence.

- *Candida* was detected in clinical samples of 14 patients (DS n=6, non-DS n=8). Metataxonomic analyses revealed differences in relative abundance of bacterial species, but no significant differences in the bacterial microbiomes of the denture-fitting surface and palate between DS and non-DS patients were evident. Importantly, however, a significant increase in the number of bacterial species was evident for the tongue microbiome of non-DS patients.

- The *in vitro* modulating capacity of bacteria toward *Candida* virulence, and the observed species-level differences in bacteria between DS and non-DS patients highlight the need for consideration of the bacterial composition of oral biofilms in the pathogenesis of DS

References

Aas, J.A., Paster, B.J., Stokes, L.N., Olsen, I. and Dewhirst, F. (2005). Defining the normal bacterial flora of the oral cavity. *Journal of clinical microbiology* [Online] **43**:5721–5732.

Abe, N., Kadowaki, T., Okamoto, K., Nakayama, K., Ohishi, M. and Yamamoto, K. (1998). Biochemical and functional properties of lysine-specific cysteine proteinase (Lys-gingipain) as a virulence factor of *Porphyromonas gingivalis* in periodontal disease. *J. Biochem. (Tokyo)* [Online] **123**:305–312.

Acharya, A., Chan, Y., Kheur, S., Jin, L.J., Watt, R.M. and Mattheos, N. (2017). Salivary microbiome in non-oral disease: A summary of evidence and commentary. *Archives of Oral Biology* [Online] **83**:169–173.

Akira, S., Uematsu, S. and Takeuchi, O. (2006). Pathogen recognition and innate immunity. *Cell* [Online] **124**:783–801.

Al-Fattani, M. a and Douglas, L.J. (2006). Biofilm matrix of *Candida albicans* and *Candida tropicalis*: chemical composition and role in drug resistance. *Journal of medical microbiology* [Online] **55**:999–1008.

Albuquerque, P. and Casadevall, A. (2012). Quorum sensing in fungi – a review. *Medical Mycology* [Online] **50**:337–345.

Alves, C.T., Wei, X., Silva, S., Azeredo, J., Henriques, M. and Williams, D.W. (2014). *Candida albicans* promotes invasion and colonisation of *Candida glabrata* in a reconstituted human vaginal epithelium. *Journal of Infection* **69**:396–407

Ansel, J., Perry, P., Brown, J., Damm, D., Phan, T., Hart, C., Luger, T. and Hefeneider, S. (1990). Cytokine modulation of keratinocyte cytokines. *The Journal of Investigative Dermatology* **94**:101–107.

Arcavi, L. and Benowitz, N.L. (2004). Cigarette smoking and infection. *Archives of Internal Medicine* [Online] **164**:2206.

Arendorf, T.M. and Walker, D.M. (1980). The prevalence and intra-oral distribution of *Candida albicans* in man. *Archives of oral biology* **25**:1–10.

Argimo, S., Wishart, J.A., Leng, R., Macaskill, S., Mavor, A., Alexandris, T., Nicholls, S., Knight, A.W., Enjalbert, B., Walmsley, R., Odds, F.C., Gow, N.A.R. and Brown, A.J.P. (2007). Developmental regulation of an adhesin gene during cellular morphogenesis in the fungal pathogen *Candida albicans*. *Eukaryotic Cell* **6**:682–692.Avila, M., Ojcius, D.M. and Yilmaz, O. (2009). The oral microbiota: living with a permanent guest. *DNA and cell biology* [Online] **28**:405–11.

Axelsson, P. and J. Lindhe (1981). Effect of controlled oral hygiene procedure on caries and periodontal disease in adults. *Journal of Clinical Periodontology* **8**:239–248.

Bachmann, S.P., VandeWalle, K., Ramage, G., Patterson, T.F., Wickes, B.L., Graybill, J.R. and López-Ribot, J.L. (2002). *In vitro* activity of caspofungin against *Candida albicans* biofilms. *Antimicrobial Agents and Chemotherapy* **46**:3591–3596.

Bagaitkar, J., Demuth, D.R. and Scott, D. a (2008). Tobacco use increases susceptibility to bacterial infection. *Tobacco induced diseases* [Online] **4**:12.

Bagge, N., Hentzer, M., Andersen, J.B., Ciofu, O., Givskov, M. and Høiby, N. (2004). Dynamics and spatial distribution of beta-lactamase expression in *Pseudomonas aeruginosa* biofilms. *Antimicrobial agents and chemotherapy* [Online] **48**:1168–74.

Baginski, M. and Czub, J. (2009). Amphotericin B and its new derivatives - mode of action. *Curr Drug Metab* [Online] **10**:459–469

Bailey, D.A., Feldmann, P.J.F., Bovey, M., Gow, N.A.R. and Brown, A.J.P. (1996). The *Candida albicans* HYR1 gene, which is activated in response to hyphal development, belongs to a gene family encoding yeast cell wall proteins. *Journal of Bacteriology* **178**:5353–5360

Baker, C.A., Desrosiers, K. and Dolan, J.W. (2002). Propranolol inhibits hyphal development in *Candida albicans*. *Antimicrobial Agents and Chemotherapy* **46**:3617–3620

Bamford, C. V., Nobbs, A.H., Barbour, M.E., Lamont, R.J. and Jenkinson, H.F. (2015). Functional regions of *Candida albicans* hyphal cell wall protein Als3 that determine interaction with the oral bacterium *Streptococcus gordonii. Microbiology (Reading, England)* **161**:18–29

Bandara, H.M.H.N., K Cheung, B.P., Watt, R.M., Jin, L.J. and Samaranayake, L.P. (2013). Pseudomonas aeruginosa lipopolysaccharide inhibits *Candida albicans* hyphae formation and alters gene expression during biofilm development. *Molecular Oral Microbiology* **28**:54–69

Barbeau, J., Séguin, J., Goulet, J.P., de Koninck, L., Avon, S.L., Lalonde, B., Rompré, P. and Deslauriers, N. (2003). Reassessing the presence of *Candida albicans* in denture-related stomatitis. *Oral surgery, oral medicine, oral pathology, oral radiology, and endodontics* [Online] **95**:51–9.

Bearon, R.N. (2003). An extension of generalized Taylor dispersion in unbounded homogeneous shear flows to run-and-tumble chemotactic bacteria. *Physics of Fluids* **15**:1552–1563

Bibel, D.J., Aly, R., Shinefield, H.R., Maibach, H.I. and Strauss, W.G. (1982). Importance of the keratinized epithelial cell in bacterial adherence. *Journal of Investigative Dermatology* [Online] **79**:250–253

Bik, E.M., Long, C.D., Armitage, G.C., Loomer, P., Emerson, J., Mongodin, E.F., Nelson, K.E., Gill, S.R., Fraser-Liggett, C.M. and Relman, D.A. (2010). Bacterial diversity in the oral cavity of 10 healthy individuals. *The ISME Journal* [Online] **4**:962–974.

Bjarnsholt, T. and Givskov, M. (2007). Quorum-sensing blockade as a strategy for enhancing host defences against bacterial pathogens. *Philosophical Transactions of the Royal Society B: Biological Sciences* [Online] **362**:1213–1222.

Blankenship, J.R. and Mitchell, A.P. (2006). How to build a biofilm: a fungal perspective. *Current opinion in microbiology* [Online] **9**:588–94.

Blot, W.J., McLaughlin, J.K., Winn, D.M., Austin, D.F., Greenberg, R.S., Preston-Martin, S., Bernstein, L., Schoenberg, J.B., Stemhagen, A. and Fraumeni, J.F. (1988). Smoking and drinking in relation to oral and pharyngeal cancer. *Cancer research* [Online] **48**:3282–3287.

Braian, C., Svensson, M., Brighenti, S., Lerm, M. and Parasa, V.R. (2015). A 3D human lung tissue model for functional studies on *Mycobacterium tuberculosis* infection. *Journal of Visualized Experiments* [Online]:1–9.

Braun, B.R., Kadosh, D. and Johnson, A.D. (2001). NRG1, a repressor of filamentous growth in *C. albicans*, is down-regulated during filament induction. *The EMBO Journal* **20**:4753–4761

Brown, A.J.P. and Gow, N.A.R. (1999). Regulatory networks controlling *Candida albicans* morphogenesis. *Trends in microbiology* **7**:333–338

Brown, G.D., Herre, J., Williams, D.L., Willment, J.A., Marshall, A.S.J. and Gordon, S. (2003). Dectin-1 mediates the biological effects of β-glucans. *The Journal of Experimental Medicine* [Online] **197**:1119–1124.

Buffie, C.G. and Pamer, E.G. (2013). Microbiota-mediated colonization resistance against intestinal pathogens. *Nature reviews. Immunology* [Online] **13**:790–801.

Burne, R.A. and Marquis, R.E. (2000). Alkali production by oral bacteria and protection against dental caries. *FEMS Microbiology Letters* **193**:1–6

Calderone, R. a and Fonzi, W. a (2001). Virulence factors of *Candida albicans*. *Trends in microbiology* [Online] **9**:327–35.

Campos, M.S., Marchini, L., Bernardes, L. a S., Paulino, L.C. and Nobrega, F.G. (2008). Biofilm microbial communities of denture stomatitis. *Oral microbiology and immunology* [Online] **23**:419–24.

Cavalcanti, I.M.G., Del Bel Cury, A.A., Jenkinson, H.F. and Nobbs, A.H. (2016). Interactions between *Streptococcus oralis, Actinomyces oris*, and *Candida albicans* in the development of multispecies oral microbial biofilms on salivary pellicle. *Molecular Oral Microbiology* [Online]:n/a-n/a.

Cavalcanti, Y.W., Morse, D.J., da Silva, W.J., Del-Bel-Cury, A.A., Wei, X., Wilson, M.J., Milward, P., Lewis, M., Bradshaw, D.J. and Williams, D.W. (2015). Virulence and pathogenicity of *Candida albicans* is enhanced in biofilms containing oral bacteria. *Biofouling:Journal of The Bioadhesion and Biofilm Research* [Online] **31**:27–38.

Chandra, J., Mukherjee, P.K., Leidich, S.D., Faddoul, F.F., Hoyer, L.L., Douglas, L.J. and Ghannoum, M. a (2001). Antifungal resistance of candidal biofilms formed on denture acrylic in vitro. *Journal of Dental Research* [Online] **80**:903–908.

Chanput, W., Mes, J., Vreeburg, R.A.M., Savelkoul, H.F.J. and Wichers, H.J. (2010). Transcription profiles of LPS-stimulated THP-1 monocytes and macrophages: a tool to study inflammation modulating effects of food-derived compounds. *Food & Function* [Online] **1**:254.

Chao, A. and Chiu, C.-H. (2016). Nonparametric estimation and comparison of species richness. *eLS* [Online]:1–11.

Chen, D., Wilkinson, C.R.M., Watt, S., Penkett, C.J., Toone, W.M., Jones, N. and Bähler, J. (2007). High-resolution crystal structure and in vivo function of a Kinesin-2 homologue in *Giardia intestinalis*. *Molecular biology of the cell* **19**:308–317

Chen, H., Fujita, M., Feng, Q., Clardy, J. and Fink, G.R. (2004). Tyrosol is a quorum-sensing molecule in *Candida albicans*. *Proceedings of the National Academy of Sciences of the United States of America* [Online] **101**:5048–52.

Chen, T., Yu, W.-H., Izard, J., Baranova, O. V, Lakshmanan, A. and Dewhirst, F. (2010). The Human Oral Microbiome Database: a web accessible resource for investigating oral microbe taxonomic and genomic information. *Database : the journal of biological databases and curation* [Online] **2010**.

Chen, X., Winckler, B., Lu, M., Cheng, H., Yuan, Z., Yang, Y., Jin, L. and Ye, W. (2015). Oral microbiota and risk for esophageal squamous cell carcinoma in a high-risk area of China. *PLoS ONE* **10**:1–16

Chen, Y., Wu, C., Chung, W. and Lee, F.S. (2002). Differential secretion of Sap4–6 proteins in *Candida albicans* during hyphae formation. *Microbiolog* **148**:3743–3754

Cho, T., Nagao, J., Imayoshi, R. and Tanaka, Y. (2014). Importance of diversity in the oral microbiota including *Candida* species revealed by high-throughput technologies. *International Journal of Dentistry* **2014**:1–5

Chowdhary, A., Anil Kumar, V., Sharma, C., Prakash, A., Agarwal, K., Babu, R., Dinesh, K.R., Karim, S., Singh, S.K., Hagen, F. and Meis, J.F. (2014). Multidrug-resistant endemic clonal strain of *Candida auris* in India. *European Journal of Clinical Microbiology and Infectious Diseases* **33**:919–926

Christensen, B.B., Sternberg, C., Andersen, J.B., Eberl, L., Møller, S., Givskov, M. and Molin, S. (1998). Establishment of new genetic traits in a microbial biofilm community. *Applied and environmental microbiology* **64**:2247–2255

Coco, B.J., Bagg, J., Cross, L.J., Jose, a, Cross, J. and Ramage, G. (2008). Mixed *Candida albicans* and *Candida glabrata* populations associated with the pathogenesis of denture stomatitis. *Oral microbiology and immunology* [Online] **23**:377–83.

Colombo, A.P.V., do Souto, R.M., da Silva-Boghossian, C.M., Miranda, R. and Lourenço, T.G.B. (2014). Microbiology of oral biofilm-dependent diseases: have we made significant progress to understand and treat these diseases? *Current Oral Health Reports* [Online].

Cone, L.A., Leung, M.M. and Hirschberg, J. (2003). *Actinomyces odontolyticus* bacteremia. *Emerging Infectious Diseases* **9**:1629–1632

Consortium, T.H.M.P. (2013). Structure, function and diversity of the healthy human microbiome. *Nature* **486**:207–214

Constant, E. and Burke, J.F. (1982). Successful use of a physiologically acceptable artificial skin in the treatment of extensive burn injury. *Plastic and Reconstructive Surgery* [Online] **70**:784.

Costa, E., Silva, S., Tavaria, F. and Pintado, M. (2014). Antimicrobial and antibiofilm activity of chitosan on the oral pathogen *Candida albicans*. *Pathogens (Basel, Switzerland)* [Online] **3**:908–19.

Costello, E.K., Lauber, C.L., Hamady, M., Fierer, N., Gordon, J.I. and Knight, R. (2009). Bacterial community variation in human body habitats across space and time. *Science* **326**:1694–1697

Costerton, J.W. (1995). Overview of microbial biofilms. *Journal of industrial microbiology* [Online] **15**:137–40.

Costerton, J.W., Cheng, K.-J., Geesey, G.G., Ladd, T.I., Nickel, J.C., Dasgupta, M. and Marrie, T.J. (1987). Bacterial biofilms in nature and disease. *Annual review of microbiology* **41**:435–464

Costerton, J.W., Lewandowski, Z., Caldwell, D.E., Korber, D.R. and Lappin-scott, H.M. (1995). Microbial biofilms. *Annual review of microbiology* **49**:711–745

Costerton, J.W., Stewart, P.S. and Greenberg, E.P. (1999). Bacterial biofilms: a common cause of persistent infections. *Science* [Online] **284**:1318–1322.

Cotter, G. and Kavanagh, K. (2000). Adherence mechanisms of *Candida albicans*. *British Journal of Biomedical Science* **57**:241–249

Creger, P.E. and Blankenship, J.R. (2018). Analysis of gene expression in filamentous cells of *Candida albicans* grown on agar plates. *Journal of biological methods* **5**:1–7

da Silva Dantas, A., Lee, K.K., Raziunaite, I., Schaefer, K., Wagener, J., Yadav, B. and Gow, N.A.R. (2016). Cell biology of *Candida albicans*-host interactions. *Current Opinion in Microbiology* [Online] **34**:111–118.

Da Silva, W.J., Seneviratne, J., Samaranayake, L.P. and Del Bel Cury, A.A. (2010). Bioactivity and architecture of *Candida albicans* biofilms developed on poly(methyl methacrylate) resin surface. *Journal of Biomedical Materials Research - Part B Applied Biomaterials* **94**:149–156

Dar-Odeh, N.S., Al-Beyari, M. and Abu-Hammad, O.A. (2012). The role of antifungal drugs in the management of stomatitis. *The International Arabic Journal of Antimicrobial Agents* **2**:1–5

del Pozo, J.L. and Patel, R. (2007). The challenge of treating biofilm-associated bacterial infections. *Clinical Pharmacology & Therapeutics* [Online] **82**:204–209.

Demarchez, M., Hartmann, D.J., Regnier, M. and Asselineau, D. (1992). The role of fibroblasts in dermal vascularization and remodeling of reconstructed human skin after transplantation onto the nude mouse. *Transplantation* [Online] **54**:317–326.

Demuth, D.R., Duan, Y., Brooks, W., Holmes, A.R., Mcnab, R. and Jenkinson, H.F. (1996). Tandem genes encode cell-surface polypeptides SspA and SspB which mediate adhesion of the oral bacterium *Streptococcus gordonii* to human and bacterial receptors. *Molecular microbiology* **20**:403–413.

Deorukhkar, S.C., Saini, S. and Mathew, S. (2014). Non-*albicans Candida* infection: an emerging threat. *Interdisciplinary Perspectives on Infectious Diseases* **2014**.

Deva, A.K., Adams, W.P. and Vickery, K. (2013). The role of bacterial biofilmsin device-associated infection. *Plastic reconstructive surgery* **132**:1328

Dewhirst, F., Chen, T., Izard, J., Paster, B.J., Tanner, A.C.R., Yu, W.-H., Lakshmanan, A. and Wade, W.G. (2010). The human oral microbiome. *Journal of bacteriology* **192**:5002–5017.

di Luca, M., Maccari, G. and Nifosí, R. (2014). Treatment of microbial biofilms in the post-antibiotic era: prophylactic and therapeutic use of antimicrobial peptides and their design by bioinformatics tools. *Pathogens and Disease* **70**:257–270.

Dinarello, C.A. (1999). IL-18: A TH1 -inducing, proinflammatory cytokine and new member of the IL-1 family. *Journal of Allergy and Clinical Immunology* **103**:11–24.

Dinarello, C.A. (2000). Proinflammatory cytokines. *Chest* [Online] **118**:503–508.

Dolan, J.W., Bell, A.C., Hube, B., Schaller, M., Warner, T.F. and Balish, E. (2004). *Candida albicans* PLD I activity is required for full virulence. *Med Mycol* [Online] **42**:439–447.

Dongari-Bagtzoglou, A. and Ebersole, J.L. (1996). Fibroblast cytokine profiles in *Actínobacillus actinomycetemcomitans*-associated periodontitis. *J periodontology* **67**:871–878.

Dongari-Bagtzoglou, A. and Kashleva, H. (2006). Development of a novel three-dimensional *in vitro* model of oral *Candida* infection. *Microbial Pathogenesis* **40**:271–278.

Dongari-Bagtzoglou, A. and Kashleva, H. (2006). Development of a highly reproducible three-dimensional organitypic model of the oral mucosa. *Nature protocols* **1**:2012–2018.

Donlan, R.M. (2001). Biofilms and device-associated infections. *Emerging Infectious Diseases* **7**:277–281.

Dunne, W.M. (2002). Bacterial adhesion: seen any good biofilms lately? *Clinical Microbiology Reviews* **15**:155–166.

Dupuy, A.K., David, M.S., Li, L., Heider, T.N., Peterson, J.D., Montano, E. a, Dongari-Bagtzoglou, A., Diaz, P.I. and Strausbaugh, L.D. (2014). Redefining the human oral mycobiome with improved practices in amplicon-based taxonomy: discovery of *Malassezia* as a prominent commensal. *PloS one* [Online] **9**:e90899.

Dwivedi, P., Thompson, A., Xie, Z., Kashleva, H., Ganguly, S., Aaron, P. and Dongari-bagtzoglou, A. (2011). Role of Bcr1-activated genes Hwp1 and Hyr1 in *Candida albicans* oral mucosal biofilms and neutrophil evasion. *PLoS ONE* **6**:e16218.

Eckhart, L., Lippens, S., Tschachler, E. and Declercq, W. (2013). Cell death by cornification. *Biochimica et Biophysica Acta - Molecular Cell Research* **1833**:3471–3480.

Eden, S.C. and Hansson, H.A. (1978). *Escherichia coli* pili as possible mediators of attachment to human urinary tract epithelial cells.. *Infection and Immunity* **21**:229–237.

Edgar, R.C. (2010). Search and clustering orders of magnitude faster than BLAST. *Bioinformatics* **26**:2460–2461.

Edgerton, M., Scannapieco, F.A., Reddy, M.S. and Levine, M.J. (1993). Human submandibular-sublingual saliva promotes adhesion of *Candida albicans* to polymethylmethacrylate. *Infection and Immunity* **61**:2644–2652.

Eick, S., Glockmann, E., Brandl, B. and Pfister, W. (2004). Adherence of *Streptococcus mutans* to various restorative materials in a continuous flow system. *Journal of oral rehabilitation* **31**:278–285.

Fábián, T.K., Hermann, P., Beck, A., Fejérdy, P. and Fábián, G. (2012). Salivary defense proteins: their network and role in innate and acquired oral immunity. *International Journal of Molecular Sciences* **13**:4295–4320.

Fang, F., Lu, W.-T., Shan, Q. and Cao, J.-S. (2014). Characteristics of extracellular polymeric substances of phototrophic biofilms at different aquatic habitats. *Carbohydrate polymers* [Online] **106**:1–6.

Felk, A., Kretschmar, M., Albrecht, A., Schaller, M., Beinhauer, S., Nichterlein, T., Sanglard, D., Korting, H.C., Schäfer, W. and Hube, B. (2002). *Candida albicans* hyphal formation and the expression of the Efg1-regulated proteinases Sap4 to Sap6 are required for the invasion of parenchymal organs. *Infection and Immunity* **70**:3689–3700.

Feller, L., Altini, M., Khammissa, R.A.G., Chandran, R., Bouckaert, M. and Lemmer, J. (2013). Oral mucosal immunity. *Oral Surgery, Oral Medicine, Oral Pathology and Oral Radiology* [Online] **116**:576–583.

Fernandes, R.A., Monteiro, D.R., Arias, L.S., Fernandes, G.L., Delbem, A.C.B. and Barbosa, D.B. (2016). Biofilm formation by *Candida albicans* and *Streptococcus mutans* in the presence of farnesol: a quantitative evaluation. *Biofouling* **32**:329–338.

Figueiral, M.H., Azul, a, Pinto, E., Fonseca, P. a, Branco, F.M. and Scully, C. (2007). Denture-related stomatitis: identification of aetiological and predisposing factors - a large cohort. *Journal of oral rehabilitation* [Online] **34**:448–55.

Filoche, S., Wong, L. and Sissons, C.H. (2010). Oral biofilms: emerging concepts in microbial ecology. *Journal of dental research* [Online] **89**:8–18.

Finlay, B.B. and Falkow, S. (1997). Common themes in microbial pathogenicity revisited. *Microbiology and molecular biology reviews : MMBR* [Online] **61**:136–69.

Fitzpatrick, D. a, Logue, M.E., Stajich, J.E. and Butler, G. (2006). A fungal phylogeny based on 42 complete genomes derived from supertree and combined gene analysis. *BMC evolutionary biology* [Online] **6**:99.

Flemming, H.-C., Neu, T.R. and Wozniak, D.J. (2007). The EPS matrix: the 'house of biofilm cells'. *Journal of bacteriology* [Online] **189**:7945–7.

Flemming, H.-C. and Wingender, J. (2010). The biofilm matrix. *Nature reviews. Microbiology* [Online] **8**:623–33.

Foster, T.J. and Höök, M. (1998). Surface protein adhesins of *Staphylococcus aureus*. *Trends in Microbiology* **6**:484–488.

Frencken, J.E., Sharma, P., Stenhouse, L., Green, D., Laverty, D. and Dietrich, T. (2017). Global epidemiology of dental caries and severe periodontitis – a comprehensive review. *Journal of Clinical Periodontology* **44**:S94–S105.

Fricks-Lima, J., Hendrickson, C.M., Allgaier, M., Zhuo, H., Wiener-Kronish, J.P., Lynch, S. V and Yang, K. (2011). Differences in biofilm formation and antimicrobial resistance of *Pseudomonas aeruginosa* isolated from airways of mechanically ventilated patients and cystic fibrosis patients. *International journal of antimicrobial agents* [Online] **37**:309–15.

Fuqua, W.C., Winans, S.C. and Greenberg, E.P. (1994). Quorum sensing in bacteria: the LuxR-LuxI family of cell density-responsive transcriptional regulators. *Journal of bacteriology* **176**:269–275.

Fux, C.A., Costerton, J.W., Stewart, P.S. and Stoodley, P. (2005). Survival strategies of infectious biofilms. *Trends in microbiology* [Online] **13**:34–40.

Fux, C.A., Stoodley, P., Hall-Stoodley, L. and Costerton, J.W. (2003). Bacterial biofilms: a diagnostic and therapeutic challenge. *Expert review of anti-infective therapy* [Online] **1**:667–83.

Gabrielli, E., Pericolini, E., Luciano, E., Sabbatini, S., Roselletti, E., Perito, S., Kasper, L., Hube, B. and Vecchiarelli, A. (2015). Induction of caspase-11 by aspartyl proteinases of *Candida albicans* and implication in promoting inflammatory response. *Infection and Immunity* **83**:1940–1948.

Galley, H.F. and Webster, N.R. (1996). The immuno-inflammatory cascade. *British Journal of Anaesthesia* **77**:11–16.

Gallico, G.G., O'Connor, N.E., Compton, C.C., Kehinde, O. and Green, H. (1984). Permanent coverage of large burn wounds with autologous cultured human epithelium. *New England Journal of Medicine* [Online] **311**:448–451.

Ganderton, L., Chawla, J., Winters, C., Wimpenny, J. and Stickler, D. (1992). Scanning electron microscopy of bacterial biofilms on indwelling bladder catheters. *European Journal of Clinical Microbiology and Infectious Diseases* **11**:789–796.

Genco, C. a, Potempa, J., Mikolajczyk-Pawlinska, J. and Travis, J. (1999). Role of gingipains R in the pathogenesis of *Porphyromonas gingivalis*-mediated periodontal disease. *Clinical infectious diseases : an official publication of the Infectious Diseases Society of America* [Online] **28**:456–65.

Gendron, R., Grenier, D. and Maheu-Robert, L.-F. (2000). The oral cavity as a reservoir of bacterial pathogens for focal infections. *Microbes and Infection* **2**:897–906.

George, K.S. and Falkler, W.A. (1992). Coaggregation studies of the *Eubacterium* species. *Oral Microbiology and Immunology* [Online] **7**:285–290.

Ghannoum, M.A., Jurevic, R.J., Mukherjee, P.K., Cui, F., Sikaroodi, M., Naqvi, A. and Gillevet, P.M. (2010). Characterization of the oral fungal microbiome (mycobiome) in healthy individuals. *PLoS Pathog* **6**:1–8.

Ghannoum, M. a and Mukherjee, P.K. (2013). The human mycobiome and its impact on health and disease. *Current Fungal Infection Reports* [Online] **7**:345–350.

Ghezzi, C.E., Marelli, B., Omenetto, F.G., Funderburgh, J.L. and Kaplan, D.L. (2017). 3D functional corneal stromal tissue equivalent based on corneal stromal stem cells and multi-layered silk film architecture. *PLoS ONE* **12**:1–18.

Gibbons, R.J., Hay, D.I., Cisar, J.O. and Clark, W.B. (1988). Adsorbed salivary proline-rich protein 1 and statherin: receptors for type 1 fimbriae of *Actinomyces viscosus* T14V-J1 on apatitic surfaces. *Infection and immunity* **56**:2990–2993.

Gibbons, R.J. and Hay, D.I. (1988). Human salivary acidic proline-rich proteins and statherin promote the attachment of *Actinomyces viscosus* LY7 to apatitic surfaces. *Infection and Immunity* **56**:439–445.

Glim, J.E., Van Egmond, M., Niessen, F.B., Everts, V. and Beelen, R.H.J. (2013). Detrimental dermal wound healing: What can we learn from the oral mucosa? *Wound Repair and Regeneration* **21**:648–660.

Gocke, R., Gerath, F. and von Schwanewede, H. (2002). Quantitative determination of salivary components in the pellicle on PMMA denture base material. *Clinical oral investigations* **6**:227–235.

Gow, N.A.R. and Hube, B. (2012). Importance of the *Candida albicans* cell wall during commensalism and infection. *Current Opinion in Microbiology* [Online] **15**:406–412.

Gow, N.A.R., Netea, M.G., Munro, C. a, Ferwerda, G., Bates, S., Mora-montes, H.M., Walker, L., Jansen, T., Jacobs, L., Tsoni, V., Brown, G.D., Odds, F.C., Meer, J.W.M. Van Der, Brown, A.J.P. and Kullberg, B.J. (2007). Immune recognition of *Candida albicans* β-glucan by dectin-1. *Journal of Infectious Diseases* **196**:1565–1571.

Gracie, J.A., Robertson, S.E. and McInnes, I.B. (2003). Interleukin-18. *Journal of Leukocyte Biology* [Online] **73**:213–224.

Granger, B.L. (2012). Insight into the antiadhesive effect of yeast wall protein 1 of *Candida albicans*. *Eukaryotic cell* [Online] **11**:795–805.

Guggenheim, B., Giertsen, E., Schüpbach, P. and Shapiro, S. (2001). Validation of an in vitro biofilm model of supragingival plaque. *Journal of Dental Research* [Online] **80**:363–370.

Hajishengallis, G. and Lamont, R.J. (2016). Dancing with the stars: how choreographed bacterial interactions dictate nososymbiocity and give rise to keystone pathogens, accessory pathogens, and pathobionts. *Trends in Microbiology* [Online] **24**:477–489.

Hall-Stoodley, L., Costerton, J.W. and Stoodley, P. (2004). Bacterial biofilms: from the natural environment to infectious diseases. *Nature reviews. Microbiology* [Online] **2**:95–108.

Hall-Stoodley, L., Nistico, L., Sambanthamoorthy, K., Dice, B., Nguyen, D., Mershon, W.J., Johnson, C., Hu, F.Z., Stoodley, P., Ehrlich, G.D. and Post, J.C. (2008). Characterization of biofilm matrix, degradation by DNase treatment and evidence of

capsule downregulation in *Streptococcus pneumoniae* clinical isolates. *BMC Microbiology* [Online] **8**:173.

Hall-Stoodley, L. and Stoodley, P. (2002). Developmental regulation of microbial biofilms. *Current Opinion in Biotechnology* [Online] **13**:228–233.

Halliwell, S.C., Smith, M.C.A., Muston, P., Holland, S.L. and Avery, S. V. (2012). Heterogeneous expression of the virulence-related adhesin Epa1 between individual cells and strains of the pathogen *Candida glabrata*. *Eukaryotic Cell* **11**:141–150.

Hannan, S., Ready, D., Jasni, A.S., Rogers, M., Pratten, J. and Roberts, A.P. (2010). Transfer of antibiotic resistance by transformation with eDNA within oral biofilms. *FEMS Immunology and Medical Microbiology* **59**:345–349.

Harrison, L.M., Hoogen, C. Van Den, Wilhelmina, C.E., Haaften, V., Tesh, V.L. and Haaften, W.C.E. Van (2005). Chemokine expression in the monocytic cell line THP-1 in response to purified shiga toxin 1 and / or lipopolysaccharides. *Infection and Immunity* [Online] **73**:403–412.

Häussler, S. and Parsek, M.R. (2010). Biofilms 2009: new perspectives at the heart of surface-associated microbial communities. *Journal of bacteriology* [Online] **192**:2941–9.

Hawser, S.P., Baillie, G.S. and Douglas, L.J. (1998). Production of extracellular matrix by *Candida albicans* biofilms. *Journal of medical microbiology* [Online] **47**:253–6.

Hawser, S.P. and Douglas, L.J. (1994). Biofilm formation by *Candida* species on the surface of catheter materials in vitro. *Infection and immunity* **62**:915–921.

Heath, A.C., DiRita, V.J., Barg, N.L. and Engleberg, N.C. (1999). A two-component regulatory system, CsrR-CsrS, represses expression of three *Streptococcus pyogenes* virulence factors, hyaluronic acid capsule, Streptolysin S, and pyrogenic exotoxin B. *Infection and immunity* **67**:5298–5305.

Heidenreich, S., Otte, B., Lang, D. and Schmidt, M. (1996). Infection by *Candida albicans* inhibits apoptosis of human monocytes and monocytic U937 cells. *Journal of Leukocyte Biology* [Online] **60**:737–743.

Hirota, K., Yumoto, H., Sapaar, B., Matsuo, T., Ichikawa, T. and Miyake, Y. (2016). Pathogenic factors in *Candida* biofilm-related infectious diseases. *Journal of applied microbiology* [Online]:1–10.

Hogan, D.A., Vik, Å.˚ and Kolter, R. (2004). A Pseudomonas aeruginosa quorum-sensing molecule influences *Candida albicans* morphology. *Molecular Microbiology* **54**:1212–1223.

Hojo, K., Nagaoka, S., Ohshima, T. and Maeda, N. (2009). Bacterial interactions in dental biofilm development. *Journal of dental research* [Online] **88**:982–90.

Hornby, J.M., Jensen, E.C., Lisec, A.D., Tasto, J., Jahnke, B., Shoemaker, R., Nickerson, K.W., Tasto, J.J. and Dussault, P. (2001). Quorum sensing in the dimorphic fungus *Candida albicans* is mediated by farnesol. *Applied and environmental microbiology* **67**:2982–2992.

Hornef, M. (2015). Pathogens, commensal symbionts, and pathobionts: Discovery and functional effects on the host. *ILAR Journal* **56**:159–162.

Hoyer, L.L. (2001). The ALS gene family of *Candida albicans*. *Trends in microbiology* **9**:176–180.

Hoyer, L.L., Green, C.B., Oh, S.-H. and Zhao, X. (2008). Discovering the secrets of the *Candida albicans* agglutinin-like sequence (*ALS*) gene family. *Medical mycology* **46**:1–15.

Hoyer, L.L. and Cota, E. (2016). *Candida albicans* agglutinin-like sequence (Als) family vignettes: a review of Als protein structure and function. *Frontiers in Microbiology* **7**:1–16.

Hsiang, M.S., Greenhouse, B. and Rosenthal, P.J. (2014). *Streptococcus oralis* and *Candida albicans* synergistically activate μ-Calpain to degrade E-cadhering from oral epithelial junctions. *Journal of Infectious Diseases*:1–2.

Hube, B., Hess, D., Baker, C.A., Schaller, M., Schäfer, W. and Dolan, J.W. (2001). The role and relevance of phospholipase D1 during growth and dimorphism of *Candida albicans*. *Microbiology* **147**:879–889.

Hube, B., Monod, M., Schofield, D.A., Brown, A.J.P. and Gow, N.A.R. (1994). Expression of seven members of the gene family encoding secretory aspartyl proteinases in *Candida albicans*. *Molecular Microbiology* **14**:87–99.

Humphrey, S.P. and Williamson, R.T. (2001). A review of saliva: normal composition, flow, and function. *Journal of Prosthetic Dentistry* **85**:162–169.

Inglis, D.O., Arnaud, M.B., Binkley, J., Shah, P., Skrzypek, M.S., Wymore, F., Binkley, G., Miyasato, S.R., Simison, M. and Sherlock, G. (2012). The *Candida* genome database incorporates multiple *Candida* species: multispecies search and analysis tools with curated gene and protein information for *Candida albicans* and *Candida glabrata*. *Nucleic acids research* [Online] **40**:D667-74.

Isolauri, E., Kirjavainen, P. V. and Salminen, S. (2002). Probiotics: a role in the treatment of intestinal infection and inflammation? *Gut* [Online] **50 Suppl 3**:III54-III59.

Jack, A.A., Daniels, D.E., Jepson, M.A., Vickerman, M.M., Lamont, R.J., Jenkinson, H.F. and Nobbs, A.H. (2015). *Streptococcus gordonii* comCDE (competence) operon modulates biofilm formation with *Candida albicans*. *Microbiology (Reading, England)* **161**:411–421.

Jacobsen, J., Nielsen, E.B., Brøndum-Nielsen, K., Christensen, M.E., Olin, H.B., Tommerup, N. and Rassing, M.R. (1999). Filter-grown TR146 cells as an in vitro model of human buccal epithelial permeability. *European journal of oral sciences* **107**:138–146.

Jakubovics, N.S. and Grant Burgess, J. (2015). Extracellular DNA in oral microbial biofilms. *Microbes and Infection* [Online]:1–7.

Jakubovics, N.S., Shields, R.C., Rajarajan, N. and Burgess, J.G. (2013). Life after death: The critical role of extracellular DNA in microbial biofilms. *Letters in Applied Microbiology* **57**:467–475.

Jayatilake, J.A.M.S., Samaranayake, L.P., Lu, Q. and Jin, L.J. (2007). IL-1α, IL-1ra and IL-8 are differentially induced by *Candida* in experimental oral candidiasis. *Oral Diseases* **13**:426–433.

Jayatilake, J.A.M.S., Samaranayake, Y.H. and Samaranayake, L.P. (2005). An ultrastructural and a cytochemical study of candidal invasion of reconstituted human oral epithelium. *Journal of oral pathology & medicine.* **34**:240–246.

Jenkinson, H.F. (2011). Beyond the oral microbiome. *Environmental Microbiology* **13**:3077–3087.Jenkinson, H.F. and Lamont, R.J. (2005). Oral microbial communities in sickness and in health. *Trends in microbiology* [Online] **13**:589–95.

Jin, Y., Samaranayake, L.P., Samaranayake, Y. and Yip, H.K. (2004). Biofilm formation of *Candida albicans* is variably affected by saliva and dietary sugars. *Archives of oral biology* [Online] **49**:789–98.

Johnson, B.P., Jensen, B.J., Ransom, E.M., Heinemann, K. a, Vannatta, K.M., Egland, K. a and Egland, P.G. (2009). Interspecies signaling between *Veillonella atypica* and *Streptococcus gordonii* requires the transcription factor CcpA. *Journal of bacteriology* [Online] **191**:5563–5.

Johnson, N. (2001). Tobacco use and oral cancer: a global perspective. *J Dent Educ* [Online] **65**:328–339.

Joo, H.-S. and Otto, M. (2013). Molecular basis of in-vivo biofilm formation by bacterial pathogens. *Chem Biol.* **19**:1503–1513.

Kadosh, D. and Johnson, A.D. (2005). Induction of the *Candida albicans* filamentous growth program by relief of transcriptional repression: a genome-wide analysis. *Molecular biology of the cell* **16**:2903–2912.

Kanda, N., Shimizu, T., Tada, Y. and Watanabe, S. (2007). IL-18 enhances IFN-γ-induced production of CXCL9, CXCL10, and CXCL11 in human keratinocytes. *European Journal of Immunology* **37**:338–350.

Katsikogianni, M. and Missirlis, Y.F. (2004). Concise review of mechanisms of bacterial adhesion to biomaterials and of techniques used in estimating bacteria-material interactions. *European Cells and Materials* **8**:37–57.

Kenney, E.B., Saxe, S.R. and Bowles, R.D. (1975). The effect of cigarette smoking on anaerobiosis in the oral cavity. *Journal of periodontology* [Online] **46**:82–5.

Keren, I., Kaldalu, N., Spoering, A.L., Wang, Y. and Lewis, K. (2004). Persister cells and tolerance to antimicrobials. *FEMS Microbiology Letters* **230**:13–18.

Keren, I., Shah, D., Spoering, A.L., Kaldalu, N. and Lewis, K. (2004). Specialized persister cells and the mechanism of multidrug tolerance in *Escherichia coli*. *Journal of bacteriology* **186**:8172–8180.

Kilian, M., Chapple, I.L.C., Hannig, M., Marsh, P.D., Meuric, V., Pedersen, A.M.L., Tonetti, M.S., Wade, W.G. and Zaura, E. (2016). The oral microbiome – an update for oral healthcare professionals. *British Dental Journal* [Online] **221**:657–666.

Kim, D., Sengupta, A., Niepa, T.H.R., Lee, B.-H., Weljie, A., Freitas-Blanco, V.S., Murata, R.M., Stebe, K.J., Lee, D. and Koo, H. (2017). *Candida albicans* stimulates

Streptococcus mutans microcolony development via cross-kingdom biofilm-derived metabolites. *Scientific Reports* [Online] **7**:41332.

Kim, S., Bao, Q., Wolyniak, M.J., Frechette, G., Lehman, R., Fox, B.K. and Sundstrom, P. (2018). Release of transcriptional repression through the HCR promoter region confers uniform expression of HWP1 on surfaces of *Candida albicans* germ tubes. *PLoS ONE* **13**:1–24.

Kinane, D.F. and Chestnutt, I.G. (2000). Smoking and periodontal disease. *Critical Reviews in Oral Biology & Medicine* [Online] **11**:356–365.

Knoke, M. and Bernhardt, H. (2006). The first description of an oesophageal candidosis by Bernhard von Langenbeck in 1839. *Mycoses* **49**:283–287.

Kolenbrander, P.E. (2000). Oral microbial communities: biofilms, interactions, and genetic systems. *Annual review of microbiology* [Online] **54**:413–37.

Kolenbrander, P.E., Andersen, R.N., Blehert, D.S., Egland, P.G., Foster, J.S. and Palmer, R.J. (2002). Communication among oral bacteria. *Microbiology and Molecular Biology Reviews* **66**:486–505.

Kraneveld, E.A., Buijs, M.J., Bonder, M.J., Visser, M., Keijser, B.J.F., Crielaard, W. and Zaura, E. (2012). The relation between oral *Candida* load and bacterial microbiome profiles in dutch older adults. *PLoS ONE* **7**:1–8.

Kruppa, M.D. (2009). Quorum sensing and *Candida albicans*. *Mycoses* [Online] **52**:1–10.

Kruppa, M.D., Krom, B.P., Chauhan, N., Bambach, A. V, Cihlar, R.L. and Calderone, R.A. (2004). The two-component signal transduction protein Chk1p regulates quorum sensing in *Candida albicans*. *Eukaryotic Cell* **3**:1062–1065.

Ku, S.C., Hsueh, P.R., Yang, P.C. and Luh, K.T. (2000). Clinical and microbiological characteristics of bacteremia caused by *Acinetobacter lwoffii*. *European journal of clinical microbiology infectious diseases official publication of the European Society of Clinical Microbiology* [Online] **19**:501–505.

Kuboniwa, M. and Lamont, R.J. (2010). Subgingival biofilm formation. *Periodontology 2000* **52**:38–52.

Kuhn, D.M., George, T., Chandra, J., Mukherjee, P.K. and Ghannoum, M. A (2002). Antifungal susceptibility of *Candida* biofilms: unique efficacy of Amphotericin B lipid formulations and echinodandins. *Antimicrobial agents and chemotherapy* **46**:1773–1780.

Kulak, Y., Arikan, a and Kazazoglu, E. (1997). Existence of *Candida albicans* and microorganisms in denture stomatitis patients. *Journal of oral rehabilitation* [Online] **24**:788–90.

Kumamoto, C. a (2002). *Candida* biofilms. *Current opinion in microbiology* [Online] **5**:608–11.

Kumamoto, C.A. and Vinces, M.D. (2005). Contributions of hyphae and hypha-co-regulated genes to *Candida albicans* virulence. *Cellular microbiology* **7**:1546–1554.

LaFleur, M.D., Kumamoto, C.A. and Lewis, K. (2006). *Candida albicans* biofilms produce antifungal-tolerant persister cells. *Antimicrobial Agents and Chemotherapy* **50**:3839–3846.

Lane, S., Birse, C., Zhou, S., Matson, R. and Liu, H. (2001). DNA array studies demonstrate convergent regulation of virulence factors by Cph1, Cph2, and Efg1 in *Candida albicans*. *The journal of biological chemistry* **276**:48988–48996.

Lane, S., Zhou, S., Pan, T., Dai, Q. and Liu, H. (2001). The basic helix-loop-helix transcription factor Cph2 regulates hyphal development in *Candida albicans* partly via Tec1. *Molecular and cellular biology* **21**:6418–6428.

Lazarevic, V., Whiteson, K., Huse, S., Hernandez, D., Farinelli, L., Østerås, M., Schrenzel, J. and François, P. (2009). Metagenomic study of the oral microbiota by Illumina high-throughput sequencing. *Journal of Microbiological Methods* [Online] **79**:266–271.

Lebeaux, D., Chauhan, A., Rendueles, O. and Beloin, C. (2013). From in vitro to in vivo models of bacterial biofilm-related infections. *Pathogens (Basel, Switzerland)* [Online] **2**:288–356.

Leberer, E., Harcus, D., Broadbent, I.D., Clark, K.L., Dignard, D., Ziegelbauer, K., Schmidt, A., Gow, N.A.R., Brown, A.J.P. and Thomas, D.Y. (1996). Signal transduction through homologs of the Ste20p and Ste7p protein kinases can trigger hyphal formation in the pathogenic fungus *Candida albicans*. *Proceedings of the National Academy of Sciences* **93**:13217–13222.

Levine, M.J., Herzberg, M.C., Levine, M.S., Ellison, S.A., Stinson, M.W., Li, H.C. and van Dyke, T. (1978). Specificity of salivary-bacterial interactions: role of terminal sialic acid residues in the interaction of salivary glycoproteins with *Streptococcus sanguis* and *Streptococcus mutans*. *Infection and Immunity* **19**:107–115.

Lewis, K. (2005). Persister cells and the riddle of biofilm survival. *Biochemistry (Moscow)* **70**:267–274.

Lewis, K. (2007). Persister cells, dormancy and infectious disease. *Nature Reviews Microbiology* [Online] **5**:48–56.

Lewis, K. (2001). Riddle of biofilm resistance. *Antimicrobial agents and chemotherapy* **45**:999–1007.

Li, Q., Wang, C., Tang, C., He, Q., Li, N. and Li, J. (2014). Dysbiosis of gut fungal microbiota is associated with mucosal inflammation in Crohn's disease. *Journal of clinical gastroenterology* [Online] **48**:513–23.

Li, Y.-H., Lau, P.C.Y., Tang, N., Svensäter, G., Ellen, R.P. and Cvitkovitch, D.G. (2002). Novel two-component regulatory system involved in biofilm formation and acid resistance in *Streptococcus mutans*. *Journal of bacteriology* **184**:6333–6342.

Li, Y., Tang, N., Aspiras, M.B., Lau, P.C.Y., Lee, J.H., Ellen, R.P. and Cvitkovitch, D.G. (2002). A quorum-sensing signaling system essential for genetic competence in *Streptococcus mutans* is involved in biofilm formation. *Journal of bacteriology* **184**:2699–2708.

Liu, H., Kohler, J. and Fink, G.R. (1994). Suppression of hyphal formation in *Candida albicans* by nutation of a STE12 homolog. *Science* **266**:1723–1726.

Liu, Y. and Filler, S.G. (2011). *Candida albicans* Als3, a multifunctional adhesin and invasin. *Eukaryotic Cell* **10**:168–173.

Livak, K.J. and Schmittgen, T.D. (2001). Analysis of relative gene expression data using real-time quantitative PCR and the 2(-Delta Delta C(T)) Method. *Methods (San Diego, Calif.)* **25**:402–408.

Lopes, J.P., Stylianou, M., Nilsson, G. and Urban, C.F. (2015). Opportunistic pathogen *Candida albicans* elicits a temporal response in primary human mast cells. *Scientific Reports* [Online] **5**:1–14.

Lopes, S.P., Ceri, H., Azevedo, N.F. and Pereira, M.O. (2012). Antibiotic resistance of mixed biofilms in cystic fibrosis: impact of emerging microorganisms on treatment of infection. *International journal of antimicrobial agents* [Online] **40**:260–3.

Lopez, C.M., Wallich, R., Riesbeck, K., Skerka, C. and Zipfel, P.F. (2014*). Candida albicans* uses the surface protein Gpm1 to attach to human endothelial cells and to keratinocytes via the adhesive protein vitronectin. *PLoS ONE* **9**.

Lu, Q., Jayatilake, J.A.M.S., Samaranayake, L.P. and Jin, L. (2006). Hyphal Invasion of *Candida albicans* Inhibits the Expression of Human β-Defensins in Experimental Oral Candidiasis. *Journal of Investigative Dermatology* [Online] **126**:2049–2056.

Lu, Y., Su, C. and Liu, H. (2014). *Candida albicans* hyphal initiation and elongation. *Trends in microbiology* **22**:704–414.

Lynch, D.P. (1994). Oral candidiasis. History, classification, and clinical presentation. *Oral Surgery, Oral Medicine, Oral Pathology* **78**:189–193.

Ma, L., Jackson, K.D., Landry, R.M., Parsek, M.R. and Wozniak, D.J. (2006). Analysis of *Pseudomonas aeruginosa* conditional psl variants reveals roles for the psl polysaccharide in adhesion and maintaining biofilm structure postattachment. *Journal of bacteriology* [Online] **188**:8213–21.

Mager, D.L., Ximenez-fyvie, L.A., Haffajee, A.D. and Socransky, S.S. (2003). Distribution of selected bacterial species on intraoral surfaces. *Journal of clinical periodontology* **30**:644–654.

Mah, T.-F., Pitts, B., Pellock, B., Walker, G.C., Stewart, P.S. and Toole, G. a O. (2003). A genetic basis for *Pseudomonas aeruginosa* biofilm antibiotic resistance. *Letters to Nature* **426**:1–5.

Mah, T.-F.C. and O'Toole, G.A. (2001). Mechanisms of biofilm resistance to antimicrobial agents. *Trends in microbiology* **9**:34–39.

Malic, S., Hill, K.E., Hayes, A., Percival, S.L., Thomas, D.W. and Williams, D.W. (2009). Detection and identification of specific bacteria in wound biofilms using peptide nucleic acid fluorescent in situ hybridization (PNA FISH). *Microbiology (Reading, England)* [Online] **155**:2603–11.

Mandlik, A., Swierczynski, A., Das, A. and Ton-That, H. (2008). Pili in Gram-positive bacteria: assembly, involvement in colonization and biofilm development. *Trends in Immunology* **16**:33–40.

Mann, E.E., Rice, K.C., Boles, B.R., Endres, J.L., Ranjit, D., Chandramohan, L., Tsang, L.H., Smeltzer, M.S., Horswill, A.R. and Bayles, K.W. (2009). Modulation of eDNA release and degradation affects Staphylococcus aureus biofilm maturation. *PLoS ONE* **4**.

Marsh, P.D. (2005). Dental plaque: biological significance of a biofilm and community life-style. *Journal of clinical periodontology* [Online] **32 Suppl 6**:7–15.

Marsh, P.D. (2004). Dental plaque as a microbial biofilm. *Caries Research* [Online] **38**:204–211.

Marsh, P.D. and Bradshaw, D.J. (1995). Dental plaque as a biofilm. *Journal of industrial microbiology* **15**:169–175.

Marsh, P.D., Moter, A. and Devine, D.A. (2011). Dental plaque biofilms: communities, conflict and control. *Periodontology 2000* [Online] **55**:16–35.

Martins, M., Uppuluri, P., Thomas, D.P., Cleary, I.A., Henriques, M., Lopez-Ribot, J.L. and Oliveira, R. (2010). Presence of extracellular DNA in the *Candida albicans* biofilm matrix and its contribution to biofilms. *Mycopathologia* **169**:323–331.

Mathé, L. and Van Dijck, P. (2013). Recent insights into *Candida albicans* biofilm resistance mechanisms. *Current Genetics* **59**:251–264.

Mayer, F.L., Wilson, D. and Hube, B. (2013). *Candida albicans* pathogenicity mechanisms. *Virulence* [Online] **4**:119–128.

McBride, B.C. and Gisslow, M.T. (1977). Role of sialic acid in saliva-induced aggregation of Streptococcus sanguis. *Infection and Immunity* **18**:35–40.

McCourtie, J. and Douglas, L.J. (1984). Relationship between cell surface composition, adherence, and virulence of *Candida albicans*. *Infection and immunity* [Online] **45**:6–12.

McKenzie, R.C. and Sauder, D.N. (1990). The role of keratinocyte cytokines in inflammation and immunity. *The Journal of Investigative Dermatology* **95**:105–107.

McLean, W.H.I. and Irvine, A.D. (2007). Disorders of keratinisation: from rare to common genetic diseases of skin and other epithelial tissues. *The Ulster medical journal* [Online] **76**:72–82.

Mehta, H., Nazzal, K. and Sadikot, R.T. (2008). Cigarette smoking and innate immunity. *Inflammation Research* **57**:497–503.

Methé, B. a, Nelson, K.E., Pop, M., Creasy, H.H., Giglio, M.G., Huttenhower, C., Gevers, D., Petrosino, J.F., Abubucker, S., Jonathan, H., Chinwalla, A.T., Earl, A.M., Fitzgerald, M.G., Fulton, R.S., Hallsworth-pepin, K., Lobos, E. a, Madupu, R., Magrini, V., Martin, J.C., Mitreva, M., Muzny, D.M., Sodergren, E.J., Wollam, A.M., Worley, K.C., Wortman, J.R., Young, S.K., Zeng, Q., Aagaard, K.M., Abolude, O.O., Allen-vercoe, E., Eric, J., Alvarado, L., Andersen, G.L., Anderson, S., Appelbaum, E., Arachchi, H.M., Armitage, G., Arze, C. a, Ayvaz, T., Baker, C.C., Begg, L., Belachew,

T., Bhonagiri, V., Bihan, M., Blaser, M.J., Bloom, T., Bonazzi, J.V., Brooks, P., Buck, G. a, Christian, J., Busam, D. a, Campbell, J.L., Canon, S.R., Cantarel, B.L., Chain, P.S., Chen, I. a, Chen, L., Chhibba, S., Chu, K., Dawn, M., Clemente, J.C., Clifton, S.W., Conlan, S., Crabtree, J., Cutting, A., Davidovics, N.J., Davis, C.C., Desantis, T.Z., Delehaunty, K.D., Dewhirst, F., Deych, E. and Ding, Y. (2012). A framework for human microbiome research. *Nature* **486**:215–221.

Miller, M.B. and Bassler, B.L. (2001). Quorum sensing in bacteria. *Annual Review of Microbiology* **55**:165–99.

Mishra, A., Wu, C., Yang, J., Cisar, J.O., Das, A. and Ton-that, H. (2010). The *Actinomyces oris* type 2 fimbrial shaft FimA mediates co-aggregation with oral streptococci, adherence to red blood cells and biofilm development. *Molecular microbiology* **77**:841–854.

Mitchell, J. (2011). *Streptococcus mitis:* Walking the line between commensalism and pathogenesis. *Molecular Oral Microbiology* **26**:89–98.

Moharamzadeh, K., Brook, I.M., Noort, R. Van, Scutt, a M. and Thornhill, M.H. (2007). Tissue-engineered oral mucosa: a review of the scientific literature. *Critical Reviews in Oral Biology & Medicine* **86**:115–124.

Mohd. Nor, N., Berahim, Z., Ahmad, A. and Kannan, T. (2016). Properties of cell sources in tissue-engineered three-dimensional oral mucosa model: a review. *Current Stem Cell Research & Therapy* [Online] **12**:52–60.

Monroe, D. (2007). Looking for chinks in the armor of bacterial biofilms. *PLoS biology* [Online] **5**:e307.

Moura, J.S., da Silva, W.J., Pereira, T., Del Bel Cury, A.A. and Rodrigues Garcia, R.C.M. (2006). Influence of acrylic resin polymerization methods and saliva on the adherence of four *Candida* species. *Journal of Prosthetic Dentistry* **96**:205–211.

Moyes, D.L., Wilson, D., Richardson, J.P., Mogavero, S., Tang, S.X., Wernecke, J., Höfs, S., Gratacap, R.L., Robbins, J., Runglall, M., Murciano, C., Blagojevic, M., Thavaraj, S., Förster, T.M., Hebecker, B., Kasper, L., Vizcay, G., Iancu, S.I., Kichik, N., Häder, A., Kurzai, O., Luo, T., Krüger, T., Kniemeyer, O., Cota, E., Bader, O., Wheeler, R.T., Gutsmann, T., Hube, B. and Naglik, J.R. (2016). Candidalysin is a fungal peptide toxin critical for mucosal infection. *Nature* [Online] **532**:64–68.

Mukherjee, P.K., Chandra, J., Kuhn, D.M. and Ghannoum, M.A. (2003). Mechanism of fluconazole resistance in *Candida albicans* biofilms: phase-specific role of efflux pumps and membrane sterols. *Infection and immunity* **71**:4333–4340.

Mukherjee, P.K., Chandra, J., Retuerto, M., Sikaroodi, M., Brown, R.E., Jurevic, R., Salata, R. a, Lederman, M.M., Gillevet, P.M. and Ghannoum, M. a (2014). Oral mycobiome analysis of HIV-infected patients: identification of Pichia as an antagonist of opportunistic fungi. *PLoS pathogens* [Online] **10**:e1003996.

Murad, A.M.A., Leng, P., Straffon, M., Wishart, J., Macaskill, S., MacCallum, D., Schnell, N., Talibi, D., Marechal, D., Tekaia, F., D'Enfert, C., Gaillardin, C., Odds, F.C. and Brown, A.J.P. (2001). NRG1 represses yeast-hypha morphogenesis and hypha-specific gene expression in *Candida albicans*. *The EMBO Journal* **20**:4742–4752.

Murray, P.A., Levine, M.J., Tabak, L.A. and Reddy, M.S. (1982). Specificity of salivary-bacterial interactions: II. Evidence for a lectin on *Streptococcus sanguis* with specificity for a NeuAcα2,3Ga1β1,3Ga1NAc sequence. *Biochemical and Biophysical Research Communications* [Online] **106**:390–396.

Murray, P.A., Levine, M.J., Reddy, M.S., Tabak, L.A. and Bergey, E.J. (1986). Preparation of a sialic acid-binding protein from *Streptococus mitis* KS32AR. *Infection and Immunity* **53**:359–365.

Mylonakis, E. and Calderwood, S. (2001). Infective endocarditis in adults. *New England Journal of Medicine* **345**:1318–1330.

Naglik, J.R., Challacombe, S.J. and Hube, B. (2003). *Candida albicans* secreted aspartyl proteinases in virulence and pathogenesis. *Microbiology and molecular biology reviews : MMBR* [Online] **67**:400–28, table of contents.

Naglik, J.R., Moyes, D.L., Wächtler, B. and Hube, B. (2011). *Candida albicans* interactions with epithelial cells and mucosal immunity. *Microbes and Infection* **13**:963–976.

Namavar, F., Sparrius, M., Veerman, E.C.I., Appelmelk, B.J. and Vandenbroucke-Grauls, C.M.J.E. (1998). Neutrophil-activating protein mediates adhesion of *Helicobacter pylori* to sulfated carbohydrates on high-molecular-weight salivary mucin. *Infection and Immunity* **66**:444–447.

Nantel, A., Dignard, D., Bachewich, C., Harcus, D., Marcil, A., Bouin, A., Sensen, C.W., Hogues, H., Hoog, M. van het, Gordon, P., Rigby, T., Benoit, F., Tessier, D.C., Thomas, D.Y. and Whiteway, M. (2009). Transcription profiling of *Candida albicans* cells undergoing the yeast-to-hyphal transition. *Molecular biology of the cell* **13**:3452–3465.

Nasidze, I., Li, J., Quinque, D., Tang, K. and Stoneking, M. (2009). Global diversity in the human salivary microbiome. :636–643.

Netea, M.G., Brown, G.D., Kullberg, B.J. and Gow, N.A.R. (2008). An integrated model of the recognition of *Candida albicans* by the innate immune system. *Nature Reviews Microbiology* [Online] **6**:67–78.

Netea, M.G., Gow, N.A.R., Munro, C. a., Bates, S., Collins, C., Ferwerda, G., Hobson, R.P., Bertram, G., Hughes, H.B., Jansen, T., Jacobs, L., Buurman, E.T., Gijzen, K., Williams, D.L., Torensma, R., McKinnon, A., MacCallum, D.M., Odds, F.C., Van Der Meer, J.W.M., Brown, A.J.P. and Kullberg, B.J. (2006). Immune sensing of *Candida albicans* requires cooperative recognition of mannans and glucans by lectin and Toll-like receptors. *Journal of Clinical Investigation* **116**:1642–1650.

Ng, W.-L. and Bassler, B.L. (2009). Bacterial quorum-sensing network achitectures. *Annu. Rev. Genet* **43**:197–222.

Nickerson, K.W., Atkin, A.L. and Hornby, J.M. (2006). Quorum sensing in dimorphic fungi: Farnesol and beyond. *Applied and Environmental Microbiology* **72**:3805–3813.

Niedermeier, W., Huber, M., Fischer, D., Beier, K., Müller, N., Schuler, R., Brinninger, a, Fartasch, M., Diepgen, T., Matthaeus, C., Meyer, C. and Hector, M.P. (2000). Significance of saliva for the denture-wearing population. *Gerodontology* **17**:104–118.

Nithyanand, P., Beema Shafreen, R.M., Muthamil, S. and Karutha Pandian, S. (2015). Usnic acid inhibits biofilm formation and virulent morphological traits of *Candida albicans*. *Microbiological Research* [Online] **179**:20–28.

Nobbs, A.H. and Jenkinson, H.F. (2015). Interkingdom networking within the oral microbiome. *Microbes and Infection* [Online] **17**:484–492.

Nobile, C.J., Andes, D.R., Nett, J.E., Smith, F.J., Yue, F., Phan, Q.-T., Edwards, J.E., Filler, S.G. and Mitchell, A.P. (2006a). Critical role of Bcr1-dependent adhesins in *C. albicans* biofilm formation *in vitro* and *in vivo* . *PLoS pathogens* [Online] **2**:e63.

Nobile, C.J., Nett, J.E., Andes, D.R. and Mitchell, A.P. (2006b). Function of *Candida albicans* adhesin Hwp1 in biofilm formation. *Eukaryotic cell* [Online] **5**:1604–10.

Nobile, C.J., Fox, E.P., Nett, J.E., Sorrells, T.R., Mitrovich, Q.M., Hernday, A.D., Tuch, B.B., Andes, D.R. and Johnson, A.D. (2011). A recently evolved transcriptional network controls biofilm development in *Candida albicans*. *Cell* [Online] **148**:126–138.

Nobile, C.J. and Mitchell, A.P. (2005). Regulation of cell-surface genes and biofilm formation by the *C. albicans* transcription factor Bcr1p. *Current Biology* **15**:1150–1155.

Nobile, C.J., Schneider, H.A., Nett, J.E., Sheppard, D.C., Filler, S.G., Andes, D.R. and Mitchell, A.P. (2008). Complementary adhesin function in *C. albicans* biofilm formation. *Current Biology* **18**:1017–1024.

O'Brien-Simpson, N.M., Veith, P.D., Dashper, S.G. and Reynolds, E.C. (2003). *Porphyromonas gingivalis* gingipains: the molecular teeth of a microbial vampire. *Curr Protein Pept Sci* **4**:409–426.

O'Brien, C.L., Allison, G.E., Grimpen, F. and Pavli, P. (2013). Impact of colonoscopy bowel preparation on intestinal microbiota. *PLoS ONE* **8**:1–10.

O'Connor, N., Mulliken, J., Banks-Schlegel, S., Kehinde, O. and Green, H. (1981). Grafting of burns with cultured epithelium prepared from autologous epidermal cells. *The Lancet* [Online] **317**:75–78.

O'Toole, G.A., Kaplan, H.B. and Kolter, R. (2000). Biofilm formation as microbial development. *Annual review of microbiology* **54**:49–79.

O'Donnell, L.E., Robertson, D., Nile, C.J., Cross, L.J., Riggio, M., Sherriff, A., Bradshaw, D.J., Lambert, M., Malcolm, J., Buijs, M.J., Zaura, E., Crielaard, W., Brandt, B.W. and Ramage, G. (2015). The oral microbiome of denture wearers Is influenced by levels of natural dentition. *Plos One* [Online] **10**:e0137717.

Odds, F.C. (1994). Pathogenesis of *Candida* infections. *Journal of the American Academy of Dermatology* [Online] **31**:S2–S5.

Offenbacher, S., Barros, S.P., Singer, R.E., Moss, K., Williams, R.C. and Beck, J.D. (2007). Periodontal disease at the biofilm-gingival interface. *J. Periodontol.* [Online] **78**:1911–1925.

Oh, K.B., Miyazawa, H., Naito, T. and Matsuoka, H. (2001). Purification and characterization of an autoregulatory substance capable of regulating the

morphological transition in *Candida albicans*. *Proceedings of the National Academy of Sciences of the United States of America* [Online] **98**:4664–8.

Okshevsky, M. and Meyer, R.L. (2014). Evaluation of fluorescent stains for visualizing extracellular DNA in biofilms. *Journal of Microbiological Methods* [Online] **105**:102–104.

Otto, M. (2008). Staphylococcal biofilms. *Current Topics in Microbiology and Immunology* **322**:207–228.

Paju, S. and Scannapieco, F.A. (2007). Oral biofilms, periodontitis, and pulmonary infections. *Oral diseases* [Online] **13**:508–12.

Palmer, R.J. (2014). Composition and development of oral bacterial communities. *Periodontology 2000* **64**:20–39.

Pappas, P.G., Kauffman, C.A., Andes, D.R., Clancy, C.J., Marr, K.A., Ostrosky-Zeichner, L., Reboli, A.C., Schuster, M.G., Vazquez, J.A., Walsh, T.J., Zaoutis, T.E. and Sobel, J.D. (2016). Clinical practice guideline for the management of candidiasis: 2016 update by the infectious diseases society of America. *Clinical infectious diseases* [Online] **62**:e1-50.

Parks, D.H. and Beiko, R.G. (2010). Identifying biologically relevant differences between metagenomic communities. *Bioinformatics* **26**:715–721.

Parsek, M.R. and Singh, P.K. (2003). Bacterial biofilms: an emerging link to disease pathogenesis. *Annual review of microbiology* [Online] **57**:677–701.

Pascual, A. (2002). Pathogenesis of catheter-related infections: lessons for new designs. *Clinical Microbiology and Infection* [Online] **8**:256–264.

Passmore, J.S., Lukey, P.T. and Ress, S.R. (2001). The human macrophage cell line U937 as an in vitro model for selective evaluation of mycobacterial antigen-specific cytotoxic T-cell function. *Immunology* **102**:146–156.

Percival, S.L., Suleman, L. and Donelli, G. (2015). Healthcare-Associated infections, medical devices and biofilms: risk, tolerance and control. *Journal of Medical Microbiology* **64**:323–334.

Pereira-Cenci, T., Deng, D.M., Kraneveld, E.A., Manders, E.M.M., Del Bel Cury, A.A., Ten Cate, J.M. and Crielaard, W. (2008). The effect of *Streptococcus mutans* and *Candida glabrata* on *Candida albicans* biofilms formed on different surfaces. *Archives of oral biology* [Online] **53**:755–64.

Periasamy, S. and Kolenbrander, P.E. (2009). *Aggregatibacter actinomycetemcomitans* builds mutualistic biofilm communities with *Fusobacterium nucleatum* and *Veillonella* species in saliva. *Infection and immunity* **77**:3542–3551.

Perry, J.D. and Freydière, A.M. (2007). The application of chromogenic media in clinical microbiology. *Journal of Applied Microbiology* **103**:2046–2055.

Phan, Q.T., Myers, C.L., Fu, Y., Sheppard, D.C., Yeaman, M.R., Welch, W.H., Ibrahim, A.S., Edwards, J.E. and Filler, S.G. (2007). Als3 is a *Candida albicans* invasin that binds to cadherins and induces endocytosis by host cells. *PLoS Biology* **5**:0543–0557.

Philpott, D.J., Girardin, S.E. and Sansonetti, P.J. (2001). Innate immune responses of epithelial cells following infection with bacterial pathogens. *Current Opinion in Immunology* [Online] **13**:410–416.

Pietrella, D., Pandey, N., Gabrielli, E., Pericolini, E., Perito, S., Kasper, L., Bistoni, F., Cassone, A., Hube, B. and Vecchiarelli, A. (2013). Secreted aspartic proteases of *Candida albicans* activate the NLRP3 inflammasome. *European Journal of Immunology* **43**:679–692.

Pinke, K.H., Freitas, P., Viera, N.A., Honório, H.M., Porto, V.C. and Lara, V.S. (2016). Decreased production of proinflammatory cytokines by monocytes from individuals presenting *Candida*-associated denture stomatitis. *Cytokine* [Online] **77**:145–151.

Polke, M., Sprenger, M., Scherlach, K., Albán-Proaño, M.C., Martin, R., Hertweck, C., Hube, B. and Jacobsen, I.D. (2017). A functional link between hyphal maintenance and quorum sensing in *Candida albicans*. *Molecular Microbiology* **103**:595–617.

Popolo, L., Degani, G., Camilloni, C. and Fonzi, W. (2017). The PHR family: the role of extracellular transglycosylases in shaping *Candida albicans* cells. *Journal of Fungi* [Online] **3**:59.

Potempa, J., Sroka, A., Imamura, T. and Travis, J. (2003). Gingipains, the major cysteine proteinases and virulence factors of *Porphyromonas gingivalis*: structure, function and assembly of multidomain protein complexes. *Current protein & peptide science* **4**:397–407.

Power, M.E., Tilman, D., Estes, J.A., Menge, B.A., Bond, W.J., Mills, L.S., Daily, G., Castilla, J.C., Lubchenco, J. and Paine, R.T. (1996). Challenges in the quest for keystones. *BioScience* [Online] **46**:609–620.

Prosser, B. la T., Taylor, D., Dix, B.A. and Cleeland, R. (1987). Method of evaluating effects of antibiotics on bacterial biofilm. *Antimicrobial Agents and Chemotherapy* **31**:1502–1506.

Ramage, G., Bachmann, S., Patterson, T.F., Wickes, B.L. and Lopez-Ribot, J.L. (2002). Investigation of multidrug efflux pumps in relation to fluconazole resistance in *Candida albicans* biofilms. *Journal of Antimicrobial Chemotherapy* [Online] **49**:973–980.

Ramage, G., Martínez, J.P. and López-Ribot, J.L. (2006). *Candida* biofilms on implanted biomaterials: a clinically significant problem. *FEMS yeast research* [Online] **6**:979–86.

Ramage, G., Saville, S.P., Wickes, B.L. and López-ribot, J.L. (2002). Inhibition of *Candida albicans* biofilm formation by farnesol, a quorum-sensing molecule. *Applied and environmental microbiology* **68**:5459–5463.

Ramage, G., Tomsett, K., Wickes, B.L., López-Ribot, J.L. and Redding, S.W. (2004). Denture stomatitis: a role for *Candida* biofilms. *Oral Surgery, Oral Medicine, Oral Pathology, Oral Radiology, and Endodontology* [Online] **98**:53–59.

Rathinavelu, S., Zavros, Y. and Merchant, J.L. (2003). *Acinetobacter lwoffii* infection and gastritis. *Microbes and Infection* **5**:651–657.

Resta-Lenert, S. and Barrett, K.E. (2003). Live probiotics protect intestinal epithelial cells from the effects of infection with enteroinvasive *Escherichia coli* (EIEC). *Gut* [Online] **52**:988–97.

Rheinwald, J.G. and Green, H. (1977). Epidermal growth factor and the multiplication of cultured human epidermal keratinocytes. *Nature* **265**:421–424.

Rheinwald, J.G. and Green, H. (1975). Serial cultivation of strains of human epidemal keratinocytes. *Cell* [Online] **6**:331–343.

Rickard, A.H., Gilbert, P., High, N.J., Kolenbrander, P.E. and Handley, P.S. (2003). Bacterial coaggregation: an integral process in the development of multi-species biofilms. *Trends in Microbiology* [Online] **11**:94–100.

Rickard, A.H., Palmer, R.J., Blehert, D.S., Campagna, S.R., Semmelhack, M.F., Egland, P.G., Bassler, B.L. and Kolenbrander, P.E. (2006). Autoinducer 2: a concentration-dependent signal for mutualistic bacterial biofilm growth. *Molecular microbiology* [Online] **60**:1446–56.

Ricucci, D. and Siqueira, J.F. (2010). Biofilms and apical periodontitis: study of prevalence and association with clinical and histopathologic findings. *Journal of Endodontics* **36**:1277–1288.

Rochex, A., Godon, J.J., Bernet, N. and Escudié, R. (2008). Role of shear stress on composition, diversity and dynamics of biofilm bacterial communities. *Water Research* [Online] **42**:4915–4922.

Rogers, H., Wei, X., Lewis, M., Patel, V., Rees, J., Walker, R., Maggio, B., Gupta, A. and Williams, D.W. (2013). Immune response and candidal colonisation in denture associated stomatitis. *Clinical and Cellular Immunology* **4**:1–7.

Rosan, B. and Lamont, R.J. (2000). Dental plaque formation. *Microbes and infection / Institut Pasteur* [Online] **2**:1599–607.

Ruhl, S., Sandberg, A.L. and Cisar, J.O. (2004). Salivary receptors for the proline-rich protein-binding and lectin-like adhesins of oral *Actinomyces* and streptococci. *Journal of Dental Research* [Online] **83**:505–510.

Samaranayake, L.P., Cheung, L.K. and Samaranayake, Y. (2002). Candidiasis and other fungal diseases of the mouth. *Dermatologic Therapy* **15**:251–269.

Samaranayake, L.P., McCourtie, J. and MacFarlane, T.W. (1980). Factors affecting the in-vitro adherence of *Candida albicans* to acrylic surfaces. *Archives of oral biology* **25**:611–615.

Samaranayake, Y.H., Bandara, H.M.H.N., Cheung, B.P.K., Yau, J.Y.Y., Yeung, S.K.W. and Samaranayake, L.P. (2014). Enteric gram-negative bacilli suppress *Candida* biofilms on Foley urinary catheters. *Apmis* **122**:47–58.

Samaranayake, Y.H., Dassanayake, R.S., Cheung, B.P.K., Jayatilake, J.A.M.S., Yeung, K.W.S., Yau, J.Y.Y. and Samaranayake, L.P. (2006). Differential phospholipase gene expression by *Candida albicans* in artificial media and cultured human oral epithelium. *Apmis* **114**:857–866.

Sands, K.M., Wilson, M.J., Lewis, M.A.O., Wise, M.P., Palmer, N., Hayes, A.J., Barnes, R.A. and Williams, D.W. (2017). Respiratory pathogen colonization of dental plaque, the lower airways, and endotracheal tube biofilms during mechanical ventilation. *Journal of Critical Care* [Online] **37**:30–37.

Sanglard, D., Hube, B., Monod, M., Odds, F.C. and Gow, N.A.R. (1997). A triple deletion of the secreted aspartyl proteinase genes *SAP4*, *SAP5*, and *SAP6* of *Candida albicans* causes attenuated virulence. *Infection and Immunity* **65**:3539–3546.

Sardi, J.C.O., Scorzoni, L., Bernardi, T., Fusco-Almeida, a M. and Mendes Giannini, M.J.S. (2013). *Candida* species: current epidemiology, pathogenicity, biofilm formation, natural antifungal products and new therapeutic options. *Journal of medical microbiology* [Online] **62**:10–24.

Satou, J., Fukunaga, A., Morikawa, A., Matsumae, I., Satou, N. and Shintani, H. (1991). Streptococcal adherence to uncoated and saliva coated restoratives. *Journal of Oral Rehabilitation* **18**:421–429.

Scannapieco, F.A. (1999). Role of oral bacteria in respiratory infection. *Journal of Periodontology* **70**:793–802.

Schaller, M., Borelli, C., Korting, H.C. and Hube, B. (2005). Hydrolytic enzymes as virulence factors of *Candida albicans*. *Mycoses* **48**:365–377.

Schaller, M., Schackert, C., Korting, H.C., Januschke, E. and Hube, B. (2000). Invasion of *Candida albicans* correlates with expression of secreted aspartic proteinases during experimental infection of human epidermis. *Journal of Investigative Dermatology* [Online] **114**:712–717.

Schelenz, S., Hagen, F., Rhodes, J.L., Abdolrasouli, A., Chowdhary, A., Hall, A., Ryan, L., Shackleton, J., Trimlett, R., Meis, J.F., Armstrong-James, D. and Fisher, M.C. (2016). First hospital outbreak of the globally emerging *Candida auris* in a European hospital. *Antimicrobial Resistance and Infection Control* [Online] **5**:1–7.

Schildberger, A., Rossmanith, E., Eichhorn, T., Strassl, K. and Weber, V. (2013). Cells exhibit different cytokine expression patterns following stimulation with lipopolysaccharide. *Mediator of Inflammation* **2013**:1–10.

Schloss, P.D., Westcott, S.L., Ryabin, T., Hall, J.R., Hartmann, M., Hollister, E.B., Lesniewski, R.A., Oakley, B.B., Parks, D.H., Robinson, C.J., Sahl, J.W., Stres, B., Thallinger, G.G., Horn, D.J. Van and Weber, C.F. (2009). Introducing mothur: open-source, platform-independent, community-supported software for describing and comparing microbial communities. *Applied and environmental microbiology* **75**:7537–7541.

Scott, J.R. and Zähner, D. (2006). Pili with strong attachments: Gram-positive bacteria do it differently. *Molecular Microbiology* **62**:320–330.

Scully, C., El-Kabir, M. and Samaranayake, L.P. (1994). *Candida* and oral candidosis: a review. *Critical Reviews in Oral Biology & Medicine* **5**:125–127.

Seerangaiyan, K., van Winkelhoff, A.J., Harmsen, H.J.M., Rossen, J.W.A. and Winkel, E.G. (2017). The tongue microbiome in healthy subjects and patients with intra-oral halitosis. *Journal of Breath Research* [Online] **11**:36010.

Sellam, A., Askew, C., Epp, E., Tebbji, F., Mullick, A., Whiteway, M. and Nantel, A. (2010). Role of transcription factor CaNdt80p in cell separation, hyphal growth, and virulence in *Candida albicans*. *Eukaryotic Cell* **9**:634–644.

Seneviratne, C.J., Jin, L. and Samaranayake, L.P. (2008). Biofilm lifestyle of *Candida*: a mini review. *Oral diseases* **14**:582–590.Sheehan, D.J., Hitchcock, C.A. and Sibley, C.M. (1999). Current and emerging azole antifungal agents. *Clinical Microbiology Reviews* **12**:40–79.

Shelburne, S.A., Sahasrabhojane, P., Saldana, M., Yao, H., Su, X., Horstmann, N., Thompson, E. and Flores, A.R. (2014). *Streptococcus mitis* strains causing severe clinical disease in cancer patients. *Emerging Infectious Diseases* **20**:762–771.

Shi, B., Wu, T., Mclean, J., Edlund, A., Young, Y., He, X., Lv, H., Zhou, X., Shi, W., Li, H. and Lux, R. (2016). The denture-associated oral microbiome in health and stomatitis. *mSphere* **1**:e00216-16.

Shibata, N., Suzuki, A., Kobayashi, H. and Okawa, Y. (2007). Chemical structure of the cell-wall mannan of *Candida albicans* serotype A and its difference in yeast and hyphal forms. *The Biochemical journal* **404**:365–372.

Shulman, J.D., Rivera-Hidalgo, F. and Beach, M.M. (2005). Risk factors associated with denture stomatitis in the United States. *Journal of oral pathology & medicine* [Online] **34**:340–6.

Silva, S., Henriques, M., Hayes, A., Oliveira, R., Azeredo, J. and Williams, D.W. (2011). *Candida glabrata* and *Candida albicans* co-infection of an in vitro oral epithelium. *Journal of oral pathology & medicine : official publication of the International Association of Oral Pathologists and the American Academy of Oral Pathology* [Online] **40**:421–7.

Silva, S., Henriques, M., Oliveira, R., Azeredo, J., Malic, S., Hooper, S.J. and Williams, D.W. (2009). Characterization of *Candida parapsilosis* infection of an in vitro reconstituted human oral epithelium. *European journal of oral sciences* [Online] **117**:669–75..

Silva, S., Hooper, S.J., Henriques, M., Oliveira, R., Azeredo, J. and Williams, D.W. (2011). The role of secreted aspartyl proteinases in *Candida tropicalis* invasion and damage of oral mucosa. *Clinical microbiology and infection : the official publication of the European Society of Clinical Microbiology and Infectious Diseases* [Online] **17**:264–72.

Silverman, R.J., Nobbs, A.H., Vickerman, M.M., Barbour, M.E. and Jenkinson, H.F. (2010). Interaction of *Candida albicans* cell wall Als3 protein with *Streptococcus gordonii* SspB adhesin promotes development of mixed-species communities. *Infection and immunity* [Online] **78**:4644–52.

Singh, J.P., Dhiman, R.K., Bedi, R.P.S. and Girish, S.H. (2011). Flexible denture base material: a viable alternative to conventional acrylic denture base material. *Contemporary clinical dentistry* [Online] **2**:313–7.

Sitheeque, M. a M. and Samaranayake, L.P. (2003). Chronic hyperplastic candidosis/candidiasis (candidal leukoplakia). *Crit Rev Oral Biol Med* **14**:253–267.

Skinner, C.E. and Fletcher, D.W. (1960). A review of the genus *Candida*. *Bacteriological reviews* **24**:397–416.

Slomiany, B.L., Murty, V.L.N., Piotrowski, J. and Slomiany, A. (1996). Salivary mucins in oral mucosal defense. *General Pharmacology* **27**:761–771.

Sohn, K., Urban, C., Brunner, H. and Rupp, S. (2003). EFG1 is a major regulator of cell wall dynamics in *Candida albicans* as revealed by DNA microarrays. *Molecular Microbiology* **47**:89–102.

Sopori, M. (2002). Science and society: effects of cigarette smoke on the immune system. *Nature Reviews Immunology* [Online] **2**:372–377.

Spiekstra, S.W., Breetveld, M., Rustemeyer, T., Scheper, R.J. and Gibbs, S. (2007). Wound-healing factors secreted by epidermal keratinocytes and dermal fibroblasts in skin substitutes. *Wound Repair and Regeneration* **15**:708–717.

Spoering, A.L. and Gilmore, M.S. (2006). Quorum sensing and DNA release in bacterial biofilms. *Current opinion in microbiology* [Online] **9**:133–7.

Stewart, P.S. and Costerton, J.W. (2001). Antibiotic resistance of bacteria in biofilms. *Lancet* [Online] **358**:135–8.

Stickler, D.J. (2014). Clinical complications of urinary catheters caused by crystalline biofilms: Something needs to be done. *Journal of Internal Medicine* **276**:120–129

.Stickler, D., Morris, N., Moreno, M.C. and Sabbuba, N. (1998). Studies on the formation of crystalline bacterial biofilms on urethral catheters. *European Journal of Clinical Microbiology and Infectious Diseases* **17**:649–652.

Stinson, M.W., Levine, M.J., Cavese, J.M., Prakobphol, A., Murray, P.A., Tabak, L.A. and Reddy, M.S. (1982). Adherence of *Streptococcus sanguis* to salivary mucin bound to glass. *Journal of dental research* [Online] **61**:1390–3.

Stoldt, V.R., Sonneborn, A., Leuker, C.E. and Ernst, J.F. (1997). Efg1p, an essential regulator of morphogenesis of the human pathogen *Candida albicans*, is a member of a conserved class of bHLH proteins regulating morphogenetic processes in fungi. *The EMBO Journal* **16**:1982–1991.

Stoodley, P., Sauer, K., Davies, D.G. and Costerton, J.W. (2002). Biofilms as complex differentiated communities. *Annual review of microbiology* [Online] **56**:187–209. Available at: http://www.ncbi.nlm.nih.gov/pubmed/12142477 [Accessed: 19 March 2014].

Stromberg, N. and Boren, T. (1992). *Actinomyces* tissue specificity may depend on differences in receptor specificity for GalNAc3-containing glycoconjugates. *Infection and immunity* **60**:3268–3277.

Sudbery, P.E. (2011). Growth of *Candida albicans* hyphae. *Nature Publishing Group* [Online] **9**:737–748..

Sudbery, P., Gow, N.A.R. and Berman, J. (2004). The distinct morphogenic states of *Candida albicans*. *Trends in microbiology* **12**:317–324.

Sun, T., Jackson, S., Haycock, J.W. and MacNeil, S. (2006). Culture of skin cells in 3D rather than 2D improves their ability to survive exposure to cytotoxic agents. *Journal of Biotechnology* **122**:372–381.

Sundstrom, P. (2006). *Candida albicans* hypha formation and virulence. *Molecular Principles of Fungal Pathogenesis*. American Society of Microbiology, pp. 45–47.

Sundstrom, P. (1999). Adhesins in *Candida albicans*. *Current Opinion in Microbiology* **2**:353–357.Sutherland, I.W. (2001). The biofilm matrix - an immobilized but dynamic microbial environment. *Trends in microbiology* [Online] **9**:222–7.

Swift, S., Throup, J.P., Williams, P., Salmond, G.P.C. and Stewart, G.S.A.B. (1996). Quorum sensing: a population density component in the determination of bacterial phenotype. *Trends in biochemical sciences* **4**:214–219.

Szajewska, H. and Mrukowicz, J.Z. (2001). Probiotics in the treatment and prevention of acute infectious diarrhea in infants and children: a systematic review of published randomized, double-blind, placebo-controlled trials. *Journal of pediatric gastroenterology and nutrition* **33 Suppl 2**:S17–S25.

Sztajer, H., Szafranski, S.P., Tomasch, J., Reck, M., Nimtz, M., Rohde, M. and Wagner-Döbler, I. (2014). Cross-feeding and interkingdom communication in dual-species biofilms of *Streptococcus mutans* and *Candida albicans*. *The ISME Journal* [Online]:1–16.

Tabak, L.A. (1995). In defense of the oral cavity: structure, biosynthesis, and function of salivary mucins. *Annual review of physiology* **57**:547–564.

Tabak, L.A., Levine, M.J., Mandel, I.D. and Ellison, S.A. (1982). Role of salivary mucins in the protection of the oral cavity. *Journal of Oral Pathology & Medicine* **11**:1–17.

Takahashi, N. (2005). Microbial ecosystem in the oral cavity: Metabolic diversity in an ecological niche and its relationship with oral diseases. *International Congress Series* [Online] **1284**:103–112.

Tande, A.J. and Patel, R. (2014). Prosthetic joint infection. *Clinical Microbiology Reviews* **27**:302–345.Taylor, P.R., Tsoni, S. V, Willment, J.A., Dennehy, K.M., Rosas, M., Findon, H., Haynes, K., Steele, C., Botto, M., Gordon, S. and Brown, G.D. (2007). Dectin-1 is required for beta-glucan recognition and control of fungal infection. *Nature Immunology* **8**:31–38.

Thein, Z.M., Samaranayake, Y. and Samaranayake, L.P. (2006). Effect of oral bacteria on growth and survival of *Candida albicans* biofilms. *Archives of oral biology* [Online] **51**:672–80.

Thein, Z.M., Samaranayake, Y. and Samaranayake, L.P. (2007). *In vitro* biofilm formation of *Candida albicans* and non-*albicans Candida* species under dynamic and anaerobic conditions. *Archives of oral biology* [Online] **52**:761–7.

Thomas, W.E., Trintchina, E., Forero, M., Vogel, V. and Sokurenko, E. V. (2002). Bacterial adhesion to target cells enhanced by shear force. *Cell* **109**:913–923.

Tlaskalová-Hogenová, H., Štěpánková, R., Hudcovic, T., Tučková, L., Cukrowska, B., Lodinová-Žádníková, R., Kozáková, H., Rossmann, P., Bártová, J., Sokol, D., Funda,

D.P., Borovská, D., Řeháková, Z., Šinkora, J., Hofman, J., Drastich, P. and Kokešová, A. (2004). Commensal bacteria (normal microflora), mucosal immunity and chronic inflammatory and autoimmune diseases. *Immunology Letters* **93**:97–108.

Tobouti, P.L., Casaroto, A.R., de Almeida, R.S.C., Ramos, S.D.P., Dionísio, T.J., Porto, V.C., Santos, C.F. and Lara, V.S. (2015). Expression of secreted aspartyl proteinases in an experimental model of *Candida albicans* -associated denture stomatitis. *Journal of Prosthodontics* [Online]:127–134.

Todaro, G.J. and Green, H. (1963). Quantitative studies of the growth of mouse embryo cells in culture and their development into established lines. *The journal of cell biology* **17**:299–313.

Tomaras, A.P., Dorsey, C.W., Edelmann, R.E. and Actis, L.A. (2003). Attachment to and biofilm formation on abiotic surfaces by Acinetobacter baumannii: Involvement of a novel chaperone-usher pili assembly system. *Microbiology* **149**:3473–3484.

Tournu, H. and Van Dijck, P. (2012). *Candida* biofilms and the host: models and new concepts for eradication. *International Journal of Microbiology* **2012**.

Turnbaugh, P.J. and Gordon, J.I. (2009). The core gut microbiome, energy balance and obesity. *The Journal of physiology* [Online] **587**:4153–8..

Turnbaugh, P.J., Hamady, M., Yatsunenko, T., Cantarel, B.L., Duncan, A., Ley, R.E., Sogin, M.L., Jones, W.J., Roe, B.A., Affourtit, J.P., Egholm, M., Henrissat, B., Heath, A.C., Knight, R. and Gordon, J.I. (2009). Human gut microbiome viewed across age and geography. *Nature* [Online] **457**:222–227.

Van Acker, H., Van Dijck, P. and Coenye, T. (2014). Molecular mechanisms of antimicrobial tolerance and resistance in bacterial and fungal biofilms. *Trends in Microbiology* [Online] **22**:326–333.

van Houte, J. (1994). Role of micro-organisms in caries etiology. *Journal of dental research* [Online] **73**:672–81.

van Staveren, W.C.G., Solís, D.Y.W., Hébrant, A., Detours, V., Dumont, J.E. and Maenhaut, C. (2009). Human cancer cell lines: experimental models for cancer cells in situ? For cancer stem cells? *Biochimica et Biophysica Acta (BBA) - Reviews on Cancer* [Online] **1795**:92–103.

Vandekerckhove, T.T.M., Watteyne, S., Willems, A., Swings, J.G., Mertens, J. and Gillis, M. (1999). Phylogenetic analysis of the 16S rDNA of the cytoplasmic bacterium *Wolbachia* from the novel host *Folsomia candida* (Hexapoda, Collembola) and its implications for wolbachial taxonomy. *FEMS Microbiology Letters* **180**:279–286.

Varkey, M., Ding, J. and Tredget, E. (2015). Advances in skin substitutes - potential of tissue engineered skin for facilitating anti-fibrotic healing. *Journal of Functional Biomaterials* [Online] **6**:547–563.

Vazquez, J.A. (2003). Invasive oesophageal candidiasis: current and developing treatment options. *Drugs* **63**:971–989.

Veerachamy, S., Yarlagadda, T., Manivasagam, G. and Yarlagadda, P.K. (2014). Bacterial adherence and biofilm formation on medical implants: A review.

Proceedings of the Institution of Mechanical Engineers, Part H: Journal of Engineering in Medicine [Online] **228**:1083–1099.

Verstrepen, K.J. and Klis, F.M. (2006). Flocculation, adhesion and biofilm formation in yeasts. *Molecular microbiology* [Online] **60**:5–15.

Vilain, S., Pretorius, J.M., Theron, J. and Brözel, V.S. (2009). DNA as an adhesin: Bacillus cereus requires extracellular DNA to form biofilms. *Applied and Environmental Microbiology* **75**:2861–2868.

Villar, C.C., Kashleva, H., Nobile, C.J., Mitchell, a P. and Dongari-Bagtzoglou, A. (2007). Mucosal tissue invasion by *Candida albicans* is associated with E-cadherin degradation, mediated by transcription factor Rim101p and protease Sap5p. *Infection and immunity* [Online] **75**:2126–35.

Vojdani, M. and Giti, R. (2015). Polyamide as a denture base material: a literature review. *J Dent Shiraz Univ Med Sci. J Dent Shiraz Univ Med Sci* **16**:1–9.

Wade, W.G. (2011). Has the use of molecular methods for the characterization of the human oral microbiome changed our understanding of the role of bacteria in the pathogenesis of periodontal disease? *Journal of clinical periodontology* [Online] **38 Suppl 1**:7–16.

Wade, W.G. (2013). The oral microbiome in health and disease. *Pharmacological research: the official journal of the Italian Pharmacological Society* [Online] **69**:137–43.

Waelti, E.R., Inaebnit, S.P., Rast, H.P., Hunziker, T., Limat, A., Braathen, L.R. and Wiesmann, U. (1992). Co-culture of human keratinocytes on post mitotic human dermal fibroblast feeder cells: production of large amounts of interleukin 6. *The Journal of Investigative Dermatology* **98**:805–808.

Walters, M.C., Roe, F., Bugnicourt, A., Franklin, M.J. and Stewart, P.S. (2003). Contributions of antibiotic penetration, oxygen limitation. *Society* **47**:317–323.

Wang, S. (2017). *3D Neuronal Innervated Corneal Tissue Model*. [Thesis]

Webb, B.C., Thomas, C.J. and Willcox, M.D.P. (1998). *Candida*-associated denture stomatitis. Aetiology and management: a review. Part 1. Factors influencing distribution of *Candida* species in the oral cavity. *Australian dental journal* **43**:45–50.

Webb, B.C., Thomas, C.J. and Willcox, M.D.P. (1998). *Candida*-associated denture stomatitis. Aetiology and management: a review. Part 2. Oral diseases caused by *Candida* species. *Australian dental journal* **43**:160–166.

Wei, X.Q., Rogers, H., Lewis, M.A.O. and Williams, D.W. (2011). The role of the IL-12 cytokine family in directing T-cell responses in oral candidosis. *Clinical and Developmental Immunology* **2011**.

Weinberg, E.D. (1975). Microbial invaders. Host's attempts to withhold iron from microbial invaders. *The journal of the American medical association* **231**:39–41.

White, P.L., Archer, A.E. and Barnes, R.A. (2005). Comparison of non-culture-based methods for detection of systemic fungal infections, with an emphasis on invasive *Candida* infections. *Journal of Clinical Microbiology* **43**:2181–2187.

White, P.L., Shetty, A. and Barnes, R.A. (2003). Detection of seven *Candida* species using the Light-Cycler system. *Journal of Medical Microbiology* **52**:229–238.

White, P.L., Williams, D.W., Kuriyama, T., Samad, S.A., Lewis, M.A.O. and Barnes, R.A. (2004). Detection of *Candida* in concentrated oral rinse cultures by real-time PCR. *Journal of clinical microbiology* **42**:2101–2107.

Williams, D.W., Jordan, R.P.C., Wei, X., Alves, C.T., Wise, M.P., Wilson, M.J. and Lewis, M. A. O. (2013). Interactions of *Candida albicans* with host epithelial surfaces. *Journal of oral microbiology* [Online] **5**:1–8.

Williams, D.W., Kuriyama, T., Silva, S., Malic, S. and Lewis, M. A. O. (2011). *Candida* biofilms and oral candidosis: treatment and prevention. *Periodontology 2000* [Online] **55**:250–65.

Williams, D.W. and Lewis, M. A. O(2011). Pathogenesis and treatment of oral candidosis. *Journal of oral microbiology* [Online] **3**:1–11.

Williams, D.W. and Lewis, M.A.O. (2000). Isolation and identification of *Candida* from the oral cavity. *Oral diseases* [Online] **6**:3–11.

Williams, P., Camara, M., Hardman, a, Swift, S., Milton, D., Hope, V.J., Winzer, K., Middleton, B., Pritchard, D.I. and Bycroft, B.W. (2000). Quorum sensing and the population-dependent control of virulence. *Philosophical transactions of the Royal Society of London. Series B, Biological sciences* [Online] **355**:667–80.

Williams, P., Winzer, K., Chan, W.C. and Cámara, M. (2007). Look who's talking: communication and quorum sensing in the bacterial world. *Philosophical transactions of the Royal Society of London. Series B, Biological sciences* [Online] **362**:1119–34.

Wilson, D., Naglik, J.R. and Hube, B. (2016). The missing link between *Candida albicans* hyphal morphogenesis and host cell damage. *PLoS Pathogens* **12**:1–5.

Winn, D.M. (2001). Tobacco use and oral disease. *J Dent Educ* [Online] **65**:306–312.

Wisplinghoff, H., Bischoff, T., Tallent, S.M., Seifert, H., Wenzel, R.P. and Edmond, M.B. (2004). Nosocomial bloodstream infections in US hospitals: analysis of 24,179 cases from a prospective nationwide surveillance study. *Clinical Infectious Diseases* [Online] **39**:309–317.

Witt, V., Wild, C. and Uthicke, S. (2011). Effect of substrate type on bacterial community composition in biofilms from the Great Barrier Reef. *FEMS microbiology letters* [Online] **323**:188–95.

Wyllie, F.S., Jones, C.J., Skinner, J.W., Haughton, M.F., Wallis, C., Wynford-Thomas, D., Faragher, R.G.A. and Kipling, D. (2000). Telomerase prevents the accelerated cell ageing of Werner syndrome fibroblasts. *Nature Genetics* **24**:16–17.

Xie, G., Chain, P.S.G., Lo, C.-C., Liu, K.-L., Gans, J., Merritt, J. and Qi, F. (2010). Community and gene composition of a human dental plaque microbiota obtained by metagenomic sequencing. *Molecular oral microbiology* **25**:391–405.

Xu, R., Sun, H.F., Williams, D.W., Jones, A. V., Al-Hussaini, A., Song, B. and Wei, X.Q. (2015). IL-34 suppresses *Candida albicans* induced tnf α production in m1 macrophages by downregulating expression of dectin-1 and tlr-2. *Journal of Immunology Research* **2015**.:1-7

Yadev, N.P., Murdoch, C., Saville, S.P. and Thornhill, M.H. (2011). Evaluation of tissue engineered models of the oral mucosa to investigate oral candidiasis. *Microbial Pathogenesis* [Online] **50**:278–285.

Yang, F., Zeng, X., Ning, K., Liu, K.-L., Lo, C.-C., Wang, W., Chen, J., Wang, D., Huang, R., Chang, X., Chain, P.S., Xie, G., Ling, J. and Xu, J. (2012). Saliva microbiomes distinguish caries-active from healthy human populations. *The ISME Journal* [Online] **6**:1–10.

Yang, G., Sau, C., Lai, W., Cichon, J. and Li, W. (2015). 3D corneal tissue model with epithelium, stroma, and innervation. *Biomaterials* **344**:1173–1178.

Yano, J., Yu, A., Jr, P.L.F. and Noverr, M.C. (2016). Transcription factors Efg1 and Bcr1 regulate biofilm formation and virulence during *Candida albicans*-associated denture stomatitis. *PLoS ONE* **11**:e0159692.

Zarco, M.F., Vess, T.J. and Ginsburg, G.S. (2012). The oral microbiome in health and disease and the potential impact on personalized dental medicine. *Oral diseases* **18**:109–120.

Zemanick, E.T., Wagner, B.D., Robertson, C.E., Stevens, M.J., Szefler, S.J., Accurso, F.J., Sagel, S.D. and Harris, J.K. (2015). Assessment of airway microbiota and inflammation in cystic fibrosis using multiple sampling methods. *Annals of the American Thoracic Society* **12**:221–229.

Zhang, K., Ren, B., Zhou, X., Xu, H.H.K., Chen, Y., Han, Q., Li, B., Weir, M.D., Li, M., Feng, M. and Cheng, L. (2016). Effect of antimicrobial denture base resin on multi-species biofilm formation. *International journal of molecular sciences* **17**:1–13.

Zhao, X., Oh, S.H., Cheng, G., Green, C.B., Nuessen, J.A., Yeater, K., Leng, R.P., Brown, A.J.P. and Hoyer, L.L. (2004). *ALS3* and *ALS8* represent a single locus that encodes a *Candida albicans* adhesin; functional comparisons between Als3p and Als1p. *Microbiology* **150**:2415–2428.

Zheng, X., Wang, Y. and Wang, Y. (2004). Hgc1, a novel hypha-specific G1 cyclin-related protein regulates *Candida albicans* hyphal morphogenesis. *EMBO Journal* **23**:1845–1856.

Zimmerli, W., Trampuz, A. and Ochsner, P.E. (2004). Prosthetic-joint infections. *N Engl J Med* **351**:1645–1654.Zobell, C.E. (1943). The effect of solid surfaces upon bacterial activity. *Journal of bacteriology*:39–56.

Appendix I

Supporting documentation for qPCR

- Melt curves for qPCR runs to confirm specificity of single product amplification

ACT1

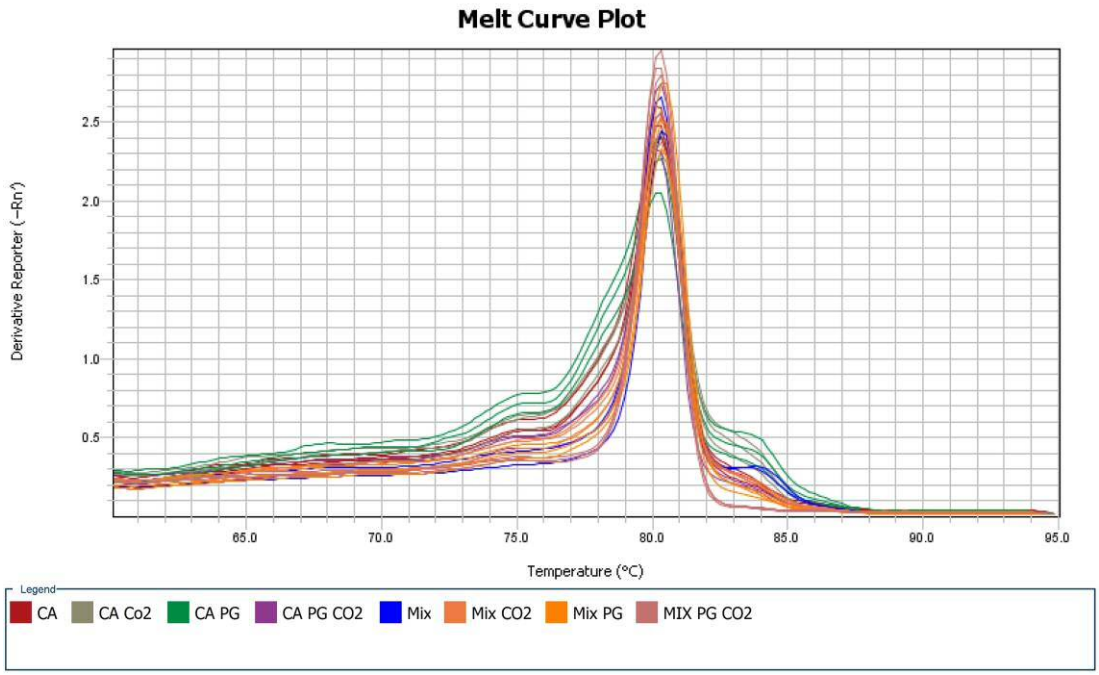
Melt Curve Plot
Derivative Reporter (-Rn')
2.5
2.0
1.5
1.0
0.5
65.0
70.0
75.0
80.0
85.0
90.0
95.0
Temperature (°C)
Legend
CA
CA Co2
CA PG
CA PG CO2
Mix
Mix CO2
Mix PG
MIX PG CO2

ALS3

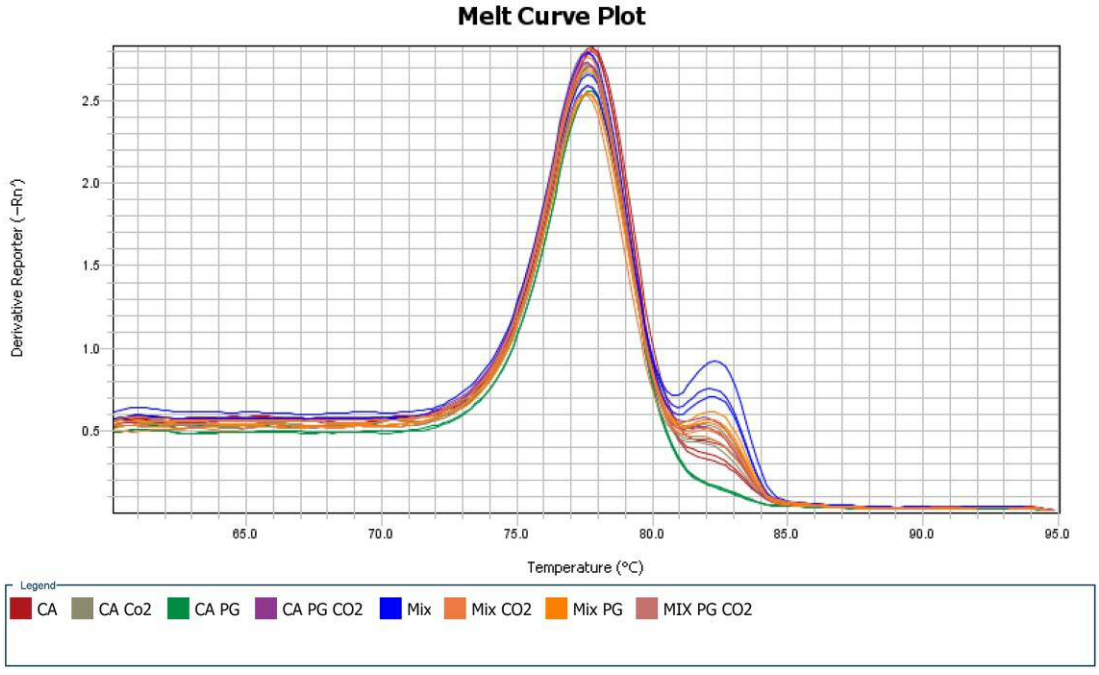
Melt Curve Plot
Derivative Reporter (-Rn')
2.5
2.0
1.5
1.0
0.5
65.0
70.0
75.0
80.0
85.0
90.0
95.0
Temperature (°C)
Legend
CA
CA Co2
CA PG
CA PG CO2
Mix
Mix CO2
Mix PG
MIX PG CO2

EPA1

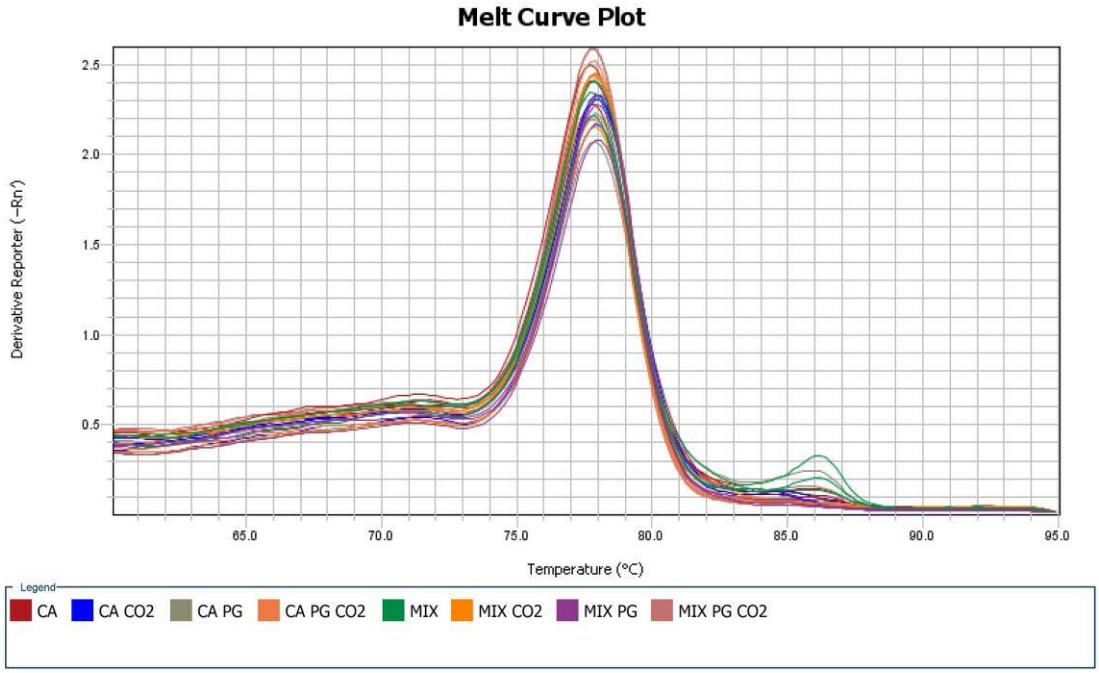
Melt Curve Plot
Derivative Reporter (-Rn')
2.5
2.0
1.5
1.0
0.5
65.0
70.0
75.0
80.0
85.0
90.0
95.0
Temperature (°C)
Legend
CA
CA CO2
CA PG
CA PG CO2
MIX
MIX CO2
MIX PG
MIX PG CO2

HWP1

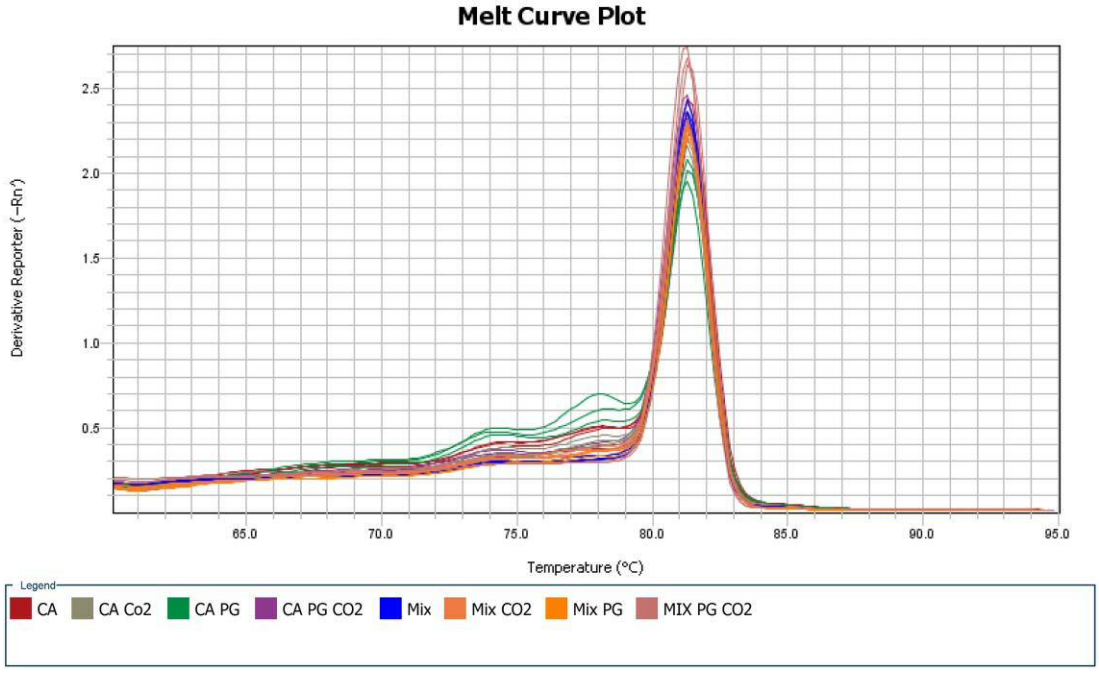
Melt Curve Plot
Derivative Reporter (-Rn')
2.5
2.0
1.5
1.0
0.5
65.0
70.0
75.0
80.0
85.0
90.0
95.0
Temperature (°C)
Legend
CA
CA Co2
CA PG
CA PG CO2
Mix
Mix CO2
Mix PG
MIX PG CO2

PLD1

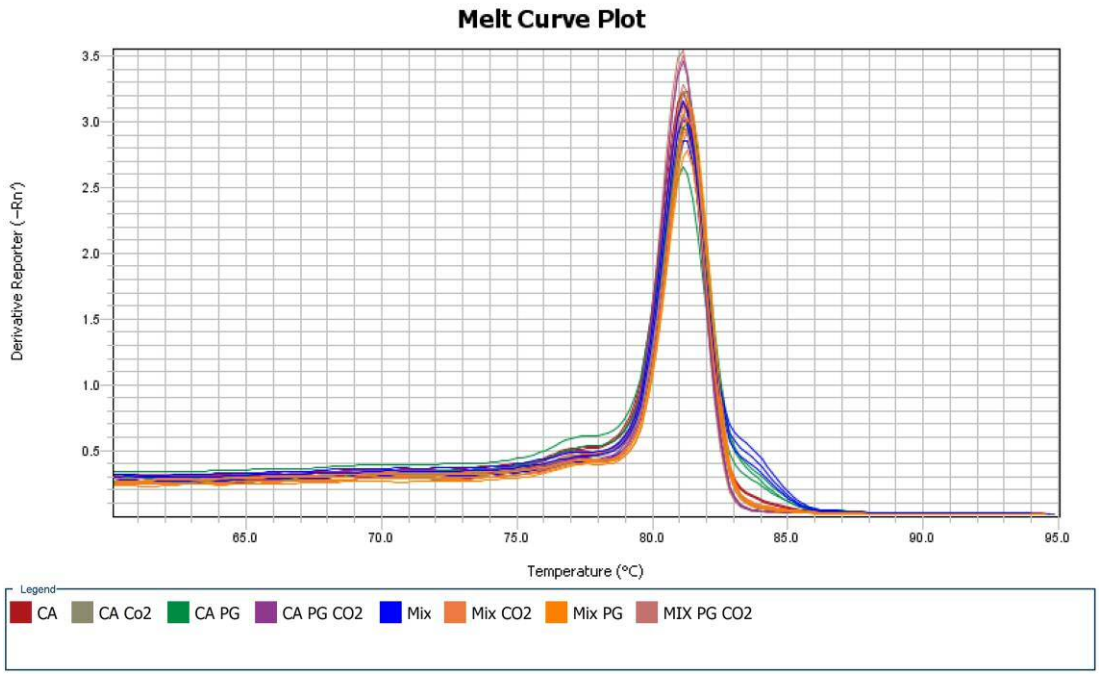
Melt Curve Plot
Derivative Reporter (-Rn')
3.5
3.0
2.5
2.0
1.5
1.0
0.5
65.0
70.0
75.0
80.0
85.0
90.0
95.0
Temperature (°C)
Legend
CA
CA Co2
CA PG
CA PG CO2
Mix
Mix CO2
Mix PG
MIX PG CO2

SAP4

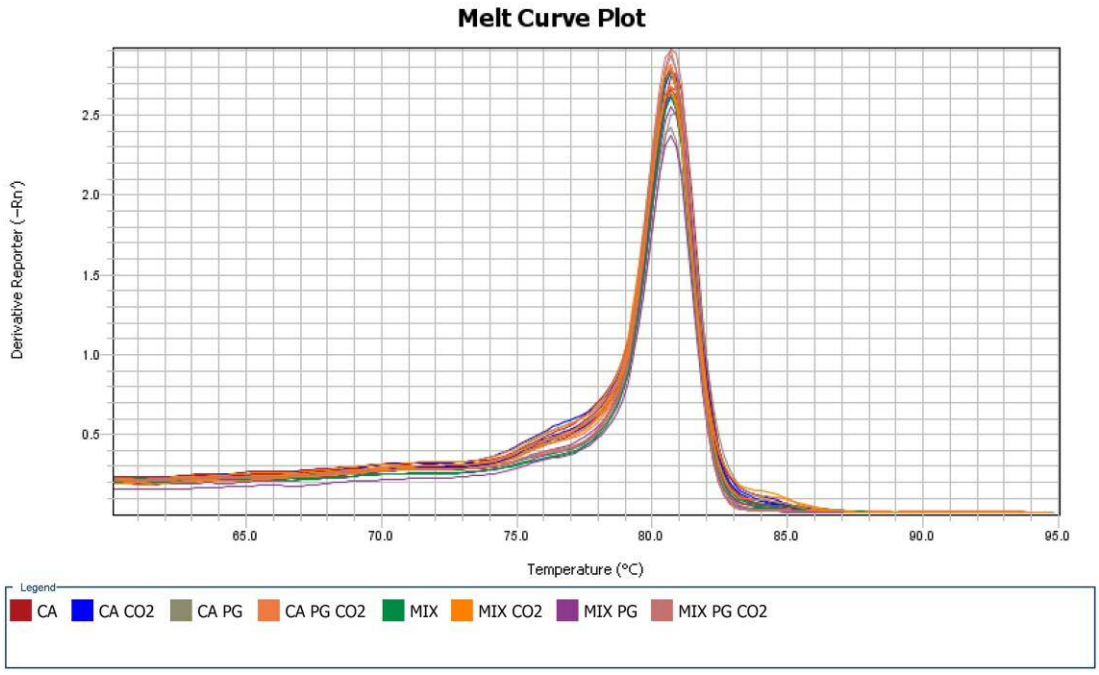
Melt Curve Plot
Derivative Reporter (-Rn')
2.5
2.0
1.5
1.0
0.5
65.0
70.0
75.0
80.0
85.0
90.0
95.0
Temperature (°C)
Legend
CA
CA CO2
CA PG
CA PG CO2
MIX
MIX CO2
MIX PG
MIX PG CO2

SAP6

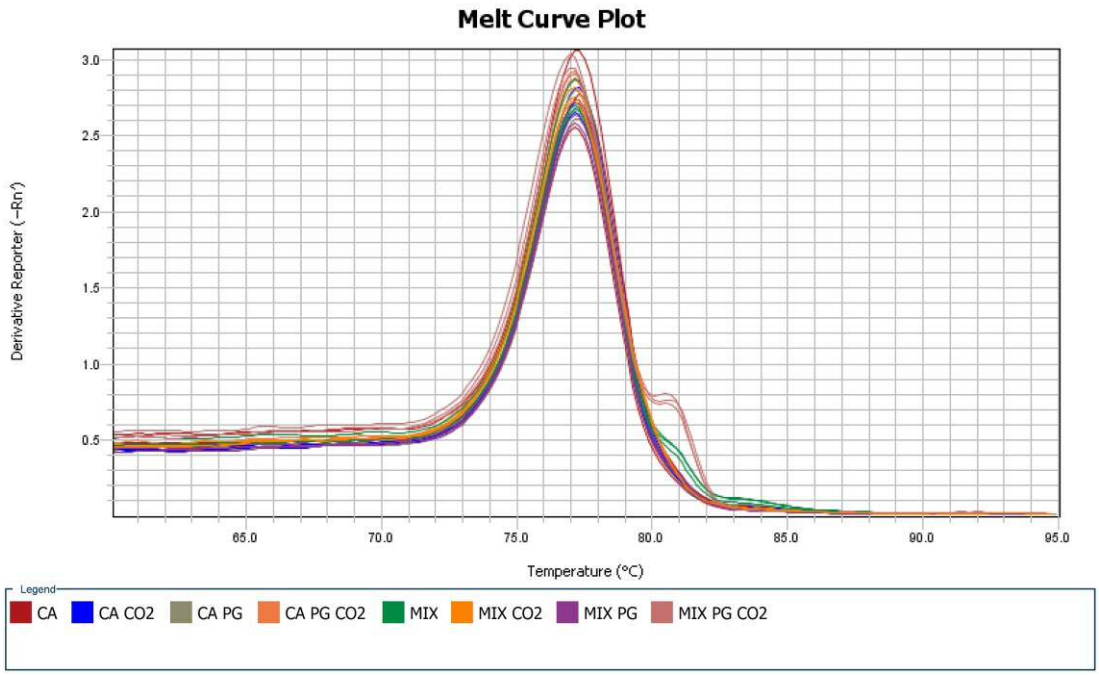
Melt Curve Plot
Derivative Reporter (-Rn')
3.0
2.5
2.0
1.5
1.0
0.5
65.0
70.0
75.0
80.0
85.0
90.0
95.0
Temperature (°C)
Legend
CA
CA CO2
CA PG
CA PG CO2
MIX
MIX CO2
MIX PG
MIX PG CO2

IL-18

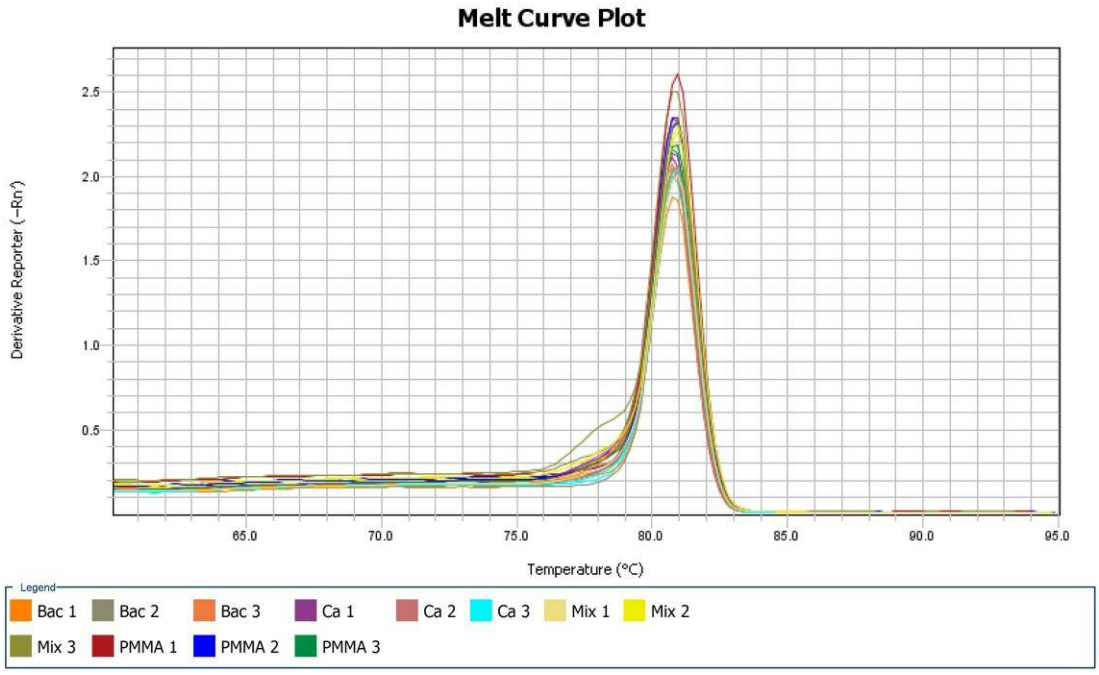
Melt Curve Plot
Derivative Reporter (-Rn')
2.5
2.0
1.5
1.0
0.5
65.0
70.0
75.0
80.0
85.0
90.0
95.0
Temperature (°C)
Legend
Bac 1
Bac 2
Bac 3
Ca 1
Ca 2
Ca 3
Mix 1
Mix 2
Mix 3
PMMA 1
PMMA 2
PMMA 3

IL12-p40

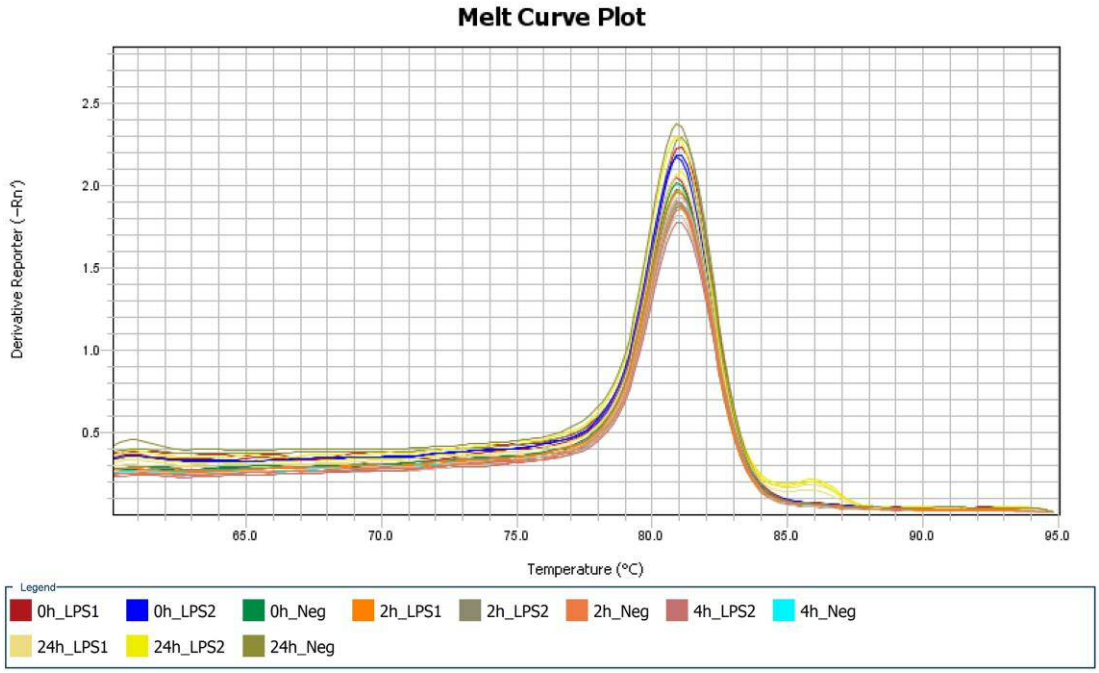

Dectin-1

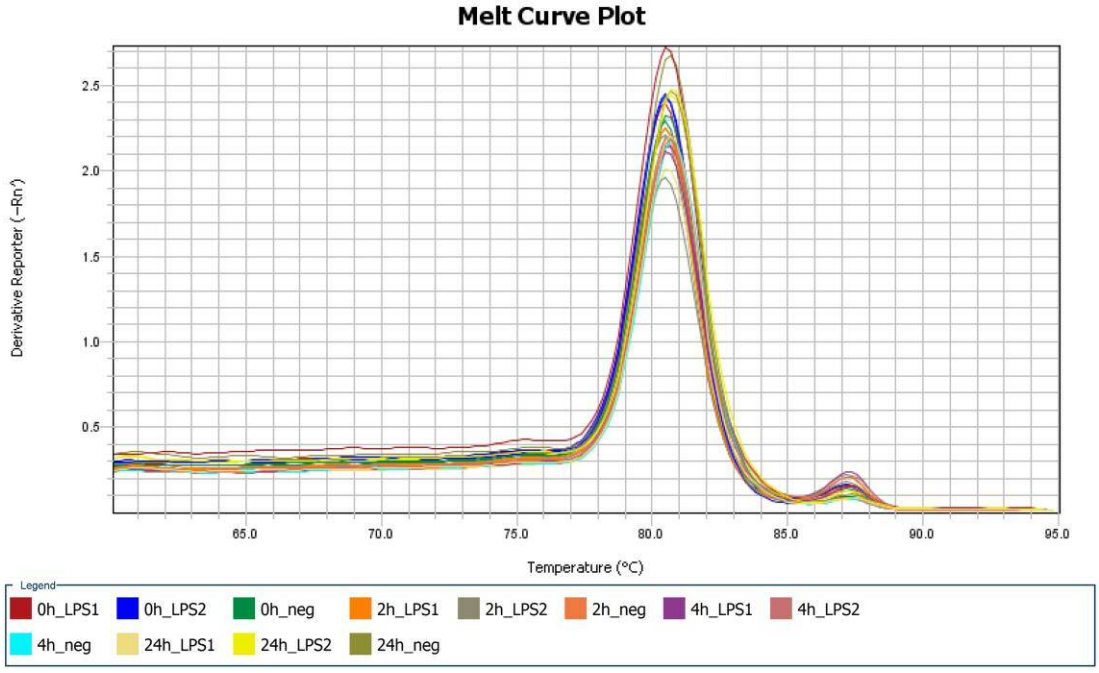

TLR2

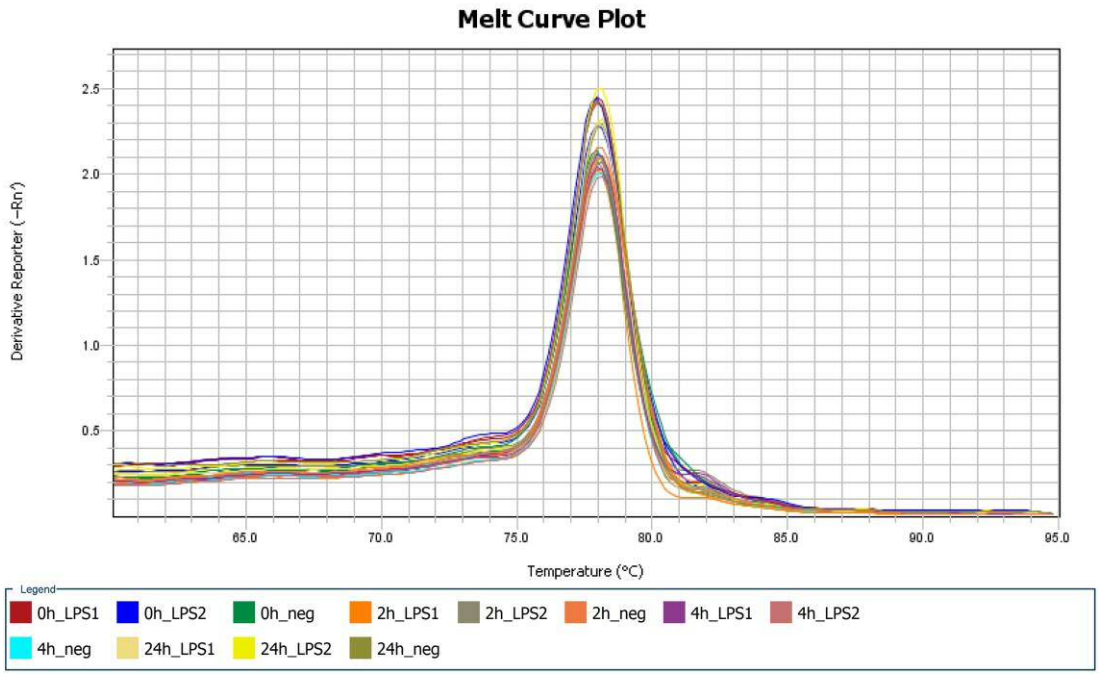
Melt Curve Plot
Derivative Reporter (-Rn')
2.5
2.0
1.5
1.0
0.5
65.0
70.0
75.0
80.0
85.0
90.0
95.0
Temperature (°C)
Legend
0h_LPS1
0h_LPS2
0h_neg
2h_LPS1
2h_LPS2
2h_neg
4h_LPS1
4h_LPS2
4h_neg
24h_LPS1
24h_LPS2
24h_neg

TLR4

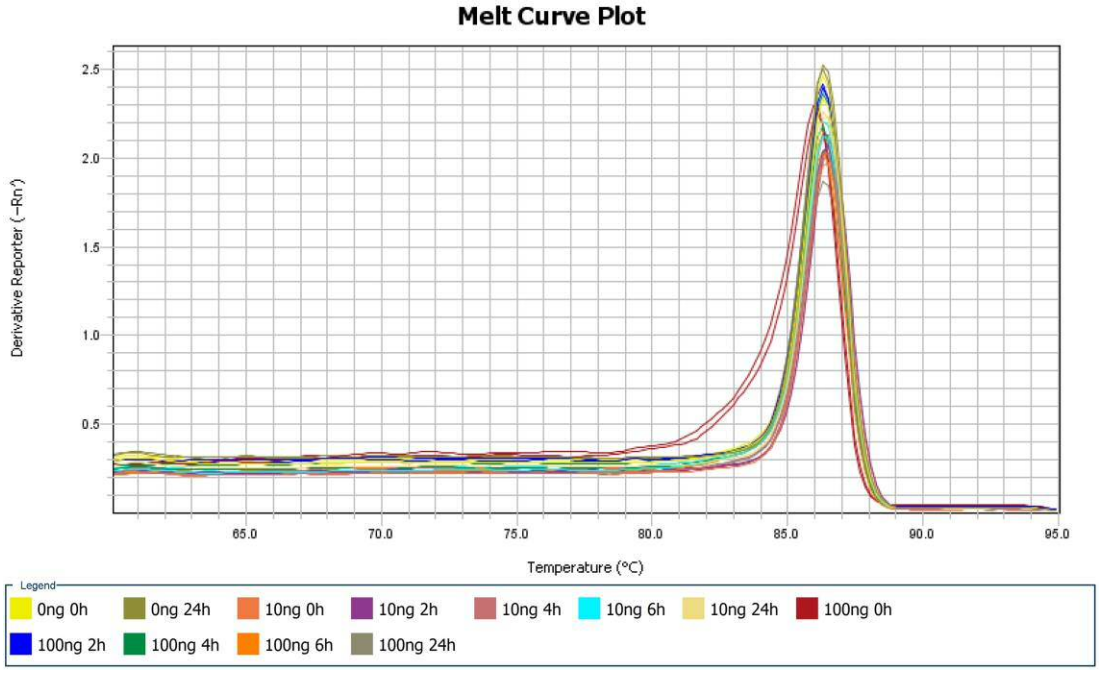
Melt Curve Plot
Derivative Reporter (-Rn')
2.5
2.0
1.5
1.0
0.5
65.0
70.0
75.0
80.0
85.0
90.0
95.0
Temperature (°C)
Legend
0ng 0h
0ng 24h
10ng 0h
10ng 2h
10ng 4h
10ng 6h
10ng 24h
100ng 0h
100ng 2h
100ng 4h
100ng 6h
100ng 24h

β-actin

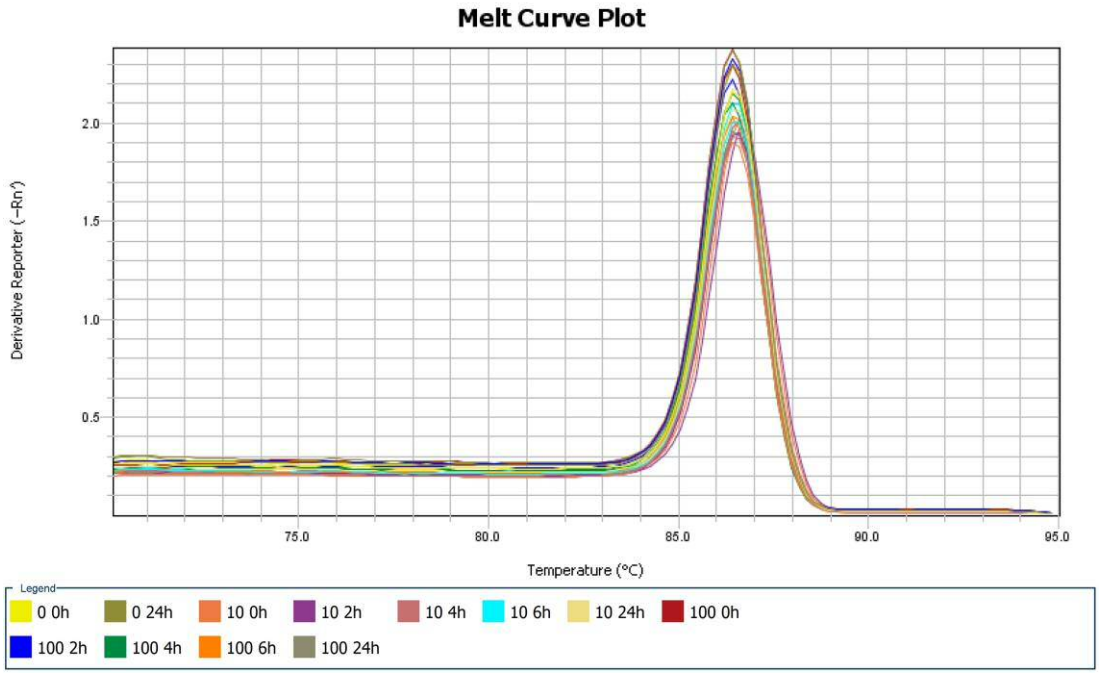
Melt Curve Plot
Derivative Reporter (-Rn')
2.0
1.5
1.0
0.5
75.0
80.0
85.0
90.0
95.0
Temperature (°C)
Legend
0 0h
0 24h
10 0h
10 2h
10 4h
10 6h
10 24h
100 0h
100 2h
100 4h
100 6h
100 24h

Appendix II

Supporting documentation for clinical study

- NHS R&D permission letter
- Study protocol
- Participant information sheet
- Patient consent form
- GP Letter
- Sponsorship letter

NHS R&D permission letter :

GIG CYMRU NHS WALES
Bwrdd Iechyd Prifysgol Caerdydd a'r Fro
Cardiff and Vale University Health Board

Ysbyty Athrofaol Cymru
University Hospital of Wales

Heath Park,
Cardiff, CF14 4XW
Phone 029 2074 7747
Fax 029 2074 3838
Minicom 029 2074 3632

Parc Y Mynydd Bychan,
Caerdydd, CF14 4XW
Ffôn 029 2074 7747
Ffacs 029 20743838
Minicom 029 2074 3632

Tel: 029 20746986
Fax: 029 20745311
CAV_Research.Development@wales.nhs.uk

From: Professor C Fegan
R&D Director
R&D Office, 2nd Floor TB2
University Hospital of Wales
Cardiff
CF14 4XW

18 February 2014

Dr Helen Rogers
School of Dentistry
College of Biomedical and Life sciences
Heath Park
Cardiff
CF14 4XY

Dear Dr Rogers

Cardiff and Vale UHB Ref and Study Title : 14/DEN/5846 : Denture Biofilms: Microbial Composition Interactions And Prevention

IRAS Project ID: 137108

The above project was forwarded to Cardiff and Vale University Health Board R&D Office by the NISCHR Permissions Coordinating Unit. A Governance Review has now been completed on the project.

Documents approved for use in this study are:

Document	Version	Date
NHS RD Form	3.5	Rec'd
SSI Form	3.5	Rec'd
Protocol	1.0	21/11/13
GP Letter	-	-
Participant Information Sheet & Consent Form	3.0	12/02/14

I am pleased to inform you that the UHB has no objection to your proposal. You have informed us that Cardiff University is willing to act as Sponsor under the Research Governance Framework for Health and Social Care.

Please accept this letter as confirmation of permission for the project to begin within this UHB.

The UHB considers that this study is likely to be suitable for adoption onto the NISCHR Clinical Research Portfolio (CRP). This is important so that the UHB can receive funding to support this study. An application for adoption should be made by

the Chief Investigator before commencing the study. If you wish to begin the study before it has been adopted, you must first obtain permission to do so from the Dental Directorate R&D Lead, Dr Vaseekaran Sivarajasingam.

If your study is adopted onto the NISCHR CRP, it will be a condition of this NHS research permission, that you will be required to regularly upload recruitment data onto the portfolio database.

To apply for adoption onto the NISCHR CRP, please go to: http://www.wales.nhs.uk/sites3/page.cfm?orgid=580&pid=31979. Once adopted, NISCHR CRP studies may be eligible for additional support through the NISCHR Clinical Research Centre. Further information can be found at: http://www.wales.nhs.uk/sites3/page.cfm?orgid=580&pid=28571

If your study is adopted onto the portfolio, please inform NISCHR PCU and the R&D Office of your portfolio ID number.

To upload recruitment data, please follow this link: http://www.crncc.nihr.ac.uk/about_us/processes/portfolio/p_recruitment Uploading recruitment data will enable NISCHR to monitor research activity within NHS organisations, leading to NHS R&D allocations which are activity driven.

May I take this opportunity to wish you success with the project and remind you that as Principal Investigator you are required to:

- Inform the R&D Office if this project has not opened within 12 months of the date of this letter. Failure to do so may invalidate R&D approval.
- Inform NISCHR PCU and the UHB R&D Office if any external or additional funding is awarded for this project in the future
- Submit any substantial amendments relating to the study to NISCHR PCU in order that they can be reviewed and approved prior to implementation
- Ensure NISCHR PCU is notified of the study's closure
- Ensure that the study is conducted in accordance with all relevant policies, procedures and legislation
- Provide information on the project to the UHB R&D Office as requested from time to time, to include participant recruitment figures

Yours sincerely,

Professor Christopher Fegan
R&D Director

CC R&D Lead, Dr Vaseekaran Sivarajasingam
CC Chief Investigator, Professor David W Williams
CC Sponsor contact, Helen Falconer, RIES Cardiff University
CC Student, Daniel Morse

Study protocol:

School of Dentistry,
Cardiff University, Heath Park,
Cardiff, CF14 4XY, UK
Tel : 029 20742541

Protocol: Denture acrylic biofilms: microbial composition, interactions and prevention

PhD Studentship Proposal:-Supervisors Dr David W Williams, Dr Melanie Wilson, Dr Xiao-Qing Wei and Prof Michael AO Lewis. School of Dentistry, College of Biomedical and Life Sciences, Cardiff University, Heath Park, Cardiff, CF14 4XY.

Background: Biofilms are defined as communities of microorganisms, that are generally attached to a surface and embedded inside an extracellular polysaccharide matrix generated by the microorganisms. Such a biofilm state appears to be the preferred mode of growth of microorganisms in natural environments, and recent estimates associate biofilms with over 65% of hospital-acquired infections.

Within the oral cavity, biofilms are present on the hard non-shedding surfaces of teeth in the form of dental plaque. Dental plaque is the archetypal biofilm and associated with two of the most prevalent infections in humans, namely dental caries and perodontal disease. Furthermore, oral biofilms can also occur on the surfaces of soft tissues, as well as prosthodontic and orthodontic devices located in the mouth.

Biofilm development on acrylic denture surfaces is promoted by poor oral hygiene, the failure to remove the denture whilst sleeping, and poor denture cleansing. The abiotic surface of the denture also means that removal of adherent microbes through 'self-renewal' of surface layers does not occur as encountered with living mucosa. In addition, the lack of salivary flow over the fitting surface of the denture limits mechanical removal of microorganisms. The significance of biofilms on dentures is that they are associated with the infection, denture stomatitis. The key microrganisms involved in denture stomatitis are believed to be fungi of the genus *Candida,* although bacterial species will also be present.

Whilst there are numerous studies investigating the microbiology of denture stomatitis, the majority are limited to the fungal component of the biofilm. By furthering awareness of the microbiology of denture biofilms insight will be gained on the involvement of bacterial species in denture stomatitis and this will lead to clinical benefit in terms of management of the condition.

Aims: This work will provide the basis of a PhD EPSRC-CASE award studentship to start in October 2013. The primary aim of this proposed research is to thoroughly characterise the microbial composition of denture biofilms, using not only cultural methods, but also, new next generation sequencing methodology (Work Package; **WP1**). Having identified the key microbial components, *in vitro* biofilms will be generated on acrylic surfaces and the distrubution of microbial species will be spatially charaterised by confocal laser scanning microscopy (CLSM) and species-specific molecular probes. This work will form the basis of **WP2**. In addition, the effect of these biofilms on oral epithelial cells and resident macrophages (cell damage and cytokine release) will be assessed. The test cell lines and oral epithelium will be from commercially available sources. Tissue macrophages are heterogeneous cell populations and macrophage responses and phenotypic differentiation will be dependent on the tissue environment adjacent to the denture biofilms. Given the inevitable close proximity of microorganisms within biofilms, it is highly likely that synergistic or antagonistic effects on virulence gene expression and host responses will occur depending on the microbial community members present. In the case of the effects on host immunity, *in vitro* studies performed in Cardiff have already demonstrated that lipopolysaccharide from Gram-negative bacteria enhances inflammatory cytokine release to subsequent *Candida* challenge. The proposed study will also examine the responses of inflammatory macrophage (M1) and anti-inflammatory macrophage (M2) against biofilm microbial challenges for cytokine production particular for IL-12 family cytokines.

In **WP3**, the effect of different bacterial components on the expression of specific *Candida* virulence factors (*e.g.* those associated with adherence, as well as hydrolytic enzymes) and the cytokine release by the oral epithelial cells interfacing with the developed biofilm will be investigated.

A key management strategy in the treatment of denture stomatitis is appropriate cleansing of the denture using antimicobial agents. Having established our *in vitro* biofilm model in **WP2** and measured the associated effects this has on tissues in **WP3**, we aim to assess the efficacy of several denture cleansing agents in **WP4.** **WP4** will involve exposure of preformed

biofilms on acrylic surfaces to denture cleansers and assessing their ability to both remove the biofilm and have cidal activity on the biofilm cells. Post-treatment the subsequent effect of the 'inhibited biofilms' on host tissue will be measured. A summary of the respective work packages is outlined below, each **WP** providing the basis of the respective Chapters within the PhD.

WP1: Analysis of microbial communities involved in denture stomatitis
This research will involve analysis of the microbial populations recovered from the fitting surfaces of dentures, tongue and palate of patients with and without denture stomatitis. Given that extensive studies have been undertaken on the *Candida* species component of the denture biofilm involved in denture stomatitis, the aim of **WP1** will be to supplement standard microbiology culture (to provide quantitative estimation and identification of both *Candida* and bacteria), with next generation sequence (NGS) analysis. As this has not previously been undertaken on these types of samples, and given the extensive amount of data generated by high-throughput sequencing, this work will essentially take the form of a pilot study and will involve the sampling of 20 patients with pre-existing denture stomatitis and 20 patients without denture stomatitis. These patients will all be attending the School of Dentistry as part of their normal oral healthcare. The patients will be identified initially by the clinician in charge of their care prior to arrangements being made for informed consent to be taken. The essential criteria for subject inclusion will be that individuals will be aged >18 years and have a full upper conventional denture. Exclusion criteria will include those patients who have used an antibiotic or antifungal within the previous 30 days, patients who undertake daily use of a steroid inhaler, systemic steroids or immunosuppressant drugs, those who have had participation in another clinical study or receipt of an investigational drug within 30 days of the screening visit. Palatal inflammation in the subjects will be assessed by the clinician and scored according to Newton's Classfication. The clinician involved in taking consent and sampling these patients will be Dr Joshua Twigg. Dr Twigg has previouis experience in taking consent from patients and has received appropriate GCP training. Appendix I provides the information sheet and consent form that will be provided to the patient.
Imprint cultures will be obtained from the denture surface in contact with the palate, the palate itself and also the tongue. These imprints will be used to inoculate blood agar to provide a total quantification of microorganisms, as well as CHROmagar for detection of *Candida* species. In addition, a swab from both the denture and palate will also be collected and will serve as a source of microbial DNA for NGS. These samples, whilst collected by the clinician, will subsequently be processed by the student undertaking the PhD. Including the time taken to acquire informed consent and clinical sampling, it is anticipated that no more than an additional 30 min of clinician time will be required for each patient. The service support costs for this work will be covered from within the funds available for the PhD.
In the case NGS, bacterial DNA will be extracted from the imprint culture using a commercial DNA extraction kit. PCR amplicon libraries will be generated using a variety of primers including covering the V1-V5 hypervariable regions of the bacterial 16S rRNA gene. Identification of the microorganisms will be conducted using the MOTHUR suite of programmes (Schloss et al., 2009). Taxonomic composition and relative abundance of phyla, genera and species within the microbial communities will be analysed using appropriate software.

WP2: Development of a clinically relevant *in vitro* model of a denture biofilm
In vitro studies will develop biofilms on acrylic surfaces. The inoculum for seeding these biofilms will be based on identified microbial species collected from WP1. A common strain of *C. albicans* will be included in all biofilms, but the bacterial component will be modified between experiments. Biofilms on acrylic surfaces will be overlaid on to a commercially available oral mucosa or one derived from commercially available cell lines. Human macrophages previously derived from human peripheral blood monocytes by culture in either M1 conditional medium or M2 conditional medium will be incorporated into this *in vitro* model. Epithelial cell damage and *Candida* tissue invasion will be investigated based on previous methodology developed by our research group.

WP3: Microbial interaction and associated effects on host cells
Using mixed *Candida* and bacterial species biofilms on acrylic surfaces and RNA extracted from infected tissues (from **WP2**), real-time PCR will be used to quantify expression the

putative *Candida* virulence factors. These factors will include agglutin-like sequence (ALS) proteins, phospholiases, and secreted aspartyl proteinases. As expression of these factors is likely to be affected by the composition of the microbial communities, the presence of particular bacterial species may then be correlated with enhanced virulence of *C. albicans*. Human cytokines will be examined using a cytokine array for the inflammatory set IL-1β, IL-8, IL-17, IFN-γ, TNFα, TGFβ and IL-10.

WP4. Antimicrobial efficacy in inhibiting denture based biofilms
Following successful construction of mixed species biofilm models and associated research into their effects on host tissue, efforts will be made to inhibit these biofilms through exposure to specific antimicrobial denture cleanser agents and mouth washes (*i.e.*. Polident, sodium hypochlorite or chlorhexidine gluconate). The efficacy of these agents on the established biofilm will be determined using total viable counts, as well as live/dead staining coupled with CLSM. In addition, biofilms treated with these agents will be introduced into our developed tissue model and the clinical benefits measured, based on tissue damage and inflammatory responses.

Participant information sheet:

Appendix I

RESEARCH PARTICIPANT INFORMATION SHEET

Denture acrylic biofilms: microorganisms involved in inflammation of the gums

Clinical Protocol

You are being invited to take part in a research study. Before you decide, it is important for you to understand why the research is being done and what it will involve. Please take time to read the following information carefully and discuss it with others if you wish.

Part 1 tells you the purpose of the study and what will happen to you if you take part.

Part 2 gives you more detailed information about the conduct of the study.

Ask us if there is anything that is not clear or if you would like more information. Take time to decide whether or not you wish to take part. Thank you for your interest in this research study.

PART 1

What is the purpose of the study?

The primary aim of this study is to investigate what microorganisms are involved in colonising dentures and causing stomatitis (inflammation of the mucous lining of the mouth).

Why have I been chosen?

You have been chosen because you meet the study entry criteria of having a full upper conventional denture and are at least 18 years of age. You may also be experiencing clinical signs of stomatitis.

Altogether, a maximum of 40 subjects will take part in this study (approximately half of whom will have clinical signs of stomatitis and approximately half of whom will not have stomatitis).

Do I have to take part in this study?

No. You are entirely free to choose whether or not to take part. If you do decide to take part, you will be asked to sign a consent form, of which you will be given a copy along with this information sheet to keep. You are still free to withdraw at any time without giving a reason.

Whether you decide to take part or not will have no influence on the subsequent treatment that you will receive in the Dental Hospital and School.

What will happen to me if I take part in this study?

If you agree to participate in this study, you must read this Research Participant Information Sheet and then sign and date the Informed Consent Form before any study procedures begin. Your involvement will be to permit microbiological samples to be collected from your denture, palate and tongue on one occasion.

The activities to be performed if you agree to participate will be as detailed below:

1. Visit 1

Upon arriving at the clinic, you will be given sufficient time to read through this information sheet and ask the clinic staff in private about any questions you may have regarding the study, before deciding whether or not to participate in the study. After you have provided your written informed consent to participate in this study, your date of birth, gender, race and smoking status will be recorded in your study booklet. The study dentist will also ask you about your medical and dental history, (including the age of your denture) and whether or not you use denture adhesive and record this in your study booklet, along with any medications you may be taking. Assuming you meet the study eligibility criteria, the study dentist will then carry out an examination of your mouth.

You may not participate in this study if you have been on another clinical study in the 30 days (1 month) before being sampled or if you have been in receipt of an antibiotic or antifungal within the previous 30 days. Similarly, patients who undertake daily use of a steroid inhaler, systemic steroids or immunosuppressant drugs, are not able to participate in this study.

2. Visit 2 – Sampling - up to 30 min

If this visit is on a separate day to visit 1, you will be asked about any medications you have taken/are taking and the study dentist will check that you are still eligible to continue in the study by asking you a few questions. Assuming you continue to meet the study eligibility criteria, the study dentist will then carry out a full examination of your mouth and ask you about any non-treatment emergent events you may have experienced. The study dentist will then remove your upper denture to determine whether or not you have clinical signs of stomatitis (as it is very unlikely that you will know whether or not you have it), and if you do have it, how much you have.

You will then undergo the following procedures/assessments:

Procedure No.	Procedure/assessment name	Why is the procedure / assessment being performed?	What will procedure/ assessment involve?
1	Inflammation index	To measure and score the inflammation in the upper oral soft tissue inside your mouth	The study dentist looking inside your mouth
2	Imprint culture	To assess microbial colonisation (yeast and bacteria) from cultures of your palate, tongue and fit surface of the denture.	The study dentist will place two separate sterile $2cm^2$ foam squares (moistened in saline) on each of the fit surface of your denture, palate and tongue for 30 seconds
3	Swab	To assess the microbial population based on the presence of the DNA of these microbes.	The study dentist will gently swab the fit surface of your denture, palate and tongue.

What do I have to do?

Attend Visit 2 (if separate from visit 1) at the allocated time, this second visit will be an already scheduled visit.
Complete all study assessments as directed.
You must **not** use denture adhesive on the day you attend the clinic.
It is important that you get back in touch should you have any concerns. The contact numbers are at the end of this information sheet.
Inform one of the study staff if you are taking part in another clinical study at present.

What are the possible disadvantages and risks of taking part?
The procedures and assessments that you will undergo are similar to those you would experience during a routine dental check-up.

The main disadvantage of taking part in the study is the inconvenience of attending for visit 2 (if required).

Are there any side effects?
There should be no side effects associated with this study.

Are there any benefits in taking part?
A possible benefit from participating in this study is that the microbial content of your denture, tongue and gums will be analysed very thoroughly and as a result you have the opportunity to contribute to a scientific investigation that may benefit others. There is also the possibility that you may not benefit from your participation in this study. There are unlikely to be any direct benefits to you as a result of taking part in this study. However, your participation will help us to understand more about the microorganisms that live on dentures and will help in the development of treatments to reduce denture related inflammation in the future..

What will happen to any samples I give?
The imprint culture samples taken will be transferred to a laboratory where they will be used to grow the microorganisms on agar media. Once cultured the microbes will be identified and used to try and replicate infection in laboratory models where they will be grown on acrylic surfaces and used to infect commercially available cells, grown in the laboratory. We can identify the bacteria and yeast recovered from your denturers present based on their genetics.

What if there is a problem?
Any complaint about the way you have been dealt with during the study or any possible harm you might suffer will be addressed. The detailed information on this is given in Part 2.

Will my taking part in the study be kept confidential?
Yes. All the information about your participation in this study will be kept confidential. These details are included in Part 2.

Contact details
If you have any further questions concerning the study, or in case of any difficulty during the study please contact:

Dr Joshua Twigg	Tel: 02920 746464 (office hours only) Tel: 07874 727549 (mobile – out of office hours)
Mrs Rita Walker	Tel: 02920 742439 (office hours only)

School of Dentistry, Cardiff University, Heath Park, Cardiff, CF14 4XY, UK.

This completes Part 1 of the Information Sheet.

If the information in Part 1 has interested you and you are considering participation, please continue to read the additional information in Part 2 before making a decision.

PART 2

What will happen if I don't want to carry on with the study?
You can withdraw from the study at any time without your medical/dental care or legal rights being affected. If you withdraw from the study we will use the data collected up to your withdrawal.

What happens if something goes wrong?
If you are harmed due to someone's negligence, then you may have grounds for a legal action but you may have to pay for it. Regardless of this, if you wish to complain, or have any concerns about any aspect of the way you have been approached or treated during the course of this study, the normal National Health Service complaints mechanisms should be available to you.

Will my taking part in this study be kept confidential?
The results will be analysed by laboratory staff, and in due course may be reviewed by the regulatory and claims approval authorities. This may involve inspection of all study-related information, but your identity will always remain strictly confidential. Your name or initials will not appear on any information collected.

Your data will be made available (within and outside the European Union) to the sponsor's employees, investigators, members of the ethics committee and/or employees of the competent supervisory authorities exclusively in anonymised form for the purposes of examining data. Your participation in the study will be treated as confidential, that is, any personally identifiable information will be held and processed under secure conditions Data will be kept on file for 15 years. You will not be referred to by name in any report or publication (in a scientific journal) of the study. Your identity will not be disclosed to any person, except in the event of a medical emergency or if required by law. You are entitled under law to access your personal data and to have any justifiable corrections made. If you wish to do so, you should request this from the investigator conducting the study.

Your anonymised data will be processed electronically to determine the outcome of this study, and to provide it to health authorities/drug regulatory agencies. Your data, which is anonymised, will not be used for any other research. If you consent to take part in this study we will notify your general practitioner (GP) of your participation.

Who is organising and funding the research?
The sponsor organising and funding this study is Cardiff University/GSK

What will happen to the results of the research study?
It is possible that the results of the study will be made available in the public domain through scientific publications and/or presentations as appropriate. Should this be the case any information about you will be anonymised as detailed in 'Confidentiality' above.

Who has reviewed the study?
This study has been reviewed and given favourable ethical approval by a Research Ethics Committee.

Intellectual property statement:
The information and any materials or items that you are given about or during the study - the type of study being performed - should be considered the confidential business information of the study sponsor. You are of course, free to discuss with your friends and family while considering whether to participate in this study or at any time when discussing your present or future healthcare.

Thank you for your help.

Patient consent form:

Screening Number:	S				

INFORMED CONSENT FORM

Denture acrylic biofilms: microorganisms involved in inflammation of the gums

Sponsor: Cardiff University

Please initial box

1. I confirm that I have read and understood the information sheet Version 3, 17th March 2016. I have had the opportunity to consider the information, ask questions and have had these questions answered satisfactorily. ☐
2. I understand that my participation is voluntary and that I am free to withdraw at any time, without giving any reason, without my medical/ dental care or legal rights being affected. ☐
3. I understand that relevant sections of any of my medical/dental notes and data collected during the study may be looked at by responsible individuals from regulatory authorities or from the NHS Trust, where it is relevant to my taking part in this research. I give permission for these individuals to have access to my records. ☐
4. I agree to take part in the above study. ☐

_____ _____
Name of Subject (print) Signature

Date (dd/mmm/yyyy):_____

_____ _____
Name of Person taking consent (print) Signature

Date (dd/mmm/yyyy):_____

For office use only (tick appropriate box):
Subject Copy ☐ *Study Site File Copy* ☐

GP Letter:

Cardiff University
Heath Park
Cardiff
CF14 4XY
Tel 02920742439

University Dental Hospital
Heath Park
Cardiff
CF14 4XY
Tel 02920746499

Dear Doctor,

RE: Patient Name. Clinical Study: Protocol: Denture acrylic biofilms: microbial composition, interactions and prevention

The above patient who is registered at your practice has given informed consent to take part in a clinical study. They have been selected since they either wear a denture and/or present with some denture stomatitis (which will be managed by routine methods here in the Dental School). A sample of oral plaque from the surface of their denture has been collected during the routine examination. There is no intervention planned as part of this study and the microbiological results of the plaque analysis will not affect the individual patient's subsequent management.

Please get in touch if you require further information.

Kind regards,

School sponsorship letter:

Research, Innovation and Enterprise Services
Director Geraint W Jones
Gwasanaethau Ymchwil, Arloesi a Menter
Cyfarwyddwr Geraint W Jones

Cardiff University
7th Floor
30 - 36 Newport Road
Cardiff CF24 0DE
Wales UK
Tel *Ffôn* +44(0)29 2087 5834
Fax *Ffacs* +44(0)29 2087 4189
Prifysgol Caerdydd
Llawr 7
30 - 36 Newport Road
Caerdydd CF24 0DE
Cymru Y Deyrnas Unedig

02 December 2013

Professor David Williams
Tissue Engineering & Reparative Dentistry
School of Dentistry
College of Biomedical & Life Sciences
Cardiff University
Heath Park
Cardiff, CF14 4XY

Dear Professor Williams,

Denture acrylic biofilms: microbial composition, interactions and prevention.

I understand that you are acting as Academic Supervisor for the above *PhD* project to be conducted by Mr Daniel Morse.

I confirm that Cardiff University agrees in principle to act as Sponsor for the above project, as required by the Research Governance Framework for Health and Social Care.

Scientific Review
I can also confirm that Scientific Review has been obtained from the Engineering and Physical Sciences Research Council (EPSRC) and the Cardiff University School of Dentistry Research Ethics Committee.

Insurance
The necessary insurance provisions will be in place prior to the project commencement. Cardiff University is insured with UMAL. Copies of the insurance certificate are attached to this letter.

Approvals
On completion of your IRAS form (for NHS REC and NHS R&D approvals), you will be required to obtain signature from the Sponsor ('Declaration by the Sponsor Representative').

Please then submit the project to the following organisations for approval:

- the appropriate Research Ethics Committee(s);
- National Institute for Social Care Health Research Permissions Coordinating Unit (NISCHR PCU- to arrange host organisation R&D approval);

Once Research, Innovation & Enterprise Services has received evidence of the above approvals, the University is considered to have accepted Sponsorship and your project may commence.

Roles and Responsibilities
As Chief Investigator you have signed a Declaration with the Sponsor to confirm that you will adhere to the standard responsibilities as set out by the Research Governance Framework for Health and Social Care. In accordance with the University's Research Governance Framework, the Chief Investigator is also responsible for ensuring that each research team member is qualified and experienced to fulfill his/her delegated roles including ensuring adequate supervision, support and training.

Roles and responsibilities are adequately detailed in the research protocol.

May I take this opportunity to remind you that, as Chief Investigator, you are required to:

- ensure you are familiar with your responsibilities under the Research Governance Framework for Health and Social Care;
- undertake the study in accordance with Cardiff University's Research Governance Framework and the principles of Good Clinical Practice;
- ensure the Research complies with the Data Protection Act 1998;
- inform Research, Innovation & Enterprise Services of any amendments to the protocol or study design, including changes to start /end dates;
- co-operate with any audit inspection of the project files or any requests from Research, Innovation & Enterprise Services for further information.

You should quote the following unique reference number in any correspondence relating to sponsorship for the above project:

SPON 1265-13

This reference number should be quoted on all documentation associated with this project.

Yours sincerely

Dr K J Pittard Davies
Head of Research Governance and Contracts
Direct line: +44 (0) 29208 79274
Email: resgov@cardiff.ac.uk

Cc: Mr Daniel Morse (Student)

School insurance documents:

Hasilwood House
60 Bishopsgate
London EC2N 4AW
Tel: 020 7847 8670
Fax: 020 7847 8689
Website: www.umal.co.uk

TO WHOM IT MAY CONCERN

26th July 2013

Dear Sir/Madam

CARDIFF UNIVERSITY
AND ALL ITS SUBSIDIARY COMPANIES

We confirm that the above Institution is a Member of U.M. Association Limited, and that the following covers are currently in place:-

PUBLIC AND PRODUCTS LIABILITY

Certificate of Entry No.	UM165/13
Period of Cover	1st August 2013 to 31st July 2014
Includes	Indemnity to Principals and includes cover whilst University employees and its students are engaged in Health and Social Care activities world-wide – excluding Medical Malpractice claims except as under
Includes	Medical Malpractice (mis-treatment) claims against the University and its employees and its students providing the latter are working under the supervision of a Medically Qualified person
Limit Of Indemnity	a) £50,000,000 any one event and in the aggregate in respect of Products Liability and Unlimited in the aggregate in respect of Public Liability b) Medical Malpractice – £10,000,000 any one event and in the aggregate
Cover provided by	U.M. Association Limited and Excess Cover Providers led by QBE Insurance (Europe) Ltd

Yours faithfully

Susan Wilkinson for U.M. Association Limited

ISO 9001 REGISTERED FIRM

U.M. Association Limited
Registered Office: Hasilwood House, 60 Bishopsgate, London EC2N 4AW
Registered in England and Wales No. 2731799

Hasilwood House
60 Bishopsgate
London EC2N 4AW
Tel: 020 7847 8670
Fax: 020 7847 8689

TO WHOM IT MAY CONCERN

26th July 2013

Dear Sir/Madam

CARDIFF UNIVERSITY AND ALL ITS SUBSIDIARY COMPANIES

Clinical Trials Coverage

We confirm that the above Institution is a Member of U.M. Association Limited, and that the following cover is currently in place in respect Clinical Trials undertaken within the United Kingdom subject to the cover terms, conditions and exceptions.

Certificate of Entry No.	UM165/13
Period of Cover	1st August 2013 to 31st July 2014
Limit of Indemnity	£30,000,000 any one claim and in the aggregate including claims costs and expenses
Basis of Cover	Legal Liability or No Fault cover
Cover provided by	U.M. Association Limited and Excess Cover Providers led by QBE Insurance (Europe) Limited
Main Cover Exclusions	i) Trials involving subjects under 5 years of age ii) Trials assisting with or altering in any way the process of conception iii) Trials investigating or participation in methods of contraception iv) Trials involving genetic engineering other than for preventing and diagnosing disease v) Trials involving drugs or surgery or nutrients vi) Trials involving persons known to be pregnant vii) Trials involving products manufactured by the University

Yours faithfully

Susan Wilkinson
For U.M. Association Limited

Appendix III

Supporting documentation

Clinical study data analysis

- Raw count data of phylotypically assigned bacterial species, grouped by sample

Species_97	score	Group	S001_D	S001_P	S001_T	S002_D	S002_P	S002_T	S003_D	S003_P	S003_T	S004_D	S004_P	S004_T	S005_T	S006_D	S006_T	S007_D	S007_P	S007_T	S008_D	S008_P	S008_T	S009_D
Streptococcus_salivarius	97.9	Otu00002	1685	27	125	128	9	259	2	25	95	8	284	1161	2569	672	2552	7	4	63	846	1103	3	783
Serratia_liquefaciens	97.3	Otu00001	0	2	2830	1	0	0	10391	9154	8437	0	2	3	1	1	0	0	0	2	0	0	0	0
Streptococcus_oralis	97.3	Otu00003	266	7	231	6703	3440	293	1	130	0	98	211	69	152	79	149	4	0	4	482	869	898	646
Pseudomonas_fluorescens	97.2	Otu00011	0	59	0	0	0	0	0	0	0	0	0	0	0	0	0	0	0	0	0	0	0	0
Streptococcus_mitis	97.6	Otu00005	1833	10	99	215	50	384	0	22	446	0	543	827	1658	1531	1567	5	4	165	1043	192	186	2464
Acinetobacter_johnsonii	97.2	Otu00004	0	36	1	1	5654	2366	0	0	0	8174	1689	684	2	0	0	2423	2096	1313	0	0	29	0
Streptococcus_unclassified	*	Otu00008	0	0	0	18	14	123	4	28	74	0	0	0	0	0	4	0	3	25	0	0	0	1
Pseudomonas_putida	97.5	Otu00006	0	681	84	0	0	0	5	0	0	43	6757	4890	1	1	0	0	0	0	9	57	1	0
Stenotrophomonas_maltophilia	97	Otu00007	1	124	4	0	0	0	0	0	2	0	0	10	0	2	0	30	0	0	0	0	0	1
Actinomyces_odontolyticus	97.3	Otu00010	49	0	83	112	51	296	4	0	2	0	1	0	165	5766	771	2	0	24	85	0	84	687
Flavobacterium_lindanitolerans	98.1	Otu00013	0	0	1	0	0	0	0	0	0	0	0	1	0	0	0	0	0	0	0	0	0	56
Enterococcus_faecalis	97.1	Otu00015	0	0	12	3	0	0	40	0	0	0	0	0	0	0	0	0	0	1	0	0	0	1
Brevundimonas_terrae		Otu00009	0	0	1	0	0	0	0	0	0	0	1	5	0	0	0	3502	1438	3232	0	0	148	0
Brevundimonas_vesicularis		Otu00014	1	3558	1	0	0	0	0	0	0	0	0	1995	0	0	1	2	555	1447	3558	1	0	0
Lactobacillus_paracasei	97.7	Otu00017	59	0	0	0	0	0	0	0	1	1	0	0	781	0	0	1	0	0	19	7602	2105	0
Massilia_aurea		Otu00012	0	0	0	0	0	0	0	0	0	0	0	0	0	0	0	0	0	0	0	0	0	0
Veillonella_parvula	97.7	Otu00022	1369	0	238	290	58	324	39	0	0	0	0	5	22	144	96	5	0	4	6	20	175	779
Haemophilus_parainfluenzae	97.6	Otu00018	0	0	62	331	89	837	147	9	185	0	0	2	1	820	1519	0	22	79	149	38	132	168
Granulicatella_adiacens		Otu00020	31	0	54	84	6	95	4	14	58	0	56	275	291	156	399	0	0	7	155	73	0	194
Rhizobium_unclassified		Otu00021	0	110	43	0	0	0	0	0	0	0	0	0	0	0	0	198	387	88	0	0	1	0
Stenotrophomonas_nitritireducens	97.3	Otu00025	0	0	0	0	0	0	0	0	0	1	1	0	2	0	0	0	0	0	0	1	0	0
Chryseobacterium_unclassified	*	Otu00016	0	0	4	0	0	0	3	0	0	0	0	0	0	0	0	1572	2086	2486	0	0	1	1
Prevotella_melaninogenica	97.3	Otu00026	1	1	0	249	61	470	0	0	0	0	0	0	1	513	232	3	0	0	0	0	0	0
Microbacterium_maritypicum	97.2	Otu00032	0	0	0	0	0	0	0	0	0	0	1	0	0	0	0	1	0	0	0	0	5125	0
Agrobacterium_tumefaciens	97.3	Otu00034	0	0	0	0	0	0	0	0	0	0	0	0	1	0	0	0	0	0	0	0	0	0
Streptococcus_oralis	97.6	Otu00024	0	8	2	53	0	64	5	10	411	0	128	256	1332	129	1101	0	3	80	230	12	0	0
Myroides_unclassified	*	Otu00028	0	0	0	0	0	0	0	0	0	0	0	0	0	0	0	0	0	0	0	0	0	0
Propionibacterium_acnes	97.7	Otu00033	2	820	1119	20	66	1	116	2	1	754	143	116	36	0	14	4	62	0	64	47	317	182
Lactobacillus_fermentum	97.2	Otu00030	3968	8	0	0	0	1	0	0	0	0	2	0	0	0	0	0	0	0	0	0	91	0
Pseudomonas_aeruginosa	97.8	Otu00039	2	70	2243	47	0	118	15	4	5	0	0	24	2	22	0	2	24	0	102	0	0	1867
Acinetobacter_lwoffii	97.5	Otu00027	0	9	39	0	1	0	0	0	0	1470	145	31	0	0	0	1	0	10	0	0	0	0
Acidovorax_unclassified		Otu00023	0	0	1	0	0	0	0	7	0	2	0	0	3763	0	0	132	363	8	0	0	1	0
Actinomyces_lingnae	97	Otu00035	184	0	26	22	6	71	5	0	21	0	0	0	0	51	69	0	0	36	0	0	0	404
Lactobacillus_rhamnosus	97.2	Otu00031	2	0	351	0	0	0	6	0	0	0	0	0	0	0	0	0	0	1	0	0	0	0
Neisseria_flavascens	97.3	Otu00036	2	0	45	414	186	2303	0	0	0	0	0	0	0	19	52	0	0	0	20	151	68	0
Haemophilus_parahaemolyticus	97.6	Otu00037	0	0	0	717	523	10	0	0	0	0	53	55	5	0	0	0	0	0	0	0	0	0
Microbacterium_testaceum		Otu00038	0	0	0	0	0	0	0	0	0	0	0	0	0	0	0	0	0	0	2672	0	770	0
Dermacoccus_nishinomiyaensis		Otu00044	0	0	98	0	0	0	1	0	0	0	0	0	0	30	0	0	0	0	0	0	0	0
Streptococcus_infantis	97.6	Otu00040	0	0	0	96	70	288	0	3	1	0	0	0	0	33	381	0	0	6	271	223	56	0
Massilia_varians	98.6	Otu00019	0	0	4	0	0	0	0	0	0	0	0	0	0	0	0	1062	1822	116	0	0	1	2
Chryseobacterium_scophthalmum		Otu00041	0	0	0	0	0	0	0	0	0	0	0	0	0	0	0	0	0	0	0	0	0	0
Prevotella_histicola	97.3	Otu00045	121	0	0	12	0	84	0	0	2	0	0	0	4	0	0	0	0	0	0	0	0	899
Moraxella_osloensis	99	Otu00050	0	2449	24	21	0	0	0	0	0	0	0	0	0	0	0	1	0	0	0	0	0	0
Fusobacterium_periodonticum		Otu00049	1	0	0	119	41	1045	0	0	0	0	0	0	0	5	0	0	0	0	0	0	0	0
Rothia_mucilaginosa	97.3	Otu00042	44	0	34	3	5	45	4	3	345	0	26	9	32	30	201	0	0	17	71	0	0	42
Lactobacillus_salivarius	97.4	Otu00043	502	6	207	0	5	0	1	0	0	0	0	0	0	0	0	0	0	0	0	0	0	0
Devosia_unclassified		Otu00029	0	0	0	0	0	0	1	0	0	0	0	0	0	0	0	801	842	476	0	0	0	0
Methylophilus_methylotrophus	97.5	Otu00061	0	0	0	0	0	0	0	0	0	0	0	0	0	0	0	0	0	0	0	0	0	0
Citrobacter_freundii	100	Otu00046	1	25	0	0	0	0	3	0	5	0	0	0	0	0	1261	0	0	1	2	0	0	0
Stenotrophomonas_unclassified		Otu00058	0	1841	0	0	0	0	0	0	0	0	0	0	0	0	0	0	0	0	0	0	0	0
Streptococcus_sanguinis	98.5	Otu00056	13	0	16	8	0	8	0	0	0	0	0	0	0	0	0	9	0	6	570	335	125	0
Gemella_haemolysans	97	Otu00051	0	0	0	204	76	8	0	3	4	82	12	18	2	0	0	0	0	0	0	0	52	0
Phormidium_sp.	97.7	Otu00048	0	0	0	0	0	1	0	1525	0	0	0	0	0	0	0	0	2	0	0	0	0	0
Leptotrichia_unclassified	*	Otu00057	2	0	0	66	17	44	0	0	0	0	0	0	0	0	0	0	0	1	0	0	0	0
Streptococcus_mitis		Otu00053	0	0	0	53	5	0	0	0	0	41	695	447	0	0	0	0	0	0	0	0	0	0
Pseudoxanthomonas_mexicana	97.3	Otu00055	0	226	0	0	0	0	0	0	0	0	0	0	0	0	0	0	7	413	0	0	0	0

Species_97	score	Group	S001_D	S001_P	S001_T	S002_D	S002_P	S002_T	S003_D	S003_P	S003_T	S004_D	S004_P	S004_T	S005_T	S006_D	S006_T	S007_D	S007_P	S007_T	S008_D	S008_P	S008_T	S009_D
Prevotella_pallens	97	Otu00064	0	0	0	85	94	339	0	0	0	0	0	0	0	0	0	0	0	4	0	0	0	0
Streptococcus_anginosus		Otu00059	0	102	1	0	0	0	0	0	0	0	0	0	9	0	0	9	0	0	0	0	121	0
Pseudorhodoferax_soli	97.8	Otu00063	0	0	0	0	0	0	0	0	0	0	0	0	0	0	0	0	0	0	0	0	0	0
beta_proteobacterium	97.5	Otu00047	0	0	0	0	0	0	0	0	0	0	0	0	0	0	0	0	0	0	0	0	0	0
Streptococcus_sp.	97	Otu00066	0	0	0	5	4	9	0	0	0	0	0	0	0	2	4	0	0	0	0	0	0	0
Porphyromonas_catoniae	98.5	Otu00069	0	1	0	140	117	128	0	0	0	0	0	0	0	0	0	0	0	2	0	1	0	0
Streptococcus_sobrinus	97.4	Otu00062	0	0	0	0	0	0	0	0	0	0	0	0	0	0	0	0	0	0	0	0	0	0
Luteimonas_cucumeris	97.6	Otu00071	0	31	0	0	0	0	0	0	0	0	0	0	0	0	0	0	0	0	0	0	0	0
Lactobacillus_unclassified		Otu00067	440	0	29	0	0	0	0	0	0	0	0	0	0	0	0	0	0	0	0	0	65	0
Acinetobacter_junii	97.2	Otu00073	0	0	0	0	0	0	0	0	0	0	0	0	0	0	0	0	0	2	0	0	0	0
Haemophilus_influenzae	97.3	Otu00081	2	13	441	22	0	1	3	0	0	0	0	0	0	0	0	0	0	0	0	0	0	0
Delftia_tsuruhatensis	97.5	Otu00060	0	0	0	0	0	0	0	0	0	0	0	0	0	0	0	418	125	101	0	0	0	0
Sphingomonas_sp.	97.3	Otu00052	0	0	0	0	0	0	0	0	0	0	0	0	0	0	0	0	0	0	0	0	0	0
Afipia_broomeae	97.3	Otu00065	0	0	0	0	0	0	0	0	786	27	0	0	0	0	0	0	0	0	0	0	0	63
Roseburia_unclassified		Otu00068	0	0	0	2	0	3	0	0	0	0	0	0	0	0	0	0	0	0	0	0	0	0
Prevotella_salivae	97.3	Otu00074	0	0	0	17	11	21	0	0	0	0	0	0	0	43	4	1	0	1	9	0	0	0
Streptococcus_unclassified	*	Otu00070	0	0	0	0	0	0	0	0	65	0	0	1	0	2	16	0	0	0	0	0	0	0
Zoogloea_ramigera	97.3	Otu00076	0	0	0	0	0	0	0	0	0	0	0	0	0	0	0	11	14	3	0	0	0	0
Gemella_sanguinis	97.1	Otu00072	0	0	0	70	6	48	0	0	0	0	0	0	0	38	274	0	0	9	43	0	0	0
Pseudomonas_unclassified		Otu00077	0	0	0	0	0	0	0	0	0	0	0	0	0	0	0	0	0	0	0	0	0	0
Prevotella_tannerae		Otu00085	0	0	59	0	0	0	0	0	0	0	0	0	0	0	0	0	33	17	0	0	0	0
Sphingobacterium_multivorum	97.6	Otu00082	0	0	0	0	0	0	0	0	0	0	0	0	0	0	0	0	0	0	0	0	0	0
Chryseobacterium_unclassified		Otu00083	0	0	0	0	0	0	0	0	0	0	0	0	0	0	0	0	0	0	0	0	0	0
Lachnoanaerobaculum_orale	97.4	Otu00075	0	0	0	10	0	25	0	0	0	0	0	0	0	348	16	1	0	0	0	0	0	0
Massilia_unclassified	*	Otu00054	0	0	0	0	0	0	0	0	0	0	0	0	0	0	0	160	373	36	0	0	1	1
Streptococcus_parasanguinis	98.8	Otu00080	0	0	0	1	0	1	0	0	0	0	0	0	0	131	43	0	0	0	62	0	0	0
Lactobacillus_fermentum	97.8	Otu00078	10	0	0	0	0	0	0	0	0	0	0	0	0	0	0	0	0	0	1	0	24	0
Sphingomonas_ursincola	97.3	Otu00079	0	0	0	0	0	0	0	0	0	0	0	0	0	0	0	0	0	0	0	0	0	0
Myroides_unclassified	*	Otu00087	0	0	0	0	0	0	0	0	0	0	0	0	0	0	0	0	0	0	0	0	0	0
Empedobacter_brevis	98.5	Otu00086	0	0	0	0	0	0	0	0	0	0	0	0	0	0	0	0	0	0	0	0	0	0
Comamonas_testosteroni	98.1	Otu00091	0	0	0	0	0	0	0	0	0	0	0	0	0	0	0	0	0	0	0	0	0	0
Streptococcus_unclassified		Otu00096	0	0	23	6	0	25	0	0	0	0	0	0	0	9	1	0	0	3	0	0	0	0
Staphylococcus_aureus	97.3	Otu00107	2	9	365	5	0	0	12	0	0	0	0	0	1	0	0	1	0	0	0	0	0	0
Streptococcus_gordonii	97.4	Otu00094	3	0	39	29	13	20	0	0	0	0	0	0	1	40	1	0	0	0	56	63	60	0
Parvimonas_micra	98.2	Otu00123	0	0	375	0	0	0	2	0	0	0	0	0	3	0	0	0	0	6	0	0	0	0
Prevotella_oris	97.3	Otu00111	0	0	37	0	0	0	0	0	0	0	0	1	0	0	0	0	0	0	0	0	0	0
Prevotella_nanceiensis	97.3	Otu00090	0	0	0	108	36	188	0	0	0	0	0	0	0	0	0	0	0	0	0	0	0	0
Mycoplasma_salivarium	98.1	Otu00135	0	0	367	0	0	0	5	0	0	0	0	0	0	0	0	0	0	0	0	0	0	0
Actinomyces_graevenitzii	98.5	Otu00100	0	0	0	0	0	1	0	0	0	0	0	0	0	0	0	0	0	1	0	0	0	351
Granulicatella_unclassified		Otu00098	0	0	0	57	38	0	0	0	0	0	0	0	0	0	0	0	0	0	0	0	0	0
Flavobacterium_lindanitolerans	97.5	Otu00097	0	0	0	0	0	0	0	0	0	0	0	0	0	0	0	0	0	0	0	0	0	0

Species_97	score	Group	S001_D	S001_P	S001_T	S002_D	S002_P	S002_T	S003_D	S003_P	S003_T	S004_D	S004_P	S004_T	S005_T	S006_D	S006_T	S007_D	S007_P	S007_T	S008_D	S008_P	S008_T	S009_D
Serratia_marcescens	97.6	Otu00099	0	0	0	0	0	0	0	0	2	0	0	0	0	0	13	0	0	0	0	0	0	0
Micrococcus_luteus	99	Otu00108	2	6	72	0	3	0	0	0	0	0	0	0	0	0	0	0	0	0	0	0	85	173
Lactobacillus_plantarum	97.2	Otu00093	0	0	0	0	0	0	0	0	0	0	0	0	0	0	0	0	0	0	0	0	1	0
Propionibacterium_acidifaciens	97.8	Otu00088	0	0	0	0	0	0	0	0	0	0	0	0	0	0	0	41	0	0	0	0	0	0
Megasphaera_micronuciformis	97.3	Otu00101	4	0	0	0	0	0	0	0	0	0	0	0	0	39	0	0	0	0	0	0	0	235
Ralstonia_sp.	97.6	Otu00114	0	0	1	0	0	0	2	0	0	0	0	0	0	0	0	0	0	0	0	0	0	0
Bradyrhizobium_sp.	97.5	Otu00116	0	0	0	0	0	0	0	0	0	0	0	0	0	0	0	0	0	0	0	0	0	0
Dermacoccus_nishinomiyaensis	97.2	Otu00118	0	0	5	0	0	0	0	0	0	0	0	0	0	2	0	0	0	0	0	0	0	0
Atopobium_parvulum	97.5	Otu00110	1	0	0	4	0	6	0	0	0	1	0	0	0	27	0	2	0	1	0	0	0	57
Campylobacter_concisus	97.9	Otu00102	0	0	0	36	4	40	0	0	1	0	0	0	0	3	1	0	0	0	0	0	0	0
Staphylococcus_warneri	100	Otu00112	0	24	0	0	0	0	0	0	0	36	0	0	0	0	0	0	0	0	0	6	80	120
Lactobacillus_vaginalis	98.6	Otu00109	240	0	0	0	0	0	0	0	0	0	0	0	0	0	0	0	0	0	0	0	0	0
Yersinia_pekkanenii	99.7	Otu00129	0	0	0	0	0	0	0	0	0	0	0	0	0	0	0	0	0	0	0	0	0	0
Flavobacterium_unclassified		Otu00133	0	0	0	0	0	0	0	0	0	0	0	0	0	0	0	0	0	0	0	0	0	0
Neisseria_sicca	97.9	Otu00122	0	0	0	3	3	39	0	0	0	0	0	0	0	0	0	0	0	0	31	89	20	0
Aeromonas_hydrophila	97	Otu00119	0	0	0	0	0	0	0	0	0	0	0	0	0	0	0	0	0	0	0	0	0	0
Bosea_unclassified		Otu00095	0	0	0	0	0	0	0	1	0	0	0	0	0	0	0	54	47	96	0	0	0	0
Actinomyces_graevenitzii	98.1	Otu00106	0	0	0	0	0	0	0	0	0	0	0	0	0	0	0	2	0	14	0	0	0	4
Diplorickettsia_unclassified	*	Otu00127	0	0	9	0	3	0	14	0	0	0	0	0	0	0	0	0	0	0	0	0	0	0
Solobacterium_moorei		Otu00115	0	0	0	13	0	14	0	0	0	0	0	0	0	31	15	0	0	0	0	0	0	0
Leptotrichia_unclassified	*	Otu00126	0	35	0	21	2	41	0	0	0	0	0	0	1	8	0	0	0	0	0	0	0	0
Streptococcus_dysgalactiae	97.6	Otu00132	0	0	0	0	0	0	0	0	0	197	0	3	0	8	0	0	0	0	0	4	0	0
Streptococcus_mitis		Otu00103	0	1	0	156	25	14	0	0	0	0	0	0	0	0	0	0	0	0	0	0	0	0
Staphylococcus_hominis	97.3	Otu00113	0	0	0	0	0	0	4	0	0	0	0	0	0	0	0	0	0	0	0	0	0	0
Prevotella_oralis	97.9	Otu00179	0	0	199	0	0	0	1	0	0	0	0	0	0	0	0	0	0	0	0	0	0	0
Variovorax_ginsengisoli	98.1	Otu00145	0	4	40	0	0	0	0	0	0	0	0	0	0	0	0	7	0	0	0	0	0	0
Corynebacterium_imitans	*	Otu00131	0	0	0	0	0	0	0	0	0	0	0	0	0	0	0	0	0	0	0	0	0	190
Shinella_kummerowiae	97.4	Otu00104	0	0	0	0	0	0	0	0	0	0	0	0	0	0	0	116	0	69	0	0	0	0
Rhizobium_mesosinicum	97.1	Otu00084	0	0	0	0	0	0	0	0	0	0	0	0	0	0	0	47	108	24	0	0	0	0
Chryseobacterium_formosense		Otu00120	0	0	0	0	0	0	0	0	0	0	0	0	0	0	0	0	0	0	0	0	0	0
Lactobacillus_kalixensis	98.5	Otu00134	0	0	0	0	0	0	0	0	0	0	0	0	0	0	0	0	0	0	0	0	0	0
Massilia_alkalitolerans	98.8	Otu00089	0	0	1	0	0	0	0	0	0	0	0	0	0	0	0	56	108	4	0	0	0	0
Pseudocitrobacter_anthropi	98.4	Otu00128	0	5	13	0	0	0	0	0	0	0	0	0	0	0	1	0	12	0	59	0	0	73
Prevotella_buccae	97.3	Otu00164	0	0	0	0	0	0	0	0	0	0	0	0	0	0	0	0	0	0	0	0	0	0
Bacteroides_unclassified	*	Otu00147	0	0	0	4	12	16	0	0	0	0	0	0	0	0	0	0	0	0	0	0	0	0
Prevotella_unclassified	*	Otu00125	0	0	0	0	0	0	0	0	0	0	0	0	0	1	0	0	0	0	0	0	0	0
Ensifer_adhaerens	97.9	Otu00105	0	0	0	0	0	0	0	0	0	0	0	0	0	0	0	14	48	9	0	0	0	0
Streptococcus_mutans	98.3	Otu00148	0	0	26	1	0	0	0	0	0	0	0	0	0	0	0	5	0	0	0	0	0	61
Actinomyces_oris	97.1	Otu00165	0	0	0	0	0	0	0	0	0	0	0	0	0	0	0	0	0	0	0	0	0	0
Stomatobaculum_longum	99.6	Otu00124	1	0	0	4	0	1	0	0	0	0	0	0	0	51	0	0	0	0	0	0	0	0
Acinetobacter_bereziniae	97.2	Otu00136	0	8	0	0	0	0	0	0	0	0	0	0	0	0	0	0	0	0	0	0	0	0
Fusobacterium_nucleatum	97.6	Otu00155	0	0	0	0	0	0	0	0	0	0	0	0	0	0	0	0	0	0	0	0	0	0
Acinetobacter_unclassified		Otu00137	0	0	0	0	0	26	0	0	0	0	0	0	0	0	0	4	0	0	0	0	0	0
Actinomyces_viscosus	97	Otu00161	9	0	0	0	0	0	0	0	0	0	0	0	0	0	0	0	0	0	0	0	0	0
Sphingomonas_unclassified		Otu00121	0	0	0	0	0	0	0	0	0	0	0	0	0	0	0	0	0	0	0	0	0	0
Streptococcus_oligofermentans	98.1	Otu00149	61	0	46	0	0	0	0	0	0	0	0	0	0	0	0	0	0	3	0	0	0	0
Alloprevotella_unclassified	*	Otu00175	0	0	0	0	0	0	0	0	0	0	0	0	0	0	0	0	0	0	0	0	0	0
Leptotrichia_shahii	97.2	Otu00130	0	0	0	0	0	0	0	0	0	0	0	0	0	0	0	0	0	0	148	0	0	0
Comamonas_aquatica	98.4	Otu00142	0	0	0	0	0	0	0	0	0	0	0	0	0	0	0	0	0	2	0	0	1	0
Rhizobium_unclassified		Otu00151	0	0	0	0	0	0	0	0	0	0	0	0	0	0	0	0	0	0	0	0	0	0
Methylobacterium_extorquens	99	Otu00150	0	3	1	0	0	0	8	15	0	0	0	0	0	0	0	0	4	5	0	0	0	0
Actinomyces_odontolyticus	98.4	Otu00153	1	0	0	0	0	1	0	0	0	0	0	0	0	7	1	0	0	0	0	0	0	2
Odoribacter_unclassified	*	Otu00184	0	0	0	0	0	0	0	0	0	0	0	0	0	0	0	0	0	0	0	0	0	0
Selenomonas_artemidis		Otu00168	0	0	0	0	0	0	0	0	0	0	0	0	0	0	0	0	0	0	0	0	0	39
Actinomyces_slackii	97.2	Otu00152	0	0	0	0	0	0	0	0	0	0	0	0	4	34	0	3	0	1	1	58	17	0
Sphingopyxis_granuli	97.6	Otu00144	0	0	0	0	0	0	0	0	0	0	0	0	0	0	0	3	0	0	0	0	0	0
Sediminibacterium_unclassified	*	Otu00154	0	0	0	0	0	0	0	0	0	0	0	0	0	3	0	1	0	0	72	0	0	48

Species_97	score	Group	S001_D	S001_P	S001_T	S002_D	S002_P	S002_T	S003_D	S003_P	S003_T	S004_D	S004_P	S004_T	S005_T	S006_D	S006_T	S007_D	S007_P	S007_T	S008_D	S008_P	S008_T	S009_D
Nocardioides_aestuarii	98.4	Otu00192	0	0	0	0	0	0	0	0	0	0	0	0	0	0	0	0	0	0	0	0	0	0
Abiotrophia_defectiva		Otu00174	0	0	0	0	0	13	0	0	0	0	0	0	0	0	0	0	0	0	13	0	0	0
Dermacoccus_nishinomiyaensis	98.8	Otu00177	0	0	3	0	0	0	0	0	0	0	0	0	0	0	0	0	0	0	0	0	0	0
Methylobacterium_gregans	98	Otu00217	0	0	122	0	0	0	1	0	0	0	0	0	0	0	0	0	0	0	0	0	0	0
Corynebacterium_segmentosum	98.5	Otu00146	0	0	33	0	0	2	0	0	0	34	0	0	0	0	0	0	0	0	0	0	0	0
Ochrobactrum_sp.	99.7	Otu00171	0	117	0	0	0	0	0	0	0	0	0	0	0	0	0	0	0	0	0	0	0	0
Actinomyces_graevenitzii	98.5	Otu00180	0	0	0	0	0	9	0	0	1	0	0	0	0	0	0	0	0	0	0	0	0	45
Lysobacter_unclassified		Otu00176	0	115	1	0	0	0	0	0	0	0	0	0	0	0	0	0	0	0	0	0	0	0
Acinetobacter_sp.	97.2	Otu00158	0	0	0	0	0	0	0	0	0	0	0	0	0	0	0	0	0	0	0	0	0	0
Brevundimonas_unclassified		Otu00092	0	0	0	0	0	0	0	0	0	0	0	0	0	0	0	2	110	1	0	0	0	0
Prevotella_unclassified	*	Otu00162	0	0	0	22	12	71	0	0	0	0	0	0	0	0	0	0	0	0	0	0	0	0
Bryobacter_unclassified	*	Otu00204	0	0	0	0	0	0	0	0	0	0	0	0	0	0	0	0	0	0	0	0	0	0
Actinomyces_unclassified	*	Otu00183	0	0	0	0	0	0	0	0	0	0	0	0	0	0	0	0	0	1	0	0	0	0
Methylobacterium_unclassified	*	Otu00182	0	0	0	0	0	0	0	0	0	0	0	0	0	0	0	0	0	0	0	0	0	0
Acinetobacter_rudis	98.2	Otu00172	0	0	0	0	0	0	0	0	0	0	0	0	0	0	0	0	0	0	0	0	0	0
Oribacterium_unclassified	*	Otu00159	0	0	1	3	0	8	0	0	0	0	0	0	0	0	54	0	0	0	0	0	0	0
Methylobacterium_goesingense	98.3	Otu00143	0	0	11	0	0	0	0	0	0	0	0	0	0	0	0	0	0	0	0	0	0	0
Massilia_timonae	98.8	Otu00243	0	1	85	0	5	0	0	0	0	0	0	0	0	0	0	0	0	0	0	0	0	0
Corynebacterium_unclassified	*	Otu00219	0	0	0	0	0	0	0	0	0	0	0	0	0	0	0	0	0	0	0	0	0	0
Devosia_riboflavina	97.9	Otu00140	0	0	0	0	0	0	0	0	0	0	0	0	0	0	0	0	0	88	0	0	1	0
Achromobacter_mucicolens	97.2	Otu00157	0	0	0	0	0	0	0	0	0	0	0	0	0	0	0	0	0	0	0	0	0	0
Rhizobium_sp.	98.6	Otu00141	0	0	0	0	0	0	0	0	0	0	0	0	0	0	0	47	8	16	0	0	0	0
Parvimonas_micra	*	Otu00203	0	0	0	0	0	0	0	0	0	0	0	0	0	0	0	0	0	0	0	0	0	0
Leptotrichia_unclassified	*	Otu00169	0	0	0	19	0	21	0	0	0	0	0	0	0	3	1	0	0	0	0	0	0	0
Streptococcus_pseudopneumoniae	98.1	Otu00163	0	0	1	4	20	0	0	1	0	1	2	1	0	0	0	0	0	0	0	0	0	1
Streptococcus_tigurinus	97.9	Otu00181	0	0	0	0	17	46	0	0	0	0	0	2	13	0	0	0	0	3	0	0	0	0
Tomitella_biformata	98.4	Otu00218	0	0	1	0	0	0	0	0	0	0	0	0	0	2	0	0	0	0	0	0	0	0
[Eubacterium]_nodatum_group_unclassified		Otu00193	0	0	0	2	7	23	0	0	0	0	0	0	0	0	0	0	0	0	0	0	0	0
Actinomyces_unclassified	*	Otu00160	0	0	0	0	0	0	0	0	0	0	0	0	0	0	0	67	0	0	0	0	0	0
Capnocytophaga_gingivalis	97.8	Otu00199	0	0	0	5	0	0	0	0	0	0	0	0	0	0	0	0	0	2	5	0	28	0
Prevotella_nigrescens	98.5	Otu00200	0	0	7	0	0	0	0	0	0	0	0	0	0	0	0	0	0	0	0	0	0	32
Terrisporobacter_unclassified		Otu00188	0	0	0	0	0	0	0	0	0	0	0	0	0	0	0	0	0	0	0	0	0	77
Pedobacter_unclassified	*	Otu00228	0	0	0	0	0	0	0	0	0	0	0	0	0	0	0	0	0	0	0	0	0	0
Oribacterium_sinus	97.7	Otu00195	0	0	0	0	0	12	0	0	0	0	0	0	0	0	3	0	0	0	0	0	0	35
Fusobacterium_nucleatum		Otu00244	0	0	63	0	0	0	1	0	0	0	0	0	0	0	0	0	0	2	0	0	0	0
Pseudomonas_putida	97.5	Otu00170	0	0	0	0	0	0	0	0	0	0	72	0	0	0	0	0	0	0	0	0	0	0
Pseudomonas_agarici	97.8	Otu00187	0	0	0	0	0	0	0	0	0	0	0	0	0	0	0	0	0	0	0	0	0	0
Sediminibacterium_salmoneum	*	Otu00210	0	0	0	0	0	0	0	0	0	0	0	0	0	0	6	0	0	0	0	0	1	15
Lactobacillus_ultunensis	97.9	Otu00242	0	0	62	0	0	0	0	0	0	0	0	0	0	0	0	0	0	0	0	0	0	0
Propionicimonas_paludicola	98.4	Otu00198	0	0	0	0	0	0	0	0	0	0	0	0	0	0	0	0	0	0	0	0	0	71
Chryseobacterium_hominis	98.4	Otu00178	0	0	0	0	0	0	0	0	0	0	0	0	0	0	0	0	0	0	0	0	0	0
Ralstonia_unclassified	*	Otu00186	0	0	0	4	1	1	0	0	0	0	0	0	0	38	0	0	0	0	0	0	0	0
Aeromonas_unclassified	*	Otu00201	0	0	0	2	0	2	0	0	0	0	0	0	0	0	0	0	0	2	0	0	0	0
Dermacoccus_nishinomiyaensis	98.4	Otu00208	0	0	1	0	0	0	0	0	0	0	0	0	0	1	0	0	0	0	0	0	0	0
Lactobacillus_crispatus	97.4	Otu00212	0	61	0	0	0	0	0	0	0	0	0	0	0	0	0	0	0	0	0	0	0	0
Ornithinimicrobium_kibberense	97.5	Otu00167	0	0	0	0	0	0	0	0	0	0	0	0	0	0	0	2	0	36	0	0	0	0
Bacillus_cereus	97.6	Otu00156	0	0	0	0	0	0	0	0	10	0	8	6	0	0	0	0	15	4	0	0	22	0
Sphingobium_herbicidovorans	99.3	Otu00230	0	0	0	0	0	0	0	0	0	0	0	0	0	0	0	0	0	0	0	0	0	0
Hydrogenophaga_defluvii	97.8	Otu00117	0	0	0	0	0	0	0	0	0	0	0	0	0	0	0	0	64	0	0	0	0	0
Microbacterium_lacticum	100	Otu00205	0	12	0	2	0	0	0	0	0	0	0	0	0	0	0	0	0	3	0	0	0	0
Alcaligenes_aquatilis	98.2	Otu00206	0	0	0	0	0	0	0	0	0	0	0	0	0	0	0	0	0	0	0	0	0	0
Rhizobium_unclassified	97	Otu00229	0	0	0	0	0	0	0	0	0	0	0	0	0	0	0	0	0	0	0	0	0	0
Devosia_sp.	97	Otu00139	0	0	0	0	0	0	0	0	0	0	0	0	0	0	0	15	32	15	0	0	0	0
Capnocytophaga_gingivalis	*	Otu00196	0	0	0	23	0	23	0	0	0	0	0	0	0	0	0	0	0	0	4	0	0	0
Halomonas_unclassified	*	Otu00275	0	0	62	0	0	0	0	0	0	0	0	0	0	0	0	0	0	0	0	0	0	0
Prevotella_unclassified	*	Otu00191	0	0	0	0	0	0	0	0	0	0	0	0	0	11	0	0	0	0	0	0	0	0

Species_97	score	Group	S001_D	S001_P	S001_T	S002_D	S002_P	S002_T	S003_D	S003_P	S003_T	S004_D	S004_P	S004_T	S005_T	S006_D	S006_T	S007_D	S007_P	S007_T	S008_D	S008_P	S008_T	S009_D
Streptococcus_sanguinis		Otu00209	0	0	0	0	0	1	0	0	0	0	0	0	0	0	0	0	0	0	28	14	3	0
Herminiimonas_arsenicoxydans	97.2	Otu00232	0	0	0	0	0	0	0	0	0	0	0	0	0	0	0	0	0	0	0	0	0	0
Pseudomonas_putida		Otu00227	0	50	0	0	0	0	0	0	0	0	8	0	0	0	0	0	0	0	0	0	0	0
Actinomyces_graevenitzii	99.4	Otu00238	0	0	0	0	0	9	0	0	3	0	0	0	0	0	0	0	0	0	0	0	0	0
Ehrlichia_unclassified	*	Otu00248	0	0	0	0	7	6	0	0	0	0	0	0	0	0	0	0	0	0	0	0	0	0
Enterococcus_faecium	98.3	Otu00283	0	0	54	0	0	0	1	0	0	0	0	0	0	0	0	0	0	0	0	0	0	0
Aminobacter_anthyllidis	98.3	Otu00166	0	0	0	0	0	0	0	0	0	0	0	0	0	0	0	41	0	15	0	0	0	0
Streptococcus_parasanguinis	98.4	Otu00221	0	0	0	0	0	1	0	0	0	0	0	1	4	1	1	0	0	0	0	0	1	0
Propionibacterium_unclassified		Otu00262	0	0	0	0	0	0	0	0	0	0	0	0	0	0	0	0	0	0	0	0	0	0
Anaeroglobus_geminatus	98.9	Otu00299	1	0	52	0	0	0	1	0	0	0	0	0	0	0	0	0	0	0	0	0	0	0
Actinomyces_oris	99.1	Otu00197	0	0	0	0	0	0	0	0	0	0	0	0	0	0	0	5	0	2	0	0	0	0
Maricurvus_unclassified	*	Otu00202	0	0	0	1	1	6	0	0	0	0	0	0	0	26	9	0	0	0	0	0	0	0
Catonella_morbi	*	Otu00211	0	0	0	21	17	9	0	0	0	0	0	0	0	0	0	0	0	0	0	0	0	0
Corynebacterium_matruchotii	97.9	Otu00271	0	0	18	0	0	0	0	0	0	0	0	0	0	0	0	0	0	0	0	0	0	8
Streptococcus_unclassified		Otu00190	0	0	0	0	0	0	0	0	1	0	0	0	39	1	2	0	0	0	1	0	0	0
Exiguobacterium_mexicanum	98	Otu00236	0	0	0	0	0	0	0	0	0	0	0	0	0	0	0	0	0	0	0	0	0	50
Pannonibacter_phragmitetus	99	Otu00263	0	0	0	0	0	0	0	0	0	0	0	0	0	0	0	0	0	0	0	0	0	0
Actinomyces_israelii	*	Otu00220	0	0	0	0	0	0	0	0	0	0	0	0	0	0	0	0	0	0	0	0	0	0
Lactococcus_lactis	99.7	Otu00246	0	44	0	0	0	0	0	0	0	0	0	0	0	0	0	0	0	0	0	0	0	0
Finegoldia_magna	98.5	Otu00189	0	0	0	0	0	0	0	0	0	0	0	0	0	0	33	0	0	0	0	0	0	0
Bavariicoccus_seileri	98.1	Otu00247	0	0	0	0	1	12	0	0	0	0	0	0	0	13	4	0	0	0	0	0	0	0
[Eubacterium]_nodatum_group_unclassified	*	Otu00256	0	0	0	0	0	0	0	0	0	0	0	0	0	0	0	0	0	0	0	0	0	0
Leptotrichia_unclassified	*	Otu00250	0	0	0	0	0	0	0	0	0	0	0	0	0	0	0	0	0	0	0	0	0	0
Sphingobacterium_faecium		Otu00213	0	0	0	0	0	0	0	0	0	0	0	0	0	0	0	0	0	0	0	0	0	0
Bergeyella_unclassified	*	Otu00224	0	0	0	6	0	0	0	0	0	0	0	0	0	0	0	0	0	0	0	0	0	0
Pseudomonas_saponiphila	98.5	Otu00234	0	0	0	0	0	0	0	0	0	0	0	0	0	0	4	0	0	0	0	0	0	0
Lactobacillus_unclassified		Otu00216	0	0	0	0	0	0	0	0	0	0	0	0	0	0	0	0	0	0	0	0	0	0
Microbacterium_hydrocarbonoxydans		Otu00173	0	0	0	0	0	0	0	0	0	0	0	0	0	0	0	3	24	15	0	0	0	0
Prevotella_shahii	97.6	Otu00237	0	0	0	5	0	12	0	0	0	0	0	0	0	0	0	0	0	0	0	0	0	0
Saccharophagus_unclassified	*	Otu00245	0	0	0	0	0	0	0	0	0	0	0	0	0	0	0	0	0	0	38	4	0	0
Treponema_socranskii	97.8	Otu00255	0	42	0	0	0	0	0	0	0	0	0	0	0	0	0	0	0	0	0	0	0	0
Shinella_unclassified	*	Otu00269	0	0	0	0	0	0	0	0	0	0	0	0	0	0	0	0	0	0	0	0	0	0
Aggregatibacter_segnis	98.1	Otu00276	0	0	32	3	0	0	1	0	0	0	0	0	0	0	0	1	0	4	0	0	0	0
Sphingomonas_paucimobilis	98.7	Otu00226	0	0	0	0	0	0	0	0	0	0	0	0	0	0	0	0	0	0	0	0	0	0
Actinomyces_odontolyticus	97.5	Otu00231	0	0	0	0	0	0	0	0	0	0	0	0	0	2	0	0	0	0	0	0	0	1
Capnocytophaga_leadbetteri	98.1	Otu00240	0	0	0	10	0	11	0	0	0	0	0	0	0	0	0	0	0	3	0	0	0	0
Pseudomonas_oryzihabitans	97.5	Otu00249	0	39	0	0	0	0	0	0	0	0	0	0	0	0	0	0	0	0	0	0	0	0
Vibrio_brasiliensis	99.1	Otu00225	0	0	0	0	0	0	0	0	0	0	38	0	0	0	0	0	0	0	0	0	0	0
Sphingobacterium_caeni	100	Otu00260	0	0	0	0	0	0	0	0	0	0	0	0	0	0	0	0	0	0	0	0	0	0
Bifidobacterium_animalis	98	Otu00257	0	0	0	3	0	0	0	0	0	0	0	0	0	1	0	0	0	0	0	0	0	0
Bacillus_wakoensis	98.3	Otu00235	0	0	2	0	0	0	2	0	0	0	0	0	0	0	0	0	0	0	0	0	0	0
Prevotella_pallens	97.9	Otu00281	0	0	0	0	3	3	0	0	0	0	0	0	0	0	0	0	0	0	0	0	0	0
Stenotrophomonas_maltophilia	97.9	Otu00254	0	0	0	0	0	0	0	0	0	0	0	0	0	0	0	0	0	0	0	0	0	0
Alloprevotella_rava		Otu00261	0	0	0	5	0	15	0	0	0	0	0	0	0	0	0	0	0	0	0	0	0	0
Rhodococcus_globerulus	97.2	Otu00138	0	0	8	0	0	0	24	0	0	0	0	0	0	0	0	0	0	0	0	0	0	0
Dyadobacter_unclassified	*	Otu00194	0	0	0	0	0	0	0	0	0	0	0	0	0	0	0	0	0	34	0	0	0	0
Ideonella_sp.	97.5	Otu00264	0	0	0	0	0	0	0	0	0	0	0	0	0	0	0	0	0	0	0	0	0	32
[Eubacterium]_nodatum_group_unclassified	*	Otu00282	0	33	0	0	0	0	0	0	0	0	0	0	0	0	0	0	0	0	0	0	0	0
Dermacoccus_nishinomiyaensis	98.8	Otu00301	0	0	0	0	0	0	0	0	0	0	0	0	0	1	0	0	0	0	0	0	0	0
Sphingobium_limneticum	98.7	Otu00308	0	0	0	0	0	0	0	0	0	0	0	0	0	0	0	0	0	0	0	0	0	0
Sphingobacterium_anhuiense	97.4	Otu00259	0	0	0	0	0	0	0	0	0	0	0	0	0	0	0	0	0	0	0	0	0	0
Pelomonas_saccharophila	100	Otu00300	0	0	0	0	0	0	0	0	0	0	0	0	2	0	0	0	0	0	0	0	0	0
Sphingomonas_desiccabilis	98.3	Otu00280	0	28	0	0	0	0	0	0	0	0	0	0	0	0	0	0	0	0	0	0	0	0
Brevundimonas_unclassified	*	Otu00284	0	28	0	0	0	0	0	0	0	0	0	0	0	0	0	0	0	0	0	0	0	0
Leucobacter_aridicollis	98.2	Otu00223	0	0	0	0	0	0	0	0	0	0	0	0	0	0	27	0	0	0	0	0	0	0
Prevotella_unclassified	*	Otu00251	0	0	0	0	0	0	0	0	0	0	0	0	0	0	0	0	0	0	0	0	0	0

Species_97	score	Group	S001_D	S001_P	S001_T	S002_D	S002_P	S002_T	S003_D	S003_P	S003_T	S004_D	S004_P	S004_T	S005_T	S006_D	S006_T	S007_D	S007_P	S007_T	S008_D	S008_P	S008_T	S009_D
Massilia_unclassified		Otu00252	0	0	0	0	0	0	0	0	0	0	0	0	0	0	0	0	0	0	0	0	0	0
Porphyromonas_unclassified	*	Otu00312	0	0	0	0	0	0	0	0	0	0	0	0	0	0	0	0	0	0	0	0	0	0
Sneathia_unclassified	*	Otu00214	0	0	0	0	0	0	0	0	0	0	0	0	0	0	0	0	6	19	0	0	0	0
Selenomonas_sputigena		Otu00328	0	0	0	0	0	0	0	0	0	0	0	0	0	0	0	0	0	0	0	0	0	0
Ochrobactrum_anthropi	100	Otu00316	0	0	0	0	0	0	0	0	0	0	0	0	0	0	0	0	0	0	0	0	0	0
Phenylobacterium_falsum	97	Otu00241	0	0	0	0	0	0	0	0	0	0	0	0	0	0	0	0	0	23	0	0	0	0
Peptostreptococcus_stomatis	97.2	Otu00268	0	0	0	0	0	17	0	0	0	0	0	0	0	0	0	0	0	2	0	0	0	0
Leptotrichia_hongkongensis	97.3	Otu00273	0	0	0	0	0	0	0	0	0	0	0	0	0	0	0	0	0	0	22	0	0	0
Fusobacterium_nucleatum		Otu00298	0	0	0	0	0	0	0	0	0	0	0	0	0	0	0	0	0	0	0	0	23	0
Fusobacterium_canifelinum	97.6	Otu00326	0	0	0	0	0	0	0	0	0	0	0	0	0	0	0	0	0	0	0	0	0	0
Mycobacterium_chelonae	99.1	Otu00270	0	0	0	0	0	0	0	0	0	0	0	0	22	0	0	0	0	0	0	0	0	0
Pseudomonas_sp.	99	Otu00272	0	0	0	0	0	0	0	0	0	0	0	0	0	0	0	0	0	0	0	0	0	0
Mycobacterium_neworleansense	98.4	Otu00289	0	0	0	0	0	0	0	0	0	0	0	0	0	0	0	0	0	0	0	0	0	0
Morganella_morganii	99.4	Otu00305	0	0	0	0	0	0	0	0	0	0	0	0	0	0	0	0	0	0	0	0	0	0
Actinomyces_slackii	98.6	Otu00370	0	0	22	0	0	0	0	0	0	0	0	0	0	0	0	0	0	0	0	0	0	0
Schwartzia_unclassified	*	Otu00207	0	0	0	0	0	0	0	0	0	0	0	0	0	0	0	0	21	0	0	0	0	0
Algoriphagus_unclassified	*	Otu00233	0	0	5	0	0	0	15	0	0	0	0	0	0	0	0	0	0	0	0	0	0	0
Selenomonas_unclassified	*	Otu00307	0	0	0	0	0	0	0	0	0	0	0	0	0	0	0	0	0	0	0	0	0	0
Pseudanabaena_sp.	100	Otu00185	0	0	0	0	0	0	0	0	0	0	0	0	0	0	0	0	20	0	0	0	0	0
Acinetobacter_guillouiae		Otu00294	0	0	0	0	0	0	0	0	0	0	0	0	0	0	0	0	0	0	0	0	0	0
Rhizobium_sp.	97.9	Otu00239	0	0	0	0	0	0	0	0	0	0	0	0	0	0	0	0	0	19	0	0	0	0
Caldicellulosiruptor_actoaceticus		Otu00266	0	0	0	0	0	0	0	0	0	0	0	0	0	0	19	0	0	0	0	0	0	0
Actinobacillus_porcitonsillarum		Otu00279	0	0	0	9	10	0	0	0	0	0	0	0	0	0	0	0	0	0	0	0	0	0
Raoultella_planticola	98.8	Otu00309	0	0	0	0	0	0	1	0	0	0	0	0	0	0	0	0	0	0	0	0	0	0
Campylobacter_concisus	*	Otu00346	0	0	0	0	0	8	0	0	0	0	0	0	0	0	0	0	0	0	0	0	0	0
Lautropia_mirabilis	100	Otu00292	0	0	0	0	0	0	0	0	0	0	0	0	0	0	0	0	0	0	18	0	0	0
Paracoccus_yeei	98.7	Otu00303	0	0	0	0	0	0	0	0	0	0	0	0	0	0	0	1	0	0	0	0	0	0
Rhodobacter_veldkampii		Otu00313	0	0	0	0	0	0	0	0	0	0	18	0	0	0	0	0	0	0	0	0	0	0
Comamonas_terrigena	98.8	Otu00325	0	0	0	0	0	0	0	0	0	0	0	0	0	0	0	0	0	0	0	0	0	0
Corynebacterium_marinum	99.4	Otu00378	0	0	18	0	0	0	0	0	0	0	0	0	0	0	0	0	0	0	0	0	0	0
Actinomyces_cardiffensis	100	Otu00380	0	0	16	0	0	0	0	0	0	0	0	0	0	0	0	0	0	2	0	0	0	0
Brevundimonas_diminuta	97.2	Otu00274	0	0	0	0	0	0	0	0	0	0	0	0	0	0	0	5	0	12	0	0	0	0
Rhodococcus_fascians	99.1	Otu00278	0	0	0	0	0	0	0	0	0	0	0	0	0	0	17	0	0	0	0	0	0	0
Veillonella_unclassified		Otu00290	0	0	0	0	0	0	0	0	0	0	0	0	0	0	0	0	0	0	0	0	0	0
Methylobacterium_adhaesivum	97.3	Otu00302	0	13	0	0	0	0	0	0	0	0	0	0	0	0	0	0	0	0	0	0	0	0
Leptotrichia_buccalis	98.1	Otu00339	0	16	0	0	0	0	0	0	0	0	0	0	0	0	0	0	0	0	0	0	0	0
Ferrimicrobium_unclassified	*	Otu00355	0	0	0	0	0	0	0	0	0	0	0	0	0	0	0	0	0	0	0	0	17	0
Paludibacter_unclassified	*	Otu00286	0	0	1	0	0	0	15	0	0	0	0	0	0	0	0	0	0	0	0	0	0	0
Pseudomonas_xanthomarina	98.1	Otu00287	0	2	0	0	0	0	0	0	0	0	0	0	0	0	0	0	0	0	0	0	0	0
Enterococcus_faecalis	99.2	Otu00311	0	0	0	0	0	0	0	0	0	0	0	0	0	0	0	0	0	0	0	0	0	0
Alcaligenes_faecalis	98.5	Otu00330	0	0	0	0	0	0	0	0	0	0	0	0	0	0	0	0	0	0	0	0	0	0
Streptococcus_australis		Otu00332	0	0	0	0	0	0	0	0	1	0	0	0	4	0	0	0	0	0	0	0	0	0
Aeromonas_bestiarum	100	Otu00358	0	0	0	0	0	0	0	0	0	0	0	0	0	0	0	0	0	0	0	0	0	0
Kingella_denitrificans	98.8	Otu00362	0	0	0	0	0	0	0	0	0	0	0	0	0	0	0	0	0	0	0	0	0	0
Massilia_haematophila	97.1	Otu00253	0	0	0	0	0	0	0	0	0	0	0	0	0	0	0	6	8	1	0	0	0	0
Ornithinimicrobium_kibberense	98.4	Otu00331	0	0	0	0	0	0	0	0	0	0	0	15	0	0	0	0	0	0	0	0	0	0
Providencia_rettgeri	99.4	Otu00342	0	0	0	1	0	0	0	0	0	0	0	0	0	0	0	0	0	0	0	0	0	0
Kocuria_rhizophila	98.5	Otu00277	0	0	0	0	0	0	0	0	0	0	0	0	0	0	0	0	0	0	0	0	0	0
Acinetobacter_sp.	99.6	Otu00293	0	0	0	0	0	0	0	0	0	0	0	0	0	0	0	0	0	0	0	0	0	0
Arthrobacter_defluvii	99.7	Otu00296	0	0	0	0	0	0	0	0	0	0	0	14	0	0	0	0	0	0	0	0	0	0
Lactobacillus_zeae	97.8	Otu00318	0	0	0	0	0	0	0	0	0	0	0	0	0	0	0	0	0	0	0	0	0	0
Brochothrix_thermosphacta	98.1	Otu00320	0	0	0	0	0	0	0	0	0	0	0	14	0	0	0	0	0	0	0	0	0	0
Acinetobacter_johnsonii	97.2	Otu00336	0	0	0	0	12	1	0	0	0	1	0	0	0	0	0	0	0	0	0	0	0	0
Pseudomonas_asplenii	97.5	Otu00347	0	0	0	0	0	0	0	0	0	0	0	9	0	0	0	0	0	0	0	0	0	0
Leptotrichia_unclassified	*	Otu00353	0	0	0	1	1	2	0	0	0	0	0	0	0	0	0	0	0	0	0	0	0	0
Prevotella_unclassified		Otu00360	0	0	0	0	0	0	0	0	0	0	0	0	0	0	0	1	0	0	0	0	0	0

Species_97	score	Group	S001_D	S001_P	S001_T	S002_D	S002_P	S002_T	S003_D	S003_P	S003_T	S004_D	S004_P	S004_T	S005_T	S006_D	S006_T	S007_D	S007_P	S007_T	S008_D	S008_P	S008_T	S009_D
Stenotrophomonas_maltophilia.	98.5	Otu00373	0	0	0	0	0	0	0	0	0	0	0	0	0	0	0	1	0	0	0	0	0	0
Acinetobacter_lwoffii	97.2	Otu00415	0	0	0	0	2	0	0	0	0	0	0	0	0	0	0	0	0	0	0	0	0	0
Bradyrhizobium_elkanii	98.3	Otu00291	0	0	0	0	0	0	0	0	0	0	0	0	0	0	0	0	0	13	0	0	0	0
Shewanella_putrefaciens	99.1	Otu00315	0	0	0	0	0	0	0	0	0	0	12	0	0	0	0	0	0	0	0	0	0	0
Granulicatella_unclassified	*	Otu00323	0	0	1	0	0	0	0	0	1	0	0	2	1	0	0	0	0	0	0	0	0	0
Paracoccus_marinus	99.3	Otu00338	0	0	0	0	0	0	0	3	0	0	10	0	0	0	0	0	0	0	0	0	0	0
Prevotella_unclassified	*	Otu00359	0	0	0	0	0	11	0	0	0	0	0	0	0	0	0	0	0	0	0	0	0	0
Pseudomonas_putida		Otu00363	0	10	0	0	0	0	0	0	0	0	0	0	0	0	0	0	0	0	0	0	0	0
Pseudochrobactrum_kiredjianiae	100	Otu00377	0	0	0	0	0	0	0	0	0	0	0	0	0	0	0	0	0	0	0	0	0	0
Sphingomonas_yanoikuyae.	98	Otu00222	0	0	0	0	0	0	0	0	0	0	0	0	0	0	0	0	12	0	0	0	0	0
Aureibacter_unclassified	*	Otu00258	0	0	5	0	0	0	7	0	0	0	0	0	0	0	0	0	0	0	0	0	0	0
Streptococcus_vestibularis		Otu00306	0	0	0	0	0	0	0	0	0	0	1	1	0	0	0	0	0	0	0	0	0	0
Devosia_limi	97	Otu00314	0	0	0	0	0	0	0	0	0	0	0	0	0	0	0	2	6	4	0	0	0	0
Intestinibacter_unclassified		Otu00324	5	0	0	0	0	0	0	0	0	0	0	0	0	0	0	0	0	0	0	0	0	0
Aridibacter_unclassified	*	Otu00285	0	0	0	0	0	0	0	0	0	0	0	0	0	0	0	0	0	0	0	0	0	0
Uruburuella_suis	98.1	Otu00329	0	0	0	0	0	0	0	0	0	0	0	0	0	0	0	0	0	0	0	0	0	0
Brevundimonas_unclassified	*	Otu00337	0	0	0	0	0	0	0	0	0	0	0	0	0	0	0	0	0	0	0	0	0	0
Prevotella_micans	97.6	Otu00344	0	0	0	0	0	0	0	0	0	0	0	0	0	0	0	0	0	0	0	0	0	0
Centipeda_periodontii	*	Otu00354	0	0	0	1	10	0	0	0	0	0	0	0	0	0	0	0	0	0	0	0	0	0
Dermacoccus_nishinomiyaensis	98.8	Otu00413	0	0	0	0	0	0	0	0	0	0	0	0	0	0	0	0	0	0	0	0	0	0
Smithella_unclassified	*	Otu00265	0	0	4	0	0	0	6	0	0	0	0	0	0	0	0	0	0	0	0	0	0	0
Phenylobacterium_kunshanense	*	Otu00288	0	0	0	0	0	0	0	0	0	0	0	0	0	0	0	0	10	0	0	0	0	0
Prevotella_oulorum	99.4	Otu00348	0	0	0	0	0	0	0	0	0	0	0	0	0	0	0	0	0	0	0	0	0	0
Capnocytophaga_sputigena	97.2	Otu00364	0	0	0	0	3	4	0	0	0	0	0	0	0	0	0	0	0	0	0	0	0	0
Actinomyces_graevenitzii	97.5	Otu00366	0	0	0	0	0	0	0	0	0	0	0	0	0	0	0	0	0	0	0	0	0	0
Burkholderia_contaminans	99.1	Otu00371	0	0	0	0	0	0	0	0	0	0	0	0	1	0	0	0	2	0	0	0	0	0
Corynebacterium_aquatimens	98.4	Otu00395	0	0	0	0	0	0	0	10	0	0	0	0	0	0	0	0	0	0	0	0	0	0
Novosphingobium_resinovorum	98.7	Otu00399	0	0	0	0	0	0	0	0	0	0	0	0	0	0	0	0	0	0	0	0	0	0
Streptococcus_infantis		Otu00418	0	0	0	0	0	0	0	0	0	0	0	0	0	0	0	0	0	0	0	0	0	0
Streptococcus_unclassified		Otu00426	0	0	0	1	0	0	0	0	0	0	0	0	1	1	1	0	0	0	0	0	0	0
Marinomonas_arenicola	98.5	Otu00430	0	10	0	0	0	0	0	0	0	0	0	0	0	0	0	0	0	0	0	0	0	0

Species_97	score	Group	S009_T	S010_P	S010_T	S011_D	S011_T	S012_D	S012_T	S013_D	S013_P	S013_T	S014_D	S014_P	S014_T	S015_D	S015_P	S015_T	S016_D	S016_P	S016_T	S017_D	S017_P	S017_T	S018_D	S018_P	S018_T	S019_D	S019_P	S019_T	Sum
Streptococcus_salivarius	97.9	Otu00002	6041	16	215	2762	3270	1230	2465	0	0	1	2	2	6668	967	91	112	35	59	278	70	50	107	65	71	89	711	2	1884	39673
Serratia_liquefaciens	97.3	Otu00001	0	1	0	0	0	0	0	1	0	0	15	0	3	0	0	0	0	0	0	0	0	1	0	0	0	0	0	1	30846
Streptococcus_oralis	97.3	Otu00003	3	125	39	25	1559	89	40	70	2070	1067	2	3	463	46	28	5	3040	67	21	0	24	8	1218	4785	354	822	0	10	30715
Pseudomonas_fluorescens	97.2	Otu00011	1	0	0	0	0	0	0	0	0	0	144	1	0	129	1222	2020	0	61	2546	31	8	0	0	30	0	4462	10972	8208	29894
Streptococcus_mitis	97.6	Otu00005	3491	0	7	904	544	855	2158	1	29	651	5	0	1908	449	44	126	58	189	112	118	57	165	37	18	283	926	1	727	27107
Acinetobacter_johnsonii	97.2	Otu00004	0	0	0	0	1	0	0	1	1	0	18	1	1	1	12	3	0	696	30	62	37	42	0	1	0	3	0	0	25378
Streptococcus_unclassified	*	Otu00008	8	0	0	0	62	8	34	9342	8407	5214	0	0	2	0	0	0	0	0	0	0	0	0	0	0	0	0	0	0	23371
Pseudomonas_putida	97.5	Otu00006	1	8	0	1	15	2787	2	0	0	1	3398	0	0	634	1422	872	211	102	369	1	429	222	0	0	0	0	0	0	23004
Stenotrophomonas_maltophilia	97	Otu00007	0	1	0	0	129	0	0	19	22	0	7	10	4	104	320	439	6773	8366	5284	213	33	2	31	41	0	0	0	0	21972
Actinomyces_odontolyticus	97.3	Otu00010	285	5	0	0	54	730	2464	0	1	0	0	0	0	152	53	78	26	116	36	44	15	22	4137	53	763	792	0	3	18011
Flavobacterium_lindanitolerans	98.1	Otu00013	0	5	0	0	0	0	0	0	0	0	0	0	1	0	0	0	0	0	0	1958	6356	6925	9	0	0	0	0	0	15312
Enterococcus_faecalis	97.1	Otu00015	0	6976	7549	0	13	8	0	2	1	0	0	0	0	4	0	0	0	5	0	0	0	0	0	0	0	0	0	0	14615
Brevundimonas_terrae		Otu00009	0	0	0	0	0	1	0	1	0	0	15	8	0	728	271	269	0	0	0	2182	816	1323	0	0	0	0	0	0	13941
Brevundimonas_vesicularis		Otu00014	0	0	1	0	1	0	0	0	0	0	0	0	1	234	5	7	0	44	318	26	477	364	0	0	0	0	0	0	12597
Lactobacillus_paracasei	97.7	Otu00017	0	0	29	776	0	155	44	0	0	0	0	0	0	0	0	0	0	0	0	0	0	0	0	0	0	0	0	0	11573
Massilia_aurea		Otu00012	0	0	0	0	12	0	0	0	0	0	0	8497	0	0	0	0	0	0	0	0	0	0	0	0	0	0	0	0	8509
Veillonella_parvula	97.7	Otu00022	189	0	0	0	48	262	91	0	125	159	0	2	0	35	5	13	1	0	4	6	19	32	191	142	1189	1544	0	32	7663
Haemophilus_parainfluenzae	97.6	Otu00018	1	0	0	0	0	30	43	1	0	291	0	0	7	3	4	188	6	30	163	4	17	29	181	415	1259	0	0	0	7262
Granulicatella_adiacens		Otu00020	215	0	6	0	4	54	258	2	7	2664	0	0	74	42	0	29	29	1	100	38	8	22	233	232	984	2	0	3	6959
Rhizobium_unclassified		Otu00021	0	2	0	0	0	0	0	0	0	0	0	0	0	0	0	4	0	0	0	4667	913	526	0	0	0	0	0	1	6940
Stenotrophomonas_nitritireducens	97.3	Otu00025	0	0	0	0	0	0	0	0	0	0	0	0	0	661	2475	3246	0	0	0	0	0	0	0	0	1	0	0	0	6388
Chryseobacterium_unclassified	*	Otu00016	0	1	0	0	0	0	0	1	0	0	0	0	0	0	0	0	0	0	0	0	0	0	0	0	0	0	0	0	6155
Prevotella_melaninogenica	97.3	Otu00026	0	0	0	0	0	90	330	184	0	0	0	0	0	0	1	63	0	0	4	0	3	2	1176	405	2164	0	0	0	5953
Microbacterium_maritypicum	97.2	Otu00032	0	0	0	0	0	0	0	0	0	0	0	1	0	0	0	0	0	174	0	0	84	5	0	0	0	0	0	0	5391
Agrobacterium_tumefaciens	97.3	Otu00034	0	0	0	0	0	4	0	0	0	0	0	0	0	2985	1974	343	0	0	0	0	0	1	0	0	0	0	0	0	5308
Streptococcus_oralis	97.6	Otu00024	1	0	0	10	160	29	2	0	1	2	0	0	886	0	0	0	22	72	19	0	3	14	0	0	65	0	0	0	5110
Myroides_unclassified	*	Otu00028	0	0	0	0	0	0	0	0	0	0	5065	0	0	0	0	0	0	0	0	0	0	0	0	0	0	0	0	0	5065
Propionibacterium_acnes	97.7	Otu00033	1	88	1	7	407	0	6	0	61	0	4	3	1	3	35	0	0	2	0	81	1	2	3	70	0	0	1	8	4671
Lactobacillus_fermentum	97.2	Otu00030	0	2	0	102	3	451	0	0	0	0	0	0	6	0	0	0	0	0	0	0	0	0	0	0	0	6	0	0	4640
Pseudomonas_aeruginosa	97.8	Otu00039	0	0	0	0	0	2	2	0	0	0	13	0	0	0	0	0	0	0	0	0	0	0	0	22	0	0	0	0	4586
Acinetobacter_lwoffii	97.5	Otu00027	0	0	0	2406	0	1	0	0	0	0	16	0	0	152	22	8	0	0	0	0	1	0	0	0	0	0	0	0	4312
Acidovorax_unclassified		Otu00023	0	0	0	0	0	0	0	0	0	0	0	0	0	0	0	0	0	0	0	0	0	0	0	0	0	0	0	0	4277
Actinomyces_lingnae	97	Otu00035	244	1	0	0	0	111	205	1	0	0	0	0	0	4	1	175	9	28	70	6	1	11	954	21	41	1093	0	21	3892
Lactobacillus_rhamnosus	97.2	Otu00031	0	0	2433	873	1	0	0	0	0	0	0	0	0	0	0	0	0	0	0	0	0	0	0	0	0	0	0	0	3667
Neisseria_flavascens	97.3	Otu00036	0	0	0	0	0	0	7	0	0	0	0	0	0	0	2	1	3	0	1	0	4	3	122	53	146	0	0	0	3602
Haemophilus_parahaemolyticus	97.6	Otu00037	0	0	0	0	0	0	0	0	0	0	0	0	0	0	0	0	0	0	1	0	0	0	202	1976	12	0	0	0	3554
Microbacterium_testaceum		Otu00038	0	0	0	0	0	0	0	0	0	0	0	0	0	0	0	0	0	0	0	0	0	4	0	0	0	0	0	0	3446
Dermacoccus_nishinomiyaensis		Otu00044	0	2958	219	0	7	2	0	1	0	0	0	0	0	2	0	0	0	5	0	0	0	0	0	0	0	0	0	0	3323
Streptococcus_infantis	97.6	Otu00040	2	0	0	0	0	6	31	3	1	111	0	0	4	94	4	41	108	234	502	0	0	0	134	25	458	0	0	0	3186
Massilia_varians	98.6	Otu00019	0	0	0	0	0	0	0	0	0	0	0	0	0	0	0	0	0	0	0	0	0	22	0	0	0	0	0	0	3029
Chryseobacterium_scophthalmum		Otu00041	0	0	0	0	0	0	1	0	0	0	0	0	0	235	1101	1435	0	0	0	0	0	0	2	0	0	0	0	0	2774
Prevotella_histicola	97.3	Otu00045	13	2	0	0	0	243	444	0	0	0	0	0	0	0	0	30	0	46	0	0	0	1	52	182	490	36	0	10	2671
Moraxella_osloensis	99	Otu00050	0	0	0	0	0	0	0	0	0	0	0	0	0	0	0	0	0	0	0	0	0	0	0	0	0	0	0	2	2497
Fusobacterium_periodonticum		Otu00049	0	0	11	7	0	0	0	0	52	0	0	0	0	0	0	0	0	113	0	2	0	3	228	152	541	0	0	0	2320
Rothia_mucilaginosa	97.3	Otu00042	36	0	2	0	12	23	36	0	27	655	0	0	389	57	0	2	1	0	22	4	8	21	0	4	58	2	0	34	2304
Lactobacillus_salivarius	97.4	Otu00043	0	0	0	1196	0	0	1	0	0	0	0	0	0	0	0	1	0	0	0	0	0	0	0	0	0	218	0	0	2137
Devosia_unclassified		Otu00029	0	0	0	0	0	0	0	0	0	0	0	0	0	0	0	0	0	0	0	0	0	0	0	0	0	0	0	0	2120
Methylophilus_methylotrophus	97.5	Otu00061	0	3	0	0	1887	2	0	0	0	0	0	13	0	99	0	0	0	1	0	0	1	1	0	0	0	0	0	0	2007
Citrobacter_freundii	100	Otu00046	328	0	0	0	0	0	0	12	0	0	108	0	0	8	59	15	0	0	0	5	2	28	0	0	0	0	0	0	1863
Stenotrophomonas_unclassified		Otu00058	0	0	0	0	0	0	0	0	0	0	0	0	0	0	0	0	0	0	0	0	0	0	0	0	0	0	0	0	1841
Streptococcus_sanguinis	98.5	Otu00056	0	2	0	0	481	0	0	0	111	1	0	0	7	0	1	0	0	43	0	0	0	0	12	2	4	0	0	0	1754
Gemella_haemolysans	97	Otu00051	0	0	0	0	2	1	3	2	0	0	0	0	10	0	3	0	359	0	0	2	0	0	30	845	8	0	0	0	1726
Phormidium_sp.	97.7	Otu00048	0	0	0	0	0	0	0	1	0	0	0	0	0	0	0	0	0	0	0	0	0	0	0	0	0	0	0	0	1529
Leptotrichia_unclassified	*	Otu00057	0	0	0	0	2	490	550	0	0	0	0	0	0	0	0	0	1	0	0	0	0	0	181	31	7	0	0	0	1392
Streptococcus_mitis		Otu00053	0	0	0	0	0	0	0	0	0	0	0	0	0	0	0	0	14	42	4	0	17	0	17	11	15	0	0	0	1361
Pseudoxanthomonas_mexicana	97.3	Otu00055	0	0	0	0	0	0	0	1	0	0	0	0	0	0	0	0	0	0	0	2	600	101	0	0	0	0	0	0	1350

Species_97	score	Group	S009_T	S010_P	S010_T	S011_D	S011_T	S012_D	S012_T	S013_D	S013_P	S013_T	S014_D	S014_P	S014_T	S015_D	S015_P	S015_T	S016_D	S016_P	S016_T	S017_D	S017_P	S017_T	S018_D	S018_P	S018_T	S019_D	S019_P	S019_T	Sum
Prevotella_pallens	97	Otu00064	0	0	0	0	0	17	29	0	0	0	0	0	0	0	0	13	0	0	0	0	0	0	68	125	549	0	0	0	1323
Streptococcus_anginosus		Otu00059	0	3	0	0	2	989	1	0	7	10	0	0	0	0	0	0	0	0	0	1	0	0	13	7	0	0	0	0	1275
Pseudorhodoferax_soli	97.8	Otu00063	0	0	0	0	0	0	0	0	0	0	0	0	0	29	36	1	0	0	0	1092	106	3	0	0	0	0	0	0	1267
beta_proteobacterium	97.5	Otu00047	0	0	0	0	2	0	0	0	0	0	0	1229	0	0	0	0	0	0	0	0	0	0	0	0	0	0	0	0	1231
Streptococcus_sp.	97	Otu00066	1	0	0	0	0	0	0	0	2	0	0	0	0	18	0	24	66	68	786	16	8	14	37	21	58	1	0	0	1144
Porphyromonas_catoniae	98.5	Otu00069	0	0	0	0	0	0	0	0	0	0	0	0	1	0	0	0	0	0	0	0	2	1	95	302	337	0	0	0	1127
Streptococcus_sobrinus	97.4	Otu00062	0	0	0	828	249	0	0	0	0	0	0	0	0	0	0	0	0	0	0	0	0	0	0	0	0	0	0	0	1077
Luteimonas_cucumeris	97.6	Otu00071	0	0	0	0	0	0	0	0	0	0	0	0	0	186	740	77	0	0	0	0	0	0	0	0	0	0	0	0	1034
Lactobacillus_unclassified		Otu00067	0	0	0	363	0	36	0	0	0	0	0	0	12	0	0	0	0	0	0	0	0	0	0	0	0	44	0	0	989
Acinetobacter_junii	97.2	Otu00073	0	0	0	0	0	1	0	0	0	0	25	0	0	601	48	2	82	31	12	158	6	13	0	0	0	0	0	0	981
Haemophilus_influenzae	97.3	Otu00081	0	0	0	0	0	0	0	0	0	0	0	0	0	0	0	0	1	0	0	0	0	0	79	381	24	0	0	0	967
Delftia_tsuruhatensis	97.5	Otu00060	0	0	0	0	0	0	0	0	0	0	24	0	1	179	21	85	0	0	0	0	0	0	0	0	0	0	0	0	954
Sphingomonas_sp.	97.3	Otu00052	0	0	0	0	2	0	0	0	0	0	0	860	0	0	0	0	0	0	0	24	0	3	0	0	0	28	0	0	917
Afipia_broomeae	97.3	Otu00065	0	0	0	0	0	0	0	0	0	0	0	0	0	0	0	0	0	0	0	0	0	0	0	0	0	0	0	0	876
Roseburia_unclassified		Otu00068	0	0	0	0	5	413	418	0	0	0	0	0	0	0	0	0	0	0	0	0	0	0	0	0	0	0	0	0	841
Prevotella_salivae	97.3	Otu00074	0	1	0	0	0	237	161	218	0	0	0	0	0	0	0	32	0	0	1	0	0	0	13	18	26	0	0	0	814
Streptococcus_unclassified	*	Otu00070	28	0	0	0	0	7	52	0	0	0	0	0	468	26	0	5	0	0	0	2	10	2	9	25	60	0	0	0	778
Zoogloea_ramigera	97.3	Otu00076	0	0	0	0	0	0	0	0	0	0	0	1	0	307	0	50	0	0	0	0	65	296	0	0	0	0	0	0	747
Gemella_sanguinis	97.1	Otu00072	0	0	0	0	0	6	9	0	0	83	0	0	0	0	4	0	0	0	12	0	6	10	15	19	53	0	0	0	705
Pseudomonas_unclassified		Otu00077	0	0	0	0	0	0	0	0	0	0	0	0	0	0	0	0	0	0	0	0	507	182	0	0	0	0	0	0	689
Prevotella_tannerae		Otu00085	0	0	0	4	542	0	2	0	0	1	0	0	0	0	0	0	0	0	0	0	0	0	0	0	0	0	0	0	658
Sphingobacterium_multivorum	97.6	Otu00082	0	0	0	0	0	1	0	0	0	0	0	1	0	329	150	169	0	0	0	0	0	0	0	0	0	0	0	0	650
Chryseobacterium_unclassified		Otu00083	0	0	0	0	0	0	0	0	0	0	0	0	0	46	301	259	0	0	0	0	0	0	0	0	0	0	0	0	606
Lachnoanaerobaculum_orale	97.4	Otu00075	1	0	0	0	5	25	104	0	0	0	0	0	0	0	0	2	0	0	10	0	4	0	7	4	23	0	0	0	585
Massilia_unclassified	*	Otu00054	0	0	0	0	0	0	0	0	0	0	0	0	0	0	0	0	0	0	0	0	0	7	0	0	0	0	0	0	578
Streptococcus_parasanguinis	98.8	Otu00080	1	0	0	0	2	2	298	0	0	0	0	0	0	1	0	1	0	0	0	0	0	0	22	0	0	1	0	0	566
Lactobacillus_fermentum	97.8	Otu00078	0	0	0	168	1	296	2	0	0	0	0	0	24	0	0	0	0	0	0	0	0	0	0	0	0	0	0	0	526
Sphingomonas_ursincola	97.3	Otu00079	0	1	0	196	1	297	0	0	0	0	0	15	0	0	0	0	0	0	0	0	0	0	0	0	0	0	0	0	510
Myroides_unclassified	*	Otu00087	0	0	0	0	0	0	0	0	0	0	492	0	0	0	0	0	0	0	0	0	0	0	0	0	0	0	0	0	492
Empedobacter_brevis	98.5	Otu00086	0	0	0	0	0	0	0	0	0	0	479	0	0	0	0	0	0	0	0	0	0	0	0	0	0	0	0	0	479
Comamonas_testosteroni	98.1	Otu00091	0	0	0	0	0	0	0	0	0	0	332	0	0	82	26	22	0	0	0	0	0	0	0	0	0	0	0	0	462
Streptococcus_unclassified		Otu00096	0	0	0	0	0	19	136	0	0	1	0	0	0	0	0	1	0	0	1	0	0	0	45	15	173	0	0	0	458
Staphylococcus_aureus	97.3	Otu00107	0	0	0	0	61	0	0	0	0	0	0	0	0	0	0	0	0	0	0	0	0	0	0	0	0	0	0	0	456
Streptococcus_gordonii	97.4	Otu00094	0	0	0	1	0	32	0	0	0	0	0	0	0	0	0	0	0	0	0	0	0	0	43	30	12	0	0	0	443
Parvimonas_micra	98.2	Otu00123	0	0	0	0	0	0	0	0	0	1	0	0	0	0	0	0	0	0	0	0	0	0	0	0	0	0	0	0	387
Prevotella_oris	97.3	Otu00111	0	0	0	1	334	2	0	0	0	0	0	1	0	0	0	0	0	0	0	0	0	0	0	0	0	0	0	0	376
Prevotella_nanceiensis	97.3	Otu00090	0	0	0	0	0	0	0	0	0	0	0	0	0	6	0	2	0	0	0	0	0	0	0	7	27	0	0	0	374
Mycoplasma_salivarium	98.1	Otu00135	0	0	0	0	0	0	0	0	0	0	0	0	0	0	0	0	0	0	0	0	0	0	0	0	0	0	0	0	372
Actinomyces_graevenitzii	98.5	Otu00100	3	0	0	0	0	3	3	0	0	0	0	0	0	0	0	5	0	0	0	0	0	0	0	0	4	0	0	0	371
Granulicatella_unclassified		Otu00098	0	0	0	0	0	0	0	0	0	0	0	0	0	0	0	0	0	0	0	0	0	0	103	164	5	0	0	0	367
Flavobacterium_lindanitolerans	97.5	Otu00097	0	0	0	0	0	0	0	0	0	0	0	0	0	0	0	0	0	0	0	72	136	141	0	0	0	0	0	0	349

Species_97	score	Group	S009_T	S010_P	S010_T	S011_D	S011_T	S012_D	S012_T	S013_D	S013_P	S013_T	S014_D	S014_P	S014_T	S015_D	S015_P	S015_T	S016_D	S016_P	S016_T	S017_D	S017_P	S017_T	S018_D	S018_P	S018_T	S019_D	S019_P	S019_T	Sum
Serratia_marcescens	97.6	Otu00099	0	0	0	0	0	0	0	0	0	0	46	0	0	1	168	81	0	0	0	0	7	27	0	0	1	0	0	0	346
Micrococcus_luteus	99	Otu00108	0	0	0	0	0	0	0	0	0	0	0	0	0	0	0	0	0	0	0	0	0	0	0	0	0	0	0	0	341
Lactobacillus_plantarum	97.2	Otu00093	0	0	338	0	0	0	0	0	0	0	0	0	0	0	0	0	0	0	0	0	0	0	0	0	0	0	0	0	339
Propionibacterium_acidifaciens	97.8	Otu00088	0	0	0	211	0	83	1	0	0	0	0	0	0	0	0	0	0	0	0	0	0	0	0	0	0	0	0	0	336
Megasphaera_micronuciformis	97.3	Otu00101	5	0	0	0	0	13	13	0	1	0	0	0	0	0	0	0	0	0	0	0	0	0	4	13	7	0	0	0	334
Ralstonia_sp.	97.6	Otu00114	0	19	0	0	0	1	0	282	7	0	0	0	0	0	0	0	4	0	0	3	5	0	0	0	0	0	0	0	324
Bradyrhizobium_sp.	97.5	Otu00116	0	0	0	0	0	0	0	0	0	0	0	0	1	321	0	0	0	0	0	0	0	0	0	0	0	0	0	0	322
Dermacoccus_nishinomiyaensis	97.2	Otu00118	0	276	28	0	0	1	0	0	0	0	0	0	0	0	0	0	0	0	0	0	0	0	0	0	0	0	0	0	312
Atopobium_parvulum	97.5	Otu00110	0	0	0	0	0	1	3	0	0	0	0	0	0	0	0	3	0	0	0	0	0	0	180	0	10	4	0	0	300
Campylobacter_concisus	97.9	Otu00102	0	0	0	0	0	60	43	0	0	0	0	0	0	2	21	0	0	15	0	0	6	6	5	53	0	0	0	0	296
Staphylococcus_warneri	100	Otu00112	0	0	0	0	0	0	1	0	0	0	2	19	0	0	0	0	0	0	0	1	0	0	0	0	0	0	0	0	289
Lactobacillus_vaginalis	98.6	Otu00109	0	0	0	3	0	0	0	0	0	0	0	0	0	0	0	0	0	0	0	0	0	0	1	0	0	28	0	2	274
Yersinia_pekkanenii	99.7	Otu00129	0	0	0	0	0	0	0	0	0	0	16	0	0	249	0	0	0	0	0	0	0	0	0	0	0	0	0	0	265
Flavobacterium_unclassified		Otu00133	0	0	0	0	0	0	0	0	0	0	0	0	0	216	0	26	0	0	0	0	0	0	0	0	0	0	0	0	242
Neisseria_sicca	97.9	Otu00122	0	0	0	0	0	0	0	0	0	2	0	0	0	0	0	0	0	0	0	0	0	0	13	12	24	0	0	0	236
Aeromonas_hydrophila	97	Otu00119	0	0	0	0	0	0	0	0	0	0	74	0	0	15	5	13	0	3	106	7	1	0	0	0	0	0	0	0	224
Bosea_unclassified		Otu00095	0	0	0	0	0	0	0	0	0	0	0	8	0	7	0	2	0	0	4	0	0	2	0	0	0	0	0	0	221
Actinomyces_graevenitzii	98.1	Otu00106	0	0	0	0	0	76	123	0	0	0	0	0	0	0	0	2	0	0	0	0	0	0	0	0	0	0	0	0	221
Diplorickettsia_unclassified	*	Otu00127	0	20	0	0	5	0	0	169	0	0	0	0	0	0	0	0	0	0	0	0	0	0	0	0	0	0	0	0	220
Solobacterium_moorei		Otu00115	0	1	0	0	46	9	20	0	0	2	0	0	0	0	1	5	0	0	3	0	0	0	43	0	16	0	0	0	219
Leptotrichia_unclassified	*	Otu00126	0	3	0	0	0	0	0	0	0	0	0	0	0	0	0	0	0	1	0	0	0	0	43	8	52	0	0	0	215
Streptococcus_dysgalactiae	97.6	Otu00132	0	0	0	0	0	0	0	0	0	0	0	0	0	0	0	0	0	0	0	0	0	0	0	0	0	0	0	0	212
Streptococcus_mitis		Otu00103	0	0	0	0	0	0	0	0	0	0	0	0	0	0	0	0	0	0	0	0	0	0	0	12	1	0	0	0	209
Staphylococcus_hominis	97.3	Otu00113	0	0	0	0	168	0	0	0	0	0	0	35	0	0	0	0	0	0	0	0	0	0	0	0	0	0	0	0	207
Prevotella_oralis	97.9	Otu00179	0	0	0	0	0	0	0	0	0	0	0	0	0	0	0	0	0	0	0	0	0	0	0	0	0	0	0	0	200
Variovorax_ginsengisoli	98.1	Otu00145	0	0	0	0	0	1	0	0	0	0	0	0	0	79	43	18	0	0	0	0	0	1	0	0	0	0	0	0	193
Corynebacterium_imitans	*	Otu00131	0	0	0	0	0	0	0	0	0	0	0	0	0	0	0	0	0	0	0	0	0	0	0	0	0	0	0	0	190
Shinella_kummerowiae	97.4	Otu00104	0	0	0	0	0	0	0	0	0	0	0	0	0	0	0	0	0	0	0	0	0	0	0	0	0	0	0	0	185
Rhizobium_mesosinicum	97.1	Otu00084	0	0	0	0	0	0	0	0	0	0	0	0	0	0	0	0	0	0	0	0	0	4	0	0	0	0	0	0	183
Chryseobacterium_formosense		Otu00120	0	0	0	0	0	0	0	0	0	0	0	0	0	0	0	0	0	0	0	0	0	183	0	0	0	0	0	0	183
Lactobacillus_kalixensis	98.5	Otu00134	0	0	0	0	0	0	0	0	0	0	0	0	0	0	0	0	0	0	0	0	0	0	0	0	0	183	0	0	183
Massilia_alkalitolerans	98.8	Otu00089	0	0	0	0	0	0	0	0	0	0	0	0	0	0	0	0	0	0	0	0	0	0	0	0	0	0	0	0	169
Pseudocitrobacter_anthropi	98.4	Otu00128	0	0	0	6	0	0	0	0	0	0	0	0	0	0	0	0	0	0	0	0	0	0	0	0	0	0	0	0	169
Prevotella_buccae	97.3	Otu00164	0	0	0	0	166	0	0	0	0	0	0	0	0	0	0	0	0	0	0	0	0	0	0	0	0	0	0	0	166
Bacteroides_unclassified	*	Otu00147	0	0	0	0	0	0	0	0	0	0	0	0	1	0	0	0	0	0	0	0	0	0	9	10	113	0	0	0	165
Prevotella_unclassified	*	Otu00125	0	0	0	0	1	87	71	0	0	0	0	0	0	0	0	3	0	0	0	0	0	0	0	0	0	0	0	0	163
Ensifer_adhaerens	97.9	Otu00105	0	1	0	0	0	0	0	0	0	0	0	0	0	19	39	32	0	0	0	0	0	0	0	0	0	0	0	0	162
Streptococcus_mutans	98.3	Otu00148	0	0	0	14	31	22	0	0	0	0	0	0	1	1	0	0	0	0	0	0	0	0	0	0	0	0	0	0	162
Actinomyces_oris	97.1	Otu00165	0	0	0	0	0	0	3	0	0	0	0	0	0	0	0	0	0	0	0	0	0	0	158	0	1	0	0	0	162
Stomatobaculum_longum	99.6	Otu00124	2	0	0	0	1	39	49	0	0	0	0	0	0	0	0	3	0	0	1	0	0	0	2	2	4	0	0	0	160
Acinetobacter_bereziniae	97.2	Otu00136	0	0	0	0	0	0	0	0	0	0	39	0	0	0	8	103	0	0	0	0	0	0	0	0	0	0	0	0	158
Fusobacterium_nucleatum	97.6	Otu00155	0	0	0	0	0	0	0	0	0	0	0	0	0	0	0	0	0	0	0	0	0	0	146	10	1	0	0	0	157
Acinetobacter_unclassified		Otu00137	0	0	0	0	0	0	0	0	0	0	0	0	0	0	0	0	0	95	3	27	0	0	0	0	0	0	0	0	155
Actinomyces_viscosus	97	Otu00161	0	0	0	0	0	0	0	0	0	0	0	0	0	0	0	0	0	0	0	0	0	0	145	1	0	0	0	0	155
Sphingomonas_unclassified		Otu00121	0	1	0	0	1	150	0	0	0	0	0	0	0	0	0	0	0	0	0	0	0	0	0	0	0	1	0	0	153
Streptococcus_oligofermentans	98.1	Otu00149	0	0	0	0	0	41	0	0	0	0	0	0	0	0	0	0	0	0	0	0	0	0	0	0	0	0	0	0	151
Alloprevotella_unclassified	*	Otu00175	0	0	0	0	0	0	0	149	0	0	0	0	0	0	0	0	0	0	0	0	0	0	0	0	0	0	0	0	149
Leptotrichia_shahii	97.2	Otu00130	0	0	0	0	0	0	0	0	0	0	0	0	0	0	0	0	0	0	0	0	0	0	0	0	0	0	0	0	148
Comamonas_aquatica	98.4	Otu00142	0	0	0	0	0	0	0	0	0	0	7	0	0	0	0	0	0	114	23	0	0	0	0	0	0	0	0	0	147
Rhizobium_unclassified		Otu00151	0	0	0	0	0	0	0	0	0	0	0	0	0	1	132	13	0	0	0	0	0	0	0	0	0	0	0	0	146
Methylobacterium_extorquens	99	Otu00150	0	0	0	0	106	0	0	0	0	0	0	1	0	0	0	0	0	0	1	0	0	0	0	0	0	0	0	0	144
Actinomyces_odontolyticus	98.4	Otu00153	6	0	0	0	0	2	9	0	0	0	0	0	0	0	0	0	1	0	2	0	0	0	84	0	0	28	0	0	144
Odoribacter_unclassified	*	Otu00184	0	0	0	0	0	0	0	136	0	0	0	0	0	0	0	0	0	0	0	0	0	0	0	0	0	0	0	0	136
Selenomonas_artemidis		Otu00168	0	0	0	0	95	0	0	0	0	0	0	0	0	0	0	0	0	0	0	0	0	0	0	0	0	0	0	0	134
Actinomyces_slackii	97.2	Otu00152	0	0	0	0	0	8	4	0	0	0	0	0	2	0	0	0	0	0	0	0	0	0	0	0	0	0	0	0	132
Sphingopyxis_granuli	97.6	Otu00144	0	0	0	0	0	0	0	0	0	0	0	13	0	0	18	12	0	0	0	0	75	10	0	0	0	0	0	0	131
Sediminibacterium_unclassified	*	Otu00154	0	0	7	0	0	0	0	0	0	0	0	0	0	0	0	0	0	0	0	0	0	0	0	0	0	0	0	0	131

Species_97	score	Group	S009_T	S010_P	S010_T	S011_D	S011_T	S012_D	S012_T	S013_D	S013_P	S013_T	S014_D	S014_P	S014_T	S015_D	S015_P	S015_T	S016_D	S016_P	S016_T	S017_D	S017_P	S017_T	S018_D	S018_P	S018_T	S019_D	S019_P	S019_T	Sum
Nocardioides_aestuarii	98.4	Otu00192	0	0	0	0	0	0	0	129	0	0	0	0	0	0	0	0	0	0	0	0	0	0	0	0	0	0	0	0	129
Abiotrophia_defectiva		Otu00174	0	0	0	0	0	0	0	0	0	0	0	0	0	0	0	0	0	0	2	0	0	0	39	31	29	0	0	0	127
Dermacoccus_nishinomiyaensis	98.8	Otu00177	0	112	7	0	2	0	0	0	0	0	0	0	0	0	0	0	0	0	0	0	0	0	0	0	0	0	0	0	124
Methylobacterium_gregans	98	Otu00217	0	0	0	0	0	0	0	0	0	0	0	0	0	0	0	0	0	0	0	0	0	0	0	0	0	0	0	0	123
Corynebacterium_segmentosum	98.5	Otu00146	0	0	0	0	1	2	0	0	0	0	0	50	0	0	0	0	0	0	0	0	0	0	0	0	0	0	0	0	122
Ochrobactrum_sp.	99.7	Otu00171	0	0	0	0	0	0	0	0	0	0	2	0	0	0	0	1	0	0	0	0	0	0	0	0	0	0	0	0	120
Actinomyces_graevenitzii	98.5	Otu00180	2	0	0	0	0	3	1	0	0	0	0	0	0	0	0	0	0	0	0	0	0	0	16	12	29	0	0	0	118
Lysobacter_unclassified		Otu00176	0	0	0	0	0	0	0	0	0	0	0	0	0	0	0	0	0	0	0	0	0	0	0	0	0	0	0	0	116
Acinetobacter_sp.	97.2	Otu00158	0	0	0	0	0	0	0	0	0	0	115	0	0	0	0	0	0	0	0	0	0	0	0	0	0	0	0	0	115
Brevundimonas_unclassified		Otu00092	0	0	0	0	0	0	0	0	0	0	0	0	0	0	0	0	0	0	0	0	0	0	0	0	0	0	0	0	113
Prevotella_unclassified	*	Otu00162	0	0	0	0	0	4	1	0	0	0	0	0	0	0	0	0	0	0	0	0	0	0	0	0	1	0	0	0	111
Bryobacter_unclassified	*	Otu00204	0	0	0	0	0	0	0	106	0	0	0	0	0	0	0	0	0	0	0	0	0	0	0	0	0	0	0	0	106
Actinomyces_unclassified	*	Otu00183	0	0	0	0	0	0	0	0	0	0	0	0	0	0	0	0	0	0	0	0	0	0	96	8	0	0	0	0	105
Methylobacterium_unclassified	*	Otu00182	0	102	0	0	0	0	0	0	0	0	0	0	0	0	0	0	0	1	0	0	0	0	0	0	0	0	0	0	103
Acinetobacter_rudis	98.2	Otu00172	0	0	0	0	0	0	0	0	0	0	102	0	0	0	0	0	0	0	0	0	0	0	0	0	0	0	0	0	102
Oribacterium_unclassified	*	Otu00159	0	0	0	0	0	0	0	0	0	0	0	0	0	0	0	0	0	0	0	0	0	0	0	27	7	0	0	0	100
Methylobacterium_goesingense	98.3	Otu00143	0	0	0	0	0	0	0	0	0	0	0	87	0	0	0	0	0	0	0	0	0	0	0	0	0	0	0	0	98
Massilia_timonae	98.8	Otu00243	0	0	0	0	0	0	0	0	0	0	0	0	0	0	0	0	0	0	0	0	0	0	0	0	0	0	0	0	91
Corynebacterium_unclassified	*	Otu00219	0	0	0	0	0	0	0	90	0	0	0	0	0	0	0	0	0	0	0	0	0	0	0	0	0	0	0	0	90
Devosia_riboflavina	97.9	Otu00140	0	0	0	0	0	0	0	0	0	0	0	0	0	0	0	0	0	0	0	0	0	0	0	0	0	0	0	0	89
Achromobacter_mucicolens	97.2	Otu00157	0	0	0	0	0	0	0	0	0	0	0	0	0	0	0	89	0	0	0	0	0	0	0	0	0	0	0	0	89
Rhizobium_sp.	98.6	Otu00141	0	0	0	0	0	0	0	6	0	0	0	0	0	0	0	10	0	0	0	0	0	0	0	0	0	0	1	0	88
Parvimonas_micra	*	Otu00203	0	0	0	0	86	1	0	0	0	0	0	0	0	0	0	0	0	0	0	0	0	0	0	0	0	0	0	0	87
Leptotrichia_unclassified	*	Otu00169	0	0	0	0	0	0	23	0	0	0	0	0	0	0	4	0	0	0	0	0	0	0	10	0	5	0	0	0	86
Streptococcus_pseudopneumoniae	98.1	Otu00163	0	0	0	0	0	0	0	0	0	0	0	0	0	0	1	0	41	3	0	0	0	0	0	9	0	0	0	0	85
Streptococcus_tigurinus	97.9	Otu00181	0	0	0	0	0	0	1	0	2	0	0	0	0	0	0	0	0	0	0	0	0	0	0	1	0	0	0	0	85
Tomitella_biformata	98.4	Otu00218	0	78	3	0	0	0	0	0	0	0	0	0	0	0	0	0	0	0	0	0	0	0	0	0	0	0	0	0	84
[Eubacterium]_nodatum_group_unclassified		Otu00193	0	0	0	0	0	0	1	0	0	0	0	0	0	0	0	8	0	0	0	0	0	0	8	2	31	0	0	0	82
Actinomyces_unclassified	*	Otu00160	0	0	0	0	0	14	0	0	0	0	0	0	0	0	0	0	0	0	0	0	0	0	0	0	0	0	0	0	81
Capnocytophaga_gingivalis	97.8	Otu00199	0	0	0	0	0	0	0	0	0	0	0	0	0	0	0	0	0	0	2	0	0	0	0	12	26	0	0	0	80
Prevotella_nigrescens	98.5	Otu00200	0	0	0	1	38	0	0	0	0	0	0	0	0	0	0	0	0	0	0	0	0	0	0	0	0	0	0	0	78
Terrisporobacter_unclassified		Otu00188	0	0	0	0	0	0	0	0	0	0	0	0	0	0	0	0	0	0	0	0	0	0	0	0	0	0	0	0	77
Pedobacter_unclassified	*	Otu00228	0	0	0	0	0	0	0	0	0	0	0	0	0	76	0	0	0	0	0	0	0	0	0	0	0	0	0	0	76
Oribacterium_sinus	97.7	Otu00195	0	0	0	0	0	7	4	0	0	0	0	0	0	0	0	5	0	0	0	0	0	0	0	4	4	0	0	0	74
Fusobacterium_nucleatum		Otu00244	0	0	5	0	0	0	2	0	0	1	0	0	0	0	0	0	0	0	0	0	0	0	0	0	0	0	0	0	74
Pseudomonas_putida	97.5	Otu00170	0	0	0	0	0	0	0	0	0	0	0	0	0	0	0	0	0	0	0	0	0	0	0	0	0	0	0	0	72
Pseudomonas_agarici	97.8	Otu00187	0	0	0	0	0	0	0	0	0	0	72	0	0	0	0	0	0	0	0	0	0	0	0	0	0	0	0	0	72
Sediminibacterium_salmoneum	*	Otu00210	0	1	0	0	49	0	0	0	0	0	0	0	0	0	0	0	0	0	0	0	0	0	0	0	0	0	0	0	72
Lactobacillus_ultunensis	97.9	Otu00242	0	0	0	0	0	10	0	0	0	0	0	0	0	0	0	0	0	0	0	0	0	0	0	0	0	0	0	0	72
Propionicimonas_paludicola	98.4	Otu00198	0	0	0	0	0	0	0	0	0	0	0	0	0	0	0	0	0	0	0	0	0	0	0	0	0	0	0	0	71
Chryseobacterium_hominis	98.4	Otu00178	0	0	0	0	0	0	0	0	0	0	0	0	0	0	0	0	63	0	7	0	0	0	0	0	0	0	0	0	70
Ralstonia_unclassified	*	Otu00186	0	0	0	0	0	0	0	0	0	0	0	0	0	0	0	3	0	0	0	0	0	0	8	1	14	0	0	0	70
Aeromonas_unclassified	*	Otu00201	0	0	0	0	0	4	9	0	0	0	0	0	0	0	0	0	0	0	0	0	0	0	37	0	14	0	0	0	70
Dermacoccus_nishinomiyaensis	98.4	Otu00208	0	65	3	0	0	0	0	0	0	0	0	0	0	0	0	0	0	0	0	0	0	0	0	0	0	0	0	0	70
Lactobacillus_crispatus	97.4	Otu00212	0	0	0	9	0	0	0	0	0	0	0	0	0	0	0	0	0	0	0	0	0	0	0	0	0	0	0	0	70
Ornithinimicrobium_kibberense	97.5	Otu00167	0	0	0	0	0	0	0	0	0	0	0	0	0	0	0	0	0	0	0	0	25	5	0	0	0	0	0	0	68
Bacillus_cereus	97.6	Otu00156	0	0	0	0	0	0	0	0	0	0	2	0	0	0	0	0	0	0	0	0	0	0	0	0	0	0	0	0	67
Sphingobium_herbicidovorans	99.3	Otu00230	0	0	0	0	0	0	0	0	0	0	0	0	0	64	0	3	0	0	0	0	0	0	0	0	0	0	0	0	67
Hydrogenophaga_defluvii	97.8	Otu00117	0	0	0	0	0	0	0	0	0	0	0	0	0	0	0	0	0	0	0	0	0	0	0	0	0	0	0	0	64
Microbacterium_lacticum	100	Otu00205	0	0	0	0	0	0	0	0	0	0	0	0	0	0	0	0	0	44	0	0	0	1	0	0	0	0	0	1	63
Alcaligenes_aquatilis	98.2	Otu00206	0	0	0	0	0	0	0	0	0	0	63	0	0	0	0	0	0	0	0	0	0	0	0	0	0	0	0	0	63
Rhizobium_unclassified	97	Otu00229	0	0	0	0	0	0	0	0	0	0	0	0	0	42	0	21	0	0	0	0	0	0	0	0	0	0	0	0	63
Devosia_sp.	97	Otu00139	0	0	0	0	0	0	0	0	0	0	0	0	0	0	0	0	0	0	0	0	0	0	0	0	0	0	0	0	62
Capnocytophaga_gingivalis	*	Otu00196	0	0	0	0	0	4	0	0	0	8	0	0	0	0	0	0	0	0	0	0	0	0	0	0	0	0	0	0	62
Halomonas_unclassified	*	Otu00275	0	0	0	0	0	0	0	0	0	0	0	0	0	0	0	0	0	0	0	0	0	0	0	0	0	0	0	0	62
Prevotella_unclassified	*	Otu00191	0	0	0	0	0	21	16	0	0	0	0	0	0	0	0	0	0	0	0	0	0	0	0	0	13	0	0	0	61

Species_97	score	Group	S009_T	S010_P	S010_T	S011_D	S011_T	S012_D	S012_T	S013_D	S013_P	S013_T	S014_D	S014_P	S014_T	S015_D	S015_P	S015_T	S016_D	S016_P	S016_T	S017_D	S017_P	S017_T	S018_D	S018_P	S018_T	S019_D	S019_P	S019_T	Sum
Massilia_unclassified		Otu00252	0	0	0	0	0	0	0	0	0	0	0	27	0	0	0	0	0	0	0	0	0	0	0	0	0	0	0	0	27
Porphyromonas_unclassified	*	Otu00312	0	0	0	0	0	0	0	0	0	0	0	0	0	0	0	0	0	0	0	0	0	0	0	16	11	0	0	0	27
Sneathia_unclassified	*	Otu00214	0	0	0	0	0	0	0	0	0	0	0	0	0	0	0	0	0	0	0	0	0	0	0	0	0	0	0	0	25
Selenomonas_sputigena		Otu00328	0	0	0	0	25	0	0	0	0	0	0	0	0	0	0	0	0	0	0	0	0	0	0	0	0	0	0	0	25
Ochrobactrum_anthropi	100	Otu00316	0	0	0	0	0	0	0	0	0	0	0	0	0	24	0	0	0	0	0	0	0	0	0	0	0	0	0	0	24
Phenylobacterium_falsum	97	Otu00241	0	0	0	0	0	0	0	0	0	0	0	0	0	0	0	0	0	0	0	0	0	0	0	0	0	0	0	0	23
Peptostreptococcus_stomatis	97.2	Otu00268	0	0	0	0	0	0	0	0	0	0	0	0	0	0	0	0	0	0	0	0	0	0	0	0	4	0	0	0	23
Leptotrichia_hongkongensis	97.3	Otu00273	0	0	0	0	0	0	0	0	0	0	0	0	0	0	0	0	0	0	0	0	0	0	0	0	1	0	0	0	23
Fusobacterium_nucleatum		Otu00298	0	0	0	0	0	0	0	0	0	0	0	0	0	0	0	0	0	0	0	0	0	0	0	0	0	0	0	0	23
Fusobacterium_canifelinum	97.6	Otu00326	0	0	0	0	0	0	0	0	0	0	0	0	0	0	0	0	0	0	0	0	0	0	11	10	2	0	0	0	23
Mycobacterium_chelonae	99.1	Otu00270	0	0	0	0	0	0	0	0	0	0	0	0	0	0	0	0	0	0	0	0	0	0	0	0	0	0	0	0	22
Pseudomonas_sp.	99	Otu00272	0	0	0	0	0	0	0	0	0	0	0	0	0	0	0	0	0	0	0	14	8	0	0	0	0	0	0	0	22
Mycobacterium_neworleansense	98.4	Otu00289	0	0	0	0	0	0	22	0	0	0	0	0	0	0	0	0	0	0	0	0	0	0	0	0	0	0	0	0	22
Morganella_morganii	99.4	Otu00305	0	0	0	0	0	0	0	0	0	0	22	0	0	0	0	0	0	0	0	0	0	0	0	0	0	0	0	0	22
Actinomyces_slackii	98.6	Otu00370	0	0	0	0	0	0	0	0	0	0	0	0	0	0	0	0	0	0	0	0	0	0	0	0	0	0	0	0	22
Schwartzia_unclassified	*	Otu00207	0	0	0	0	0	0	0	0	0	0	0	0	0	0	0	0	0	0	0	0	0	0	0	0	0	0	0	0	21
Algoriphagus_unclassified	*	Otu00233	0	1	0	0	0	0	0	0	0	0	0	0	0	0	0	0	0	0	0	0	0	0	0	0	0	0	0	0	21
Selenomonas_unclassified	*	Otu00307	0	0	0	4	0	17	0	0	0	0	0	0	0	0	0	0	0	0	0	0	0	0	0	0	0	0	0	0	21
Pseudanabaena_sp.	100	Otu00185	0	0	0	0	0	0	0	0	0	0	0	0	0	0	0	0	0	0	0	0	0	0	0	0	0	0	0	0	20
Acinetobacter_guillouiae		Otu00294	0	0	0	0	0	0	0	0	0	0	20	0	0	0	0	0	0	0	0	0	0	0	0	0	0	0	0	0	20
Rhizobium_sp.	97.9	Otu00239	0	0	0	0	0	0	0	0	0	0	0	0	0	0	0	0	0	0	0	0	0	0	0	0	0	0	0	0	19
Caldicellulosiruptor_actoaceticus		Otu00266	0	0	0	0	0	0	0	0	0	0	0	0	0	0	0	0	0	0	0	0	0	0	0	0	0	0	0	0	19
Actinobacillus_porcitonsillarum		Otu00279	0	0	0	0	0	0	0	0	0	0	0	0	0	0	0	0	0	0	0	0	0	0	0	0	0	0	0	0	19
Raoultella_planticola	98.8	Otu00309	0	0	0	0	0	0	0	0	0	0	16	1	0	0	0	1	0	0	0	0	0	0	0	0	0	0	0	0	19
Campylobacter_concisus	*	Otu00346	0	0	0	0	0	0	0	0	0	0	0	0	0	0	0	0	0	0	0	0	0	0	10	0	1	0	0	0	19
Lautropia_mirabilis	100	Otu00292	0	0	0	0	0	0	0	0	0	0	0	0	0	0	0	0	0	0	0	0	0	0	0	0	0	0	0	0	18
Paracoccus_yeei	98.7	Otu00303	0	0	17	0	0	0	0	0	0	0	0	0	0	0	0	0	0	0	0	0	0	0	0	0	0	0	0	0	18
Rhodobacter_veldkampii		Otu00313	0	0	0	0	0	0	0	0	0	0	0	0	0	0	0	0	0	0	0	0	0	0	0	0	0	0	0	0	18
Comamonas_terrigena	98.8	Otu00325	0	0	0	0	0	0	0	0	0	0	0	0	0	0	7	11	0	0	0	0	0	0	0	0	0	0	0	0	18
Corynebacterium_marinum	99.4	Otu00378	0	0	0	0	0	0	0	0	0	0	0	0	0	0	0	0	0	0	0	0	0	0	0	0	0	0	0	0	18
Actinomyces_cardiffensis	100	Otu00380	0	0	0	0	0	0	0	0	0	0	0	0	0	0	0	0	0	0	0	0	0	0	0	0	0	0	0	0	18
Brevundimonas_diminuta	97.2	Otu00274	0	0	0	0	0	0	0	0	0	0	0	0	0	0	0	0	0	0	0	0	0	0	0	0	0	0	0	0	17
Rhodococcus_fascians	99.1	Otu00278	0	0	0	0	0	0	0	0	0	0	0	0	0	0	0	0	0	0	0	0	0	0	0	0	0	0	0	0	17
Veillonella_unclassified		Otu00290	10	0	0	0	0	1	5	0	0	0	0	0	0	0	0	1	0	0	0	0	0	0	0	0	0	0	0	0	17
Methylobacterium_adhaesivum	97.3	Otu00302	0	0	0	0	0	0	0	0	0	0	0	4	0	0	0	0	0	0	0	0	0	0	0	0	0	0	0	0	17
Leptotrichia_buccalis	98.1	Otu00339	0	0	0	0	0	0	0	0	0	0	0	0	0	0	0	0	0	0	0	0	0	0	0	0	1	0	0	0	17
Ferrimicrobium_unclassified	*	Otu00355	0	0	0	0	0	0	0	0	0	0	0	0	0	0	0	0	0	0	0	0	0	0	0	0	0	0	0	0	17
Paludibacter_unclassified	*	Otu00286	0	0	0	0	0	0	0	0	0	0	0	0	0	0	0	0	0	0	0	0	0	0	0	0	0	0	0	0	16
Pseudomonas_xanthomarina	98.1	Otu00287	0	0	0	0	0	13	0	0	0	0	0	0	0	0	0	0	0	0	0	0	0	1	0	0	0	0	0	0	16
Enterococcus_faecalis	99.2	Otu00311	0	12	4	0	0	0	0	0	0	0	0	0	0	0	0	0	0	0	0	0	0	0	0	0	0	0	0	0	16
Alcaligenes_faecalis	98.5	Otu00330	0	0	0	0	0	0	0	0	0	0	16	0	0	0	0	0	0	0	0	0	0	0	0	0	0	0	0	0	16
Streptococcus_australis		Otu00332	9	0	0	0	0	0	1	0	0	0	0	0	1	0	0	0	0	0	0	0	0	0	0	0	0	0	0	0	16
Aeromonas_bestiarum	100	Otu00358	0	0	0	0	0	0	0	0	0	0	9	0	0	0	0	7	0	0	0	0	0	0	0	0	0	0	0	0	16
Kingella_denitrificans	98.8	Otu00362	0	0	0	0	16	0	0	0	0	0	0	0	0	0	0	0	0	0	0	0	0	0	0	0	0	0	0	0	16
Massilia_haematophila	97.1	Otu00253	0	0	0	0	0	0	0	0	0	0	0	0	0	0	0	0	0	0	0	0	0	0	0	0	0	0	0	0	15
Ornithinimicrobium_kibberense	98.4	Otu00331	0	0	0	0	0	0	0	0	0	0	0	0	0	0	0	0	0	0	0	0	0	0	0	0	0	0	0	0	15
Providencia_rettgeri	99.4	Otu00342	0	0	0	0	0	0	0	0	0	0	14	0	0	0	0	0	0	0	0	0	0	0	0	0	0	0	0	0	15
Kocuria_rhizophila	98.5	Otu00277	0	0	0	0	0	0	0	0	11	0	0	3	0	0	0	0	0	0	0	0	0	0	0	0	0	0	0	0	14
Acinetobacter_sp.	99.6	Otu00293	0	0	0	14	0	0	0	0	0	0	0	0	0	0	0	0	0	0	0	0	0	0	0	0	0	0	0	0	14
Arthrobacter_defluvii	99.7	Otu00296	0	0	0	0	0	0	0	0	0	0	0	0	0	0	0	0	0	0	0	0	0	0	0	0	0	0	0	0	14
Lactobacillus_zeae	97.8	Otu00318	0	0	14	0	0	0	0	0	0	0	0	0	0	0	0	0	0	0	0	0	0	0	0	0	0	0	0	0	14
Brochothrix_thermosphacta	98.1	Otu00320	0	0	0	0	0	0	0	0	0	0	0	0	0	0	0	0	0	0	0	0	0	0	0	0	0	0	0	0	14
Acinetobacter_johnsonii	97.2	Otu00336	0	0	0	0	0	0	0	0	0	0	0	0	0	0	0	0	0	0	0	0	0	0	0	0	0	0	0	0	14
Pseudomonas_asplenii	97.5	Otu00347	0	0	0	0	0	0	0	0	0	0	0	0	0	0	5	0	0	0	0	0	0	0	0	0	0	0	0	0	14
Leptotrichia_unclassified	*	Otu00353	0	0	0	0	0	6	4	0	0	0	0	0	0	0	0	0	0	0	0	0	0	0	0	0	0	0	0	0	14
Prevotella_unclassified		Otu00360	0	0	0	0	13	0	0	0	0	0	0	0	0	0	0	0	0	0	0	0	0	0	0	0	0	0	0	0	14

Species_97	score	Group	S009_T	S010_P	S010_T	S011_D	S011_T	S012_D	S012_T	S013_D	S013_P	S013_T	S014_D	S014_P	S014_T	S015_D	S015_P	S015_T	S016_D	S016_P	S016_T	S017_D	S017_P	S017_T	S018_D	S018_P	S018_T	S019_D	S019_P	S019_T	Sum
Streptococcus_sanguinis		Otu00209	0	0	0	0	0	0	0	0	9	0	0	0	0	0	0	0	0	5	0	0	0	0	1	0	0	0	0	0	61
Herminiimonas_arsenicoxydans	97.2	Otu00232	0	0	0	0	0	0	0	0	0	0	0	0	0	61	0	0	0	0	0	0	0	0	0	0	0	0	0	0	61
Pseudomonas_putida		Otu00227	0	0	0	0	0	0	0	0	0	0	0	0	0	0	0	0	0	0	0	0	0	0	0	0	0	0	0	0	58
Actinomyces_graevenitzii	99.4	Otu00238	0	0	0	0	0	0	1	0	0	0	0	0	0	0	0	1	0	0	0	16	0	0	8	0	19	0	0	0	57
Ehrlichia_unclassified	*	Otu00248	0	0	0	0	9	0	0	35	0	0	0	0	0	0	0	0	0	0	0	0	0	0	0	0	0	0	0	0	57
Enterococcus_faecium	98.3	Otu00283	0	0	0	0	0	0	2	0	0	0	0	0	0	0	0	0	0	0	0	0	0	0	0	0	0	0	0	0	57
Aminobacter_anthyllidis	98.3	Otu00166	0	0	0	0	0	0	0	0	0	0	0	0	0	0	0	0	0	0	0	0	0	0	0	0	0	0	0	0	56
Streptococcus_parasanguinis	98.4	Otu00221	0	0	0	0	0	0	3	0	0	6	0	0	1	35	0	0	0	1	1	0	0	0	0	0	0	0	0	0	56
Propionibacterium_unclassified		Otu00262	0	0	0	0	55	0	0	0	0	0	0	0	0	0	0	0	0	0	0	0	0	0	0	0	0	0	0	0	55
Anaeroglobus_geminatus	98.9	Otu00299	0	0	0	0	0	0	0	0	0	0	0	0	0	0	0	0	0	0	0	0	0	0	0	0	0	0	0	0	54
Actinomyces_oris	99.1	Otu00197	0	0	0	0	1	43	1	0	0	0	0	0	0	0	0	0	0	1	0	0	0	0	0	0	0	0	0	0	53
Maricurvus_unclassified	*	Otu00202	0	0	0	0	0	0	0	0	0	0	0	0	0	0	0	0	0	0	0	0	0	0	6	2	2	0	0	0	53
Catonella_morbi	*	Otu00211	0	0	0	0	0	0	5	0	0	0	0	0	0	0	0	0	0	0	0	0	0	0	0	0	1	0	0	0	53
Corynebacterium_matruchotii	97.9	Otu00271	0	26	0	0	0	0	0	0	0	0	0	0	0	0	0	0	0	0	0	0	0	0	0	0	0	0	0	0	52
Streptococcus_unclassified		Otu00190	3	0	0	0	1	0	1	0	0	0	0	0	2	0	0	0	0	0	0	0	0	0	0	0	0	0	0	0	51
Exiguobacterium_mexicanum	98	Otu00236	0	0	0	0	0	0	0	0	0	0	0	0	0	0	0	0	0	0	0	0	0	0	0	0	0	0	0	0	50
Pannonibacter_phragmitetus	99	Otu00263	0	0	0	0	50	0	0	0	0	0	0	0	0	0	0	0	0	0	0	0	0	0	0	0	0	0	0	0	50
Actinomyces_israelii	*	Otu00220	0	0	0	0	0	49	0	0	0	0	0	0	0	0	0	0	0	0	0	0	0	0	0	0	0	0	0	0	49
Lactococcus_lactis	99.7	Otu00246	0	0	0	4	0	0	0	0	0	0	0	0	0	0	0	0	0	0	0	0	0	0	0	0	0	0	0	0	48
Finegoldia_magna	98.5	Otu00189	0	0	0	0	0	0	0	0	0	0	0	10	0	0	4	0	0	0	0	0	0	0	0	0	0	0	0	0	47
Bavariicoccus_seileri	98.1	Otu00247	0	1	0	0	0	0	1	0	0	0	0	0	0	0	0	1	0	0	0	0	0	0	0	0	14	0	0	0	47
[Eubacterium]_nodatum_group_unclassified	*	Otu00256	0	0	0	0	47	0	0	0	0	0	0	0	0	0	0	0	0	0	0	0	0	0	0	0	0	0	0	0	47
Leptotrichia_unclassified	*	Otu00250	0	0	0	0	0	0	0	0	0	0	0	0	0	0	0	0	0	0	0	0	0	0	34	0	12	0	0	0	46
Sphingobacterium_faecium		Otu00213	0	0	0	0	0	0	0	0	0	0	0	0	0	0	0	45	0	0	0	0	0	0	0	0	0	0	0	0	45
Bergeyella_unclassified	*	Otu00224	0	0	0	0	0	0	0	0	0	15	0	0	0	0	0	0	0	0	1	0	0	2	3	0	17	0	0	0	44
Pseudomonas_saponiphila	98.5	Otu00234	0	0	0	0	0	0	0	0	0	0	40	0	0	0	0	0	0	0	0	0	0	0	0	0	0	0	0	0	44
Lactobacillus_unclassified		Otu00216	0	0	0	0	0	0	0	0	0	0	0	0	0	0	0	0	0	43	0	0	0	0	0	0	0	0	0	0	43
Microbacterium_hydrocarbonoxydans		Otu00173	0	0	0	0	0	0	0	0	0	0	0	0	0	0	0	0	0	0	0	0	0	0	0	0	0	0	0	0	42
Prevotella_shahii	97.6	Otu00237	0	0	0	0	0	0	0	0	0	0	0	0	0	0	0	0	0	0	0	0	0	0	4	11	10	0	0	0	42
Saccharophagus_unclassified	*	Otu00245	0	0	0	0	0	0	0	0	0	0	0	0	0	0	0	0	0	0	0	0	0	0	0	0	0	0	0	0	42
Treponema_socranskii	97.8	Otu00255	0	0	0	0	0	0	0	0	0	0	0	0	0	0	0	0	0	0	0	0	0	0	0	0	0	0	0	0	42
Shinella_unclassified	*	Otu00269	0	0	0	0	0	0	0	0	0	0	0	0	0	40	0	2	0	0	0	0	0	0	0	0	0	0	0	0	42
Aggregatibacter_segnis	98.1	Otu00276	0	0	0	0	0	0	0	0	0	0	0	0	0	0	0	0	0	0	0	0	0	0	0	0	0	0	0	0	41
Sphingomonas_paucimobilis	98.7	Otu00226	0	0	0	0	0	0	0	0	0	0	0	0	0	0	0	0	2	36	1	0	0	0	0	0	0	0	0	0	39
Actinomyces_odontolyticus	97.5	Otu00231	0	0	0	0	0	2	1	0	0	0	0	0	0	1	0	0	1	0	1	0	0	0	16	0	0	14	0	0	39
Capnocytophaga_leadbetteri	98.1	Otu00240	0	0	0	0	0	0	0	0	0	0	0	0	0	0	0	0	0	0	0	0	0	0	0	0	15	0	0	0	39
Pseudomonas_oryzihabitans	97.5	Otu00249	0	0	0	0	0	0	0	0	0	0	0	0	0	0	0	0	0	0	0	0	0	0	0	0	0	0	0	0	39
Vibrio_brasiliensis	99.1	Otu00225	0	0	0	0	0	0	0	0	0	0	0	0	0	0	0	0	0	0	0	0	0	0	0	0	0	0	0	0	38
Sphingobacterium_caeni	100	Otu00260	0	0	0	0	0	0	0	0	0	0	0	0	0	23	0	15	0	0	0	0	0	0	0	0	0	0	0	0	38
Bifidobacterium_animalis	98	Otu00257	0	0	0	0	0	4	22	0	0	0	0	0	0	0	0	7	0	0	0	0	0	0	0	0	0	0	0	0	37
Bacillus_wakoensis	98.3	Otu00235	0	0	0	0	32	0	0	0	0	0	0	0	0	0	0	0	0	0	0	0	0	0	0	0	0	0	0	0	36
Prevotella_pallens	97.9	Otu00281	0	0	0	0	0	1	0	0	0	0	0	0	0	0	0	0	0	0	0	0	0	0	2	2	25	0	0	0	36
Stenotrophomonas_maltophilia	97.9	Otu00254	0	0	3	0	0	0	0	0	0	0	1	0	0	1	13	17	0	0	0	0	0	0	0	0	0	0	0	0	35
Alloprevotella_rava		Otu00261	0	0	0	0	0	5	10	0	0	0	0	0	0	0	0	0	0	0	0	0	0	0	0	0	0	0	0	0	35
Rhodococcus_globerulus	97.2	Otu00138	0	0	0	0	0	0	0	0	0	0	0	0	0	0	0	0	0	0	0	0	0	2	0	0	0	0	0	0	34
Dyadobacter_unclassified	*	Otu00194	0	0	0	0	0	0	0	0	0	0	0	0	0	0	0	0	0	0	0	0	0	0	0	0	0	0	0	0	34
Ideonella_sp.	97.5	Otu00264	0	0	0	0	0	0	0	0	0	0	0	0	0	0	0	0	0	0	0	1	0	0	0	0	0	0	0	0	33
[Eubacterium]_nodatum_group_unclassified	*	Otu00282	0	0	0	0	0	0	0	0	0	0	0	0	0	0	0	0	0	0	0	0	0	0	0	0	0	0	0	0	33
Dermacoccus_nishinomiyaensis	98.8	Otu00301	0	29	0	0	0	0	0	0	0	0	0	0	0	0	0	0	0	0	0	0	0	0	0	0	0	0	0	0	30
Sphingobium_limneticum	98.7	Otu00308	0	0	0	0	0	0	0	0	0	0	0	0	0	30	0	0	0	0	0	0	0	0	0	0	0	0	0	0	30
Sphingobacterium_anhuiense	97.4	Otu00259	0	0	0	0	0	0	0	0	0	0	0	0	0	0	0	29	0	0	0	0	0	0	0	0	0	0	0	0	29
Pelomonas_saccharophila	100	Otu00300	0	0	0	0	22	0	0	0	0	0	2	0	0	0	0	0	0	0	0	0	0	0	0	3	0	0	0	0	29
Sphingomonas_desiccabilis	98.3	Otu00280	0	0	0	0	0	0	0	0	0	0	0	0	0	0	0	0	0	0	0	0	0	0	0	0	0	0	0	0	28
Brevundimonas_unclassified	*	Otu00284	0	0	0	0	0	0	0	0	0	0	0	0	0	0	0	0	0	0	0	0	0	0	0	0	0	0	0	0	28
Leucobacter_aridicollis	98.2	Otu00223	0	0	0	0	0	0	0	0	0	0	0	0	0	0	0	0	0	0	0	0	0	0	0	0	0	0	0	0	27
Prevotella_unclassified	*	Otu00251	0	0	0	0	0	27	0	0	0	0	0	0	0	0	0	0	0	0	0	0	0	0	0	0	0	0	0	0	27

Species_97	score	Group	S009_T	S010_P	S010_T	S011_D	S011_T	S012_D	S012_T	S013_D	S013_P	S013_T	S014_D	S014_P	S014_T	S015_D	S015_P	S015_T	S016_D	S016_P	S016_T	S017_D	S017_P	S017_T	S018_D	S018_P	S018_T	S019_D	S019_P	S019_T	Sum
Stenotrophomonas_maltophilia.	98.5	Otu00373	0	0	0	0	0	0	0	0	0	0	0	0	0	0	1	12	0	0	0	0	0	0	0	0	0	0	0	0	14
Acinetobacter_lwoffii	97.2	Otu00415	0	0	0	0	0	0	0	0	0	0	1	0	0	0	0	0	0	0	0	0	0	0	0	0	0	0	0	11	14
Bradyrhizobium_elkanii	98.3	Otu00291	0	0	0	0	0	0	0	0	0	0	0	0	0	0	0	0	0	0	0	0	0	0	0	0	0	0	0	0	13
Shewanella_putrefaciens	99.1	Otu00315	0	0	0	0	0	0	0	0	0	0	1	0	0	0	0	0	0	0	0	0	0	0	0	0	0	0	0	0	13
Granulicatella_unclassified	*	Otu00323	0	0	0	0	0	0	0	0	0	0	0	0	0	1	0	0	1	0	5	0	0	0	0	0	1	0	0	0	13
Paracoccus_marinus	99.3	Otu00338	0	0	0	0	0	0	0	0	0	0	0	0	0	0	0	0	0	0	0	0	0	0	0	0	0	0	0	0	13
Prevotella_unclassified	*	Otu00359	0	0	0	0	0	0	0	0	0	0	0	0	0	0	0	0	0	0	0	0	0	0	0	0	2	0	0	0	13
Pseudomonas_putida		Otu00363	0	0	0	0	0	0	0	0	0	0	3	0	0	0	0	0	0	0	0	0	0	0	0	0	0	0	0	0	13
Pseudochrobactrum_kiredjianiae	100	Otu00377	0	0	0	0	0	0	0	0	0	0	13	0	0	0	0	0	0	0	0	0	0	0	0	0	0	0	0	0	13
Sphingomonas_yanoikuyae.	98	Otu00222	0	0	0	0	0	0	0	0	0	0	0	0	0	0	0	0	0	0	0	0	0	0	0	0	0	0	0	0	12
Aureibacter_unclassified	*	Otu00258	0	0	0	0	0	0	0	0	0	0	0	0	0	0	0	0	0	0	0	0	0	0	0	0	0	0	0	0	12
Streptococcus_vestibularis		Otu00306	0	0	0	4	0	2	0	0	0	0	0	0	0	0	0	0	0	0	0	0	0	0	0	0	0	1	0	3	12
Devosia_limi	97	Otu00314	0	0	0	0	0	0	0	0	0	0	0	0	0	0	0	0	0	0	0	0	0	0	0	0	0	0	0	0	12
Intestinibacter_unclassified		Otu00324	0	0	0	0	0	0	0	0	0	0	0	7	0	0	0	0	0	0	0	0	0	0	0	0	0	0	0	0	12
Aridibacter_unclassified	*	Otu00285	0	0	0	0	0	0	0	0	11	0	0	0	0	0	0	0	0	0	0	0	0	0	0	0	0	0	0	0	11
Uruburuella_suis	98.1	Otu00329	0	0	0	0	0	0	0	0	0	0	11	0	0	0	0	0	0	0	0	0	0	0	0	0	0	0	0	0	11
Brevundimonas_unclassified	*	Otu00337	0	0	0	0	0	0	0	0	0	0	0	0	0	0	0	0	0	0	0	0	0	11	0	0	0	0	0	0	11
Prevotella_micans	97.6	Otu00344	0	0	0	11	0	0	0	0	0	0	0	0	0	0	0	0	0	0	0	0	0	0	0	0	0	0	0	0	11
Centipeda_periodontii	*	Otu00354	0	0	0	0	0	0	0	0	0	0	0	0	0	0	0	0	0	0	0	0	0	0	0	0	0	0	0	0	11
Dermacoccus_nishinomiyaensis	98.8	Otu00413	0	11	0	0	0	0	0	0	0	0	0	0	0	0	0	0	0	0	0	0	0	0	0	0	0	0	0	0	11
Smithella_unclassified	*	Otu00265	0	0	0	0	0	0	0	0	0	0	0	0	0	0	0	0	0	0	0	0	0	0	0	0	0	0	0	0	10
Phenylobacterium_kunshanense	*	Otu00288	0	0	0	0	0	0	0	0	0	0	0	0	0	0	0	0	0	0	0	0	0	0	0	0	0	0	0	0	10
Prevotella_oulorum	99.4	Otu00348	0	0	0	0	0	10	0	0	0	0	0	0	0	0	0	0	0	0	0	0	0	0	0	0	0	0	0	0	10
Capnocytophaga_sputigena	97.2	Otu00364	0	0	0	0	0	0	0	0	0	0	0	0	0	0	0	0	0	0	0	0	0	0	0	0	3	0	0	0	10
Actinomyces_graevenitzii	97.5	Otu00366	0	0	0	0	0	1	6	0	0	0	0	0	0	0	0	0	0	0	0	0	0	0	0	0	3	0	0	0	10
Burkholderia_contaminans	99.1	Otu00371	0	0	0	4	1	0	0	0	0	0	0	0	0	1	0	0	1	0	0	0	0	0	0	0	0	0	0	0	10
Corynebacterium_aquatimens	98.4	Otu00395	0	0	0	0	0	0	0	0	0	0	0	0	0	0	0	0	0	0	0	0	0	0	0	0	0	0	0	0	10
Novosphingobium_resinovorum	98.7	Otu00399	0	0	0	0	0	0	0	0	0	0	0	0	0	0	0	0	0	0	0	0	0	10	0	0	0	0	0	0	10
Streptococcus_infantis		Otu00418	0	0	0	0	0	0	0	0	0	0	0	0	0	0	0	0	0	0	0	0	0	0	8	0	2	0	0	0	10
Streptococcus_unclassified		Otu00426	0	0	0	0	0	0	0	0	0	0	0	6	0	0	0	0	0	0	0	0	0	0	0	0	0	0	0	0	10
Marinomonas_arenicola	98.5	Otu00430	0	0	0	0	0	0	0	0	0	0	0	0	0	0	0	0	0	0	0	0	0	0	0	0	0	0	0	0	10

Appendix IV

Peer-reviewed published manuscript incorporating work from Chapters 2 and 4

Cavalcanti *et al*., (2015)

Biofouling, 2015
Vol. 31, No. 1, 27–38, http://dx.doi.org/10.1080/08927014.2014.996143

Virulence and pathogenicity of *Candida albicans* is enhanced in biofilms containing oral bacteria

Yuri Wanderley Cavalcanti[a,b]*, Daniel James Morse[b], Wander José da Silva[a], Altair Antoninha Del-Bel-Cury[a], Xiaoqing Wei[b], Melanie Wilson[b], Paul Milward[b], Michael Lewis[b], David Bradshaw[b,1] and David Wynne Williams[b]

[a]*Piracicaba Dental School, State University of Campinas, Piracicaba, SP, Brazil;* [b]*Tissue Engineering & Reparative Dentistry, School of Dentistry, Cardiff University, Cardiff, UK*

(*Received 22 October 2014; accepted 2 December 2014*)

This study examined the influence of bacteria on the virulence and pathogenicity of candidal biofilms. Mature biofilms (*Candida albicans*-only, bacteria-only, *C. albicans* with bacteria) were generated on acrylic and either analysed directly, or used to infect a reconstituted human oral epithelium (RHOE). Analyses included *Candida* hyphae enumeration and assessment of *Candida* virulence gene expression. Lactate dehydrogenase (LDH) activity and *Candida* tissue invasion following biofilm infection of the RHOE were also measured. *Candida* hyphae were more prevalent ($p < 0.05$) in acrylic biofilms also containing bacteria, with genes encoding secreted aspartyl-proteinases (SAP4/SAP6) and hyphal-wall protein (HWP1) up-regulated ($p < 0.05$). *Candida* adhesin genes (ALS3/EPA1), SAP6 and HWP1 were up-regulated in mixed-species biofilm infections of RHOE. Multi-species infections exhibited higher hyphal proportions ($p < 0.05$), up-regulation of IL-18, higher LDH activity and tissue invasion. As the presence of bacteria in acrylic biofilms promoted *Candida* virulence, consideration should be given to the bacterial component when managing denture biofilm associated candidoses.

Keywords: biofilm; *Candida albicans*; candidosis; co-infection; RHOE; virulence

Introduction

The fungal genus *Candida* contains over 150 species, several of which are frequent commensal colonisers of humans. Most often, commensal carriage of *Candida* occurs at moist mucosal surfaces, such as those of the oral cavity and vagina (Peleg et al. 2010; Gow et al. 2011). *Candida albicans* is the species most frequently encountered, growing as yeast, pseudohyphal or hyphal forms. In cases where there is host debilitation, or where there is a change in the local environment promoting *Candida* overgrowth, infection (referred to as candidosis) may follow (Peleg et al. 2010; Gow et al. 2011). Candidoses are the most prevalent human fungal infections, and whilst systemic infection can occur, most manifest superficially on the oral and vaginal mucosa (Peleg et al. 2010; Gow et al. 2011).

There are several putative *C. albicans* virulence factors, including secreted aspartyl proteinases (SAPs), phospholipases, expression of surface adhesins and the ability to grow as hyphae (Gow et al. 2011). Hyphal growth protects *C. albicans* from phagocytosis and promotes invasion of host epithelial surfaces. *Candida* species are also adept at growing as biofilms on oral surfaces including those of the oral mucosa and prosthetic biomaterials, and these biofilms are resistant to removal by the action of salivary flow and host defence molecules.

Candida-associated denture stomatitis is the most prevalent form of oral candidosis, occurring in > 65% of denture wearers (Williams et al. 2011). The infection occurs after the formation of biofilms on poorly cleansed, denture acrylic surfaces (Pereira-Cenci et al. 2010; Williams et al. 2011; Williams & Lewis 2011; Teles et al. 2012). Denture stomatitis presents as areas of erythema on the palatal mucosa overlying the denture. *Candida* biofilms serve as reservoirs of infectious agents, largely protected from host removal mechanisms (Williams et al. 2011; Williams & Lewis 2011). This protected environment for denture biofilms arises from poor salivary flow over the upper denture surface and the nature of the non-shedding acrylic material leading to colonising organisms not being removed by the sloughing action, which would occur with epithelial surfaces.

Although most attention in denture stomatitis has been given to the *Candida* component of the biofilm, and particularly to *C. albicans*, bacteria also co-exist with *Candida* within denture biofilms (Morales & Hogan 2010; Peleg et al. 2010; Pereira-Cenci et al. 2010; Teles et al. 2012; Xu et al. 2014). However, the role of bacteria in denture stomatitis remains uncertain and has received little attention. The fact that bacteria will undoubtedly alter the local environment, as well as modulate host immune responses towards *Candida* (Morales

*Corresponding author. Email: CavalcantiY@cardiff.ac.uk
[1]Denture Care & Family Health New Product Research, GlaxoSmithKline, Weybridge, UK

& Hogan 2010; Peleg et al. 2010), suggests their presence could both directly and indirectly effect progression of denture stomatitis. Evidence exists for bacterial influence in other forms of oral candidosis, most notably in acute erythematous candidosis, where receipt of broad-spectrum antibiotic therapy is a known risk factor (Morales & Hogan 2010; Peleg et al. 2010; Williams & Lewis 2011).

Bacteria could be directly involved in the infection, or could modulate the pathogenicity of *Candida*. Indeed, *Streptococcus gordonii* has recently been found to trigger the virulence attributes of *Candida* (Bamford et al. 2009; Shirtliff et al. 2009; Diaz, Xie, et al. 2012; Ricker et al. 2014), and other streptococci could act similarly (Xu et al. 2014). It is also known that receipt of broad-spectrum antibiotics predisposes to oral candidosis, and whilst this may be due to reduced microbial competition allowing the proliferation of *Candida* (Juárez Tomás et al. 2011; Purschke et al. 2012), it may also relate to changes in immune responses by the host as a result of a reduced bacterial load.

Candida–host interactions have been investigated using different model systems (Green et al. 2004; Negri et al. 2011; Xu et al. 2014). A commercially available reconstituted human oral epithelium (RHOE; SkinEthic Laboratories, Nice, France) represents a reproducible and standardised tissue suitable for modelling the interaction between *Candida* and epithelial cells (Silva et al. 2011; Yadev et al. 2011). However, the RHOE has not previously been used to model mature biofilm interactions.

The aim of this study was to examine the effect of a bacterial component on the virulence and pathogenicity of *Candida* biofilms. In addition, the study assessed epithelial cell responses to the different biofilm compositions. The intention was to gain insight into the importance of bacteria within *Candida* biofilm-mediated infections, such as denture stomatitis.

Materials and methods

Microorganisms and culture preparation

C. albicans ATCC 90028, *Streptococcus mutans* ATCC 25175, *Streptococcus sanguinis* ATCC 10556, *Actinomyces viscosus* ATCC 15987 and *Actinomyces odontolyticus* NCTC 9935 were used to develop biofilms on acrylic coupons. *C. albicans* was maintained on Sabouraud's Dextrose Agar (SDA; Oxoid, Basingstoke, UK) and bacterial species were cultured on Blood Agar (BA) (blood agar base; Oxoid) supplemented with 5% (v/v) defibrinated horse blood (TCS Biosciences, Buckingham, UK). Isolates were subcultured in Brain Heart Infusion liquid medium (BHI; Oxoid) for 24 h at 37°C. *C. albicans*, *S. mutans* and *S. sanguinis* were cultured aerobically, whilst *A. viscosus* and *A. odontolyticus* were cultured anaerobically. Microbial cells were harvested by centrifugation (3,000 × *g* for 5 min) and the resulting cell pellets washed (× 2) in phosphate buffered saline (PBS; pH 7.0). Cell pellets were resuspended in Dulbecco's Modified Eagle Medium (DMEM; Life Technologies, Paisley, UK) supplemented with 10% (v/v) Foetal Bovine Serum (FBS; Life Technologies) and 50 mM glucose. The cell density was adjusted to an optical density of 1.0 at 600 nm using a spectrophotometer (DiluPhotometer™; Implen, Westlake Village, CA, USA). To produce inocula for biofilms on acrylic coupons, a 200-fold dilution of each standardised suspension was prepared in sterile culture medium (DMEM supplemented with 10% (v/v) FBS). The concentration of microorganisms in each inoculum corresponded to ~1×10^5 colony forming units (CFU) ml^{-1} of *C. albicans* and ~1×10^7 CFU ml^{-1} of the bacteria.

Preparation of acrylic coupons for biofilm development

Heat-polymerised acrylic resin (QC-20; Dentsply Int, Inc., Weybridge, UK) was prepared according to the manufacturer's instructions and fabricated into disc-shaped (10 mm diameter, 2 mm thickness) coupons. Acrylic coupons were finished using a horizontal polisher (model APL-4; Arotec, São Paulo, Brazil) with progressively finer aluminium oxide papers (320-, 400-, and 600-grit). The surface roughness was standardised to 0.30 ± 0.02 μm. Prior to use, acrylic coupons were ultrasonically cleaned with 70% (v/v) alcohol and sterile ultra-purified water (20 min) to remove surface debris. The coupons were immersed in sodium hypochlorite solution (2 g l^{-1}) for 5 min and then thoroughly rinsed with sterile water. Coupons were maintained in sterile distilled water until use. Acrylic coupons were then immersed in artificial saliva (2.5 g l^{-1} mucin, 0.25 g l^{-1} sodium chloride, 0.2 g l^{-1} potassium chloride, 0.2 g l^{-1} calcium chloride, 2.0 g l^{-1} yeast extract, 5.0 g l^{-1} protease peptone and 1.25 ml l^{-1} of 40% urea) overnight at 37°C under gentle agitation (75 rpm).

Development of in vitro biofilms on acrylic coupons

The biofilms generated consisted of *C. albicans* (single species biofilms), *C. albicans* with the four different bacterial species (mixed-species biofilms), and bacteria-only biofilms. To produce these biofilms, acrylic coupons were placed in the wells of a 24-well plate and overlaid with 2 ml of microbial inoculum. After an initial adherence period of 2 h, the culture medium was removed and 2 ml of fresh culture medium (DMEM supplemented with 10% (v/v) FBS and 50 mM glucose) added to each well. The coupons were then incubated aerobically for 72 h at 37°C in an orbital shaking incubator (75 rpm). The culture medium was changed every 24 h to maintain biofilm growth. After 72 h, acrylic biofilms were collected for

analysis, or used to overlay specimens of RHOE (SkinEthic Laboratories, Nice, France). Analysis of biofilms on acrylic coupons (n = 12) was performed in three independent experiments, using four samples per group on each occasion.

Biofilm infection of reconstituted human oral epithelium (RHOE)

Commercially available RHOE was used in combination with the biofilms on acrylic coupons to produce an *in vitro* model of denture stomatitis. The RHOE provided the contact epithelium for previously developed single (*C. albicans*), mixed-species (*C. albicans* and bacteria) and bacteria-only biofilms on acrylic coupons. Acrylic coupons without biofilm served as non-infected controls.

Acrylic coupons, with or without biofilm, were overlaid on the surface of RHOE (n = 6) and incubated for 12 h at 37°C, in a 5% (v/v) CO_2 atmosphere, under saturated humidity. After incubation, the acrylic was removed and the tissues bisected. Total RNA was extracted from one half of the tissue, with the remainder processed for histological analysis. Culture medium (Maintenance Medium without antibiotics, SkinEthic Laboratories) was also retained and used to measure lactate dehydrogenase (LDH) activity originating from the RHOE. Analysis of RHOE (n = 6) was performed on two independent occasions, using three samples per group.

Analysis of acrylic biofilms

Prior to undertaking experiments with RHOE, initial studies directly examined biofilms developed on the acrylic coupons. Biofilms generated over 72 h were recovered from acrylic surfaces (n = 12) by vigorous vortex mixing for 60 s. Biofilm cells were pelleted by centrifugation and then resuspended in 1 ml of PBS. Serial decimal dilutions of the suspensions were cultured on SDA and BA using a drop-counting technique. SDA and BA plates were incubated aerobically at 37°C for 24 h and 48 h, respectively, and the resulting CFU ml^{-1} determined.

An 800-µl volume of the biofilm suspension was also centrifuged and the cell pellet resuspended in RNALater (Life Technologies) and stored at –20°C prior to RNA extraction and qPCR analysis.

In situ biofilms on acrylic coupons (n = 6 for each group, analysed on two independent occasions) were also examined by confocal laser-scanning microscopy (CLSM), using a Leica TCS SP2 AOBS spectral confocal microscope (Leica Microsystems GmbH, Wetzlar, Germany). CLSM was used to assess the quantity and viability of biofilms, as well as the proportion of *C. albicans* hyphae. Biofilms were stained with 10 µl of SYTO-9 (25 µM; Molecular Probes, Paisley, UK) to assess cell viability, and 10 µl of concanavalin-A conjugated with Alexa Fluor® 594 (25 µM; Molecular Probes) to detect *Candida*.

Representative images (125 µm × 125 µm) of both dye-channels, SYTO-9 (green) and concanavalin-A (red), were obtained from a minimum of five different fields of view for each of three replicate specimens in two independent experiments. Images were analysed using ImageJ 1.46r (Wayne Rasband, National Institute of Health, Bethesda, MD, USA). The red channel, representative of *C. albicans*, was used to quantify yeast and hyphae. The green channel was used to ascertain cell viability within the biofilms. Images were first adjusted using the function of threshold intensity and *C. albicans* yeast and hyphal forms separately quantified using the 'Analyze Particles' tool of the software.

RNA extraction and synthesis of cDNA for qPCR

RNA was extracted from both biofilms on acrylic coupons (n = 12) and the RHOE (n = 6) that had been overlaid with biofilms and controls. Extraction of total RNA involved initial resuspended cells from biofilms and/or RHOE in lysis buffer (RLT Buffer, QIAGEN, Crawley, UK) containing 1% (v/v) β-mercaptoethanol. Cells were disrupted by high-speed homogenisation with glass beads in a Mini-Bead-Beater-8 (Stratech Scientific, Soham, UK). Total nucleic acid was obtained after separation with phenol:chloroform:isoamyl alcohol (25:24:1) (Sigma-Aldrich, Poole, UK) and total RNA was recovered after DNAse I (QIAGEN) treatment using the RNeasy Mini Kit (QIAGEN) according to the manufacturer's instructions. The integrity and purity of the total RNA was assessed by gel electrophoresis, and the total RNA concentration was spectrophotometrically determined by measuring absorbance ratio at $260/280_{nm}$ (NanoVue, GE Healthcare, Little Chalfont, UK) and standardised to 200 ng ml^{-1}. Reverse transcription reactions for cDNA synthesis included 5 µl of total RNA (200 ng $µl^{-1}$) template, 1 µl of 10 mM dNTPs, 1 µl of 50 µg ml^{-1} random primers, 1 µl of 25 U $µl^{-1}$ RNasin RNase inhibitor, 5 µl of M-MLV reaction buffer (× 5) and 1 µl of 200 U $µl^{-1}$ M-MLV (Promega, Southampton, UK). Molecular grade water was added to give a final reaction volume of 25 µl. The reaction mix was incubated at 70°C for 5 min, followed by incubation at 37°C for 60 min. The resulting cDNA was stored at –20°C prior to use for qPCR.

qPCR analysis of acrylic biofilms and infected RHOE

Primers used in qPCR analysis are presented in Table 1 and designed from full-length gene sequences obtained from the nucleotide platform in PubMed using Primer3 software (Koressaar & Remm 2007; Untergasser et al.

Table 1. Forward (FW) and reverse (RV) primers used for qPCR.

Target gene	Sequence (5′ → 3′)
ACT1 – *C. albicans* actin housekeeping gene (*C. albicans*)	FW – TGCTGAACGTATGCAAAAGG
	RV – TGAACAATGGATGGACCAGA
ALS1 – Human β-actin agglutinin-like sequence (*C. albicans*)	FW – CCCAACTTGGAATGCTGTTT
	RV – TTTCAAAGCGTCGTTCACAG
ALS3 – Agglutinin-like sequence (*C. albicans*)	FW – CTGGACCACCAGGAAACACT
	RV – GGTGGAGCGGTGACAGTAGT
EPA1 – Epithelial adhesin (*C. albicans*)	FW – ATGTGGCTCTGGGTTTTACG
	RV – TGGTCCGTATGGGCTAGGTA
SAP4 – Secreted aspartyl proteinase (*C. albicans*)	FW – GTCAATGTCAACGCTGGTGTCC
	RV – ATTCCGAAGCAGGAACGGTGTCC
SAP6 – Secreted aspartyl proteinase (*C. albicans*)	FW – AAAATGGCGTGGTGACAGAGGT
	RV – CGTTGGCTTGGAAACCAATACC
HWP1 – Hyphal wall protein (*C. albicans*)	FW – TCTACTGCTCCAGCCACTGA
	RV – CCAGCAGGAATTGTTTCCAT
PLD1 – Phospholipase D (*C. albicans*)	FW – GCCAAGAGAGCAAGGGTTAGCA
	RV – CGGATTCGTCATCCATTTCTCC
β-actin – Housekeeping gene (human cells)	FW – GAGCACAGAGCCTCGCCTTTGCCGAT
	RV – ATCCTTCTGACCCATGCCCACCATCACG
IL-18 – Interleukin 18 (human cells)	FW – CCTTCCAGATCGCTTCCTCTCGCAACAA
	RV – CAAGCTTGCCAAAGTAATCTGATTCCAGGT
Dectin1 – Cellular membrane receptor (human cells)	FW – ACAGCAATGAGGCGCCAAGGAGGAGATG
	RV – GGAGCAGAAAGAAAAGAGCTCCCAAATGCT

2012). The specificity of each primer was confirmed using primer-BLAST (Ye et al. 2012), which compared the respective sequences with databases of *C. albicans* and human genomes. In addition, primer specificity for qPCR was confirmed in preliminary studies involving extracted genomic DNA. The targeted putative virulence genes of *C. albicans* were ALS1 and ALS3 (agglutinin-like sequence), EPA1 (epithelial adhesin), SAP4 and SAP6 (secreted aspartyl proteinases), HWP1 (hyphae wall protein) and PLD1 (phospholipase D). In the case of RHOE, expression of genes encoding IL-18 (an interleukin) and Dectin-1 (a *Candida* receptor) was determined. ACT1 and β-actin served as reference genes for *C. albicans* and human cells, respectively.

Triplicate qPCRs were performed in 96-well plates in an ABI Prism 7000 instrument (Life Technologies). Each 20-µl reaction comprised 2 µl of cDNA, 10 µl (×2) of SYBR-Green PCR Master Mix (Precision Master Mix; Primer Design, Southampton, UK), 1 µl of each primer (10 mM), and 6 µl of molecular biology grade water. The thermal cycle profile comprised of initial denaturation at 95°C for 2 min, followed by 40 cycles of denaturation at 95°C for 15 s, primer annealing at 58°C for 30 s and primer extension at 72°C for 30 s. A final extension at 72°C for 2 min was performed, followed by cooling at 4°C. A dissociation stage at 60°C was used to generate a melting curve for verification of the amplified product.

After qPCR, the threshold was adjusted according to the amplification curves of all evaluated genes. Comparison between groups was made based on the cycle number at which both the target and reference genes reached threshold cycle (Ct) fluorescence. Analysis of relative gene expression was achieved according to the $^{\Delta\Delta}$Ct method (Bustin et al. 2009).

Lactate dehydrogenase (LDH) activity in the culture medium of infected RHOE

LDH activity was measured in RHOE culture medium (n = 6, for each group) using an LDH Cytotoxicity Assay kit as recommended by the manufacturer (Thermo Fisher Scientific, Cramlington, UK). Experiments were performed in triplicate, with control samples for normalisation purposes. The LDH activity of RHOE infected with biofilms was compared to uninfected controls.

Histological assessment of damage and candidal invasion of infected RHOE

RHOE damage and invasion of the epithelium by *C. albicans* was determined by light microscopy and CLSM. RHOE for histological analysis was initially fixed in 10% (v/v) neutral buffered formalin (Leica Biosystems, Newcastle-upon-Tyne, UK) for 48 h. Tissues were dehydrated through an increasing alcohol concentration series and then infiltrated with paraffin wax. Sections (20 µm) were placed on microscope slides and de-waxed in xylene, with subsequent rehydration using water. Selected sections for light microscopy were stained using the Periodic Acid-Schiff (PAS) technique.

For fluorescence *in situ* hybridisation (FISH) and CLSM analysis, sections were treated with 10 mg ml^{-1} lysozyme (30 min, 37°C) and incubated in 1 × citrate buffer (pH 6.0, 30 min, 55°C; Sigma-Aldrich). Sections were then exposed to fluorescent probes specific either for *C. albicans*, bacteria or epithelial cells at 55°C for 60 min. *Candida* was detected using the Yeast Traffic Light® PNA FISH® kit (AdvanDx, Vedbaek, Denmark) in combination with concanavalin-A conjugated with Alexa Fluor® 594 (1 µg $µl^{-1}$; Life Technologies) (Malic et al. 2007). Bacteria were detected using the universal bacterial Cy3 labelled peptide nucleic acid (PNA) probe (Bac-Uni1CY3; 300 nM; probe sequence: CTGCCTCCCGTAGGA) specific for bacterial 16S rRNA (Malic et al. 2009). Epithelial cells were treated with 20 µg ml^{-1} of pan-cytokeratin antibody (C11) (sc8018, Santa Cruz Biotechnology, Heidelberg, Germany) followed by an Alexa Fluor® 488-labelled goat anti-Mouse IgG (H+L) antibody (5 µg $µl^{-1}$; Life Technologies) plus a nucleic acid dye (Hoechst 33342; 1 µg $µl^{-1}$) (trihydrochloride-trihydrate; Life Technologies) (Malic et al. 2007). Tissue sections were mounted using Vectashield (H-1000, Vector Laboratories, Peterborough, UK) fade-retarding mount. The CLSM parameters were as described earlier.

Statistical analysis

Statistical analysis was undertaken using Sigma Plot v. 11.3 (Systat Software Inc., London, UK) at 5% significance. The assumptions of equality of variances and normal distribution of errors were evaluated for each variable. When data were not normally distributed, they were logarithmically transformed. Comparison between parameters (viable cells number, hyphae enumeration and gene expression) for single and mixed-species biofilms, as well as candidal gene expression was by independent *t*-test ($\alpha < .05$). LDH activity and epithelial cell gene expression were analysed by one-way ANOVA. *Post hoc* comparisons of one-way ANOVA tests were performed using Tukey's Honestly Significant Difference (HSD) test.

Results

Analysis of biofilms on acrylic coupons and infected RHOE

Both *C. albicans*-only and mixed-species biofilms extensively colonised acrylic surfaces after 72 h growth (Figure 1). The number of viable *C. albicans* in single-species biofilms (3.7×10^7 CFU ml^{-1}) was not statistically different ($p > 0.05$) from those in mixed-species biofilms, where *C. albicans* appeared as the predominant organism (1.6×10^8 CFU ml^{-1}).

CLSM (Figures 2 and 3) confirmed the findings of culture and interestingly revealed higher proportions of hyphae in mixed-species acrylic biofilms compared with *C. albicans*-only biofilms. Significantly ($p < 0.01$) higher hyphal proportions (Figure 3) were seen in both mixed species biofilms colonising the acrylic (5.6%) and infecting RHOE (13.4%). Hyphal elements in the mixed-species biofilms also appeared more developed than those in *C. albicans*-only biofilms (Figure 2).

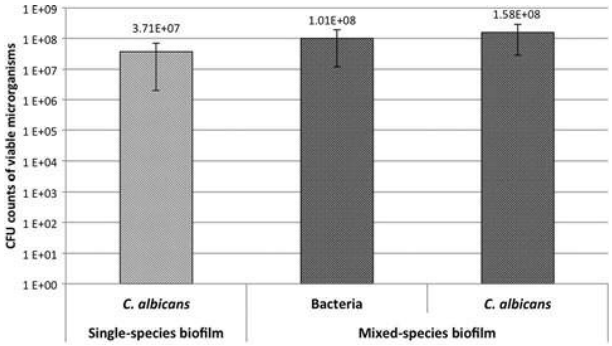

Figure 1. CFU ml^{-1} in single-species (*C. albicans* only, $n = 12$) and mixed-species (*S. mutans*, *S. sanguinis*, *A. viscosus*, *A. odontolyticus* and *C. albicans*, $n = 12$) biofilms. Bars show averages and SDs within each group.

Gene expression of *C. albicans* adhesins differed between biofilms developed on acrylic and infected RHOE (Figure 4A), with higher expression of both ALS1 and ALS3 evident in *C. albicans*-only biofilms on acrylic ($p < 0.05$). Interestingly, significantly ($p < 0.01$) higher expression of *C. albicans* ALS3 and EPA1 genes occurred in RHOE infected by mixed-species biofilms compared with RHOE infected by *C. albicans*-only biofilms.

Similarly, expression of *C. albicans* SAP4 and SAP6 genes (Figure 4B) was significantly ($p < 0.05$) higher in mixed-species biofilms on acrylic compared with *C. albicans*-only biofilms. For infected RHOE, expression of SAP4 was similar for *C. albicans*-only biofilms and mixed-species biofilms, whilst SAP6 expression was significantly ($p < 0.05$) up-regulated in the latter.

Expression of *C. albicans* PLD1 (Figure 4C) was equivalent for all biofilm types. However, expression of the *C. albicans* hyphal wall protein gene (HWP1) (Figure 4C) was significantly ($p < 0.01$) higher in mixed-species biofilms on acrylic and RHOE mixed infections, compared with *C. albicans*-only biofilms and associated infections.

With regards to the responses of RHOE to biofilm infection (Figure 4D), expression of human interleukin-18 (IL-18) and Dectin-1 (a cell receptor for *C. albicans* primarily associated with immune cells) were analysed. Expression of IL-18 was up-regulated for RHOE infected by mixed-species biofilms, relative to other biofilms types ($p < 0.05$). Dectin-1 expression was equivalent for RHOE infected by mixed species and *C. albicans*-only biofilms ($p < 0.05$).

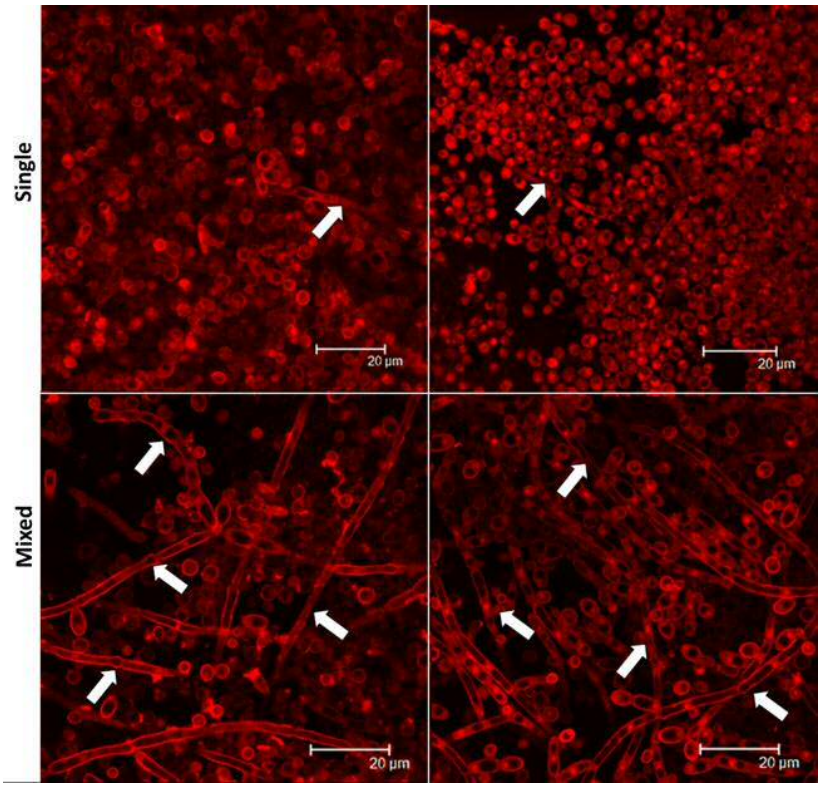

Figure 2. Representative CLSM images of single-species (*C. albicans*-only) biofilms (upper) and mixed-species (*S. mutans*, *S. sanguinis*, *A. viscosus*, *A. odontolyticus* and *C. albicans*) biofilms (lower) on an acrylic surface. *C. albicans* was stained with concanavalin-A conjugated with Alexa Fluor® 594. The white arrows highlight the presence of hyphae in both biofilm types. Note that hyphae in mixed-species biofilms appear more developed than those in single-species biofilms.

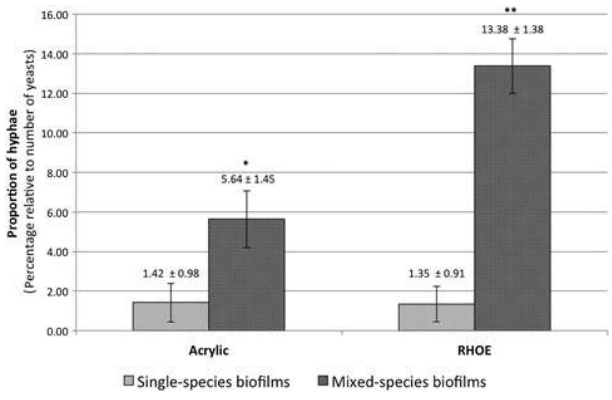

Figure 3. Proportion (%) of hyphae relative to the total number of *C. albicans* yeast in single and mixed-species biofilms (n = 6, per group) on acrylic and in infected RHOE. Bars show averages and SDs within each group. *Shows a statistically higher proportion of hyphae relative to single-species biofilms. **Shows a statistically higher proportion of hyphae relative to single-species biofilms and to mixed-species biofilm developed on acrylic.

Analysis of RHOE damage based on LDH activity (Figure 5), revealed that both *C. albicans*-only, and mixed-species biofilms resulted in significantly ($p < 0.05$) higher tissue damage compared with uninfected and bacteria-only biofilms. The tissue damage caused by mixed-species biofilms was significantly ($p < 0.01$) higher than for all other infection types.

The increased damage caused by mixed-species biofilms was also histologically confirmed using light microscopy (Figure 6) and CLSM analysis (Figure 7). Microscopy revealed higher numbers of *C. albicans* hyphae (proportion of *C. albicans* in hyphal form: 13.4%) in mixed-species biofilm infections, which extensively invaded the epithelial tissue. Although *C. albicans*-only biofilms demonstrated lower invasion and reduced proportions of hyphae compared to mixed-species biofilms (Figures 6 and 7), the damage observed for this group was significantly higher than that for the bacteria-only infection and uninfected controls. It was apparent that bacteria-only infections produced limited tissue damage compared to uninfected controls.

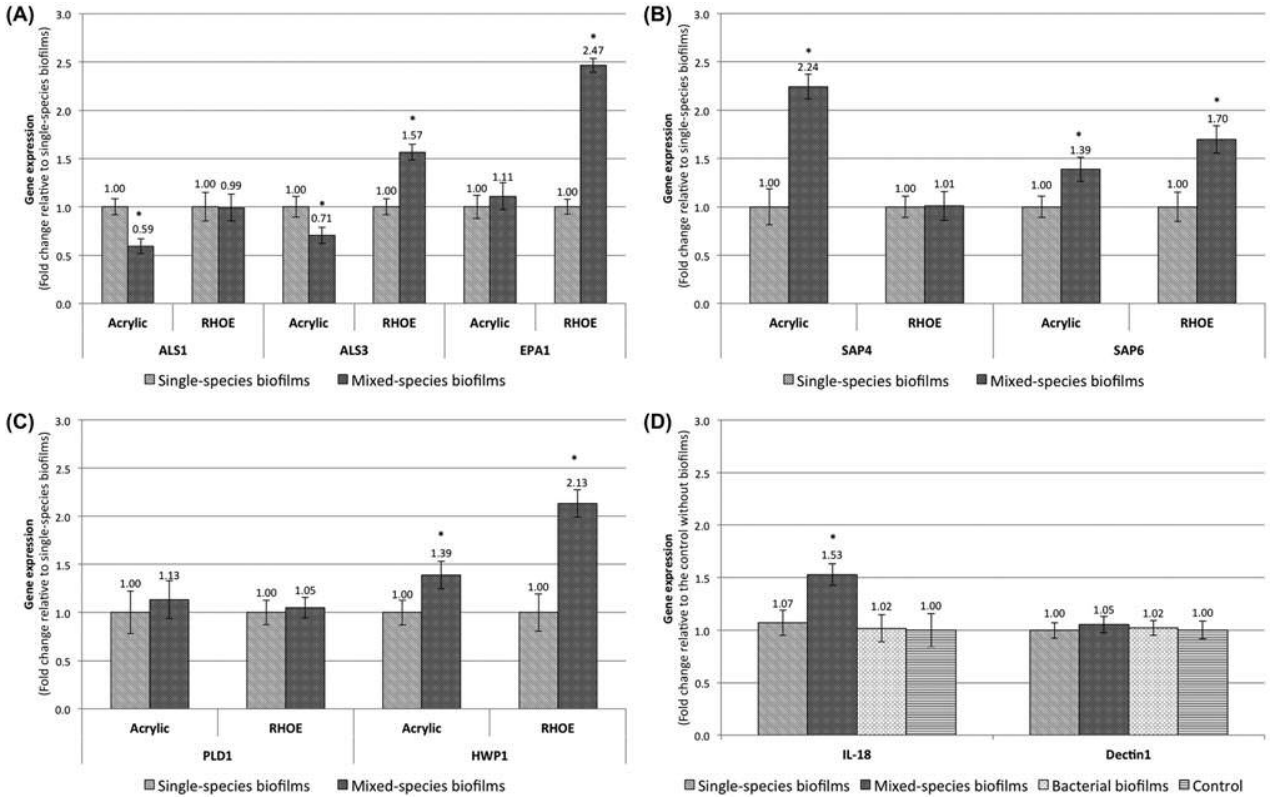

Figure 4. Relative gene expression in single and mixed-species biofilms on acrylic (n = 12), or in biofilms infecting RHOE (n = 6) of (A) *C. albicans* adhesins (ALS1, ALS3 and EPA1); (B) *C. albicans* secreted aspartyl proteinases (SAP4 and SAP6); and (C) *C. albicans* phospholipase D (PLD1) and hyphal wall protein (HWP1). (D) Relative gene expression of human interleukin 18 (IL-18) and of a human epithelial cell receptor for *C. albicans* (Dectin-1), in RHOE samples (n = 6) infected with single-*Candida* biofilm, mixed-species biofilm, bacterial biofilm, or control (without infection). *C. albicans* target genes were normalised using the *C. albicans* housekeeping gene (ACT1). Human target genes were normalised using a human housekeeping gene (β-actin). Analysis of quantitative RT-PCR was made by the $^{\Delta\Delta}$Ct method. Single-species biofilms were used as reference samples for expression *C. albicans* genes. Control RHOE samples (uninfected) were used as reference samples for expression of human genes. Bars show averages and SDs within each group. *Statistically different gene expression relative to controls (single-species biofilms – for analysis of *Candida* genes expression; uninfected samples – for analysis of human genes expression).

Discussion

Candida–bacteria interaction will invariably occur when associated together in oral biofilms. Mutualistic interactions between *C. albicans* and streptococci have previously been reported (Diaz, Xie, et al. 2012; Diaz, Strausbaugh, et al. 2014; Ricker et al. 2014; Xu et al. 2014) and were confirmed in the present study. Other studies have shown antagonistic interactions between *C. albicans* and other bacteria, such as *Lactobacillus* (Juárez Tomás et al. 2011) and *Pseudomonas aeruginosa* (Purschke et al. 2012; Méar et al. 2013). Such antagonism could occur due to bacterial-derived and quorum sensing regulated molecules such as pyocyanin and hydrogen peroxide (Hogan et al. 2004; Morales & Hogan 2010; Tian et al. 2013). To date, there have been limited studies examining the role oral bacteria play in directly influencing *C. albicans* virulence.

The aim of the present study was to compare *C. albicans* virulence attributes in biofilms on acrylic containing *C. albicans*-only, or biofilms also including selected oral bacteria. *Streptococcus* and *Actinomyces* species were the selected bacteria, as these are known primary colonisers of the oral cavity and are present in denture biofilms (Pereira-Cenci et al. 2010; Teles et al. 2012). In addition to examining biofilms on acrylic, the pathogenicity of these biofilms was compared by interfacing them with the surface of RHOE.

Importantly, the results show that *C. albicans* hyphal proliferation and expression of several putative candidal virulence genes significantly increased in the presence of bacteria. Associated with this, was enhanced RHOE damage and tissue invasion by *C. albicans* hyphae in mixed species biofilm infections, along with increased expression of the IL-18 gene (encoding a pro-inflammatory cytokine).

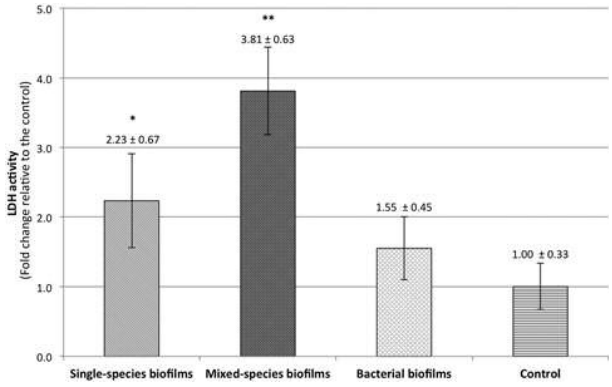

Figure 5. Relative LDH activity measured in the culture medium supernatant of RHOE tissues (n = 6, for each group) after 12 h incubation of samples infected with single-species *Candida* biofilm, mixed-species biofilm, bacteria only biofilm, or control (devoid of infection). Basal culture medium was used to 'blank' samples and the fold change calculations were based on a control group. Bars show averages and SDs within each group. *Statistically higher LDH activity relative to control and to bacterial biofilm. **Statistically higher LDH activity relative to control, single-species (*C. albicans*) and bacterial biofilms.

Enhanced *C. albicans* hyphal development in biofilms with bacteria and subsequent significant tissue invasion in RHOE could arise from direct interaction between bacteria and *C. albicans*. Indeed, it is known that streptococci interact with the cell-wall proteins of *Candida* (Bamford et al. 2009; Diaz, Xie, et al. 2012; Ricker et al. 2014) and inhibit farnesol-mediated hyphal suppression (Morales & Hogan 2010; Gow et al. 2011). Furthermore, bacterial metabolites (Purschke et al. 2012; Ricker et al. 2014) may influence biochemical pathways involved in candidal and hyphal transition. Some secreted bacterial quorum sensing molecules (eg competence-stimulating peptide secreted by *S. mutans*, and autoinducer-2 secreted by *Aggregatibacter actinomycetemcomitans*) have been reported to inhibit hyphal formation (Jarosz et al. 2009; Bachtiar et al. 2014).

Furthermore, it is likely that bacteria in mixed species biofilms affect the local environment by changing parameters such as nutrient or carbon dioxide levels, which are factors known to be involved in *C. albicans* hyphal transition and virulence (Morales & Hogan 2010; Gow et al. 2011; Lu et al. 2013; Buu & Chen 2014). Environmental pH can influence yeast–hyphal transition (Bensen et al. 2004; Gow et al. 2011) and co-cultivation of *C. albicans* with streptococci would lower the environmental pH, possibly inactivating the *C. albicans* transcription factor (Rim101 pathway) involved in hyphal morphogenesis (Bensen et al. 2004; Gow et al. 2011). Excessive environmental changes would, however, have been partially mitigated through daily medium replacement.

Hyphal growth of *C. albicans* is generally regarded as more pathogenic than yeast (Dalle et al. 2010; Martin et al. 2011; Kuo et al. 2013), with the former able to migrate and invade tissues (Gow et al. 2011; Diaz, Xie, et al. 2012). Perhaps unsurprisingly, associated with increased hyphal development was the concurrent up-regulation of HWP1, along with SAP4 and SAP6, which are genes implicated in *C. albicans* hyphal development (Jayatilake et al. 2006; Nailis et al. 2010; Zhu & Filler 2010; Martin et al. 2011; Alves et al. 2014).

With regards to expression of *C. albicans* putative virulence genes, only ALS1 and ALS3 were up-regulated in *C. albicans*-only biofilms on acrylic, and these are associated with substratum adhesion (Hoyer 2001; Zhu & Filler 2010; Méar et al. 2013). Interestingly, similar down-regulation has previously been demonstrated in mixed species biofilms on abiotic surfaces (Park et al. 2014). ASL1 is associated with biofilm maturation (Nailis et al. 2010; Zhu & Filler 2010) and its reduced expression caused by bacteria has been linked to altered nutrient availability, with associated slower biofilm development (Buu & Chen 2014; Park et al. 2014). ALS3 is a hyphal-specific cell surface protein and receptor for the streptococcal adhesins SspA and SspB (Bamford et al. 2009; Diaz, Xie, et al. 2012; Diaz, Strausbaugh, et al. 2014). The fact that higher hyphal proportions were present in mixed species acrylic biofilms would have presumably led to elevated ALS3 expression. However, this was not seen. It might be that the hyphal development arose prior to ALS3 being down-regulated due to bacterial factors.

Phospholipase D expression by *C. albicans* was not affected by bacteria and might indicate constitutive expression, corroborating previous findings (Nailis et al. 2010; Alves et al. 2014).

Other *C. albicans* putative virulence genes, related to hyphal proliferation (HWP1) and secretion of aspartyl proteinases (SAP4 and SAP6) were up-regulated in mixed species biofilms on acrylic. HWP1 is related to hyphal proliferation and substratum adhesion (Nailis et al. 2010; Zhu & Filler 2010; Martin et al. 2011; Alves et al. 2014), whilst SAP4 and SAP6 are associated with yeast–hyphal transition and tissue invasion (Naglik et al. 2003; Jayatilake et al. 2006; Naglik, Moyes, et al. 2008; Dalle et al. 2010; Martin et al. 2011). Given the changes to the *C. albicans* phenotype in the presence of bacteria in biofilms on acrylic, it was hypothesised that an increased pathogenic effect would be apparent when these biofilms were overlaid on RHOE. In these studies, the presence of bacteria led to enhanced expression of putative *Candida* virulence genes related to cell wall adhesins (ALS3 and EPA1), secreted aspartyl proteinases (SAP6) and hyphal proliferation (HWP1). Unsurprisingly, enhanced tissue invasion by *C. albicans* in the mixed species biofilms was associated with significantly

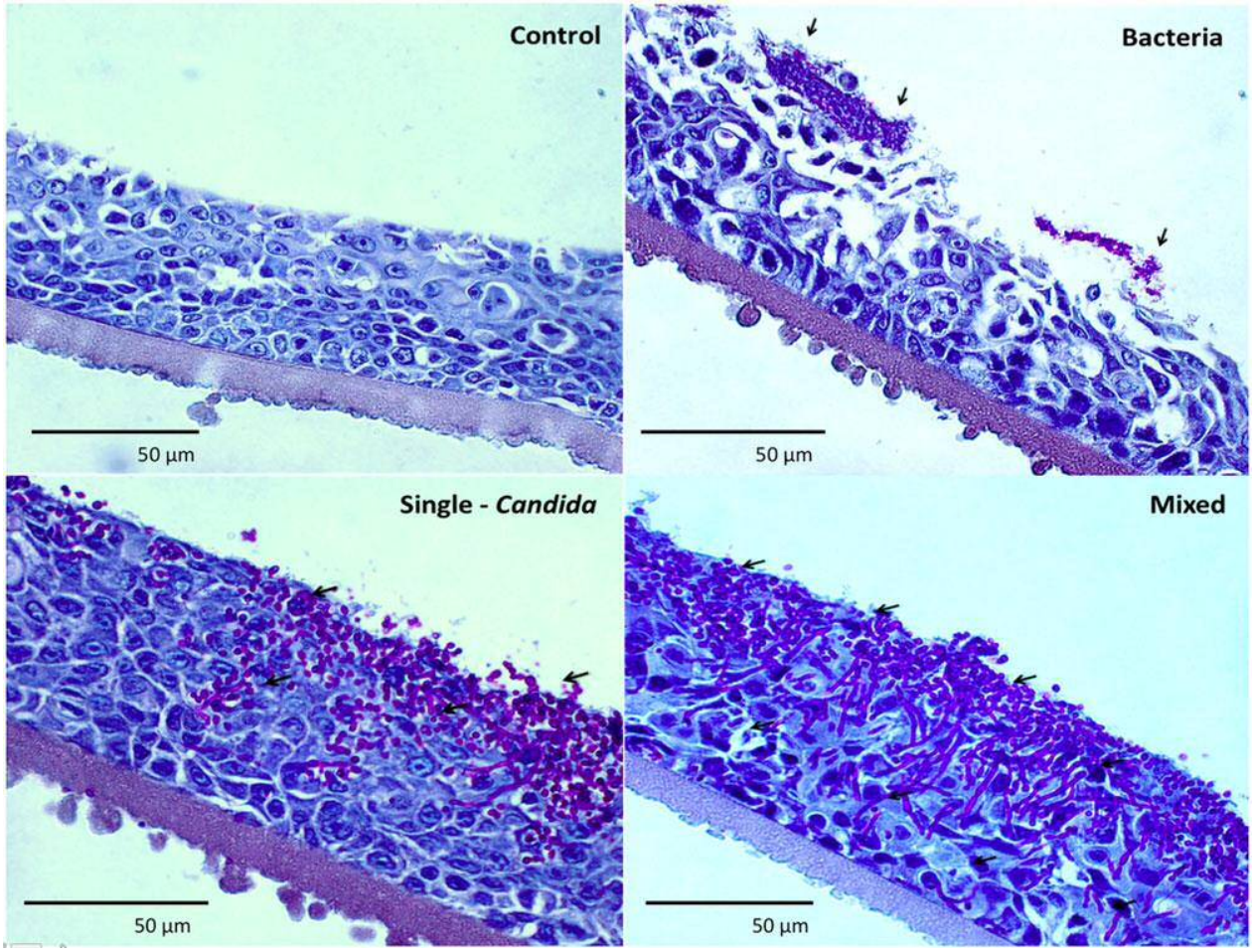

Figure 6. Representative light microscope images of fixed RHOE (n = 6, for each group) stained with PAS. Groups were comprised of healthy RHOE (control – upper left), and RHOE infected with bacterial biofilm (upper right); single-species *C. albicans* biofilm (lower left); or with mixed-species biofilm (lower right). Arrows show biofilms infecting tissues and invading the epithelia. Hyphae were seen in both single-species (*C. albicans*) and mixed-species biofilms but higher proportions of *C. albicans* hyphae and invasion were detected in mixed-species biofilms.

higher tissue damage, as determined by the LDH assay. Also, the increased proportion of *C. albicans* hyphae in mixed infections may have been responsible for the enhanced RHOE immune response seen by up-regulation of the gene encoding human interleukin IL-18 (Tardif et al. 2004; Martin et al. 2011; Kuo et al. 2013; Lowman et al. 2014).

Enhanced expression of ALS3 and EPA1 in mixed species biofilms infecting RHOE indicate that *C. albicans* adhesion to epithelial cells might also be increased in the presence of bacteria. The EPA1 gene translates a specific adhesin to epithelial cells (Kuhn & Vyas 2012), whilst ALS3 adhesin binds to the specific host cell receptors E-cadherin and N-cadherin (Zhu & Filler 2010; Liu & Filler 2011). Interestingly, the RHOE appeared to negate the previously observed lower ALS3 expression in mixed biofilms and two factors might explain this. Firstly, invasion of hyphae into the RHOE might protect against inhibitory effects of the bacteria, and secondly, the RHOE might provide additional nutrients to limit bacterial impact.

The mechanism by which the bacterial component of the biofilm induced the observed changes in *C. albicans* remains unclear. The effect could be due to several factors, eg alteration of environmental parameters including nutrient limitation, hypoxia, or specific effects such as inhibition of the farnesol pathway of hyphal suppression (Morales & Hogan 2010; Peleg et al. 2010; Gow et al. 2011; Lu et al. 2013; Buu & Chen 2014). Since many studies have shown antagonism of *C. albicans* by other bacteria (Hogan et al. 2004; Tian et al. 2013), studies assessing specific probiotics and quorum sensing molecules to manage candidal infection might also be of future value in this regard.

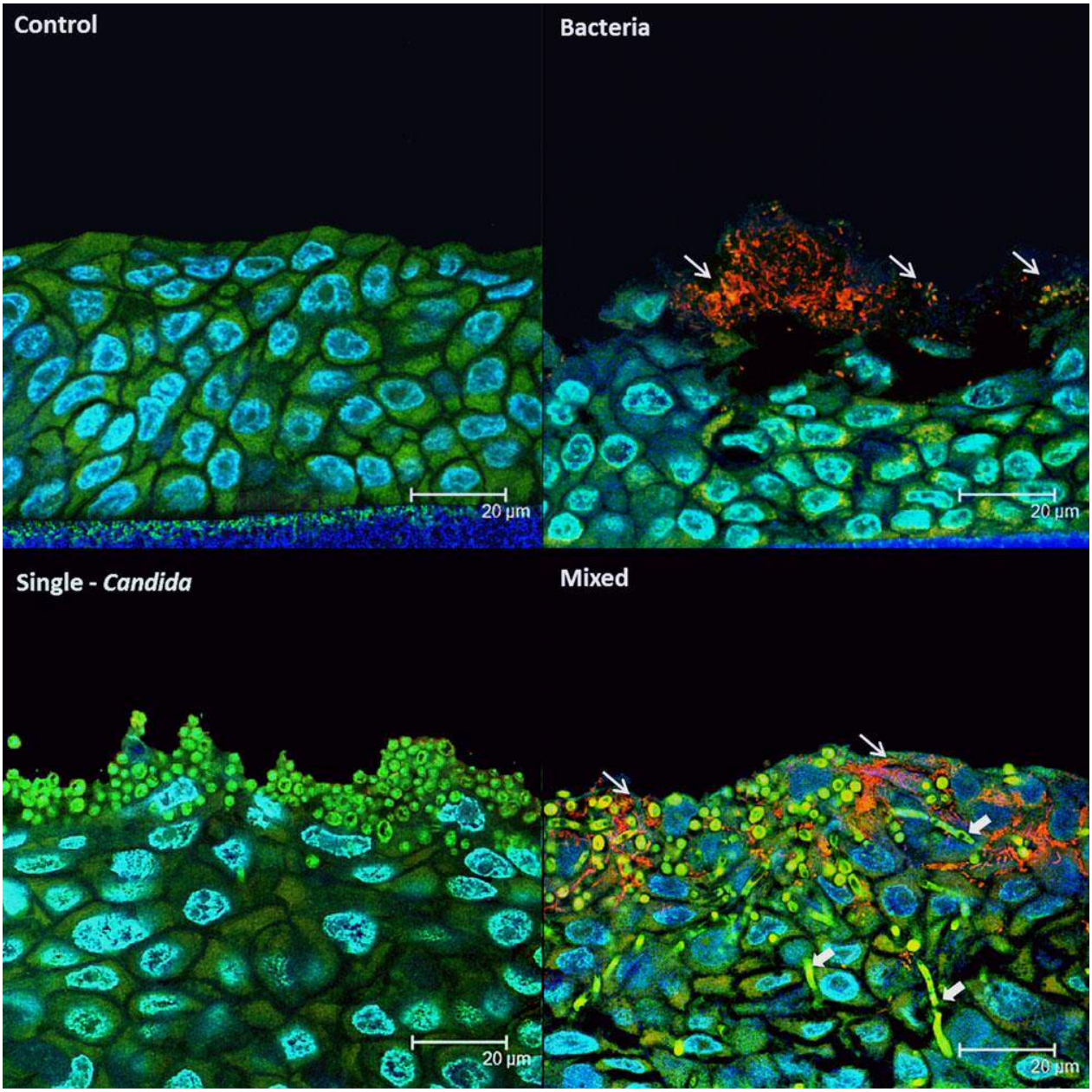

Figure 7. Representative CLSM images of fixed RHOE (n = 6, for each group) stained with fluorescent probes, after FISH. Groups comprised of healthy RHOE (control – upper left), and RHOE infected with bacterial biofilm (upper right); single-species *C. albicans* (lower left); or with mixed-species biofilm (lower right). Light arrows show bacterial species detected by a universal PNA probe (seen in red) in both bacterial and mixed-species biofilms. Bold arrows show hyphae and *C. albicans* invading the epithelium. A higher proportion of hyphae and invasion were detected in mixed-species biofilms. Epithelial nuclei were stained blue by Hoechst staining and epithelial cells were detected using pan-cytokeratin immunofluorescence. *Candida* was stained green by a PNA probe (YTL kit) and the cell wall was stained red by concanavalin-A conjugated lectin (Alexa Fluor® 594). Bacterial cells stained red following hybridisation with a bacterium-specific PNA probe.

This study found that an important factor in biofilm pathogenicity was the influence of the oral bacterial component on *C. albicans*. It may well be the case that different bacterial components modulate *C. albicans* pathogenicity *in vivo*, either by enhancing or reducing it. Since most attention in managing denture stomatitis has previously been directed towards the colonising *Candida*, based on these findings, further consideration should be given to the oral bacterial component of denture biofilms.

Conclusion

The presence of specific bacteria promotes proliferation of *C. albicans* hyphae and leads to enhanced tissue invasion and damage in mixed species biofilms. Higher virulence and pathogenicity of *Candida* biofilms was associated with up-regulation of virulence genes related to cell adhesion, hyphal proliferation and secreted aspartyl proteinases. These results are important, as in oral candidosis involving denture biofilms, progression and management of the infection may in part be dependent on the bacterial component present, an aspect that is frequently not a primary focus during clinical management.

Acknowledgements

The input of Mrs Kath Allsopp for processing and sectioning tissue samples is gratefully acknowledged.

Conflict of interest disclosure statement

No potential conflict of interest was reported by the author(s).

Funding

This work was supported by the following research funding agencies: CAPES (Brazil) under research grant [grant number 007355/2013-00]; FAPESP (Brazil) under research grant [grant number 2012/07436-6]; and GlaxoSmithKline under EPSRC-CASE award.

References

Alves CT, Wei XQ, Silva S, Azeredo J, Henriques M, Williams DW. 2014. *Candida albicans* promotes invasion and colonisation of *Candida glabrata* in a reconstituted human vaginal epithelium. J Infect. 69:396–407.

Bachtiar EW, Bachtiar BM, Jarosz LM, Amir LR, Sunarto H, Ganin H, Meijler MM, Krom BP. 2014. AI-2 of *Aggregatibacter actinomycetemcomitans* inhibits *Candida albicans* biofilm formation. Front Cell Infect Microbiol. 4:94. doi:10.3389/fcimb.2014.00094.

Bamford CV, d'Mello A, Nobbs AH, Dutton LC, Vickerman MM, Jenkinson HF. 2009. *Streptococcus gordonii* modulates *Candida albicans* biofilm formation through intergeneric communication. Infect Immun. 77:3696–3704.

Bensen ES, Martin SJ, Li M, Berman J, Davis DA. 2004. Transcriptional profiling in *Candida albicans* reveals new adaptive responses to extracellular pH and functions for Rim101p. Mol Microbiol. 54:1335–1351.

Bustin SA, Benes V, Garson JA, Hellemans J, Huggett J, Kubista M, Mueller R, Nolan T, Pfaffl MW, Shipley GL, et al. 2009. The MIQE guidelines: minimum information for publication of quantitative real-time PCR experiments. Clin Chem. 55:611–622.

Buu LM, Chen YC. 2014. Impact of glucose levels on expression of hypha-associated secreted aspartyl proteinases in *Candida albicans*. J Biomed Sci. 21:22.

Dalle F, Wächtler B, L'Ollivier C, Holland G, Bannert N, Wilson D, Labruère C, Bonnin A, Hube B. 2010. Cellular interactions of *Candida albicans* with human oral epithelial cells and enterocytes. Cell Microbiol. 12:248–271.

Diaz PI, Strausbaugh LD, Dongari-Bagtzoglou A. 2014. Fungal-bacterial interactions and their relevance to oral health: linking the clinic and the bench. Front Cell Infect Microbiol. 4:101. doi:10.3389/fcimb.2014.00101.

Diaz PI, Xie Z, Sobue T, Thompson A, Biyikoglu B, Ricker A, Ikonomou L, Dongari-Bagtzoglou A. 2012. Synergistic interaction between *Candida albicans* and commensal oral streptococci in a novel *in vitro* mucosal model. Infect Immun. 80:620–632.

Gow NA, van de Veerdonk FL, Brown AJ, Netea MG. 2011. *Candida albicans* morphogenesis and host defence: discriminating invasion from colonization. Nat Rev Microbiol. 10:112–122.

Green CB, Cheng G, Chandra J, Mukherjee P, Ghannoum MA, Hoyer LL. 2004. RT-PCR detection of *Candida albicans* ALS gene expression in the reconstituted human epithelium (RHE) model of oral candidiasis and in model biofilms. Microbiol. 150:267–275.

Hogan DA, Vik A, Kolter R. 2004. A *Pseudomonas aeruginosa* quorum-sensing molecule influences *Candida albicans* morphology. Mol Microbiol. 54:1212–1223.

Hoyer LL. 2001. The ALS gene family of *Candida albicans*. Trends Microbiol. 9:176–180.

Jarosz LM, Deng DM, Van der Mei HC, Crielaard W, Krom BP. 2009. *Streptococcus mutans* competence-stimulating peptide inhibits *Candida albicans* hypha formation. Eukaryot Cell. 8:1658–1664.

Jayatilake JA, Samaranayake YH, Cheung LK, Samaranayake LP. 2006. Quantitative evaluation of tissue invasion by wild type, hyphal and SAP mutants of *Candida albicans*, and non-albicans *Candida* species in reconstituted human oral epithelium. J Oral Pathol Med. 35:484–491.

Juárez Tomás MS, Saralegui Duhart CI, De Gregorio PR, Vera Pingitore E, Nader Macías ME. 2011. Urogenital pathogen inhibition and compatibility between vaginal *Lactobacillus* strains to be considered as probiotic candidates. Eur J Obstet Gynecol Reprod Biol. 159:399–406.

Koressaar T, Remm M. 2007. Enhancements and modifications of primer design program Primer3. Bioinformatics. 23:1289–1291.

Kuhn DM, Vyas VK. 2012. The *Candida glabrata* adhesin Epa1p causes adhesion, phagocytosis, and cytokine secretion by innate immune cells. FEMS Yeast Res. 12:398–414.

Kuo ZY, Chuang YJ, Chao CC, Liu FC, Lan CY, Chen BS. 2013. Identification of infection- and defense-related genes via a dynamic host-pathogen interaction network using a *Candida albicans*-zebrafish infection model. J Innate Immun. 5:137–152.

Liu Y, Filler SG. 2011. *Candida albicans* Als3, a multifunctional adhesin and invasin. Eukaryot Cell. 10:168–173.

Lowman DW, Greene RR, Bearden DW, Kruppa MD, Pottier M, Monteiro MA, Soldatov DV, Ensley HE, Cheng SC, Netea MG, Williams DL. 2014. Novel structural features in *Candida albicans* hyphal glucan provide a basis for differential innate immune recognition of hyphae versus yeast. J Biol Chem. 289:3432–3443.

Lu Y, Su C, Solis NV, Filler SG, Liu H. 2013. Synergistic regulation of hyphal elongation by hypoxia, CO_2, and nutrient conditions controls the virulence of *Candida albicans*. Cell Host Microbe. 14:499–509.

Malic S, Hill KE, Hayes A, Percival SL, Thomas DW, Williams DW. 2009. Detection and identification of specific bacteria in wound biofilms using peptide nucleic acid fluorescent *in situ* hybridization (PNA FISH). Microbiology. 155:2603–2611.

Malic S, Hill KE, Ralphs JR, Hayes A, Thomas DW, Potts AJ, Williams DW. 2007. Characterization of *Candida albicans* infection of an *in vitro* oral epithelial model using confocal laser scanning microscopy. Oral Microbiol Immunol. 22:188–194.

Martin R, Wächtler B, Schaller M, Wilson D, Hube B. 2011. Host-pathogen interactions and virulence-associated genes during *Candida albicans* oral infections. Int J Med Microbiol. 301:417–422.

Méar JB, Kipnis E, Faure E, Dessein R, Schurtz G, Faure K, Guery B. 2013. *Candida albicans* and *Pseudomonas aeruginosa* interactions: more than an opportunistic criminal association? Med Mal Infect. 43:146–151.

Morales DK, Hogan DA. 2010. *Candida albicans* interactions with bacteria in the context of human health and disease. PLoS Pathog. 6:e1000886.

Naglik JR, Challacombe SJ, Hube B. 2003. *Candida albicans* secreted aspartyl proteinases in virulence and pathogenesis. Microbiol Mol Biol Rev. 67:400–428.

Naglik JR, Moyes D, Makwana J, Kanzaria P, Tsichlaki E, Weindl G, Tappuni AR, Rodgers CA, Woodman AJ, Challacombe SJ, et al. 2008. Quantitative expression of the *Candida albicans* secreted aspartyl proteinase gene family in human oral and vaginal candidiasis. Microbiology. 154:3266–3280.

Nailis H, Kucharíková S, Ricicová M, Van Dijck P, Deforce D, Nelis H, Coenye T. 2010. Real-time PCR expression profiling of genes encoding potential virulence factors in *Candida albicans* biofilms: identification of model-dependent and -independent gene expression. BMC Microbiol. 10:114. doi:10.1186/1471-2180-10-114.

Negri M, Botelho C, Silva S, Lopes LM, Henriques M, Azeredo J, Oliveira R. 2011. An *in vitro* evaluation of *Candida tropicalis* infectivity using human cell monolayers. J Med Microbiol. 60:1270–1275.

Park SJ, Han K-H, Park JY, Choi SJ, Lee K-H. 2014. Influence of bacterial presence on biofilm formation of *Candida albicans*. Yonsei Med J. 55:449–458.

Peleg AY, Hogan DA, Mylonakis E. 2010. Medically important bacterial-fungal interactions. Nat Rev Microbiol. 8:340–349.

Pereira-Cenci T, da Silva WJ, Cenci MS, Cury AA. 2010. Temporal changes of denture plaque microbiologic composition evaluated *in situ*. Int J Prosthodont. 23:239–242.

Purschke FG, Hiller E, Trick I, Rupp S. 2012. Flexible survival strategies of *Pseudomonas aeruginosa* in biofilms result in increased fitness compared with *Candida albicans*. Mol Cell Proteomics. 11:1652–1669.

Ricker A, Vickerman M, Dongari-Bagtzoglou A. 2014. *Streptococcus gordonii* glucosyltransferase promotes biofilm interactions with *Candida albicans*. J Oral Microbiol. 6:23419. doi:10.3402/jom.v6.23419.

Shirtliff ME, Peters BM, Jabra-Rizk MA. 2009. Cross-kingdom interactions: *Candida albicans* and bacteria. FEMS Microbiol Lett. 299:1–8.

Silva S, Henriques M, Hayes A, Oliveira R, Azeredo J, Williams DW. 2011. *Candida glabrata* and *Candida albicans* co-infection of an *in vitro* oral epithelium. J Oral Pathol Med. 40:421–427.

Tardif F, Goulet JP, Zakrazewski A, Chauvin P, Rouabhia M. 2004. Involvement of interleukin 18 in the inflammatory response against oropharyngeal candidiasis. Med Sci Monit. 10:BR239–249.

Teles FR, Teles RP, Sachdeo A, Uzel NG, Song XQ, Torresyap G, Singh M, Papas A, Haffajee AD, Socransky SS. 2012. Comparison of microbial changes in early redeveloping biofilms on natural teeth and dentures. J Periodontol. 83:1139–1148.

Tian J, Weng LX, Zhang YQ, Wang LH. 2013. BDSF inhibits *Candida albicans* adherence to urinary catheters. Microb Pathog. 64:33–38.

Untergasser A, Cutcutache I, Koressaar T, Ye J, Faircloth BC, Remm M, Rozen SG. 2012. Primer3–new capabilities and interfaces. Nucleic Acids Res. 40:e115.

Williams D, Lewis M. 2011. Pathogenesis and treatment of oral candidosis. J Oral Microbiol. 3:5771. doi:10.3402/jom.v3i0.5771.

Williams DW, Kuriyama T, Silva S, Malic S, Lewis MA. 2011. *Candida* biofilms and oral candidosis: treatment and prevention. Periodontol 2000. 55:250–265.

Xu H, Sobue T, Thompson A, Xie Z, Poon K, Ricker A, Cervantes J, Diaz PI, Dongari-Bagtzoglou A. 2014. Streptococcal co-infection augments *Candida* pathogenicity by amplifying the mucosal inflammatory response. Cell Microbiol. 16:214–231.

Yadev NP, Murdoch C, Saville SP, Thornhill MH. 2011. Evaluation of tissue engineered models of the oral mucosa to investigate oral candidiasis. Microb Pathog. 50:278–285.

Ye J, Coulouris G, Zaretskaya I, Cutcutache I, Rozen S, Madden TL. 2012. Primer-BLAST: a tool to design target-specific primers for polymerase chain reaction. BMC Bioinf. 13:134. doi:10.1186/1471-2105-13-134.

Zhu W, Filler SG. 2010. Interactions of *Candida albicans* with epithelial cells. Cell Microbiol. 12:273–282.

Appendix V

Peer-reviewed published manuscript incorporating work from Chapters 3 and 4

Morse *et al*., (2018)

JOURNAL OF MEDICAL MICROBIOLOGY

RESEARCH ARTICLE

Morse *et al.*, *Journal of Medical Microbiology*

DOI 10.1099/jmm.0.000677

MICROBIOLOGY SOCIETY

OPEN MICROBIOLOGY

Denture-associated biofilm infection in three-dimensional oral mucosal tissue models

Daniel J. Morse,[1,*] Melanie J. Wilson,[1] Xiaoqing Wei,[1] Michael A. O. Lewis,[1] David J. Bradshaw,[2] Craig Murdoch[3] and David W. Williams[1]

Abstract

Purpose. *In vitro* analyses of virulence, pathogenicity and associated host cell responses are important components in the study of biofilm infections. The *Candida*-related infection, denture-associated oral candidosis, affects up to 60 % of denture wearers and manifests as inflammation of palatal tissues contacting the denture-fitting surface. Commercially available three-dimensional tissue models can be used to study infection, but their use is limited for many academic research institutions, primarily because of the substantial purchase costs. The aim of this study was to develop and evaluate the use of *in vitro* tissue models to assess infections by biofilms on acrylic surfaces through tissue damage and *Candida albicans* virulence gene expression.

Methodology. *In vitro* models were compared against commercially available tissue equivalents (keratinocyte-only, SkinEthic; full-thickness, MatTek Corporation). An *in vitro* keratinocyte-only tissue was produced using a cancer-derived cell line, TR146, and a full-thickness model incorporating primary fibroblasts and immortalised normal oral keratinocytes was also generated. The *in vitro* full-thickness tissues incorporated keratinocytes and fibroblasts, and have potential for future further development and analysis.

Results. Following polymicrobial infection with biofilms on acrylic surfaces, both in-house developed models were shown to provide equivalent results to the SkinEthic and MatTek models in terms of tissue damage: a significant (P<0.05) increase in LDH activity for mixed species biofilms compared to uninfected control, and no significant difference (P>0.05) in the expression of most *C. albicans* virulence genes when comparing tissue models of the same type.

Conclusion. Our results confirm the feasibility and suitability of using these alternative *in vitro* tissue models for such analyses.

INTRODUCTION

Biofilms are highly significant in human infection, and these complex polymicrobial communities of micro-organisms can develop on biotic or abiotic surfaces [1, 2]. They develop according to a defined series of events, and are highly structured, with distinct microenvironments within the EPS supporting the growth of a diverse range of micro-organisms [2–7]. A key component of this is their inherent antimicrobial tolerance [8] and resistance to host defence molecules and mechanisms. Biofilms frequently occur on the surfaces of medical devices and are often implicated in healthcare-associated infections [9–14]. It is well documented that the oral cavity (with numerous different surfaces such as the surface of teeth, gingival tissue and mucosa) can support the growth of up to 1000 different species of micro-organisms, including bacteria [15–17] and fungi [18]. Dental plaque is a well-studied example of a polymicrobial biofilm in the oral cavity [19, 20] and is responsible for the most prevalent human infections, namely dental caries and periodontal disease.

Received 6 November 2017; Accepted 3 January 2018

Author affiliations: [1]Oral and Biomedical Sciences, School of Dentistry, Cardiff University, Cardiff, UK; [2]GlaxoSmithKline Consumer Healthcare, Weybridge, Surrey, UK; [3]School of Clinical Dentistry, University of Sheffield, Sheffield, UK.

***Correspondence:** Daniel J. Morse, morsedj@cardiff.ac.uk

Keywords: biofilm; tissue model; candidosis; denture stomatitis; oral mucosa; infection.

Abbreviations: ALI, air–liquid interface; ANOVA, analysis of variance; Ct, cycle threshold; DMEM, Dulbecco's modified Eagle's medium; DMEM/F12, Dulbecco's modified Eagle's medium supplemented with Ham's F12; DS, *Candida*-associated denture stomatitis; EPS, extracellular polymeric substances; FT, full thickness; HKC, Heath-killed *Candida*; LDH, lactate dehydrogenase; LP, lamina propria; LPS, lipopolysaccharide; MTA, material transfer agreement; NCTC, National Collection of Type Cultures; PMMA, poly(methyl methacrylate); RHOE, reconstituted human oral epithelium; SE, stratified epithelium.

Two supplementary figures are available with the online version of this article.

Dental prostheses are common, particularly in the elderly population, and serve to maintain normal oral function and aesthetic appearance. Dentures are one such example, where, unlike living epithelia, this acrylic material lacks a natural sloughing capacity and, coupled with the inevitable formation of a salivary pellicle on the denture surface [21], serves to aid the establishment and retention of biofilms.

Chronic erythematous candidosis (*Candida*-associated denture stomatitis; DS) is a frequent oral infection that affects up to 60 % of denture wearers [22] and is associated with biofilms containing fungi of the genus *Candida*. DS presents as areas of inflammation on the palatal mucosa in close proximity to the denture acrylic, the extent of which is classified according to Newton's classification [23]. The infection occurs as a result of poor oral and denture hygiene, along with a number of other predisposing factors, including tobacco use, diabetes and impaired immunocompetence [24–26].

Candida are generally regarded as the main causative agents of DS and current management strategies target the fungal component. However, it is becoming increasingly apparent that bacteria and *Candida* interact within biofilms [27], and the role of bacteria in the pathogenesis, and thus the prognosis and management, of DS warrants further evaluation.

Tissue models are valuable tools for *in vitro* analysis of the pathogenicity of biofilms and associated host cell responses. Several commercially available constructs have been used to undertake such investigations [27–30], and they are necessary to gain greater insight into the complex relationship between host and microbes, particularly in the context of biofilm infections.

Two types of keratinocyte-only oral mucosal epithelium tissue models are commercially available, namely SkinEthic Reconstituted Human Oral Epithelium (RHOE) (EpiSkin, Lyon, France) and EpiOral (MatTek Corporation, Ashland, MA, USA). In addition, there is a full-thickness oral mucosa model incorporating a fibroblast-populated *lamina propria* composed of collagen and overlaid with keratinocytes (EpiOral FT, MatTek Corporation).

Keratinocyte-only models are comparatively simplistic, containing the epithelial layer, but lack a collagen matrix and fibroblast cells. Thus, potential analyses are limited when compared to full-thickness tissue models. Furthermore, the commercially available models provided are 'static', i.e. they are 'ready-to-use' products, with no potential to incorporate additional cells, such as immune cells or endothelial cells, to make them more representative of normal tissues.

This study developed and evaluated two *in vitro* tissue models as alternatives to the commercially available constructs, and for the first time used them to assess the effects of infection with denture biofilms. Specifically, the biofilm pathogenicity and host cell responses toward DS infections were analysed.

METHODS

Cell culture and conditions

TR146 keratinocytes (obtained from Cancer Research UK) were cultured in Dulbecco's modified Eagle's medium (DMEM; 11965–092, Life Technologies) supplemented with 4.5 g glucose l^{-1}, 10 % (v/v) foetal bovine serum (FBS), 2.5 mM L-glutamine, and 100 U penicillin ml^{-1} and 100 µg streptomycin ml^{-1} (Life Technologies). The cells were cultured and maintained in T75/T175 culture flasks in a humidified incubator at 37 °C with 5 % CO_2, 95 % air.

Primary human oral fibroblasts isolated from biopsies obtained from the buccal and gingival oral mucosa from patients during routine dental procedures with written, informed consent [31] (ethical approval number 09/H1308/66) kindly provided by Dr Helen Colley, University of Sheffield, were cultured in DMEM supplemented with 4.5 g glucose l^{-1}, 10 % (v/v) FBS, 2.5 mM L-glutamine, 100 U penicillin ml^{-1} and 100 µg streptomycin ml^{-1} in T175 flasks in a humidified incubator at 37 °C with 5 % CO_2, 95 % air.

FNB6 keratinocytes (obtained from Dr Keith Hunter, University of Sheffield, MTA provided by Cancer Research UK) were cultured in DMEM supplemented with 4.5 g glucose l^{-1}, 10 % (v/v) FBS, 2.5 mM L-glutamine, and 100 U penicillin ml^{-1} and 100 µg streptomycin ml^{-1} in T175 flasks in a humidified incubator at 37 °C with 5 % CO_2, 95 % air. Gamma-irradiated mouse-3T3 fibroblast cells were co-cultured at a density of approximately 3×10^5 cells per flask as a feeder layer.

Isolation of type I rat tail collagen

Rat tail type I collagen was isolated from the tails of Wistar rats. Briefly, surgically removed rat tails were folded and twisted approximately 4–5 cm from the base to expose the collagen fibres. The fibres were removed, washed in sterile PBS and dissolved for 7 days in 0.1 M sterile acetic acid at 4 °C with continuous stirring. The collagen was freeze-dried, redissolved in 0.1 M acetic acid to a stock concentration of 5 mg collagen ml^{-1}, and then stored at 4 °C.

Keratinocyte-only tissue model

TR146 cells were washed with PBS, and 3 ml of 0.25 % (w/v) trypsin-EDTA solution (Life Technologies, UK) was added to the flasks. The flasks were then incubated for 5 min to detach cells. The cells were collected into sterile plastic universal containers, centrifuged to pellet at 1500 rev min^{-1} for 5 min, and then suspended at $1–2\times10^6$ cells ml^{-1} in fresh keratinocyte DMEM culture medium [DMEM/F12 was supplemented with 4.5 g glucose l^{-1}, 10 % (v/v) FBS, 2.5 mM L-glutamine, 10 ng epidermal growth factor ml^{-1}, 0.5 µg insulin ml^{-1}, 1.8×10^4 U cholera toxin ml^{-1} and 5 µg adenine ml^{-1}]. A 500 µl volume of the standardised cell suspension was added to each 12 mm diameter (0.4 µm pore size) polycarbonate cell culture insert (PIHP01250, Merck Millipore) and then 2 ml of fresh keratinocyte DMEM was added to the well. The cells were incubated to allow attachment for 48 h, after which the medium was removed from both the insert and the well, and

600 µl fresh keratinocyte DMEM was added to the well. The medium was replenished every 2 days to maintain growth, taking care not to disturb the tissue, but removing any excess medium from inside the insert if necessary.

Co-culture tissue model

Full-thickness oral mucosal models were produced as previously described. [32, 33] Primary human oral fibroblasts were washed and detached form the culture flasks with 0.25 % trypsin-EDTA, centrifuged and suspended at 1×10^6 cells ml^{-1} in DMEM. The collagen mixture was then prepared (sufficient for ten inserts), containing 1 ml of reconstitution buffer (22 mg sodium bicarbonate ml^{-1}, 20 mM HEPES buffer, 0.062 M NaOH), 1 ml 10×DMEM (Sigma), 0.83 ml FBS, 0.1 ml L-glutamine and 6.73 ml collagen type 1 dissolved in 0.1 M acetic acid (5 mg collagen ml^{-1} extracted from rat tails), and kept on ice. The collagen mixture was gently but thoroughly mixed by hand, and the pH was adjusted by the addition of 1 M NaOH to be neutral. Fibroblasts were added into the collagen mixture (at a final concentration of 2.5×10^5 cells per insert) and mixed gently until homogenous, and then 500 µl of the collagen and cell mixture was added to each insert. The plates were incubated at 37 °C in 5 % CO_2, 95 % air for 30 min to allow the collagen to set, and then 2 ml of DMEM added to the well and the plates returned to the incubator. After 48 h incubation, cultured TR146 or FNB6 keratinocytes were detached with 0.25 % trypsin-EDTA and suspended to 1×10^6 cells ml^{-1} in DMEM, before 500 µl of the cell suspension was added to each insert on top of the collagen and fibroblasts. These cells were cultured for a further 48 h and then brought to the air–liquid interface (ALI). Culture medium was removed from the inside of the insert and the well, and 600 µl of fresh keratinocyte medium [DMEM, Hams F12, supplemented with 10 % (v/v) FBS, 100 U penicillin ml^{-1}, 100 µg streptomycin ml^{-1}, 0.625 µg amphotericin B ml^{-1}, 0.025 µg adenine ml^{-1}, 1.36 ng 3,3,5-tri-iodothymine ml^{-1}, 5 µg apo-transferrin ml^{-1}, 4 µg hydrocortisone ml^{-1}, 5 ng epidermal growth factor ml^{-1}, 8.47 ng cholera toxin ml^{-1} and 5 µg insulin ml^{-1}) was added to the well, leaving the cells in the insert at the ALI. These models were cultured for a further 14 days, with the medium being replenished every 2 days. Two days prior to the tissue model infection, the growth medium was adjusted to exclude the use of penicillin/streptomycin.

Receipt and processing of commercial mucosal tissue models

Both the EpiSkin and MatTek Corporation tissue models were transported with the models set in 'agar-like' culture medium to restrict movement during transport, and upon receipt they were placed into fresh 12-well plates with fresh maintenance medium as provided by the manufacturer. The models were incubated in 5 % CO_2 in a humidified incubator for at least 4 h prior to infection.

Biofilm infection of tissue models

Circular acrylic [poly-(methyl methacrylate); PMMA] coupons (approximately 10 mm diameter, 2 mm thickness) were prepared and sterilised. These coupons were then preconditioned overnight with an artificial saliva solution [2.5 g porcine stomach mucin l^{-1} (Sigma), 0.35 g sodium chloride l^{-1}, 0.2 g potassium chloride l^{-1}, 0.2 g calcium chloride dehydrate l^{-1}, 2 g yeast extract l^{-1}, 1 g Lab-Lemco powder l^{-1} (Sigma), 5 g proteose peptone l^{-1} (Sigma) and 1.25 ml 40 % (w/v) urea solution l^{-1}]. The biofilms were prepared on the acrylic coupons as detailed previously [27]. Briefly, the biofilms were grown on PMMA coupons and contained the following micro-organisms: single-species *Candida albicans* ATCC 90028, bacteria-only (*Streptococcus sanguinis* ATCC 10556, *S. gordonii* ATCC 10558, *Actinomyces viscosus* ATCC 15987 and *A. odontolyticus* NCTC 9935) and mixed species (*C. albicans* plus oral bacteria). The biofilms were prepared by the inoculation of 100 µl of each micro-organism suspension from a standardised concentration (as measured by optical density at 600 nm; a density of 1.0 for *C. albicans* and densities of 0.08–0.10 for bacterial cultures) for 2 h. Non-adhered cells were then removed and fresh medium was added to the wells. The biofilms were cultured for 72 h with daily medium change.

Immediately prior to tissue infection, the tissue culture medium was replaced with fresh culture medium, and the acrylic coupons with and without biofilms were inverted and placed in direct contact with the tissue models and incubated at 37 °C in 5 % CO_2, 95 % air for 12 h. Post-infection, the acrylic coupons were carefully removed with forceps, and the tissue models were cut out of the insert with a scalpel and bisected. One section was used for histopathological processing and imaging, and the other was added immediately to 350 µl buffer RLT (Qiagen) with 1 % (v/v) β-mercaptoethanol and 500 µl phenol:chloroform:isoamyl alcohol (25 : 24 : 1, Sigma) and kept on ice prior to RNA extraction.

Histopathological preparation and analysis of tissue models

Tissue models were fixed in 10 % (v/v) formal saline and then subjected to dehydration and formalin/paraffin fixation in a pathology cassette using Leica ASP300S processor. The samples were sectioned at 5 µm thickness and stained with haematoxylin and eosin using an automated staining machine (Thermo GLX Linistainer, Thermo Scientific).

RNA extraction, purification and synthesis of cDNA

RNA was extracted using an RNeasy Mini-prep kit (Qiagen) and reverse-transcribed to cDNA using a reverse-transcription kit (Primer Design, UK) according to manufacturer's instructions, as described by Cavalcanti *et al.* [27].

qPCR analysis of tissue model infections

Real-time qPCR was performed as described previously [27]. The targeted putative virulence genes of *C. albicans* were *ALS1*, *ALS3* (agglutinin-like sequences), *EPA1* (epithelial adhesin), *SAP4* and *SAP6* (secreted aspartyl proteinases), *HWP1* (hyphal wall protein) and *PLD1* (phospholipase D), the primer sequences of which are detailed in Table 1. Human interleukin-18 (IL-18) was also evaluated for

Table 1. *Candida* and human gene primer sequences used in qPCR analysis

Target gene	Sequence (5′ → 3′)
ACT1 – housekeeping gene	FW – TGCTGAACGTATGCAAAAGG
	RV – TGAACAATGGATGGACCAGA
ALS1 – agglutinin-like sequence	FW – CCCAACTTGGAATGCTGTTT
	RV – TTTCAAAGCGTCGTTCACAG
ALS3 – agglutinin-like sequence	FW – CTGGACCACCAGGAAACACT
	RV – GGTGGAGCGGTGACAGTAGT
EPA1 – epithelial adhesin	FW – ATGTGGCTCTGGGTTTTACG
	RV – TGGTCCGTATGGGCTAGGTA
HWP1 – hyphae wall protein	FW – TCTACTGCTCCAGCCACTGA
	RV – CCAGCAGGAATTGTTTCCAT
PLD1 – phospholipase D	FW - GCCAAGAGAGCAAGGGTTAGCA
	RV – CGGATTCGTCATCCATTTCTCC
SAP4 – secreted aspartyl proteinase	FW – GTCAATGTCAACGCTGGTGTCC
	RV – ATTCCGAAGCAGGAACGGTGTCC
SAP6 – secreted aspartyl proteinase	FW – AAAATGGCGTGGTGACAGAGGT
	RV – CGTTGGCTTGGAAACCAATACC
β-actin – human housekeeping gene	F – GAGCACAGAGCCTCGCCTTTGCCGAT
	R – ATCCTTCTGACCCATGCCCACCATCACG
IL-18 – human interleukin 18 (pro-inflammatory cytokine)	F – CCTTCCAGATCGCTTCCTCTCGCAACAA
	R – CAAGCTTGCCAAAGTAATCTGATTCCAGGT

keratinocyte-only tissue model infections as described previously [27]. The primer sequences for the human genes are also detailed in Table 1. Analysis of relative gene expression was performed according to the $^{\Delta\Delta}$Ct method [34].

Monocyte cell responses to bacterial lipopolysaccharide and heat killed *C. albicans*

THP-1 monocytes were cultured in RPMI 1640 medium (Life Technologies), supplemented with 10 % (v/v) FBS and 2 mM L-glutamine. The cells were seeded at a density of 2×10^5 cells ml^{-1} in six-well plates prior to lipopolysaccharide (LPS) or heat-killed *C. albicans* (HKC) challenge. *C. albicans* cells were cultured overnight in yeast nitrogen base supplemented with 100 mM glucose as previously described [27], and heated in a water bath at 95 °C for 10 min. Heat-killing efficacy was confirmed by negative agar culture on Sabouraud dextrose agar. Bacterial LPS (isolated from *Escherichia coli*, Sigma) was prepared at a stock concentration of 1 mg ml^{-1} in PBS and diluted in RPMI 1640 (Life Technologies), supplemented with 10 % (v/v) FBS and 2 mM L-glutamine. THP-1 cells were cultured overnight in the presence or absence of 100 ng LPS ml^{-1}, and then challenged overnight with HKC at varying densities. The cell culture conditioned medium was collected and stored at −80 °C.

Quantification of secreted IL-23 cytokine protein by enzyme linked immunosorbent assay (ELISA)

IL-23 ELISA was performed on cell culture-conditioned medium using the Ready-Set-Go kit (eBioscience, Thermo Fisher Scientific) according to the manufacturer's instructions. The resulting concentration of IL-23 in the conditioned medium was determined by plotting sample absorbance against the standard curve.

Lactate dehydrogenase (LDH) activity of infected tissue models

Supernatant (n=3 for each group) was collected for the analysis of cell damage via lactate dehydrogenase activity assay (Pierce LDH cytotoxicity assay; Fisher Scientific, Cramlington, UK) according to the manufacturer's instructions, and the results were normalised to acrylic-only (no biofilm) controls.

Statistical analysis

Statistical analysis was performed with Prism version 6.0c (GraphPad Software, La Jolla, CA, USA). One-way ANOVA followed by Tukey's multiple comparisons test was used to evaluate statistical differences between samples at 95 % confidence.

RESULTS

In vitro tissue model culture

The development of an *in vitro* keratinocyte-only tissue model was achieved. This involved using different cell seeding densities and incubation periods, and it was compared to the SkinEthic RHOE model for tissue depth and structure (Fig. 1a). The cell densities, namely 5×10^5 (Fig. 1b, c), and 1×10^6 (Fig. 1d, e) cells per insert, and different incubation periods, including 5 days (Fig. 1b, d), and 10 days (Fig. 1c, e), showed varied tissue depths, but the observed cell morphology was typical of viable keratinocytes at all densities and incubation periods. The tissue depth was consistent across the supporting membrane for each tissue section, with the presence of tight cell-to-cell junctions being evident. Reduced tissue thickness was apparent at the lower seeding densities [5×10^5 cells per insert (Fig. 1b, c) compared with 1×10^6 cells (Fig. 1d, e)] per insert, but the thickness was similar to that of SkinEthic RHOE.

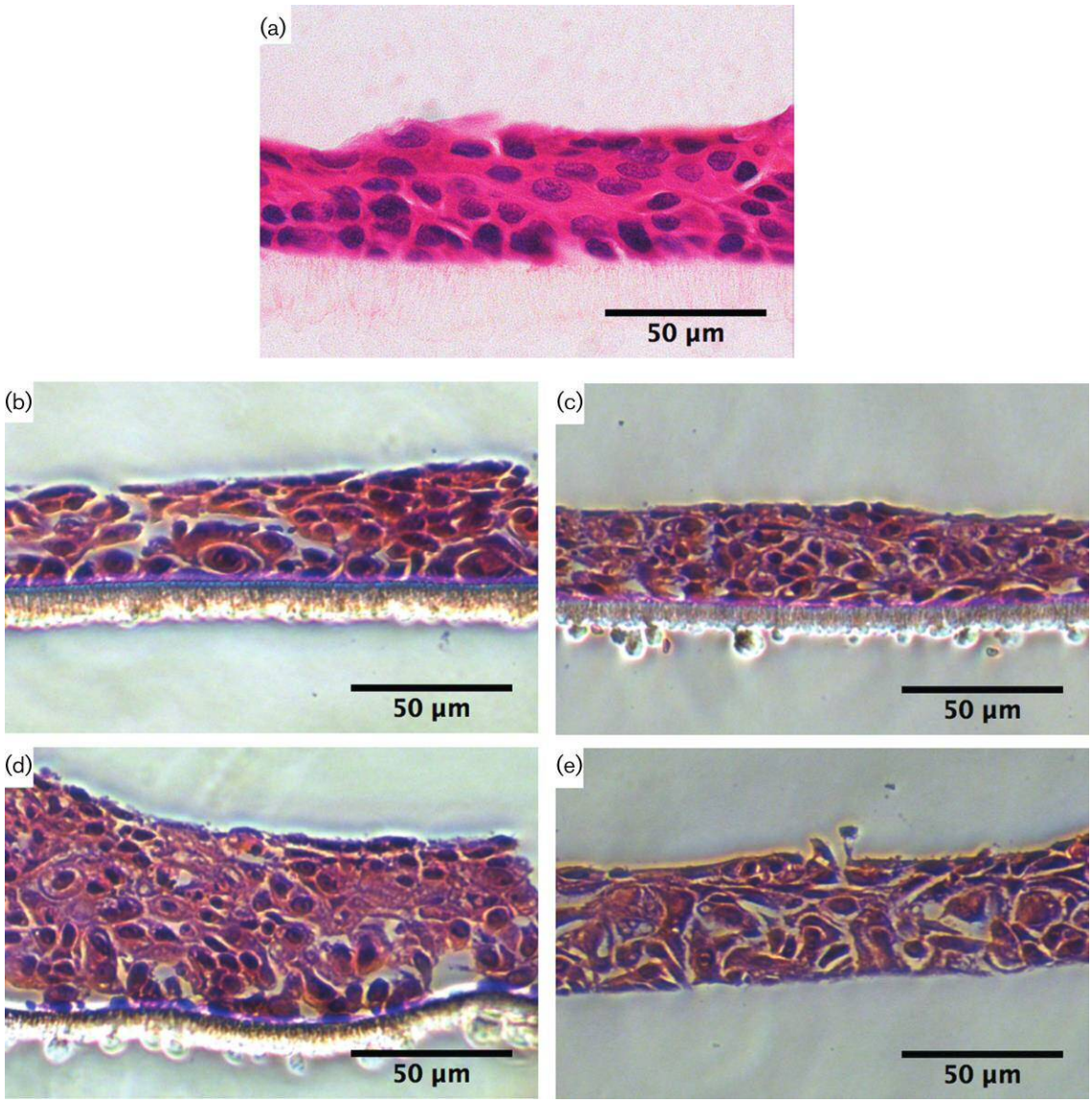

Fig. 1. Representative light microscopy images of the *in vitro* keratinocyte-only tissue model, sectioned at 5 µm thickness. (a) SkinEthic reconstituted human oral epithelia (RHOE) tissue; (b) *in vitro* keratinocyte-only tissue seeded with 5×10^5 cells cultured for 5 days; (c) *in vitro* keratinocyte-only tissue seeded with 5×10^5 cells cultured for 10 days; (d) *in vitro* keratinocyte-only tissue seeded with 1×10^6 cells cultured for 5 days; (e) *in vitro* keratinocyte-only tissue seeded with 1×10^6 cells cultured for 10 days. Stained with haematoxylin and eosin. The scale bar represents 50 µm.

Growth at 5 days (following seeding with 1×10^6 cells) resulted in a tissue thickness that was greater than that observed in the SkinEthic RHOE tissues. There were small differences in tissue thickness across the membrane, but no differences in cellular morphology for 5- or 10-day cultures. All of the models showed good stratification and limited cell differentiation.

During the development of the method, the importance of the ALI was noted. When the models were cultured submersed in culture medium, the thickness of the tissue was greatly reduced (Fig. 2) compared to those cultured at the ALI, and thus all of the tissue models were then cultured at the ALI to ensure good stratification of the epithelium. Culturing at the ALI is also known to promote keratinisation of the epithelium, which is present in normal oral mucosa, whereas when the culturing is submersed, keratinisation is restricted.

The development of the *in vitro* full-thickness tissue model development was more complex than that for the keratinocyte-only models. The required growth period was significantly longer: approximately 2 weeks, compared to just 5 days for the keratinocyte-only models. The longer culture

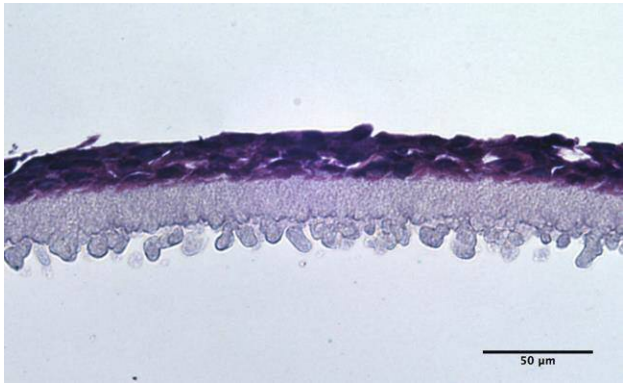

Fig. 2. Light microscopy image showing a very thin epithelium when culturing is performed with medium covering the cells (e.g. not at the air–liquid interface). Stained with haematoxylin and eosin. The scale bar represents 50 µm.

period was necessary to achieve maturation of the cells and the establishment of a stratified epithelium (SE; Fig. 3a). As observed with the keratinocyte-only tissue models, consistent epithelial thickness was again evident across the membrane. Fig. 3(a) demonstrates a thick *lamina propria* (LP), with fibroblasts populating the collagen matrix relatively sparsely. Additionally, epithelial cell differentiation was observed within the SE layer, with several distinct keratinocyte morphologies visible. Also present was a basement membrane (a darker, more densely packed area of epithelium), with layers of stratification towards the upper region, where some keratinisation was evident.

When the cancer cell line TR146 was used in place of immortalised normal oral keratinocytes, the results were somewhat different (Fig. 3b) to those for immortalised normal oral keratinocytes (Fig. 3a). Specifically, whilst a number of layers of keratinocytes were visible in the epithelium, their organisation was substantially different. There was a reduction in the overall thickness of the epithelium, a lack of distinctly defined stratified layers, with no distinct basement membrane cells, and little cellular differentiation. The cellular morphology also appeared to be less representative of normal oral mucosa compared with models developed using immortalised normal oral keratinocytes. Furthermore, no keratinisation of the epithelium was evident, as was also observed with keratinocyte-only tissue models, which were developed using the same cell line.

Denture-associated biofilm infection of keratinocyte-only tissues

Infection of the SkinEthic RHOE tissues with mature biofilms developed on denture acrylic resulted in the same pattern of tissue damage as previously reported [27]. The tissue damage, as measured by lactate dehydrogenase (LDH) activity, showed that bacteria-only biofilm infections induced an increase in damage compared with acrylic coupons with no biofilms, although this was not statistically significant ($P>0.05$). However, a significant ($P<0.05$) increase occurred with *C. albicans*-only biofilms, and a further significant ($P<0.01$) increase in tissue damage was observed with mixed-species (bacteria and *C. albicans*) biofilms (Fig. 4a).

Biofilm infection of the *in vitro* keratinocyte-only models (Fig. 4b) resulted in a similar pattern of damage to that observed with infections of the SkinEthic RHOE. A significant ($P<0.01$) increase in tissue damage was caused by

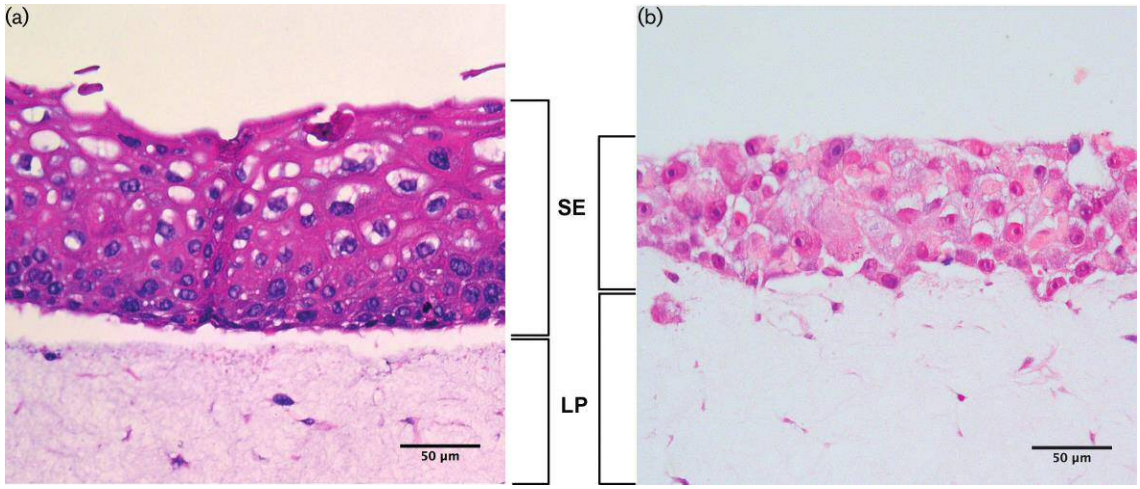

Fig. 3. (a) *In vitro* full-thickness mucosal tissue using primary oral cells. Clear distinct layers of fibroblast-populated *lamina propria* (LP) in collagen, with good stratification and differentiation of the epithelia (SE). (b) *In vitro* full-thickness mucosal tissue using primary fibroblasts, with TR146 cancer-derived keratinocytes. Note the substantial lack of cellular maturation and organisation, and the reduced epithelial stratification compared with tissues developed using immortalised normal oral keratinocytes. Stained with haematoxylin and eosin. The scale bar represents 50 µm.

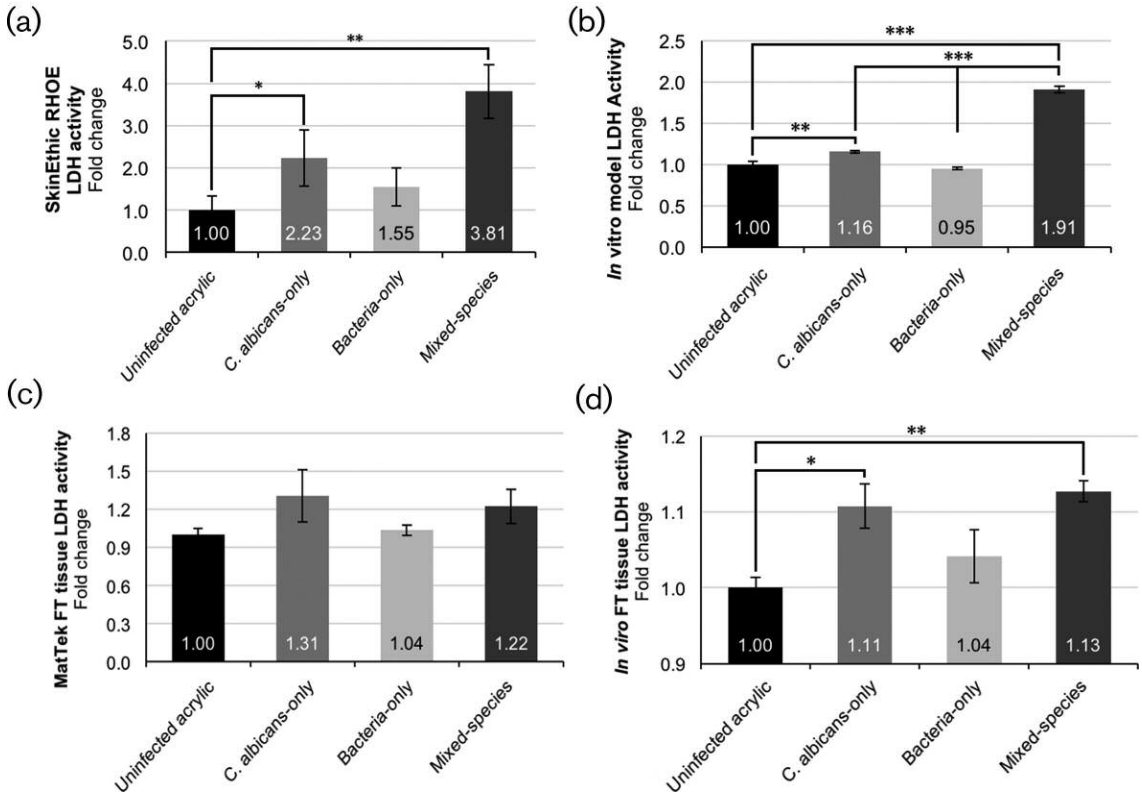

Fig. 4. Biofilm-induced tissue damage as measured by the lactate dehydrogenase activity assay of infections. The results are expressed as fold change, normalised against an acrylic-only (no biofilm) control. (a) SkinEthic RHOE, (b) *in vitro* keratinocyte-only tissue, (c) MatTek EpiOral full-thickness tissue and (d) *in vitro* full-thickness tissue. All of the tissues show a similar pattern of damage; the largest increase in tissue damage is induced by mixed-species biofilms, compared to single-species and uninfected control acrylic coupons.

C. albicans-only biofilms relative to the acrylic coupons with no biofilms, and a further significant (P<0.001) increase was observed with mixed-species biofilm infections relative to both the *C. albicans*-only biofilms and bacteria-only biofilms, and the uninfected acrylic coupons.

Denture-associated biofilm infection of full-thickness tissue models

A similar pattern of biofilm-induced tissue damage to the keratinocyte-only tissue models was evident with the MatTek EpiOral full-thickness tissue models; an increase in the damage caused by *C. albicans*-only and mixed-species biofilms, but no clear difference with bacteria-only biofilms. These differences, when compared with the uninfected acrylic coupons only, were not statistically significant (P>0.05) (Fig. 4c). However, *in vitro* full-thickness tissue model infections (Fig. 4d) once again showed a similar pattern of tissue damage, but with a significant (P<0.05) increase in LDH activity caused by *C. albicans*-only biofilm infections, and a similar, but even more significant (P<0.01), increase in mixed-species biofilms. Furthermore, as previously observed, no significant (P>0.05) differences in tissue damage were observed with infection using bacteria-only biofilms.

C. albicans gene expression profile during biofilm infection of tissue models

The relative levels of expression of putative *C. albicans* virulence genes were compared to those of the housekeeping control gene, *ACT1*, and relative to a *C. albicans*-only biofilm control infection. The expression of all *C. albicans* virulence genes, with the exception of *ALS1,* followed the same pattern when compared between mixed-species biofilm infection of tissues of the same type, e.g. SkinEthic RHOE versus *in vitro* keratinocyte-only, and MatTek EpiOral full-thickness versus *in vitro* full-thickness tissues. Some variation in the extent of gene expression was evident, which highlights the innate variability of biofilms.

In order to establish whether there were differences between the commercial and in-house tissues with regard to the infecting biofilms, comparisons were again made of tissue models of the same type; namely SkinEthic RHOE versus *in vitro* keratinocyte-only tissues, and MatTek EpiOral versus *in vitro* full-thickness tissues. Overall, no significant differences in *C. albicans* gene expression were observed between infections of tissues of the same type for *ALS3, EPA1, HWP1, PLD1, SAP4* or *SAP6* genes. A significant (P<0.01)

increase in the expression of *ALS1* was observed in *in vitro* full-thickness tissues compared with MatTek EpiOral, and a larger increase in the expression of *SAP4* was also observed in biofilms used to infect the *in vitro* full-thickness tissue compared with MatTek EpiOral tissues, but this difference was not statistically significant.

The expression of the genes involved in adhesion, biofilm initiation and maturation, and formation of *C. albicans* hyphae (Fig. 5a; agglutinin-like sequences, *ALS1*, *ALS3*; epithelial adhesin 1, *EPA1*) was increased in mixed-species biofilms relative to *C. albicans*-only biofilms, and showed little difference between the different tissue infections, with the exception of *ALS1* in the MatTek EpiOral infections, where a decrease in expression was observed.

The *C. albicans* genes involved in pathogenicity by cell invasion and damage (Fig. 5b; phospholipase D1, *PLD1*; secreted aspartyl proteases, *SAP4*, *SAP6*) were also increased in the mixed-species biofilms for each of the tissue models. A significant increase in the gene expression of *SAP4* was observed in the SkinEthic RHOE tissue infections compared with MatTek EpiOral tissue infections, but no significant differences were observed between tissue models of the same type. Additionally, although there was no apparent increase in the expression of hyphal wall protein 1 (Fig. 5a; *HWP1*) expression during the infections in this study, we have previously shown that a significant proportion of hyphae are present relative to yeast cells [27] in these biofilms, and there was a substantial presence of hyphae in the microscopy of the tissue infection histological sections.

Histological analyses of full thickness tissue model infections

The ability to perform histological analysis proved useful for determining the extent of infection, particularly with regard to damage to the epithelium, as previously evaluated with the RHOE keratinocyte-only model [27]. This study therefore focused on the evaluation of full-thickness tissue infections for histological analysis.

The infections of *in vitro* full-thickness tissues (Fig. 6) and MatTek EpiOral tissues (Figs 7 and 8) showed some variation in the extent of the visible tissue damage caused by the infecting biofilms. This correlated with the variable LDH activity results previously described (Fig. 4c, d). Fig. 6(a) shows little to no damage caused by the acrylic coupon itself

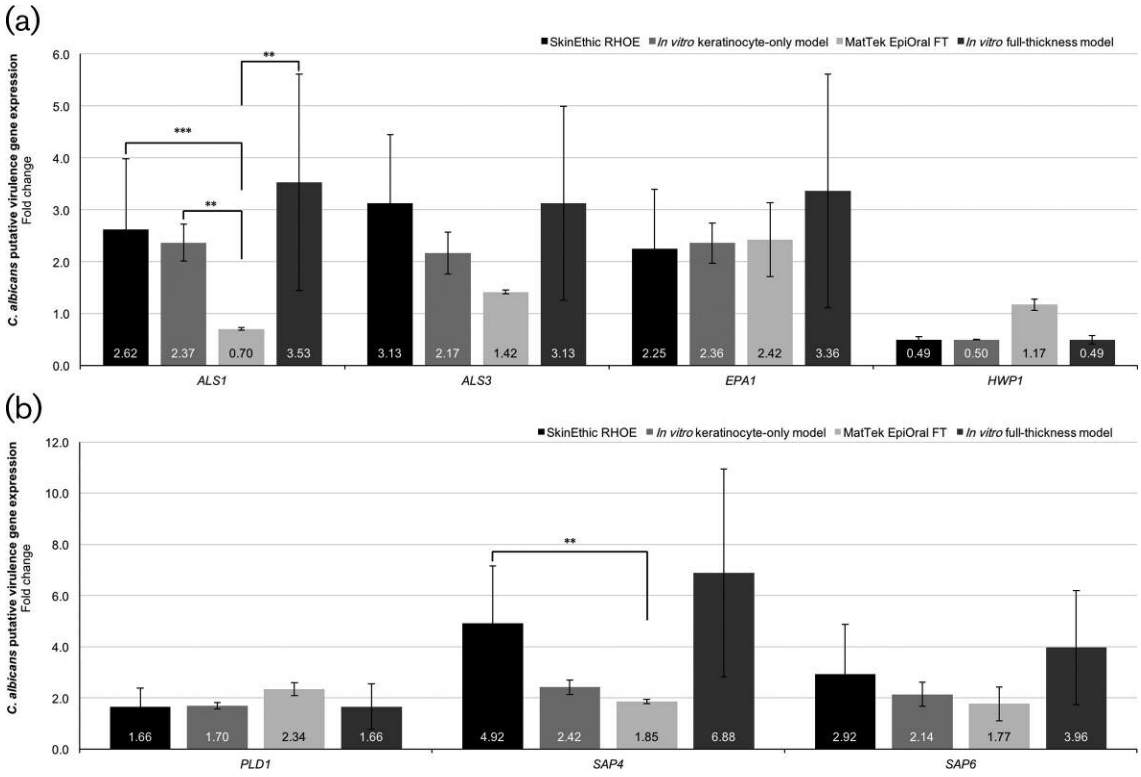

Fig. 5. Expression of putative *Candida albicans* virulence genes of mixed-species biofilms post-tissue infection. The results are expressed as the fold change of samples relative to the housekeeping gene ACT1 against a normalised *C. albicans*-only biofilm control. No significant differences in *C albicans* gene expression were observed between tissue models of the same type (e.g. SkinEthic RHOE versus *in vitro* keratinocyte only, or MatTek EpiOral full-thickness versus *in vitro* full-thickness tissues) with the exception of full-thickness tissues for the *ALS1* gene.

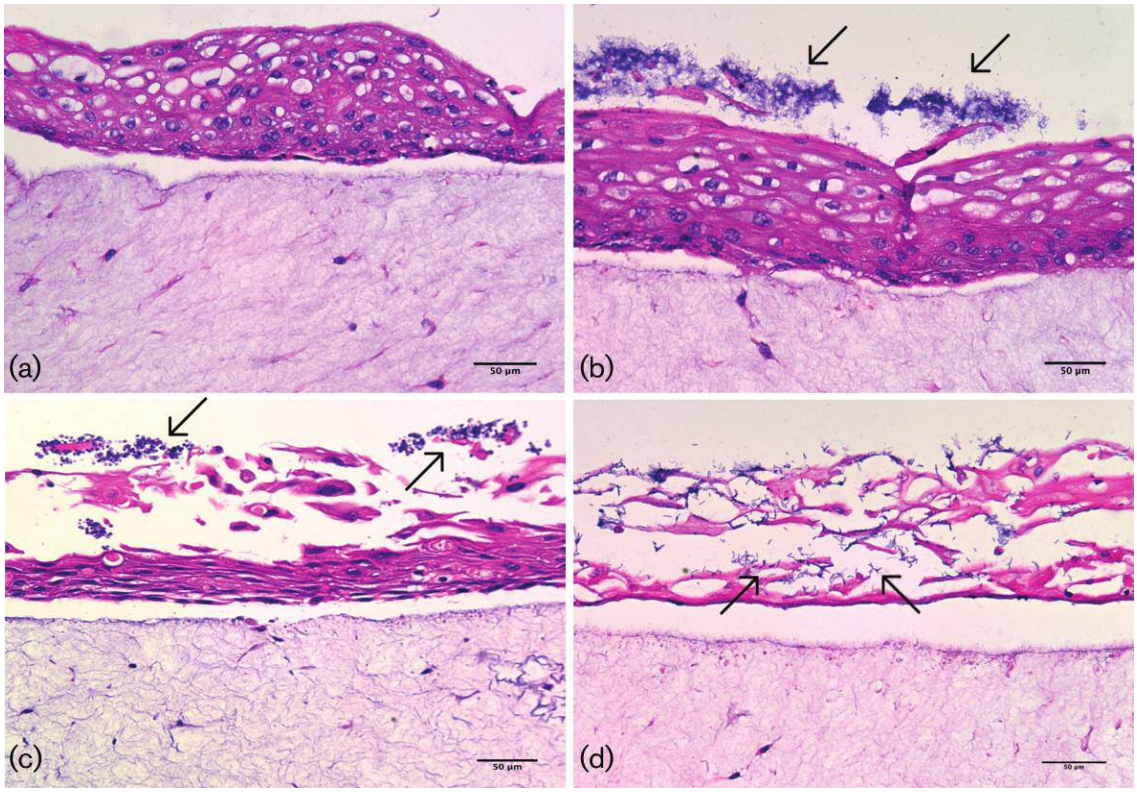

Fig. 6. Typical light microscopy images of (a) full-thickness tissue after infection with acrylic coupons only (no biofilm), showing no damage to epithelium; (b) full-thickness tissue after infection with bacteria-only biofilm, showing slight tissue damage and clustering of biofilms on the epithelial surface (indicated by arrows); (c) full-thickness tissue after infection with *Candida albicans*-only biofilm, showing substantial epithelial damage and biofilms clustered on the surface of the epithelium (indicated by arrows); (d) full-thickness tissue after infection with mixed-species biofilm, showing extensive epithelial damage and microbial invasion through the epithelium (indicated by arrows). Stained with haematoxylin and eosin. The scale bar represents 50 µm.

on the *in vitro* full-thickness tissues, as was also observed with the MatTek EpiOral full-thickness tissues (Fig. 7a), and similarly with bacteria-only biofilms in both tissue models (Figs 6b, and 7b). *C. albicans*-only biofilms caused substantial damage to *in vitro* full-thickness tissues (Fig. 6c) and some damage in MatTek EpiOral tissues (Fig. 7c), although to a lesser extent than *in vitro* tissues. Mixed-species biofilms caused substantial damage to the *in vitro* tissues, where there was significant penetration and epithelial invasion of *C. albicans* hyphae and bacteria. Some damage was observed in the MatTek EpiOral tissues when they were analysed histologically (Fig. 7d), which correlates with the LDH analysis, as previously discussed, and although the penetration and invasion of *C. albicans* hyphae was evident (Fig. 8), it was to a lesser extent than was observed in *in vitro* full-thickness tissues.

Information on the data underpinning the results presented here, including how to access them, can be found in the Cardiff University data catalogue at http://doi.org/10.17035/d.2017.0044151363.

DISCUSSION

Three-dimensional tissue model development, limitations and advantages

Oral biofilms are of considerable clinical importance, and the ability to research the microbial interactions that underpin biofilm biology *in vitro* is important to understand and combat these infections. When *in vitro* tissue models provide valid and reproducible results, they are preferable, as they may remove the need for animal experimentation, a desirable characteristic for many funding bodies.

Commercially available tissue constructs have been used extensively to investigate infections [27–30, 35, 36]. Cavalcanti *et al.* [27] used such constructs to study denture biofilm infection using SkinEthic RHOE. This study is, however, the first to evaluate the use of both keratinocyte-only and full-thickness *in vitro* tissue models for denture biofilm infections, with a specific emphasis on biofilm-induced tissue damage in order to evaluate the *in vitro* tissues as an alternative to the commercially available constructs. The

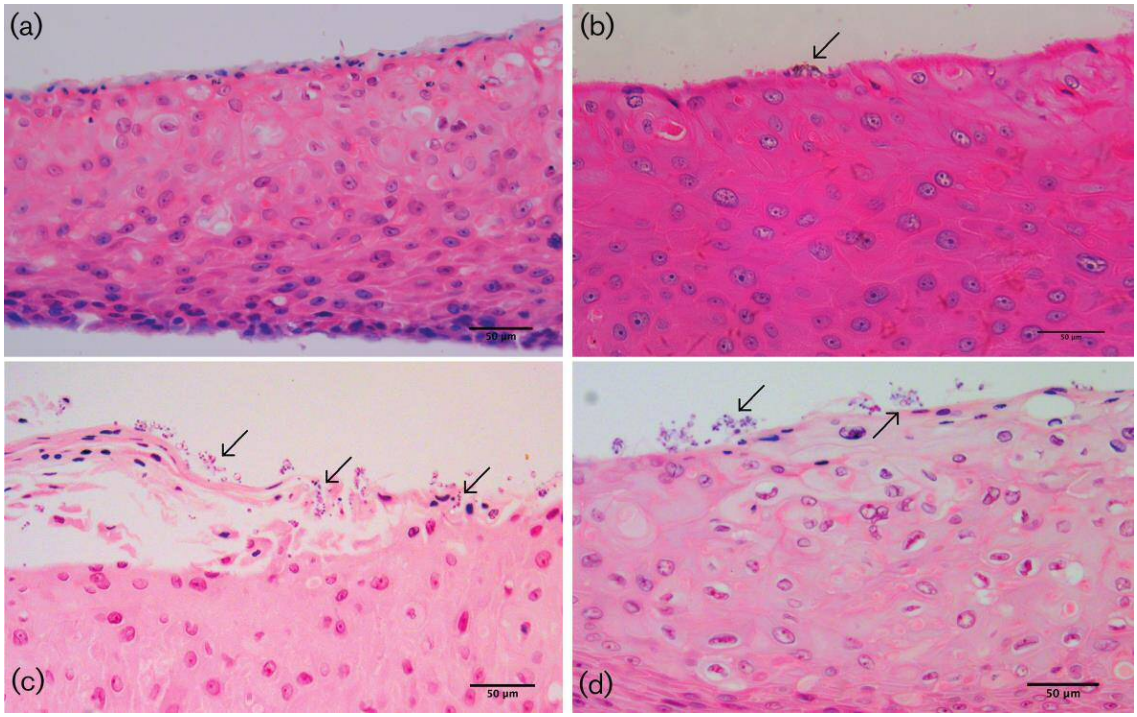

Fig. 7. Typical light microscopy images of (a) MatTek full-thickness tissue after infection with acrylic coupons only (no biofilm), showing no damage to epithelium; (b) MatTek full-thickness tissue after infection with bacteria-only biofilm, showing very slight tissue damage and clustering of biofilms on the epithelial surface (indicated by arrows); (c) MatTek full-thickness tissue after infection with *Candida albicans*-only biofilm, showing slight epithelial damage and biofilms clustered on the surface of the epithelium (indicated by arrows); (d) MatTek full-thickness tissue after infection with mixed-species biofilm, showing slight epithelial damage and biofilms clustered on the surface of the epithelium (indicated by arrows). Stained with haematoxylin and eosin. The scale bar represents 50 µm.

primary aim was to evaluate them in terms of a more cost-effective way of investigating biofilm infections of tissues, particularly in this study, related to infections associated with the oral mucosa.

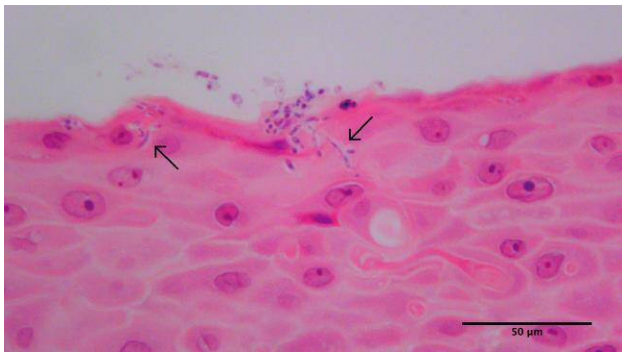

Fig. 8. Representative light microscope image of the mixed-species biofilm infection of MatTek full-thickness tissues, demonstrating tissue damage caused by invading *Candida albicans* and bacteria as a result of biofilm infection. Stained with haematoxylin and eosin. The scale bar represents 50 µm.

The detection of secreted molecules in response to infection is dependent on the type and duration of the infection, as some cytokines typically take longer to accumulate in the supernatant to a level sufficient for detection with many assays, and therefore it takes longer to determine true differences between infections [35]. The biofilms used in this study were considered to be too pathogenic for sustained cytokine production to be allowed to proceed to a level that would be detectable in an *in vitro* assay without complete tissue destruction, but visual representation of tissue damage and microbial invasion was clearly evident.

Biofilm infection varies between tissue types

This study aimed to compare commercially available and *in vitro* tissue models, both keratinocyte-only and full thickness, where we observed good similarity between the tissue models of the same type. The pattern of LDH activity was consistent between keratinocyte-only tissue models, as was *C. albicans* virulence gene expression. Additionally, the measurement of the relative expression of the *IL-18* gene in single versus mixed-species biofilms via RT-qPCR was also consistent between these models (Fig. S1, available in the online version of this article).

Some differences were observed in the infections using full-thickness tissues, primarily the extent of damage induced by the biofilms (Figs 6 and 7). Visually, very substantial damage was evident in the *in vitro* full-thickness tissues, with severe disruption of the epithelium (Fig. 6), whereas the relative extent of damage was reduced with MatTek full-thickness tissues. It was noted, however, that the epithelium of MatTek tissues, which by its very nature is an excellent natural physical barrier to the external environment, was more highly keratinised. Tissue invasion was observed in mixed-species infections of the MatTek tissues, although not to the same extent as seen in the *in vitro* tissues. Thus, although the same overall pattern of damage and invasion was evident in both *in vitro* and MatTek tissues, the duration of the infection with respect to MatTek tissues may not have been sufficient to demonstrate the pathogenicity of the infection that we have become accustomed to in previous studies. Furthermore, cornification of the tissue models may occur if, for example, they are extended long past the optimum culture period. This can subsequently influence tissue viability and responses to infection.

It is known that the pro-inflammatory cytokine interleukin-18 (IL-18) can stimulate monocyte cells to mature and induce phagocytosis of pathogens, and that monocyte cells can produce inflammatory cytokines of their own, including IL-23, the production of which during *in vitro* investigations was shown to be increased in a dose-dependent manner as a result of *C. albicans* challenge with prior stimulation by the bacterial LPS (Fig. S2). Furthermore, *IL-18* gene expression was up-regulated during mixed-species infection in this study and was also previously observed by Cavalcanti *et al.* [27].

Commercially available tissue models do not allow for the incorporation of immune cells within the tissues, but there is scope for continued development with *in vitro* full-thickness tissues to achieve this. The incorporation of immune cells may allow for cell-to-cell communication to be evaluated, along with the potential for the migration of immune cells to clear the infection to be monitored. This study is the first step in determining suitable models with which further development can be pursued. Neither the SkinEthic RHOE or MatTek EpiOral full-thickness tissues appear to provide benefits that outweigh the use or further development of *in vitro* tissue models, and there is a substantial cost benefit in using *in vitro* tissues, despite the increased manpower required to culture the *in vitro* tissues compared with simply purchasing them ready-made. There are clear advantages in using these for future studies instead of the commercially available tissues.

Conclusions

The main findings of this study were the successful development of reproducible *in vitro* oral mucosal tissue models, and the observation that these in-house models were comparable to commercially available constructs for the study of denture-associated biofilm infections. This work highlights the flexibility, advantages and future potential of using *in vitro* tissues compared with static, commercially available constructs, and in particular the substantial cost benefit of doing so.

Funding information
This work was completed as part of an EPSRC-GlaxoSmithKline case award PhD studentship.

Acknowledgements
The input of Mr Luke Jennings, Dr Lucie Hadley and Dr Helen Colley of the School of Clinical Dentistry, University of Sheffield, and their expertise, advice and continued support relating to full-thickness tissue model culture are gratefully acknowledged. We are also grateful for the support of Ms Sue Wozniak and Ms Hayley Pincott, who assisted with the preparation and sectioning of samples for histological analysis, and for the histological expertise provided by Dr Adam Jones.

Conflicts of interest
The authors declare that there are no conflicts of interest.

Ethical statement
Primary human oral fibroblasts were isolated from biopsies obtained from the buccal and gingival oral mucosa from patients during routine dental procedures with written, informed consent (ethical approval number 09/H1308/66), and were kindly provided by Dr Helen Colley, University of Sheffield, for use in this study.

References

1. Flemming HC, Wingender J. The biofilm matrix. *Nat Rev Microbiol* 2010;8:623–633.
2. Costerton JW, Stewart PS, Greenberg EP. Bacterial biofilms: a common cause of persistent infections. *Science* 1999;284:1318–1322.
3. Sutherland IW. The biofilm matrix—an immobilized but dynamic microbial environment. *Trends Microbiol* 2001;9:222–227.
4. Costerton JW, Cheng KJ, Geesey GG, Ladd TI, Nickel JC *et al.* Bacterial biofilms in nature and disease. *Annu Rev Microbiol* 1987;41:435–464.
5. Hall-Stoodley L, Stoodley P. Developmental regulation of microbial biofilms. *Curr Opin Biotechnol* 2002;13:228–233.
6. Bradshaw DJ, Marsh PD, Allison C, Schilling KM. Effect of oxygen, inoculum composition and flow rate on development of mixed-culture oral biofilms. *Microbiology* 1996;142:623–629.
7. Bradshaw DJ, Marsh PD, Watson GK, Allison C. Role of *Fusobacterium nucleatum* and coaggregation in anaerobe survival in planktonic and biofilm oral microbial communities during aeration. *Infect Immun* 1998;66:4729–4732.
8. Fux CA, Costerton JW, Stewart PS, Stoodley P. Survival strategies of infectious biofilms. *Trends Microbiol* 2005;13:34–40.
9. Trautner BW, Darouiche RO. Role of biofilm in catheter-associated urinary tract infection. *Am J Infect Control* 2004;32:177–183.
10. Ramage G, Martínez JP, López-Ribot JL. *Candida* biofilms on implanted biomaterials: a clinically significant problem. *FEMS Yeast Res* 2006;6:979–986.
11. Wolcott RD, Rhoads DD, Bennett ME, Wolcott BM, Gogokhia L *et al.* Chronic wounds and the medical biofilm paradigm. *J Wound Care* 2010;19:45–53.
12. Gendreau L, Loewy ZG. Epidemiology and etiology of denture stomatitis. *J Prosthodont* 2011;20:251–260.
13. Djeribi R, Bouchloukh W, Jouenne T, Menaa B. Characterization of bacterial biofilms formed on urinary catheters. *Am J Infect Control* 2012;40:854–859.
14. Percival SL, Suleman L, Vuotto C, Donelli G. Healthcare-associated infections, medical devices and biofilms: risk, tolerance and control. *J Med Microbiol* 2015;64:323–334.
15. Aas JA, Paster BJ, Stokes LN, Olsen I, Dewhirst FE. Defining the normal bacterial flora of the oral cavity. *J Clin Microbiol* 2005;43:5721–5732.

16. **Dewhirst FE, Chen T, Izard J, Paster BJ, Tanner AC *et al.*** The human oral microbiome. *J Bacteriol* 2010;192:5002–5017.
17. **Wade WG.** The oral microbiome in health and disease. *Pharmacol Res* 2013;69:137–143.
18. **Ghannoum MA, Jurevic RJ, Mukherjee PK, Cui F, Sikaroodi M *et al.*** Characterization of the oral fungal microbiome (mycobiome) in healthy individuals. *PLoS Pathog* 2010;6:e1000713–1000718.
19. **Ritz HL.** Microbial population shifts in developing human dental plaque. *Arch Oral Biol* 1967;12:1561–1568.
20. **Marsh PD.** Dental plaque as a microbial biofilm. *Caries Res* 2004; 38:204–211.
21. **Edgerton M, Levine MJ.** Characterization of acquired denture pellicle from healthy and stomatitis patients. *J Prosthet Dent* 1992;68: 683–691.
22. **Salerno C, Pascale M, Contaldo M, Esposito V, Busciolano M *et al.*** *Candida*-associated denture stomatitis. *Med Oral Patol Oral Cir Bucal* 2011;16:e139–e143.
23. **Newton AV.** Denture sore mouth: a possible aetiology. *Br Dent J* 1962;112:357–360.
24. **Williams DW, Kuriyama T, Silva S, Malic S, Lewis MA.** *Candida* biofilms and oral candidosis: treatment and prevention. *Periodontol 2000* 201155:250–265.
25. **Shulman JD, Rivera-Hidalgo F, Beach MM.** Risk factors associated with denture stomatitis in the United States. *J Oral Pathol Med* 2005;34:340–346.
26. **Rogers H, Wei X-Q, Lewis MAO, Patel V, Rees J *et al.*** Immune response and candidal colonisation in denture associated stomatitis. *J Clin Cell Immunol* 2013;4:1–7.
27. **Cavalcanti YW, Morse DJ, da Silva WJ, del-Bel-Cury AA, Wei X *et al.*** Virulence and pathogenicity of *Candida albicans* is enhanced in biofilms containing oral bacteria. *Biofouling* 2015;31:27–38.
28. **Silva S, Henriques M, Oliveira R, Azeredo J, Malic S *et al.*** Characterization of *Candida parapsilosis* infection of an *in vitro* reconstituted human oral epithelium. *Eur J Oral Sci* 2009;117:669–675.
29. **Silva S, Hooper SJ, Henriques M, Oliveira R, Azeredo J *et al.*** The role of secreted aspartyl proteinases in *Candida tropicalis* invasion and damage of oral mucosa. *Clin Microbiol Infect* 2011;17:264–272.
30. **Yadev NP, Murdoch C, Saville SP, Thornhill MH.** Evaluation of tissue engineered models of the oral mucosa to investigate oral candidiasis. *Microb Pathog* 2011;50:278–285.
31. **Colley HE, Hearnden V, Jones AV, Weinreb PH, Violette SM *et al.*** Development of tissue-engineered models of oral dysplasia and early invasive oral squamous cell carcinoma. *Br J Cancer* 2011; 105:1582–1592.
32. **Jennings LR, Colley HE, Ong J, Panagakos F, Masters JG *et al.*** Development and characterization of *in vitro* human oral mucosal equivalents derived from immortalized oral keratinocytes. *Tissue Eng Part C Methods* 2016;22:1108–1117.
33. **Wayakanon K, Thornhill MH, Douglas CW, Lewis AL, Warren NJ *et al.*** Polymersome-mediated intracellular delivery of antibiotics to treat *Porphyromonas gingivalis*-infected oral epithelial cells. *FASEB J* 2013;27:4455–4465.
34. **Bustin SA, Benes V, Garson JA, Hellemans J, Huggett J *et al.*** The MIQE guidelines: minimum information for publication of quantitative real-time PCR experiments. *Clin Chem* 2009;55:611–622.
35. **Jayatilake JA, Samaranayake YH, Samaranayake LP.** An ultrastructural and a cytochemical study of candidal invasion of reconstituted human oral epithelium. *J Oral Pathol Med* 2005;34:240–246.
36. **Dongari-Bagtzoglou A, Kashleva H.** Development of a novel three-dimensional *in vitro* model of oral *Candida* infection. *Microb Pathog* 2006;40:271–278.